

Some pages of this thesis may have been removed for copyright restrictions.

If you have discovered material in Aston Research Explorer which is unlawful e.g. breaches copyright, (either yours or that of a third party) or any other law, including but not limited to those relating to patent, trademark, confidentiality, data protection, obscenity, defamation, libel, then please read our [Takedown policy](#) and contact the service immediately (openaccess@aston.ac.uk)

The Single Drop Drying of Heat-Sensitive Materials

Abid Ali Sayed

Doctor of Philosophy

The University of Aston in Birmingham

April 1995

This copy of the thesis has been supplied on the condition that anyone who consults it is understood to recognise that its copyright rests with the author and that no quotation from the thesis and no information derived from it may be published without proper acknowledgement.

Abstract

The literature relating to the principles and practice of drying of materials, particularly those susceptible to thermal degradation or undesirable loss of volatile components, has been reviewed.

Single droplets of heat-sensitive materials were dried whilst suspended in a horizontal wind tunnel from a specially-designed, rotating thermocouple which enabled direct observation of drying behaviour and continuous measurement of droplet temperature as drying progressed.

The effects of drying air temperature and initial solids concentration on the potency of various antibiotics, viz. ampicillin, chloramphenicol, oxytetracycline, streptomycin, and tetracycline, were assessed using a modified Drug Sensitivity Testing technique. Only ampicillin was heat-sensitive at temperatures above 100°C, e.g. at an air temperature of 115°C its zone diameter was reduced from 100% to 45%.

Selected enzymes, viz. dextran sucrose and invertase, were also dried and their residual activities determined by High Performance Liquid Chromatography. The residual activity of dextran sucrose was rapidly reduced at temperatures above 65°C, and the residual activity of invertase reduced rapidly at temperatures above 65°C but drying with short residence times will retain most its activity.

The performance of various skin-forming encapsulants, viz. rice and wheat starch, dextrin, coffee, skim milk, fructose, gelatine 60 and 150 Bloom, and gum arabic, was evaluated to determine their capabilities for retention of ethanol as a model volatile, under different operating conditions. The effects of initial solids concentration, air velocity and temperature were monitored for each material tested. Ethanol content was analysed by Gas Liquid Chromatography and in some cases dried crusts were removed for examination. Volatiles retention was concluded to depend in all cases upon the rate and nature of the skin formation and selective diffusion phenomena.

The results provided further insight into the inter-relationship between temperature, residence time and thermal degradation of heat-sensitive materials. They should also assist in selection of the preferred dryer for such materials, and of the operating parameters to enable maximum retention of the required physico-chemical characteristics in the dried materials.

Key words: single droplet drying, volatiles retention, antibiotics, enzymes, encapsulants, spray drying, freeze drying, heat-sensitive materials

Acknowledgement

I am indebted to my supervisor, Dr Clive Mumford, for his continual encouragement throughout the duration of this study.

I would like to thank my family for their patience and their encouragement to bring this study to its completion and all my fellow students in the Mass Transfer Lab for their friendship.

The contribution of Dr HM Hassan to the experimentation on volatiles retention in convective drying is also acknowledged.

Dedication

To the Guardian of the Time.

Contents

TITLE PAGE	1
ABSTRACT	2
ACKNOWLEDGEMENT	3
DEDICATION	4
CONTENTS	5
LIST OF FIGURES	13
LIST OF TABLES	30
1: INTRODUCTION	32
1.1: THE NATURE OF DRYING	33
1.2: SURFACE EVAPORATION - EFFECT OF EXTERNAL CONDITIONS	35
1.3: EFFECTS OF INTERNAL CONDITIONS	37
1.3.1: DIFFUSION	38
1.3.2: CAPILLARY FLOW	38
1.4: MASS TRANSFER ACROSS A PHASE BOUNDARY	39
1.4.1: THE TWO FILM THEORY	41
1.4.2: THE PENETRATION THEORY	41
1.4.3: THE FILM PENETRATION THEORY	42
1.4.4: THE BOUNDARY LAYER THEORY	42
1.5: MOISTURE CONTENTS OF SOLIDS	42

1.6: CLASSIFICATION OF SOLIDS	43
2: MECHANISMS OF DRYING	45
2.1: DETERMINATION OF DRYING CHARACTERISTICS	45
2.2: PERIODS OF DRYING	46
2.3: METHODS OF DRYING	48
2.3.1: CONVECTIVE DRYING	50
2.3.2: CONDUCTION DRYING	51
2.3.3: RADIATION DRYING	53
2.3.4: DIELECTRIC DRYING	53
2.3.5: FREEZE DRYING	55
2.3.6: VACUUM DRYING	55
2.4: SELECTION OF PREFERRED DRYER FOR HEAT-SENSITIVE PRODUCTS	56
3: HEAT-SENSITIVE MATERIALS	58
3.1: PHARMACEUTICALS	58
3.2: ENZYMES	60
3.3: FLAVOURS	62
3.3.1: THE 'SELECTIVE DIFFUSION' THEORY FOR FLAVOUR RETENTION	64
3.4: MECHANISM OF THERMAL DEGRADATION	66
3.5: OTHER FORMS OF DEGRADATION	68
3.5.1: ENZYMATIC REACTIONS	68
3.5.2 CHEMICAL REACTIONS IN FOODS	69
3.5.2.1: The Maillard reaction	69
3.5.2.2: Lipid oxidation	69
3.5.2.3: Protein denaturation	70
3.5.3: STRUCTURAL DEGRADATION	71

4:	DRYING TECHNIQUES FOR HEAT-SENSITIVE MATERIALS	73
4.1:	FREEZE DRYING	75
4.1.1:	THE FREEZE DRYING PROCESS	78
4.1.2:	TYPES OF FREEZE DRYERS	83
4.2:	SPRAY DRYING	83
4.2.1:	ATOMISATION	88
4.2.2:	DROP SIZE AND SIZE DISTRIBUTION	88
4.2.3:	CHAMBER DESIGN	90
4.2.3.1:	Air-droplet contact systems	91
4.2.4:	ANCILLARY EQUIPMENT	91
4.2.4.1:	Air heaters	92
4.2.4.2:	Fans	92
4.2.4.3:	Powder separators	92
4.2.5:	THERMAL EFFICIENCY	93
4.2.6:	APPLICATIONS OF SPRAY DRYING	94
4.2.7:	ADVANTAGES/DISADVANTAGES OF SPRAY DRYING	94
4.3:	VACUUM DRYERS	96
4.3.1:	VACUUM TRAY DRYERS	96
4.3.2:	VACUUM DRUM DRYERS	97
4.3.3:	VACUUM BAND DRYERS	97
4.3.4:	VACUUM DOUBLE CONE DRYERS	97
4.3.5:	VACUUM PADDLE DRYERS	98
5:	SINGLE DROPLET EVAPORATION AND DRYING	99
5.1:	SINGLE DROPLETS OF PURE LIQUIDS	101
5.1.1:	DROPLET EVAPORATION UNDER NATURAL CONVECTION	101
5.1.2:	DROPLET EVAPORATION UNDER FORCED CONVECTION	102
5.1.2.1:	The mass transfer approach	102
5.1.2.2:	The heat transfer approach	106
5.1.3:	DROPLET EVAPORATION IN HIGH TEMPERATURES	107

5.2: EVAPORATION FROM DROPLETS WITH DISSOLVED OR SUSPENDED SOLIDS	111
5.3: FLAVOUR RETENTION	120
5.4 THE DRYING OF ENZYMES	139
5.5: THE DRYING OF PHARMACEUTICALS	144
 6: EXPERIMENTAL INVESTIGATION	 154
6.1: SELECTION OF APPARATUS AND MATERIALS	154
6.1.1: APPARATUS SELECTION	154
6.1.2: MATERIALS SELECTION	154
6.2: APPARATUS	155
6.2.1: CONSTRUCTION	155
6.2.1.1: The air supply	155
6.2.1.2: Modifications to allow use of nitrogen as drying gas	159
6.2.1.3: The working section	159
6.2.2: COMMISSIONING/OPERATION OF THE APPARATUS	167
6.2.2.1: Commissioning	167
6.2.2.2: Operation	167
6.2.3: EXPERIMENTAL PROCEDURE & DATA TREATMENT	168
6.3: MATERIALS	170
6.3.1: FLAVOUR ENCAPSULANTS	170
6.3.1.1: Gum arabic	170
6.3.1.2: Rice starch	170
6.3.1.3: Coffee	171
6.3.1.4: Wheat starch	171
6.3.1.5: Gelatine	171
6.3.1.6: Dextrin	172
6.3.1.7: Skim milk	172
6.3.2: ANTIBIOTICS	172
6.3.2.1: Ampicillin	173
6.3.2.2: Streptomycin	173
6.3.2.3: Tetracycline	173

6.3.2.4: Oxytetracycline	180
6.3.2.5: Chloramphenicol	180
6.3.3: ENZYMES	180
6.3.3.1: Dextran sucrose	180
6.3.3.2: Invertase	181
6.4: ANALYTICAL TECHNIQUES	181
6.4.1: DRUG SENSITIVITY TESTING (DST)	181
6.4.1.1: Preparation of bacterial cultures	182
6.4.1.2: Preparation of the agar plates	182
6.4.1.3: Seeding the agar plates	185
6.4.1.4: Setting-up the assay	185
6.4.1.5: Reading the plates	188
6.4.2: GAS LIQUID CHROMATOGRAPHY	189
6.4.2.1: Components of the GLC	189
6.4.2.1.1: Carrier gas supply	190
6.4.2.1.2: Sample injection system	190
6.4.2.1.3: Columns	191
6.4.2.1.4: Detection systems	192
6.4.2.2: Operation of the GLC	193
6.4.2.3: Sample preparation and analysis	194
6.4.3: FOURIER TRANSFORM INFRA-RED SPECTROPHOTOMETRY	195
6.4.3.1: Components of an IR spectrophotometer	196
6.4.3.2: Detectors	196
6.4.3.3: Solid sample preparation	198
6.4.3.4: IR Fourier transform spectrophotometer	199
6.4.4: HIGH PERFORMANCE LIQUID CHROMATOGRAPHY	200
6.4.4.1: Components of an HPLC system	200
6.4.4.1.1: Degassing system	200
6.4.4.1.2: Pumps	201
6.4.4.1.3: Pre-columns	201
6.4.4.1.4: Sample injectors	202
6.4.4.1.5: Analytical columns	202
6.4.4.1.6: Detectors	204
6.4.4.2: The HPLC system used in this study	204

6.5: FREEZE-DRYING	206
7: RESULTS	207
7.1: FLAVOUR ENCAPSULANTS	207
7.1.1: THE EFFECT OF INITIAL CONCENTRATION	208
7.1.1.1: Rice starch	208
7.1.1.2: Wheat starch	212
7.1.1.3: Dextrin	217
7.1.1.4: Fructose	222
7.1.1.5: Sucrose	225
7.1.1.6: Skim milk	227
7.1.1.7: Coffee	231
7.1.1.8: Gelatine 60	234
7.1.1.9: Gelatine 150	236
7.1.1.10: Gum arabic	236
7.1.2: THE EFFECT OF AIR VELOCITY	239
7.1.2.1: Rice starch	239
7.1.2.2: Wheat starch	243
7.1.2.3: Dextrin	247
7.1.2.4: Fructose	249
7.1.2.5: Sucrose	249
7.1.2.6: Skim milk	253
7.1.2.7: Coffee	256
7.1.2.8: Gelatine 60	259
7.1.2.9: Gelatine 150	259
7.1.2.10: Gum arabic	260
7.1.3: THE EFFECT OF TEMPERATURE	264
7.1.3.1: Rice starch	264
7.1.3.2: Wheat starch	267
7.1.3.3: Dextrin	270
7.1.3.4: Fructose	273
7.1.3.5: Skim milk	276
7.1.3.6: Coffee	279
7.1.3.7: Gelatine 60	282

7.1.3.8: Gelatine 150	284
7.1.3.9: Gum arabic	287
7.2: ANTIBIOTICS	290
7.2.1: THE EFFECT OF INITIAL CONCENTRATION	293
7.2.1.1: Ampicillin	293
7.2.1.2: Chloramphenicol	297
7.2.1.3: Oxytetracycline	303
7.2.1.4: Streptomycin	308
7.2.1.5: Tetracycline	313
7.2.2: THE EFFECT OF TEMPERATURE	318
7.2.2.1: Ampicillin	318
7.2.2.2: Chloramphenicol	322
7.2.2.3: Oxytetracycline	326
7.2.2.4: Streptomycin	330
7.2.2.5: Tetracycline	334
7.2.3: THE EFFECT OF DRYING IN AN INERT MEDIUM (NITROGEN)	338
7.2.3.1: Ampicillin	338
7.2.3.2: Chloramphenicol	341
7.2.3.3: Streptomycin	341
7.2.3.4: Tetracycline	346
7.3: ENZYMES	349
7.3.1: DEXTRAN SUCRASE	349
7.3.2: INVERTASE	351
7.4: FREEZE DRYING	353
7.4.1: ANTIBIOTICS	353
7.4.1.1: Ampicillin	354
7.4.1.2: Chloramphenicol	354
7.4.1.3: Oxytetracycline	354
7.4.1.4: Streptomycin	354
7.4.1.5: Tetracycline	354
7.4.2: FLAVOUR ENCAPSULANTS	357
7.5: FTIR SPECTROSCOPY RESULTS	362

8:	DISCUSSION OF RESULTS	368
8.1:	EXPERIMENTAL TECHNIQUE	369
8.1.1:	LOSS OF VOLATILES	370
8.1.2:	POSSIBLE STRATEGIES FOR VOLATILES RETENTION	379
8.2:	ANTIBIOTICS	382
8.3:	ENZYMES	383
9:	CONCLUSIONS AND RECOMMENDATIONS FOR FURTHER WORK	385
9.1:	CONCLUSIONS	385
9.2:	RECOMMENDATIONS FOR FURTHER STUDIES	387
10:	NOMENCLATURE	389
11:	REFERENCES	392
12:	APPENDICES	402
12.1.	APPENDIX A - AIR/WATER SYSTEM PROPERTIES	402
12.2.	APPENDIX B - MATERIAL SPECIFICATION SHEETS	403
12.3.	APPENDIX C - PAPERS SUBMITTED FOR PUBLICATION	413

List of Figures

Figure 2.1	A typical drying rate for a hygroscopic product at constant drying conditions.	46
Figure 2.3	Convective drying (a) open loop (b) closed loop circulation.	52
Figure 2.4.	Drum dryer - an example of a conductive dryer.	52
Figure 3.1.	Effect of heat on proteins.	61
Figure 3.2.	Effect of water concentration in aqueous solutions upon the diffusion coefficient of water and acetone	64
Figure 3.3.	The effect of water concentration on diffusion coefficients of acetone and water.	65
Figure 4.2.	Model for uniformly retreating ice front in freeze drying	80
Figure 4.4.	Layout of a typical spray drying plant. Single rotary atomiser, co-current operation with or without application of swirl.	85
Figure 4.5.	Spray dryer configuration (a) Co-current	86
Figure 4.5.	Spray dryer configuration (b) Counter-current	87
Figure 5.1.	Drying rate for sodium sulphate droplets	115
Figure 5.2.	Drying rate for droplet of organic liquid	115
Figure 5.3.	Effect of initial concentration of maltodextrin on ethanol retention.	128
Figure 5.6.	Loss of SF ₆ with 20% w/w glucose	137
Figure 5.7.	Loss of SF ₆ with 20% w/w sucrose	137
Figure 5.8.	Loss of SF ₆ with 20% w/w maltodextrin	138
Figure 5.9.	Loss of SF ₆ with 5% w/w coffee	138
Figure 5.10.	Effect of immobilisation on the thermo-stability of alcohol-oxidase	142

Figure 5.11.	Thermo-inactivation of dry immobilised alcohol-oxidase	142
Figure 5.12.	Effect of temperature on pyrethrins content.	145
Plate 5.13.	Electron photomicrographs of di-sodium cromoglycate (a) mechanically micronised, (b) spray dried.	147
Plate 5.15.	Electron photomicrograph of di-sodium cromoglycate (a) mechanically micronised, (b) spray dried, and (c) spray dried after storage at 60% humidity.	151
Figure 5.16.	Diazepam tablet formulations [top] and the corresponding dissolution profiles [bottom]	152
Figure 6.1.	Arrangement for air supply to the working section.	156
Plate 6.2.	Photograph of air supply to working section.	158
Figure 6.3.	The working section of the apparatus.	160
Plate 6.4.	Photograph showing the working section of the apparatus	161
Plate 6.5.	Photograph to show the location of (a) the wet bulb and (b) the dry bulb thermocouples	162
Figure 6.6:	Diagram representing the electric motor analogy used to provide the rotating electrical linkage for the thermocouple.	164
Figure 6.7.	Split in support shaft to prevent heat transfer to the droplet.	166
Figure 6.8.	Example of hard copy of the droplet temperature history	166
Plate 6.10.	Photomicrographs showing (a) rice starch [top], and (b) dextrin [bottom].	174
Plate 6.10.	Photomicrographs showing (c) wheat starch [top], and (d) skim milk [bottom].	175
Plate 6.10.	Photomicrographs showing (e) gelatine 60 Bloom [top], and (f) gelatine 150 Bloom [bottom].	176
Plate 6.10.	Photomicrographs showing (g) gum arabic [top], and (h) ampicillin [bottom].	177

Plate 6.10.	Photomicrographs showing (i) streptomycin [top], and (j) chloramphenicol [bottom].	178
Plate 6.10.	Photomicrographs showing (k) tetracycline [top], and (l) oxytetracycline [bottom].	179
Figure 6.12.	Variation in agar gel thickness affecting drug diffusion	184
Figure 6.14.	Three methods of antibiotic application to seeded agar plates (a) filter paper disc [top], (b) cylinder filled with antibiotic [middle], and (c) well cut into the agar [bottom].	186
Figure 6.16.	Components of a GLC.	190
Figure 6.18.	Components of an FTIR spectrophotometer.	198
Figure 6.19.	Components of an HPLC system.	201
Figure 6.20.	Types of particles used in liquid chromatography	203
Figure 6.21.	Detectability differences for microbore and conventional columns. (A) large porous particles, (B) pellicular particles, and (C) micro-porous particles.	203
Figure 7.1a	The effect of initial concentration on the retention of ethanol in rice starch solutions at ambient temperature ($T=25^{\circ}\text{C}$).	209
Figure 7.1b	The drying rate and droplet temperature history for the rice starch solutions.	209
Figure 7.2a	The effect of initial concentration on the retention of ethanol in rice starch solutions at $T=62^{\circ}\text{C}$.	210
Figure 7.2b	The drying rate and droplet temperature history for the rice starch solutions.	210
Figure 7.3a	The effect of initial concentration on the retention of ethanol in wheat starch solutions at ambient temperature ($T=25^{\circ}\text{C}$).	213
Figure 7.3b	The drying rate and droplet temperature history for the wheat starch solutions.	213

Figure 7.4a	The effect of initial concentration on the retention of ethanol in wheat starch solutions at $T=42^{\circ}\text{C}$.	214
Figure 7.4b	The drying rate and droplet temperature history for the wheat starch solutions.	214
Figure 7.5a	The effect of initial concentration on the retention of ethanol in wheat starch solutions at $T=62^{\circ}\text{C}$.	215
Figure 7.5b	The drying rate and droplet temperature history for the wheat starch solutions.	215
Figure 7.6a	The effect of initial concentration on the retention of ethanol in dextrin solutions at ambient temperature ($T=25^{\circ}\text{C}$).	218
Figure 7.6b	The drying rate and droplet temperature history for the dextrin solutions.	218
Figure 7.7a	The effect of initial concentration on the retention of ethanol in dextrin solutions at $T=42^{\circ}\text{C}$.	219
Figure 7.7b	The drying rate and droplet temperature history for the dextrin solutions.	219
Figure 7.8a	The effect of initial concentration on the retention of ethanol in dextrin solutions at $T=62^{\circ}\text{C}$.	220
Figure 7.8b	The drying rate and droplet temperature history for the dextrin solutions.	220
Figure 7.9a	The effect of initial concentration on the retention of ethanol in fructose solutions at ambient temperature ($T=25^{\circ}\text{C}$).	223
Figure 7.9b	The drying rate and droplet temperature history for the fructose solutions.	223
Figure 7.10a	The effect of initial concentration on the retention of ethanol in fructose solutions at $T=62^{\circ}\text{C}$.	224
Figure 7.10b	The drying rate and droplet temperature history for the fructose solutions.	224

Figure 7.11a The effect of initial concentration on the retention of ethanol in sucrose solutions at ambient temperature ($T=25^{\circ}\text{C}$).	226
Figure 7.11b The drying rate and droplet temperature history for the sucrose solutions.	226
Figure 7.12a The effect of initial concentration on the retention of ethanol in skim milk solutions at ambient temperature ($T=25^{\circ}\text{C}$).	229
Figure 7.12b The drying rate and droplet temperature history for the skim milk solutions.	229
Figure 7.13a The effect of initial concentration on the retention of ethanol in skim milk solutions at $T=62^{\circ}\text{C}$.	230
Figure 7.13b The drying rate and droplet temperature history for the skim milk solutions.	230
Figure 7.14a The effect of initial concentration on the retention of ethanol in coffee solutions at ambient temperature ($T=25^{\circ}\text{C}$).	232
Figure 7.14b The drying rate and droplet temperature history for the coffee solutions.	232
Figure 7.15a The effect of initial concentration on the retention of ethanol in coffee solutions at $T=62^{\circ}\text{C}$.	233
Figure 7.15b The drying rate and droplet temperature history for the coffee solutions.	233
Figure 7.16a The effect of initial concentration on the retention of ethanol in gelatin 60 solutions at ambient temperature ($T=25^{\circ}\text{C}$).	235
Figure 7.16b The drying rate and droplet temperature history for the gelatin 60 solutions.	235
Figure 7.17a The effect of initial concentration on the retention of ethanol in gelatine 150 solutions at ambient temperature $T=25^{\circ}\text{C}$.	237
Figure 7.17b The drying rate and droplet temperature history for the gelatine 150 solutions.	237

Figure 7.18a The effect of initial concentration on the retention of ethanol in gum arabic solutions at ambient temperature ($T=25^{\circ}\text{C}$).	238
Figure 7.18b The drying rate and droplet temperature history for the gum arabic solutions.	238
Figure 7.19a The effect of air flowrate on the retention of ethanol in 20% rice starch solutions at ambient temperature $T=25^{\circ}\text{C}$.	240
Figure 7.19b The drying rate and droplet temperature history for the 20% rice starch solutions.	240
Figure 7.20a The effect of air flowrate on the retention of ethanol in 20% rice starch solutions at $T=42^{\circ}\text{C}$.	241
Figure 7.20b The drying rate and droplet temperature history for the 20% rice starch solutions.	241
Figure 7.21a The effect of air flowrate on the retention of ethanol in 20% rice starch solutions at $T=62^{\circ}\text{C}$.	242
Figure 7.21b The drying rate and droplet temperature history for the 20% rice starch solutions.	242
Figure 7.22a The effect of air flowrate on the retention of ethanol in 20% wheat starch solutions at ambient temperature $T=25^{\circ}\text{C}$.	244
Figure 7.22b The drying rate and droplet temperature history for the 20% wheat starch solutions.	244
Figure 7.23a The effect of air flowrate on the retention of ethanol in 20% wheat starch solutions at $T=42^{\circ}\text{C}$.	245
Figure 7.23b The drying rate and droplet temperature history for the 20% wheat starch solutions.	245
Figure 7.24a The effect of air flowrate on the retention of ethanol in 20% wheat starch solutions at $T=62^{\circ}\text{C}$.	246
Figure 7.24b The drying rate and droplet temperature history for the 20% wheat starch solutions.	246

Figure 7.25a	The effect of air flowrate on the retention of ethanol in 20% dextrin solutions at ambient temperature $T=25^{\circ}\text{C}$.	248
Figure 7.25b	The drying rate and droplet temperature history for the 20% dextrin solutions.	248
Figure 7.26a	The effect of air flowrate on the retention of ethanol in 20% fructose solutions at ambient temperature $T=25^{\circ}\text{C}$.	250
Figure 7.26b	The drying rate and droplet temperature history for the 20% fructose solutions.	250
Figure 7.27a	The effect of air flowrate on the retention of ethanol in 20% fructose solutions at $T=62^{\circ}\text{C}$.	251
Figure 7.27b	The drying rate and droplet temperature history for the 20% fructose solutions.	251
Figure 7.28a	The effect of air flowrate on the retention of ethanol in 20% sucrose solutions at $T=62^{\circ}\text{C}$.	252
Figure 7.28b	The drying rate and droplet temperature history for the 20% sucrose solutions.	252
Figure 7.29a	The effect of air flowrate on the retention of ethanol in 20% skim milk solutions at ambient temperature $T=25^{\circ}\text{C}$.	254
Figure 7.29b	The drying rate and droplet temperature history for the 20% skim milk solutions.	254
Figure 7.30a	The effect of air flowrate on the retention of ethanol in 20% skim milk solutions at $T=62^{\circ}\text{C}$.	255
Figure 7.30b	The drying rate and droplet temperature history for the 20% skim milk solutions.	255
Figure 7.31a	The effect of air flowrate on the retention of ethanol in 20% coffee solutions at ambient temperature $T=25^{\circ}\text{C}$.	257
Figure 7.31b	The drying rate and droplet temperature history for the 20% coffee solutions.	257

Figure 7.32a The effect of air flowrate on the retention of ethanol in 20% coffee solutions at $T=62^{\circ}\text{C}$.	258
Figure 7.20b The drying rate and droplet temperature history for the 20% coffee solutions.	258
Figure 7.33a The effect of air flowrate on the retention of ethanol in 20% gelatine 60 solutions at ambient temperature $T=25^{\circ}\text{C}$.	261
Figure 7.33b The drying rate and droplet temperature history for the 20% gelatine 60 solutions.	261
Figure 7.34a The effect of air flowrate on the retention of ethanol in 20% gelatine 150 solutions at ambient temperature $T=25^{\circ}\text{C}$.	262
Figure 7.34b The drying rate and droplet temperature history for the 20% gelatine 150 solutions.	262
Figure 7.35a The effect of air flowrate on the retention of ethanol in 20% gum arabic solutions at ambient temperature $T=25^{\circ}\text{C}$.	263
Figure 7.35b The drying rate and droplet temperature history for the 20% gum arabic solutions.	263
Figure 7.36a The effect of temperature on the retention of ethanol in 20% rice starch solutions.	265
Figure 7.36b The drying rate and droplet temperature history for the 20% rice starch solutions.	265
Figure 7.37a The effect of temperature on the retention of ethanol in 20% rice starch solutions.	266
Figure 7.37b The drying rate and droplet temperature history for the 20% rice starch solutions.	266
Figure 7.38a The effect of temperature on the retention of ethanol in 20% wheat starch solutions.	268
Figure 7.38b The drying rate and droplet temperature history for the 20% wheat starch solutions.	268

Figure 7.39a The effect of temperature on the retention of ethanol in 20% wheat starch solutions.	269
Figure 7.39b The drying rate and droplet temperature history for the 20% wheat starch solutions.	269
Figure 7.40a The effect of temperature on the retention of ethanol in 20% dextrin solutions.	271
Figure 7.40b The drying rate and droplet temperature history for the 20% dextrin solutions.	271
Figure 7.41a The effect of temperature on the retention of ethanol in 20% dextrin solutions.	272
Figure 7.41b The drying rate and droplet temperature history for the 20% dextrin solutions.	272
Figure 7.42a The effect of temperature on the retention of ethanol in 20% fructose solutions.	274
Figure 7.42b The drying rate and droplet temperature history for the 20% fructose solutions.	274
Figure 7.43a The effect of temperature on the retention of ethanol in 20% fructose solutions.	275
Figure 7.43b The drying rate and droplet temperature history for the 20% fructose solutions.	275
Figure 7.44a The effect of temperature on the retention of ethanol in 20% skim milk solutions.	277
Figure 7.44b The drying rate and droplet temperature history for the 20% skim milk solutions.	277
Figure 7.45a The effect of temperature on the retention of ethanol in 20% skim milk solutions.	278
Figure 7.45b The drying rate and droplet temperature history for the 20% skim milk solutions.	278

Figure 7.46a	The effect of temperature on the retention of ethanol in 20% coffee solutions.	280
Figure 7.46b	The drying rate and droplet temperature history for the 20% coffee solutions.	280
Figure 7.47a	The effect of temperature on the retention of ethanol in 20% coffee solutions.	281
Figure 7.47b	The drying rate and droplet temperature history for the 20% coffee solutions.	281
Figure 7.48a	The effect of temperature on the retention of ethanol in 20% gelatine 60 solutions.	283
Figure 7.48b	The drying rate and droplet temperature history for the 20% gelatine 60 solutions.	283
Figure 7.49a	The effect of temperature on the retention of ethanol in 20% gelatine 60 solutions.	285
Figure 7.49b	The drying rate and droplet temperature history for the 20% gelatine 60 solutions.	285
Figure 7.50a	The effect of temperature on the retention of ethanol in 20% gelatine 150 solutions.	286
Figure 7.50b	The drying rate and droplet temperature history for the 20% gelatine 150 solutions.	286
Figure 7.51a	The effect of temperature on the retention of ethanol in 20% gum arabic solutions.	288
Figure 7.51b	The drying rate and droplet temperature history for the 20% gum arabic solutions.	288
Figure 7.52a	The effect of temperature on the retention of ethanol in 20% gum arabic solutions.	289
Figure 7.52b	The drying rate and droplet temperature history for the 20% gum arabic solutions.	289

Plate 7.53	Photograph showing re-growth of organisms on previously cleared zones	291
Plate 7.54	Photograph showing re-growth of organisms on previously cleared zones	292
Figure 7.55a	Variation in zone diameter with initial concentration of ampicillin at ambient air temperature ($T=23^{\circ}\text{C}$)	294
Figure 7.55b	The drying rate and droplet temperature history for the ampicillin solutions.	294
Figure 7.56a	Variation in zone diameter with initial concentration of ampicillin at 65°C air temperature.	295
Figure 7.56b	The drying rate and droplet temperature history for the ampicillin solutions.	295
Figure 7.57a	Variation in zone diameter with initial concentration of ampicillin at 90°C air temperature.	296
Figure 7.57b	The drying rate and droplet temperature history for the ampicillin solutions.	296
Figure 7.58a	Variation in zone diameter with initial concentration of ampicillin at 115°C air temperature	298
Figure 7.58b	The drying rate and droplet temperature history for the ampicillin solutions.	298
Figure 7.59a	Variation in zone diameter with initial concentration of chloramphenicol at air temperature ($T=23^{\circ}\text{C}$).	299
Figure 7.59b	The drying rate and droplet temperature history for the chloramphenicol solutions.	299
Figure 7.60a	Variation in zone diameter with initial concentration of chloramphenicol at 65°C air temperature.	300
Figure 7.60b	The drying rate and droplet temperature history for the chloramphenicol solutions.	300

Figure 7.61a	Variation in zone diameter with initial concentration of chloramphenicol at 90°C air temperature.	301
Figure 7.61b	The drying rate and droplet temperature history for the chloramphenicol solutions.	301
Figure 7.62a	Variation in zone diameter with initial concentration of chloramphenicol at 115°C air temperature.	302
Figure 7.62b	The drying rate and droplet temperature history for the chloramphenicol solutions.	302
Figure 7.63a	Variation in zone diameter with initial concentration of oxytetracycline at air temperature (T=23°C).	304
Figure 7.63b	The drying rate and droplet temperature history for the oxytetracycline solutions.	304
Figure 7.64a	Variation in zone diameter with initial concentration of oxytetracycline at 65°C air temperature.	305
Figure 7.64b	The drying rate and droplet temperature history for the oxytetracycline solutions.	305
Figure 7.65a	Variation in zone diameter with initial concentration of oxytetracycline at 90°C air temperature.	306
Figure 7.65b	The drying rate and droplet temperature history for the oxytetracycline solutions.	306
Figure 7.66a	Variation in zone diameter with initial concentration of oxytetracycline at 115°C air temperature.	307
Figure 7.66b	The drying rate and droplet temperature history for the oxytetracycline solutions.	307
Figure 7.67a	Variation in zone diameter with initial concentration of streptomycin at air temperature (T=23°C).	309
Figure 7.67b	The drying rate and droplet temperature history for the streptomycin solutions.	309

Figure 7.68a	Variation in zone diameter with initial concentration of streptomycin at 65°C air temperature.	310
Figure 7.68b	The drying rate and droplet temperature history for the streptomycin solutions.	310
Figure 7.69a	Variation in zone diameter with initial concentration of streptomycin at 90°C air temperature.	311
Figure 7.69b	The drying rate and droplet temperature history for the streptomycin solutions.	311
Figure 7.70a	Variation in zone diameter with initial concentration of streptomycin at 115°C air temperature.	312
Figure 7.70b	The drying rate and droplet temperature history for the streptomycin solutions.	312
Figure 7.71a	Variation in zone diameter with initial concentration of tetracycline at air temperature (T=23°C).	314
Figure 7.71b	The drying rate and droplet temperature history for the tetracycline solutions.	314
Figure 7.72a	Variation in zone diameter with initial concentration of tetracycline at 65°C air temperature.	315
Figure 7.72b	The drying rate and droplet temperature history for the tetracycline solutions.	315
Figure 7.73a	Variation in zone diameter with initial concentration of tetracycline at 90°C air temperature.	316
Figure 7.73b	The drying rate and droplet temperature history for the tetracycline solutions.	316
Figure 7.74a	Variation in zone diameter with initial concentration of tetracycline at 115°C air temperature.	317
Figure 7.74b	The drying rate and droplet temperature history for the tetracycline solutions.	317

Figure 7.75a	Variation in zone diameter of 10% ampicillin solution with gas temperature.	319
Figure 7.75b	The drying rate and droplet temperature history for the 10% ampicillin solutions.	319
Figure 7.76a	Variation in zone diameter of 20% ampicillin solution with air temperature.	320
Figure 7.76b	The drying rate and droplet temperature history for the 20% ampicillin solutions.	320
Figure 7.77a	Variation in zone diameter of 40% ampicillin solutions with air temperature.	321
Figure 7.77b	The drying rate and droplet temperature history for the 40% ampicillin solutions.	321
Figure 7.78a	Variation in zone diameter of 10% chloramphenicol solution with gas temperature.	323
Figure 7.78b	The drying rate and droplet temperature history for the 10% chloramphenicol solutions.	323
Figure 7.79a	Variation in zone diameter of 20% chloramphenicol solution with air temperature.	324
Figure 7.79b	The drying rate and droplet temperature history for the 20% chloramphenicol solutions.	324
Figure 7.80a	Variation in zone diameter of 40% chloramphenicol solution with air temperature.	325
Figure 7.80b	The drying rate and droplet temperature history for the 40% chloramphenicol solutions.	325
Figure 7.81a	Variation in zone diameter of 10% oxytetracycline solution with gas temperature.	327
Figure 7.81b	The drying rate and droplet temperature history for the 10% oxytetracycline solutions.	327

Figure 7.82a	Variation in zone diameter of 20% oxytetracycline solution with air temperature.	328
Figure 7.82b	The drying rate and droplet temperature history for the 20% oxytetracycline solutions.	328
Figure 7.83a	Variation in zone diameter of 40% oxytetracycline solution with air temperature.	329
Figure 7.83b	The drying rate and droplet temperature history for the 40% oxytetracycline solutions.	329
Figure 7.84a	Variation in zone diameter of 10% streptomycin solution with gas temperature.	331
Figure 7.84b	The drying rate and droplet temperature history for the 10% streptomycin solutions.	331
Figure 7.85a	Variation in zone diameter of 20% streptomycin solution with air temperature.	332
Figure 7.85b	The drying rate and droplet temperature history for the 20% streptomycin solutions.	332
Figure 7.86a	Variation in zone diameter of 40% streptomycin solution with air temperature.	333
Figure 7.86b	The drying rate and droplet temperature history for the 40% streptomycin solutions.	333
Figure 7.87a	Variation in zone diameter of 10% tetracycline solution with gas temperature.	335
Figure 7.87b	The drying rate and droplet temperature history for the 10% tetracycline solutions.	335
Figure 7.88a	Variation in zone diameter of 20% streptomycin solution with air temperature.	336
Figure 7.88b	The drying rate and droplet temperature history for the 20% streptomycin solutions.	336

Figure 7.89a Variation in zone diameter of 40% streptomycin solution with air temperature.	337
Figure 7.89b The drying rate and droplet temperature history for the 40% streptomycin solutions.	337
Figure 7.90a Variation in zone diameter of 10% ampicillin solution with drying atmosphere at ambient temperatures	339
Figure 7.90b The drying rate and droplet temperature history for the 10% ampicillin solutions.	339
Figure 7.91a Variation in zone diameter of 10% ampicillin solution with drying atmosphere at 115°C gas temperature.	340
Figure 7.91b The drying rate and droplet temperature history for the 10% ampicillin solutions.	340
Figure 7.92a Variation in zone diameter of 10% chloramphenicol solution with drying atmosphere at ambient temperatures	342
Figure 7.92b The drying rate and droplet temperature history for the 10% chloramphenicol solutions.	342
Figure 7.93a Variation in zone diameter of 10% chloramphenicol solution with drying atmosphere at 115°C gas temperature.	343
Figure 7.93b The drying rate and droplet temperature history for the 10% chloramphenicol solutions.	343
Figure 7.94a Variation in zone diameter of 10% streptomycin solution with drying atmosphere at ambient temperatures	344
Figure 7.94b The drying rate and droplet temperature history for the 10% streptomycin solutions.	344
Figure 7.95a Variation in zone diameter of 10% streptomycin solution with drying atmosphere at 115°C gas temperature.	345
Figure 7.95b The drying rate and droplet temperature history for the 10% streptomycin solutions.	345

Figure 7.96a Variation in zone diameter of 10% tetracycline solution with drying atmosphere at ambient temperatures	347
Figure 7.96b The drying rate and droplet temperature history for the 10% tetracycline solutions.	347
Figure 7.97a Variation in zone diameter of 10% tetracycline solution with drying atmosphere at 115°C gas temperature.	348
Figure 7.97b The drying rate and droplet temperature history for the 10% tetracycline solutions.	348
Figure 7.98a The effect of temperature on the enzyme activity of dextran sucrase.	350
Figure 7.98b The drying rate and droplet temperature history for the dextran sucrase solutions.	350
Figure 7.99a The effect of temperature on the enzyme activity of invertase.	352
Figure 7.99b The drying rate and droplet temperature history for the invertase solutions.	352
Figure 7.100 Variation in zone diameter with initial concentration of ampicillin.	355
Figure 7.101 Variation in zone diameter with initial concentration of chloramphenicol	355
Figure 7.102 Variation in zone diameter with initial concentration of streptomycin.	356
Figure 7.103 Variation in zone diameter with initial concentration of oxytetracycline.	356
Figure 7.104 Variation in zone diameter with initial concentration of tetracycline.	358
Figure 7.105 Effect of freeze-drying on the retention of ethanol in various solutions.	358

Figure 7.106 Effect of freeze-drying on the retention of ethanol in various solutions.	359
Figure 7.107 Effect of freeze-drying on the retention of ethanol in various solutions.	359
Figure 7.108 Effect of freeze-drying on the retention of ethanol in various solutions.	361
Figure 7.109 FTIR spectra for ampicillin dried at 115°C.	363
Figure 7.110 FTIR spectra for chloramphenicol dried at 115°C.	364
Figure 7.111 FTIR spectra for oxytetracycline dried at 115°C.	365
Figure 7.112 FTIR spectra for streptomycin dried at 115°C.	366
Figure 7.113 FTIR spectra for tetracycline dried at 115°C.	367
Figure 8.1: The relationship between the drying material and its surroundings	368
Figure 8.2: The retention of ethanol in 20% solutions of the various encapsulants at 25°C	372
Figure 8.3: The retention of ethanol in 20% solutions of the various encapsulants at 40°C	373
Figure 8.4: The retention of ethanol in 20% solutions of the various encapsulants at 65°C	374
Figure 8.5: The retention of ethanol in 20% solutions of the various encapsulants at 89°C	375
Figure 8.6: The retention of ethanol in 40% solutions of the various encapsulants at 25°C	376
Figure 8.7: The retention of ethanol in 20% solutions of the various encapsulants at 112°C	377
Figure 8.8: Drying characteristics of single droplets	380

List of Tables

Table 2.2:	Typical residence times in different dryer types	49
Table 3.4:	Effect of treatment upon availability of beef protein	71
Table 4.1:	Preservation of final product quality for Bakers Yeast	74
Table 4.3:	Frozen layer and maximum dry surface temperatures in typical freeze drying operations	82
Table 5.4:	Effect of the addition of gelatine on the retention of acetone	131
Table 5.5:	The influence of flavour solvent upon the retention of flavour compounds during spray drying.	133
Table 5.14:	Percentages of disodium cromoglycate particles reaching and remaining in the various stages during in vitro inhalation tests with the drug having been stored at the given humidities	148
Table 5.17:	Capsule formulation [top] and associated plasma diazepam levels of human volunteers [bottom]	153
Table 6.9:	Exposure times for the heat-sensitive materials	169
Table 6.11:	Target organisms for the antibiotics	182
Table 6.13:	The adapted Latin square, the numbers represent the inoculum number.	185
Table 6.15:	Experimentally-determined appropriate dilutions	187
Table 6.22:	Characteristics of chromatography detectors	205

1: Introduction

The drying of a material is often the final essential operation in a manufacturing process. Hence it deals with the finished product so that quality control, to avoid physical and chemical degradation, may be a prime consideration. In the majority of processing industries, drying is carried out for a combination of reasons which include:

- i) ease of handling - packaging, handling, and transportation of a dry product are easier and cheaper, because of the reduction in weight and/or volume ,
- ii) to provide, or retain, identifiable properties in the material e.g. to maintain the free-flowing nature of salt or the freedom from agglomeration of detergent powders, or to produce seasoned timber less prone to warpage,
- iii) to improve shelf-life (particularly for food products). A dry food product is less susceptible to microbial spoilage because microbial activity is inhibited in a dry environment. The risk of unfavourable oxidative and enzymatic reactions is also reduced,
- iv) to assist downstream processing e.g. a dry solid may be mixed more uniformly with other materials to yield a homogeneous product,
- v) to provide a material with an acceptable appearance, e.g. as with granulated coffee which is also readily dissolved in water, or freeze dried food products.

The present study was concerned with factors which determine the onset and rate of thermal degradation, including the loss of volatile constituents other than water, during drying. Although any drying process is system-specific (since, as discussed later, the means of moisture retention and transfer within the solid are critical features), the mechanisms involved are similar so that generalisations could be drawn as to the preferred selection of operating

parameters e.g. surface area to mass ratio, gas or surface temperature, initial feed condition, and residence time. The value of some additives was also assessed. The type of dryer and operating conditions likely to be suitable in any particular application, and the use and limitations of small-scale drying tests may be deduced from the literature review and the results.

1.1: The nature of drying

Drying normally describes the process of thermally removing volatile substances, usually water but sometimes a solvent, from a material to yield a solid product. (This definition excludes the partial drying of a solid by mechanical means, e.g. squeezing / expression , or centrifugation / filtration). The method, and efficiency of, heat transfer and potential for energy recovery are therefore important considerations in many processes.

The moisture is present in two forms - bound and unbound. Bound moisture is held in loose chemical combination, present as a trapped liquid solution within the solid, or even trapped within the microstructure of the solid. It therefore exerts a vapour pressure less than that of pure water at the same temperature. Unbound moisture is the moisture content in excess of the bound moisture i.e. it is retained in the solid and exerts an equilibrium vapour pressure equal to that of water at the same temperature.

Unbound moisture may be present in one of two forms:

- i) funicular state - a continuous liquid state exists within the porous body,
- ii) pendular state - the liquid around and between discrete particles is discontinuous so that the moisture is interspersed by air bubbles.

In the funicular state, liquid movement to the external surface of the material takes place by capillary action. As the moisture is removed , the continuity of the liquid phase gradually breaks-up due to suction of air into pores leaving

isolated pockets of moisture (pendular state), with capillary flow occurring only on a localised scale. When the material is close to 'bone dry', the moisture which is held as a monolayer of molecules on the pore walls is removed mainly by vapour flow (Strumillo & Kudra, 1986).

When a wet solid is subjected to thermal drying, two processes occur simultaneously:

- i) transfer of energy, mainly as heat, from the surrounding environment to evaporate the surface moisture, and
- ii) transfer of internal moisture to the surface of the solid and its subsequent evaporation due to process (i).

The rate at which drying is accomplished is governed by the rate at which these two processes proceed. Heat transfer from the surroundings to the wet solid occurs as a result of convection, conduction, or radiation, and in some cases as a result of a combination of these effects. The method selected depends upon the throughput of material, its drying characteristics and physical form, the importance of avoiding contamination or degradation, the feed condition and many other parameters.

In convective drying, heat is transferred to the surface of the wet solid from a gas and is then conducted from the surface to the interior. In conductive drying, e.g. with a drum dryer, the heat is applied to the underside of the solid or solution / slurry. However, in dielectric, radio frequency or microwave drying, the energy is supplied to generate heat internally within the solid which then flows to the exterior surfaces.

Process (i), the removal of water from the material surface depends upon the external conditions of temperature, air flow rate and humidity, pressure, and area of exposed surface available for evaporation. Process (ii), the movement of moisture internally within the solid is a function of the physical nature of

the solid, the temperature, and its moisture content; thus in convective drying it cannot be altered significantly by altering the gas temperature and velocity.

In a drying operation, either heat transfer or the various modes of mass transfer may be the limiting factor governing the drying rate, although they both proceed simultaneously throughout the drying cycle.

1.2: Surface evaporation - effect of external conditions

External drying conditions, such as temperature, humidity, and flow rate of the hot gas, are important during the initial stages of convective drying when unbound surface moisture is being removed. Surface evaporation is controlled by the diffusion of vapour from the surface of the solid into the surrounding atmosphere through a thin film of air in contact with the surface.

Since drying involves the interphase transfer of mass when a gas is brought into contact with the liquid, in which it is essentially insoluble, it is necessary to be familiar with the equilibrium characteristics of the wet solid.

As the moisture is generally removed by the drying air or hot gases, and as the ability of these gases to pick up the moisture will be determined by their temperature and humidity, it is also necessary to consider the properties of the air - water system, some of which are discussed in Appendix B.

From Coulson & Richardson (1977):

$$\text{Rate of heat transfer from gas to liquid} = h.A.(\theta - \theta_w) \quad 1.1$$

where,

h = heat transfer coefficient,

A = surface area, and

θ_w = wet bulb temperature

θ = air temperature.

$$\text{Mass rate of vaporisation} = ((h_D \cdot A \cdot M_W) / (RT)) \cdot (P_{W0} - P_W)$$

where,

h_D = mass transfer coefficient,

R = universal gas constant, and

M_W = molecular mass of water

P_W = partial pressure of water vapour

P_{W0} = vapour pressure of water at θ_w

T = temperature

$$\begin{aligned} \text{Mass rate of vaporisation} &= ((h_D \cdot A \cdot M_W) / (RT)) \cdot (P - P_W)_{\text{mean}} \cdot (H_W - H), \\ &= h_D \cdot A \cdot \rho_A (H_W - H) \end{aligned}$$

where,

H = humidity, mass of water carried per unit mass of dry air

H_W = humidity of saturated air at θ_w

ρ_A = density of air at its mean partial pressure.

Heat transfer required to cause vaporisation at this rate

$$= h_D \cdot A \cdot \rho_A (H_W - H) \cdot (\lambda) \quad 1.2$$

where λ is the latent heat of vaporisation of water

At equilibrium, the rates of heat transfer given by equations 1.1 and 1.2 above must be equal.

Hence,

$$h \cdot A \cdot (\theta - \theta_w) = h_D \cdot A \cdot \rho_A \cdot \lambda \cdot (H_w - H) \quad 1.3$$

$$h (\theta - \theta_w) / h_D \rho_A \lambda = (H_w - H)$$

$$(H - H_w) = - h (\theta - \theta_w) / h_D \rho_A \lambda \quad 1.4$$

Therefore, wet bulb temperature θ_w depends only upon the temperature and humidity of the drying air.

1.3: The effects of internal conditions

As a result of heat transfer to a wet solid, a temperature gradient develops within the solid, whilst moisture evaporation occurs from the surface. This promotes a migration of moisture from within the solid to the surface. Migration occurs through one or more mechanisms viz. diffusion, capillary flow, the influence of internal pressures set up by shrinkage during drying and, in the case of conduction drying, through repeated vaporisation and re-condensation of moisture.

An understanding of this internal movement of moisture is necessary when it is the controlling factor, e.g. when drying is carried out to low final moisture contents below a critical value. Variables such as air quality, which normally enhance the rate of surface evaporation through their effect upon the gas film heat and mass transfer coefficients, become less important.

1.3.1: Diffusion

Lewis, in 1921, and Newman, in 1932, proposed that the main mechanism of moisture migration was that of diffusion. In 1929, Sherwood proposed that drying occurred either:

- i) by the movement of moisture as a liquid through the pores to the surface and its subsequent evaporation from the surface, or
- ii) by the diffusion of water vapour through the pores after liquid vaporisation below the surface of the solid, and its subsequent transfer to the surrounding gas.

1.3.2: Capillary flow

The capillary theory of drying has been put forward in order to explain the migration of moisture. The basic importance of pore space between granular particles was first pointed out by Slichter in 1897 in connection with the movement of moisture in soils.

With the evaporation of the surface moisture during the constant-rate period, a liquid meniscus forms at the entrance of the pores which exist in a porous solid. The formation of the meniscus leads to the setting-up of capillary forces between the liquid and the solid, a concept first introduced by Buckingham in 1907. These forces cause the moisture to migrate from the interior to the exterior of the solid. Pore size affects the capillary force in that smaller pores produce stronger capillary forces than larger pores.

At the critical moisture content, some of the menisci begin to retreat into the pores and there is a gradual decrease in the wetted external surface area. Thus, although the drying rate per unit area of wetted surface remains constant, there is a decrease in the drying rate based upon the total external surface, giving rise to the first falling-rate period.

As more moisture is removed, the external surface dries completely until the remaining moisture is insufficient to maintain a continuous phase linking all the interior pores. The remaining moisture retreats to small isolated pockets within the solid, and the gas now penetrates into the pores to form the continuous phase.

Heat transfer, which now occurs by conduction through the solid to the moisture pockets, causes the vaporisation of the remaining moisture which diffuses in the gas phase to the surface and is subsequently removed by the drying air.

1.4: Mass transfer across a phase boundary

Contact between two phases during most diffusional mass transfer processes, such as evaporation and droplet drying, allows diffusion of vapour from one phase to the other. The existence of a concentration gradient across the interface provides the driving force for mass transfer, which continues until the concentration gradient has been reduced to zero, either by the evaporation of the liquid, or the saturation of the gas.

Mass transfer can take place in either a gas phase or liquid phase, or in both simultaneously (Coulson & Richardson, 1977). The rate of transfer of gas 'a', in a mixture of two gases 'a' and 'b', is determined not only by the rate of diffusion of 'a', but also the behaviour of 'b'. The molar rate of transfer of 'a' per unit area is given by Fick's law:

$$N_a = - D_{ab} (dC_a / dy) \quad 1.5$$

where

N_a is the molar rate of diffusion per unit area,

D_{ab} is the diffusivity of 'a' in 'b',

C_a is the concentration of 'a', and

y is the distance in the direction of diffusion.

And, the rate of diffusion of 'b' in 'a' is given by:

$$N_b = - D_{ba} (dC_b / dy)$$

Similarly, the rate of transfer of material in the liquid phase is represented by an equation similar to equation 1.5 above except that D_{ab} is replaced by D_l , the liquid phase diffusivity, to give:

$$N_a = - D_l (dC_a / dy)$$

Upon integration, this yields:

$$N_a = - D_l \frac{C_{a2} - C_{a1}}{y_2 - y_1}$$

where C_{a1} and C_{a2} are the molar concentrations of 'a' at two points y_1 and y_2 .

In most of the important applications of mass transfer, such as distillation, liquid-liquid extraction, *etc.*, there is transfer of material across an interface. The mass transfer rate between two fluids will depend upon the physical properties of the two phases, the concentration gradient, the interfacial area, and the degree of turbulence. Mass transfer equipment is, therefore, designed to provide a large area of contact between the phases, to promote turbulence within each of the fluids, and to optimise the concentration driving force.

In most industrial applications, the interfacial area is not precisely known. Hence, a number of mechanisms have been put forward to represent conditions in the region of the phase boundary.

1.4.1: The two film theory

The two film theory, proposed by Whitman in 1923, assumes that there is no turbulence at the interface and that the interface can be replaced by two hypothetical layers in which transfer is by molecular diffusion alone, and the concentration gradient resides only in these two layers. Mass transfer is treated as a steady-state process, and therefore the theory can only be applied if the time for the establishment of the concentration gradients is negligible compared to the time taken for mass transfer, or if the capacity of the films is negligible. The rate of transfer is then proportional to the diffusivity.

1.4.2: The penetration theory

The penetration theory of Higbie, in 1935, was based on the assumption that mass transfer took place as result of unsteady-state molecular diffusion. It is assumed that eddies in the fluid bring an element of fluid to the interface where it is exposed to the second phase for a definite interval of time, after which the surface element is mixed with the bulk again. Hence, fluid which has an initial composition corresponding to that of the bulk fluid remote from the interface is suddenly exposed to the second phase. It is further assumed that the surface layers immediately reach equilibrium, that unsteady state molecular diffusion occurs, and that the element is remixed after a fixed period of time. Unlike in the two film theory, the rate of transfer is proportional to the square root of the diffusivity.

1.4.3: The film penetration theory

A theory incorporating both of the two previous theories was proposed by Toor and Marchello in 1958. This regards the resistance to mass transfer as being in the laminar film at the interface, and mass transfer as an unsteady-state process. Mass transfer is assumed to take place as in the penetration theory, with the exception that the resistance is confined to the finite film, and the material that traverses the film is completely and immediately mixed with the bulk of the fluid. For short exposure times, when none of the diffusing materials has reached the far side of the film, the process occurs as in the penetration theory. But for longer exposure times, when a steady concentration gradient has been developed, the process occurs as in the two film theory.

1.4.4: The boundary layer theory

When a fluid flows over a solid surface, a velocity gradient is set up in the boundary layer. The existence of a temperature gradient and a concentration gradient between the surface and the fluid, will set up simultaneous heat and mass transfer processes, respectively between the surface and the fluid. Frossling applied this to evaporating droplets of nitrobenzene, aniline and water, and proposed that the rate of mass transfer was proportional to the diffusivity raised to a power of 0.67 (Hassan, 1991).

1.5: Moisture contents of solids

The moisture contained in a wet solid or liquid solution exerts a vapour pressure dependent upon the nature of the moisture, the nature of the solid, and the temperature. A wet solid exposed to a continuous supply of fresh gas

continues to lose moisture until the vapour pressure of the moisture in the solid is equal to the partial pressure of the vapour in the gas.

The solid and gas are then in equilibrium, and the moisture content of the solid is the equilibrium moisture content under the prevailing conditions. Further exposure to this air for indefinitely long periods will not cause any additional moisture loss. Exposing the solid to air of lower relative humidity could further reduce the moisture content of the solid.

1.6: Classification of solids

Solids have been classified by van Brackel in 1980 according to the presence / absence of pore space and to the bound / unbound moisture content. Although only applicable to homogeneous media, these classifications are:

a) non-hygroscopic capillary porous media such as sand, crushed minerals, polymer particles, and some ceramics. Such media:

- i) have a clearly recognisable pore space. This space is filled with liquid if the capillary porous media is completely saturated, and is filled with air when completely dry,
- ii) contain a negligible amount of physically-bound moisture, i.e. the media is non-hygroscopic, and
- iii) do not shrink during drying.

b) hygroscopic porous media such as clay, molecular sieves, wood, textiles.

Such media:

- i) have a clearly recognisable pore space,
- ii) contain a large amount of physically-bound moisture, and

iii) shrink during the initial stages of drying.

c) non-porous, colloidal media such as soap, glue, some polymers (e.g. nylon) and various food products. Such media:

i) do not have any pore space (evaporation occurs only at the surface),
and

ii) contain all their moisture in a physically-bound state.

2: Mechanisms of drying

As mentioned earlier, moisture in a solid may be present in either a bound or unbound condition. There are two methods of removing unbound moisture:

a) evaporation, by conduction, as occurs in roller dryers when the moisture is evaporated by raising the moisture temperature to its boiling point. The vapour pressure of moisture on the solid surface is equal to the atmospheric pressure. If the material being dried is heat sensitive, then the temperature at which evaporation occurs (i.e. the boiling point) could be lowered by lowering the pressure (vacuum evaporation). If the pressure is lowered below the triple point, then no liquid phase can exist and the moisture in the product is frozen. The addition of heat causes sublimation of the ice directly to water vapour, as in freeze drying.

b) vaporisation, by convection, i.e. the drying is carried out by passing warm air (or gas) over the product to be dried. The air is cooled by the product, and the moisture is transferred into the air and removed. In this case the saturation vapour pressure of the moisture over the solid surface is less than atmospheric pressure.

2.1: Determination of drying characteristics

Determination of the drying characteristics of any specific solid are essential for the selection of a suitable dryer. Information is also required on the solid handling characteristics, equilibrium moisture conditions, temperature sensitivities, and the temperature limits attainable with a particular heat source.

- i) humidity measurement (Audu, 1973, Ali, 1985, *etc.*)
- ii) continuous weighing (Hassan, 1991)
- iii) intermittent weighing (Charlesworth & Marshall, 1960, Furuta *et. al.*, 1984, *ibid*, 1985)

2.2: Periods of drying

The behaviour of any product depends upon its moisture content. During the first stage of drying, the constant-rate period illustrated in Figure 2.1, the surface contains free moisture. Vaporisation takes place from there (Charlesworth & Marshall, 1960, Fortes & Okos, 1980, *etc.*), and some shrinkage may occur as the moisture interface recedes into the solid. In this stage of drying, which may not always be present or be of short duration e.g. with a slurry, the rate-limiting step is the diffusion of water vapour across the air-moisture interface.

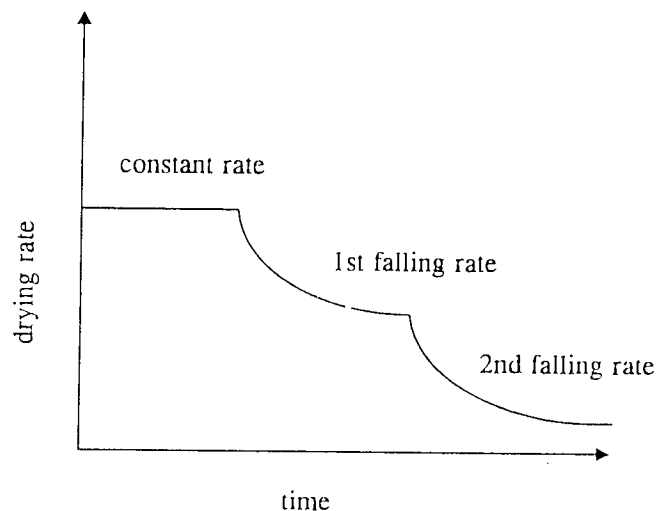


Figure 2.1 A typical drying rate for a hygroscopic product at constant drying conditions.

To calculate the drying rate under these conditions, the relationships for diffusion of vapour from a liquid surface into a gas may be used, the simplest of these being:

$$W = K_G A (P_S - P_W) \quad 1.5$$

where

W = mass evaporation rate

K_G = diffusional transfer coefficient

A = surface area

P_S = vapour pressure of water

P_W = partial pressure of water vapour in the air stream

The rate of drying in the constant-rate period is given by, after equation 1.4:

$$-dW / dt = (h A \Delta T / \lambda) = K_G A (P_S - P_W) \quad 1.6$$

where

dW / dt is the rate of moisture loss

ΔT is the temperature difference between the air and the surface.

The mass transfer coefficient is usually expressed in terms of humidity rather than pressure difference, i.e.:

$$K_G A (P_S - P_W) \cong k_A (H_S - H) \quad 1.7$$

The rate of drying is thus determined by h , ΔT , and A , and not by the conditions inside the solid (Perry & Chilton, 1974). ' h ' depends upon the air velocity and the direction of flow, and it has been found that:

$h = CG'^{0.8}$ where G' is the mass flow rate of air in kg/sm^2 (Coulson & Richardson, 1978).

Towards the end of this constant-rate period, moisture has to be transported from the inside to the surface e.g. by diffusion or capillary forces and the drying rate may still be constant. When the average moisture content has reached a critical moisture content, the drying rate falls giving rise to the second stage. In this first falling-rate period unsaturated surface drying proceeds until the surface film of liquid is entirely evaporated. The rate controlling process is the mechanism by which internal moisture is transferred to the surface.

On further drying (the third stage), which is not always exhibited, the rate at which moisture may move through the solid as a result of concentration gradients between the deeper parts and the surface is the rate controlling process. During this stage, some of the moisture bound by sorption is removed. As the moisture concentration is lowered by drying, the rate of internal moisture movement decreases. The rate of drying falls even more rapidly than before but, given sufficient time, drying continues until the moisture content falls to an equilibrium value depending upon the humidity of the surrounding air.

2.3: Methods of drying

Although moisture removal from wet materials can be carried out by mechanical dewatering processes, such as filtration, extrusion, or pressing, the process of drying commonly implies moisture evaporation involving simultaneous processes of heat and mass transfer.

Because of the vast number of materials that are dried, and the differing methods of supplying the heat, it is difficult to classify all possible drying methods.

One commonly used classification is based upon the mode of heat transfer e.g. conduction, convection, or radiation. Residence time within a dryer is also

used to classify dryers, as is shown in Table 2.2. Clearly those dryers which can achieve a given degree of drying in the shortest residence time at any

Dryer type		Typical residence time
1. Convection		
	belt conveyor	10 - 60 min
	flash dryer	0 - 10 sec
	fluid bed	10 - 60 min
	rotary dryer	10 - 60 min
	spray dryer	10 - 30 sec
	tray dryer (batch)	1 - 6 hr
	tray dryer (continuous)	10 - 60 min
2. Conduction		
	drum dryer	10 - 30 sec
	steam jacket rotary dryer	10 - 60 min
	steam tube rotary dryer	10 - 60 min
	tray dryer (batch)	1 - 6 hr
	tray dryer (continuous)	10 - 60 min

Table 2.2: Typical residence times in different dryer types (after Schlunder, 1982).

specific temperature are preferable for heat sensitive materials; hence the popularity of spray drying for certain foodstuffs, since they can be operated co-currently such that the hottest gas contacts the wettest solid. These dryers naturally vary in the type of feed they are able to handle, e.g. some dryers like

spray and drum dryers can accommodate solutions or slurries, whereas fluidised beds require a particulate feed.

2.3.1: Convective drying

Convective, or direct, drying is possibly the most common method of drying particulate solids; the heat is supplied by heated air or gas flowing over the surface of, or through, the solid. Heat for evaporation is supplied by convection to the exposed surface of the material and the evaporated moisture is transported away by the drying medium. Hot air is the most common drying medium, although waste gases, superheated steam, *etc.*, can also be used. Evidently, a problem with the use of hot flue gases in some applications is the potential for cross-contamination of the drying material, e.g. if it is a food stuff.

When highly flammable, unstable, or explosive mixtures or materials saturated with organic solvents have to be dried, inert gases, e.g. nitrogen, are used in a closed loop drying system. In such a system, the evaporated moisture has to be removed from the circulating gas by a condenser / liquid separator arrangement. Figure 2.3 shows both closed and open loop circulation used in convective drying.

In such dryers, during the initial constant-rate period, the solid surface approaches or attains the wet bulb temperature corresponding to the air temperature and humidity at the same location. However in the falling-rate period, the solids temperature approaches the dry bulb temperature of the air. As mentioned earlier, these factors make convective drying more suitable for the drying of heat-sensitive materials.

Examples of convective dryers include air suspension dryers, e.g. fluid bed, flash, or spray dryers, and air impingement dryers for papers / pulp. More details on drying methods are given in Chapter 4.

2.3.2: Conduction drying

Conduction, or indirect, dryers are more suitable for thin products or very wet solids. The heat for evaporation is supplied through heated surfaces, either moving or stationary, placed within the dryer to support or convey the solids. Apart from the mode of heat transfer, a fundamental difference between such indirect dryers and direct (convective) dryers is that the heat and mass transfer paths are co-current.

The amount of heat transferred to the drying surface not only depends upon the thermal conductivity of the material of the heating surface but also on the heat transfer coefficient from the heating medium to the surface. Common heating media include steam, molten metals, and organic liquids, which enable high values of heat transfer coefficients to be attained.

Since all the heat for moisture evaporation passes through the material layer, the thermal efficiency of conductive drying is higher than convective drying where most of the heat flows over the material and may be wasted into the outlet air (Strumillo & Kudra, 1986, Menon & Mujumdar, 1987). However, higher product contact temperatures tend to be required so that dryers with extended residence times, as shown in Table 2.2, tend to be unsuitable for heat sensitive materials, particularly if relatively thick layers are involved.

Examples of indirect dryers include paddle dryers for drying of pastes, rotary dryers with internal steam tubes, and drum dryers, (see Figure 2.4), for drying thin slurries.

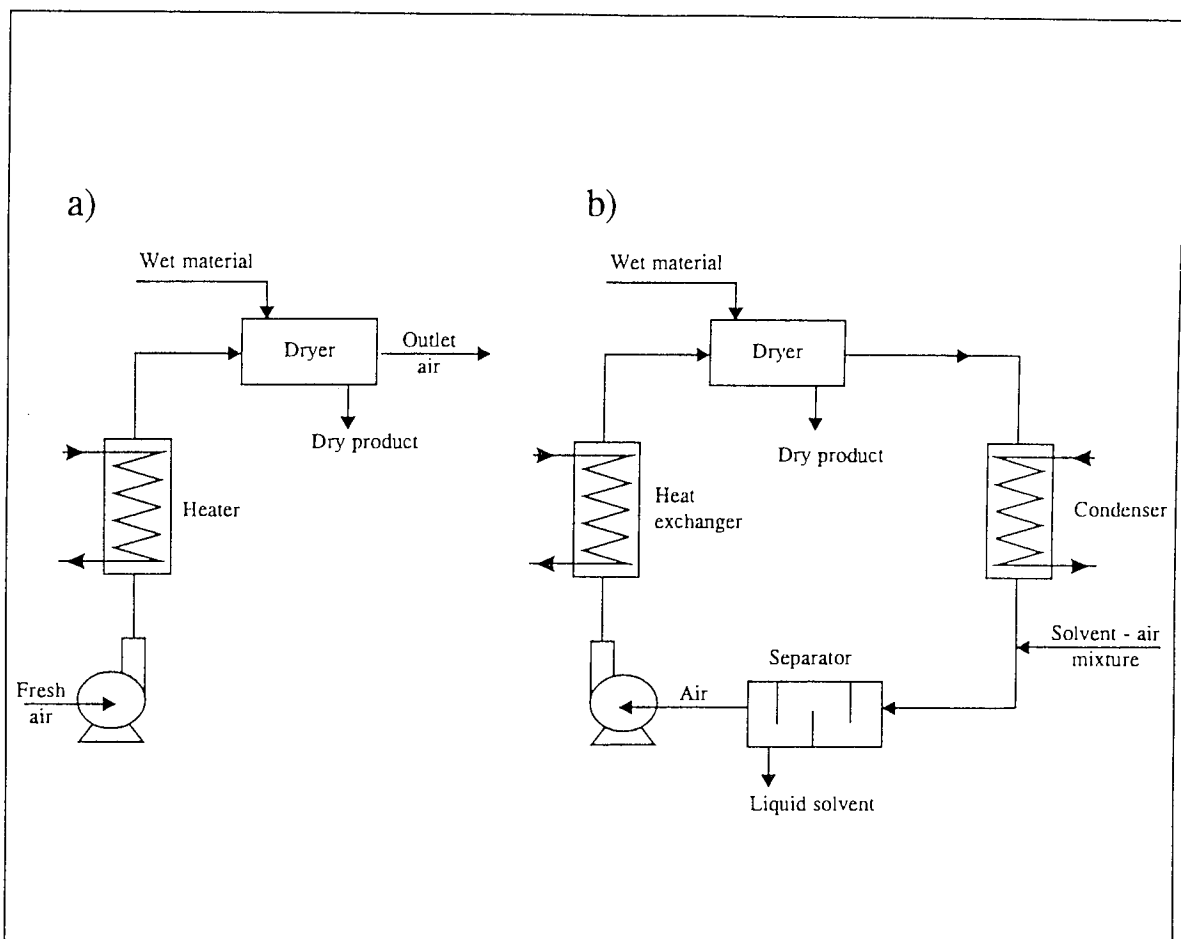


Figure 2.3 Convective drying (a) open loop (b) closed loop circulation.

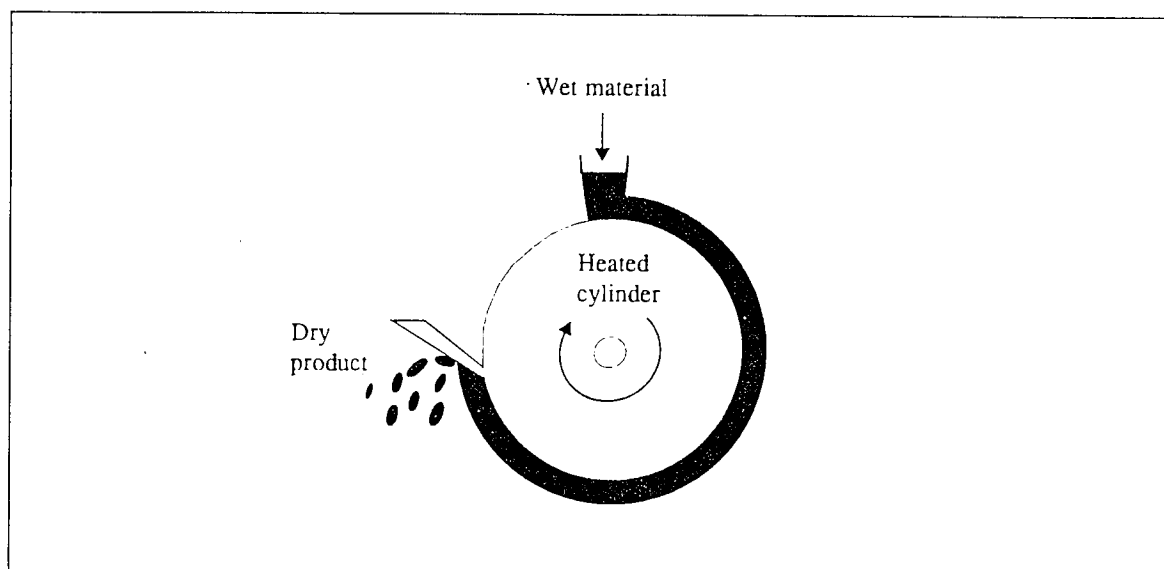


Figure 2.4. Drum dryer - an example of a conductive dryer.

2.3.3: Radiation drying

In radiation drying, the thermal energy is supplied to a wet material by electromagnetic radiation in the $0.76\mu\text{m} - 400\mu\text{m}$ waveband. Radiation within this infra-red region penetrates into the material and causes vibration of the molecules which creates the heating effect.

Because of the relatively small penetration depth of these infra-red waves, radiation drying is mainly used in the drying of thin materials such as films, coatings, and paints. Moisture transport within the material and the diffusion of the vapour from the solid, in radiation drying, is similar to that in convective and conductive drying.

2.3.4: Dielectric drying

In dielectric drying, the thermal energy is generated within material placed in an electromagnetic field, in the radio frequency or microwave region. Due to the rapid changes in the direction of the electromagnetic field, the dipoles of the dielectric or polar liquids alter their orientation which causes heat generation as a result of molecular friction (Stuchley & Stuchley, 1983).

The thermal effect of the electromagnetic energy absorption is proportional to the dielectric constant, i.e. the higher the dielectric constant, the greater is the electromagnetic energy absorption. Table 2.5 shows typical materials that heat poorly and those that heat well.

Since the dielectric constant of water is considerably higher than most of the solids to be dried, heat is generated in the wet parts of the materials. With internal heat generation, mass transfer is primarily due to the total pressure gradient established as a result of the rapid vapour generation within the material (Lyons *et. al.*, 1972); most of the moisture is vaporised before leaving the material.

If the material is initially very wet, and the pressure inside increases very rapidly, liquid may be removed from the material under the influence of a total pressure gradient. The higher the initial moisture, the greater is the influence of the pressure gradient upon the total mass removal. Thus a 'pumping action' forces moisture, often as vapour, to the surface. This leads to very rapid drying without the need to overheat the surrounding atmosphere and hence avoids case-hardening or other surface overheating phenomena.

Heat well	Heat poorly
water	hydrocarbons
halogenated hydrocarbons (unsymmetrical)	halogenated hydrocarbons (symmetrical)
alcohols	alkali hydrides .eg. salt
aldehydes	inorganic oxides eg alumina
ketones	some elements eg sulphur
amides	boron nitride
amines	mica
nitrates	
cyanides	
proteins	
acid anhydrides	
ferrites	
ferro-electrics	
ionic solutions	

Table 2.5: The heating properties of various materials in dielectric drying (after White, 1973).

Examples of the application of dielectric drying are to be found in a variety of industries including the lumber industry, e.g. in the drying and manufacture of plywood, the paper industry to dry the paper and coating materials, the food industry in the post-bake drying of biscuits, and the ceramics industry where drying times, which were of the order of 24 hours in high temperature ovens because of the insulating nature of the ceramics, have been reduced to 20 - 22 minutes (Schiffman, 1987). One unsuccessful attempt to use microwave drying utilised a domestic microwave oven. The domestic microwave oven was found to be grossly under-powered compared to an industrial microwave unit, 650W for a domestic oven compared to 300 kW for an industrial unit (Sud & Woollatt, 1993).

2.3.5: Freeze drying

Freeze drying is based upon the sublimation of frozen moisture from the material in the drying chamber where the pressure is below the triple point value (Mujumdar *et. al.*, 1980, Liapis, 1980). The heat required for sublimation is supplied by radiation, or conduction, at such a rate that the temperature of the material is not raised above 0°C (Strumillo & Kudra, 1986). After the moisture sublimates to a vapour, it is removed by mechanical vacuum pumps or steam ejectors.

Because of its particular advantages, freeze drying is used for heat sensitive materials such as vaccines and pharmaceutical materials, enzymes, and foodstuffs. Further details are given in Chapter 4.

2.3.6: Vacuum drying

Vacuum drying is based upon the removal of moisture from a material by lowering the pressure inside the drying chamber. Materials that are

thermolabile or easily oxidisable, especially when wet, can be dried in vacuum dryers.

2.4: Selection of preferred dryer for heat-sensitive products

The majority of chemical, biochemical, and natural products from industry undergo drying at some stage of processing for a number of reasons, e.g. materials need to have a particular moisture content for subsequent processing / pelleting, to reduce their weight, powders must be dried to suitable moisture contents to allow satisfactory packaging, and low moisture levels are required with some materials to retard degradation.

Excessive drying is wasteful; since more energy is consumed, and hence more expense involved, than necessary and over-drying often results in a degraded product.

The need for consistent product quality, dependent upon the end use of the product, imposes constraints on the choice of dryer. For many bulk chemicals, handling considerations determine moisture content requirements; flavour retention, palatability, and rehydration properties are important for foodstuffs; timber must retain its strength and decorative properties after drying.

The end moisture content, which determines the drying time and drying conditions, is largely governed by the storage and stability requirements of the material. Factors including degradation, phase changes, staining, discoloration, and dust flammability give rise to temperature restrictions; thermal sensitivity dictates the maximum temperature to which the material can be exposed for the drying time.

The foregoing summary demonstrates that the selection of a dryer is based upon a number of criteria which include:

- i) properties (thermal and physico-chemical) of the material to be dried,
- ii) the required form (powder / agglomerate) of the dried material,
- iii) dried product value,
- iv) initial and final moisture contents
- v) sensitivity, of the drying material, to degradation, and
- vi) quality control requirements.

This latter criterion may even result in a preference for energy-inefficient batch drying over a more efficient continuous type of dryer, e.g. with pharmaceutical products.

The dryer of choice for large quantities of pumpable heat sensitive materials would be a spray dryer in a co-current configuration because:

- a) short residence times can be achieved with spray dryers (see Table 2.2 for details), and
- b) the driest, most sensitive product is exposed to the lowest gas temperature.

Very high value heat-sensitive products, e.g. plasma, vaccines, antibiotics, *etc.*, are freeze dried. Freeze drying is an expensive process but the cost of obtaining the dried product is offset by the value of the dried product.

It should also be noted that a combination of dryers can be used to produce a desired product; an example of this is the use of a fluid bed dryer after spray drying of milk and coffee to produce agglomerate particles which disperse easily when rehydrated.

3: Heat-sensitive materials

The term 'heat-sensitive' encompasses a wide range of materials with limited tolerances to high temperatures or those that can tolerate such high temperatures for only short periods of time. The vast majority of these heat-sensitive materials are in daily usage, but because of their high intrinsic value, they must be dried with great care to ensure that there is no decline in product quality.

Heat-sensitive products range from inorganic colours / organic dyes and coffee to exotic examples such as flavours, antibiotics, vaccines, enzymes, and hormones.

3.1: Pharmaceuticals

Pharmaceuticals represent a whole range of chemical / biological substances ranging from relatively cheap and easy-to-dry materials, such as acetyl salicylic acid, to extremely valuable and difficult-to-dry products, such as hormones and antibiotics. In many cases, an inert gas must be used to prevent oxidation, and the vapour removed is often a toxic or flammable solvent. In most cases, the drying gas must be carefully filtered and processed to avoid contamination of the final product.

The manufacture of pharmaceuticals, in tablet form, is generally carried out in three stages:

- i) synthesis of the intermediate products,
- ii) final synthesis of the drug, and
- iii) manufacture of the tablets.

After the second stage, and often after the first, if the intermediate product is to be processed elsewhere, these products are dried. Granulation, a necessary step before tableting, often accompanies drying. Raff *et. al.*, in 1961, showed that spray drying produced pharmaceuticals that were readily tableted.

Solutions and thin slurries of drugs can be spray dried; particles of dry product obtained in such a way are very fine, thus after mixing with other components and granulation, they can be used directly for tableting. There is little risk of overheating, because of the high evaporation rates, when the spray drying operation is co-current; hence highly-sensitive materials can be spray dried. Although open-cycle spray dryers can be used to dry pharmaceuticals, closed-cycle dryers are needed to recover the organic solvents used to precipitate the substrates, which would otherwise be lost (Strumillo *et. al.*, 1988, and Kjaergaard, 1974). Closed-cycle spray dryers are also used for micro-encapsulation of pharmaceuticals by using polymeric coating materials dissolved in the feed to the dryer.

In the production of certain pharmaceuticals, such as antibiotics, the powders obtained by spray drying of low concentration aqueous solutions have low bulk density; higher bulk density antibiotics can be obtained by partly precipitating the feed. High bulk density antibiotics are produced from suspensions of precipitated substrates in organic solvents. After filtration, several pharmaceutical products form pastes which can be spray dried if they are pumpable; pastes that are too thick must be thinned with solvents or by disintegration of their structure.

Spray dried pharmaceutical products show high release and absorption rates compared to physically-prepared mixtures (Bootsma *et. al.*, 1989).

3.2: Enzymes

Enzymes are natural catalysts in biological systems with striking characteristics of enormous catalytic power and specificity (Masters, 1988). They are nitrogenous organic catalysts produced by living cells and cannot be synthesised (Barzana-Garcia *et. al.*, 1986). Enzymes are normally very heat-sensitive, 'wet' heat being more damaging than 'dry' heat (Desrosier, 1970), and hence, mild drying temperatures are necessary. The addition of additives, e.g. inorganic salts, polymers, *etc.*, further minimises heat damage (Kirby, 1990).

The thermally unstable, or heat-labile, nature of proteins and enzymes requires mild drying conditions such as low temperature operation, or very fast rate, high temperature drying. However, the use of high temperature, short residence time operations such as spray drying can result in the loss of product quality (Zakarian & King, 1982, van der Bruel *et. al.*, 1971, and Taylor & Hoare, 1988). For example, the spray drying of a heat-sensitive enzyme, such as alkaline phosphatase, can result in high levels of enzyme loss even at relatively low outlet temperatures, e.g. 85° to 95°C , (Daeman & van der Stege, 1982, and Daeman *et. al.*, 1983), while heat stable enzymes such as α -amylase are relatively easily spray dried (Wijlhuizen, 1979, Yamamoto *et. al.*, 1985, and Taylor & Hoare, 1988).

The increase in the rate of reaction by enzyme catalysts is caused by a reduction in the activation energy. Given an activation energy level typical for many reactions, ($\cong 12\text{kcal/mol}$), reaction rates approximately double for every 10°C rise in temperature. Thus, for every 10°C rise in temperature, the amount of enzyme required for a given conversion can theoretically be halved (Wasserman, 1984).

Although operating at high temperatures is advantageous, all enzymes eventually lose their catalytic activity as the temperature is increased. This thermal inactivation may be either reversible or irreversible, (see Figure 3.1).

The fact that enzymes are proteins imposes a limit on the maximum temperature to which they can be subjected in aqueous solution.

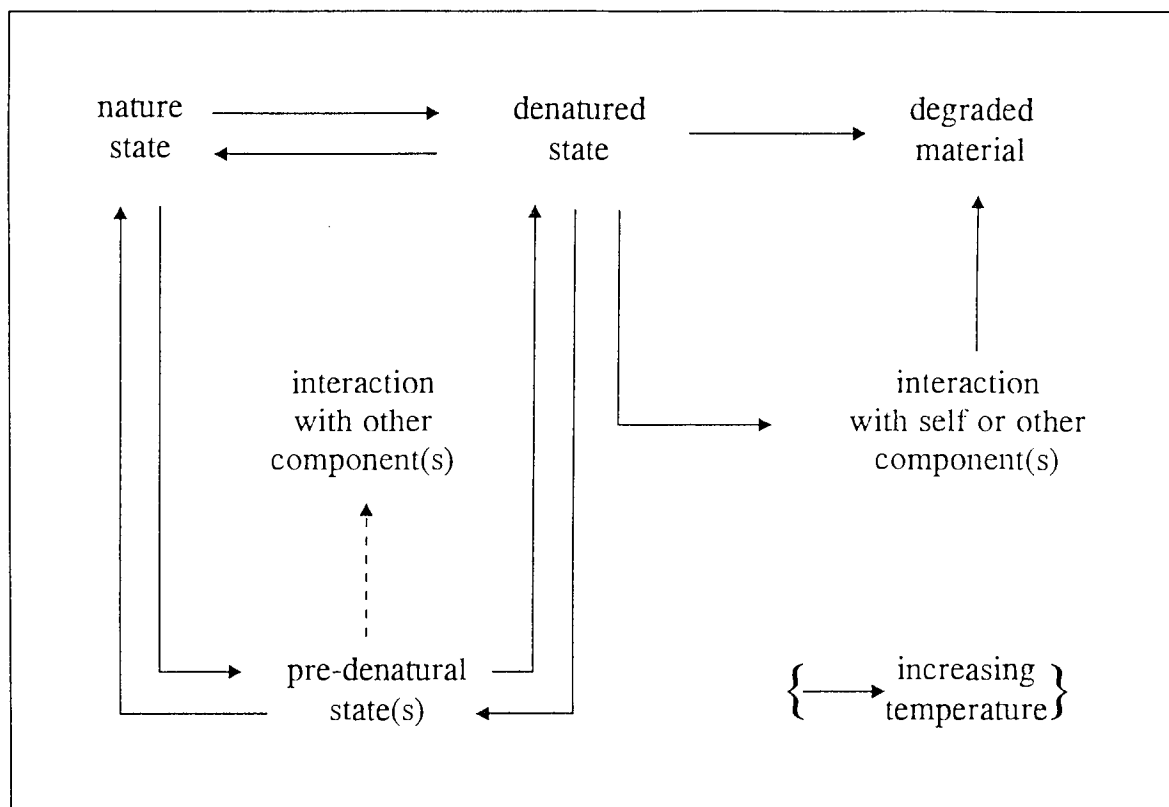


Figure 3.1. Effect of heat on proteins (after Hassan, 1991)

Hence to make economical use of enzymes, there is a need to enhance their thermostability. Several methods are used to enhance the stability of enzymes including isolation from thermophilic organisms, use of recombinant DNA techniques, and physical / chemical methods such as immobilisation and micro-encapsulation (Kirby, 1990). Another method of enzyme stabilisation is dehydration; Zaks & Klibanov, in 1984, found that the thermostability of porcine pancreatic lipase at 100°C was greatest at low water content. The highest thermostability cited in the literature is for dry enzymes, e.g. prolonged heating at 160°C - 200°C is required to fully inactivate dry trypsin, and dry lysozyme resists one hour of heating at 140°C (Barzana Garcia *et. al.*, 1985).

3.3: Flavours

The characteristic aroma of many liquid foods, including coffee, tea, and fruit juices, is caused by a complex mixture of volatile organic compounds, many of which are present in the ppm (parts per million) range, with boiling points between -80° (hydrogen sulphide) and 280°C (vanillin). At the ppm levels, nearly all of these compounds are much more volatile than water, and direct spray drying of the materials containing them leads to very high flavour losses in the exhaust air flow, with resultant loss in product quality (Thijssen, 1970, Menting *et. al.*, 1970, Rulkens & Thijssen, 1972, Kerkhof & Thijssen, 1974, King, 1974, Zakarian & King, 1982, Kieckbusch & King, 1980, King, 1988, Masters, 1988).

Flavour losses are prevented in several ways including the use of additives (e.g. gelatine, maltodextrin), to enhance flavour retention (Tsujimoto *et. al.*, 1985, Yamamoto *et. al.*, 1985, Kieckbusch & King, 1980, Heath, 1985, King, 1988, Masters, 1988), encapsulation of the flavours in water soluble coatings (Furuta *et. al.*, 1985, Reineccius, 1982, Heath, 1985, Inglett *et. al.*, 1988, Masters, 1988, Kirby, 1990), and increasing the solids in the feed to the spray dryer (Reineccius, 1982). In instant coffee production, the oils which provide the characteristic aroma may be removed prior to spray drying and then re-added further downstream in the processing.

At present, large quantities of flavours are stabilised whilst spray drying by encapsulation in a solid edible film. Gum arabic is very suitable as a coating to enhance flavour retention (Randall *et. al.*, 1989); the degree of volatile retention is influenced by the speed of formation and completion of the protective film. The film of gum arabic is formed during the early stages of droplet evaporation, during which most of the volatile loss has been reported (Kieckbusch & King, 1980, Tsujimoto *et. al.*, 1985), and is permeable to water but not to many flavour compounds, thus allowing the water to evaporate without significant loss of flavour.

Increasing the solids content of the feed to the spray dryer enhances flavour retention, (Reineccius *et. al.*, 1982, King, 1990), partly because a high starting solids content requires minimal drying to provide a semi-permeable film through which the water continues to evaporate while the flavour compounds are retained. However, high solids content also results in a more viscous feed and may render atomisation difficult. High viscosities tend to limit convection currents within the drying droplets and would also slow volatile diffusion to the drying surface (Reineccius *et. al.*, 1982).

3.3.1: The 'selective diffusion' theory for flavour retention

A mechanism of selective diffusion which would lead to enhanced flavour / aroma retention was first proposed by Thijssen in the mid-1960s. This concept is based upon the differing behaviour of the diffusion coefficient of water, in concentrated solutions, compared to the diffusion coefficients of other materials, as shown in Figure 3.2.

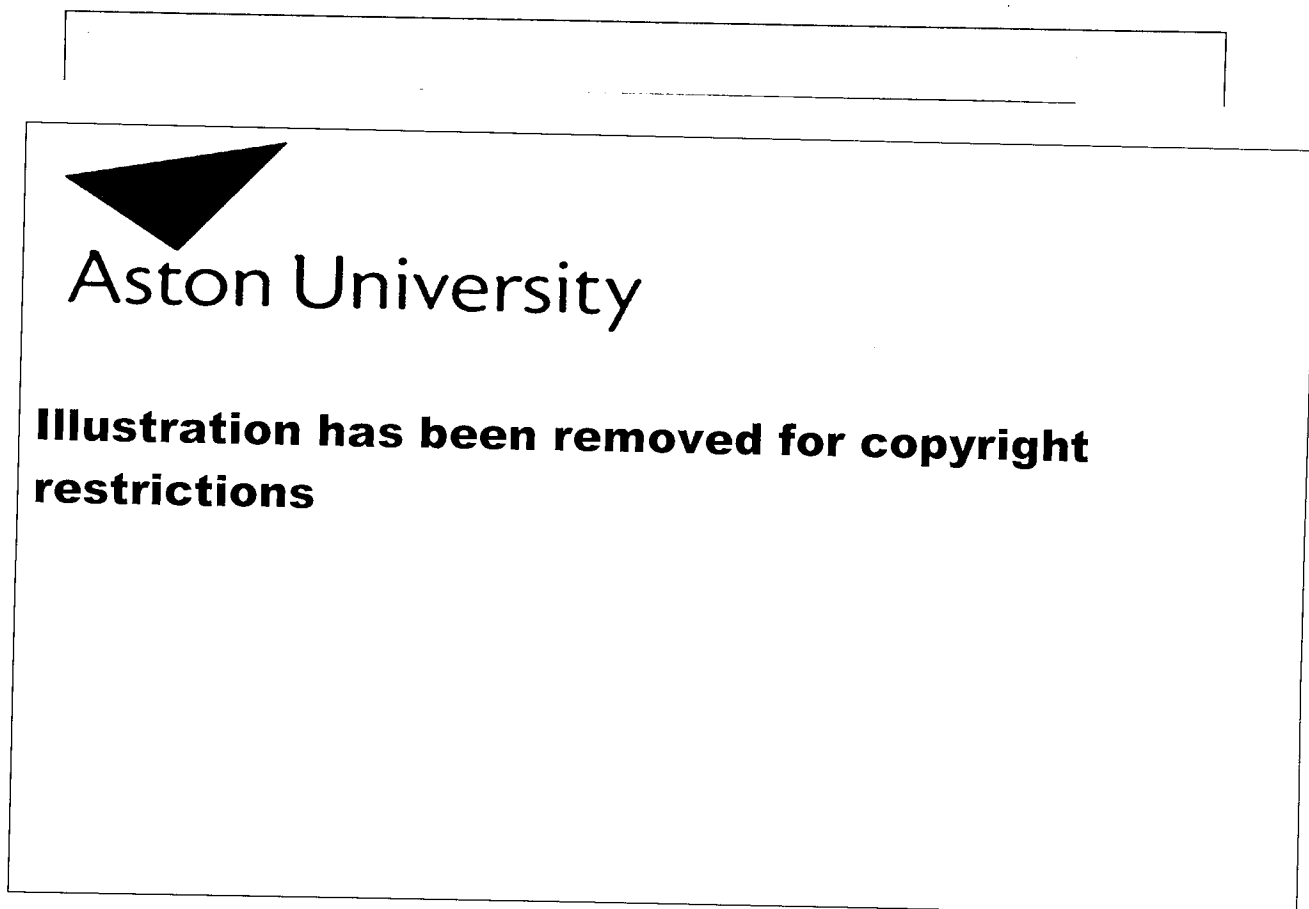


Figure 3.2. Effect of water concentration in aqueous solutions upon the diffusion coefficient of water and acetone (King, 1990).

Figure 3.2, shows that the diffusion coefficients of water and other solutes decrease substantially as the water concentration decreases in aqueous solutions of carbohydrate and other food-related products. The diffusion coefficient of water, however, decreases much less than the diffusion coefficients of other substances; this behaviour is general and applies to many

different organic solutes and mixtures of dissolved solids (Bomben *et. al.*, 1973). The result of this general phenomenon, as illustrated in Figure 3.3, whereby the diffusion coefficients of other substances become much less than that of water above some dissolved solids content, is that the water will diffuse faster than the other substances. Hence, if such a high dissolved solids content could be achieved at the surface of a drying material, before substantial loss of the volatile flavour / aroma, the remainder of the volatiles would be retained at the expense of the water which would be lost because it would diffuse faster (King, 1990).

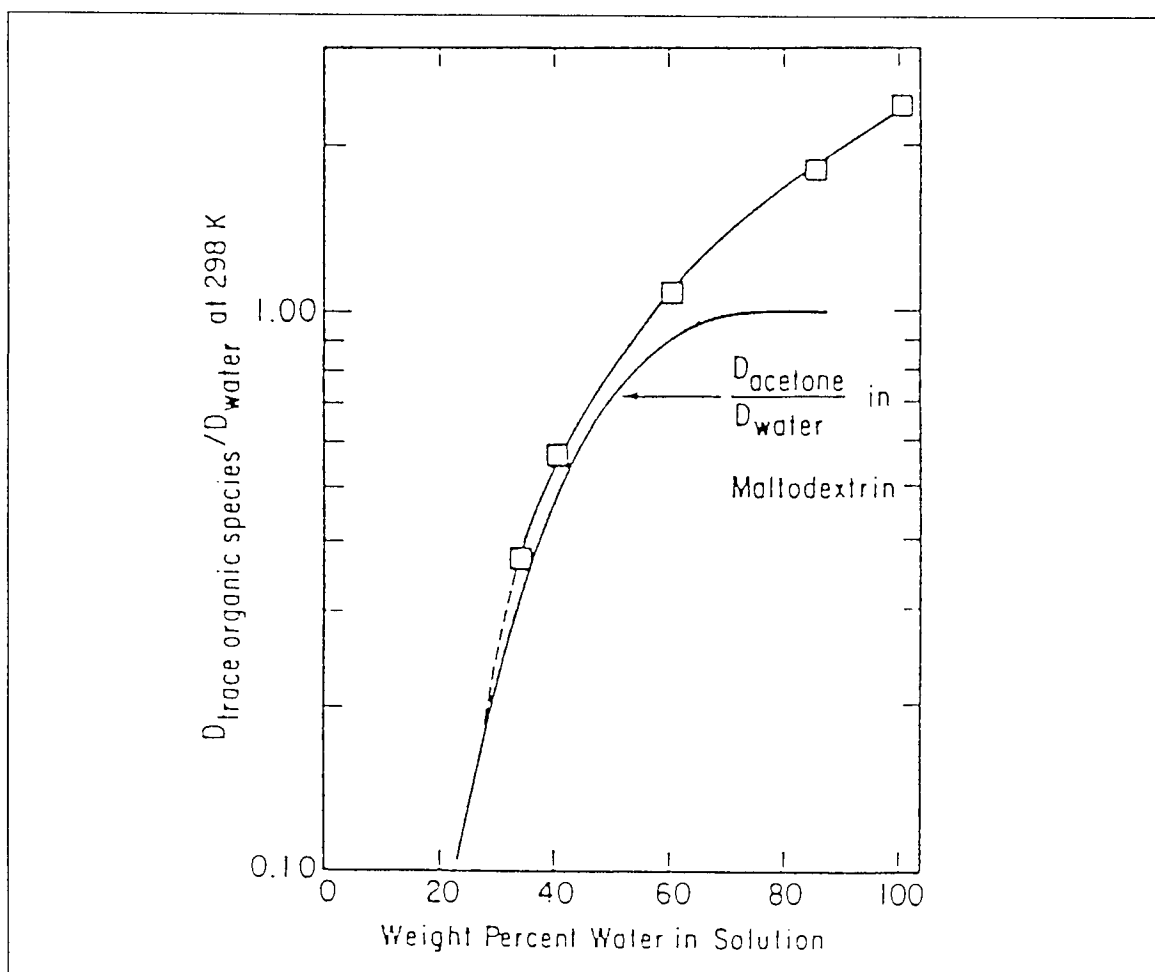


Figure 3.3. The effect of wter concentration on diffusion coefficients of acetone and water

The existence of selective diffusion has been verified in a number of ways which include:

- i) measurements of diffusion coefficients under carefully controlled conditions (Menting *et. al.*, 1970, Chandrasekaran & King, 1972),
- ii) variation in operating parameters of spray and freeze drying result in volatiles retention as predicted by the selective diffusion theory (Thijssen & Rulkens, 1970, Kerkhof & Thijssen, 1977, King, 1977), and
- iii) losses have been modelled, upon the basis of measured diffusion coefficients, from suspended droplets under controlled conditions (Menting & Hoogstag, 1967, Kerkhof & Shoeber, 1974).

3.4: Mechanism of thermal degradation

An increased temperature, in association with time of exposure to this elevated temperature, associated with dehydration, affect the quality of the heat-sensitive material. In terms of chemical kinetics, this loss of quality, or thermal degradation, can be visualised as the decomposition of a particular chemical compound.

This decomposition, for a single mono-molecular reaction, may be expressed as:



where,

N = original compound

DN = decomposed compound, and

k = reaction rate constant (dependent upon temperature)

The dependence of k upon temperature is often described by:

$$k \propto e^{-(E/RT)}$$

where,

E = activation energy of the reaction,

R = gas constant, and

T = absolute temperature, (Karel, 1988).

Since expression 3.1, above, represents the loss of compound N , the rate of loss of this compound can be described as:

$$\frac{d[N]}{dt} = -k[N] \quad 3.2$$

where,

$[N]$ = concentration of compound N , and

$\frac{d[N]}{dt}$ = rate of loss of compound N .

Assuming that the rate constant k is a true constant, and the concentration of N changes only as a result of the reaction, then equation 3.2 may be integrated with the appropriate boundary conditions to result in equation 3.3 below:

$$-\ln \frac{[N]}{[N]_0} = kt \quad 3.3$$

where,

$[N]_0$ = the initial concentration of compound N .

The rate constant k , is dependent upon temperature, as shown above, so that thermal degradation can be reduced by:

- i) significantly reducing the temperatures to which the material is exposed for any extended period of time, as in the case of freeze dryers, or
- ii) permitting only very short exposure times (e.g. <30s) to high temperatures, as in spray dryers (see table 2.2).

3.5: Other forms of degradation

Changes, including chemical and enzymatic conversions, and physical changes, in a material during dehydration are in part due to the unit operations that convert the raw material to the final dry product. All changes depend upon temperature, water activity, and time, and hence upon temperature and moisture profiles as a function of time. Many changes occur prior to drying and during storage after drying.

3.5.1: Enzymatic reactions

Enzymatic reactions occur during both drying and storage. When enzymatic reactions are undesirable, either the enzymes have to be inactivated prior to drying, or the drying conditions have to be selected such that rapid inactivation occurs. An example of this is the enzymatic browning caused by the enzyme polyphenol oxidase which causes phenolic compounds to oxidise to orthoquinones at a pH between 5 and 7, the enzyme being inactivated irreversibly at pH<5 (Lee, 1992). The reaction can be minimised during the drying process by operating the dryer under an inert atmosphere to prevent oxidation, or under vacuum.

3.5.2 Chemical reactions in foods

The main reactions which are generally considered during drying are:

- i) the Maillard reaction, or non-enzymatic browning,
- ii) lipid oxidation, and
- iii) protein denaturation.

These reactions are heat and moisture sensitive, and are hence strongly influenced by drying.

3.5.2.1: The Maillard reaction

Discoloration of the product, often a desirable effect in foods (Genskow, 1988), is caused by non-enzymatic browning, or the Maillard reaction. Although the reaction does not need high temperatures to occur, (non-enzymatic browning has been known to occur in products stored at 3°C to 8°C), the rate of reaction increases markedly with temperature. The Maillard reaction proceeds in aqueous solution, but it occurs much more readily at low moisture levels, and is often associated with foods that have been thermally dehydrated (Whitfield, 1992). Prevention of the Maillard reaction from occurring could be achieved by drying thermally to a moisture content at which the browning becomes a problem, and then completing the process by freeze drying.

3.5.2.2: Lipid oxidation

Lipid oxidation, a series of degradation reactions, causes rancidity and off-flavours, and also induces other deteriorative reactions in proteins, amino acids, and other food components (Whitfield, 1992). The oxidation of lipids in

foods is greater at higher temperatures than at low temperatures of dehydration (Desrosier, 1970). Lipid oxidation can be prevented by:

- i) the removal of oxygen during drying by drying in an inert atmosphere or under vacuum (Genskow, 1988),
- ii) the addition of antioxidants to protect the lipids (Desrosier, 1970, Genskow, 1988), and
- iii) allowing the Maillard reaction to occur as the products from this reaction exert an antioxidative effect (Whitfield, 1992).

3.5.2.3: Protein denaturation

Protein denaturation, (which in some cases is reversible), is usually defined as any conformational modification, without any alteration of the primary structure, that causes a change in the functional properties of the protein. Thermal denaturation of proteins generally takes place between 55° and 80°C; enzymes, being more susceptible to the effects of temperature, begin to denature at temperatures as low as 45°C. Decreased solubility, by the heat-induced exposure of hydrophobic groups resulting in the aggregation of unfolded protein molecules, often accompanies denaturation (Pace, 1983). A reduction or loss of biological activity and increased water absorption, susceptibility to protease digestion, and increase in intrinsic viscosity also accompanies thermal denaturation (Yada *et. al.*, 1992).

The biological value of dried protein is dependent upon the method of drying. Prolonged exposure to high temperature can render the protein less useful in the diet; conversely low temperature treatments (as shown by Table 3.4), increase the digestibility of protein over the native untreated protein (Desrosier, 1970).

Treatment	Pepsin digest residue (PDR)
Beef (fresh frozen)	76
Beef (fresh cooked)	77
Beef (dehydrated 2% moisture)	77
Beef (rehydrated)	78
Beef (frozen fresh stored 12 months -20°F)	68
Beef (dehydrated 2% moisture stored 12 months -20°F; flexible packing)	81
Beef (dehydrated 8% moisture stored 12 months 70°F flexible packing)	76
Beef (dehydrated 2% moisture stored 12 months 100°F canned)	80
Beef (dehydrated 8% moisture stored 12 months 100°F canned)	76

Table 3.4: Effect of treatment upon availability of beef protein (after Adachi *et. al.*, 1958) (high PDR indicates increased digestibility of the protein)

3.5.3: Structural degradation

Structural changes occur during a dehydration process, and include shrinkage of cells and case hardening.

Shrinkage, in general, affects product quality by reducing wettability, changing product texture and decreasing product absorbency. Shrinkage is a result of capillary collapse, a normal occurrence as the fluid evaporates from a capillary. The degree of collapse is affected by a number of mechanisms which include surface tension, and electrostatic forces.

Case hardening, in the case of a drying droplet, may cause the droplet to eventually explode releasing its contents and also producing undesirable 'fines'. Case hardening may similarly occur with slabs, e.g. in tray dryers.

In the present study, the heat-sensitive materials chosen were flavours, pharmaceuticals, and enzymes.

4: Drying techniques for heat-sensitive materials

The moisture content and water activity of any biological product can affect its physico-chemical and microbiological stability. These factors, either separately or in combination, can result in loss of material, reduced quality, decreased efficacy or reduced acceptability, and, consequential, economic loss. Hence, the need to reduce moisture content and thereby water activity.

The drying of heat-sensitive materials that are of low volume but high cost, such as enzymes, flavours, *etc.*, is an important down-stream processing operation that has gained renewed interest with the advent of biotechnology.

Owing to the complex structure and variety of biological substances, the dryer type and working parameters should be chosen for each specific application. Clearly because of the heat-sensitivity of the substances, special attention should be paid to the temperature at which drying is to occur and the period of exposure to it. Improperly-chosen drying temperatures may cause thermal decomposition of biosynthesis products, changes of biological and biophysical functions, and even death of micro-organisms which are required for product end-use.

Research by other workers such as Karpov & Ulunov, 1982, has shown that no practical drying methods allow the retention of 100% of the biological properties of the input product. Data, in Table 4.1, on the preservation of final product quality for Bakers Yeast demonstrates the problem. Surprisingly, however, the drum dryer, involving direct contact heat transfer which is generally synonymous with higher contact temperatures, apparently out-performed the spray dryer. Therefore, the selection of a proper drying method and optimum process conditions are essential to guarantee a high quality yield.

There are two main groups of drying methods for heat-sensitive materials; firstly, the drying of biosynthesis products in the form of biological solutions or suspensions; and, secondly, where the structure of the biological material is changed by admixture with other porous substances (carriers). Many biosynthetic products can be dried either on carriers or with them, e.g. amino acids, yeasts, antibiotics, *etc.*. The choice of method depends on the type and properties of the biological product, the mode of utilisation of the final p


T	 Aston University Content has been removed for copyright reasons	
st		
dt		
fl		
bi		
va		
fl		
sp		
fre		
fre		
fre		

Table 4.1: Preservation of final product quality for Bakers Yeast (Karpov & Ulunev, 1982)

The main method of drying for high cost heat-sensitive materials is freeze drying, (Goldblith *et. al.*, 1975, Karpov & Ulunev, 1982, Mackey, 1984, Rowe

& Snowman, 1976), as it ensures the highest quality of the final product. This is demonstrated in Table 4.1. However, because of its high capital and operating costs, freeze drying is usually only used for expensive heat-sensitive products which cannot be satisfactorily dried by other methods.

More generally spray drying is used to dry products of biosynthesis (Masters, 1991, Karpov & Ulunev, 1982). The properties of the materials being dried determine the construction of the dryer to be used. The dryers differ considerably with regard to their aerodynamics, type of heat carrier, energy source, re-circulation of the drying agent, output, initial solution concentrations, *etc.*.

Amongst the other methods of dispersion drying of heat-sensitive materials cited in the literature are fluidized beds, vibro-fluidized bed dryers, spouted bed dryers and pneumatic dryers (Strumillo & Kudra, 1986).

4.1: Freeze drying

Certain biological materials, pharmaceuticals and foodstuffs, which may not be heated even to moderate temperatures, i.e. 37°C, in ordinary drying may be freeze dried. The substance to be dried is usually frozen initially by exposure to very cold air. The water or other solvent is then displaced as vapour by sublimation from the frozen material in a vacuum chamber; the solvent vapour is removed by pumps or steam ejectors.

Generally, freeze drying produces the highest quality food product obtainable by any drying method. A major factor in this is the structural rigidity, or integrity, afforded by the frozen substance at the surface where sublimation occurs. This rigidity, to a large extent, prevents the collapse of the solid matrix remaining after drying, resulting in a non-shrunken structure in the dried product that facilitates rapid and almost complete rehydration when water is subsequently added. Hence, freeze drying is used for dehydrating

foods such as coffee which dissolves easily in water. An unusual example of the ease of rehydration of freeze-dried material was the use of freeze dried vitreous humour, at a higher concentration than normal, injected into the posterior chamber of the eye to cure detached retina (Goldblith *et. al.*, 1971). (Resultant swelling of the freeze-dried material caused the detached retina to be pushed back into place).

Freeze drying of foods and biological materials also possesses the advantage that it results in little loss of flavour or aroma. The low processing temperatures, the relative absence of liquid water, and the rapid transition of any local region of the material being dried from a fully-hydrated to a nearly completely dehydrated state minimise the degradation reactions that normally occur in ordinary drying processes such as non-enzymatic browning, protein denaturation, and enzymatic reactions. Hence, freeze dried coffee attracts a premium over the spray dried material.

Within any food material, some non-frozen water (bound water) will unavoidably be present during freeze drying, but there is often a very sharp transition temperature for the still wet region during drying below which the product quality improves markedly (Mellor, 1978). This improvement shows that sufficient water is frozen to give the beneficial product characteristics of freeze drying.

Freeze drying is, however, an expensive form of dehydration for foods because of the slow drying rate and the use of vacuum. The cost of processing is offset to some extent by the lack of need for refrigerated handling and storage that would otherwise be necessary.

Systematic freeze drying is a procedure applied mainly to three broad bands of biological materials:

i) non-living matter, e.g. blood, plasma, enzymes, hormone solutions, and foodstuffs,

- ii) surgical transplants, which are made non-viable so that the host cells can grow on them as the skeleton, including artery, bone, and skin, and
- iii) living cells that are to remain viable for long periods of time, e.g. bacteria, yeasts, viruses, but not mammalian cells.

Freeze drying requires very low pressures or high vacuum in order to produce a satisfactory drying rate. If the water were in a pure state, the drying could occur at or near 0°C at an absolute pressure of 4.58mm Hg. However because the water usually exists in a combined state or solution, the material must be kept at or below 0°C to retain the water as a solid phase; hence most freeze drying is done below -10°C at an absolute pressure of 2mm Hg or lower.

In summary, freeze drying is a multiple operation in which the material to be dried is:

- i) frozen hard by low temperature cooling (pre-freezing),
- ii) dried by direct sublimation of the frozen solvent, generally under reduced pressure (i.e. under vacuum), and
- iii) stored in the dry state under controlled conditions (e.g. free from oxygen and water vapour).

If correctly processed, most freeze-dried material can be stored in such a way for an unlimited period of time whilst retaining a substantial proportion of its initial physical, chemical, biological, and organoleptic properties. For example 90% quality was retained for Bakers Yeast in tests listed in Table 4.1. The material also remains available at any time for immediate reconstitution. In most cases this is done by the addition of the exact amount of solvent that has been extracted, thus providing a reconstituted product with an appearance and structure which closely resembles the original material.

Vaccines and pharmaceutical materials are very often reconstituted in physiological solutions, quite different from the original solvent extracted,

which are best suited for intra-muscular/veinous injections. Freeze-dried organisms, such as marine animals, plants, or tissue extracts, can be the starting point of an extraction process using non-aqueous solvents to isolate biologically active substances.

4.1.1: The freeze drying process

Freeze drying is usually a batch process, in which the initial freezing may be performed outside the dryer or by evaporation under vacuum. Rapid freezing results in:

- i) smaller crystals being formed - this lessens damage to the walls of organic cells, permits a higher sublimation rate, and reduces forces (due to expansion) on the container, and
- ii) reduced risk of producing highly concentrated solutions before freezing is completed.

Slow freezing may, however, result in a higher survival rate for bacteria and other cells.

In freeze drying there is, initially, a short constant-rate drying period during which bulk or hydrodynamic vapour flow takes place; this is followed by a long falling-rate period during which vapour transfer occurs by diffusion. The constant-rate period occurs principally when sublimation takes place from a free ice surface with a gradient in total pressure but, as the ice interface recedes below the surface of the material being dried, the resistance impeding the vapour flow becomes increasingly effective. This period, therefore, gives way to a falling-rate period with diffusive flow, and mass transfer is the controlling factor (Mellor, 1978).

The most widely used freeze drying process relies upon the heat being supplied from the surrounding gases to the surface of the material being dried

(Mellor, 1978, King, 1971). The heat is then transferred by conduction through the drying layer to the ice surface.

Referring to the model developed by King in 1971, as shown in Figure 4.2, the heat flux to the surface of the material is transferred by convection and within the dry solid by conduction to the sublimation surface. The heat flux to the surface is equal to that conducted through the dry solid, assuming steady state conditions, and is given by:

$$q = h (T_e - T_s) = (k / \Delta L) (T_s - T_f) \quad 4.1$$

where,

q = heat flux (W/m^2),

h = external heat transfer coefficient ($\text{W/m}^2\text{K}$),

T_e = external temperature of gas (K),

T_s = surface temperature of the dry solid (K),

T_f = temperature of the sublimation layer (K),

k = effective thermal conductivity of the dry solid (W/mK), and

ΔL = thickness of the dry layer (m).

Similarly, the mass flux of the water vapour from the sublimation front is given by:

$$N_w = (D' / R T \Delta L) (P_{fw} - P_{sw}) = k_g (P_{sw} - P_{ew}) \quad 4.2$$

where,

N_w = water vapour flux ($\text{kg mol/m}^2\text{s}$),

D' = average effective diffusivity in the dry layer (m^2/s),

k_g = external mass transfer coefficient ($\text{kg mol/m}^2\text{s}$),

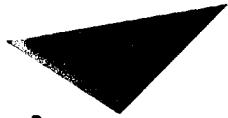
P_{ew} = partial pressure of water vapour in external gas phase (N/m^2),

P_{sw} = partial pressure of water vapour at surface (N/m^2),

P_{fw} = partial pressure of water vapour in equilibrium with the sublimation front (N/m^2),

R = gas constant, and

T = average temperature of the dry layer (K).



Aston University

Illustration has been removed for copyright restrictions

Figure 4.2. Model for uniformly retreating ice front in freeze drying
(King, 1971)

The coefficients h and k_g , determined by the gas velocities and characteristics of the dryer, are constant; the values of T , determined by the gas velocities and characteristics of the dryer, are constant; the values of T_e and P_{ew} are set by external operating conditions; and the values of k and D' are determined by the nature of the dried material. P_{fw} is uniquely determined by T_f , since it is the equilibrium vapour pressure of ice at that temperature.

The relationship between heat flux and mass flux at steady state is given by:

$$q = \Delta H_S N_W \quad 4.3$$

where,

$$\Delta H_S = \text{latent heat of sublimation of ice (2840 kJ/kg)}$$

Substituting for q (from equation 4.1) and N_W (from equation 4.2) into equation 4.3 gives:

$$\begin{aligned} & (T_e - T_f) / ((1 / h) + (\Delta L / k)) \\ & = \Delta H_S ((P_{fw} - P_{ew}) / ((1 / k_g) + (R T \Delta L / D'))) \end{aligned} \quad 4.4$$

As T_e , and hence T_S , is raised to increase the drying rate, two limits may be imposed:

- i) T_S must not become too high to risk thermal damage, and
- ii) T_f must be kept well below the melting point of ice.

When $k/\Delta L$ is small compared to k_g and $D' / R T \Delta L$, the outer surface limit will be reached first as T_S is raised; the process is thus said to be heat transfer controlled, and k must be raised to increase the drying rate. If the melting point temperature limit is reached first, the process is then mass transfer controlled, and hence to raise the drying rate, D' must be raised.

The frozen layer temperature must be maintained below the melting point, which may be more than 10°C below the melting point of ice. Typical ice temperatures in the freeze drying of foods under conditions in which the total pressure was primarily due to water vapour and the heat transfer was via the dry layer are shown in Table 4.3.

food material	chamber pressure (mm Hg)	maximum surface temp (°C)	frozen layer temp (°C)
chicken (diced)	0.95	60	-20
strawberry slices	0.45	70	-15
orange juice	0.05 - 0.1	49	-43
guava juice	0.05 - 0.1	43	-37
shrimp	0.1	52	-29
shrimp	0.1	79	-18
salmon steaks	0.1	79	-29
beef, quick frozen	0.5	60	-14
beef, slow frozen	0.5	60	-17

Table 4.3: Frozen layer and maximum dry surface temperatures in typical freeze drying operations (after Goldblith *et. al.*, 1975)

Factors controlling the drying time are related by:

$$t_d = (L^2 \rho (M_1 - M_2) \Delta H_S) / (8k (T_S - T_f)) \quad 4.5$$

where

t_d = drying time (s),

ρ = bulk density of the dry product (kg/m^3),

M_1 = initial moisture content, and

M_2 = final moisture content in the dry layer (Fellows, 1992).

4.1.2: Types of freeze dryers

There are three main types of freeze dryer:

- i) rotary spin freeze dryers - these are used for liquids, which are rotated in a bowl during freezing so that they are spread around the container walls,
- ii) cabinet shelf dryers (the most common type) - in these the solids are heated by conduction through the tray; alternatively granules are spread in a thin layer and the heat supplied by radiation from above, and
- iii) manifold freeze dryers - which are used for drying the contents of large numbers of small capacity containers.

4.2: Spray drying

The process of, spray drying transforms a pumpable fluid feed into a dried product in a single operation (Dloughy & Gauvin, 1960, Wijlhuizen *et. al.*, 1979, Sano & Keey, 1982, Furuta *et. al.*, 1984, Ali *et. al.*, 1988).

The fluid is atomised using a rotating wheel or nozzle, and the spray of droplets, generally in the size range 20µm to 200µm, immediately comes into contact with a flow of hot drying gas, usually air. The resulting rapid evaporation maintains a low droplet temperature so that high drying air temperatures can be applied without affecting the product.

The time of drying the droplets is very short in comparison with other drying processes. Thus in designs with cyclone-like air flow patterns the residence time may be 3 to 6 seconds; in designs with more languid counter-current or co-current flow patterns it is of the order of 25 to 30 seconds.

Low product temperatures and short residence times permit the spray drying of very heat-sensitive products (Strumillo *et. al.*, 1988, Taylor &

Hoare, 1988). Spray drying is used to dry pharmaceuticals, foods, dairy products, blood plasma, numerous organic/inorganic chemicals, ceramic powders, detergents, and other products.

The spray drying process involves three basic stages:

- i) atomisation of the pumpable feed,
- ii) mixing of the spray and drying medium (air), and moisture evaporation, and
- iii) separation of the dry products from the exhaust air.

Each stage is carried out according to the dryer design and operation, and, together with the physical and chemical properties of the feed, determines the characteristics of the final product.

The design of spray dryers, (a typical layout of which is shown in Figure 4.4), ranges from very simple to very complex, dependent upon the fluid to be dehydrated. The main differences in the designs are the variations in atomising devices, in air flow patterns, in gas-heating systems, and in separating and collecting systems. Figure 4.5 shows two common configurations of spray dryer, i.e. co-current and counter-current.

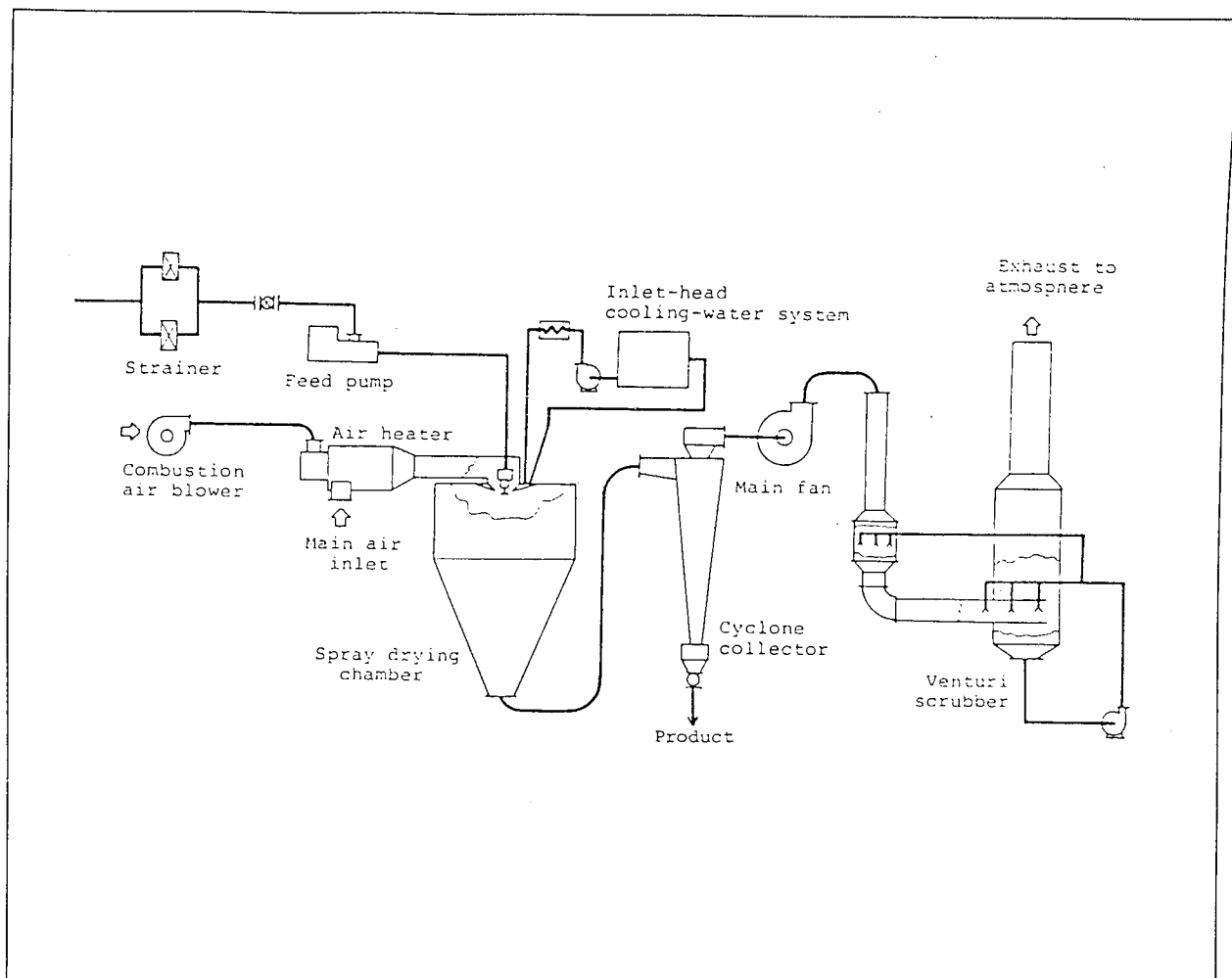


Figure 4.4. Layout of a typical spray drying plant. Single rotary atomiser, co-current operation with or without application of swirl.

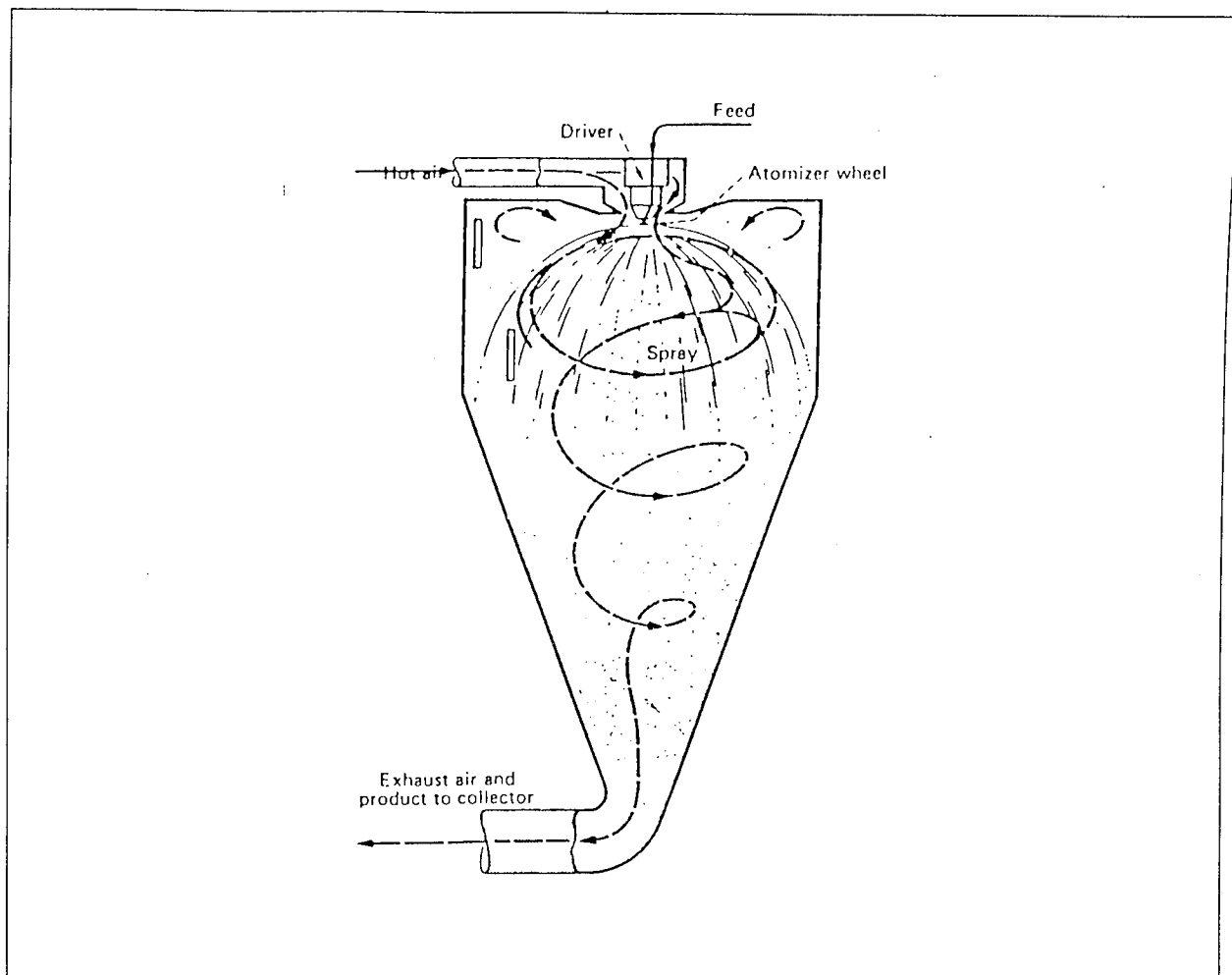


Figure 4.5. Spray dryer configuration (a) Co-current

Swirling increases the particle residence time and may be introduced deliberately

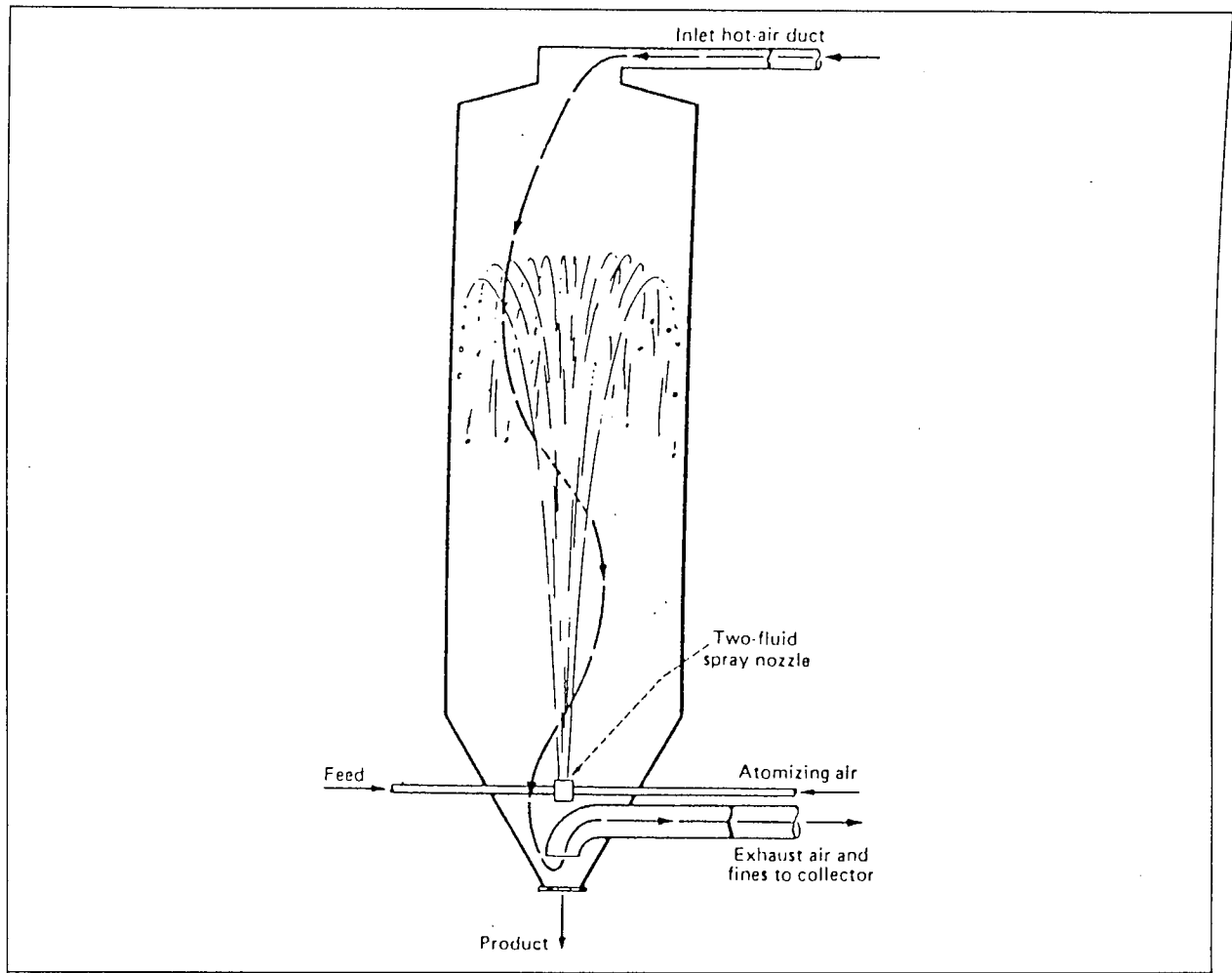


Figure 4.5. Spray dryer configuration (b) Counter-current

Insertion of spray at the top, via a multitude of atomisers with product leaving at the bottom is more common. In some designs additional rows of atomisers are spaced along the tower.

4.2.1: Atomisation

Atomisation is the process of liquid bulk break-up into a myriad of individual droplets to form a spray. It is the most important operation in spray drying, since the type of atomiser determines the energy required to form the spray, the size and size distribution of the drops, and their trajectory and speed. The final particle size, (which also affects the residence time) is critically dependent on the size distribution. The design of the spray drying chamber is also influenced by the choice of atomiser. The drop size distribution establishes the surface available for heat transfer and thus the drying rate.

Although three general types of atomiser are available, the most commonly used are the rotary wheel and the pressure nozzle single-fluid atomisers. Pneumatic two-fluid nozzles are rarely used; ultrasonic atomisers are a recent development of pneumatic nozzles but have not yet reached commercial application.

The selection of atomiser is based upon considerations such as availability, flexibility, energy consumption, or the particle size distribution of the dry product. In many cases, rotary and nozzle atomisers can be used equally successfully, but there are differences in the dry product characteristics, bulk density, and shape between the wheel and nozzle atomisers. In cases where both wheel and nozzle atomisers produce similar spray patterns, the wheel atomiser is usually preferred because of its greater flexibility.

4.2.2: Drop size and size distribution

Consumer requirements and further processing usually determine the dry powder characteristics and specified quality. The single most important factor affected by the operating conditions of atomisation is the quality of the powder. The rate of drying and the residence time are, as already mentioned,

drop-size dependent. Furthermore, the mechanisms of drying and hence the product morphology are similarly affected (Walton, 1994).

Hence it is necessary to know how the particle size and size distribution are affected by the various parameters in order to meet the required bulk density and quality of the dry powder. Particle size and distribution are related to the size of droplets and their size distribution. Hence, in order to control the powder properties, it is necessary as a first step to successfully predict the droplet size.

The spray characteristics are defined by the mean size of the droplet and the size distribution. The Sauter mean diameter is used to characterise the droplet swarm together with the size distribution. This is defined as the ratio of the total droplet volume to the total droplet surface area, i.e.:

$$D_{3,2} = (\sum D_i^3 f_i) / (\sum D_i^2 f_i)$$

where, f_i is the number frequency of the droplet size D_i .

The Sauter mean diameter corresponds to the particle diameter with the same surface-to- volume ratio as the entire spray or powder sample. Sometimes, the median diameter, D_M , is also used in spray drying calculations.

The log-normal and Rosin-Rammler distributions are the most common distributions used in spray drying process calculations. The log-normal distribution, used to represent sprays from wheel atomisers, has two parameters, the geometric mean diameter D_{GM} and the geometric standard deviation S_G , and has the mathematical form:

$$\frac{d(N)}{d(D)} = \frac{1}{D S_G} \sqrt{2\pi} \exp \frac{-(\log D - \log D_{GM})^2}{2S_G^2}$$

where N is the number of droplets counted.

The log-normal distribution also enables determination of the quantities for evaluation of the dispersion factor D_q , which characterises the homogeneity of the spray.

$$D_q = (D_{95} - D_5)/D_{3,2}$$

where D_{95} and D_5 are the droplet diameters at the 95% and 5% probability respectively.

The Rosin-Rammler distribution, used to represent sprays from nozzles, is empirical and relates the volume percentage oversize, V_D , to droplet diameter D ; it has the mathematical formula:

$$V_D = 100 - ((D/D_R)^{D_q})$$

where D_q , again, is the dispersion factor and D_R is the Rosin-Rammler mean diameter. It is the droplet diameter above which 36.8% of the entire spray volume lies.

4.2.3: Chamber design

The type of atomiser in use and the air-fluid contact system, in general, determine the chamber design. The required characteristics of the dry product and production rate are determined by the selection of atomiser and air-fluid layout. If heat-sensitive material is to be dried, then attention must be paid to the temperature profile of the drying air along the drying chamber. The droplet trajectory, mainly the trajectory of the largest droplet, also requires consideration since the size of the chamber must be such that the largest droplet in the spray is sufficiently dry before it reaches the chamber wall. This reduces the formation of partially dried material build-up on the chamber walls; such material would have an extended residence time leading to degradation and even charring.

The chamber shape depends upon the type of atomiser used because the spray angle determines the trajectory of the droplets, and hence the diameter and height of the drying chamber.

4.2.3.1: Air-droplet contact systems

There are three basic types of air-droplet contact systems in use in spray drying systems, two of which are shown in Figure 4.5:

- i) co-current, where the falling droplets are in contact with the air flowing in the same direction. This is used with both wheel atomisation, when fine particles are required, and nozzles, for coarse particles. If there is a constant-rate period, the initial drying occurs with the droplet at the wet-bulb temperature of the inlet air only.
- ii) counter-current, where the drying air flows against the falling droplets/particles. This is used usually with nozzles and for materials that require coarse particles, or special porosity, or high bulk density, e.g. detergents. The final product temperature is higher than that of the exit air.
- iii) mixed flow contact is employed when a coarse product is required and the size of the drying chamber is limited. This has so far been the most economical for materials that can withstand exposure to high temperatures in the dry form. The temperature of the chamber wall that comes into contact with the particles / droplets must be lower than the melting point of the product being dried to prevent baking-on.

4.2.4: Ancillary equipment

The ancillary equipment used generally depends upon the spray dryer process layout, but some are common and these are discussed below.

4.2.4.1: Air heaters

Direct heaters may be used if the material can safely come into contact with the products of combustion, otherwise indirect heaters must be used. The type of heater depends upon the required temperature of the drying air and on the availability of the heat source.

4.2.4.2: Fans

High flow rates of drying air, used in spray drying, are generally obtained using centrifugal fans. A two fan system is usually used; the main fan is situated after the product recovery equipment and the supply fan in the inlet duct to the drying chamber. Two fans enable better control of the pressure in the chamber. With a single fan after the cyclone the whole system operates under a high negative pressure. The operating pressure in a drying chamber determines the amount of powder in the exhaust air, and hence the capacity of the cyclones and their collecting efficiency.

4.2.4.3: Powder separators

Powder separators must separate the dry product from the drying air at the highest possible efficiency and collect the powder. Dry separators, i.e. cyclones, bag filters, or electrostatic precipitators, are used for the principal dry product separation and collection. Wet separators, i.e. wet scrubbers, wet cyclones, or irrigation fans, are used for the final air cleaning and hence are situated after the dry collectors.

In a dry cyclone, centrifugal force is used to move the particles towards the wall and separate them from the air core around the axis. Air and the product particles swirl down the cyclone where the particles are collected and leave the cyclone; the clean air flows upwards and leaves from the top.

A single or multi cyclone system may be used depending upon:

- i) size characteristics to determine the smallest particle size that can be separated,
- ii) overall cyclone efficiency, and
- iii) pressure drop over the unit.

Two characteristics used to define cyclone efficiency are the critical particle diameter (the particle size that is completely removed from the airstream) and the cut size (the particle diameter for which 50% collection efficiency is achieved).

4.2.5: Thermal efficiency

The efficiency of the spray drying operation is defined as the ratio of the heat used in evaporation to the total heat input.

Thus,

$$\eta = \frac{M_{ch} \lambda}{L_A (T_A - T_{WB}) (C_{PA}) + M_F (T_F - T_{WB}) C_{PF}}$$

where,

M_{ch} = chamber evaporation capacity,

λ = latent heat of evaporation,

L_A = air flow rate,

M_F = feed flow rate,

C_{PA} = heat capacity of air,

C_{PF} = heat capacity of the feed,

T_A = air temperature ,

T_F = feed temperature, and

T_{WB} = wet bulb temperature.

4.2.6: Applications of spray drying

Spray drying has enabled many industries to meet dried product specifications most desirable for subsequent processing or direct consumer usage (Wijlhuizen *et. al.*, 1979, Daeman & van der Stege, 1982, Furuta *et. al.*, 1984, Sano & Keey, 1985). It is used in all major industries ranging from production in the most delicate conditions in food and pharmaceutical manufacture through to the high-tonnage outputs within such heavy chemical fields as mineral ores and clays (King, 1974, Zakarian & King, 1982).

A wide range of foodstuffs is spray dried; these include coffee, dried eggs, milk, soups, and baby foods. General household items, e.g. detergents, are also spray dried. Pharmaceuticals, e.g. antibiotics, are produced under aseptic conditions as finely-divided powders which are subsequently tabletted; the spray dried powder form is ideal for rapid assimilation into target body organs (Bootsma *et. al.*, 1989). Many cosmetics rely on spray drying for their constituents, e.g. face powders. Wall tiles are made from spray dried clays; paints contain spray dried pigments; spray dried kaolin is used in the manufacture of paper (Masters, 1991).

4.2.7: Advantages/disadvantages of spray drying

The main advantages of spray drying are:

- i) product properties and quality are more effectively controlled,

- ii) heat-sensitive foods, biological products, and pharmaceuticals can be dried at atmospheric pressure and low temperature (Strumillo *et. al.*, 1988, Taylor & Hoare, 1988),
- iii) high throughput in continuous operation using relatively simple equipment (Zakarian & King, 1982),
- iv) problems of corrosion and choice of materials for construction of equipment are simplified, because the product comes into contact with the equipment surfaces in a substantially anhydrous state,
- v) spray dryers can be used in multi-stage drying processes, e.g. spray dryers coupled to fluidized bed dryers are used in the dairy industry to produce milk powders that have coarse and free flowing agglomerated particles, and also in systems with closed circulation of inert gas as the drying medium, which protects the heat-sensitive material against decomposition, oxidation, *etc.*, and
- vi) spray drying produces relatively uniform, spherical particles with nearly the same proportion of non-volatile compounds as in the liquid feed.

Amongst the disadvantages of spray drying are:

- i) there is some deposition of the drying material on the dryer walls, necessitating the continuous removal of these deposits from the walls either by compressed air or by mechanical means. This agglomeration and deposition can be prevented by the addition of fillers to the feed solution, which form a film on the surface of the drying material, thereby preventing it from sticking to the walls (Strumillo *et. al.*, 1988),
- ii) spray drying fails if a high density product is required,
- iii) spray drying, in general, is inflexible; a unit for fine atomisation may not be able to produce a coarse product, and vice-versa,
- iv) the feed must be pumpable (Sano & Keey, 1982),

- v) there is a high initial investment cost, and
- vi) product recovery and dust collection increase the cost of drying.

4.3: Vacuum dryers

Materials that are thermo-labile or easily oxidisable, especially when wet, can be dried in vacuum dryers. Various types of vacuum dryers are in use for drying of pharmaceutical products.

4.3.1: Vacuum tray dryers

Vacuum tray, or shelf, dryers are indirect-heated batch dryers consisting of a vacuum chamber, containing heated trays (shelves) to support the drying material, and one or two doors (depending upon size of drying chamber). Vacuum is applied to the chamber and the vapour removed and subsequently condensed outside the chamber, in a condenser. Vacuum tray dryers are used extensively for the drying of heat-sensitive or easily-oxidisable materials. Because of the intrinsic value of the materials being dried, the labour costs involved with such drying is insignificant. The advantages with vacuum tray drying include:

- i) easy solvent recovery,
- ii) dusty materials can be dried without excessive losses,
- iii) small quantities can be dried because of the batchwise nature of drying, and
- iv) hygroscopic materials can be dried at temperatures below those required in atmospheric dryers.

4.3.2: Vacuum drum dryers

Double or single drum dryers are also used, under vacuum, for the drying of heat-sensitive materials. Because of the increased capital costs compared to atmospheric drum dryers, these vacuum dryers are used to dry expensive materials such as antibiotics under sterile conditions. The volatile solvents are also easily recoverable in these dryers.

4.3.3: Vacuum band dryers

Vacuum band dryers are suitable for all types of paste-like materials. Wet material is dried as it is transported on a moving band, and heat is supplied by infra red low-temperature radiators or by contact with heated bands.

4.3.4: Vacuum double cone dryers

Vacuum double cone dryers, operated in batch mode, are suitable for drying wet granular materials. The heat necessary to evaporate the moisture is supplied from the steam-heated dryer walls. They are rotated upon their axis and the tumbling effect:

- i) keeps a thin layer on the hot, drying surface, thus allowing heat / mass transfer into / out of the wet material, and
- ii) constantly provides a 'new' layer to be dried.

Because of the intense nature of the blending, these dryers can be used in the preparation of tableting formulations. They are especially suited to perform consecutive chemical reaction - drying cycles, with the necessary reagents being supplied via a feed tube into the drying chamber.

4.3.5: Vacuum paddle dryers

Continuously operated, steam heated, vacuum paddle dryers are suitable for the drying of both paste-like and granular materials. A horizontal rotating shaft fitted with paddles continually scrapes product from the walls and mixes and transports it along the length of the dryer. With the fitting of suitable condensers, the evaporating solvents can be fully recovered.

5: Single droplet evaporation and drying

Studies of the evaporation of pure liquid drops initiated the development of single droplet drying techniques, firstly by Maxwell in 1890 who observed the evaporation of pure liquid drops in a stationary environment. Frossling, in 1938, extended this further when he took the relative motion between the droplet and the air into consideration resulting in the well-known equation:

$$Sh = 2 (1 + \beta Re^{0.5} Sc^{0.33}) \quad 5.1$$

where $\beta = 0.276$

The studies of pure liquid droplets were later extended to cover evaporation from liquids containing dissolved and / or suspended solids mainly by Ranz & Marshall in 1952, who empirically confirmed the validity of equation 5.1 but with β as 0.3.

The techniques, used by Ranz & Marshall, and others, were to suspend either a single droplet from a filament or fine thermocouple, (e.g. Yamamoto *et. al.*, 1985) or a stream of droplets in a wind tunnel or an oven, (e.g. Greenwald & King, 1982, Alexander & King, 1985) where the conditions of the drying air could be carefully controlled. Alternatively the drops were allowed to free-fall in a temperature-controlled wind tunnel.

The successful use of an inverted air velocity profile to maintain a drop in free-flight has been achieved by a number of workers (e.g. Miura *et. al.*, 1977, Akbar, 1988, Oteng-Attakora, 1995) by careful control of the air velocity to match the terminal velocity of the droplet. Droplets, with diameters between 1.5mm and 2.0mm, have also been suspended within an electrostatic or an ultrasonic field (Toei & Furuta, 1982, Furuta *et. al.*, 1982).

Although other methods of droplet suspension have been used, the method of physically suspending a droplet in a controlled airstream, from the end of a thin glass filament, or nozzle, or very fine thermocouple has been at the forefront in the study of the evaporation process (e.g. Charlesworth & Marshall, 1960, Sano & Keey, 1982, Yamamoto *et. al.*, 1985, El-Sayed, 1990, Bains, 1990, Hassan, 1991, Yamamoto & Sano, 1992, Verderber & King, 1992, Sunkel & King, 1993, Walton, 1994). Once the droplet has been suspended, the necessary measurements can be made of droplet weight, size, temperature. Visual recordings of the behaviour of the drying droplet are also possible, using high speed video or cine cameras. Dried particles can also be recovered for microscopic examination of their morphology, sectioning, or porosity measurements (Audu, 1973).

These methods of droplet suspension, viz. free-flight and physical suspension, are the only direct methods of observing particulate drying phenomena, but they have their limitations, e.g.

- i) the suspended droplet (with diameters of between 0.2mm and 2.0 mm) can be as much as twice the size of droplets in a spray dryer (in which diameters are between 10 μ m and 1000 μ m), hence the surface area to mass ratio and distances for internal moisture transport differ,
- ii) the physical support may act as a heat source transferring heat to the droplet by conduction,
- iii) the relatively large droplet size may cause the droplet to oscillate, thereby facilitating mass transfer (Oteng-Attakora, 1995), and
- iv) the lack of free rotation, with a physical support, may lead to differences in the drying rates, the windward side having a higher drying rate than the leeward side (Frossling, 1938).

5.1: Single droplets of pure liquids

The study of evaporation of pure liquid droplets was, as stated previously, commenced by Maxwell in 1890 and later taken up by Frossling in 1938 to result in equation 5.1.

Because of the wide variety of experiments carried out on the evaporation of pure liquid droplets, the literature has been divided into the following categories;

- i) evaporation under natural convection,
- ii) evaporation under forced convection, and
- iii) evaporation under high temperature conditions.

5.1.1: Droplet evaporation under natural convection

Droplet evaporation under natural convection was first studied by Maxwell for pure liquid drops on a flat surface in still air. Subsequent work was conducted on droplets suspended from thin filaments. This approximated more closely to the evaporation from free droplets, as the drops retained their spherical shape thus allowing convective mass and heat transfer over the whole surface.

Optical measurements were made, using a travelling microscope, of the changes in diameter of an evaporating droplet suspended from a glass filament at the centre of a spherical glass vessel with an internal diameter of 20mm (Langstroth *et. al.*, 1950). Evaporation rates were determined of droplets, 2.8mm in diameter, of water and a number of organic liquids. Although corrections were made for radiation and the finite size of the vessel, no account was made for the heat gain through the glass filament.

Steinberger & Treybal, in 1960, studied benzoic acid spheres, 12.7mm, 19.1mm, and 25.4mm in diameter, suspended in a water-filled, 'circulation-

free' Dewar flask, for a day. The resultant solution, from the dissolution of the benzoic acid spheres, was titrated the following day for its benzoic acid content. They proposed the correlations:

i) for $(Gr.Sc) \leq 10^8$

$$Sh_0 = 2.0 + 0.569 (Gr.Sc)^{0.25} \quad 5.2$$

and,

ii) for $(Gr.Sc) > 10^8$

$$Sh_0 = 2.0 + 0.254 (Gr.Sc)^{0.33} \quad 5.3$$

5.1.2: Droplet evaporation under forced convection

A knowledge of the mechanisms of evaporation from droplets travelling relative to a drying medium is essential for the understanding of convective drying. Most of the studies previously conducted into evaporation processes have been carried out using stationary droplets placed in a gas stream. The more significant studies are listed below according to their consideration of either mass or heat transfer.

5.1.2.1: The mass transfer approach

Ranz & Marshall, 1952, studied the rate of evaporation of single droplets, ranging from 0.6 to 1.1mm in diameter, of water, benzene, and aniline, suspended at the end of a glass capillary tube attached to a micro burette, above a stream of dry air at temperatures of between 85°C to 220°C and with a Reynolds number between 0 and 200. The droplet was maintained at a constant diameter by the continual supply of liquid from the micro-burette, to the suspended droplet. Thus the rate of evaporation of evaporation equalled the rate of supply of liquid from the micro-burette. They confirmed the results

obtained by Frossling and derived the heat and mass transfer equations:

$$Nu = 2.0 + 0.6 Re^{0.5} Pr^{0.33} \quad 5.4$$

and

$$Sh = 2.0 + 0.6 Re^{0.5} Sc^{0.33} \quad 5.5$$

From their results, they considered that initially evaporation proceeds as though the droplet was saturated, regardless of the average solute concentration in the droplet, until the formation of a skin or crust. This assumption was, however, disputed by Charlesworth & Marshall, 1960, who, in turn, proposed that the droplet of a solution evaporated initially as a pure liquid droplet until the formation of a crust over the whole surface of the droplet.

Although stationary suspended droplet studies provided insight into the fundamentals of evaporation from liquid droplets, they are limited in that the windward side of the droplet will have a faster drying rate than the leeward side. This was observed by Frossling in the evaporation of naphthalene spheres, when the evaporation rate from the windward side was approximately ten times greater than the rate from the leeward side. To overcome this problem, studies have been conducted with rotating droplets where the droplet is subjected uniformly to the heat and mass transfer phenomena.

Kinzer & Gunn in 1951 conducted theoretical and experimental investigations, using instantaneous photography, of the evaporation of water droplets at temperatures in the range 0°C to 40°C. Charged droplets, 10 µm to 140 µm in diameter, were allowed to free fall through a tube with detector rings, with hydrodynamic forces supporting the larger droplets. Their results confirmed the work of Frossling as they obtained the same relationship as equation 5.1, with $\beta = 0.23$ for $100 < Re < 1600$, and :

i) for $Re < 0.9$, the wind factor was unity, i.e. $\beta = 0$,

- ii) there was an increase in the wind factor with increasing Re ; the value of β increased to 0.46 for $Re = 4$, and
- iii) β eventually fell to 0.23 with $Re = 100$.

The method of keeping the droplet diameter constant, as used by Ranz & Marshall, was also used by Hsu *et. al.* (1954) to measure the evaporation rates of droplets of heptane 1.8mm in diameter at 37°C with $70 < Re < 300$. Particular attention was given to the droplet shape, as the large droplet size and the low surface tension of heptane combined to produce non-spherical droplets, e.g. droplets on the end of fine capillaries (0.1mm) were pear-shaped compared to the truncated spheres at the end of wide-mouthed capillaries (0.8mm). They found that there was an increase in the evaporation rate when the droplets were non-spherical, oblate spheroids giving higher evaporation rates than pendant droplets.

A theoretical analysis of the influence of internal circulation upon the rate of mass transfer from spherical fluid particles was presented by Bowman *et. al.*, in 1961. It was assumed that internal circulation affected the external flow pattern, thereby reducing the resistance to mass transfer into the external fluid. This was illustrated by the work of Ward *et. al.*, in 1962, who measured the rates of mass transfer in four liquid-liquid systems, viz.:

- i) water droplets into cyclohexane,
- ii) cyclohexane droplets into water,
- iii) isobutanol droplets into water, and
- iv) toluene droplets into water.

Their results showed that there was a four to six times enhancement of mass transfer in droplets with internal circulation compared with droplets with no internal circulation. These results also confirmed an earlier suggestion of

Fuchs (1959) that internal circulation within a drop may enhance heat and mass transfer.

The proposal that mass transfer by natural and forced convection were additive was made by Steinberger & Treybal, in 1960, following work with cast spheres of benzoic acid in a stream of water and propylene glycol. They proposed:

$$Sh = Sh_0 + 0.347 (Re Sc^{0.5})^{0.62} \quad 5.6$$

where

Sh_0 is the contribution from natural convection obtained from equation 5.2 or 5.3.

A review of investigations in this area of research, by Pei *et. al.* in 1962, showed that only Steinberger & Treybal assumed that forced and natural convection were additive; all other researchers had suggested that there was a gradual transition from forced to natural convection, and vice-versa, and the two were not additive.

Kinard *et. al.* (1963), reviewed theoretical approaches to the estimation of mass transfer from single spheres, and considered separately the boundary layer in the windward and leeward sides. They found that boundary theory was unable to accurately predict mass transfer because it neglected the rear surface of the sphere. Selected data from previous work on mass transfer by forced convection by Ranz & Marshall (1952), Garner & Suckling (1958), and Steinberger & Treybal (1960) were used to develop the following equation:

$$Sh = 2.0 + Sh_0 + 0.45 Re^{0.5} Sc^{0.33} + 0.00484 Re Sc^{0.33} \quad 5.7$$

5.1.2.2: The heat transfer approach

Heat transfer to the droplet, suspended from a filament / thermocouple, capillary, or nozzle in the various studies on droplet evaporation, occurs as a combination of convection, conduction, and, radiation. Hence, there is heat transfer into the droplet, via the suspension device, which must be considered as an extra heat source when evaluating heat and mass transfer rates.

Tsubouchi & Sato, 1960, investigated heat transfer between single drops and a fluid by using thermistor beads (ranging from 0.3mm to 2.0mm in diameter) suspended in a wind tunnel. By measuring the changes in resistance, and knowing the supplied current and voltage, they were able to deduce the heat dissipated and the temperatures attained by the thermistor. They obtained the following correlation for heat transfer:

$$Nu = 2.0 + 0.5 Re^{0.5} \quad 5.8$$

for $0.3 < Re < 3000$

Heated spheres, ranging from 6.0mm to 60.0mm in diameter, made from carbon steel and brass placed in wind tunnels were used by Yuge in 1960 to compare the effect upon heat transfer, of flow patterns, i.e. cross-flow, counter-flow, and parallel-flow. The resultant expression was:

$$Nu = 2.0 + 0.493 Re^{0.5} \text{ for } 10 < Re < 1.8 \times 10^3 \quad 5.9$$

and

$$Nu = 2.0 + 0.3 Re^{0.5564} \text{ for } 1.8 \times 10^3 < Re < 1.5 \times 10^5 \quad 5.10$$

Experiments on heat transfer, measured in air and water, for internally heated copper spheres, and mass transfer, measured by observing the dissolution of naphthalene spheres in air, for $10 < Re < 10^4$, were conducted by Rowe *et. al.* in 1965. They obtained the following heat and mass transfer correlations:

i) for air

$$\text{Nu} = 2 + 0.69 \text{Re}^{0.5} \text{Pr}^{0.33} \quad 5.11$$

$$\text{Sh} = 2 + 0.69 \text{Re}^{0.5} \text{Sc}^{0.33} \quad 5.12$$

ii) for water

$$\text{Nu} = 2 + 0.79 \text{Re}^{0.5} \text{Pr}^{0.33} \quad 5.13$$

$$\text{Sh} = 2 + 0.79 \text{Re}^{0.5} \text{Sc}^{0.33} \quad 5.14$$

5.1.3: Droplet evaporation in high temperatures

During the evaporation of a droplet, there is heat transfer to the surface of the droplet which causes the liquid to vaporise; the resultant vapour is removed from the surface by diffusion. In the case of a high temperature environment, there is a considerable increase in the sensible heat required to raise the liquid surface temperature to that of the surrounding gas, which results in a reduction in the amount of heat for vaporisation. Ranz, in 1956, demonstrated that the heat available for evaporation, in a high temperature environment i.e. $>300^\circ\text{C}$, was as little as 25% of the total heat transferred, the remainder being absorbed by the cold vapour in its radial flow from the droplet.

In 1955, Marshall, whilst studying droplet evaporation at high air temperatures, developed a differential heat balance over a spherical shell through which heat transfer was inwards towards the droplet and mass transfer outwards. Solution of this differential equation, ignoring variations in thermal conductivity and heat capacity of the gas film caused by temperature and concentration gradients, resulted in an expression for the temperature, T , as a function of distance, x , through the gas film surrounding the droplet.

$$\frac{T - T_s}{T_a - T_s} = e^{-E/x} - \frac{e^{-E/r_1}}{e^{-E/r_2}} - e^{-E/r_1} \quad 5.15$$

where,

r_1 = radius of the evaporating droplet,

r_2 = outer radius of the gas film, and

$$E = m C_{pv} / 4 \pi k_v$$

C_{pv} = heat capacity of the diffusing vapour,

k_v = thermal conductivity of the film, and

m = mass flow rate.

Equation 5.15 yields a value for the Nusselt number when differentiated at the droplet surface, thus:

$$Nu = \frac{2(E / r_1)}{e^{E(1/r_1 - 1/r_2)} - 1} \quad 5.16$$

Hoffman & Gauvin, in 1960, conducted a study on the evaporation rates of droplets, ranging from 0.4mm to 1.4mm in diameter, of water, methanol, pentane, and benzene within an electrically-heated stainless steel sphere containing superheated vapour. The experiments were conducted at temperatures ranging from 100°C to 500°C, and the evaporating droplets were photographically recorded. Their results, which showed that at high temperatures the rate of evaporation was not governed by the rate of heat transfer by natural convection but depended upon a transfer number B , were represented by the expression:

$$Nu = 3.2 (B^{0.97} / B') \cdot Pr^{0.33} \quad 5.17$$

where

$B = (C_{pa} \Delta T / \lambda)$ not allowing for heat transfer by radiation, and

$$B' = (C_{pa} \Delta T) / ((\lambda - (q_e / N_A)) \text{ allowing for heat transfer by radiation.}$$

This equation is limited in its usefulness as it is only valid when the vapour and the walls of the spheres are at the same temperature.

The evaporation of water, methanol, or benzene from porous, hollow spheres, 6.35mm to 12.7mm in diameter, and at temperatures between 204°C and 337°C, were studied by Pei & Gauvin, in 1962. The rates were correlated by the expression:

$$Nu = (3.32 / B) (Re^{0.5} Pr^{0.33}) (Gr / Re^2)^{0.007} \quad 5.18$$

However, the value of the term with an exponent of 0.007, in this case (Gr/Re^2) , will tend to unity, thereby making it insignificant.

Pei *et. al.*, in 1963, used a modified version of the apparatus of Hoffman & Gauvin, and demonstrated that the contributions of forced and natural convection were not additive and that there was a gradual transition from one to the other. However, they were unable to produce an expression to account for this dependency. Using superheated steam at temperatures ranging from 150°C to 750°C with $5.5 < Re < 510$, they concluded that the effects of natural convection were negligible for $Gr/Re^2 < 0.2$, and forced convection effects were negligible for $Gr/Re^2 > 10$.

Frazier & Hellier, (1969), investigated the rapid vaporisation of pure liquid droplets in a high temperature gas stream, using a stream of Freon 113 droplets with a mean diameter of 440µm passing through an air jet at 669°C. A photographic record was made of the vaporisation process. The mass transfer coefficient was out by a factor of four compared to that obtained by Ranz & Marshall. These results of Frazier & Hellier were later re-calculated by Crosby & Stewart, (1970), to yield a smaller (33%) difference between the predicted and observed values.

Toei and his associates, (1966), studied the evaporation of water droplets into a stream of superheated steam and air and obtained the expression:

$$Sh = (P_{bm} / P) (2 + 0.65 Re^{0.5} Sc^{0.33}) \quad 5.19$$

where P_{bm} is the average partial pressure in the boundary layer.

The evaporation of water droplets, 230 μ m to 1130 μ m in diameter, suspended on the end of a 50 μ m glass fibre in a horizontal wind tunnel in a stream of either superheated steam or air with $64 < Re < 250$ was studied by Lee & Ryley in 1968. They evaluated the rates of evaporation by optical measurements of the droplet using a travelling microscope. Neglecting the effects of radiation, they obtained a similar correlation to Ranz & Marshall except that their coefficient was 0.74.

Trommelen & Crosby, (1970), investigated the evaporation of water droplets 1.56mm in diameter in superheated steam and air at velocities of between 1.6m/s to 2.1m/s and at temperatures between 150°C and 250°C. The droplet was suspended at the end of a thermocouple fixed into the end of a fine horizontal glass fibre, which allowed the droplet weight and temperature to be measured simultaneously. They found that at equal temperatures and velocities, the rate of evaporation was greater for air than superheated steam, and this difference decreased at higher temperatures. Their results confirm the work of Toei *et. al.* and also that the heat transfer coefficients for the evaporation of droplets of pure liquids are applicable to both air and superheated vapour. Their analysis accounted for heat transfer by radiation and conduction through the thermocouple wires, but they used the cross-section area of the wires in their estimation of the latter, which underestimates the area of the junction by at least a factor of four.

Audu, (1973), in his investigations into the rates of evaporation of droplets suspended from a rotating nozzle in a horizontal wind tunnel, proposed a temperature correction factor, for temperatures greater than 46°C, and obtained the expression:

$$\text{Sh} = 2.0 + 0.44 \left[\frac{T_a - T_s}{T_{\text{amb}}} \right]^{-0.008} \text{Re}^{0.5} \text{Sc}^{0.33} \quad 5.20$$

Here, again the term with the exponent of -0.008 will tend to unity thus rendering the term insignificant; thus the proposed correction factor will have an insignificant effect upon the whole expression.

5.2: Evaporation from droplets with dissolved or suspended solids

Ranz & Marshall undertook studies on the evaporation of solutions of sodium chloride or ammonium nitrate, a suspension of a green insoluble dye, and reconstituted dried whole milk. They assumed that during the constant-rate period, the evaporation proceeded as though the surface of the droplet was saturated at all times regardless of the concentration within the droplet. This hypothesis was later questioned by Charlesworth & Marshall who proposed that the droplet of a solution evaporated initially as a pure liquid droplet until the formation of a crust over the whole surface of the droplet, after which the droplet behaviour was controlled by the nature of the crust, i.e. whether the crust was porous, non-porous, *etc.*. Obviously this neglects the phenomenon of skin formation.

Trommelen & Crosby, (1970), also investigated the characteristics of four food products and various inorganic salts using superheated steam and air as the drying media. They found that, with the exception of the droplets of skim milk and sodium sulphate, all the materials dried faster in air than in superheated steam.

Miura *et. al.*, (1977), classified materials thus:

- i) crust forming, e.g. sodium sulphate, sodium chloride, and ammonium chloride, *etc.*,

- ii) skin forming , e.g. skim milk, gelatine, *etc.*, and
- iii) neither skin nor crust forming, e.g. bentonite.

Audu & Jeffreys, in 1975, in their investigations of the drying of sodium sulphate and detergent droplets suspended from a rotating nozzle in a horizontal wind tunnel, proposed a crust thickness model based upon the material balance of moisture in the surrounding air. However their calculated values were as much as 20% higher than the observed experimental values. They also proposed a crust mass transfer coefficient, k_c , expressed as:

$$k_c = (D_v \varepsilon^{1.5}) / \psi \quad 5.21$$

where

D_v = molecular diffusivity,

ε = crust porosity, and

ψ = crust thickness.

For the systems used in the study, the crust provided 64.2% of the total resistance for sodium sulphate droplets, and 97.5% for detergent droplets. There were some limitations in the experimental methodology, since although a rotating droplet was studied,:

- i) additional heat was provided to the droplet through the stainless steel nozzle,
- ii) an hygrometer was used to measure the humidity of the airstream before and after the droplet to determine the rate of drying. (This method, although feasible, requires the hygrometer to be very sensitive and accurate, and the air to be of an homogeneous humidity), and
- iii) it did not provide for the droplet temperature histories.

Sano & Keey, (1982), with the assumption that the droplet inflates and ruptures to yield a hollow sphere when the equilibrium vapour pressure of the

moisture inside the droplet exceeds the pressure of the ambient air, proposed equations to describe the evaporation of moisture from single droplets containing colloidal material. In their calculations, they assumed:

- a) that only a single inflation and rupture occurred, (whereas other workers, e.g. El-Sayed *et. al.*, (1990), have observed inflation-deflation cycles), and
- b) provided that there was a conservation of mass, either
 - i) the maximum radius did not change, and the void radius increased because of the loss of moisture, or
 - ii) the outer radius shrank, but the void radius remained constant.

Their experiments with skim milk droplets, at temperatures between 100°C and 150°C, correlated better with the assumption that the void radius remained constant. In order to correlate their experimental results with theoretical values, they had to assign an inflation ratio ($= R_{\max} / R_0$) of 0.88; conversely an inflation ratio of 1.1 was needed to agree with the results of Trommelen and Crosby (1970) at the same temperatures and moisture contents.

To describe the drying characteristics of stationary single droplets in the falling-rate period, Cheong, (1983), developed the receding interface model using an improved version of the technique of Trommelen & Crosby. He measured droplet weight and temperature simultaneously with a cleverly designed filament thermocouple. The thermocouple was made from a 50µm nickel wire, inserted into a glass filament 0.18mm to 0.2mm in diameter, to expose approximately 0.5mm of the wire from the end of the filament. A thin film of copper was deposited onto the filament, and the necessary junction of dissimilar metals, a pre-requisite for the generation of an emf, was made at the exposed end of the nickel wire. The resultant unit measured both the droplet temperature, and, from the deviation from the horizontal, the droplet weight.

Three equations were derived, which upon solution yielded values for crust thickness, core temperature, and droplet weight all as a function of time. The

model, although it predicted the crust thicknesses quite well, did not consider the constant-rate period or the effects of fractures, or blow holes. Hence, it does not allow for the loss in weight of the droplet due to the solids, vapour, or liquid loss during rupture, blowholes, and overestimates the weight after crust formation.

Cheong, in his work with sodium sulphate, observed a sudden fall in the core temperature of the droplet at 33°C; this fall was attributed to the absorption of heat in the melting of the crystals of sodium sulphate. Although Ali, in 1985, also measured the core temperatures of sodium sulphate, he failed to detect this temperature fluctuation at 33°C. In this current study this fall in the core temperature of the droplet of sodium sulphate was observed at approximately 36°C.

Ali *et. al.*, in 1988, used the same apparatus as Audu (1975) to study the drying rates of sodium sulphate and a number of organic dyes. The drying rates for sodium sulphate and an organic dye are shown in Figures 5.1 and 5.2. A scanning electron microscope was used to examine the resultant dry crusts, which were classified as crystalline porous, rough non-crystalline, or very smooth and non-porous. Crust formation was dependent upon air velocity and temperature, and the initial moisture content. Thus, drying after crust formation will always be specific to the nature of the material being dried.

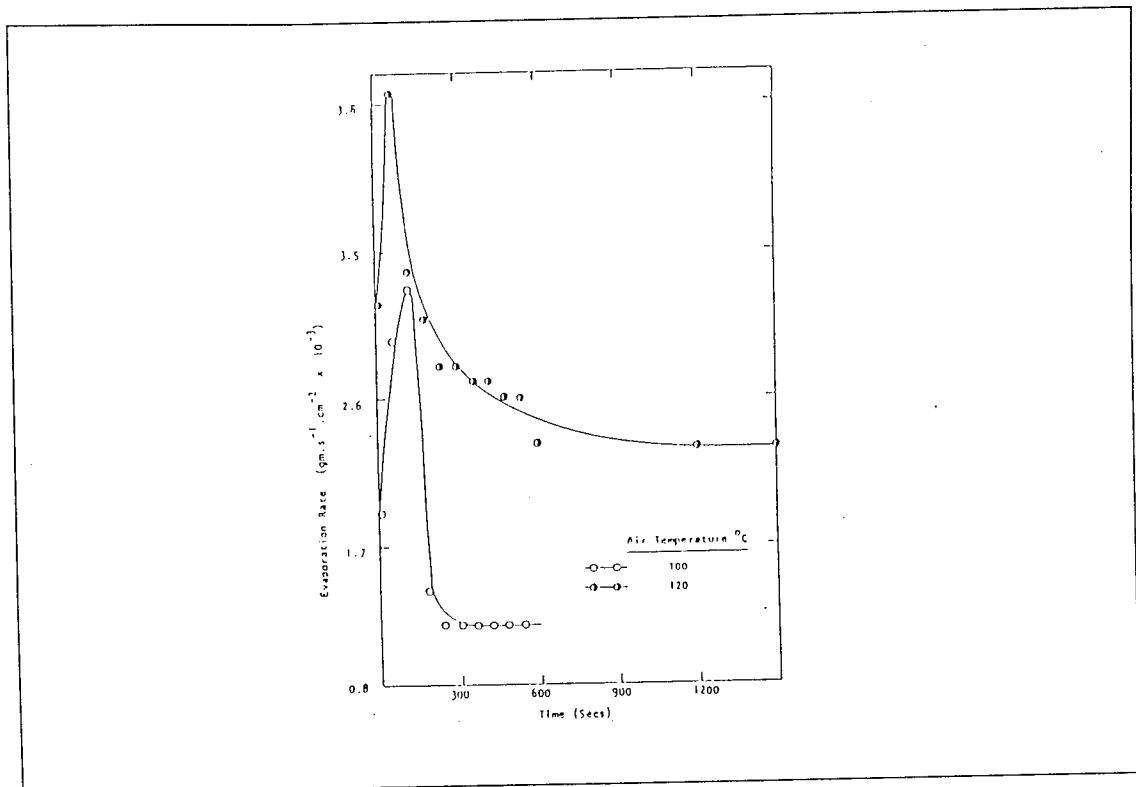


Figure 5.1. Drying rate for sodium sulphate droplets (Ali, *et.al.*, 1988)

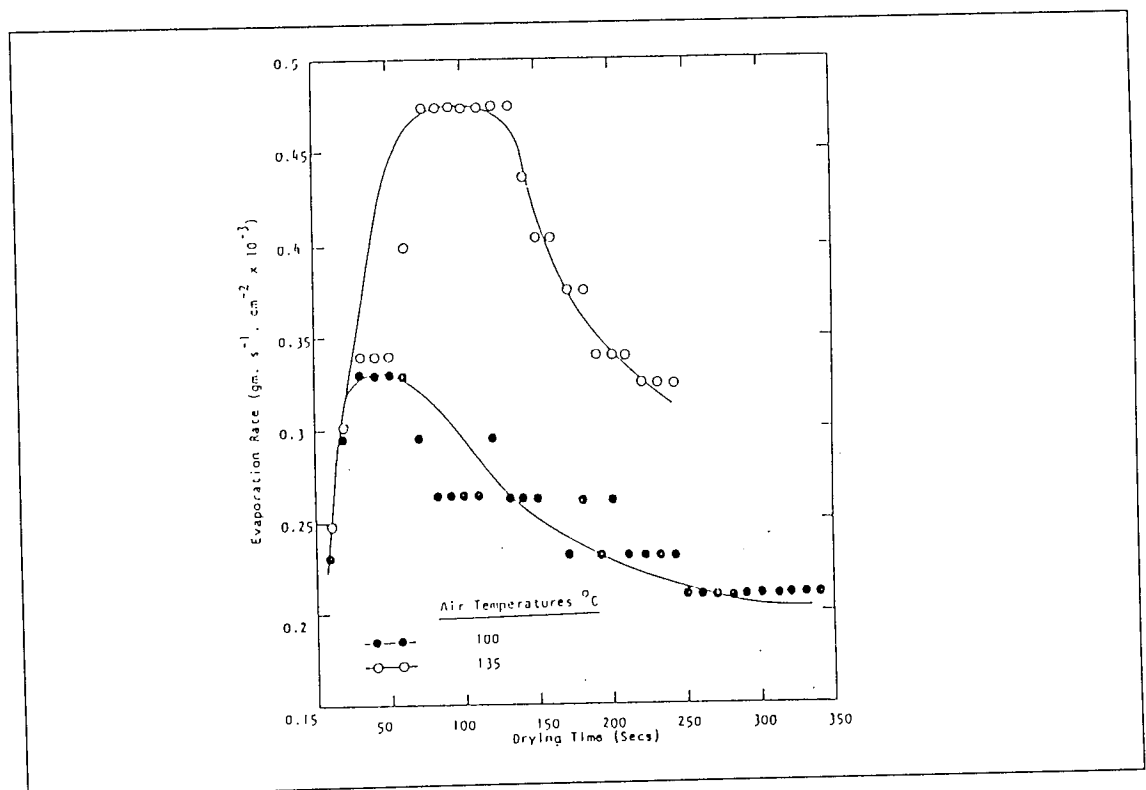


Figure 5.2. Drying rate for droplet of organic liquid (Ali *et.al.*, 1988)

By using techniques similar to those of Charlesworth & Marshall, Nesic (1988) investigated the drying of droplets of colloidal silica, water, sodium sulphate, and skim milk under different drying conditions with air temperatures ranging from 20°C to 200°C and air velocities between 0.1m/s and 2.0 m/s. Water was chosen to test the experimental technique and procedure; skim milk and sodium sulphate were chosen as real solutions. Colloidal silica was chosen because of its known characteristics of forming a porous crust by agglomeration of the primary particles, i.e. the insoluble silicon oxide spheres, as drying progresses.

A model was proposed for droplet evaporation, based upon a number of assumptions, to describe the complete drying process from the initial heating-up period through the constant-rate period, the first falling-rate period (brought on by the development of a crust, by either crystallisation, or agglomeration, which hinders vapour diffusion), through to boiling, (where the droplet undergoes inflation / deflation leading to cracking or bursting of the droplet), and the second falling-rate period, (where the bonded moisture is being removed from an otherwise dry particle). The assumptions used to arrive at this model included:

- i) temperature gradient within the droplet is neglected,
- ii) upon the droplet boiling, there is no temperature or concentration gradient,
- iii) non-spherical shape, oscillations, and other changes in the droplet form are neglected,
- iv) the coefficients for heat and mass transfer are those for the steady state and not for the unsteady state conditions, and
- v) heat of crust formation (the heat of crystallisation) is neglected.

Good agreement was obtained between the predicted and observed results using the chosen materials.

With the filament thermocouple technique developed by Cheong, Bains (1990) studied the drying characteristics of single droplets of inorganic salts, viz. sodium sulphate, sodium chloride, potassium sulphate, copper sulphate, and sodium acetate. A modified version of Cheong's receding interface model was proposed, which covered both the constant-rate period, prior to the formation of the crust, and the subsequent falling-rate period. Numerical solution of the model allowing for the variation in core temperature, droplet weight, and crust thickness, provided good agreement between predicted and observed results for materials that formed rigid crusts, i.e. sodium sulphate, sodium chloride, potassium sulphate, and copper sulphate. For the lower initial solids content droplets of sodium acetate, the results were not as predicted, because of the formation of a non-rigid skin; but, at the higher initial solids content, there was good agreement between the observed and the expected results.

Hassan, in 1991, performed experiments using a modified version of the apparatus used by Audu (1973) and Ali (1985), and classified materials into three according to the mechanisms of crust/skin formation during the drying process:

- i) type 1, typified by custard and starch, where the skin formation was due to gelatinisation at high temperatures,
- ii) type 2, typified by gelatine, where the formation of the skin was immediate upon the commencement of the drying process, and
- iii) type 3, e.g. skim milk and fructose, where the skin appeared at a certain stage of the drying process.

A model was proposed to predict the point of appearance of the skin in type 1 materials. Good agreement was demonstrated between the expected and observed times of the appearance of the skin for the limited range of materials studied.

The apparatus modifications introduced by Hassan were that:

- a) the nozzles used to suspend the droplets were made from glass to minimise heat transfer via the nozzle,
- b) the droplet suspension device could be attached to a sensitive balance, thus allowing continuous measurement of the changes in droplet weight as drying proceeded, and
- c) continual monitoring of the droplet temperature was achieved by a stationary thermocouple which was inside the droplet at all times.

Although much improved from that of Audu and Ali, some shortfalls in this technique remained, e.g.:

- i) the droplet was always hemispherical instead of spherical,
- ii) the rotating nozzle with the stationery thermocouple arrangement may interfere with the internal circulations within the droplet, and
- iii) there was a significant potential source of error in the measurement of the droplet weight which was at least 1000 times less than the weight of the nozzle (the nozzle weighed 50g whilst the droplet before exposure to the drying process typically weighed at approximately 30-40 mg).

Hassan & Mumford (1993) reported that a porous crust formed on materials of type 1 at low temperatures and that skin formation due to swelling of the granules of the material only occurred at temperatures $>150^{\circ}\text{C}$. Variation in the solute concentrations had little or no effect upon the drying rate, but doubling the air velocity effectively doubled the drying rate. Skin formation was almost immediate with materials of type 2, with the rate of skin formation being dependent upon the solute concentration; increasing the solute concentration increased the rate of skin formation. The droplet formed a skin at a certain stage in the drying process dependent upon the drying conditions and the solute concentration.

Walton (1994), experimented with rotating droplets suspended at the end of a thin glass filament in a horizontal wind tunnel, to study the effect of solute concentration, air velocity and temperature, and the degree of aeration of the suspension upon the morphology of the drying particles. A VHS video recorder was used to record the changes in morphology as the drying process progressed. A number of interesting phenomena were observed, such as inflation/deflation of the droplets (which would enhance mass transfer), the occurrence of blow holes, and the formation of protrusions away from the main body of the droplet (which would also provide for enhanced mass transfer), *etc.*. A scanning electron microscope was used to study the crusts collected off the glass filament to gain some insight into the effects of the different variables, such as degree of aeration, air temperature and velocity, on the particle morphology.

Amongst the drawbacks of the apparatus used by Walton was the non-availability of any droplet temperature histories of the drying droplets, the variation in droplet size due to the use of an ordinary syringe to suspend the droplets, and the method of droplet suspension on the glass filament. Although not essential for his study, additional information regarding the droplet, such as temperature, which could have been made available, would have proved useful in understanding the observed phenomena.

The apparatus used in the current study was similar to that used by Walton, but the droplet was suspended on a rotating thermocouple. This allowed the droplet temperature histories to be recorded. The use of an Eppendorf pipettor allowed the accurate suspension of 10 μ l droplets onto the end of the rotating thermocouple, thus enabling inter-droplet comparisons to be made.

5.3: Flavour retention

For food products, the need to retain the characteristic flavour of the product being dried is of paramount commercial importance. The loss of such volatiles as flavours in the exhaust air from the dryers may hence represent an economic loss. Hence the need to optimise flavour retention during drying.

Flavour retention can be enhanced in a number of ways which include the use of less harsh drying regimes, such as freeze drying or spray drying. Encapsulants, e.g. gum arabic, may be added to contain the flavours within an edible shell which readily dissolves in water to release the flavour when required. Other methods have included the removal of the flavour components prior to the drying stage and their subsequent re-addition after drying, as happens during the drying of coffee.

A considerable amount of research has been conducted along various avenues into flavour retention/loss. This section deals with some of the work that has already taken place.

In 1970, when considering the loss of aroma during the drying of coffee extract, Thijssen first proposed the theory of selective diffusion. This is based on the fact that at a certain critical dissolved solids content, the diffusion coefficients of the other substances become less than that of the water, thus leading to the conservation of those species in preference to the water. Working with coffee extract, from which the natural flavour had been removed and replaced with 'model' flavours, e.g. methanol, acetone, *etc.*, dried in an experimental co-current spray dryer, the relative volatilities of the model flavours were found to be insignificant in their influence upon flavour retention compared to the dissolved solids content of the feed. The loss of volatile flavours during spray drying was explained to be due to the formation of blowholes during the expansion of the droplets as a consequence of skin formation over the surface of the droplet.

Subsequent work, in the same year, by Menting *et. al.* on the loss of a model flavour (acetone) from slabs of a starch (maltodextrin) matrix showed that the loss of a flavour component is determined by its volatility relative to water and its diffusion coefficient. They proposed that for maximum volatiles retention, there would have to be a dry surface layer which would be impervious to the flavour component and selectively permeable to water. They found that with the spray drying of foods at an initial solids content of 50%, the retention of flavours is somewhere between 50% and 80% because of the inflation/deflation phenomenon experienced by the droplets.

Rulkens & Thijssen, studied the effect of process variables upon the retention of volatiles in 1972. Volatile retention was apparently independent of the relative volatilities but was determined by the diffusion coefficients of the volatiles in the drying droplets. Aqueous solutions of maltodextrin were spiked with 0.1% w/w model flavours, such as acetone, methanol, and propanol, and spray dried in an experimental spray dryer with a pressure nozzle atomiser; the dried powder was collected and dissolved in water for subsequent analysis by gas chromatography for its volatiles content. Results obtained by them showed that there was increased retention with increasing molecular size of the volatile, and with increased solids content and viscosity (but the viscosity must remain low enough for proper atomisation). The variation with molecular size suggests that real flavours would exhibit improved retention, particularly if their volatilities are also less, compared with the model compounds studied. At high feed concentrations and with inlet air temperatures above 210°C, they found that there was a decrease in volatiles retention. It was thought feasible to achieve retentions greater than 90% with optimisation of the process conditions.

Chandrasekaran & King, also in 1972, studied the retention of trace volatile components in aqueous solutions of fructose, glucose, and sucrose which simulated food liquids during freeze drying. The aqueous solutions were prepared with 1% to 2% gelatine thoroughly mixed with the dry sugar; hot

water was added to this dry mixture, and when the solution had cooled to room temperature, the solution was spiked with 0.5 volume % ethyl acetate, the simulated volatile. The resultant solution was then dried in a freeze dryer, a description of which is given in their paper, and the dry slab was dissolved in 3ml of distilled water. The amount of ethyl acetate in each dry slab was determined by flame ionisation of 2.5ml of the 3ml sample. The results correlated quite well with those of Rulkens & Thijssen, except that while Rulkens & Thijssen believed that the diffusion coefficient remained constant at a value equal to that of the binary diffusivity of the volatile component in water at high dilution, Chandrasekaran & King expected the coefficient to vary with the dissolved solids content in a complex relationship.

In 1974, Kerkhof & Thijssen conducted experiments to study the effects of extractive drying upon the retention of methanol, n-propanol, and n-pentanol in aqueous solutions of dextrin and maltodextrin. Extractive drying is a means of dehydration in which the water is removed by means of contact with a water-absorbing second phase. Droplets of the model food solutions were dispersed in the extraction liquid, polyethylene glycol (PEG) 400. The extractive drying was conducted, batchwise, in a 1 litre tank, with four baffles and an eight-blade impeller, which contained the PEG 400 into which 55ml of the aqueous solutions were added as a stream of droplets ranging from 0.2mm to 2.0mm in diameter. After extraction for 30 minutes, the product was filtered and treated to wash off any adhering PEG; this was followed by gas chromatography to measure the aroma retention. The conclusions reached by Kerkhof & Thijssen were that extractive drying could lead to high flavour retentions provided:

- i) the selective diffusion behaviour evident in air and freeze-drying can be retained, i.e. no appreciable amount of extraction liquid should penetrate into the material being dried,
- ii) the droplets remain rigid from the beginning of their formation, so that no extra losses can occur because of distortion of the droplet or internal

circulation, (clearly this would depend upon drop size and the degree of turbulence), and

iii) the removal of water from the droplet should be very fast with respect to the internal water transport velocity, i.e. the extraction liquid should be hygroscopic and the continuous phase mass transfer coefficient should be high.

Large losses in volatiles near the pressure nozzle spraying the liquid feed were reported by Kieckbusch & King, in 1980, when studying the retention of volatile acetates (ethyl, propyl, butyl, and pentyl acetates) during atomisation in spray drying. They used an experimental spray drying chamber, 0.17m in diameter and 0.40m in length, in which heated air contacted the sprayed liquid co-currently. The spray was collected with a refrigerated probe, designed to capture a continuous stream of droplets and minimise air flow disturbance and the additional volatiles loss during sampling. The droplets were analysed for their volatiles content using gas chromatography.

The losses of the volatiles as a function of distance from the nozzle showed the effects of operating conditions, the nature of the feed solution, and the type of nozzle. Increasing the concentration of the feed solutions provided a slight gain in volatile retention, but there was a selective gain in the retention of the higher molecular weight acetates over the lighter molecular weight acetates with increasing feed concentrations.

Changes in the spray distribution produced by slight variations in the nozzle cone angle substantially affected the retention. A large loss of volatiles occurred at short distances from the nozzle, when the amount of water evaporated was still small, e.g. there was <30% retention of ethyl acetate when approximately 7% of the water had evaporated. There was no apparent effect on retention by increasing the air flow rate.

Attempts were made to reduce the loss of volatiles in the proximity of the nozzle by:

- i) provision of a conical shield for the film and early spray, but the improvement in the retention was negligible,
- ii) providing a gas stream saturated with propyl acetate to blanket the nozzle; although there was an increase in the retention of volatiles, it was not sufficient to justify the extra consumption of propyl acetate in the feed, and
- iii) addition of a vegetable oil emulsion to the feed as an extraction liquid; this enhanced volatiles retention as well as altering the spray pattern by shortening the liquid film. The latter is an interesting observation since thin sheets and sheet disruption mechanisms, together with high relative velocities, e.g 40 m/s, can be anticipated to cause high rates of volatiles mass transfer.

Zakarian & King, in 1982, continuing from where Kieckbusch & King had left off, studied the effects of a dispersed oil phase in the feed upon the retention of volatiles, particularly in the region close to the atomiser. Commercially available peanuts and sucrose were blended to result in a 40% w/w emulsion which was later added to a 19 litre feed tank; an emulsifying agent, Tween 81, was added to the mixture to stabilise the emulsion. The apparatus used was exactly as that of Kieckbusch & King; the concentration of the retained volatiles was determined by flame ionisation and gas chromatography.

Measurements of the retention of ethyl, butyl, and pentyl acetates with no oil phase agreed closely with those of Kieckbusch & King; the retention increased with increasing molecular weight of the volatiles, indicating liquid-phase mass-transfer control as previously found by Kieckbusch & King (1980). They concluded that the effect of the added oil was:

a) physical, in that the oil:

- i) decreased the length of the coherent spray sheet,
- ii) increased the spray angle, and
- iii) increased the size and the spread of the drop sizes, and

b) chemical, in that the oil extracted the volatile compounds, according to their oil-water partition coefficient, into the dispersed oil phase.

The overall effect of the addition of the oil into the dispersed phase was to increase the retention of the volatiles in the oil phase during drying, but to decrease the retention in the oil-free feed.

Reineccius *et. al.*, in 1982, in their attempt to explain the unexpected high retention of food flavours, with boiling points much lower than that of water, made use of Thijssen's selective diffusion theory. They explained this phenomenon by the fact that during the drying process a film of high solids material forms on the surface of the drying droplet. This partially dried film is permeable to water molecules, which are small in comparison to most flavour molecules; the flavour molecules, partly because of their relative size, are unable to diffuse through this barrier and, hence, are trapped within the drying droplet. They proposed that the factors which determine flavour retention during spray drying were those which affected flavour loss until the formation of the semi-permeable film around the droplet. These include the time necessary for the formation of the semi-permeable membrane, and the molecular diameter and vapour pressure of the flavour compounds.

The role of molecular diameter in flavour retention is apparent, i.e. the larger the molecule, the more slowly it would diffuse to the interface where evaporation was occurring, thereby being retained. Vapour pressure would have an effect upon the loss of flavour compounds until the formation of the semi-permeable film, the driving force for the evaporation being the difference in the vapour pressure of a component in solution compared to the vapour pressure in the air above the solution. Compounds which exhibited high vapour pressures in solution would be lost to a greater extent than those with lower vapour pressures.

The time needed for the development of the semi-permeable film around the droplet also determines the flavour retention. The longer the time necessary

for the formation of the semi-permeable film, the greater the loss of volatile flavours. The time needed for the formation of such a film is influenced by:

- i) infeed solids composition - infeed solids above 50% have been shown to have minimal flavour loss,
- ii) infeed temperature - a low infeed temperature was shown to provide a better flavoured spray dried coffee,
- iii) infeed composition - using encapsulants, such as gum arabic, mixed with the infeed allowed more flavour retention, and
- iv) dryer inlet temperatures - as the inlet air temperature increases, the rate of film formation increases, thereby increasing flavour retention until such a temperature was reached which caused inflation/deflation of the droplet causing flavour loss.

Furuta *et. al.*, in 1984, studied, both theoretically and experimentally, the effects of drying upon the retention of ethanol, a simulated flavour component, during drying of a single drop of maltodextrin solution containing the ethanol. They suspended a 5 μ l droplet of the ethanol/maltodextrin mixture on the end of a fine glass filament which was subsequently placed at the centre of a drying air stream. The droplet was weighed at intervals, thereby giving a droplet weight profile during drying; after each weighing, the droplet was discarded and replaced with a fresh droplet, i.e. the weight was not monitored continually but at discrete points during the drying process. Another similar-sized droplet, placed at the end of a thermocouple in the drying air stream, was used to provide the droplet temperature histories during drying. Although a temperature history of the drying droplet was obtained, it was not necessarily the same as that for the droplet from which the retention was being measured. In the current study, the temperature histories did correspond to the particular drying droplets, as the droplet core temperature was monitored continually throughout the drying. The dry droplet was collected after the appropriate drying time, dissolved in 100 μ l of distilled

water, and the resultant solution analysed for its ethanol content using gas chromatography; the resultant data were scattered and inconclusive.

Theoretical analysis of the retention of the ethanol was based on the assumptions that:

- i) for simplicity, the droplet consisted of three components - water, dissolved solid, and trace flavour component,
- ii) transfer of these components occurred only by molecular diffusion, and
- iii) no bubbles or crystals appear during the drying.

With the equations formulated by Kerkhof & Schoeber (1974), Furuta *et. al.* derived more equations which would describe the retention of a volatile component during drying.

Results from their experiments showed that substantial losses of the ethanol occurred in the initial periods of drying during the constant-rate period. The appearance of a dry film on the surface of the droplet coincided with the retention of the ethanol. There was fairly good agreement between the numerically calculated values and the experimentally observed values of ethanol retention; thus they provided another validation for the selective diffusion theory.

The variation of initial concentration of the maltodextrin caused a variation in the retention of the ethanol; the higher the concentration, the more the retention of the ethanol, as illustrated in Figure 5.3.

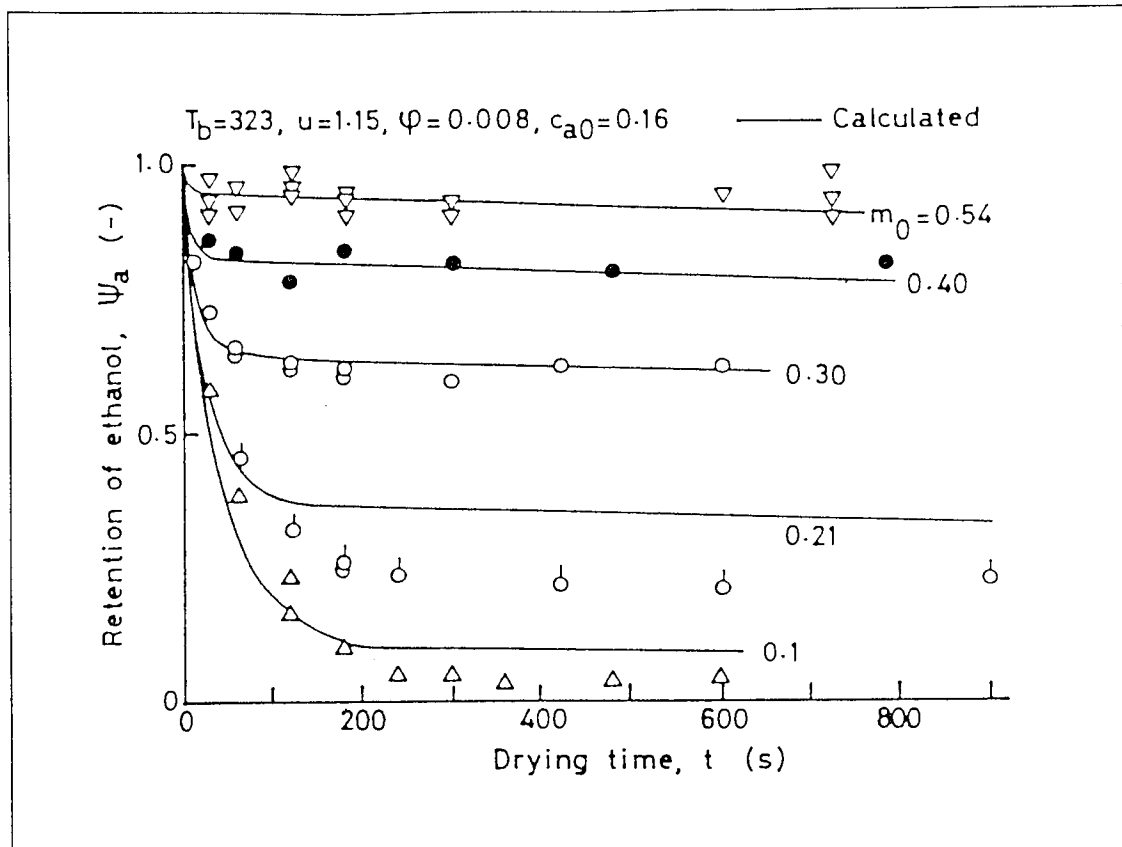


Figure 5.3. Effect of initial concentration of maltodextrin on ethanol retention.

The temperature of the drying air also played a part in the retention of the ethanol such that there was increased final retention with increasing temperature. This was explained by the rate of appearance of the dry film over the droplet which allowed selective diffusion of water; the higher the temperature, the more rapid was the appearance of this dry film.

Furuta *et al.*, in 1985, repeated their previous experiments but with additional materials, viz. gelatine, skim milk, sugar (sucrose, maltose, and glucose) and protein (egg albumin) solutions. They again measured the droplet weights at discrete time intervals, and the temperature histories were measured for different droplets to those collected for subsequent ethanol content analysis.

Considering the effect of droplet expansion, at high air temperatures, upon the retention of ethanol, the droplets were found to expand in different ways:

- i) at relatively low temperatures, e.g. 110°C, the bubble which formed inside the droplet expanded almost coaxially to result in the droplet drying as a spherical shell,
- ii) at temperatures slightly greater than 110°C, many bubbles were generated at different points within the droplet, leading to the formation of a honeycombed structure upon drying, and
- iii) at even more elevated temperatures, e.g. >130°C, the droplet expanded violently and suddenly burst to produce protuberances sticking out from the droplet surface; this bursting exposed liquid inside the droplet to the drying air. They concluded that with expansion of the droplet, the retention of ethanol was reduced because of the increased internal circulation within the expanding droplet and also with the bursting of the droplet exposing the liquid inside to the drying air.

With respect to the influence of the various solutions to the retention of ethanol, they found that:

- i) with the sugar solutions, the retention was higher with increasing molecular weight of the sugar, i.e. there was greater retention with sucrose (MW = 342) than with glucose (MW = 180),
- ii) with the protein solutions, there was a sharp fall in retention, similar to that for the sugar solutions, followed by a gradual but continual decline in the retention throughout the drying period, and
- iii) the retention obtained with solutions of skim milk were similar to those with the sugar solutions. This was explained by regarding the skim milk as a solution of a mixture of sugars and proteins, with the sugar components protecting the ethanol.

Heath, in a short review of flavour encapsulation in 1985, considered the formation of the selectively permeable film, characterised by most of the accepted food encapsulants such as gum arabic and modified starches, which selectively allowed the smaller water molecules to diffuse through leaving the hydrophobic, larger and more volatile flavour molecules inside the drying droplet. He concluded that although the overall flavour losses were small (<5%), the loss of some of the more volatile components would be relatively higher, resulting in a change in the flavour profile. Thus care was needed, to allow for this loss, in the preparation of the feed into the dryer.

In 1985, Tsujimoto *et. al.*, worked with solutions of maltodextrin with 1% w/w acetone spray dried in a co-current spray dryer, to study volatiles loss during spray drying. Increasing the initial concentration was found to enhance the retention of acetone. Losses in the proximity of the nozzle region were found to be dominant with low solute concentrations. The addition of 1% w/w gelatine to the 40% maltodextrin solution considerably enhanced the retention of acetone, as illustrated in Table 5.4. It was therefore suggested that it was the addition of the gelatine that reduced the volatiles loss in the nozzle region and not the increase in viscosity associated with the increased initial solute concentration.

King, in his review of the control of food quality factors in spray drying also in 1985, suggests that loss of volatiles was greatest near the atomiser before there was sufficient drying of the droplet surface for the mechanism of selective diffusion to become dominant. The addition of a dispersed oil phase in the feed had the effect of altering the film break-up mechanism and the drop-size distribution, and led to extraction of the volatiles into the oil phase thereby enhancing retention of flavours. The effect of foaming, as a result of mechanical mixing, causing additional volatiles loss.

solution	viscosity (Pa s)	% relative retention
dextrin 40%	22.0×10^{-3}	0.6
dextrin 40% + 1% gel	28.0×10^{-3}	50.2
dextrin 50%	58.0×10^{-3}	9.1

Table 5.4: Effect of the addition of gelatine on the retention of acetone

(where relative retention is the ratio of final to initial ethanol content)

In another review of the spray drying of foods and volatiles retention, King, in 1988, suggested that volatiles loss during spray drying could be attributed to:

- i) the initial losses occurred from the expanding sheet issuing from the atomiser, the greater the length of this sheet, the greater the volatiles loss, (with enhanced transport due to the turbulence within the liquid),
- ii) the losses due to diffusion after the formation of the droplets and the cessation/absence of oscillations and internal circulations, and
- iii) additional losses, although uncharacterised as yet, due to morphological changes of the droplets, such as frothing, expansion, and cratering/blowholes.

Kim Ha & Reineccius, in 1988, studied the effect of different solvents upon flavour retention during spray drying. An artificially prepared model flavour was added to the desired solvent (in the ratio 9 parts solvent to 1 part flavour) together with a 30% w/w solution of gum arabic prior to spray drying in a Niro spray dryer. With inlet and outlet temperatures of 200°C and 100°C respectively, approximately 15kg of water was evaporated per hour. Flavour retention was measured using the acetone precipitation technique, with the ratio of the quantity of each flavour compound being measured in the infeed and in the reconstituted spray dried powder yielding the percent retention. Their results, shown in Table 5.5, illustrated the fact that there was, as expected, an improvement in flavour retention when a fat soluble flavour solvent was used in the flavour formulation. This was because the flavour

compounds formed an emulsion and exhibited both a reduced vapour pressure (relative to being dispersed in water) and greater resistance to diffusion resulting in less evaporative losses during drying.

The enhanced flavour retention with the propylene glycol as compared with the ethanol was explained by the fact that, although neither of these two provide any lowering of the vapour pressure or any reduction in the diffusivity of the flavour compound, the ethanol promoted the 'ballooning' of the droplets caused by the vaporisation of the ethanol inside the droplet. This expansion of the droplets would produce particles with a greater surface area and thinner walls which would enhance the loss of volatiles, and therefore reduce overall flavour retention.

Inglett *et. al.*, in 1988, worked with a number of oligosaccharides to encapsulate orange oil during spray drying to achieve maximum flavour retention. The work was prompted by the limitations afforded by the encapsulants that were currently available, viz.:

i) chemically-modified starches, although possessing good emulsifying properties, were shown to provide good retention of volatiles but could not provide protection from oxidation,

Flavour compound	Flavour Solvent			
	ethanol	propylene glycol	triethyl citrate	vegetable oil
Diacetyl	23	39	65	59
Ethyl acetate	19	25	41	29
Ethyl propionate	30	26	61	50
Ethyl butyrate	52	52	77	70
Butyl acetate	52	50	76	81
2-Heptanone	61	66	81	81
Ethyl valerate	70	72	91	84
Benzaldehyde	82	63	78	70
Limonene	84	90	92	86
Acetophenone	80	91	97	96
Phenyl ethyl alcohol	80	86	100	90
Benzyl acetate	83	88	100	96
Methyl salicylate	83	84	97	95
Carvone	84	88	99	99
Methyl anthranilate	86	97	103	100
Ethylmethyl phenyl glycidate	100	103	102	98
Isoeugenol	92	97	100	101
β -Ionone	100	103	99	91
Ethyl hexanoate	84	91	98	90

Table 5.5: The influence of flavour solvent upon the retention of flavour compounds during spray drying.

ii) partially-hydrolysed starches, e.g. maltodextrin, provided excellent protection against oxidation, but because of the lack of emulsification, they provided poor volatiles retention, and

iii) gum arabic, which provided good retention but limited protection from oxidation.

The oligosaccharides were prepared from the action of α -amylase on waxy maize, ordinary maize, amylo maize, wheat, rice, cassava, and potato. A homogenised mixture of 25% w/w orange oil in a 50% w/w aqueous solution of each modified starch was spray dried in a co-current spray dryer with inlet and outlet temperatures at 200°C and 100°C respectively.

No obvious relationship was found between the origin of the oligosaccharide and the retention of the orange oil, with the retentions ranging from 42% for the waxy corn to 72% for the amylo maize. They studied the spray dried orange oil for shelf life, by the appearance of limonene epoxide on the surface of the dried particles, to see whether the particular encapsulant used afforded any protection from oxidation. The results showed that shelf life was related to the starch oligosaccharide composition. Amylo maize, which has a dextrose equivalent (DE) value of 18, and the highest proportion of large oligosaccharides and the smallest proportion of small oligosaccharides, had the poorest shelf life; Potato starch (DE = 18) had a similar composition and similar shelf life. Other starches with higher DEs, i.e. with a higher proportion of smaller oligosaccharides, had a better shelf life. This suggested that the presence of the smaller oligosaccharides, i.e. higher DEs, promoted oxidative stability by forming a much more effective oxygen barrier.

In 1990, King, in another review of spray drying and the retention of volatiles made the analogy of the initial pre-freezing stage in freeze drying, in which the concentrating effect enhances retention of volatiles, to that of the early build-up of a high concentration of dissolved solids during spray drying to assist in volatiles retention. From the work done by his colleagues and

himself, King suggested a number of improvements to the drying process which would help in the retention of volatiles:

- i) feed concentration - increasing the feed concentration markedly improved the volatiles retention as it lowered the diffusion coefficients of the dissolved solids and reduced the initial concentration gradient needed to achieve the critical surface concentration to allow selective diffusion to occur,
- ii) inlet air temperature - hotter air would result in better volatiles retention because the faster drying would impose steeper internal water concentration gradients, but this must be balanced with the possibility of greater thermal degradation,
- iii) existence of an oil phase in the feed - the oil phase aided the retention of volatiles by extracting the volatiles into the oil phase. However, although this aided volatiles retention, it suppressed the olfactory response of the reconstituted product for a given solute concentration, and
- iv) change of feed composition to alter the morphology of the droplets. The changes in morphology, such as expansion and blowholes, of the drying droplet affected the retention of volatiles. Therefore it was suggested that the feed could be altered in some way to reduce such morphological changes and, hence, result in better volatiles retention.

A novel technique to measure the instantaneous rates of volatiles loss was developed by Verderber & King in 1992. They used a highly volatile compound, sulphur hexafluoride (SF_6), in aqueous solutions of glucose, sucrose, maltodextrin, and coffee extract, suspended as a droplet from a hollow fibre (attached to a syringe which contained the simulated flavour) in a drying airstream of pure (99.99%) nitrogen at 150°C . The gas was sampled downstream from the droplet, and analysed for its SF_6 content using a gas chromatograph coupled to an electron capture detector, (which is very highly sensitive to halogenated compounds). A video recorder was used to follow the morphological changes undergone by the drying droplet.

Their results demonstrated that there was an initial release of the SF₆ in the early stages of drying before the onset of selective diffusion, after which there was little or no release of the SF₆ until (as shown by Figures 5.6, 5.7, 5.8, and 5.9) changes occurred in morphology of the droplets:

- i) cycles of balloon-like expansion, bursting and collapse of the droplet were experienced by the glucose and sucrose droplets,
- ii) the maltodextrin droplets tended to froth and roll within themselves, and
- iii) the droplets of coffee extract formed protrusions, as reported earlier by El-Sayed *et. al.* (1990), which provided the extra surface area from where the volatile SF₆ could be lost.

In 1993, Sunkel & King studied the effect of particle morphology upon volatiles retention, again using SF₆ as the volatile, in solutions of coffee extract, non-fat milk (assumed to be skim milk), and maltodextrin suspended as a droplet at the end of a hollow fibre in a drying gas stream of pure nitrogen. Again, the SF₆ concentrations were measured continually as in the previous study of Verderber & King (1992) using an electron capture detector, and the droplet morphology was simultaneously recorded on video tape. The SF₆ losses were related to changes in droplet morphology during drying.

Their results correlated with those of Verderber & King, 1992, in that with droplets of coffee extract and maltodextrin there was a substantial increase in SF₆ losses later in drying, corresponding to the periods of morphological development - formation of protrusions for coffee extract and repeated expansion, bursting, and collapse of the maltodextrin droplets. With the non-fat milk, the development and sustenance of a smooth skin resulted in a reduction in the loss of SF₆ later on during drying.

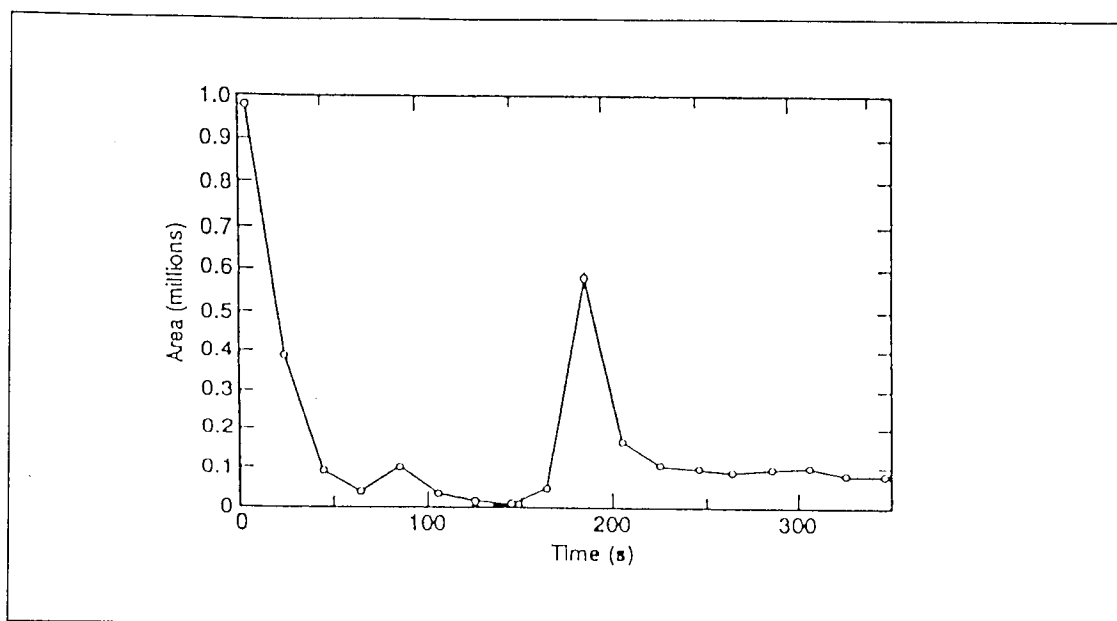


Figure 5.6. Loss of SF_6 with 20% w/w glucose

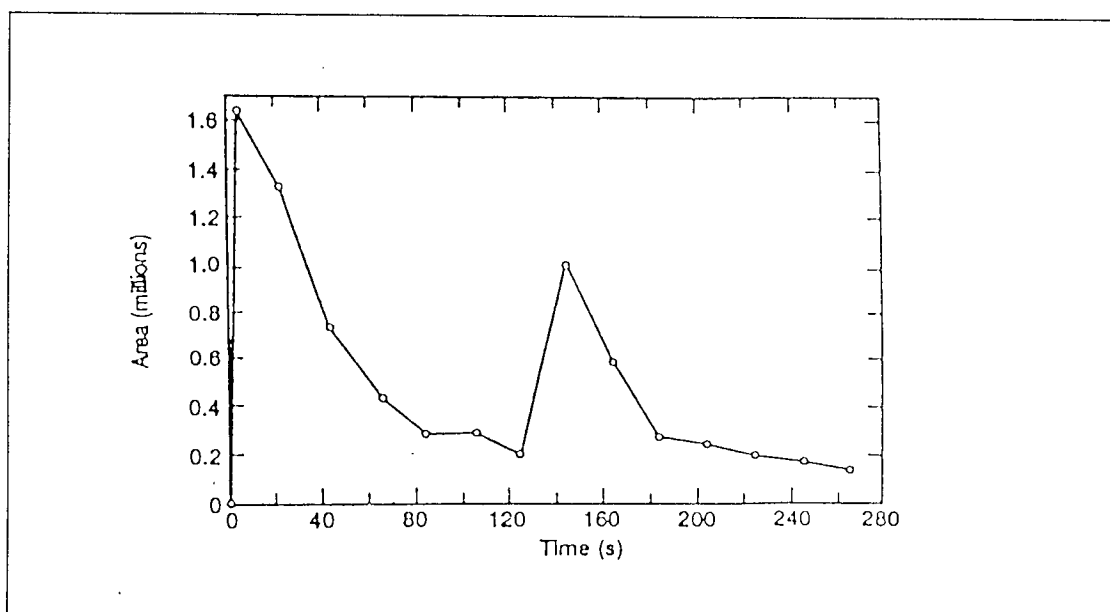


Figure 5.7. Loss of SF_6 with 20% w/w sucrose

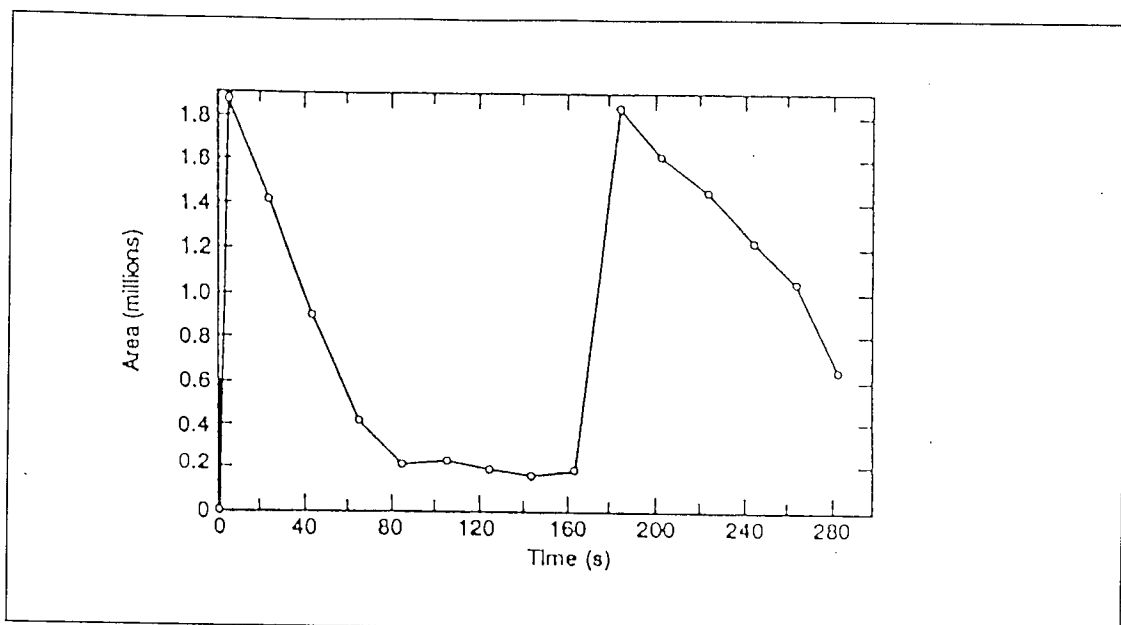


Figure 5.8. Loss of SF₆ with 20% w/w maltodextrin

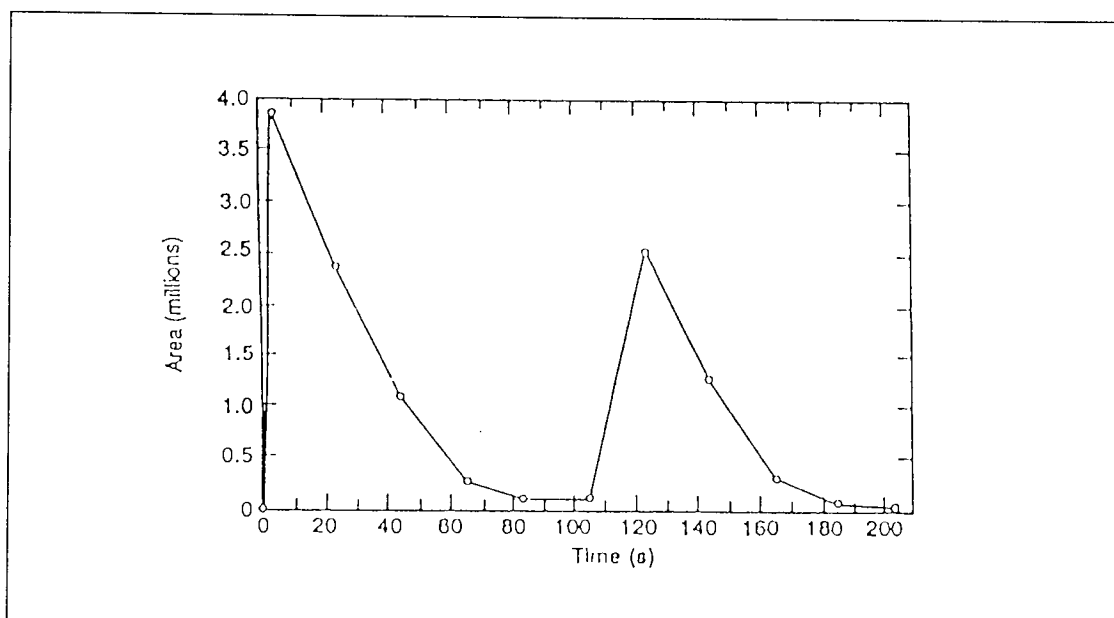


Figure 5.9. Loss of SF₆ with 5% w/w coffee

Walton, 1994, in his study of the morphology of drying droplets, also conducted some experiments on the retention of volatiles. In the apparatus, described earlier, he studied the effects of solute concentration, drying temperature, and particle morphology upon the retention of volatiles using ethanol as the model volatile and solutions/slurries of sodium chloride, skim milk, and silica. Ethanol concentrations were measured with a gas chromatograph.

The effect of solute concentration was similar to that described by previous workers, e.g King and his associates, i.e. increasing the initial solids content lead to increased volatiles retention. There was an optimum temperature above which there was a decrease in final retention of the volatile, because of droplet expansion and collapse after bursting. Experiments on the effect of particle morphology produced predictable results:

- i) the particles which formed a crystalline (sodium chloride) or agglomerate (silica) structure upon drying had a reduced retaining effect, and
- ii) the skim milk formed a skin, after a certain drying time, which enhanced the retention of the volatile.

5.4 The drying of enzymes

Enzymes are powerful natural catalysts with great substrate specificity, and are more easily damaged by 'wet' heat than 'dry' heat. Given that at higher temperatures, enzymatic conversions would involve smaller quantities of enzyme, there is a need to enhance the thermostability of the enzymes. This is achieved by several methods including dehydration, micro-encapsulation, and isolation from thermophilic organisms.

Although the literature cites the importance of thermostabilised enzymes, the mechanisms of enhanced thermostabilisation by dehydration are not known. It may result from the hindered unfolding of the protein macromolecule in a water-free solid phase.

In a theoretical study of the inactivation of phosphatase during the spray drying of skim milk, Wijlhuizen *et. al.*, in 1979, developed a model where the enzyme was immobile with respect to the dissolved solids. Their computed results correlated well to the experimental work of Daeman.

They concluded that:

- i) increasing the drying air temperature leads to a greater degradation of the enzyme,
- ii) increasing the initial solids concentration leads to a smaller increase in the thermal degradation, and
- iii) increasing the ratio of the gas bubble, inside the droplet, and droplet size caused less thermal degradation of the enzyme because of the faster drying process resulting from the shorter diffusion distance.

Daeman & van der Stege conducted a study on the destruction of enzymes and bacteria during spray drying in 1982. They used the enzymes alkaline phosphatase, rennin, and α -amylase and the bacteria *Serratia marcescens* and a *Staphylococcus* strain C131 dried in a commercial co-current spray dryer to study the effect of air temperature, initial solids concentration, and droplet size upon residual activity of the enzymes.

The effect of inlet air temperature was found to be negligible compared to that of the outlet air; this was expected because the inlet air temperature would contact the wettest particles and the outlet air temperature would contact the driest particles. Also, the drying of a more concentrated feed resulted in more inactivation. For the effect of droplet size, they assumed that the temperature would be the same for all sizes of droplets, but that the drying time would be longer for larger droplets. Hence, it was concluded that the destruction of the enzymes and bacteria would be greater in the larger droplets.

Further work along similar avenues was done by Daeman *et. al.* in 1983. They analysed the process of spray drying to determine where the actual destruction of the enzymes and bacteria took place. Samples were collected, from various points in the spray dryer, on trays cooled with liquid nitrogen to halt any

further degradation of the samples. They found that, as before, there was a decrease in activity of the enzyme as drying proceeded, but this was countered by the increased thermoresistance provided by the increasing total solids content of the droplets. The overall result was a reduction in enzyme activity, but not complete inactivation of the enzyme. With increasing outlet air temperatures, the enzyme inactivation started at lower total solids content.

A model developed by Liou *et. al.*, in 1985, to study enzyme inactivation was successfully correlated with experimental results of the inactivation of soybean lipoxygenase. The model was based upon the diffusion equation for a binary system, the heat balance of the drying particle, and the equations describing enzyme inactivation kinetics. The experiment was conducted with a slab of gel containing the immobilised enzyme; after set time periods, the enzyme gel was removed from the drying cell and analysed for its residual activity.

Yamamoto *et. al.*, in 1985 studied single droplets to ascertain the effects of oxidation and pH during drying on the enzyme inactivation using glucose oxidase, alkaline phosphatase, and alcohol dehydrogenase. They also developed a theoretical model, which was verified experimentally. It was concluded that the effects of thermal inactivation of the enzyme must be considered together with the effects of oxidation and pH.

In a study of enzyme thermostability in 1986, Barzana-Garcia *et. al.* worked with the enzyme alcohol oxidase, immobilised onto DEAE cellulose. The effect of dehydration and not the immobilisation onto a solid matrix was found to afford the enhanced thermoresistance. The soluble and dry enzyme preparations were suspended in phosphate buffer (0.01M) at pH 7.5 and incubated at 60°C, and the residual enzyme activity measured at different times. The residual enzyme activity was measured by spectrophotometric analysis, at $\lambda = 480\text{nm}$, of the hydrogen peroxide formation from ethanol, a reaction catalysed by the enzyme alcohol oxidase.

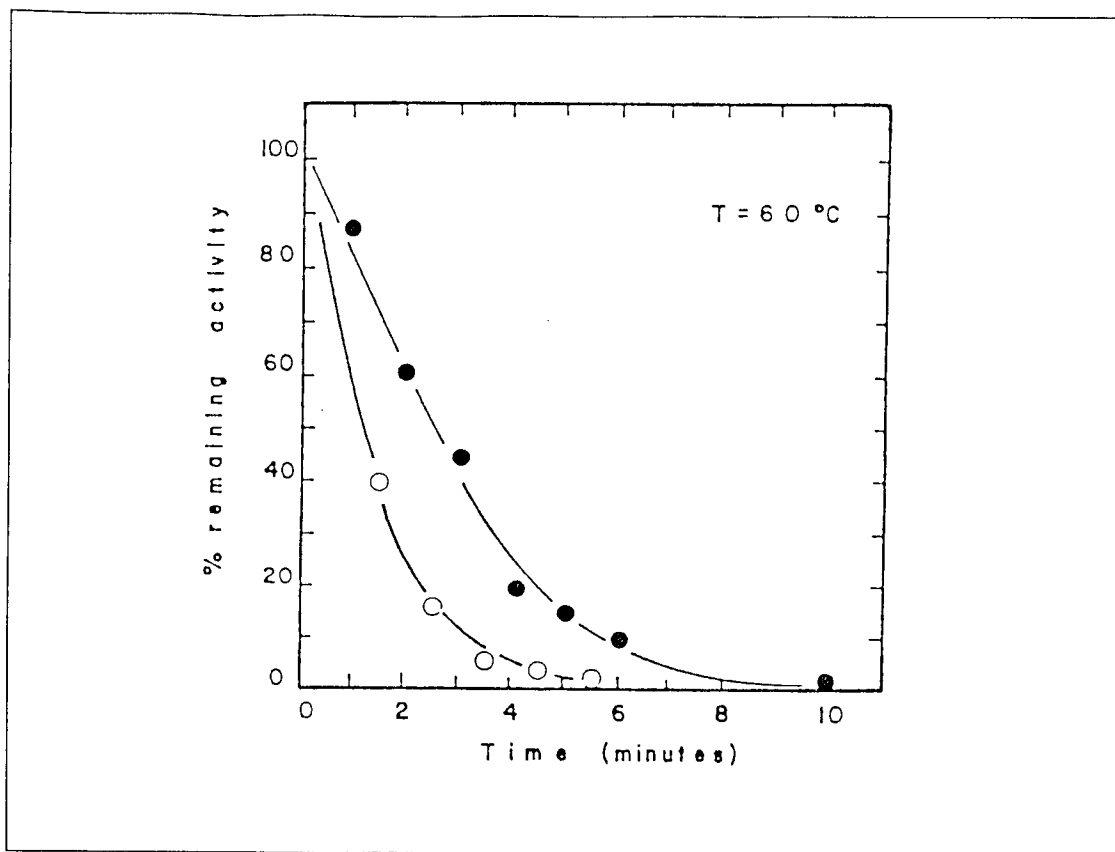


Figure 5.10. Effect of immobilisation on the thermo-stability of alcohol-oxidase (solid symbol - dehydrated enzyme, open symbol - liquid enzyme)

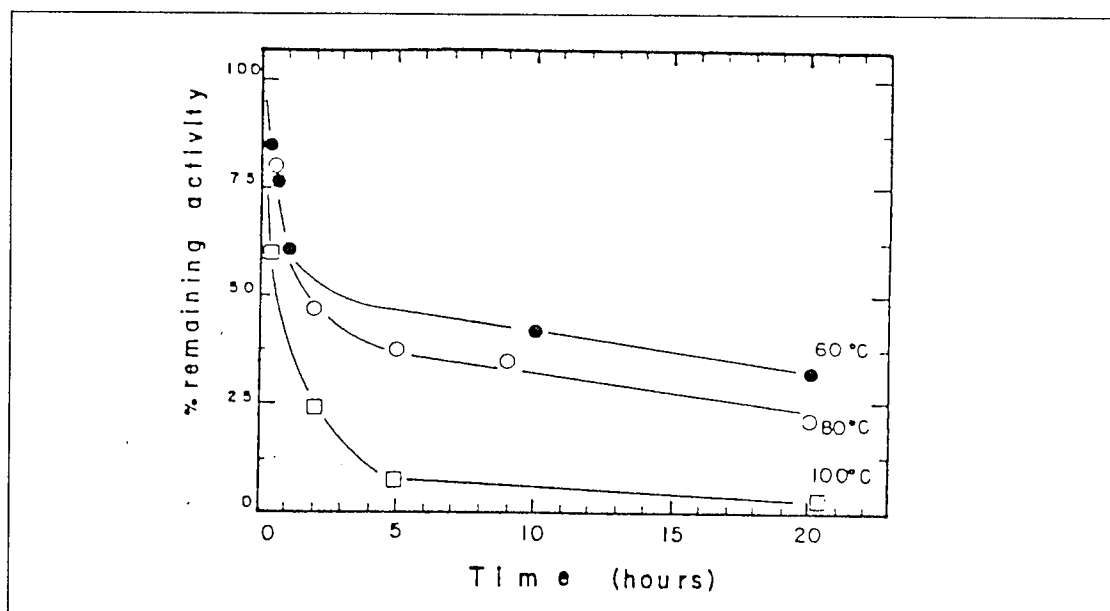


Figure 5.11. Thermo-inactivation of dry immobilised alcohol-oxidase

The results, shown in Figure 5.10, demonstrated that, although both enzyme preparations had short half-lives, the dehydrated enzyme ($t_{1/2} = 3$ minutes) was slightly more stable than the liquid enzyme ($t_{1/2} < 2$ minutes).

Dry preparations of the enzyme powder were incubated at elevated temperatures to determine the denaturation kinetics of the dehydrated enzyme, the residual enzyme activity being measured as before. Results, shown in Figure 5.11, demonstrated that dehydration dramatically increased the thermostability of the enzyme, e.g with reference to Figures 5.10 and 5.11, the $t_{1/2}$ at 60°C was found to have increased from less than 2 minutes to approximately 3 hours.

Taylor & Hoare, in 1988, studied the drying of the enzyme glucose oxidase in a continuous band vacuum dryer. It was observed that with increasing vacuum, there was increased drying, and that at the two pressures studied, (4,250Pa and 20,000Pa), there was no loss in enzyme activity during the entire drying process. However, with a vacuum lower than 25,000Pa the extent of dewatering prior to drying affected the loss of enzyme activity.

Yamamoto & Sano, in 1992, worked with single droplets of sugar solutions containing either of the enzymes β -galactosidase, glucose oxidase, and alkaline phosphatase, measured the residual enzyme activity as a function of drying time. The droplets were suspended from a glass filament, and subjected to a constant drying temperature and a flat velocity profile air flow. Periodically, the droplet weight was measured, by the deflection of the glass beam balance, after the air flow had been momentarily stopped; the droplet temperature was continually recorded with the thermocouple inserted into the droplet. After the set drying period, the droplets were removed from the filament, dissolved in the appropriate buffer solution, and the residual enzyme activity was assayed.

The loss of enzyme activity was not as great as in aqueous solutions even when the air temperature was quite high, e.g. 80°C to 85°C. The droplet size had a significant influence upon the final enzyme activity; high enzyme

retention was correlated with small droplet size and moderate air temperatures for the drying process. The choice of dissolved sugars, known to be good stabilisers of enzymes, was also found to be important. The enzyme retention became lower with increasing molecular weight of the sugars, i.e. enzyme inactivation increased with a decrease in the number of hydroxyl groups per molecule of the sugar. As previously demonstrated by Yamamoto *et. al.* (1985), the use of foamed droplets also increased the retention of enzyme activity.

In the present study, droplets of pure enzyme solution were dried on the end of a rotating thermocouple suspended in a drying air stream, and the droplet temperature was continually monitored. With hindsight, the use of dissolved sugars, to facilitate comparison of the results with those of Yamamoto *et. al.* and others, or the evaluation of the use of encapsulants upon retention of enzyme activity may have yielded more significant data. (Such studies are discussed further in the recommendations for further work, Chapter 9).

5.5: The drying of pharmaceuticals

Pharmaceuticals represent a wide variety of different chemical or biological substances ranging from relatively cheap and easy-to-dry materials, such as acetylsalicylic acid, through to expensive and difficult-to-dry products, such as hormones. Hence there is a need to determine the drying characteristics of the various pharmaceuticals to enable the appropriate selection of the dryer to dry such products.

Githinji, in 1980, investigated the effect of drying at various temperatures upon pyrethrum flowers, the source of a potent but environmentally friendly insecticide (pyrethrins), to demonstrate that the use of excessive drying temperatures and overdrying resulted in the loss of pyrethrins. The flowers were arranged in a mono-layer on wire-mesh trays to allow for efficient circulation of air and the removal of water vapour, and dried in an air oven at

temperatures from 60°C to 160°C at 20°C intervals. After specific time intervals, the flowers were removed and analysed spectrophotometrically for their pyrethrins content. Results, shown in Figure 5.12, confirmed that drying of the pyrethrum flowers at high air temperatures and for prolonged periods of time had a detrimental effect upon the pyrethrins. To allow for sufficient drying rate with minimal loss of the pyrethrins, it was recommended to dry the pyrethrum flowers at 80°C.

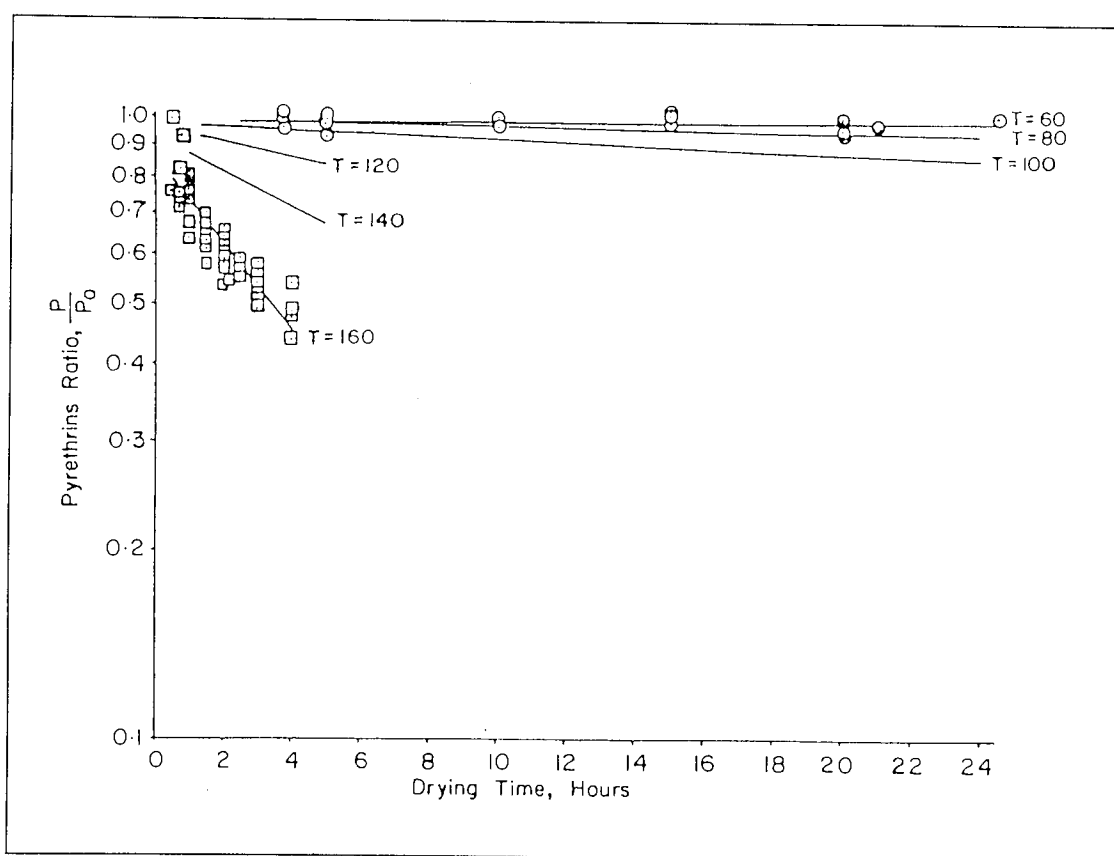


Figure 5.12. Effect of temperature on pyrethrins content.

Vidgren *et al.*, in 1988, studied the in vitro effects of two forms of the anti-asthmatic drug, disodium cromoglycate; two forms of preparation of the drug were used to ascertain the most suitable method of preparation. The two chosen modes of drug preparation to yield particles of the optimum size range, of between 0.5µm and 7.0µm for inhaled drug particles, were:

- i) mechanical micronisation - using an air jet mill with two passes to complete the milling process, and
- ii) spray drying - a 6% w/w disodium cromoglycate solution was spray dried in a laboratory scale spray dryer, with the inlet and outlet air temperatures at 180°C and 80°C respectively, and a feed rate of 60 litres per minute.

The physical difference between the two modes of preparation are clearly visible in the electron micrographs, shown in Plate 5.13. The resultant particles were then dispersed into the liquified propellant (Freon, P12 and Freon, P114) with an homogeniser and filled into aerosol containers; each 50µl dose of the reconstituted drug contained 1mg of active substance. The drugs were delivered to a simulated upper respiratory tract, constructed from bent tubing, which was subsequently dismantled into its constituent parts, each part being carefully washed with pure water to collect any drug that may have collected onto each part. The water was evaporated from the resultant suspension, and the samples then re-suspended in phosphate buffer and subjected to spectrophotometric analysis at $\lambda = 238\text{nm}$. Results from their experiments showed that the spray dried particles stuck to the imitation throat more than the micronised particles since the spray dried particles were more cohesive.

Vidgren *et. al.*, in 1989, extended this work to study the effect of different humidities upon the usefulness of disodium cromoglycate as an anti-asthmatic drug. Using the same modes of sample preparation and in-vitro testing methodologies as their previous study of 1988, they found that the fractions below 7.1µm could be deposited at the site of most therapeutic benefit in the lungs. Their results, shown in Table 5.14, illustrate that for the mechanically micronised form of the drug, approximately 30% of the drug is available irrespective of the relative humidities of the air in which the drug had been stored after preparation. This could be explained by the observation that most of the water was absorbed inside the micronised particles.

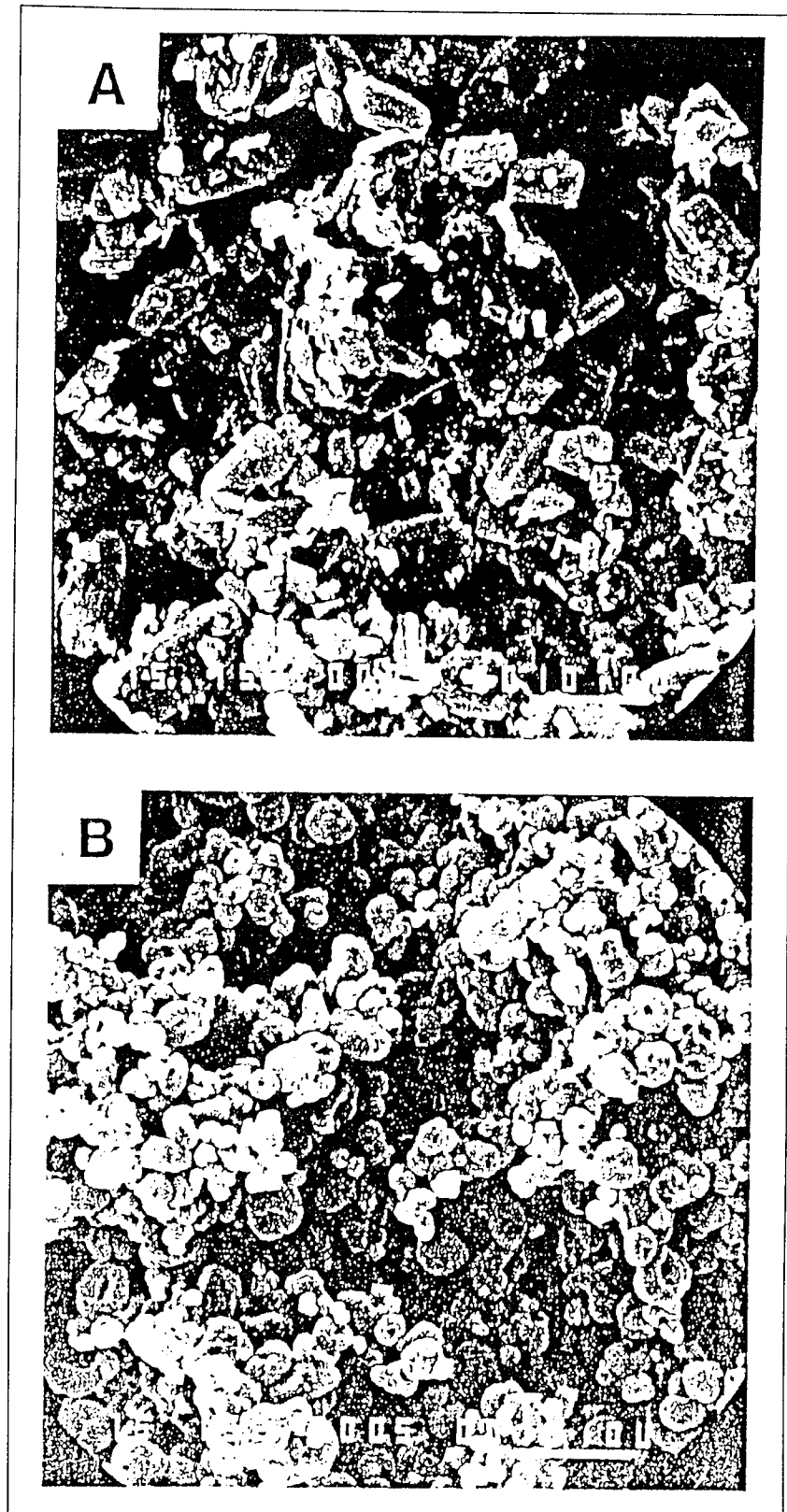


Plate 5.13. Electron photomicrographs of di-sodium cromoglycate
(a) mechanically micronised, (b) spray dried.



Aston University

Content has been removed for copyright reasons

Table 5.14 Percentages of disodium cromoglycate particles reaching and remaining in the various stages during in vitro inhalation tests with the drug having been stored at the given humidities (Vidgren *et. al.*, 1989).

However the spray dried particles, which were affected by the humidity of the air in which the drug had been stored after preparation, were very difficult to deliver to the effective part of the lungs. This was explained using electron microscopy which showed the larger agglomerates formed by the spray dried drug upon exposure to humid air, as shown in Plate 5.15.

In 1989, Bootsma *et. al.* studied the use of cyclodextrins as complexing agents for lipophilic drug molecules, such as diazepam. The advantage of the complexed form of the drug compared to the pure form included chemical and

physical stability and improved bioavailability. The diazepam- β -cyclodextrin complexes were formed by spray drying in a laboratory scale spray dryer with an inlet air temperature of 170°C and an outlet air temperature of 70°C, and a feed flow rate of 750ml per minute.

As illustrated by Figure 5.16, the spray dried diazepam- β -cyclodextrin complex had a greatly increased dissolution rate ($130\mu\text{g}/\text{cm}^2/\text{min}$) compared to that of pure diazepam ($7\mu\text{g}/\text{cm}^2/\text{min}$). In vivo studies conducted on human volunteers, with the levels of diazepam in the plasma measured by HPLC, also showed that the absorption of the spray dried diazepam- β -cyclodextrins was also greater compared to pure diazepam, as illustrated by Table 5.17.

Takeuchi *et. al.*, investigated the use of various aqueous polymers (Eudragit) to provide controlled release tablets, using theophylline microspheres from spray drying solutions of the following compositions:

i)	Eudragit L30D	100ml
	PEG 6000 (a plasticiser)	3.0g
	Theophylline (to form a suspension)	40.0g
	Water	1000ml
	Aerosil (colloidal silica)	5.0g
ii)	Eudragit E30D	50ml
	Theophylline (to form a suspension)	100.0g
	Water	950ml
	Aerosil (colloidal silica)	5.0g, and
iii)	Eudragit L100-55	15.5g
	PEG 6000 (a plasticiser)	1.5g
	Theophylline (to form a solution)	15.0g
	2% Ammonia water	1000ml
	Aerosil (colloidal silica)	2.0g

The particle morphology of the spray dried particles depended upon the drug to polymer ratio in the formulation. They evaluated the dissolution of the

various preparations of the spray dried particles and the theophylline release was measured spectrophotometrically at $\lambda = 270\text{nm}$. The rates of dissolution of the various polymers showed that with the both Eudragit L30D and L100-55 there was a rapid release of theophylline at pH 6.8 and a sustained release at pH 1.2; this was attributed to the solubility of the polymers in the test solution at pH 6.8. Conversely, the Eudragit E30D provided a sustained release of theophylline in both the test solutions, thereby making the E30D the better choice for possible usage in drug formulations for taste masking, insulation, or oxygen-stabilisation.

A literature search to find reports of any previous work along the avenues intended in the current study upon the effect of drying on pharmaceuticals proved fruitless. Although the preceding studies did not reveal any information on the fundamentals of the drying of pharmaceuticals, they have been included as they have demonstrated that drugs produced by spray drying were still viable, dissolved easier, and were often more readily assimilated. Hence the relevance of the current study, and others, on the fundamental drying behaviour and morphology of spray dried particles is established.

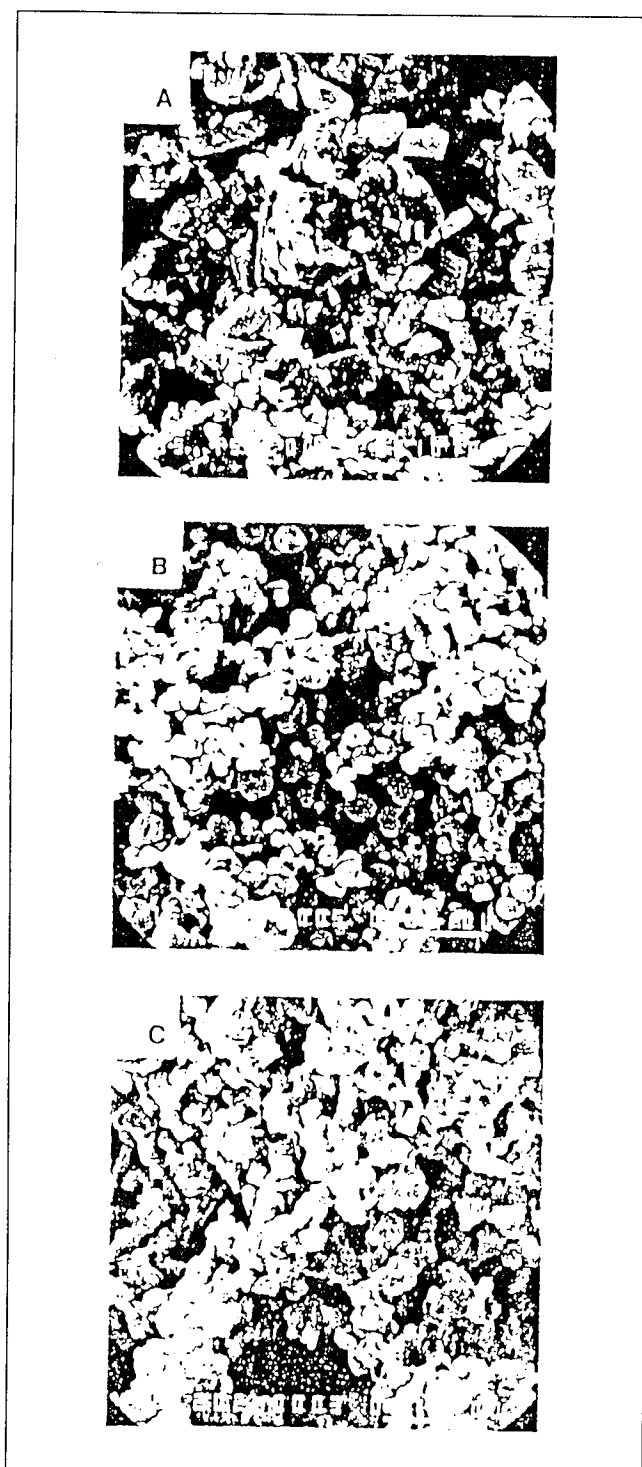


Plate 5.15. Electron photomicrograph of di-sodium cromoglycate (a) mechanically micronised, (b) spray dried, and (c) spray dried after storage at 60% humidity.

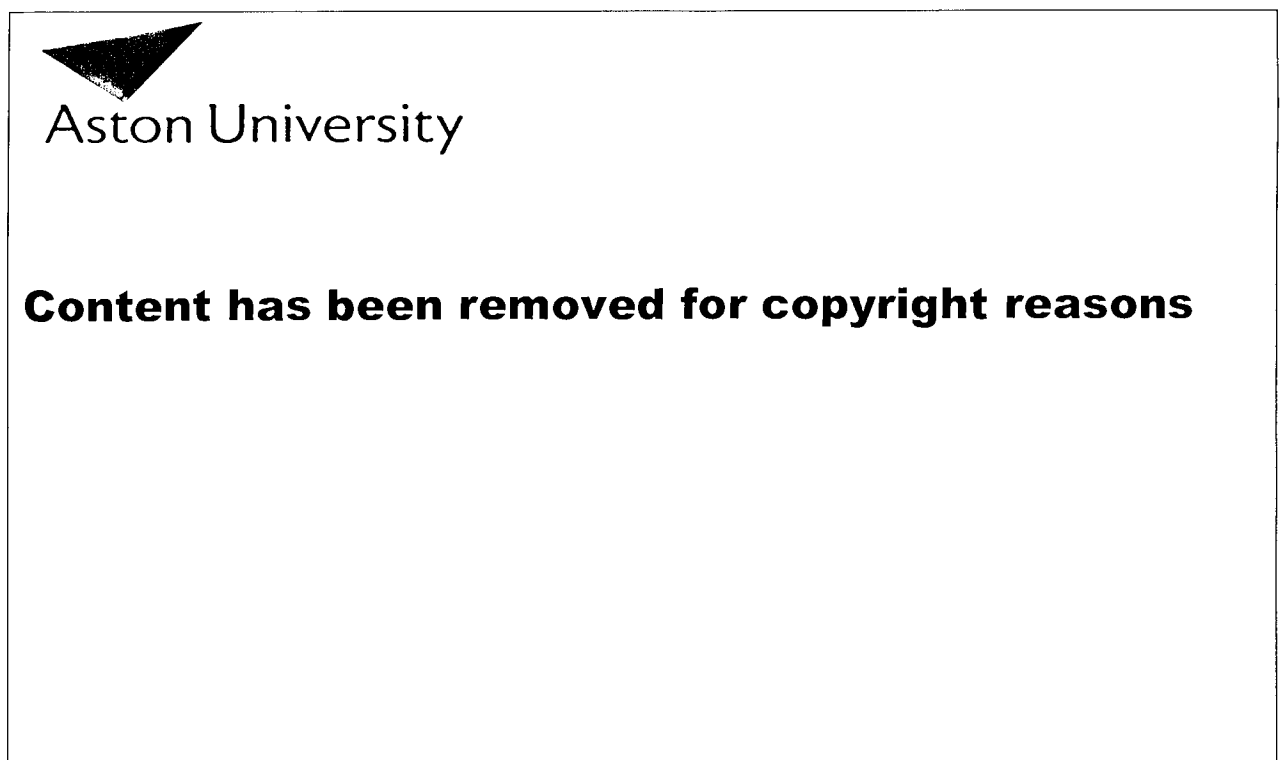
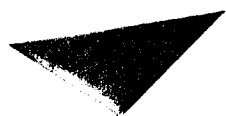


Figure 5.16. Diazepam tablet formulations [top] and the corresponding dissolution profiles [bottom] (Bootsma *et. al.*, 1989).



Aston University

Content has been removed for copyright reasons



Aston University

Content has been removed for copyright reasons

Table 5.17. Capsule formulation [top] and associated plasma diazepam levels of human volunteers [bottom] (Bootsma et.al., 1989)

6: Experimental Investigation

The first stage in the experimental investigation was the selection of representative materials to dry and of the scientific procedures to perform this dehydration and the subsequent analyses.

6.1: Selection of apparatus and materials

6.1.1: Apparatus selection

The design of the apparatus was based upon that used by Walton (1994), but with significant differences e.g. individual droplets were suspended on a rotating thermocouple whereas in Walton's apparatus they were suspended on a rotating glass filament. Although Hassan (1991) also measured droplet temperatures with a thermocouple during the drying process, that thermocouple was stationary whilst the droplet rotated around it. In the present study, the thermocouple and the suspended droplet rotated together. Thus, unlike in the case of Hassan's thermocouple which would be adversely affected by the formation of thick crusts preventing it from rotating freely, this thermocouple had complete freedom of rotation irrespective of crust formation.

6.1.2: Materials selection

The materials used were selected for a number of reasons:

- i) The flavour encapsulants were selected to test the skin / crust formation hypothesis posed by Hassan in 1991,

ii) ethanol was chosen as the simulated flavour because of the ease of detection by gas chromatography and its relatively low retention time of approximately 3 minutes as compared to iso-propanol which had a retention time of 5-6 minutes at the particular operating parameters of the gas chromatograph. (In hindsight, the choice of ethanol as the simulated flavour was restrictive in value because at low concentrations of water, it forms an azeotrope with the water. Moreover it is now clear that molecular weight of the volatile, i.e. its relative diffusivity, is an important variable.),

iii) the antibiotics were chosen because they are in common use and were believed to be reasonably heat stable except for ampicillin, which is fairly heat sensitive (Lambert, 1992), and

iv) the enzymes, dextran sucrose and invertase, were chosen because of their ready availability.

6.2: Apparatus

The apparatus comprised of two basic sections:

i) the air supply section, in which the air could be conditioned prior to reaching the suspended droplet, and

ii) the working section, in which the individual droplets were suspended.

6.2.1: Construction

6.2.1.1: The air supply

The apparatus set up to supply the air is illustrated in Figure 6.1 and Plate 6.2. It consisted of an air reservoir, a rotameter, a heater, an air dehydrator, and a

copper pipeline with strategically placed valves to control the air flow rate and direction.

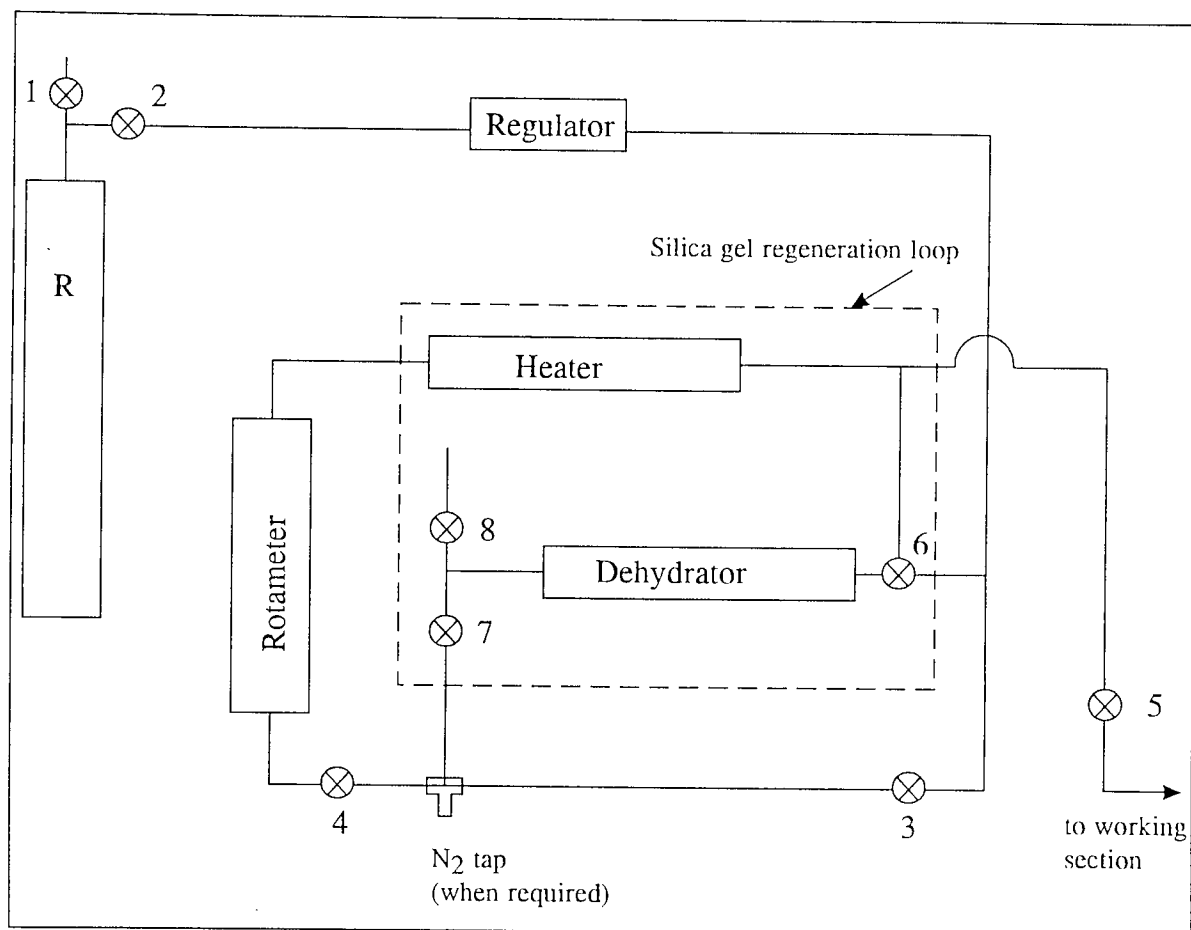


Figure 6.1. Arrangement for air supply to the working section.

In operation (referring to Figure 6.1),

- valves (1) and (2) controlled the air flow from the mains supply into the reservoir and the apparatus respectively,
- switching off valve (3) diverted the air flow to the dehydrator,
- valve (4) controlled the flow rate (in conjunction with the rotameter) to the heater,
- valve (5) switched on, or off, the air supply to the working section,

- opening valves (6) and (7) and closing off valve (3) permitted the use of dehydrated air,
- closing valves (3) and (7) and opening valves (6) and (8) allowed the hot air to pass over the silica gel and the molecular sieve in the dehydrator, for the purpose of regeneration.

The reservoir R prevented any variations in the air pressure in the circuit due to any fluctuations in the mains supply pressure. The heater was a 240V, 2kW Secomac heater (Secomac Ltd., Stanmore, London) controlled by a Variac. The rotameter was a metric 14 with a Duralumin float. The rotameter was calibrated using an analogue anemometer, with the probe located centrally in the wind tunnel.

The pipeline was constructed of standard copper pipe; the section prior to the heater was of 15mm i.d. and the section of the heater was of 22mm i.d..

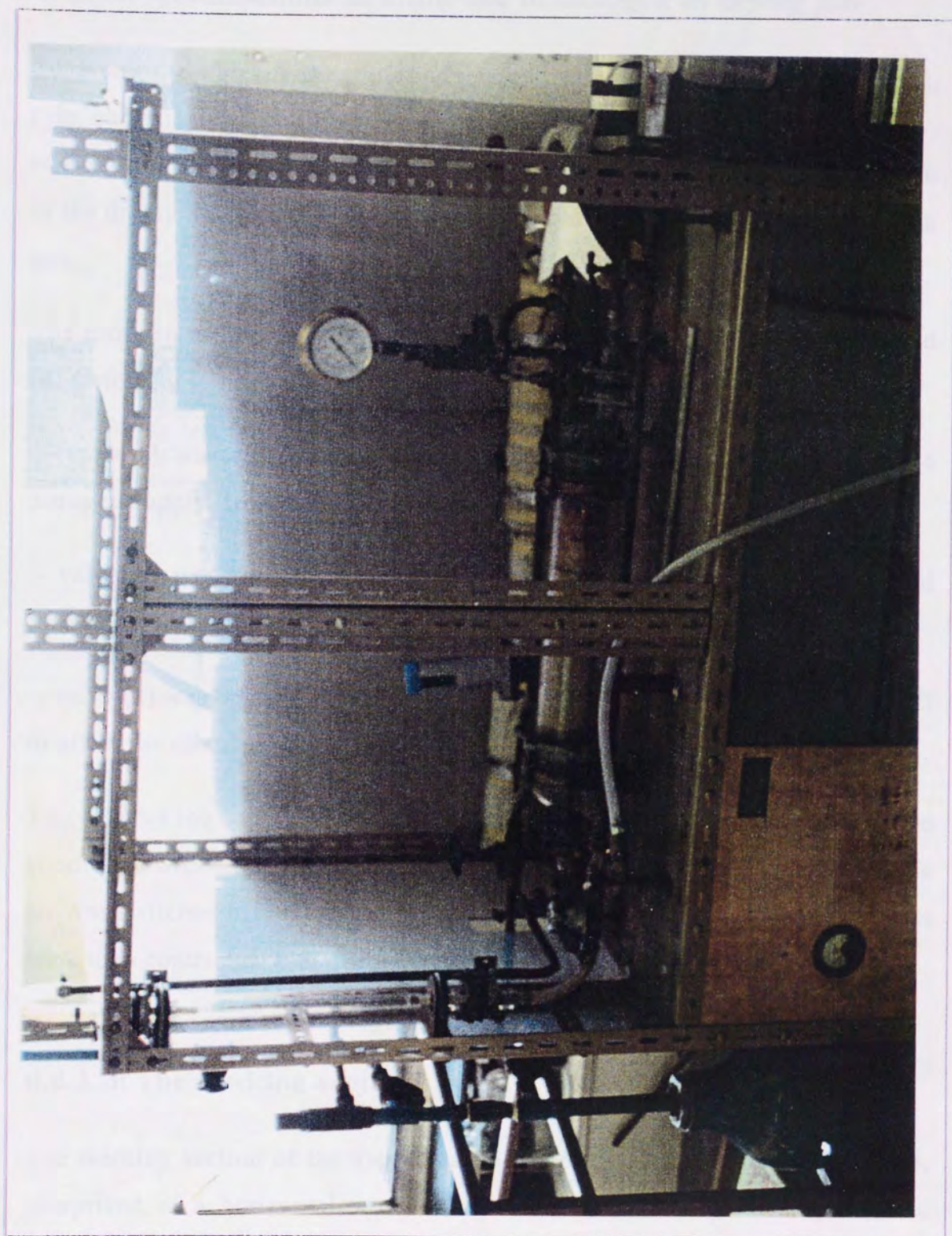


Plate 6.2. Photograph of air supply to working section.

6.2.1.2: Modifications to allow use of nitrogen as drying gas

To determine whether the antibiotics, which exhibited some effect on drying, (viz. chloramphenicol 10% w/w, ampicillin 10% w/w, streptomycin 10% w/w, and tetracycline 20% w/w), were affected by the high temperatures or oxygen in the drying air, the apparatus was run with pure (99%) nitrogen as the drying gas.

The nitrogen supply was connected at the 'T' junction between valves (3) and (4) (referring to Figure 6.1). The flow of nitrogen was controlled as follows:

- valve(3) was closed to switch off the air supply to the heater, and the nitrogen supply, from the attached cylinder, was switched on
- valve (4) was then opened to allow the nitrogen to flow to the heater, and then onto the working section
- valve (3) was opened, valve (4) closed, and the nitrogen supply switched off to allow the circulation of air through the apparatus.

To conserve the supply of nitrogen, the apparatus was brought to steady state conditions with air as the drying medium. Once at the required conditions, the air was switched off and the apparatus purged with nitrogen. The experiments were then conducted with nitrogen as the drying gas.

6.2.1.3: The working section

The working section of the apparatus, illustrated in Figure 6.3 and Plate 6.4, comprised of a horizontal wind tunnel made from 28mm i.d. copper tube enclosed in a perspex box to provide a constant environment. The box had the following dimensions, 500mm length, 200mm depth, and 150mm height.

A semi-cylindrical section of the copper tube was removed to allow the rotating thermocouple to fit into the wind tunnel. Since this removal could

have caused disturbance of the air flow patterns around the droplet, this section was covered with a similar clear perspex tube section with a hole to allow for the insertion of the rotating thermocouple. The clear perspex tube allowed the suspended droplet to be viewed with ease.

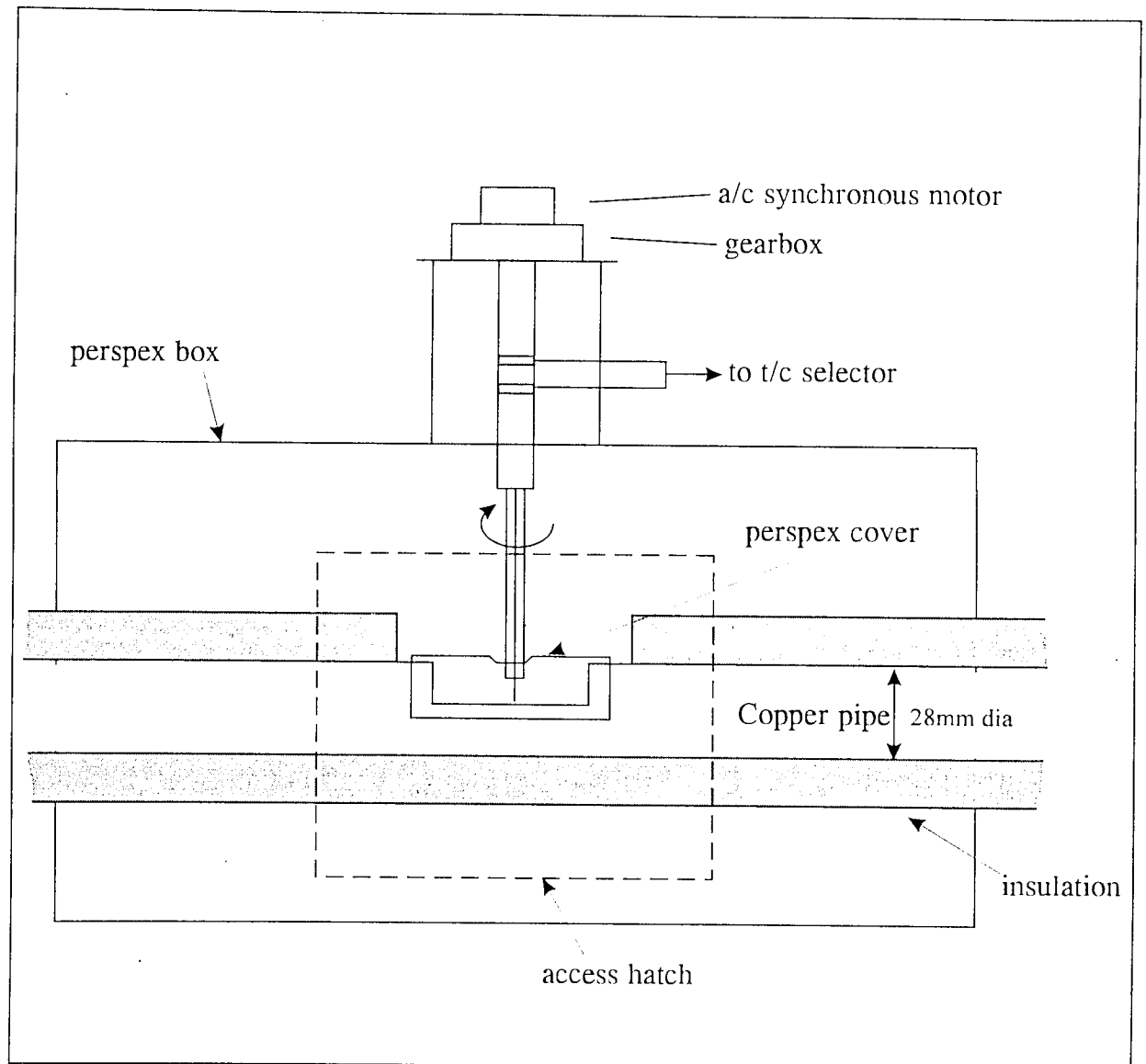


Figure 6.3. The working section of the apparatus.

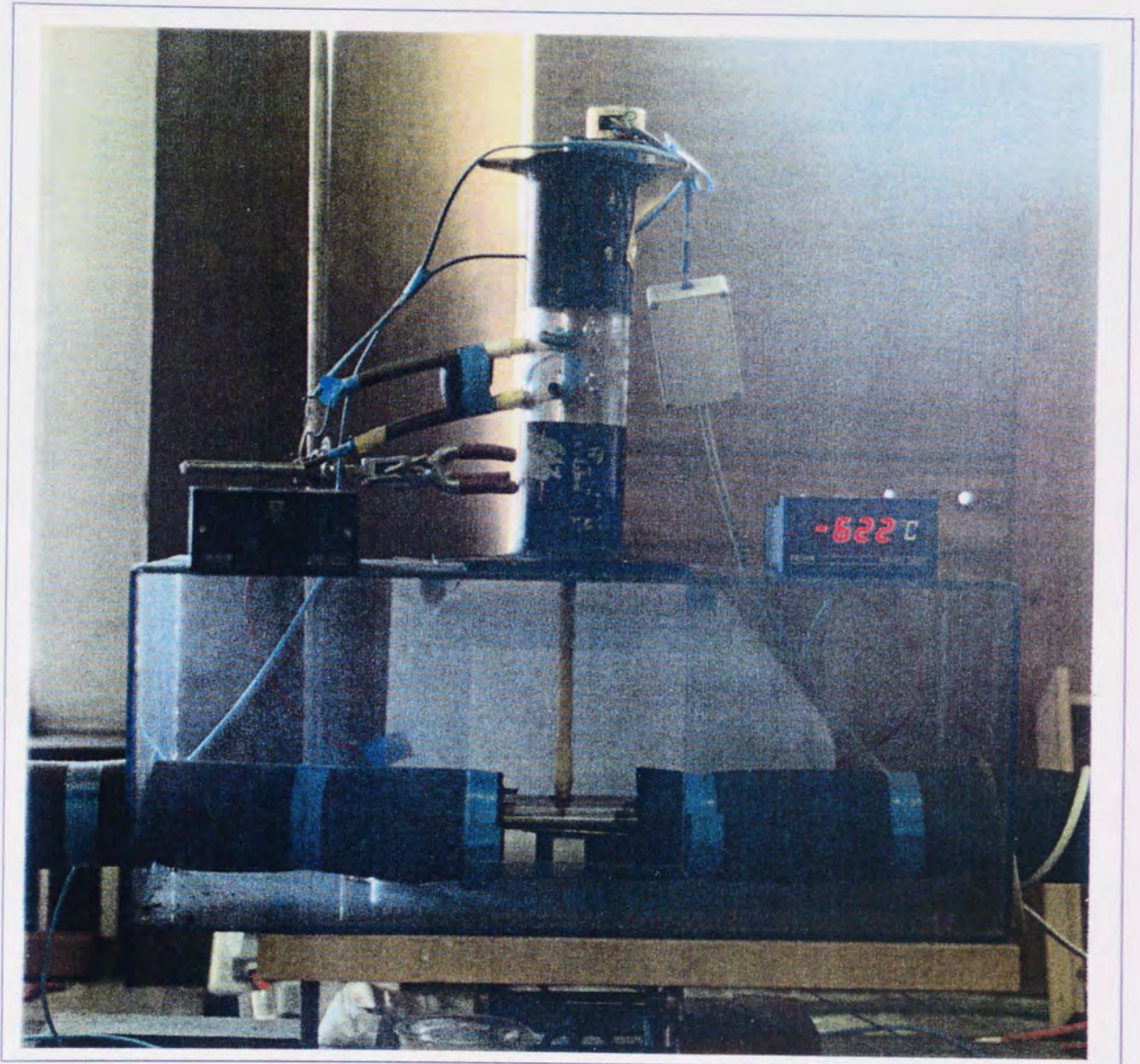


Plate 6.4. Photograph showing the working section of the apparatus

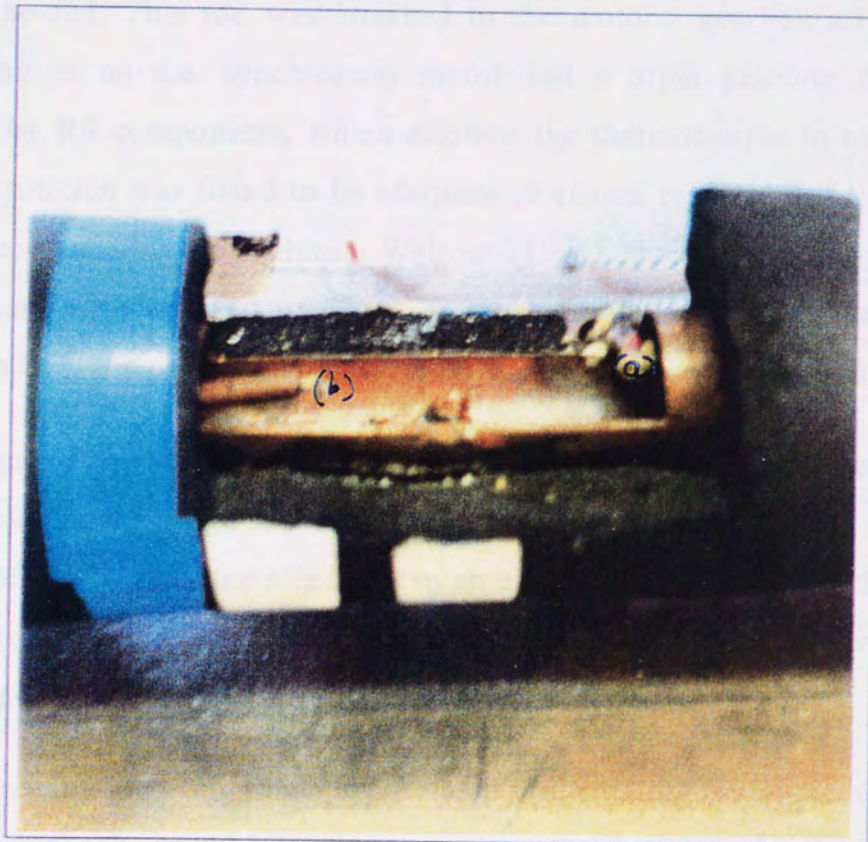


Plate 6.5. Photograph to show the location of (a) the wet bulb and (b) the dry bulb thermocouples

Two thermocouples were also housed within the wind tunnel - one upstream from the rotating thermocouple to measure the dry bulb temperature of the air, and one downstream of it to measure the wet bulb temperature; this thermocouple was kept wetted by a wick immersed in a water reservoir soldered to the side of the wind tunnel.

The rotating thermocouple was constructed from a hypodermic needle thermocouple (RS Components Ltd., Birmingham) mounted in a hollowed-out, insulated brass rod, with the thermocouple wires emerging from a hole in the side of the rod. This rod was attached to the motor / gearbox arrangement comprising of an a.c. synchronous motor and a 5rpm gearbox unit, both supplied by RS components, which allowed the thermocouple to rotate. The speed of rotation was found to be adequate to ensure each side of the droplet experienced similar conditions; Walton (1994) used a similar rotation arrangement with a speed of 3rpm; faster rotation would have caused the droplet to be flung off the thermocouple by centripetal / centrifugal forces.

The design of the rotating thermocouple necessitated the development of a rotating electrical linkage to the thermocouple. This was achieved by using the analogy of the brushes and slip-rings in an electric motor. The slip-rings were formed from the bared wires of the thermocouple and the brushes were made from copper and copper / nickel strips as illustrated in Figure 6.6.

Before installation into the apparatus, the rotating thermocouple was thoroughly bench tested. To improve the electrical contact between the brushes and the slip-rings, a number of electrically conducting medical gels were used:

- i) electrode gel (used for electro-cardiograms), and
- ii) ultrasound gel (used for ultrasound scans).

Although electrical contact was improved, use of these gels created a problem since they tended to run down the brass rod. This problem was solved by using a more viscous gel, TENS gel, applied to the thermocouple in-situ via a syringe. However, the use of the more viscous gel created a different problem in that it tended to react with the electrodes resulting in oxidation which caused the brushes to jump off the slip-rings and give erroneous readings.

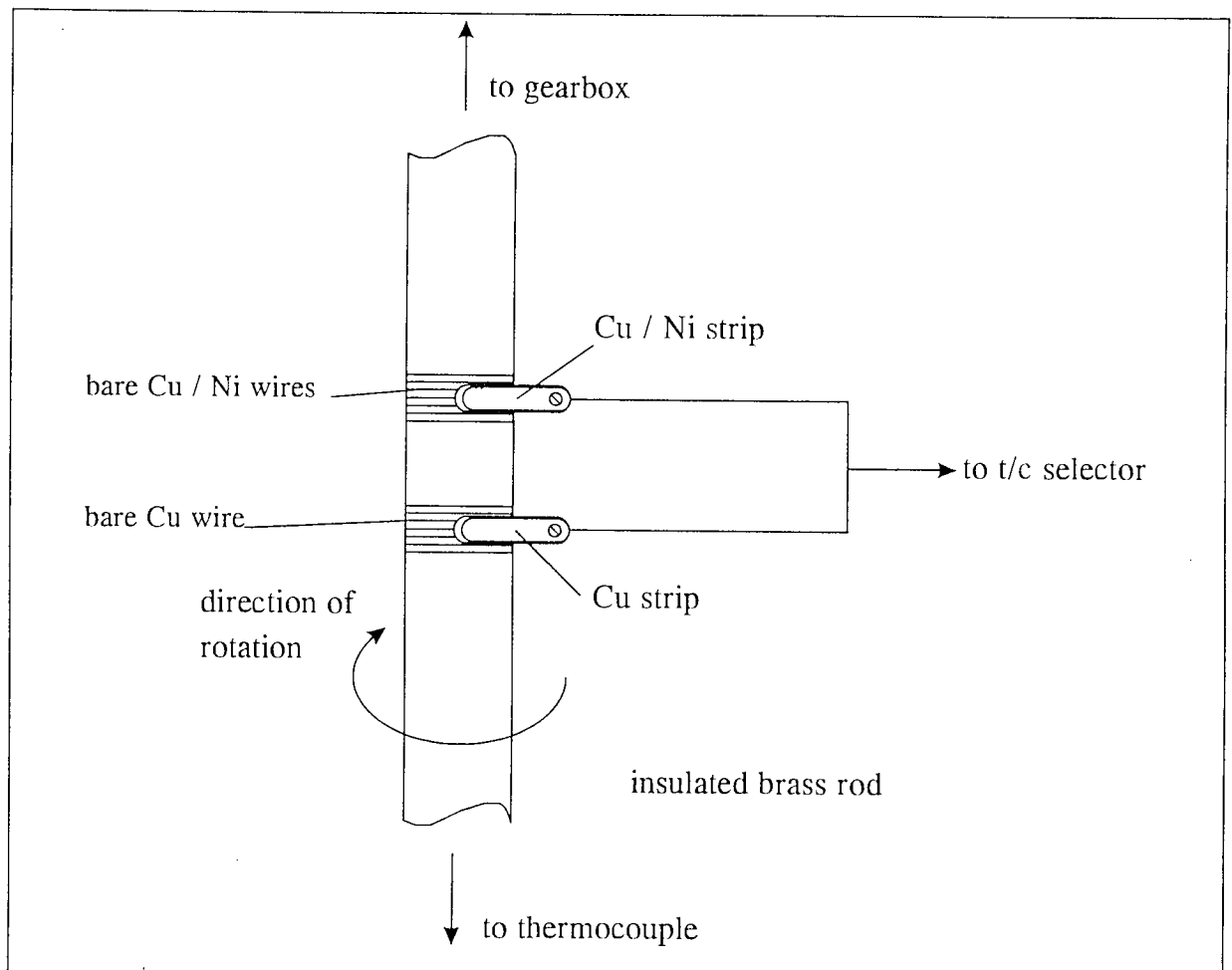


Figure 6.6: Diagram representing the electric motor analogy used to provide the rotating electrical linkage for the thermocouple.

To overcome the problems found to be associated with the gels, their use was discontinued; the electrical contact was improved by using a pair of helical compression springs. These physically forced the brushes onto the slip-rings and gave an improved electrical contact.

The shaft of the thermocouple support rod was insulated with a ceramic insulating tape to prevent the hot drying air from heating the shaft, so minimising the conduction of heat to the droplet from the heated shaft. Furthermore, the hollow shaft was cut and the end which housed the thermocouple was isolated from the main body to prevent heat transfer, as illustrated in Figure 6.7. The two parts were kept separate by a tight-fitting p.t.f.e. hollow cylinder super-glued in place, and the complete shaft was then insulated with the ceramic insulating tape.

The thermocouples used in this study were of type T (copper-copper/nickel) which cover the temperature range -40°C to $+400^{\circ}\text{C}$, and are accurate to $\pm 1^{\circ}\text{C}$. They were obtained from both Comark Ltd, Littlehampton, West Sussex, England, and RS Components Ltd.. All the thermocouples were linked upto a single digital temperature display via a thermocouple selector unit, supplied by Comark Ltd., which allowed upto twelve thermocouples to be linked to one display. The temperature display, supplied by RS Components Ltd., was also accurate to $\pm 1^{\circ}\text{C}$.

In addition to the digital temperature display, the output from the rotating thermocouple was linked to a JJ Lloyd CR652S y-t chart recorder (JJ Lloyd Instruments Ltd., Southampton, England) which enabled a hard copy of the droplet temperature history, as shown in Figure 6.8, to be readily obtained.

All the thermocouples were calibrated against a mercury-in-glass thermometer, (a standard calibration technique), using water, prior to being incorporated into the apparatus.

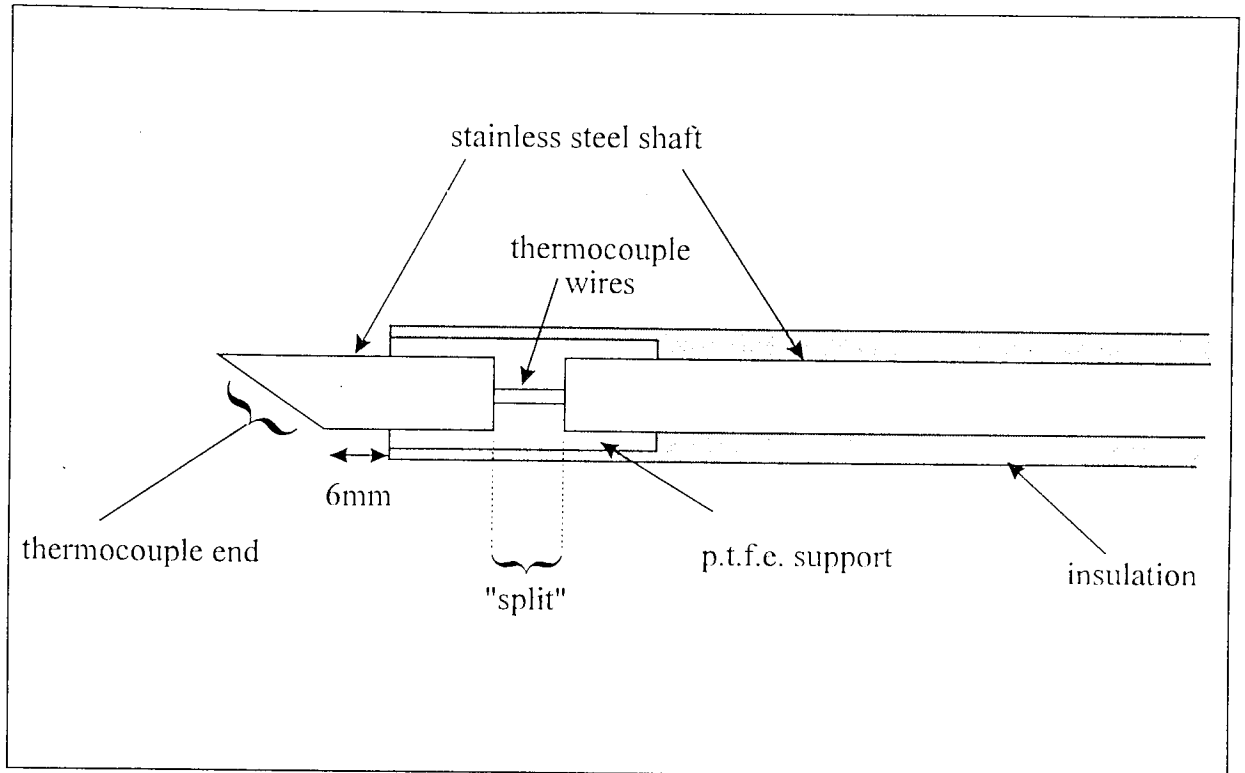


Figure 6.7. Split in support shaft to prevent heat transfer to the droplet.

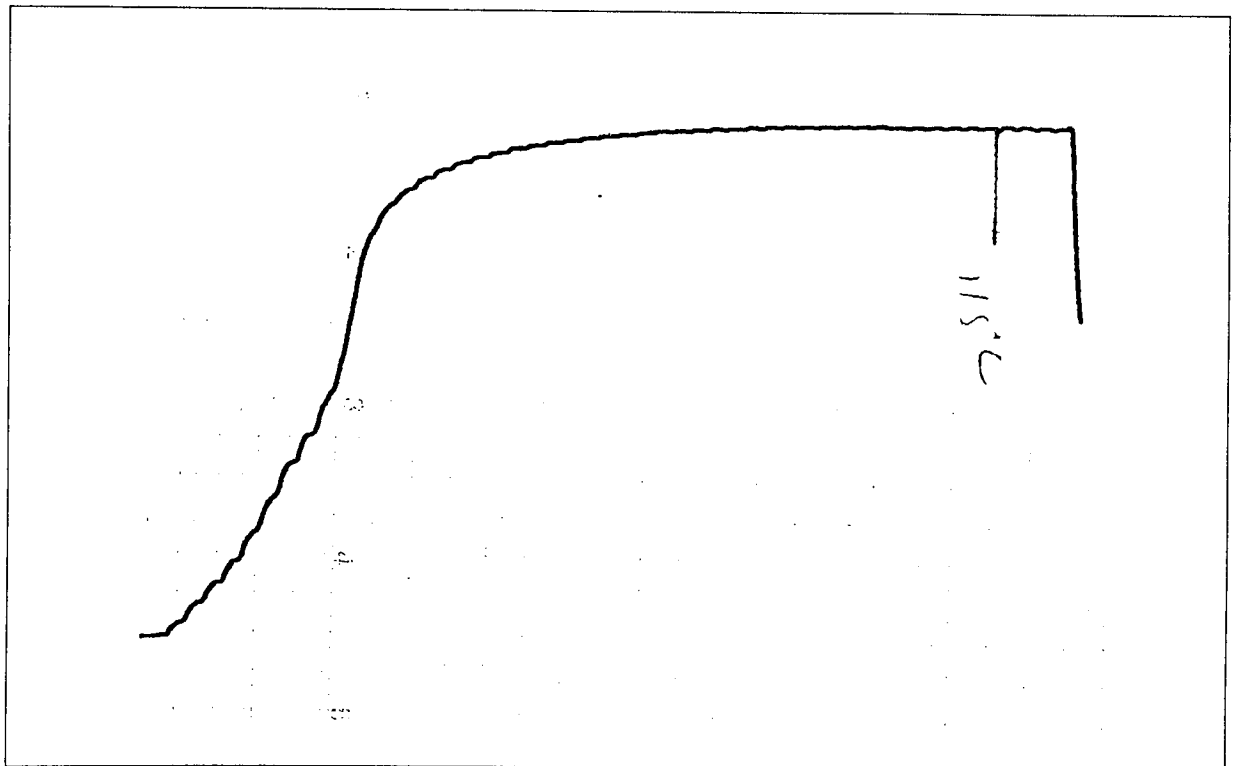


Figure 6.8. Example of hard copy of the droplet temperature history

6.2.2: Commissioning/Operation of the apparatus

6.2.2.1: Commissioning

The rotameter and the heater control Variac were calibrated; the performances of all the thermocouples were also tested, and found to be accurate to $\pm 1^\circ\text{C}$. The performance of the rotating thermocouple was tested, using droplets of distilled water suspended onto the tip of the rotating thermocouple, and found to be satisfactory.

Following commissioning trials with distilled water, saturated sodium sulphate solution was used as the stock solution. Initial results of the temperature measurement using the rotating thermocouple demonstrated a fall before increasing again. This fall in temperature correctly mirrored the melting of the sodium sulphate crystals on the rotating thermocouple. This phenomenon has also been reported by Hassan in 1991 during a study of skin forming materials and by Cheong *et. al.* (1986).

Results confirmed that the rotating thermocouple measured the temperature inside the droplet rather than the surface temperature. The surface temperature was the wet bulb temperature, the rotating thermocouple always indicating higher.

6.2.2.2: Operation

The appropriate heater and rotameter settings, from the apparatus commissioning data, were used to obtain the required air temperature and flow rate. The air flow rates were chosen to be similar to those in the study of skin forming materials (Hassan, 1991) to allow a comparison between his skin formation hypothesis and the results from this study. The apparatus attained steady state within approximately two hours of being switched on. Once

steady state had been reached, as indicated by a steady flow rate and constant dry and wet bulb temperatures, single droplets were suspended onto the end of the rotating thermocouple. Initially, the droplet was suspended using a syringe and a hypodermic needle, but inter-drop size variations of 20% - 40% were associated with this method; it was, therefore, rejected.

Subsequently, an Eppendorf 4710 1-10 μ l pipettor was used to suspend a 10 μ l droplet onto the rotating thermocouple; this pipettor dispensed 10 μ l with an accuracy of $\pm 1\%$.

To suspend a droplet, the rotating thermocouple was stopped and the droplet carefully positioned onto the thermocouple. The droplets of some formulations were quite easy to suspend, whilst others, e.g. the antibiotic streptomycin, required several attempts. Each droplet was exposed to a specific drying condition for a given period of time, measured by a countdown timer. After the set times, the whole rotating thermocouple assembly was removed, allowing the (dry) droplet to be removed from the end into 1.5ml Eppendorf micro centrifuge tubes.

6.2.3: Experimental procedure and data treatment

The experimental regime was identical for each of the heat-sensitive materials under investigation. After the preparation of the various solutions, the droplets were suspended / collected as listed in Table 6.9. (Tube 0 contained three drops (30 μ l) of 'untreated' solution to be used as the reference). Each tube contained three droplets that had undergone identical treatment.

Each Eppendorf tube was labelled and weighed, using a Mettler AE50 balance accurate to ± 0.0001 g prior to use and re-weighed after the droplets had been collected. All the weights were referred to the untreated droplets weight (tube 0) to calculate the water / solvent loss during the drying. The contents of each tube were re-constituted accordingly before being analysed using the

various tests. To reduce the problems associated with the amount of headspace above the liquid into which the ethanol could evaporate, and thereby give erroneous retention values upon subsequent gas chromatograph analysis, tubes with a smaller volume (0.5 ml instead of 1.5ml) were used for the collection of the droplets of flavour encapsulants.

The drying rate, as illustrated in the graphs, was evaluated as:

$$\text{drying rate} = (m_2 - m_1) / (t_2 - t_1)$$

where

m_2 = droplet mass at t_2

m_1 = droplet mass at t_1

and $(t_2 - t_1)$ is the corresponding time interval

Tube number	time of exposure (minutes)	
	antibiotic / enzyme	flavour encapsulant
0	0	0
1	1	0.5
2	2	1
3	4	2
4	5	3
5	10	5
6	/	10

Table 6.9: Exposure times for the heat-sensitive materials

6.3: Materials

All the materials were obtained from Sigma Chemical Co Ltd of Poole, Dorset, UK, unless otherwise stated. Their specifications are given in Appendix B and their photomicrographs are shown in Plate 6.10 (a to l). They were all stored at ambient temperature (between 18°C and 20°C) unless otherwise stated, and distilled water was used throughout to prepare the various solutions / suspensions. The solutions / suspensions were prepared from previously dried solids, and they do not necessarily accurately reproduce the characteristics or properties of the native materials, e.g. in the case of detergents, additives are subsequently incorporated into the dry powders.

6.3.1: Flavour encapsulants

As stated previously, the encapsulants were chosen for their skin / crust formation characteristics. The chosen materials are listed below, together with their batch, code numbers, and source.

6.3.1.1: Gum arabic

Gum arabic is a branched polymer of galactose, rhamnose, arabinose and glucuronic acid, and is derived from the acacia tree. The gum arabic used in this study was coded G9752 and was from lot # 20H0130; when mixed with water, it formed a colloidal suspension.

6.3.1.2: Rice starch

The rice starch was obtained from BDH/Merck Ltd. of Atherstone, Warwickshire, UK, and its code number was 30263 and lot # 4350530J. Upon mixing with water, the starch formed a suspension. Constant agitation with a

magnetic stirrer (with the speed controller set at position 2) was needed to maintain the particles in suspension.

6.3.1.3: Coffee

The coffee solution was made using commercially-prepared freeze dried coffee granules (Nescafe Gold Blend, Nestle) from batch # 1345MRX.

6.3.1.4: Wheat starch

The wheat starch had been purified by heat hydrolysis, and was from lot # 75F0605 code # S-2760. It formed a colloidal suspension upon mixing, with the magnetic stirrer, with water.

6.3.1.5: Gelatine

The gelatine was of Type A, which was derived from acid-cured porcine skin. (Type B gelatine is derived from lime-cured tissue). Gelatine of two different type 'Bloom' numbers was used, viz. 60 Bloom and 150 Bloom. The Bloom number is an indicator of the strength of the gels produced; the higher the Bloom number, the stronger the gel.

The 60 Bloom gelatine had the code # G-6144 and lot # 75F0605, whilst the 150 Bloom gelatine (obtained from BDH/Merck Ltd.) was coded 33046 and lot # 6981630J. Upon mixing with water, the gelatine crystals absorbed it and swelled to form a gel.

6.3.1.6: Dextrin

Hydrolysis of starch, either by heat or acid, produces dextrin, which is more water soluble than the native starch. (Water solubility increases with the progression of the hydrolysis).

The dextrin used in this study was obtained from BDH/Merck Ltd. coded 33046 and lot # 6981780K. Upon mixing with water, with continuous agitation with a magnetic stirrer for approximately one hour, the dextrin eventually dissolved completely.

6.3.1.7: Skim milk

The skim milk used was from a commercial preparation, 'Marvel' - a spray dried instant skim milk powder. The agglomerated powder dissolved easily when mixed with water.

6.3.2: Antibiotics

The antibiotics used in this study were chosen because they are in common use, fairly heat-stable (except for ampicillin), and also because of the availability of suitable target organisms for sensitivity testing. All the antibiotics were obtained from Sigma Chemical Co Ltd. With the exception of streptomycin, which was soluble, they formed suspensions when mixed with water; continuous agitation with a magnetic stirrer was necessary to prevent the particles from falling out of suspension.

6.3.2.1: Ampicillin

Ampicillin (D[-] α -aminobenzylpenicillin) trihydrate (code # A-6140, lot # 80H0914) was used; it was stored in a refrigerator. Its chemical formula is $C_{16}H_{19}N_3O_4S \cdot 3H_2O$. Ampicillin is bactericidal to growing cells as it inhibits cell wall synthesis (it inhibits the peptidoglycan cross-linking in the cell wall (Bryan & Godfrey, 1991)).

6.3.2.2: Streptomycin

Streptomycin sulphate (code # S-6501 lot # 39F0749) was used in this study. When not in use, the antibiotic was stored in a refrigerator. Streptomycin is bactericidal in that it binds to the S12 protein of the 30S ribosomal sub-unit, causing mis-translation, hence inhibiting protein synthesis (Davies, 1991).

6.3.2.3: Tetracycline

The tetracycline used in this study had code # T-3258 and was from lot # 118F0636, with a chemical formula $C_{22}H_{24}N_2O_8$. Any unused antibiotic was stored in a freezer at $-5^{\circ}C$. Tetracycline is a bacteriostatic antibiotic; it binds onto the 30S ribosome thus preventing the binding of the aminoacyl-tRNA to the ribosome. This action inhibits the synthesis of protein by preventing the translation step (Neu, 1991).

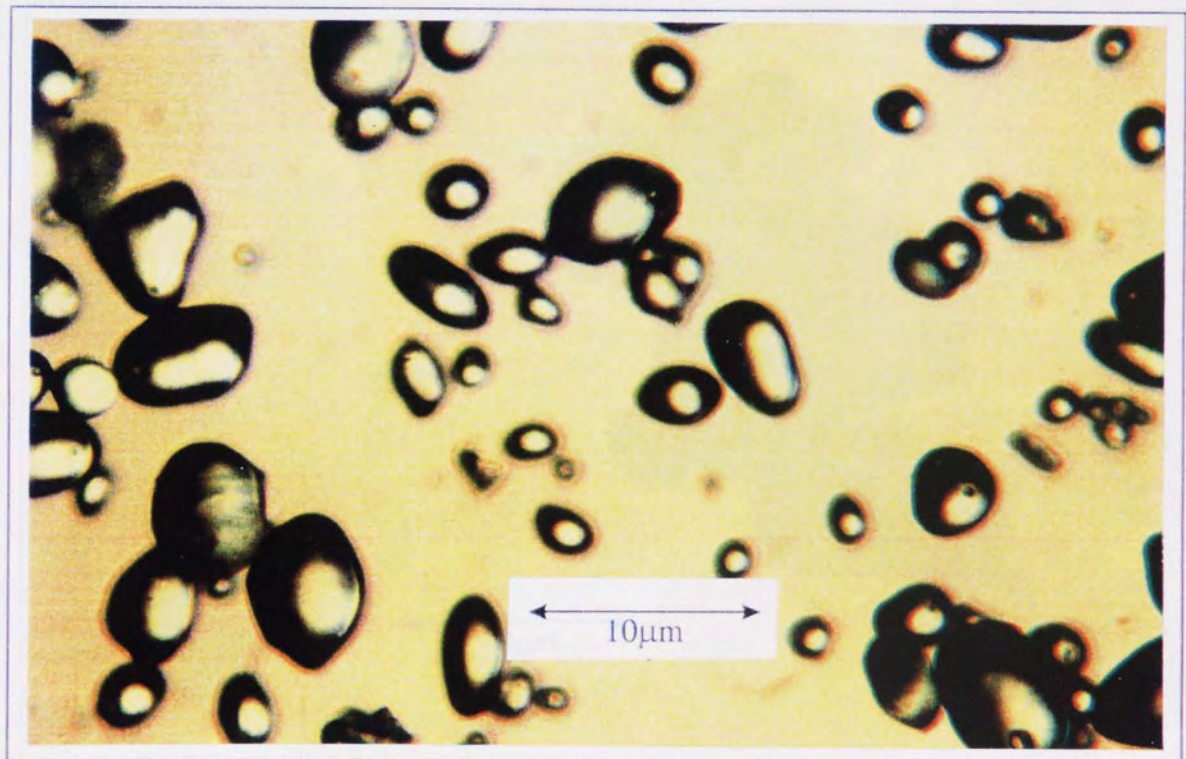
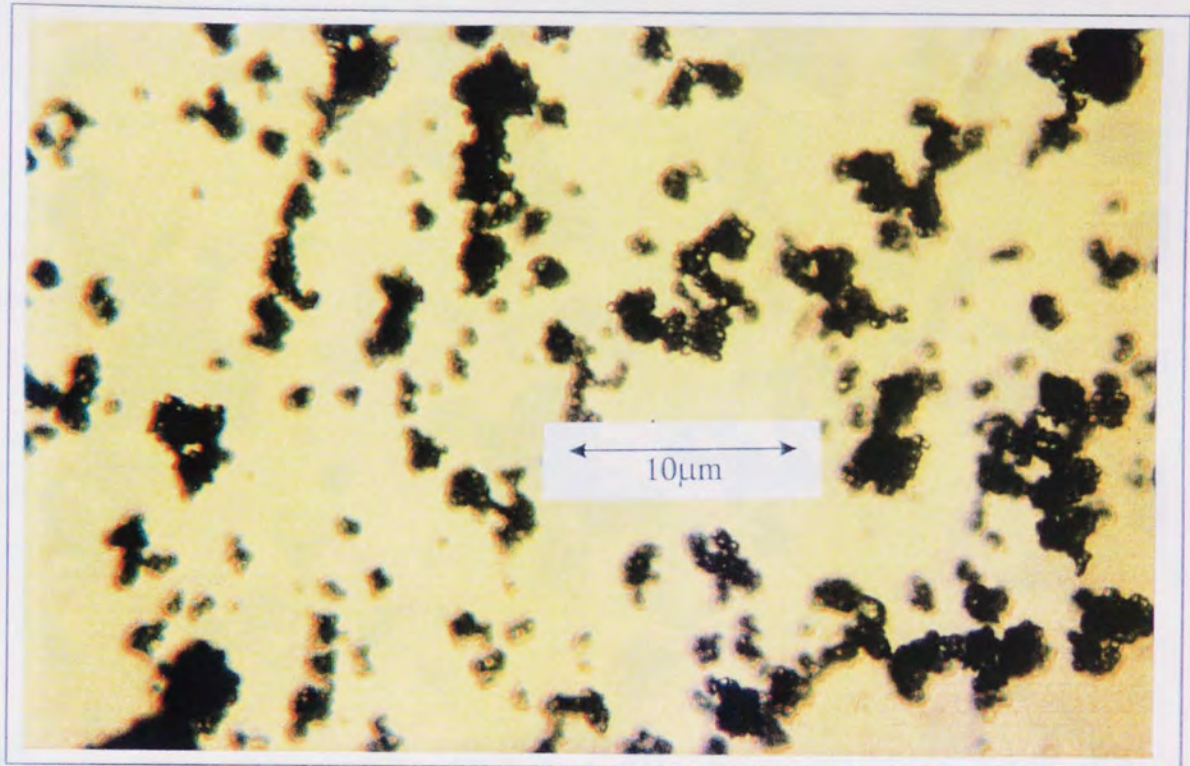


Plate 6.10. Photomicrographs showing (a) rice starch [top], and (b) dextrin [bottom].

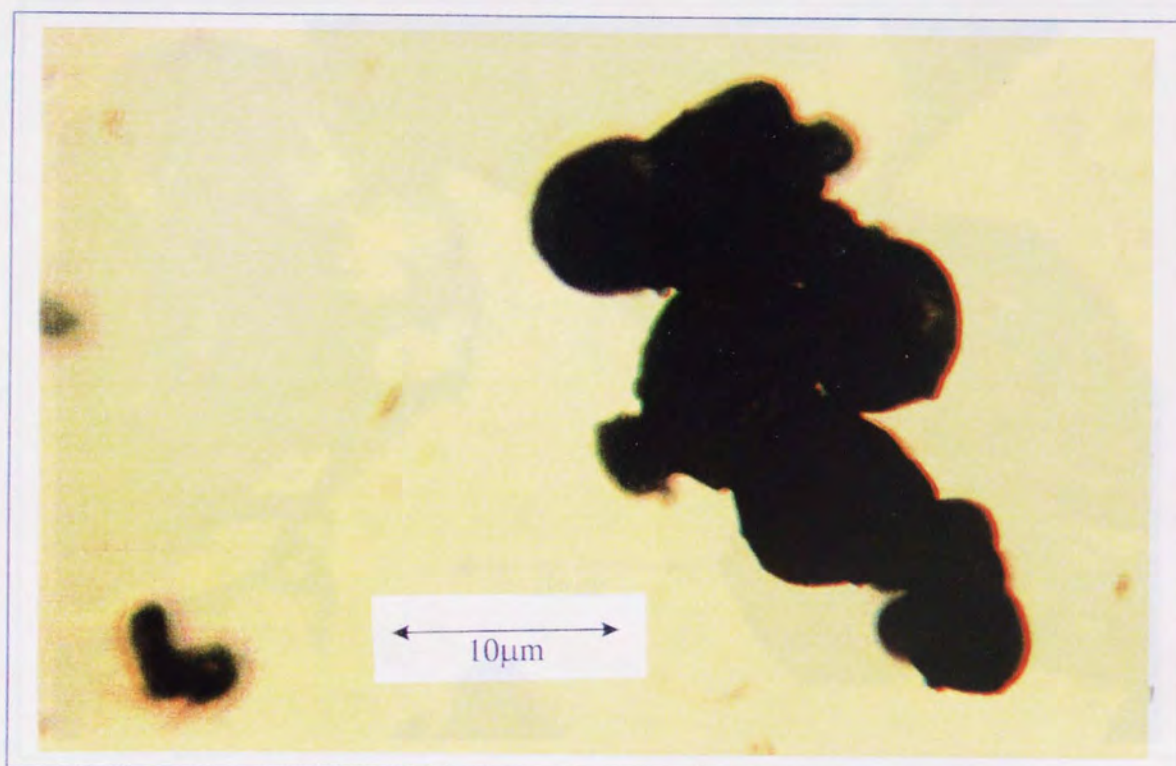
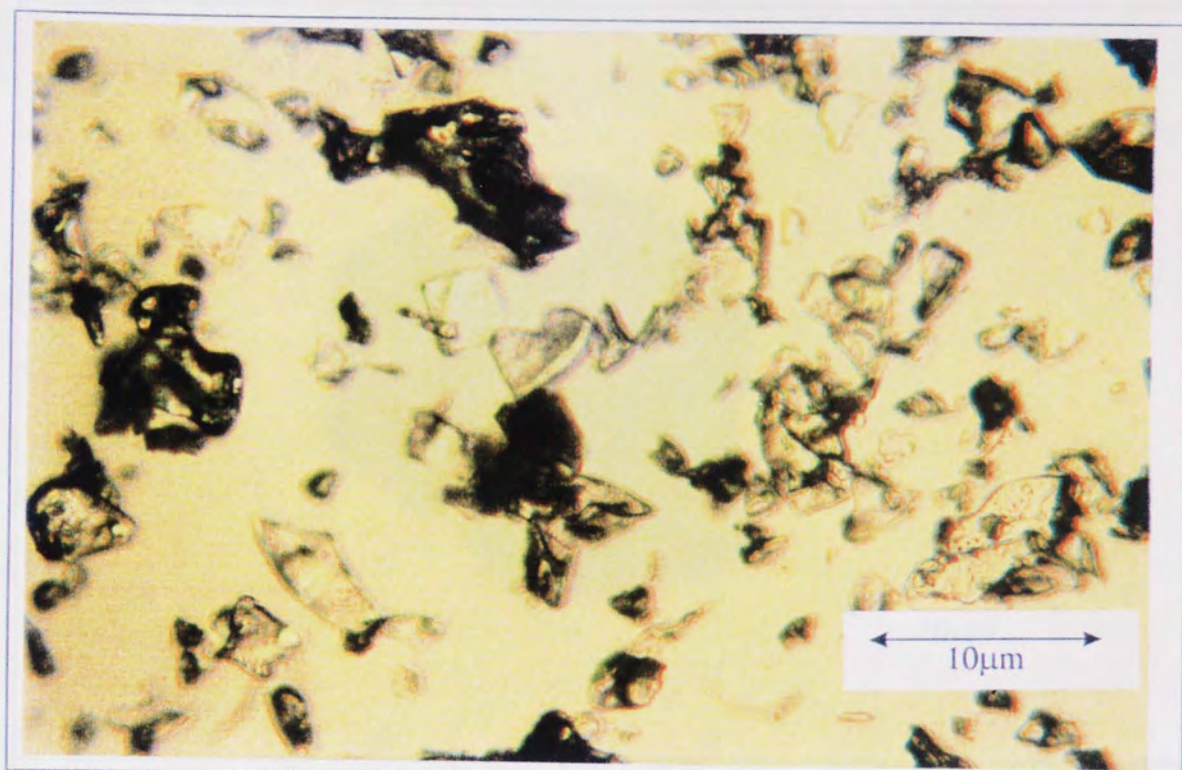


Plate 6.10. Photomicrographs showing (c) wheat starch [top], and (d) skim milk [bottom].

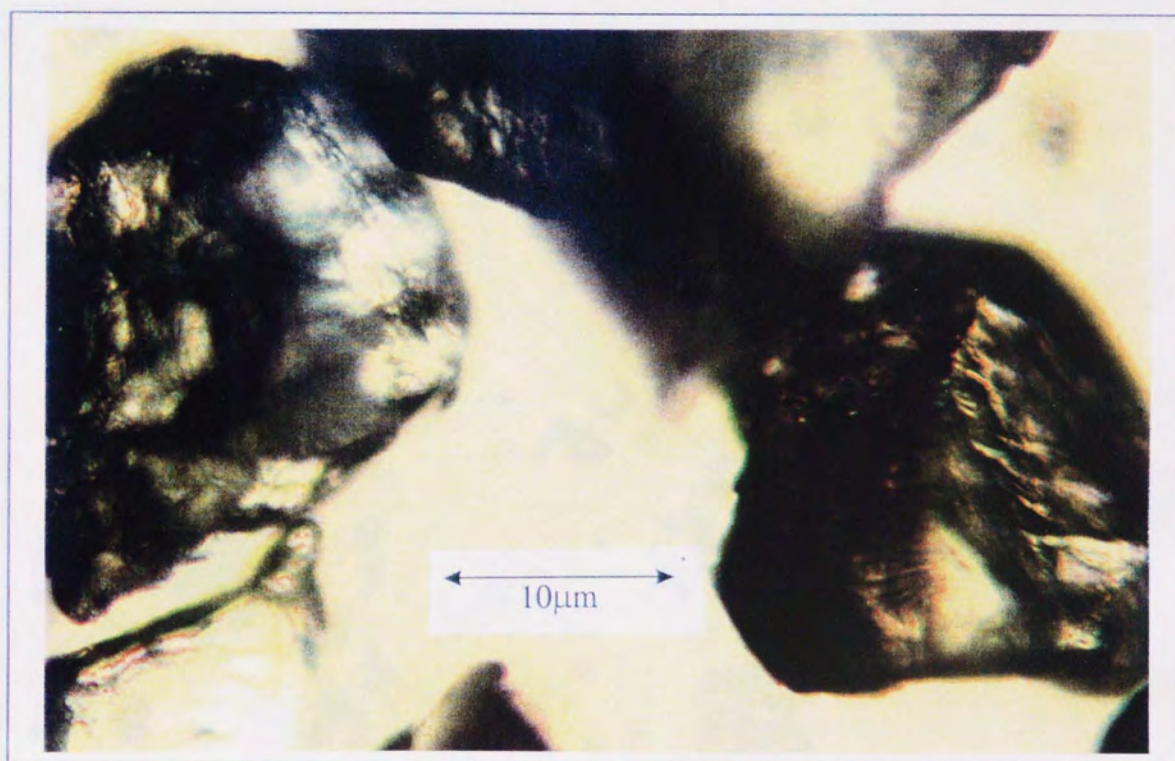


Plate 6.10. Photomicrographs showing (e) gelatine 60 Bloom [top], and (f) gelatine 150 Bloom [bottom].

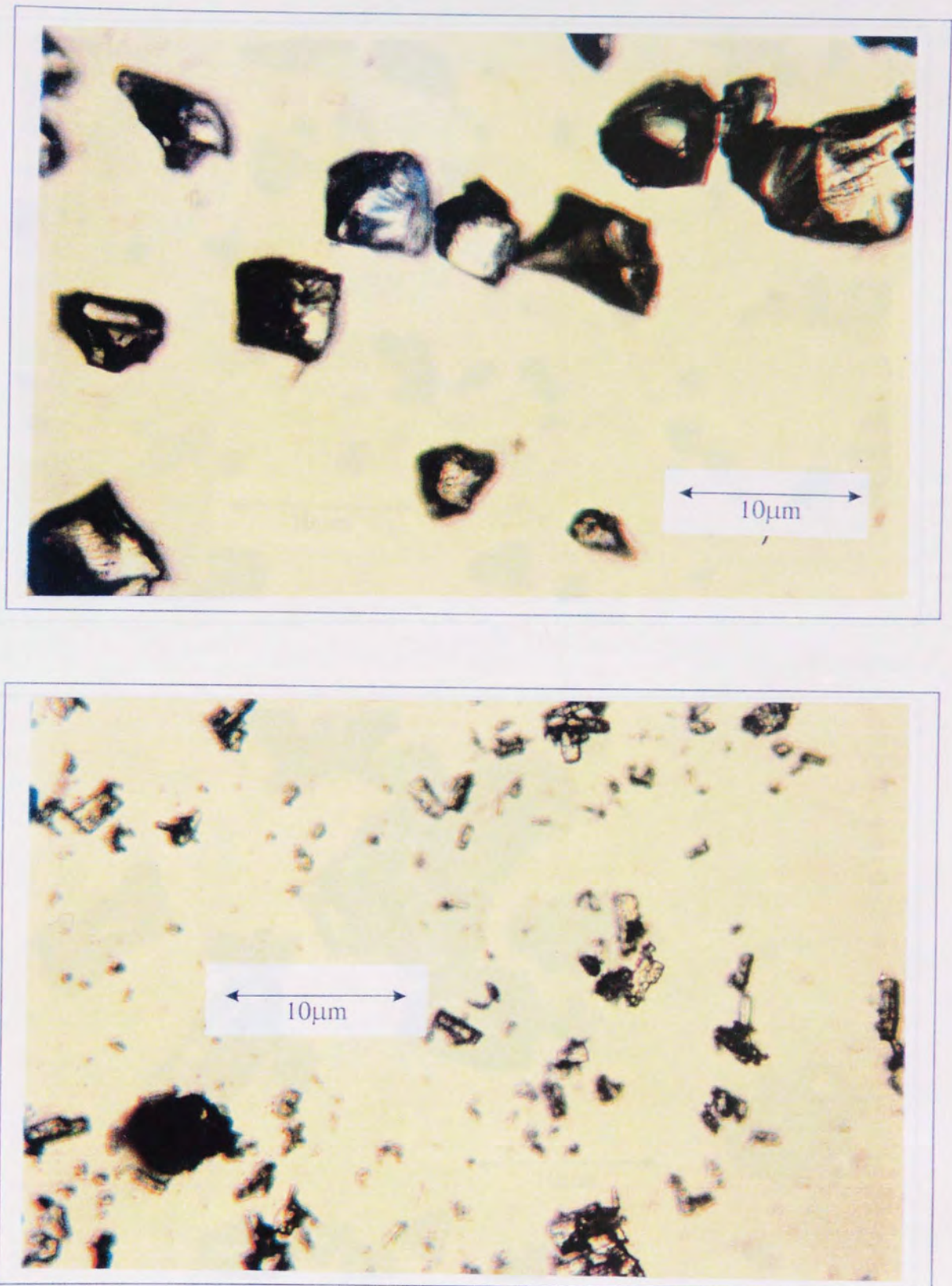


Plate 6.10. Photomicrographs showing (g) gum arabic [top], and (h) ampicillin [bottom].

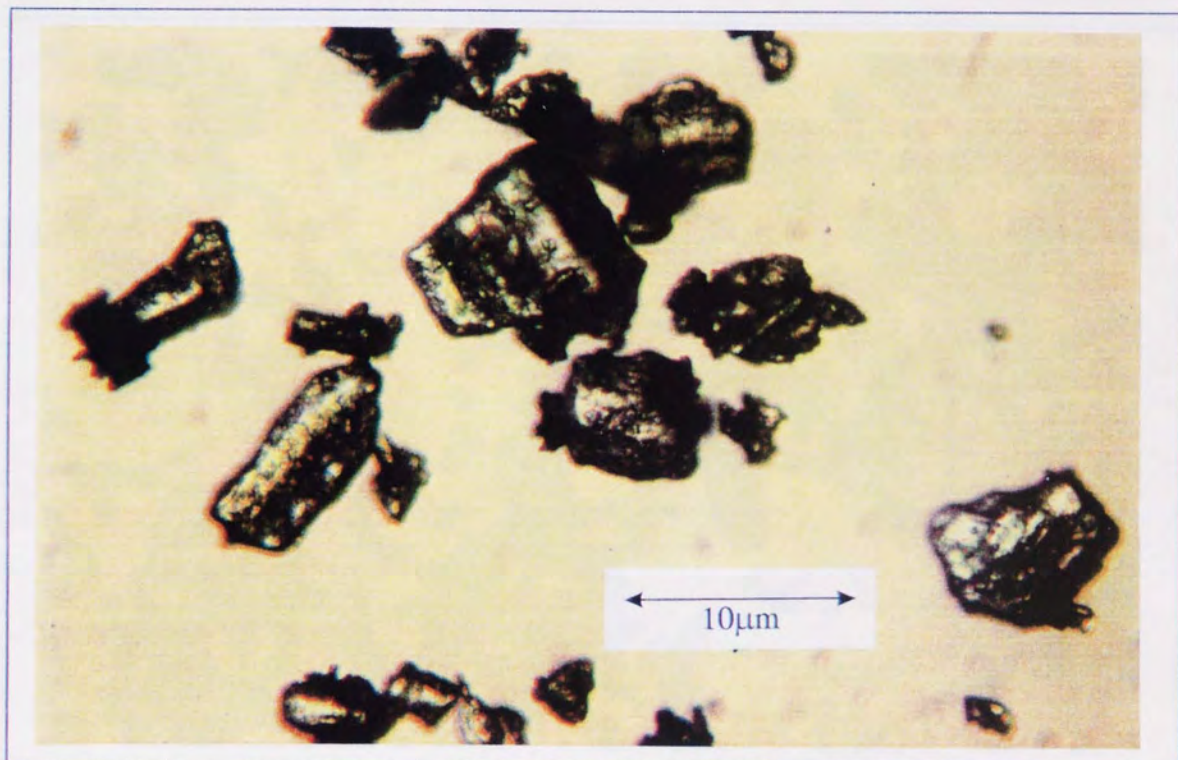
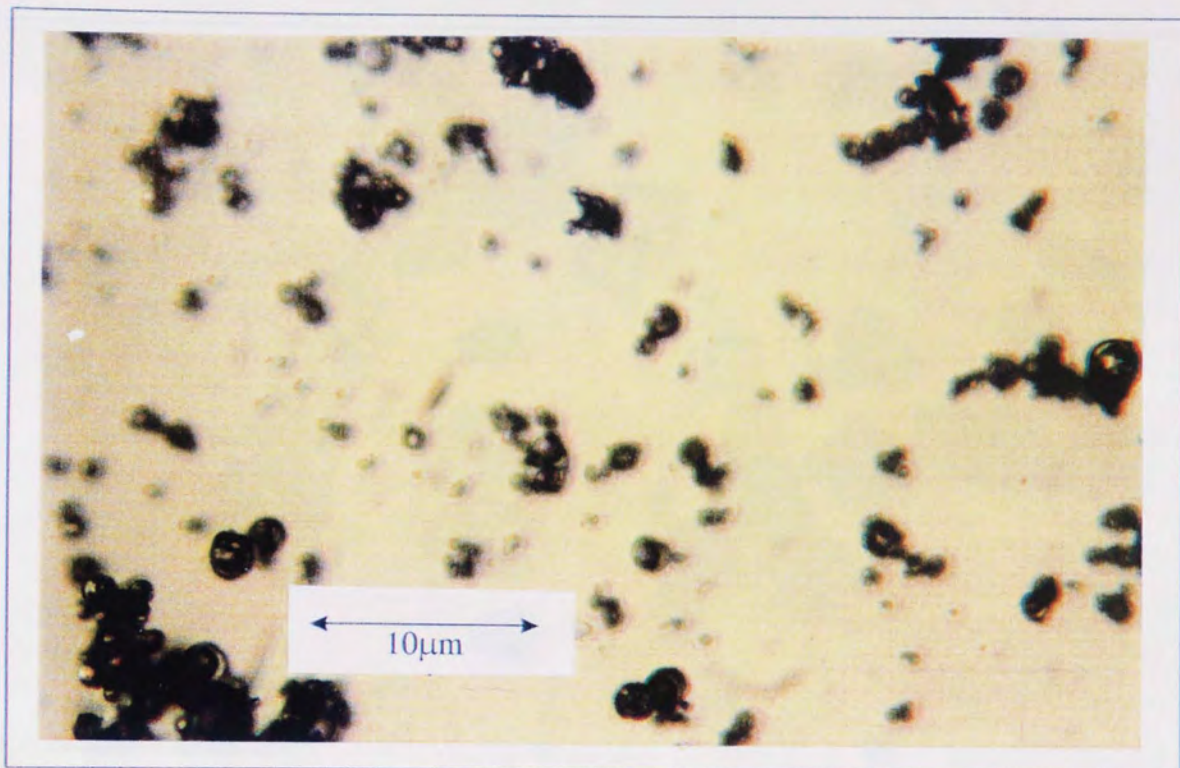


Plate 6.10. Photomicrographs showing (i) streptomycin [top], and (j) chloramphenicol [bottom].

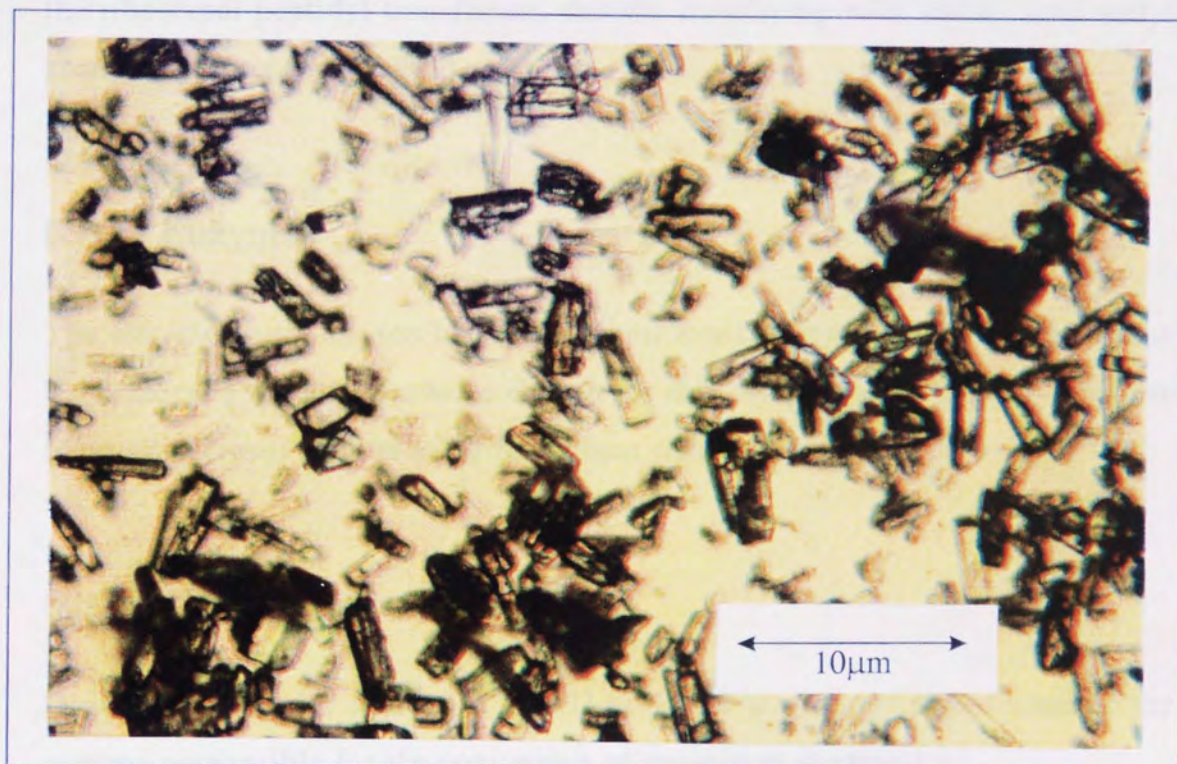
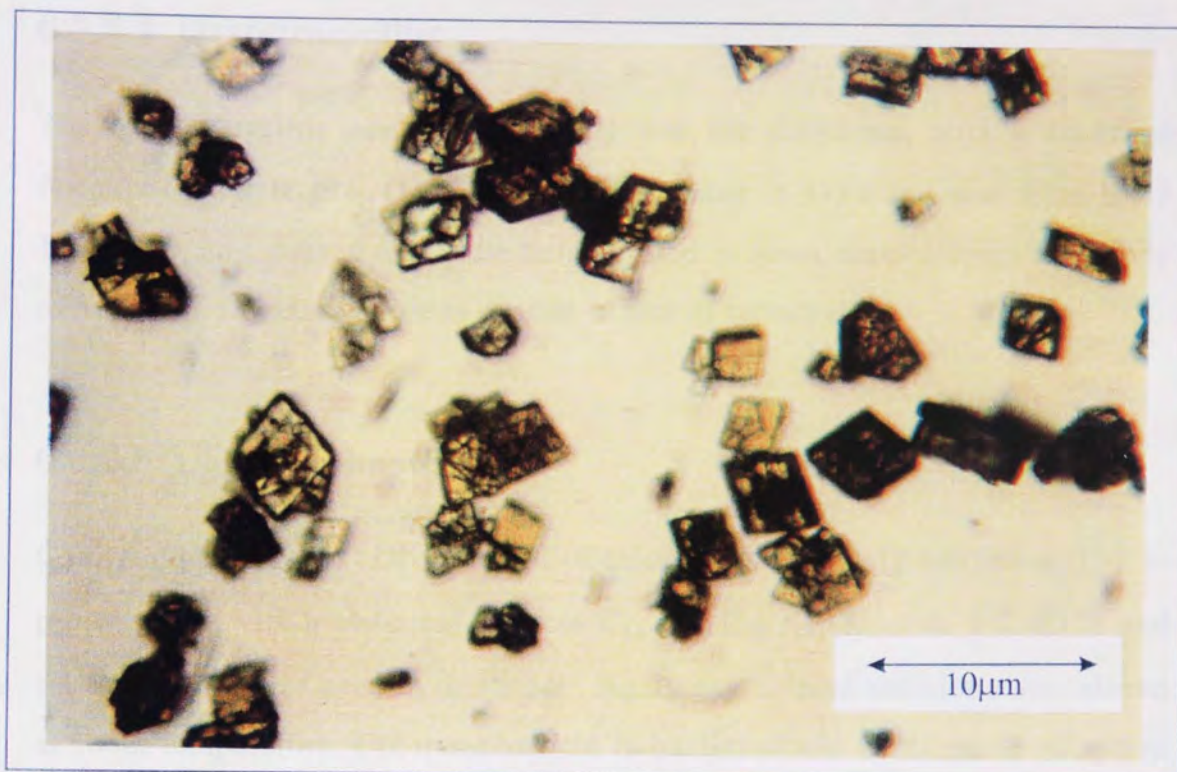


Plate 6.10. Photomicrographs showing (k) tetracycline [top], and (l) oxytetracycline [bottom].

6.3.2.4: Oxytetracycline

The oxytetracycline used in this study was the dihydrate, with a chemical formula of $C_{22} H_{24} N_2 O_9 \cdot 2H_2O$. It was coded O-5750 and was from lot # 116F0364, any unused antibiotic being stored at room temperature. The mode of action of oxytetracycline is similar to that of tetracycline.

6.3.2.5: Chloramphenicol

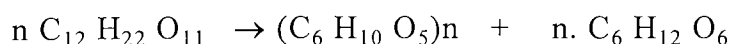
Chloramphenicol, or D[-] threo-2-dichloroacetamido-1-[p-nitrophenyl]-1,3-propanediol, with a chemical formula $C_{11} H_{12} Cl_2 N_2 O_5$, code # C-0378 and lot # 10H0724 was used in this study. Again any unused antibiotic was stored at room temperature. Chloramphenicol is bacteriostatic in its mode of action by inhibiting protein biosynthesis. It binds to the 50S ribosome at the site of the ribosomal peptidyl transferase, thereby interfering with amino acid acetyl group migration (Neu, 1991).

6.3.3: Enzymes

The enzymes were chosen because of their availability from the Fermentation Laboratory. Two enzymes were chosen for this study, one being heat-sensitive (dextran sucrose) and the other fairly heat stable (invertase).

6.3.3.1: Dextran sucrose

Dextran sucrose, (or sucrose: 1,6 α D glucan 6 α glucosyl transferase) is the enzyme responsible for the conversion of sucrose to dextran i.e.:



sucrose → dextran + fructose

(Barker & Ajongwen, 1991).

Dextran sucrose is an extra-cellular inducible bacterial enzyme produced in the presence of sucrose; the enzyme used in this study was derived from *Leuconostoc mesenteroides* (strain B-152). The optimum working conditions for this enzyme are pH 5.0 - 5.3 and temperature range 25°C to 30°C; hence this enzyme is heat-sensitive.

6.3.3.2: Invertase

The enzyme, invertase, is used commercially to convert sucrose into a glucose / fructose mixture commonly known as 'invert sugar'. The optimum pH and temperature ranges for invertase to work are 4 - 5 and 55°C to 60°C respectively (Ganetsos, 1990); hence this enzyme is fairly heat stable.

6.4: Analytical techniques

This section describes the methodologies of the analytical techniques employed in this study, viz. gas liquid chromatography, Fourier transform infra-red spectrophotometry, drug sensitivity testing, and high performance liquid chromatography.

6.4.1: Drug sensitivity testing (DST)

DST using susceptible target organisms is a standard pharmacological technique. It involves the use of 'seeded agar lawns' and the use of aseptic techniques throughout the procedure.

The choice of susceptible organisms is shown in Table 6.11. Although *Bacillus pumilus* is the preferred organism for tetracycline and

oxytetracycline, *Bacillus subtilis* was used since it is also susceptible to these antibiotics.

6.4.1.1: Preparation of bacterial cultures

The first stage in DST is the preparation of the bacterial cultures. The required organisms were removed from a freezer where they had been stored at -18°C. A loopful of cells from each culture was inoculated into 50ml aliquots of sterile nutrient broth. The resultant flasks were then placed onto a shaker, to keep the nutrient broth agitated, in a warm room (at 37°C) for an overnight incubation. The bacterial cells in these flasks provided the target organisms for the DST.

Antibiotic	Target organism	Strain number
chloramphenicol	<i>Escherichia coli</i>	NCTC 9700
streptomycin	<i>Bacillus subtilis</i>	NCTC 8236
oxytetracycline	<i>Bacillus pumilus</i>	NCTC 8241
tetracycline	<i>Bacillus pumilus</i>	NCTC 8241
ampicillin	<i>Sarcinia lutea</i>	not known

Table 6.11: Target organisms for the antibiotics

6.4.1.2: Preparation of the agar plates

The petri dishes used for DST were special square plates (24mm * 24mm), Nunc bio-assay dishes (manufactured by A/S Nunc, Denmark DK4000), and were re-used after sterilisation. Sterilisation comprised of washing the dishes thoroughly with antibacterial soap, and allowing to dry, before wiping with a clean tissue soaked with 70% v/v denatured ethanol.

The agar used was Oxoid D.S.T. agar (code CM261) obtained from Unipath Ltd, Basingstoke, England, and was made up as follows:

- i) 40g of the dehydrated media was suspended in one litre of distilled water,
- ii) the media was dissolved completely by carefully boiling so as to avoid burning the agar at the bottom, and
- iii) the dissolved media was then sterilised by autoclaving at 121°C for fifteen minutes.

After sterilisation, the media was then kept in a warm cabinet (at approximately 60°C) to cool and to keep it liquid until use. When the media was cool, but still liquid, it was dispensed into previously sterilised bio-assay trays in 150ml aliquots. This volume resulted in agar gels that were approximately 3mm in height.

Variation in thickness of the agar gel affects the drug diffusion into the agar as shown in Figure 6.12. In very thick pour plates, the three-dimensional diffusion can result in a semi-circular zone of inhibition being smaller at the bottom and larger at the surface. When the agar is very thin, the amount of drug that is available for diffusion is greater, thus resulting in larger zones of inhibition (Barry & Fay, 1973).

Once poured, the trays were left on a flat surface, to obtain a uniform thickness gel, until the gel had set. The trays were then placed in the warm room (at 37°C) for approximately half an hour with their covers removed to allow the surface of the gels to dry. Each bio-assay tray was labelled on the base for identification.

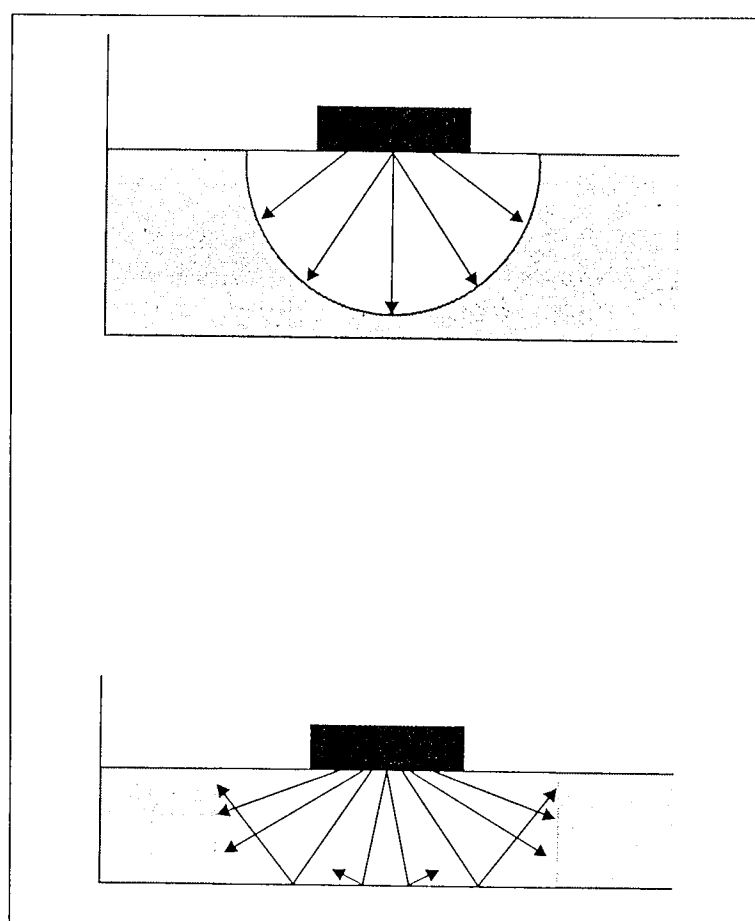


Figure 6.12. Variation in agar gel thickness affecting drug diffusion

6.4.1.3: Seeding the agar plates

Once prepared, the agar plates were 'seeded' with the bacterial cultures. One plate was used for each culture. The seeding procedure was:

- i) prepare a 1/10 dilution of the 'neat' culture,
- ii) pour this diluted culture onto the surface of the agar plate,
- iii) swirl the plate around, wetting the whole surface,
- iv) pour off the excess liquid, and
- v) drain the remainder with a sterile disposable Pasteur pipette.

6.4.1.4: Setting-up the assay

After surface seeding the agar plate, the next step was to introduce the antibiotic into the agar. The technique used was an adaptation of the 'Latin square' technique used in pharmacology. This basically divides the plate into thirty six squares (as shown in Figure 6.13), allowing, in this case, each sample to be tested in triplicate. A mark was made on the base of the tray to enable the correct orientation of the tray to be maintained throughout.

1	7	5	2	12	6
4	3	10	9	4	8
8	6	14	1	7	2
2	11	4	11	10	5
9	12	6	9	3	8
5	10	3	12	7	1

Table 6.13: The adapted Latin square, the numbers represent the inoculum number.

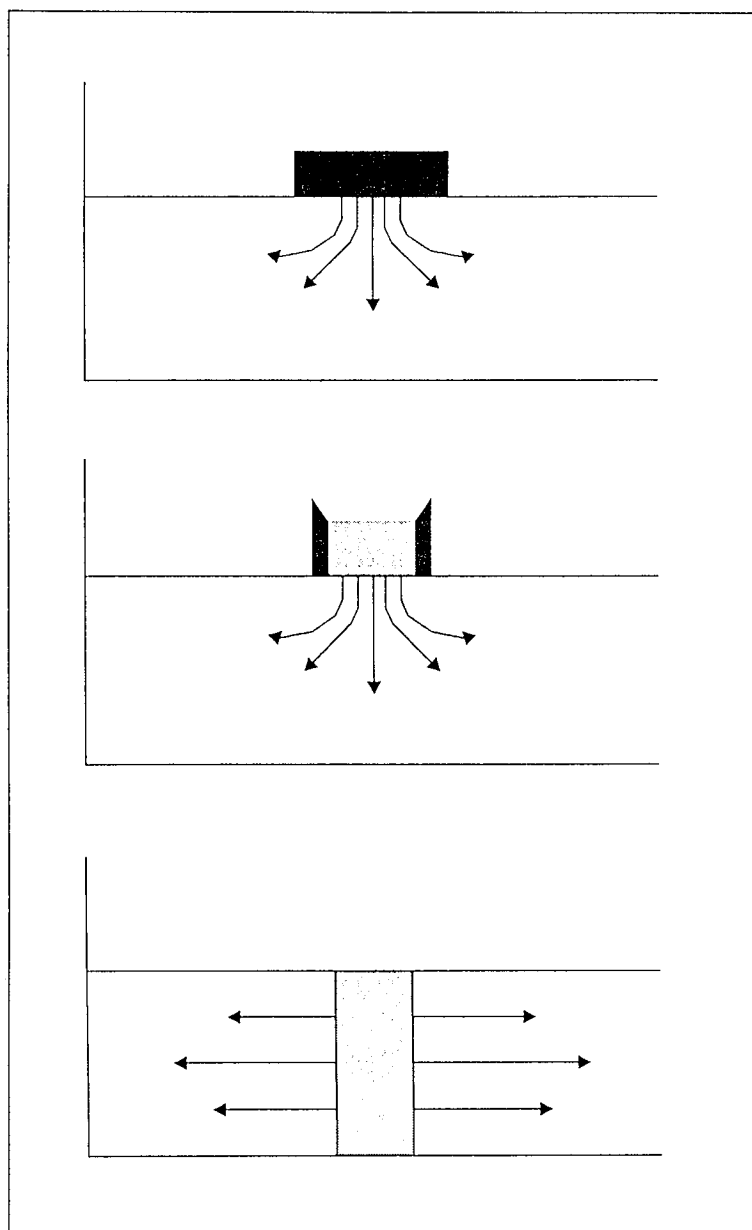


Figure 6.14. Three methods of antibiotic application to seeded agar plates (a) filter paper disc [top], (b) cylinder filled with antibiotic [middle], and (c) well cut into the agar [bottom].

There are three basic ways of applying antibiotics to seeded agar plates (as shown in Figure 6.14):

- i) filter paper discs saturated with the antibiotic may be applied to the surface of the agar,
- ii) glass, or metal, cylinders may be applied to the agar surface and then filled with the antibiotic solution, and
- iii) wells may be cut into the agar which are then filled with the antibiotic solution.

Using the Latin square framework as a guide, thirty six wells were cut, centrally in each square, using the wider end of a sterile glass Pasteur pipette. The appropriate re-constituted antibiotic, corresponding to the number in the grid, was then inoculated into each well. A standard sample volume of 20µl of antibiotic was used throughout.

To overcome the problems associated with excessively large inhibition zones, e.g. overlapping / intersection of the various zones thereby giving inaccurate readings of zone diameter, an appropriate dilution of each antibiotic was experimentally determined, as illustrated in Table 6.15.

Antibiotic	Dilution
chloramphenicol	10^{-3}
streptomycin	10^{-3}
tetracycline	10^{-4}
oxytetracycline	10^{-4}
ampicillin	10^{-4}

Table 6.15: Experimentally-determined appropriate dilutions.

The tray was then left undisturbed for approximately two hours, to allow the antibiotic to diffuse from the wells into the surrounding agar, before incubating the tray at 37°C for 18 to 24 hours.

6.4.1.5: Reading the plates

If a seeded tray is incubated without an antibiotic, the result would be a uniform growth of bacteria on the surface (a so-called 'lawn'). However, if the agar is inoculated with antibiotic, there is inhibition of growth in circular regions, of varying diameter, around the wells; the greater the inhibition, the bigger the zone of inhibition. The zone of growth inhibition is a result of the antibiotic diffusing into the agar; the further the diffusion, the bigger the zone. The rate of diffusion, driven by the antibiotic concentration gradient, is also affected by the size and shape of the antibiotic molecule and the overall ionic charge. The size of this zone of inhibition is a measure of the effectiveness of the antibiotic against the micro-organism.

The zone diameter was measured, not on the plate, but from an image of the plate projected onto the wall using an overhead projector. This process greatly increased the accuracy of the measurement because of the increased magnification (i.e. ten times); the percentage error was reduced from approximately 10% to less than 2%.

To reduce any risk of optical aberrations at the edges, the zone being measured was always positioned at the centre, which had been previously marked. Thus the plate was moved to align each zone above the centre after each set of measurements.

Two diameters were measured at right angles to each other, using a standard 300mm ruler, and an average recorded as the zone diameter. Values were hence obtained for zone diameter for each antibiotic at the various temperatures and times of exposure to these conditions.

All the zone diameters were compared to the zone diameter of the untreated antibiotic to give a relative zone diameter, which was then plotted against the corresponding time of exposure.

6.4.2: Gas liquid Chromatography

In gas liquid chromatography (GLC) the components of a vaporised sample are separated as a consequence of partition between a mobile gaseous phase and a stationary phase held in a column. This concept was first described by Martin & Synge in 1941, and demonstrated experimentally in 1952 by James & Martin.

GLC has two main functions:

- a) to perform separations, and
- b) to complete an analysis, viz.:
 - i) qualitative identification using retention times, and
 - ii) peak heights or areas to provide qualitative information.

6.4.2.1: Components of the GLC

A GLC system, shown diagrammatically in Figure 6.16, consists of four basic units:

- i) carrier gas supply,
- ii) sample injection system,
- iii) separation column, in a thermostatted oven, and
- iv) detection system.

6.4.2.1.1: Carrier gas supply

A chemically inert carrier gas, such as helium, argon, nitrogen, out of pressurised tanks, is used, the flow rate being controlled by a regulator. The gas supply often contains a molecular sieve to remove water and other impurities from the gas.

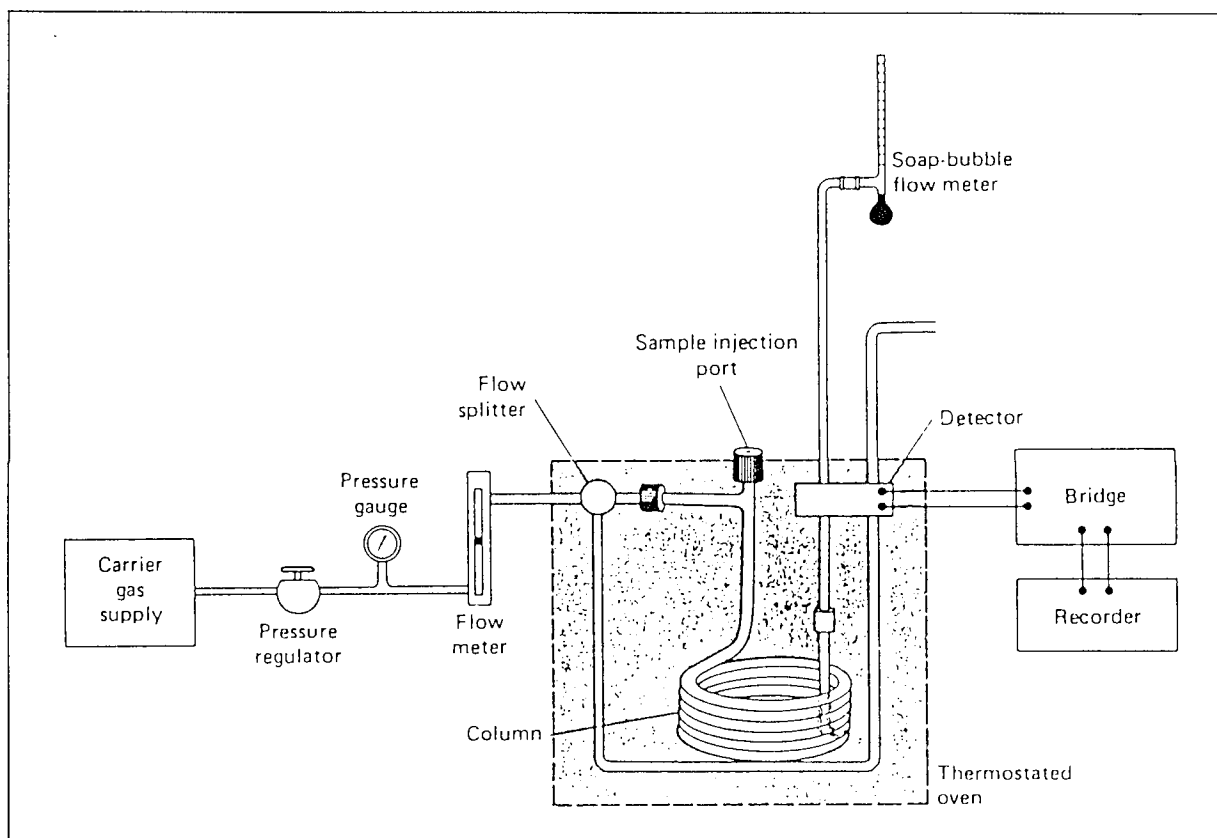


Figure 6.16. Components of a GLC.

6.4.2.1.2: Sample injection system

Column efficiency dictates that the sample is of a suitable size, and that it is introduced as a 'plug' of vapour; slow injection of over-sized samples causes band spreading and poor resolution. A micro-syringe is used to inject liquid samples through a rubber or silicone septum into a heated sample port located

at the head of the column. For ordinary analytical columns, sample sizes vary from tenths of a microlitre to ten microlitres.

6.4.2.1.3: Columns

Two types of column are used in GLC, capillary and packed columns. Capillary columns comprise of capillary tubing, of between 0.3mm and 0.5mm internal diameter, the bore of which is coated with a very thin film ($\sim 1\mu\text{m}$) of the liquid phase. Because capillary columns have a negligible pressure drop, they can be very long (10m to 100m or more) (Skoog & West, 1986, Lochmuller, 1987); but they have very low sample capacities ($<0.01\mu\text{l}$). This can be increased by coating the inside of the tube with a porous material, such as graphite, a metal oxide, or a silicate.

Packed columns are made of glass or metal tubes of 1mm to 8mm inside diameter; stainless steel tubing is used in situations where aluminium and copper tubes form catalytically active oxide films that make them undesirable for sensitive compounds such as steroids (Lochmuller, 1987).

The tubes are filled with small, uniform, spherical particles, (which have good mechanical strength, are inert at elevated temperatures, and are uniformly wetted by the liquid phase), which are coated with the stationary phase. The two most common packing materials, derived from diatomaceous earths are firebrick (sold under the trade names Chromosorb P, C22, and Sterchamol), and kieselguhr (sold under the trade names Chromosorb W, Celite, Embacel, and Celatom). The tubes, ranging from 2m to 20m in length, are folded or coiled, so that they can easily fit inside a thermostatted oven. The optimum temperature is that which gives the faster elution time together with adequate resolution of the components.

The properties of the immobilised phase in the column include:

- i) it must not be very volatile, ideally the boiling point must be at least 200°C above the maximum operating temperature of the column,
- ii) thermal stability, and
- iii) chemical inertness.

6.4.2.1.4: Detection systems

The three most common detectors used in GLC are those using thermal conductivity, flame ionisation, and electron capture. The first measures changes in thermal conductivity, which is different for different gases. The second and third type respond to changes in electron current, the electrons being produced in a flame by burning the sample, or by exposing the sample to a radioactive source.

6.4.2.1.41: Thermal conductivity sensor

The thermal conductivity sensor (TCD), or katherometer, is a simple detector that produces a large signal which requires no amplification. The detector cell has either two or four sensing elements, made of either platinum, tungsten, or a thermistor, arranged in a Wheatstone bridge circuit. In the four element model, two elements in the opposing arms of the bridge circuit are surrounded by the carrier gas flowing in a reference stream, and the other pair by carrier gas flowing out of the columns; thus the thermal conductivity of the carrier gas is cancelled. The TCD is reliable, simple, non-destructive, and moderately sensitive; it responds to essentially all compounds. It has a concentration detection limit of $5 - 10 \times 10^{-6}$ g/ml of eluant gas (Lochmuller, 1987).

6.4.2.1.4.2: Flame ionisation detector

The flame ionisation detector (FID) has a wide linear range and high sensitivity, and is quite reliable. It consists of a hydrogen-air flame polarised

in an electrostatic field. The flame ignites and ionises the combustible components as the carrier gas passes onto it, after which the ions (mainly carbon compounds) are collected at the electrodes, producing a current. The FID does not respond fully to oxygenated carbons, such as carbonyls, and carboxylic acids. However, it does not respond at all to water or atmospheric gases (N_2 , O_2 , CO_2 , *etc.*), making it ideally suitable for analysis in aqueous solutions and atmospheric samples. The response is proportional to the number of carbon atoms, but diminishes with increasing substitution by halogens, amines, or other electron-capturing species. The limit of detection for the FID is $1 - 5 \times 10^{-9}$ g/ml of eluant gas.

6.4.2.1.4.3: Electron capture detector

The electron capture detector (ECD) takes advantage of the affinity of certain functional groups for free electrons (the reason for loss of sensitivity in the FID). The carrier gas is passed through a cell containing a β -emitter, such as ^{63}Ni , which ionises the carrier gas molecules to produce electrons which migrate to the anode under an applied voltage of 1-100V. An electron capturing species eluting from the column reacts with the electrons to form an ion or neutral molecule which is swept from the cell; the net result being a reduction in the number of electrons found at steady state, or a drop in the standing current. (A peak in ECD detection is really a detector current valley, since the maximum current is found in the absence of electron capturing species).

The response is very non-linear, but a linear range can be achieved by pulsing the polarising voltage. The detection limit of the ECD is approximately 1×10^{-12} g/ml of eluant gas. The ECD is insensitive to amines, alcohols, and hydrocarbons, but very sensitive to electro-negative functional groups such as halogens, anhydrides, and nitro-groups.

6.4.2.2: Operation of the GLC

The GLC used in this study was the Perkin Elmer Sigma 2B gas chromatograph. It had a Porapak Q column (Alltech Chromatography, Carnforth, Lancashire, England), which was made from stainless steel tubing 1.8m long and 63mm (0.25") internal diameter. Helium was used as the carrier gas, with a flow rate of 30ml per minute; and the detector was the FID. The column temperature was set at 220°C, whilst the detector and injector port were maintained at 250°C. A sample volume of 2.5µl was introduced into the GLC using a 10µl Hamilton syringe. The FID was linked to a Spectra Physics SP4100 computing integrator, (Spectra-Physics (UK) Ltd., Hertfordshire), which provided details such as peak shape, peak area, and retention times for the components.

6.4.2.3: Sample preparation and analysis

After the appropriate drying times, each droplet was collected into a pre-weighed 0.5ml centrifuge tube, and re-constituted with distilled water to its original weight (with respect to the untreated droplets). Each tube contained three droplets, i.e. an untreated volume of 30µl. An extra 30µl of distilled water was added to each tube to increase the volume available for analysis. This addition did not affect the overall results because all the tubes were treated similarly; also, the results were all relative to the untreated sample. The sample in each tube was then thoroughly mixed using a whirlimixer. The tubes were then centrifuged, at 3000rpm for thirty minutes, to separate the suspended solids and the solvent, and then left in a refrigerator overnight before analysing the supernatant.

A sample of 2.5µl was then taken from each tube and injected into the GLC; the first sample was the one which had the lowest concentration of ethanol and the last was the highest concentration sample; the syringe was washed in ether in between each sample.

The resultant peak areas, for each sample set, were compared to the peak area of the untreated sample in the set, i.e. tube 0, to give the relative ethanol remaining in the sample after drying (i.e. the relative retention of ethanol). Hence, values were obtained for the relative retention for each flavour encapsulant at the various temperatures / air flow rates and times of exposure to these conditions allowing the graphs of relative retention, for the given drying times, to be plotted.

6.4.3: Fourier transform infra-red spectrophotometry

Infra-red (IR) spectrophotometry is a form of absorption spectroscopy which has been traditionally used to obtain detailed structural and bonding information for many types of molecules.

An infra-red absorption spectrum, often contains a large number of sharp maxima and minima. It is this multitude of peaks that imparts specificity to the spectrum; no two compounds give identical spectra. Peaks useful for the identification of functional groups are located in the shorter wavelength region of the infra-red spectrum (below $8.5\mu\text{m}$). Table 6.17 gives the positions characteristic for some common functional groups. Although the identification of the functional groups can be used to identify a compound, the entire spectrum from $2.5\mu\text{m}$ to $15\mu\text{m}$ must be compared for a more positive identification.

In conventional spectroscopy, the sample experiences only a small element of the available frequencies (or wavelengths) at one time; the resultant plot of intensity versus frequency (or wavenumber) is known as a frequency domain spectrum. By contrast, in Fourier transform spectroscopy, the sample experiences all the frequencies (or wavelengths) in the region of interest at all times instead of only a small portion at a time, resulting in a time-domain spectrum which is then converted by a Fourier transform, using a digital computer, into the conventional frequency-domain spectrum.

6.4.3.1: Components of an IR spectrophotometer

The basic components of any spectrophotometer are similar, (as shown in Figure 6.18):

- i) a source of electromagnetic energy,
- ii) an analyser to sort out the energies modified by the sample,
- iii) a detector of these energies, and
- iv) a recorder.

Because of the complexity of IR spectra, most commercial instruments are of the double beam type which cancel background absorption caused by atmospheric gases such as CO₂ and H₂O. The radiation from the source is split into two beams, one passing through the sample and the other through the reference compartment. The beams are then transmitted in pulses by a series of mirrors and slits through the monochromator, and then focussed onto the detector. The in-coming beam is modulated by a Michelson interferometer, (described in Kincaid, 1987), to convert the in-coming radiation to a frequency that can be followed by the detector. The information from the detector is digitised using analogue to digital converters and processed mathematically using computers to generate the conventional frequency-domain spectrum.

6.4.3.2: Detectors

The two general classes of IR detector in use are:

- i) photon detectors, based upon the photoconductive effect that occurs in some semi-conductors, e.g. lead sulphide, which are sensitive to radiation between 1 μm and 3 μm wavelength and have a response time of 10 μs , and

ii) thermal detectors, in which the absorption of IR radiation produces a heating effect, which in turn alters a physical property, e.g. electrical resistance, of the detector, e.g. a thermopile, made from several thermocouples connected together, which in turn has a response time of approximately 100ms.



Aston University

Content has been removed for copyright reasons

Table 6.17: Some characteristic IR absorption peaks (Skoog & West, 1986).

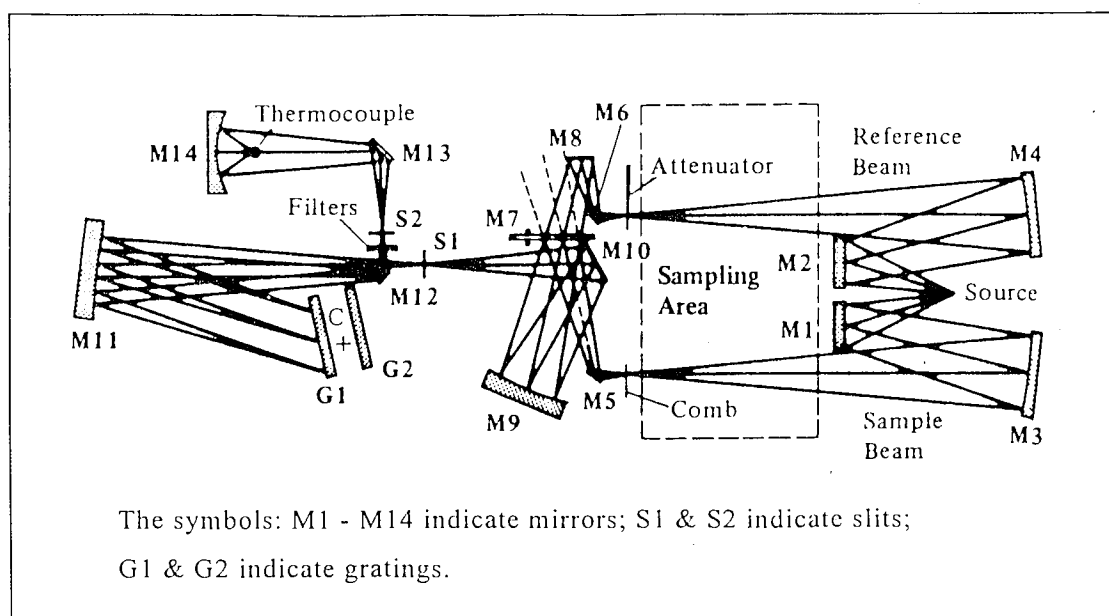


Figure 6.18. Components of an FTIR spectrophotometer.

A recent development is the pyroelectric detector, based upon the fact that some crystals, e.g. tri-glycine sulphate, deuterated tri-glycine sulphate, possess an internal electric polarisation resulting from the alignment of electric dipole moments. The absorption of IR radiation causes a change in this polarisation. If such a crystal is placed between two electrodes in an external circuit, current will flow to balance the charge re-distribution. The pyroelectric effect, since it depends on the rate of change of temperature and not on the absolute value, responds only to modulated radiation and not to the slowly varying background radiation. Such detectors have a much faster response time and are used widely in Fourier transform IR spectrophotometers.

6.4.3.3: Solid sample preparation

The most commonly used sampling method is the KBr disc technique. Before the various dry droplets could be used in any FTIR analysis, any residual moisture within the drops was removed by placing the tubes containing the

droplets inside a dessicator containing dehydrated silica gel for approximately one month. The reason for this was that the peaks from any residual moisture would tend to mask any other peaks from other functional groups that may be present.

Each of the KBr discs used in this study was prepared as illustrated below:

- i) a small quantity of the dry sample was ground in a marble pestle and mortar, with some dry IR quality KBr, until they were well mixed,
- ii) the mixture was then transferred to an evacuable die 13mm in diameter. It was carefully dropped onto the floor of the die so as to produce an even layer,
- iii) the die was then connected to a vacuum pump and placed in a Perkin Elmer 15 tonne hydraulic press. It was pressed at two tonnes for thirty seconds and then ten tonnes for four minutes, and
- iv) the pressure was released, and the die removed from the press. The resultant KBr disc was carefully removed from the die, so as not to damage the thin disc that had been formed, and placed into the sample holder; the sample holder was then inserted into the sample chamber of the instrument.

Fifteen such KBr discs were prepared for the antibiotics.

6.4.3.4: IR Fourier transform spectrophotometer

The instrument used in this study was a Perkin Elmer 1710 IR Fourier transform spectrophotometer, which had a He-Ne class II laser, with its power $<0.4\text{mW}$ and output wavelength of 633nm, as the source of IR radiation; a caesium iodide beam splitter was used to split the beam. The output from the detector was linked via an IBM-clone computer to an Hewlett-Packard HP-7475A x-y plotter which plotted the resultant frequency domain spectrum for each sample. The computer program which controlled the instrument was the Perkin Elmer 1710 IR Data Manager version C.

The FTIR, controlled by on-screen menus, was set to scan the sample ten times from wavenumber 4000cm^{-1} to 450cm^{-1} , with a 2.0cm^{-1} resolution. The resultant frequency-domain spectra were stored onto disc for further analysis / manipulation, e.g. overlaying of the plots.

6.4.4: High performance liquid chromatography

Chromatography is a group of separation methods that allow the separation, isolation, and identification of closely related components of complex mixtures.

The development of packing materials from large porous particles ($\sim 50\mu\text{m}$ diameter) to microporous particles ($\sim 5\mu\text{m}$ to $10\mu\text{m}$ diameter) greatly enhanced the separation efficiency; but reasonable flow rates, with microporous particles, could only be achieved with high pressure pumps, thus high performance (pressure) liquid chromatography (HPLC).

6.4.4.1: Components of an HPLC system

The components of a typical HPLC system are shown in Figure 6.19.

6.4.4.1.1: Degassing system

The solvents used must be degassed to prevent interference from bubbles which would otherwise form in the column and detector systems. A convenient method of solvent treatment is to filter the solvent through a millipore filter under vacuum; this removes gases as well as suspended solids from the solvent.

6.4.4.1.2: Pumps

Most HPLC pumps have outputs of between 4000 and 6000psig, with a flow rate of at least 3ml per minute. The most popular type of pump is a reciprocating pump; this alternately sucks in the mobile phase from the reservoir (low pressure side), then delivers the pump volume to the column (high pressure side). This provides a pulsed flow which must be subsequently damped.

6.4.4.1.3: Pre-columns

Pre-columns, with chemically identical packing as in the analytical column but larger particle size, are used to remove impurities from the solvent, thus preventing contamination of the analytical column. In addition, the pre-column saturates the mobile phase with the liquid making up the stationary phase, thereby preventing stripping of the stationary phase from the analytical column.

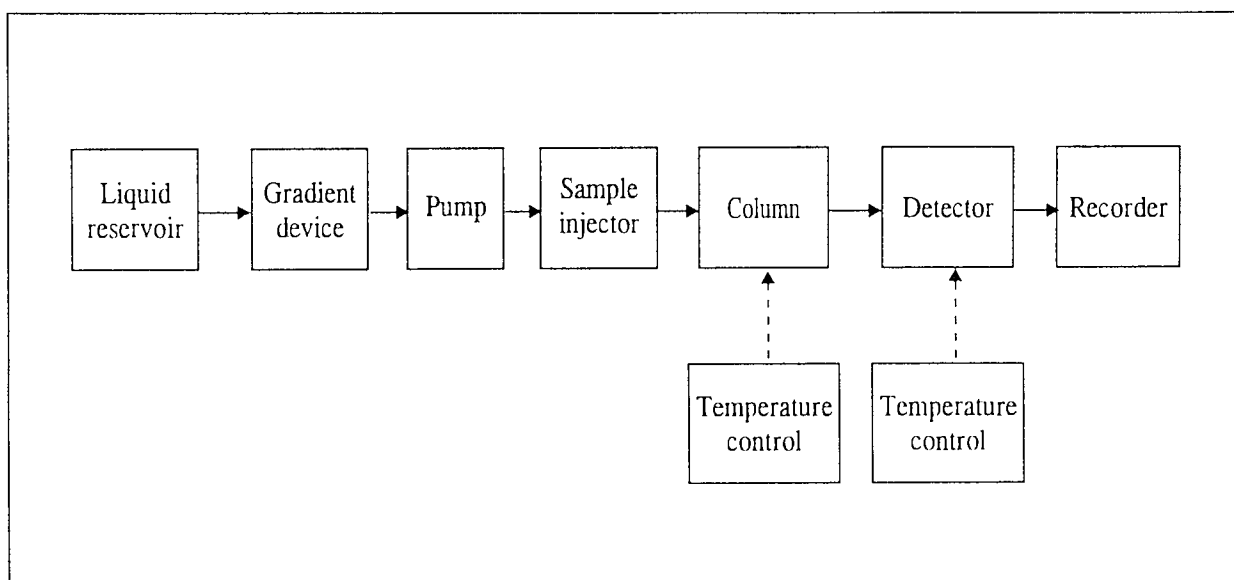


Figure 6.19. Components of an HPLC system.

6.4.4.1.4: Sample injectors

For forced flow systems as in HPLC, the sample injector is located between the pump and the analytical column; the most commonly used injector is the loop injector. In the load position, the sample is forced through the loop by a syringe. Once the loop is completely filled, the valve core is rotated automatically; the high pressure pump forces the mobile phase through the loop and displaces the sample onto the column. Auto-samplers are used for automatic injection of samples.

6.4.4.1.5: Analytical columns

Analytical columns for HPLC are constructed of either heavy walled glass tube or precision bore stainless steel for high pressures (above 600psi). A recent trend in HPLC has been the use of more efficient columns with smaller internal diameters; this has been made possible firstly by the development of pellicular packing particles (average particle diameter of 37 μ m to 50 μ m) and subsequently of porous micro-particles (with average diameter of 5 μ m to 10 μ m). Pellicular particles, as shown in Figure 6.20, consist of a solid non-porous core (usually a glass bead 40 μ m in diameter) with a thin porous outer shell (usually 1 μ m to 3 μ m thick) made from silica gel, alumina, resin, or polyamide.

A typical HPLC column ranges from 15cm to 150cm in length with an inside diameter of approximately 2mm to 3mm (Skoog & West, 1986). Column temperature is maintained either by placing the column in an oven, or by using a water jacket around the column. There are several advantages in using small internal diameter, or microbore, columns, e.g.:

- i) solvent consumption is reduced, and
- ii) there is increased detector sensitivity; with the same sample volume, the narrow peak widths give an increased peak concentration (provided the

column is not over-loaded), thus giving greater sensitivity at the detector, as shown in Figure 6.21.

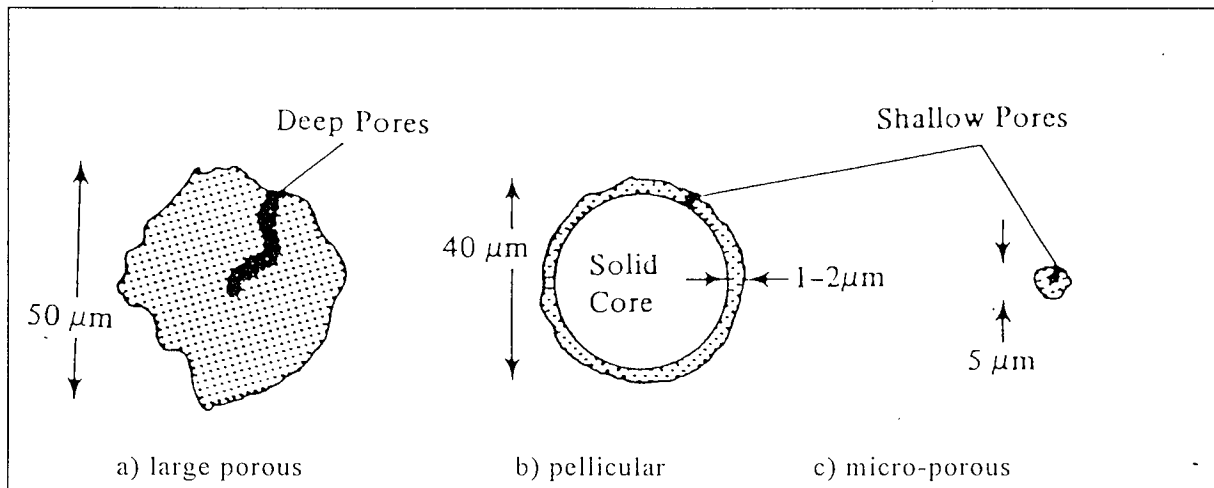


Figure 6.20. Types of particles used in liquid chromatography

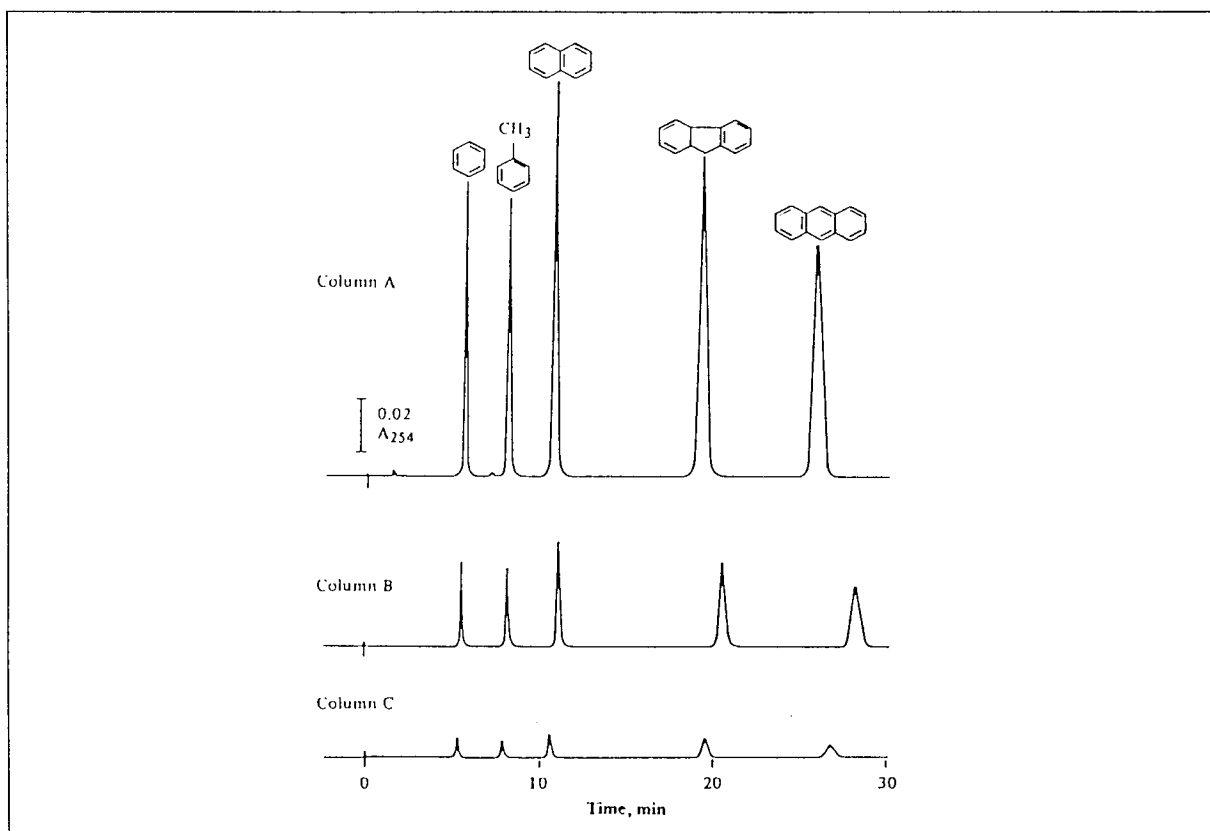


Figure 6.21. Detectability differences for microbore and conventional columns. (Column A) large porous particles, (Column B) pellicular particles, and (Column C) micro-porous particles.

6.4.4.1.6: Detectors

The substances eluting from a column can be measured either by:

- i) an automatic fraction collector, that collects a defined volume of eluent for analysis, or
- ii) a continuous detection device placed at the exit of the column.

The detector can be selective (i.e. it detects ultra violet absorbing or fluorescent compound only) or universal (i.e. it detects all components).

The continuous detectors most often used in HPLC (as illustrated in Table 6.22) are based on ultra-violet or visible absorbtion, fluorescence, electrochemistry, and differential refractometry, and are commercially available. These detectors are generally less sensitive than GLC detectors.

6.4.4.2: The HPLC system used in this study

A 30cm long Aminex HPX-87C column (supplied by Biorad (UK) Ltd., Hemel Hempstead) with an internal diameter of 0.78mm was used as the analytical column. The column packing was the calcium form of 8% divinylbenzene cross-linked resin. The column was operated at 85°C, and protected with LiChroCart RP-18 pre-columns (BDH/Merck Ltd., Atherstone, Warwickshire).

The eluent, prepared with distilled water containing 0.02% w/v calcium acetate to maintain the calcium form of the resin, was degassed by heating to 80°C and pre-filtered using a 0.45µm sintered metal filter before being pumped into the analytical column using a Biorad 1330 pump (Biorad (UK) Ltd.) at a flow rate of 0.5ml per minute.



Aston University

Content has been removed for copyright reasons

Table 6.22: Characteristics of chromatography detectors (Skoog & West, 1986)

The samples were filtered with 5.0 μ m and 0.45 μ m disposable filters (Gelman Sciences, Northampton, UK) to remove particulate impurities and to prolong the life of the analytical and guard columns. The enzyme samples were denatured by heat treatment in boiling water for five minutes. A Talbot ASI-3 autosampler (Talbot Instruments Ltd., Cheshire, UK) was used to inject the samples onto the columns.

The detector system used was of the continuous detection type based upon differential refractometry, using a Biorad 1750 refractive index monitor (Biorad (UK) Ltd.). measuring the differential refractive index between the pure eluent and the eluent from the analytical column. The output from the refractive index monitor was linked to a Spectra-Physics SP4270 integrator (Spectra-Physics (UK) Ltd., Hertfordshire) which provided a chromatogram where the resolved components were identified by their retention times, and

the component concentrations were determined by the areas under the peaks on the chromatograms.

6.5: Freeze-drying

30 μ l aliquots of the various solutions / suspensions of the flavour encapsulants and antibiotics were dispensed into 0.5ml micro-centrifuge tubes which were subsequently placed into the drying chamber of an Edwards Manifold Freeze Dryer (Edwards High Vacuum, Crawley, Sussex, England) for the same periods of time as for the air drying of the single droplets. After each set period, the 0.5ml micro-centrifuge tube, containing the specific materials, was removed from the drying chamber and sealed. The material was then analysed for respective properties, viz. volatiles retention and residual potency, using the methods detailed earlier in this chapter.

7: Results

To investigate the effect of drying upon materials, various materials were chosen to be representative of their particular group. The materials chosen were flavour encapsulants, pharmaceuticals, and enzymes. The choice of flavour encapsulants was based upon the work of Hassan (1991) on the formation of a skin / crust which could have a significant bearing upon flavour retention. Antibiotics were used as representative of pharmaceuticals, because of the existence of standard methods of testing which could be easily modified to suit this study. Enzymes were chosen because of their increased thermoresistance resulting from dehydration. The straight line connections of the data points do not imply an inter-point relationship.

7.1: Flavour encapsulants

The chosen flavour encapsulants were dissolved / suspended in distilled water; a simulated flavour, ethanol, was added to the mixture. Individual droplets were suspended on the end of a thermocouple in a drying air stream; after set time intervals they were removed for analysis of residual ethanol content using a gas chromatograph. (The method of analysis is detailed in Chapter 6).

The effects, upon the retention of the simulated flavour in each of the flavour encapsulants, of variations in initial concentration, air flow rate, and drying air temperature were evaluated. The measure of relative retention was calculated from the ratio of the ethanol content at a particular time to the initial ethanol content of the untreated sample.

A value $t_{1/2}$ was assigned to the time at which the value of the relative retention had fallen to half its initial value, i.e. when there was 50% retention. The various concentrations of the suspensions / solutions have been assigned

codes for ease of reference, i.e. solution A for the 10%, solution B for the 20%, and solution C for the 40% concentration solutions / suspensions.

7.1.1: The effect of initial concentration

Series of experiments were conducted with the various encapsulants to determine the effect of the initial concentration of each encapsulant upon flavour retention. The results are presented graphically.

7.1.1.1: Rice starch

Starches, in general, vary because of their amylose content (a linear polysaccharide, composed of 1,4 linked α -D-glucopyranosyl units, which increases gel strength) and amylopectin content (a highly branched molecule, of 1,4 linked α -D-glucopyranosyl units with the branches occurring at the 1,6 α -D-linkages, which causes a decrease in the gel strength and viscosity)

Rice starch, with particles generally of 3 μ m to 8 μ m in diameter (Bemiller, 1992), dispersed easily in cold water but did not remain in suspension without continuous agitation with a magnetic stirrer. The addition of 1.0ml of the simulated flavour (ethanol) did not cause any apparent changes in the solubility characteristics of the starch.

Referring to Figure 7.1a, at $T = 25^{\circ}\text{C}$, there was no significant difference in the retention of the ethanol with the 10% and 20% concentrations of rice starch. Both concentrations exhibited a decrease in the retention of 50% within the first minute of drying. With the 40% suspension, there was a very sharp fall in retention down to approximately 20% within the first thirty seconds of exposure to the drying air. After two minutes of drying, all three concentrations behaved similarly, eventually attaining very low retentions (<5%) after ten minutes of drying.

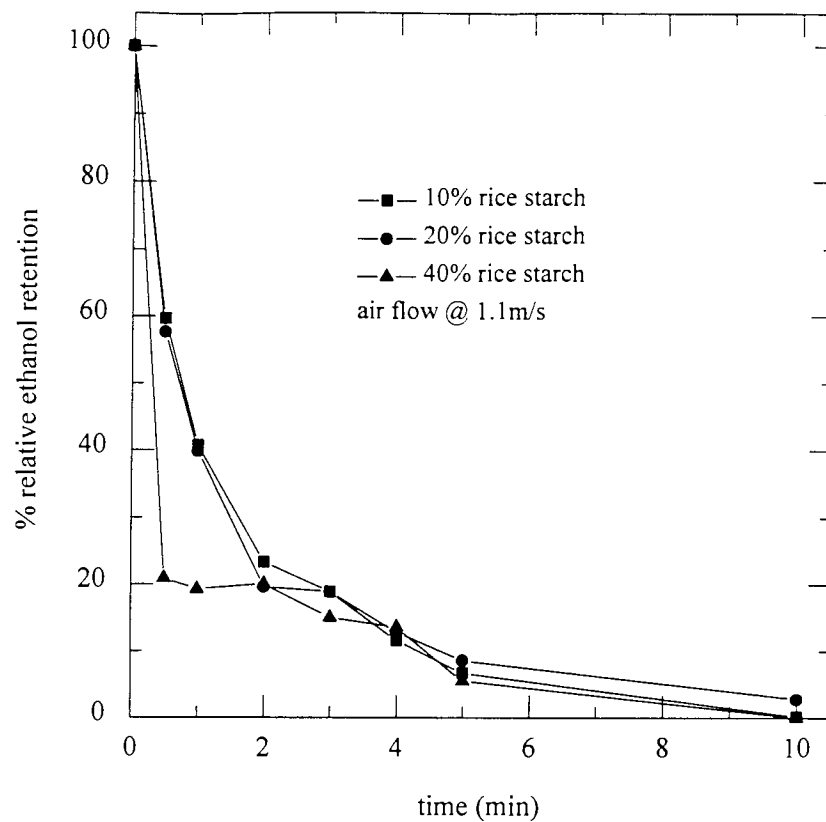


Figure 7.1a

The effect of initial concentration on the retention of ethanol in rice starch solutions at ambient temperature ($T = 25^{\circ}\text{C}$)

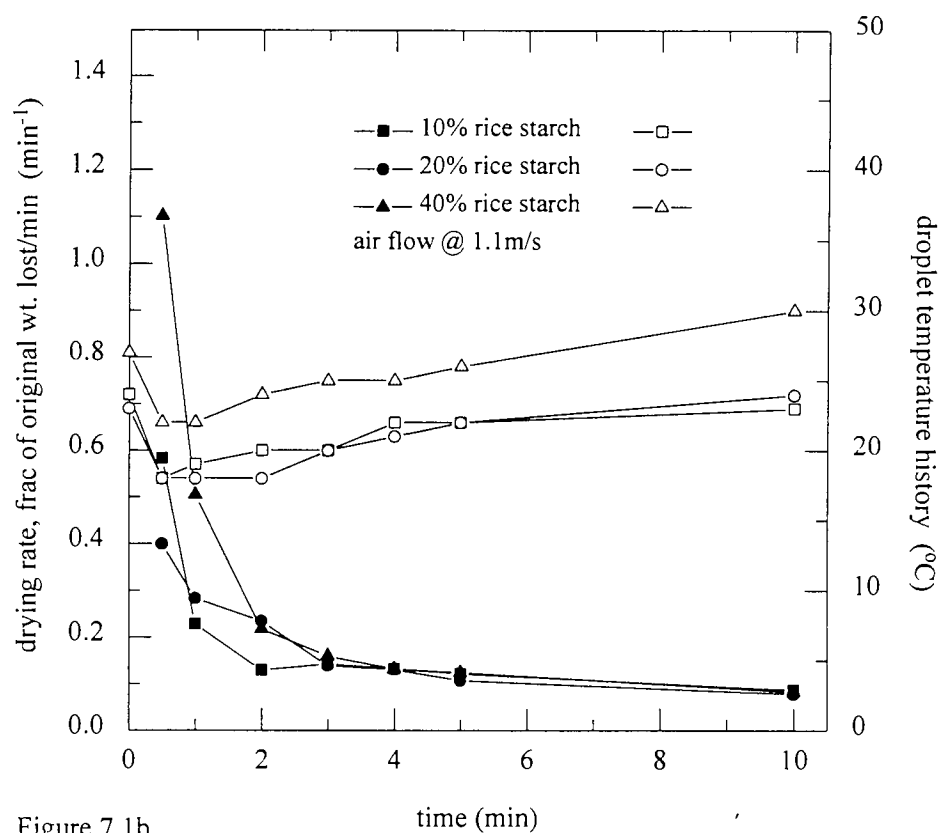


Figure 7.1b

The drying rate [solid symbols] and droplet temperature history [open symbols] for rice starch solutions

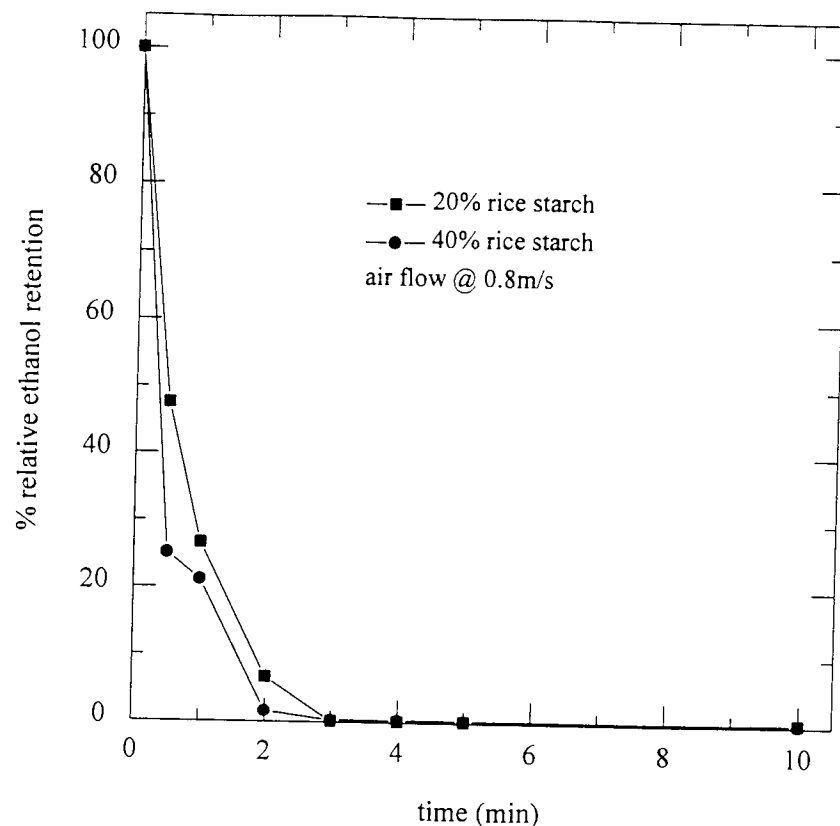


Figure 7.2a

The effect of initial concentration on the retention of ethanol in rice starch solutions at $T = 62^{\circ}\text{C}$

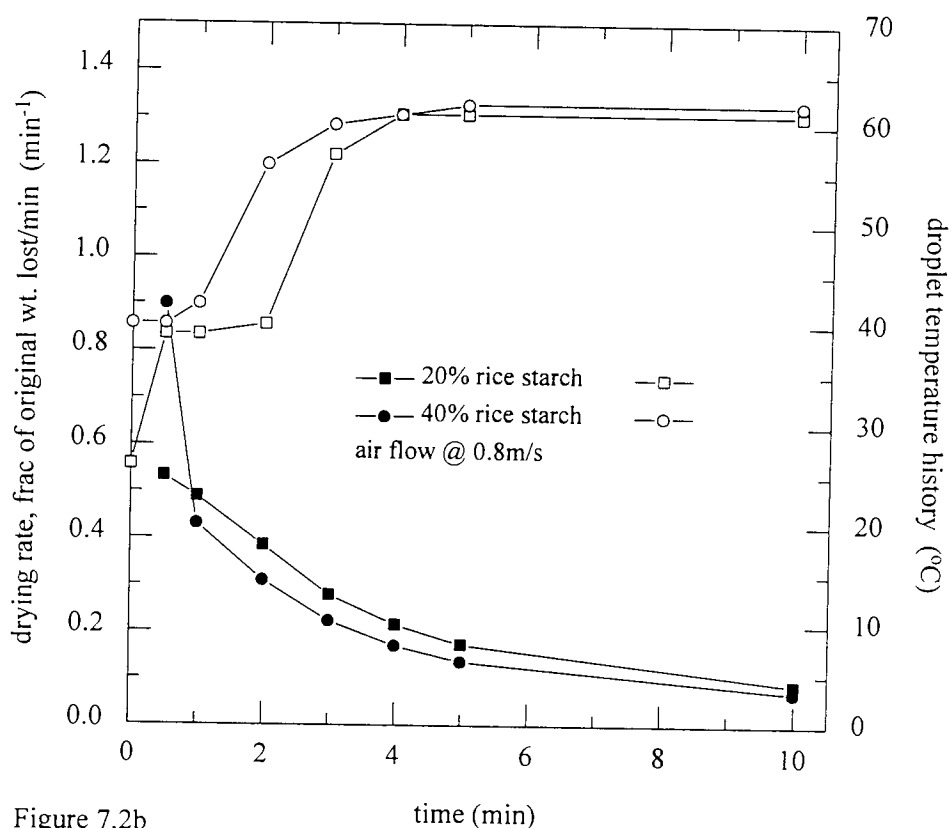


Figure 7.2b

The drying rate [solid symbols] and droplet temperature history [open symbols] for rice starch solutions

Figure 7.1b shows the drying rates and the temperature histories for the drying droplets. Initial droplet temperatures fell to the prevalent wet bulb temperature before a gradual increase towards the temperature of the drying air. There was an initial rapid drying rate within the first two minutes of exposure to the drying air, followed by a much slower drying rate; no constant-rate period was observed at any time prior to the first falling-rate period. This suggests that in the first falling-rate period, the rice starch particles, by forming an open structure crust during drying, allowed water to transfer rapidly to the surface by capillary action for subsequent evaporation. Thus there was a rapid initial drying rate. Subsequently in the second falling-rate, the water was brought to the surface by diffusion, because of the setting up of concentration gradients. The rate was very slow because very little water was left in the droplet, i.e. the concentration driving force was small.

Figure 7.2a illustrates the effect of concentration at 62°C. Both solutions B and C exhibited a similar trend in that $t_{1/2}$ for both was less than one minute. Within three minutes, the retention had been reduced to zero. (Solution A was not used because of its similarity with the 20% concentration suspension).

Referring to Figure 7.2b, solution C displayed two falling-rates whilst solution B had only one falling-rate period. Differences between the times spent at the prevalent wet bulb temperature are also evident, with solution C remaining at the wet bulb temperature for only 30 seconds, and solution B for 90 seconds. This suggests that moisture was lost more rapidly from the higher concentration suspension, as shown by the earlier rise in droplet temperature. The droplet temperature stayed at the wet bulb temperature because of the evaporating moisture, but when there was a reduction in the moisture being evaporated, the droplet temperature began to increase towards that of the drying air. After four minutes of exposure to the drying air, the droplets had attained the temperature of the drying air.

The above results demonstrate that there was little, or no, effect of initial concentration upon the retention of the volatile flavour since the rice starch

formed a suspension in the water. As a consequence there was no depression of the vapour pressure of either water or ethanol.

At these drying temperatures, the rice starch droplets formed a crust upon drying. However these crusts were of a porous nature, as illustrated in Plate 7.1, and had little effect upon the retention of the flavour. Rice starch, as shown by Hassan & Mumford, 1993, forms a skin at very high drying temperatures ($>150^{\circ}\text{C}$) where the individual granules gelatinise, i.e. there is a collapse in the molecular order resulting in irreversible changes, such as granule swelling, within the starch granules (Bemiller, 1992).

7.1.1.2: Wheat starch

Wheat starch has an amylose content of 27%, an average particle diameter of between $5\mu\text{m}$ and $25\mu\text{m}$, and a gelatinisation temperature of between 62°C and 70°C . Hence drying at temperatures beyond these temperatures should result in the formation of a smooth skin which should be resistant to mass flow, thereby resulting in increased ethanol retention.

Suspensions of 10% and 20% concentration were used to study the effect of initial concentration upon flavour retention. It proved impractical to use a 40% suspension because of the difficulty in pipetting such a viscous droplet.

At a temperature of 25°C , shown in Figure 7.3a, droplets of wheat starch of both concentrations showed similar behaviour in their retention. Again, $t_{1/2}$ was approximately thirty seconds, but the final retention values were significantly greater than those with the rice starch at the same temperature. The significant effect of initial concentration upon the retention of ethanol was again evident; solution A resulting in less retention than solution B (approximately 3% for solution A and almost 10% for solution B).

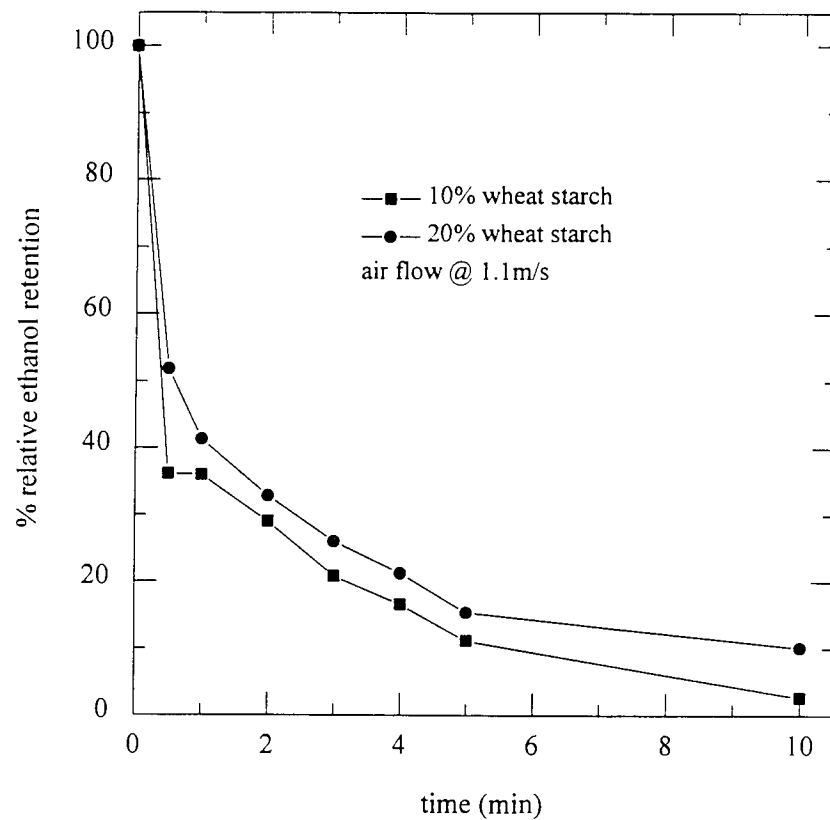


Figure 7.3a

The effect of initial concentration on the retention of ethanol in wheat starch solutions at ambient temperature $T=25^{\circ}\text{C}$

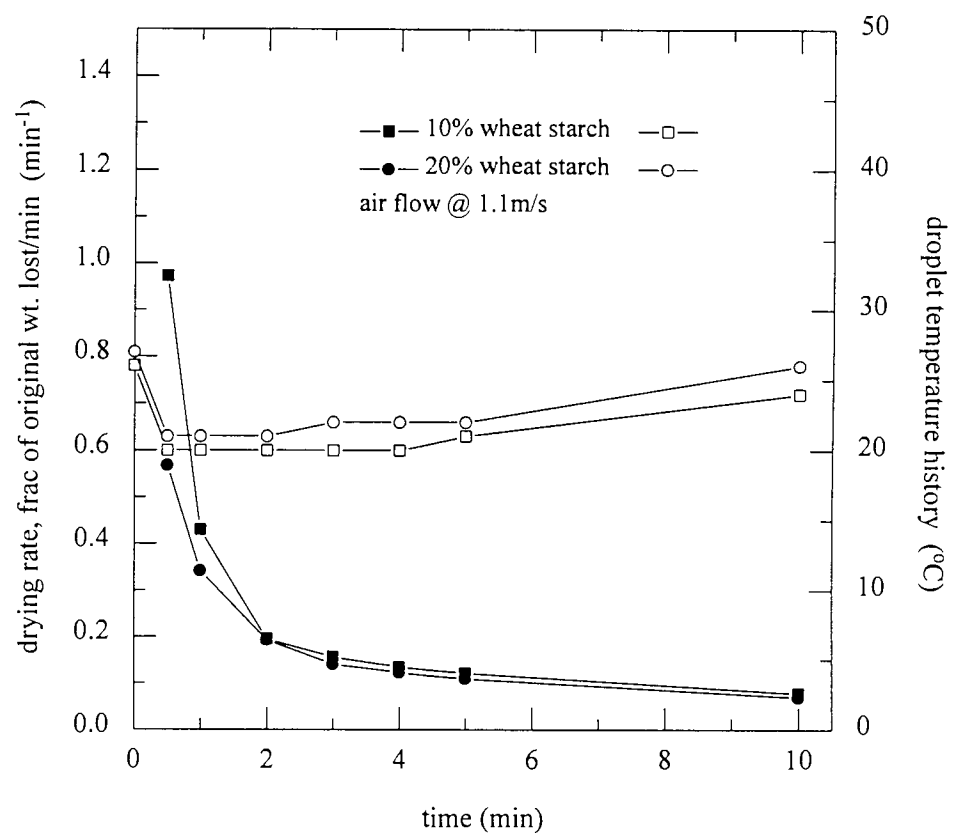


Figure 7.3b

The drying rate [solid symbols] and droplet temperature history [open symbols] for wheat starch solutions

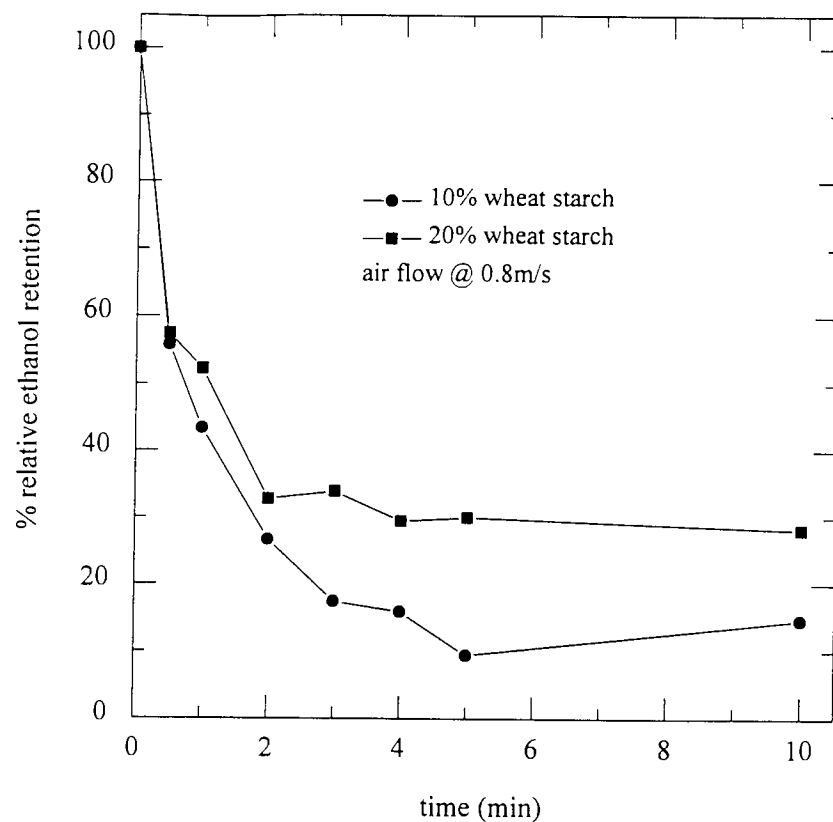


Figure 7.4a

The effect of initial concentration on the retention of ethanol in wheat starch solutions at 42°C

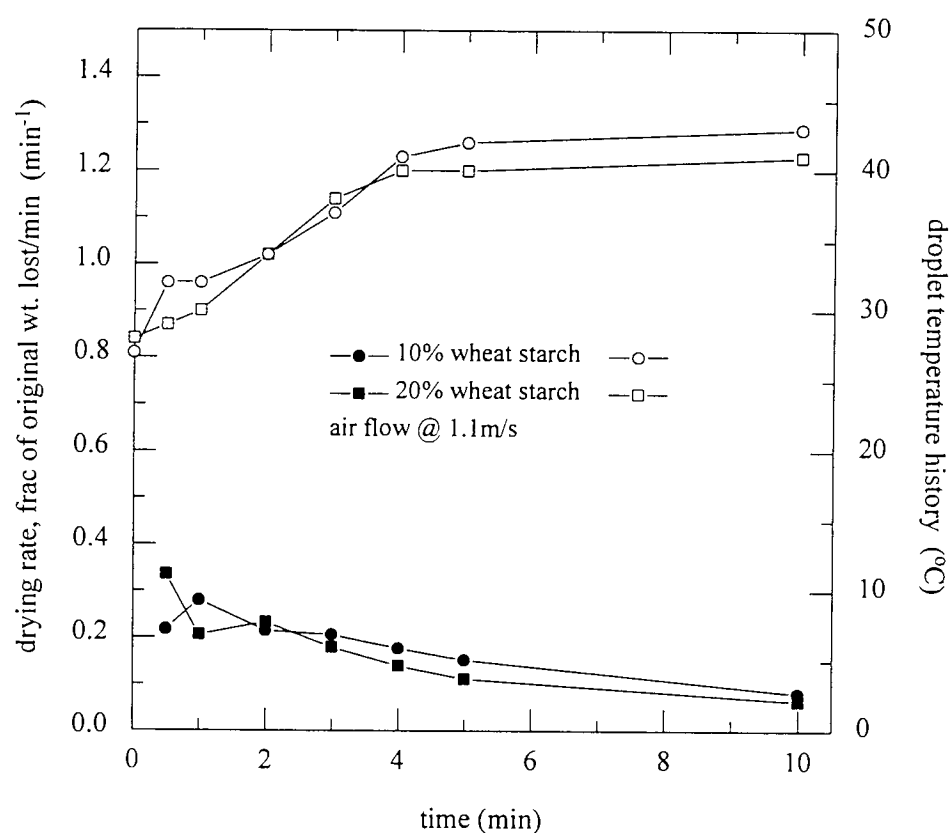


Figure 7.4b

The drying rate [solid symbols] and droplet temperature history [open symbols] for wheat starch solutions

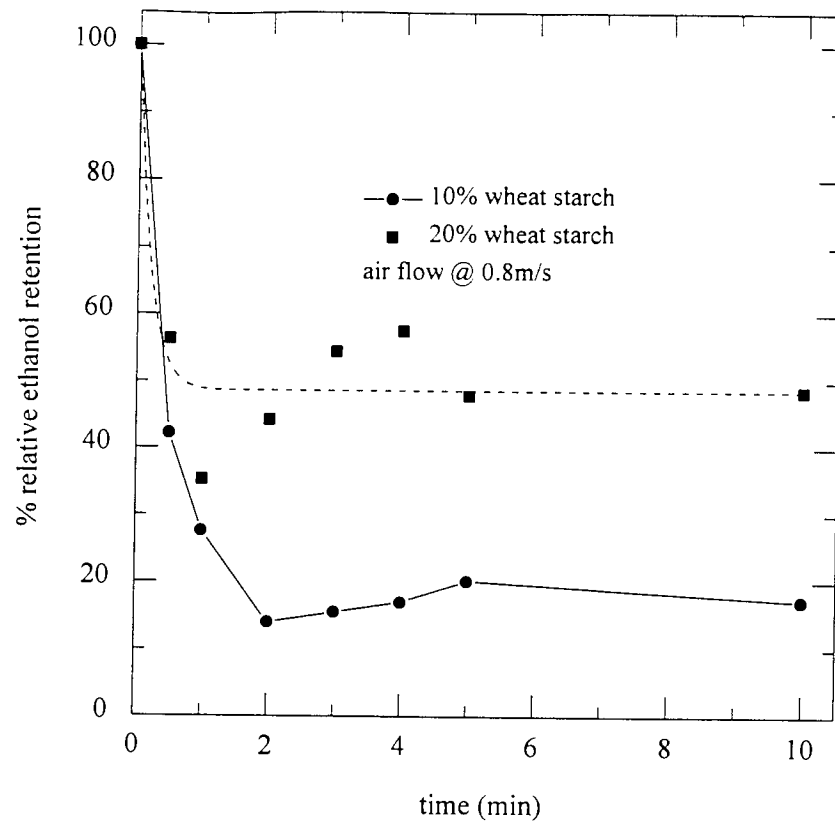


Figure 7.5a

The effect of initial concentration on the retention of ethanol in wheat starch solutions at 62°C

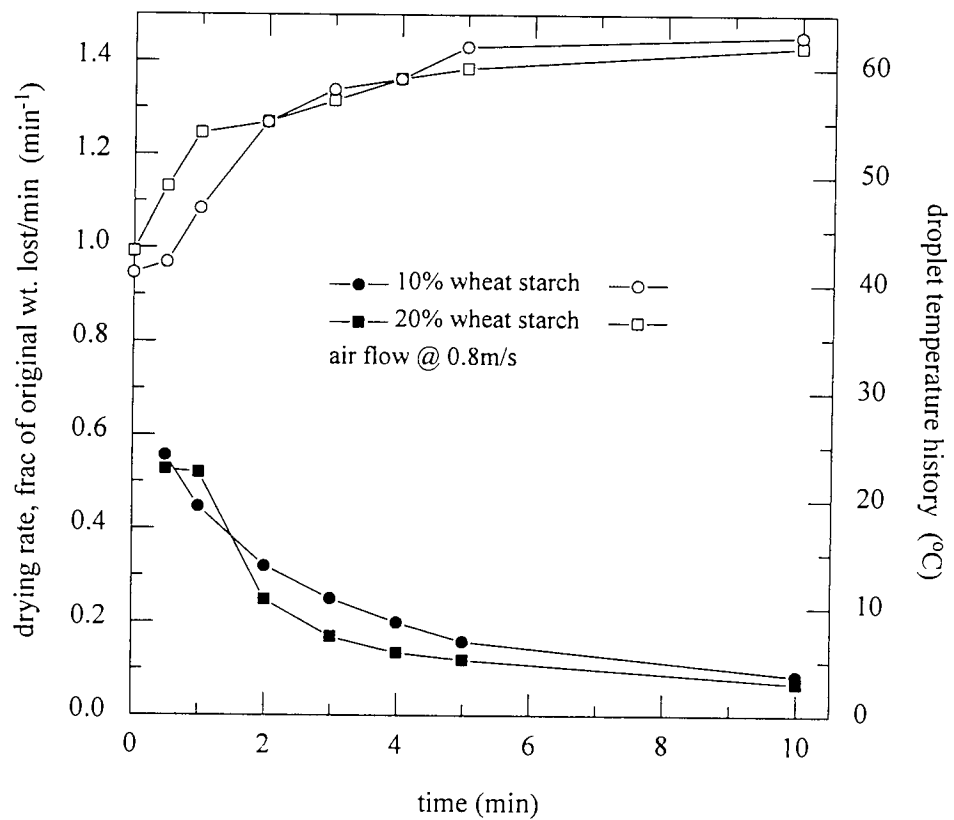


Figure 7.5b

The drying rate [solid symbols] and droplet temperature history [open symbols] for wheat starch solutions

The temperature histories, shown in Figure 7.3b, illustrate that again there was a fall in droplet temperature to the wet bulb temperature before a gradual increase to the temperature of the drying air. The drying rates show that there was a more rapid falling-rate for solution A than for solution B, suggesting that the skin formed at the lower concentration was porous to moisture thereby resulting in more initial loss than at the higher concentration. After two minutes, the drying rates equalised suggesting that the skin must have reached a critical thickness necessary for the effective prevention of loss of moisture, and hence the ethanol.

Figure 7.4a shows that by increasing the air temperature to 40°C, $t_{1/2}$ increased slightly to just above one minute for solution B and just under one minute for solution A. A greater final retention was also evident; 15% for solution A and 30% for solution B.

Referring to Figure 7.4b, the temperature histories for both the concentrations are similar, there was a steady increase in the droplet temperature, until after 4 minutes exposure, the droplets attain the drying air temperature. The drying rates were also similar, showing only one falling-rate period for both concentrations. The steady increase in the droplet temperature, coupled with the drying rates, suggests that there was a reduction in evaporation from the surface, resulting in enhanced ethanol retention.

At 62°C, i.e. at the gelatinisation temperature of the wheat starch, shown in Figure 7.5a, the $t_{1/2}$ was again less than thirty seconds, but the final retention increased to 50% for solution B and 20% for solution A. At $t = 1$ min, there was a decrease in the value of retention of solution B possibly because of the morphological effects upon the droplet, such as inflation / deflation and rupturing of the skin / crust, as reported by Sayed *et. al.*, 1995.

Figure 7.5b shows that there was a steady increase in droplet temperature towards the drying air temperature, again suggesting a reduction in moisture migration to the surface (and its subsequent evaporation to keep the droplet

temperature constant). The drying rates for both the concentrations were also similar, with only one falling-rate period in each case. The results again suggest that the critical thickness of skin had formed to allow a reduction in moisture, and hence ethanol, loss.

On exposure to the drying air, a wheat starch droplet, with the absorbed water, immediately forms a partly dried skin on the surface of the droplet (Hassan & Mumford, 1993). This skin, shown in Plate 7.2, offers increased resistance to mass flow, and this accounts for the increasing retention of the simulated flavour. The higher initial concentration of the wheat starch results in greater retention because of the formation of a thicker skin. The increase in viscosity with increasing starch concentrations also provides an increased resistance to the diffusion of the volatile flavour to the surface but this is likely to be of a lower order of magnitude.

7.1.1.3: Dextrin

Dextrins are a product of the decomposition of polysaccharides by chemical or physical means. Although they have the same empirical formula, they have a lower molecular weight than the native starch. In contrast to starch, however, dextrins are soluble in water (Heimann, 1980).

With reference to Figure 7.6a, it is evident that at ambient temperature, there was an increase in the final retention of ethanol with an increase in initial concentration, i.e.:

- i) for solution A, the retention was less than 5%,
- ii) for solution B, the retention was 10%, and
- iii) for solution C, the retention was 40%.

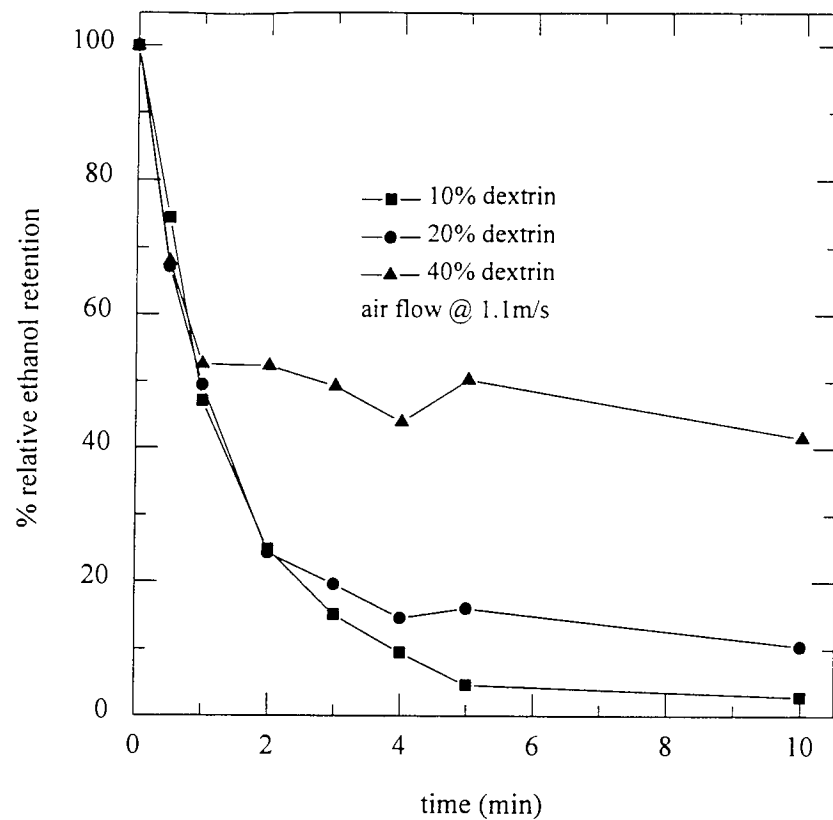


Figure 7.6a

The effect of initial concentration on the retention of ethanol in dextrin solutions at ambient temperature ($T=25^{\circ}\text{C}$)

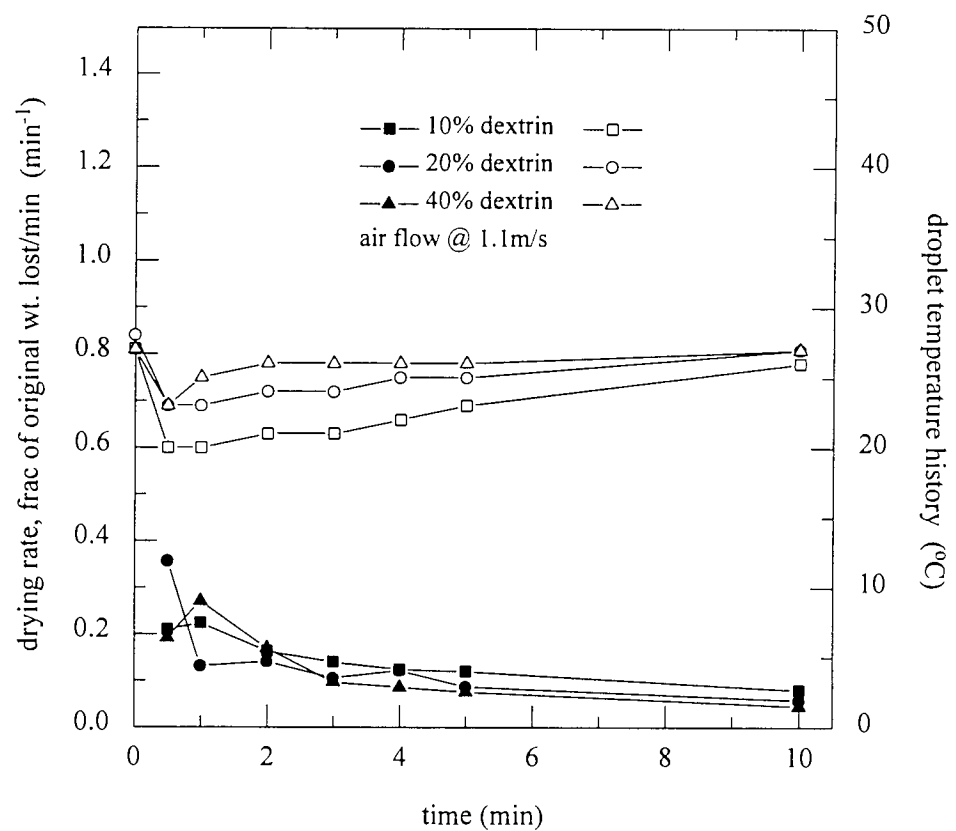


Figure 7.6b

The drying rate [solid symbols] and droplet temperature history [open symbols] for dextrin solutions

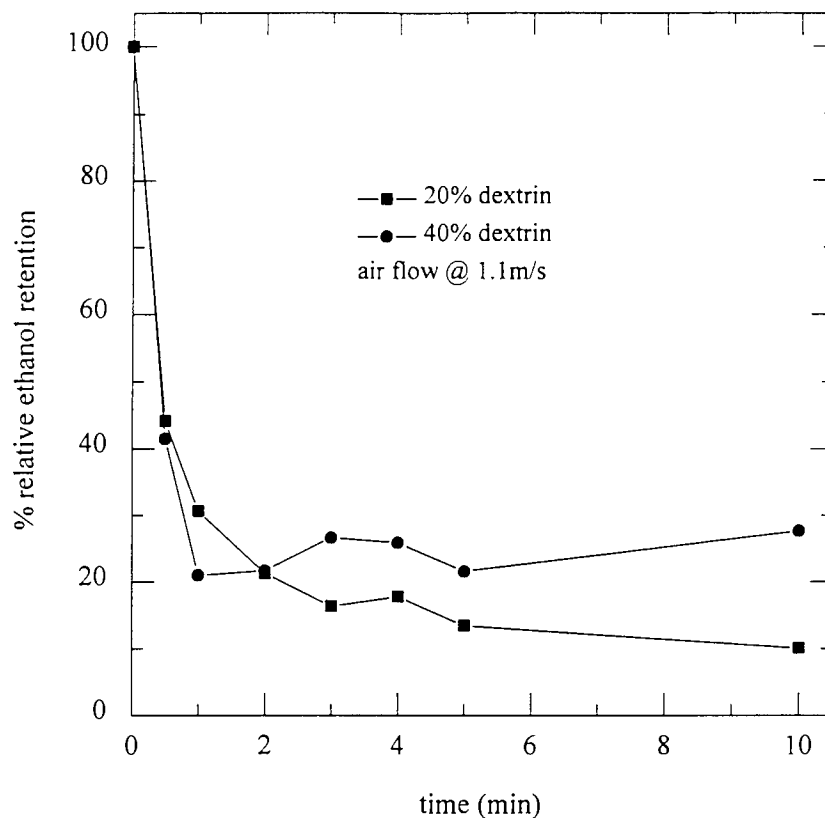


Figure 7.7a

The effect of initial concentration on the retention of ethanol in dextrin solutions at 42°C

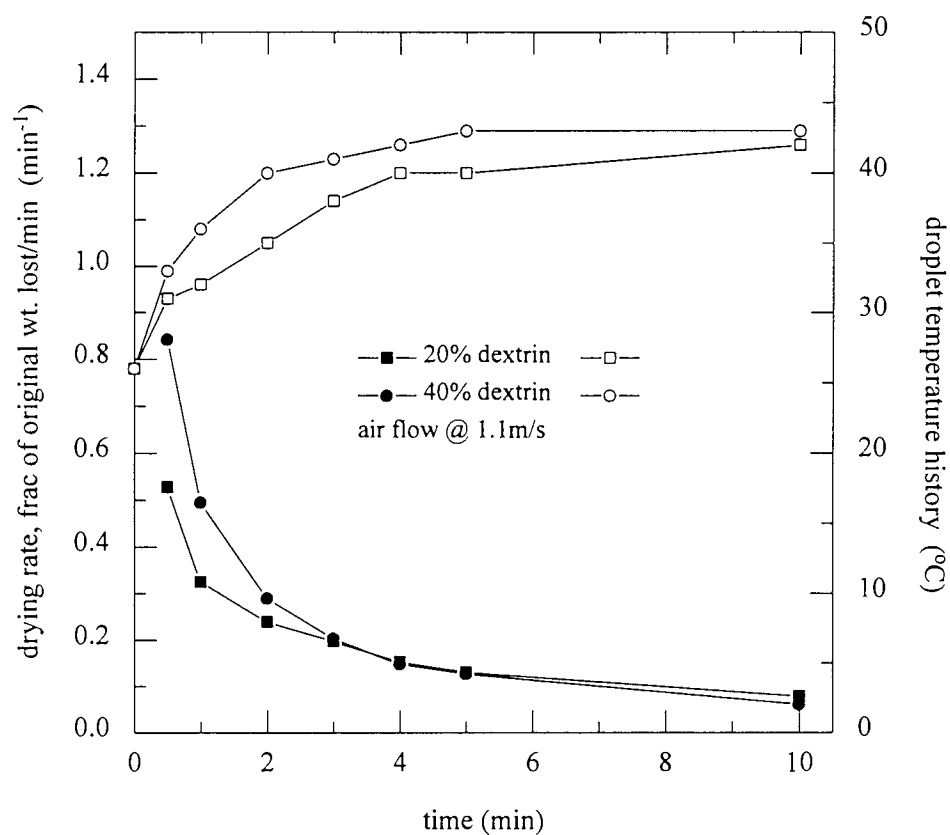


Figure 7.7b

The drying rate [solid symbols] and droplet temperature history [open symbols] for dextrin solutions

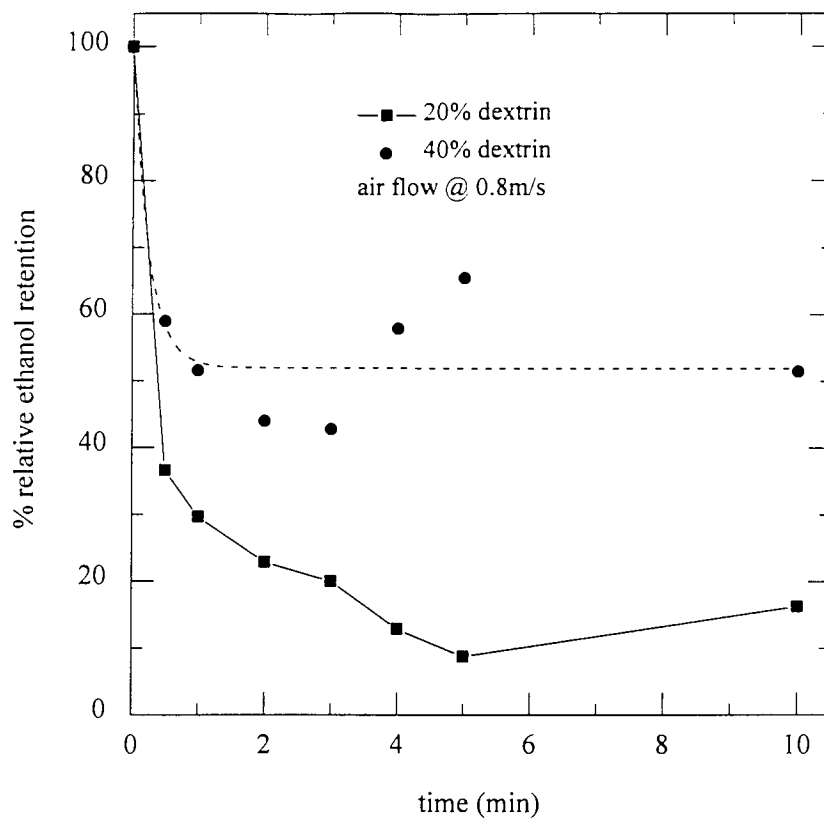


Figure 7.8a

The effect of concentration on the retention of ethanol in dextrin solutions at 62°C

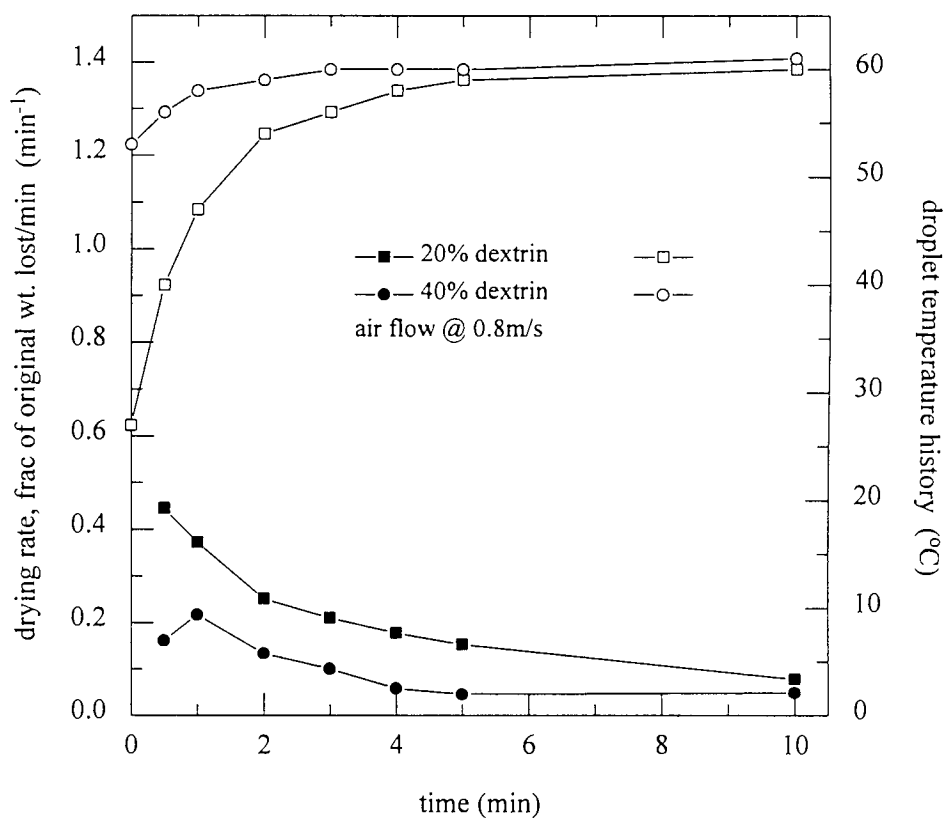


Figure 7.8b

The drying rate [solid symbols] and droplet temperature history [open symbols] for dextrin solutions

This phenomenon, of increasing retention with increasing concentration, has also been reported by other workers such as Furuta *et. al.*, 1984, and Tsujimoto *et. al.*, 1985. Although there was increased retention with increasing concentration, $t_{1/2}$ was the same for all three solutions, i.e. $t_{1/2} = 1$ minute. This time could correspond to that after which there was skin formation on the droplet surface. The greater the initial concentration, the thicker the skin, thereby preventing the loss of moisture (and ethanol) from the droplet.

Figure 7.6b shows that at all three concentrations, the droplet temperature initially fell to the wet bulb temperature before increasing steadily to the drying temperature. Also, there was only one very gently decreasing falling-rate period evident for all three concentrations; this again suggests there was a reduction in the loss of moisture from the droplets.

By increasing the air temperature to 42°C, with reference to Figure 7.7a, there was little change in retention except that the $t_{1/2}$ was reduced to thirty seconds for both solutions B and C. There was no change in the final retention for solution B, but for solution C, the final retention was reduced to less than 30%.

The temperature histories, shown in Figure 7.7b, show a rapid increase in the droplet temperature to the prevalent drying air temperature. The drying rates show two falling-rate periods, the first falling-rate, shown by the reduced retention of ethanol, and the second falling-rate, where the drying rate is slow, with the droplets gradually reaching equilibrium with the drying air, shown by the levelling off of the ethanol retention graph (Figure 7.7a).

Referring to Figure 7.8a, the increase in the temperature to 62°C resulted in a marked effect of concentration upon the retention. The $t_{1/2}$ for solution B remained close to thirty seconds, but increased for solution C to ninety seconds. Also the final retentions for both the solutions were increased to 50% for solution C and approximately 15% for solution B. The low ethanol

retention values, at $t = 4$ and 5 minutes, for solution B were probably due to morphological changes, such as droplet expansion, which would enhance mass transfer and reduce ethanol retention. Similarly at the same times, the droplets of solution C showed a markedly higher ethanol retention than the trend shown by the preceding points. This may be explained by the fact that droplet expansion, a random occurrence, may not have occurred in this case to result in the higher ethanol retention.

Figure 7.8b shows that there was a rapid increase in temperature of the droplets of solution B compared to solution C partly because the droplets of solution B experienced a lower initial temperature ($<30^{\circ}\text{C}$). The drying rates show only one falling-rate period for both concentrations; with the drying rate for solution B greater than that for solution C. This would suggest that there was an increased resistance to mass transfer with the higher initial concentration solution, explaining the resultant increased ethanol retention for solution C.

7.1.1.4: Fructose

Fructose is a hexose sugar found in large amounts in sweet fruits, and is difficult to crystallise (Heimann, 1980). It is hygroscopic and easily forms an aqueous solution.

The effect of concentration on the retention of ethanol was evaluated for two concentrations, viz. 20% and 40%, and at two temperatures, ambient and 62°C .

At ambient temperature, in Figure 7.9a, the behaviour of both solutions was similar upto $t = 2$ minutes after which, at the lower concentration, the final retention value is zero but that for solution C, the final retention is approximately 7%.

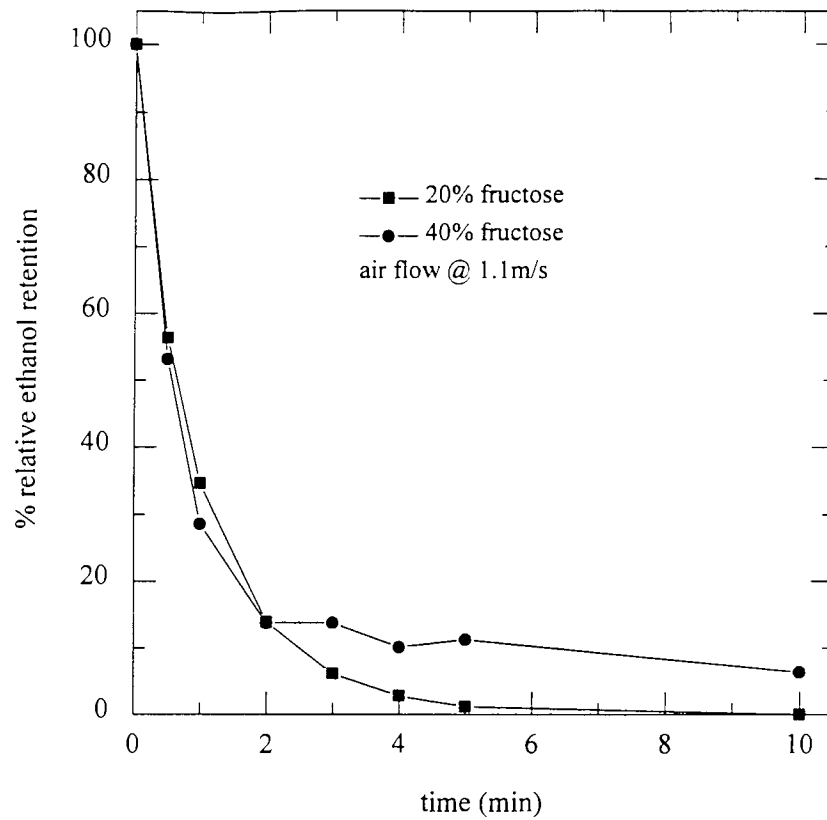


Figure 7.9a

The effect of initial concentration on the retention of ethanol in fructose solutions at ambient temperature ($T=25^{\circ}\text{C}$)

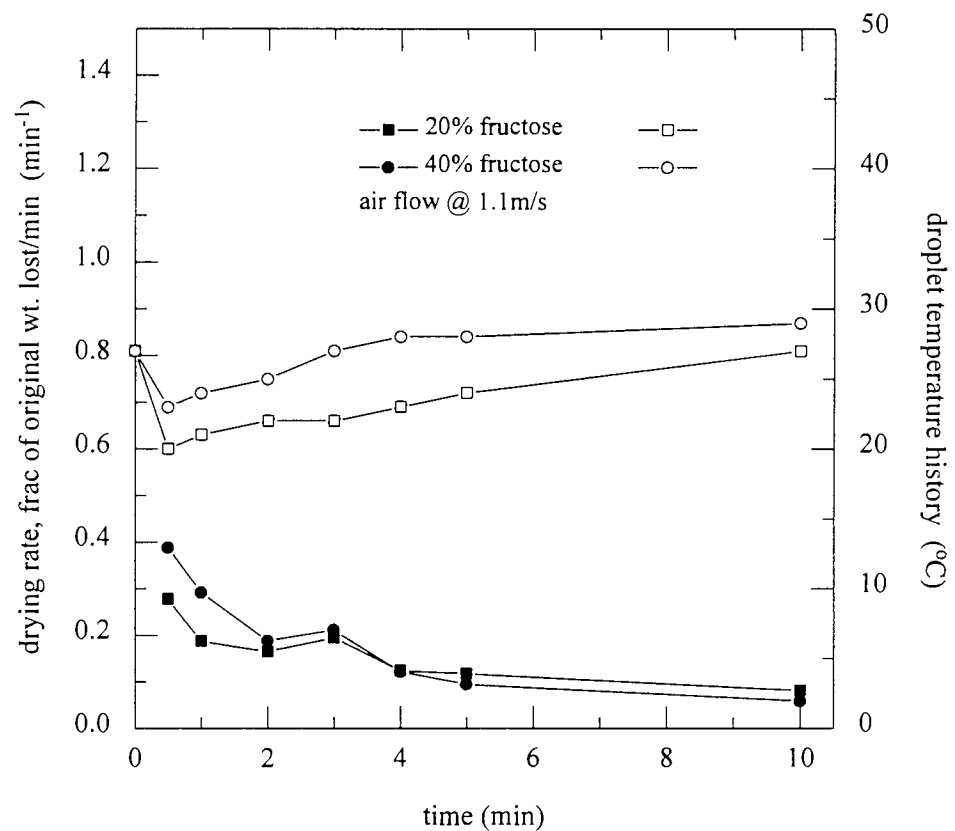


Figure 7.9b

The drying rate [solid symbols] and droplet temperature history [open symbols] for fructose solutions

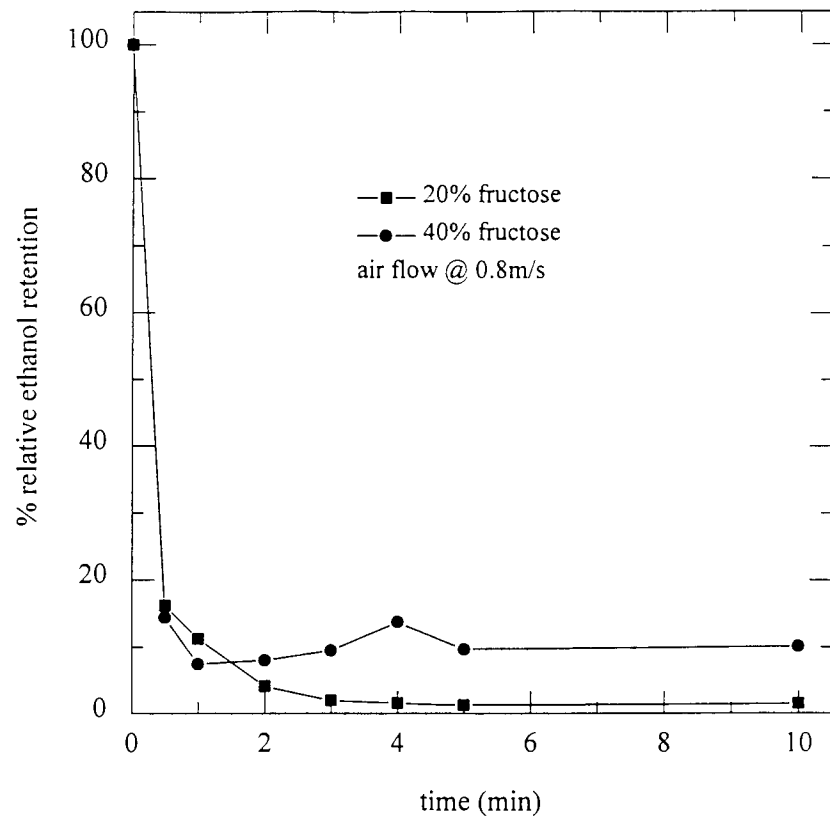


Figure 7.10a

The effect of initial concentration on the retention of ethanol in fructose solutions at 62°C

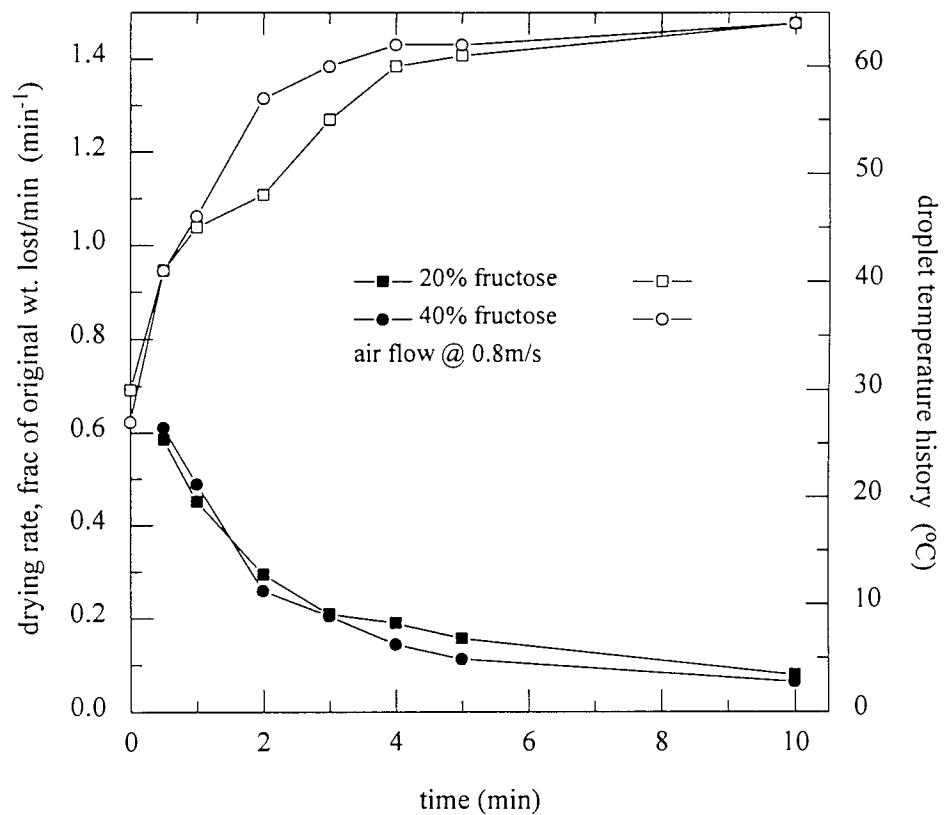


Figure 7.10b

The drying rate [solid symbols] and droplet temperature history [open symbols] for fructose solutions

The $t_{1/2}$ for both solutions was approximately one minute. The slight increase with an increase in initial concentration could be partially explained by the more rapid formation of a viscous solution, which would hinder molecular diffusion, at the higher concentration. The decrease in water concentration would also have caused a decrease in the diffusivity coefficients with the flavour diffusivity decreasing much faster than that of the water (Kerkhof & Thijssen, 1974).

Referring to Figure 7.9b, which shows the droplet temperature histories and corresponding drying rates, the droplet behaviour was similar at both concentrations. The temperature initially fell to the wet bulb temperature before increasing gradually to that of the drying air. The drying rates show only one falling-rate period; the faster rate in the first two minutes explains the ethanol loss which occurred in this time.

At the higher temperature, i.e. 62°C, the $t_{1/2}$ for both solutions had been reduced to under thirty seconds, as shown in Figure 7.10a. There was no gradual onset of the loss of volatiles, but the loss was sudden, levelling to approximately 10% and 2% for solutions C and B respectively.

Figure 7.10b shows that the droplet temperatures, for both concentrations, increased rapidly to reach the drying air temperature within 4 minutes of exposure to the drying air. Again only one falling-rate period is in evidence, but with a steeper gradient compared to that at 25°C. This suggests that the temperature driving force was the major influence upon the loss of ethanol from the droplets.

7.1.1.5: Sucrose

Referring to Figure 7.11a, at ambient temperature (25°C), there was little or no effect of initial concentration, on the retention of ethanol, upto $t = 2.0$ minutes, after which the two retention traces diverge. Both solutions B and C

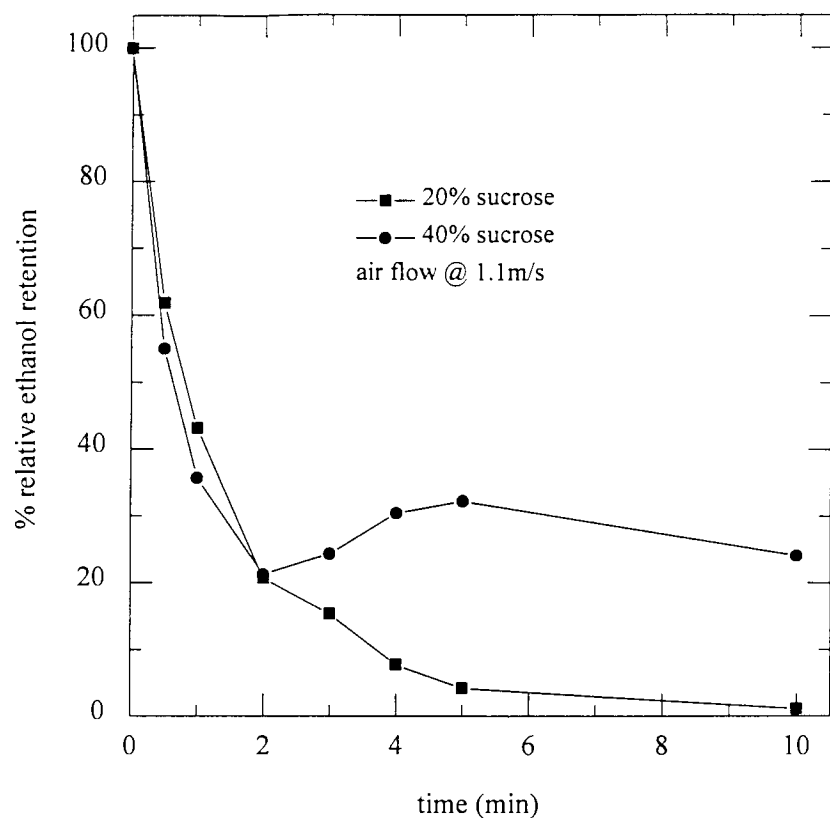


Figure 7.11a

The effect of initial concentration on the retention of ethanol in sucrose solutions at ambient temperature ($T=25^{\circ}\text{C}$)

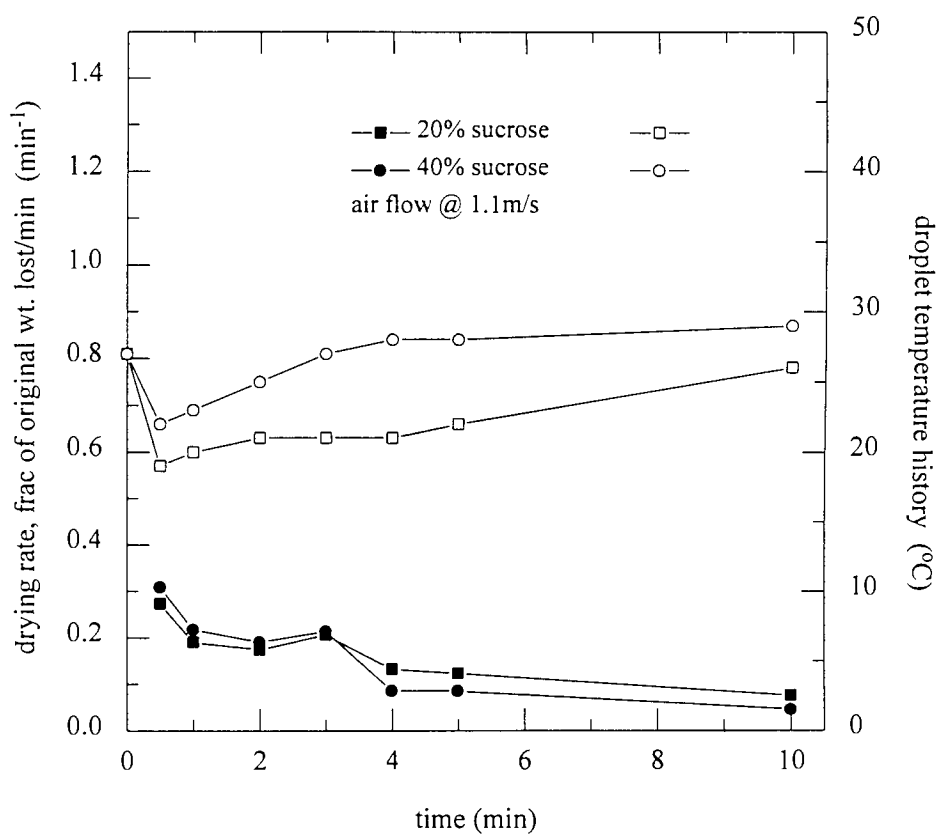


Figure 7.11b

The drying rate [solid symbols] and droplet temperature history [open symbols] for sucrose solutions

had the same $t_{1/2}$ (\cong one minute). The formation of a more viscous liquid, at the higher concentration, which hindered molecular diffusion could probably account for the increased retention at the higher concentration. The increased retention could also be accounted for by the decreasing diffusivity of the volatile flavour as the drying process progressed. The final retention values were zero for solution B and approximately 24% for solution C.

Figure 7.11b again shows that the droplet temperature fell to the wet bulb temperature before the gradual increase to the prevalent air temperature, suggesting that initially there was evaporation from the wet surface. The gradual increase in temperature, and the one falling-rate period, suggest that this subsequently changed to diffusion controlled evaporation.

7.1.1.6: Skim milk

Skim milk was chosen as the encapsulant in preference to ordinary pasteurised milk because the latter contains fat molecules in suspension which would affect the nature of skin formation.

At 25°C, shown in Figure 7.12a, the $t_{1/2}$ was one minute for solution B and nearer two minutes for solution C, i.e. the $t_{1/2}$ was effectively doubled by the doubling of the initial concentration from 20% to 40%. As drying progressed, the retention in solution B gradually decreased until a final value of approximately 10% was attained, whilst the final retention with solution C approached 44%. The increased retention with the higher concentration solution would probably be accounted for by the rapid formation of a skin, which thickens with increasing drying time, providing an increased resistance to mass transfer by vapour diffusion (Hassan & Mumford, 1993).

Referring to Figure 7.12b, there was only one similar falling-rate period for both concentrations. As regards the droplet temperatures, droplets of solution B initially fell to the wet bulb temperature before increasing unlike

those from solution C, which gradually increased upto the drying air temperature. This suggests that for the lower concentration, there was evaporation from a wet surface, but for the higher concentration, solution C, only diffusion-controlled evaporation was occurring from the droplet surface.

At 65°C, illustrated in Figure 7.13a, there was little change to the retention of solution C, there is only a slight increase in final retention to 48%. But with solution B, although $t_{1/2}$ remained at one minute, there was almost a three-fold increase in the final retention value from approximately 10% to 36%. This was probably due to rapid formation of a vapour resistant skin which effectively contained the diffusing vapour leading to greater retention.

Figure 7.13b shows that there was a rapid increase in the droplet temperature for solution B; this suggests that the interior of the droplet was being heated, i.e. there was little or no evaporation from a wet surface. This would probably result from the formation of a skin which was resistant to mass transfer. Hence, the rapid increase in temperature, coupled with the increased retention of ethanol for solution B, is consistent with the formation of a skin, which was resistant to mass transfer, formed on the droplet surface.

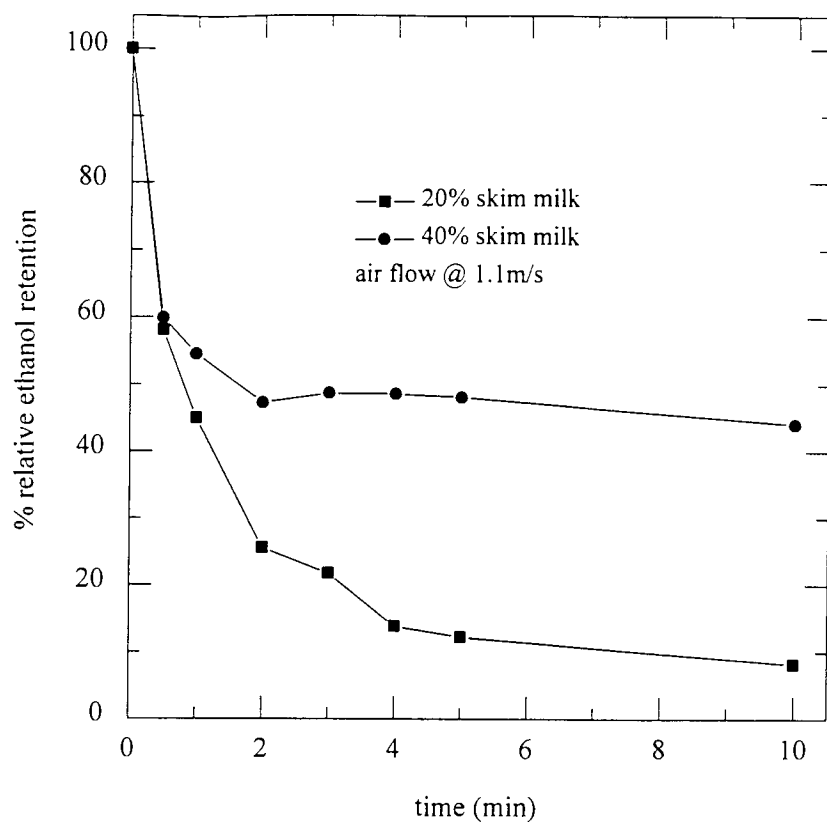


Figure 7.12a

The effect of initial concentration on the retention of ethanol in skim milk solutions at ambient temperature ($T=25^{\circ}\text{C}$)

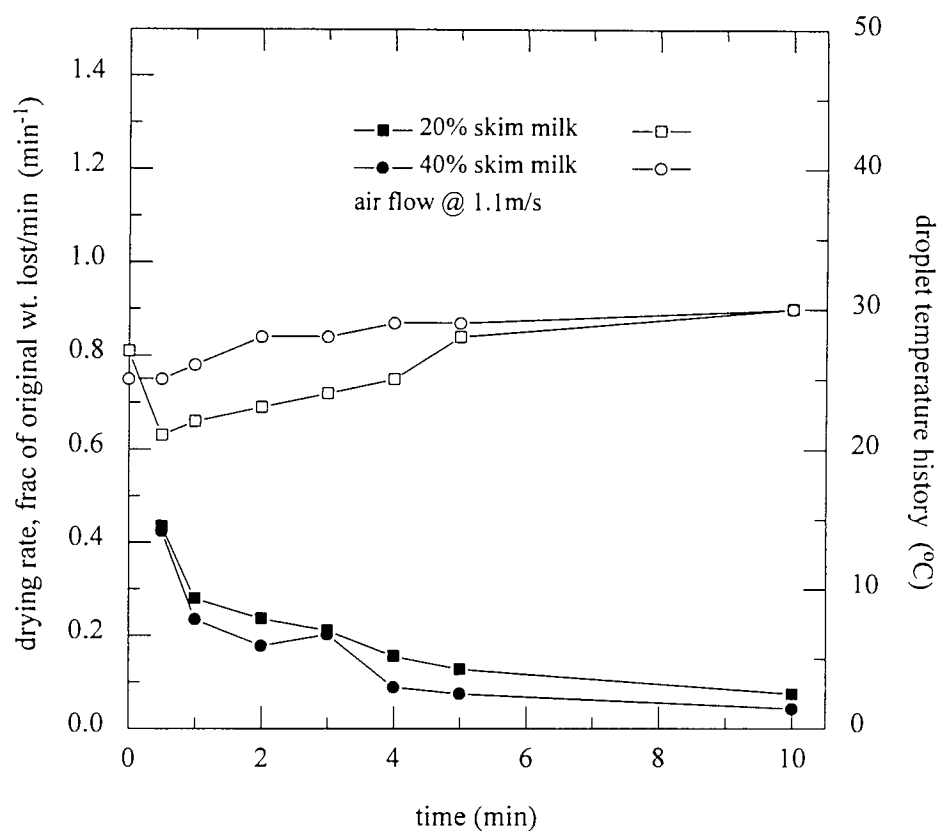


Figure 7.12b

The drying rate [solid symbols] and droplet temperature history [open symbols] for skim milk solutions

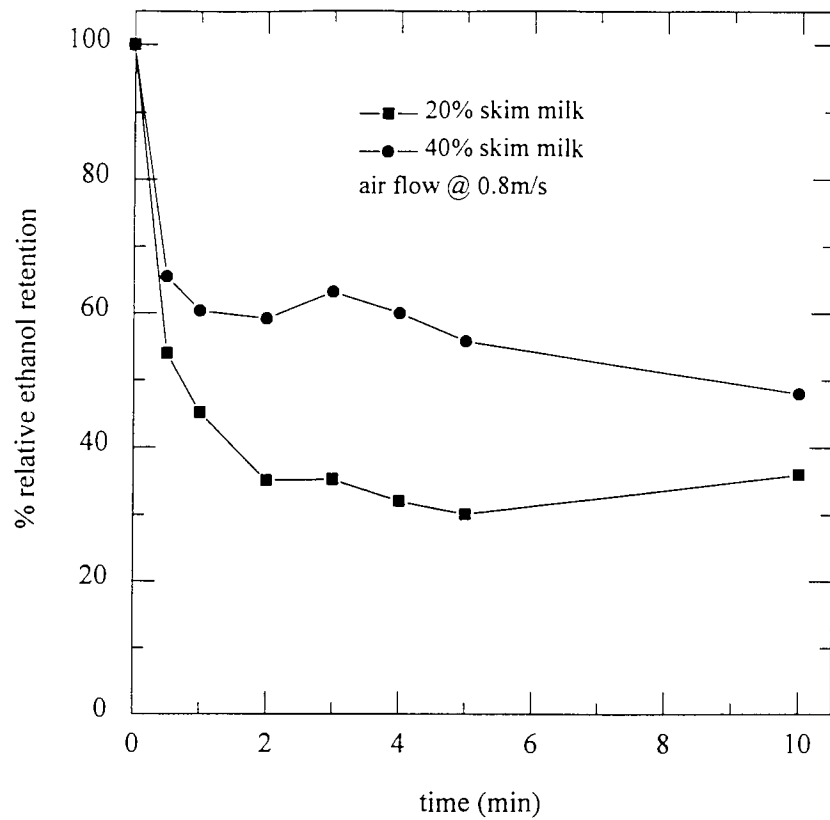


Figure 7.13a

The effect of initial concentration on the retention of ethanol in skim milk solutions at 62°C

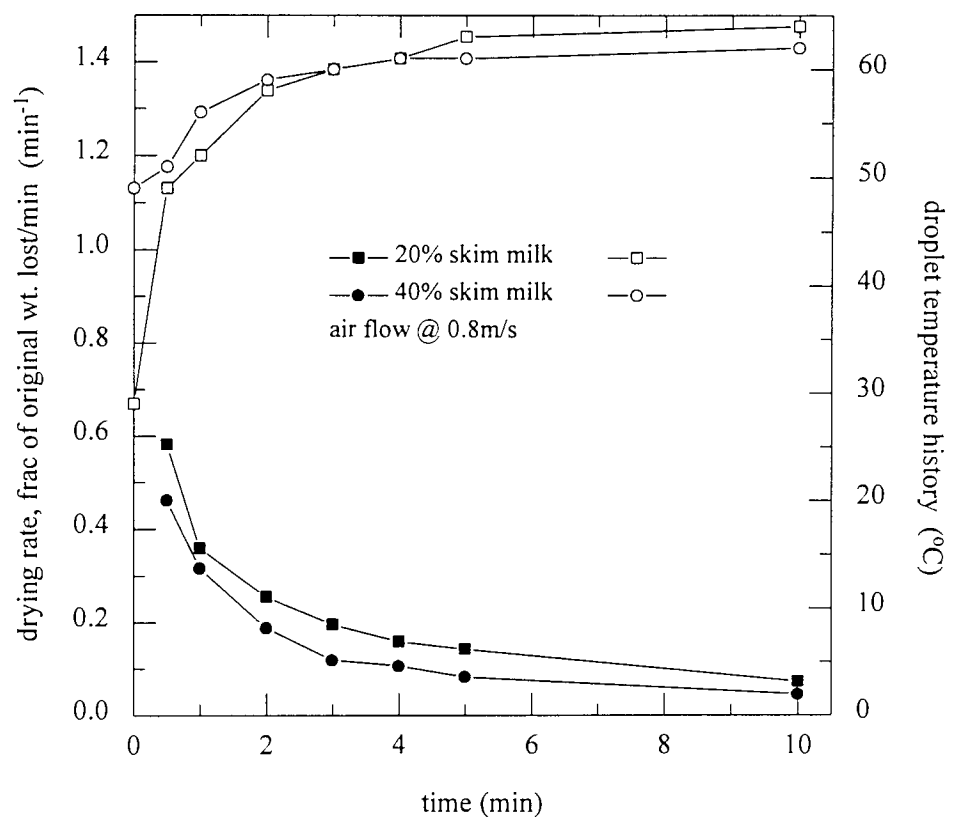


Figure 7.13b

The drying rate [solid symbols] and droplet temperature history [open symbols] for skim milk solutions

7.1.1.7: Coffee

The droplets of coffee of both concentrations and at ambient temperature (25°C) demonstrated a similar trend in their retention histories, as illustrated in Figure 7.14a, except that with solution B $t_{1/2}$ = 2.0 minutes and for solution C $t_{1/2} \cong 4.0$ minutes, and the values of final retention are 30% and 50% for solutions B and C respectively. An explanation for this could be the faster formation of a skin on the droplet of solution C compared to that of solution B.

As shown in Figure 7.14b, there is only one falling-rate period for both solutions, and the droplet temperature histories are also similar for both.

With reference to Figure 7.15a, both solutions had a similar $t_{1/2}$ ($\cong 1.0$ minute) and the trends in ethanol retention were similar upto $t = 3.0$ minutes, after which there was increased retention with solution C compared to solution B. However there was no overall difference in the final values of retention for each solution at the two temperatures, except for the reduction in $t_{1/2}$ at the higher temperature.

Figure 7.15b shows that the droplet temperatures, especially for solution B, increased rapidly towards the drying air temperature. After approximately 3 minutes, the increase occurs at a much reduced rate. This, coupled with the observed ethanol retention, would tend to suggest that the loss of ethanol in the first three minutes of drying is governed by the temperature driving force, after which a resistant skin forms which reduces further loss from the droplet. Again there is only one falling-rate period.

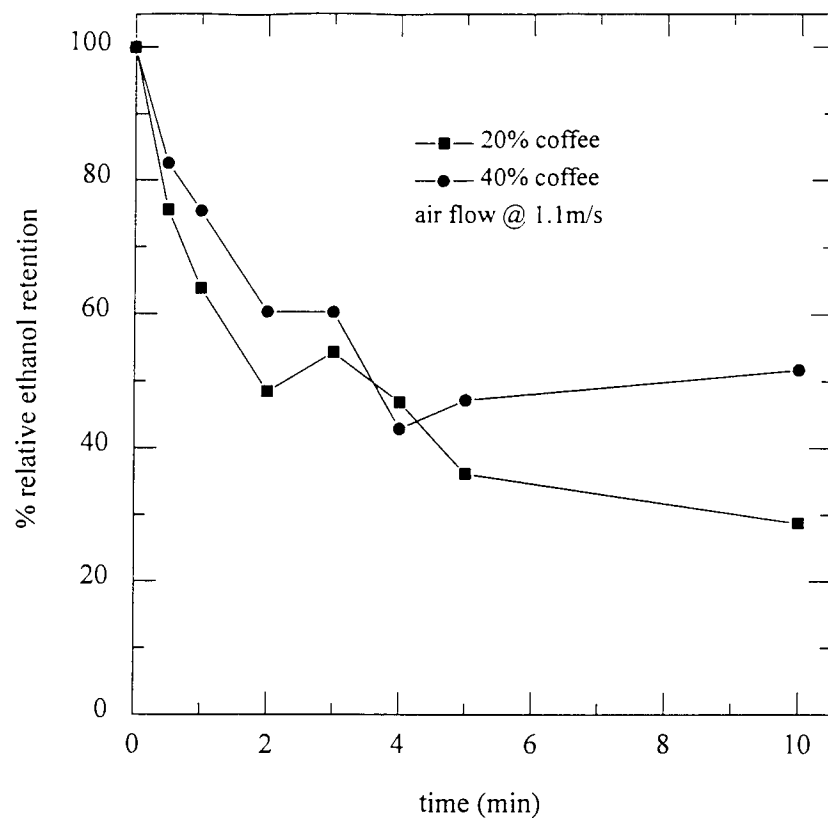


Figure 7.14a

The effect of initial concentration on the retention of ethanol in coffee solutions at ambient temperature ($T=25^{\circ}\text{C}$)

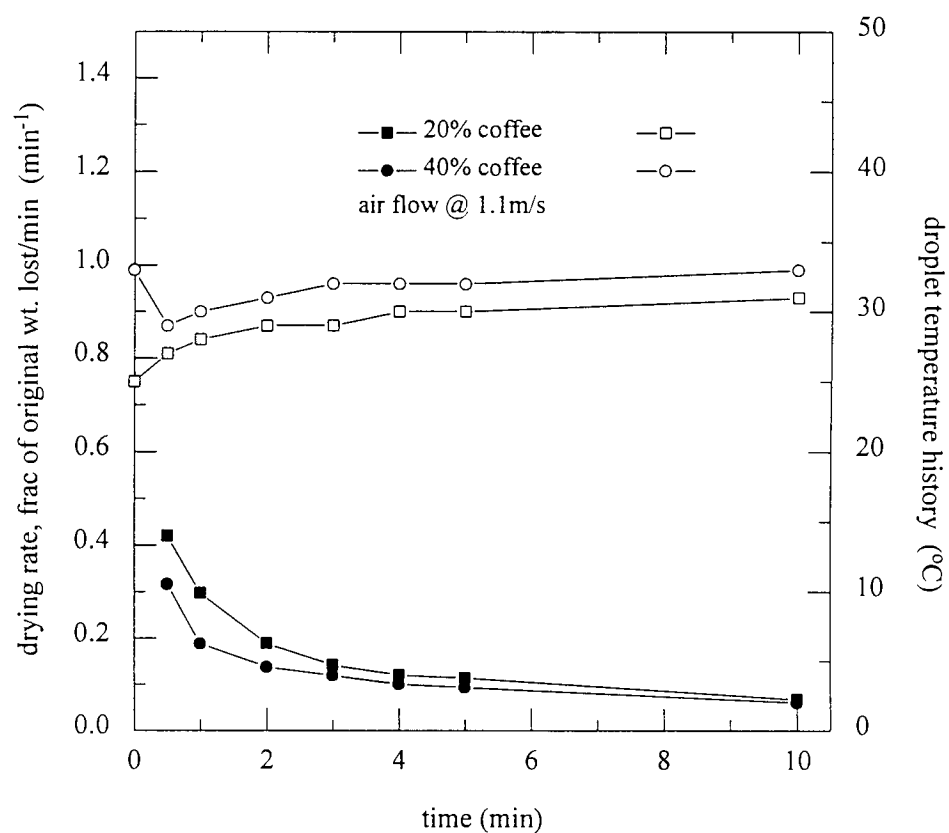


Figure 7.14b

The drying rate [solid symbols] and droplet temperature history [open symbols] for coffee solutions

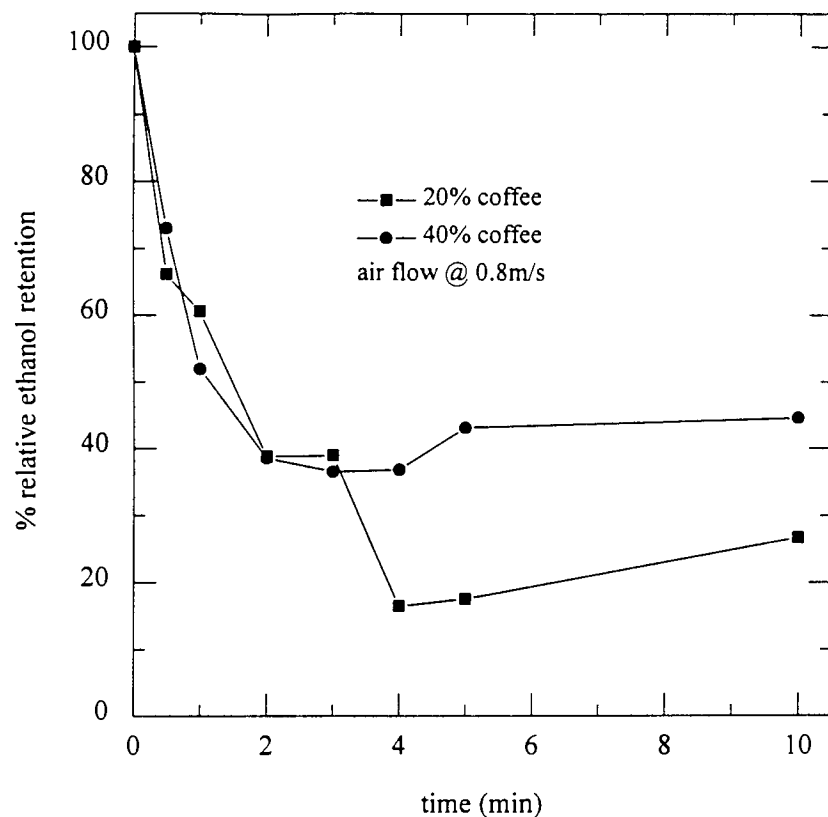


Figure 7.15a

The effect of initial concentration on the retention of ethanol in coffee solutions at 62°C

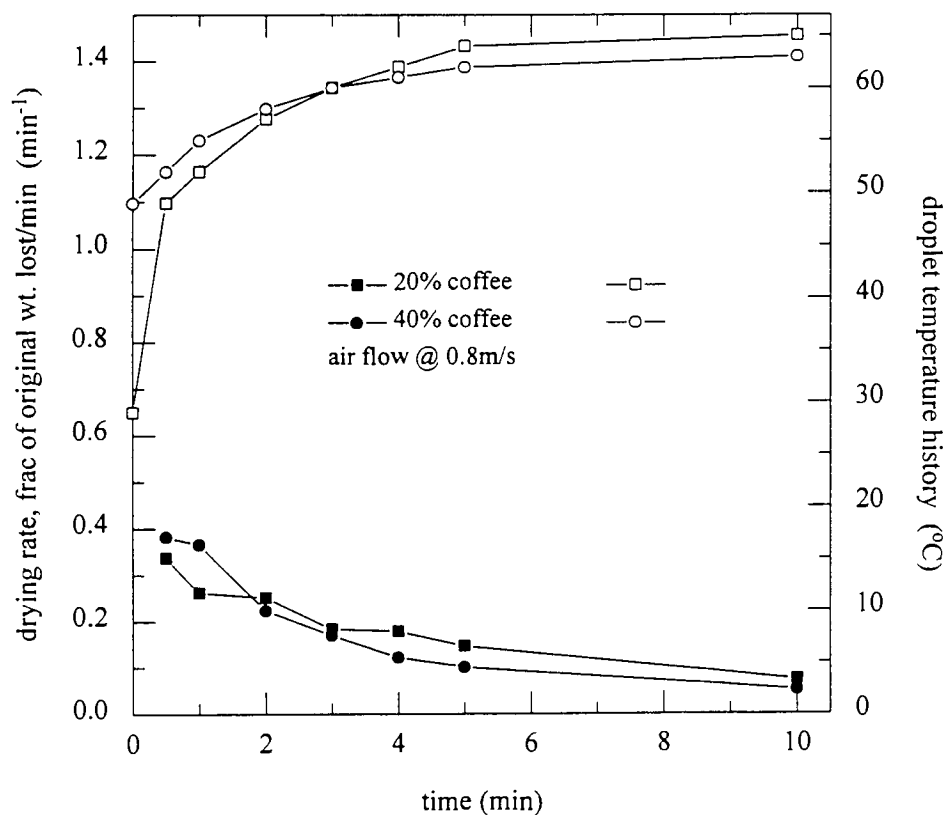


Figure 7.15b

The drying rate [solid symbols] and droplet temperature history [open symbols] for coffee solutions

7.1.1.8: Gelatine 60

The effect of initial concentration of gelatine 60 is illustrated in Figure 7.16a. At ambient temperature, the $t_{1/2}$ values for both solutions was less than thirty seconds, with a final retention of 10% and 30% for solutions B and C respectively. An increase in retention was found at $t = 3, 4,$ and 5 minutes before the final retention value at $t = 10$ minutes for solution C. A possible explanation for this behaviour could be the uneven mixing of the granules and the solvent (water / ethanol) when the solvent was added to the gelatine granules as they rapidly absorbed the solvent to form a gel, i.e. the droplets could have been sampled from pockets with a higher ethanol content, giving rise to increased retentions.

If these three points are ignored, the trend for both solutions is similar except for the higher retention with solution C, attributed to the higher concentration causing a reduction in the diffusivity of the volatile flavour in accordance with the selective diffusion theory.

Figure 7.16b illustrates that droplets of both concentrations initial fell to the wet bulb temperature. The drying rates show two falling-rate periods. The lower concentration droplet showed a steeper drying rate, i.e. there was more localised wet surface evaporation on the droplets of solution B than of solution C.

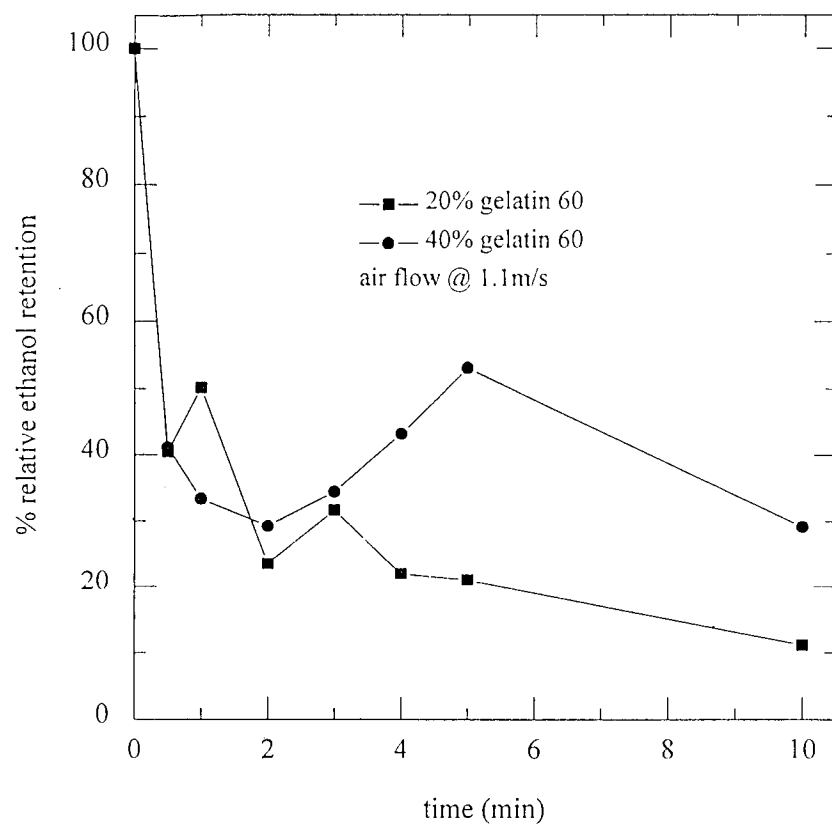


Figure 7.16a

The effect of concentration on the retention of ethanol in gelatin 60 solutions at ambient temperature ($T=25^{\circ}\text{C}$)

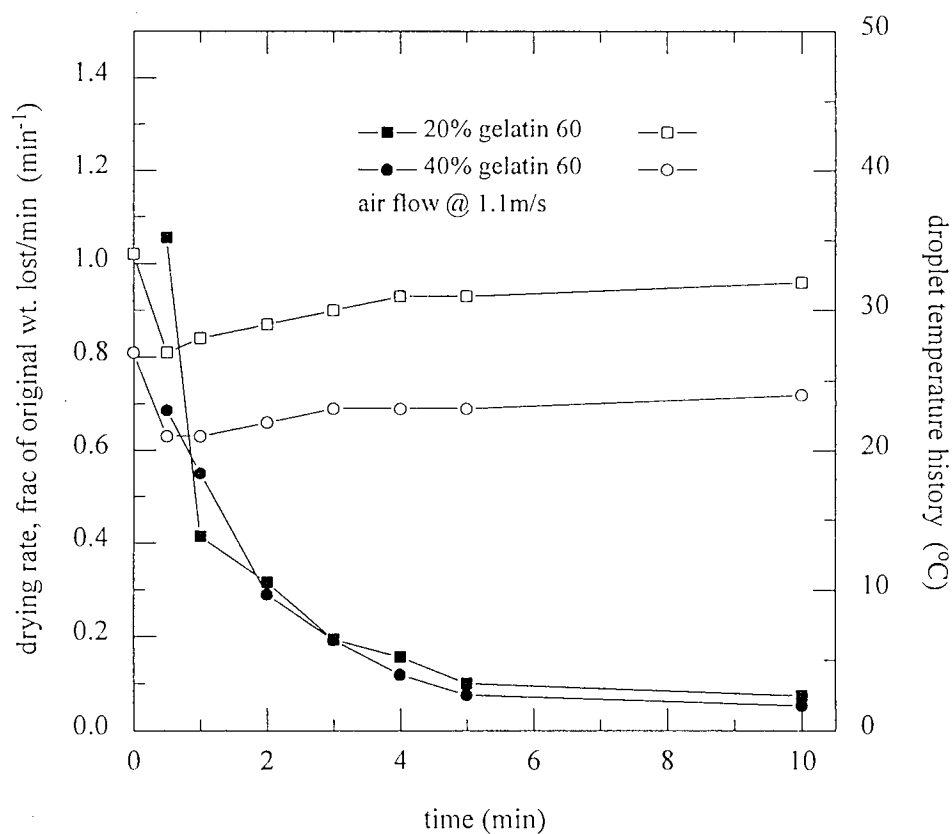


Figure 7.16b

The drying rate [solid symbols] and droplet temperature history [open symbols] for gelatin 60 solutions

7.1.1.9: Gelatine 150

The gel formed by gelatine 150 is stronger than that formed by gelatine 60. Therefore the skin formed by gelatine 150 should be more resistant to mass transfer by vapour diffusion, and hence result in higher retention values. Figure 7.17a illustrates this contention as the final retention values are increased especially for solution B from 10% to 25%; there was a slight change for solution C with retention increasing from 30% to 35%. There also was a difference in $t_{1/2}$ between the two solutions; $t_{1/2} \leq 30$ s for solution B $t_{1/2} = 1$ minute for solution C. A similar explanation could be used here because as the water is lost, there is a decrease in the diffusivity of the volatile flavour, thereby causing an increase in volatiles retention.

Figure 7.17b shows a similar trend, for both concentrations, in their temperature histories and drying rates. After approximately 2 minutes of drying, the drying rate levels off to almost a constant-rate; this would tend to suggest that the skin which formed at any drying temperature (Hassan & Mumford, 1993) was better at preventing moisture, and thus volatiles, loss.

7.1.1.10: Gum arabic

Gum arabic is composed of highly branched acidic protein-polysaccharides, is highly soluble and has a low viscosity, a 20% w/w solution resembling a thin sugar syrup in body and flow properties (Bemiller, 1992).

The effect of initial concentration on the retention of ethanol with solutions of gum arabic at 25°C, shown in Figure 7.18a, reveal that $t_{1/2}$ (= 30 s) was very similar for both solution B and C. The final retention values were also similar, with 21% for solution B and 15% for solution C. A repeat experiment for solution C resulted in a final retention value of 18%, showing that the technique was reproducible.

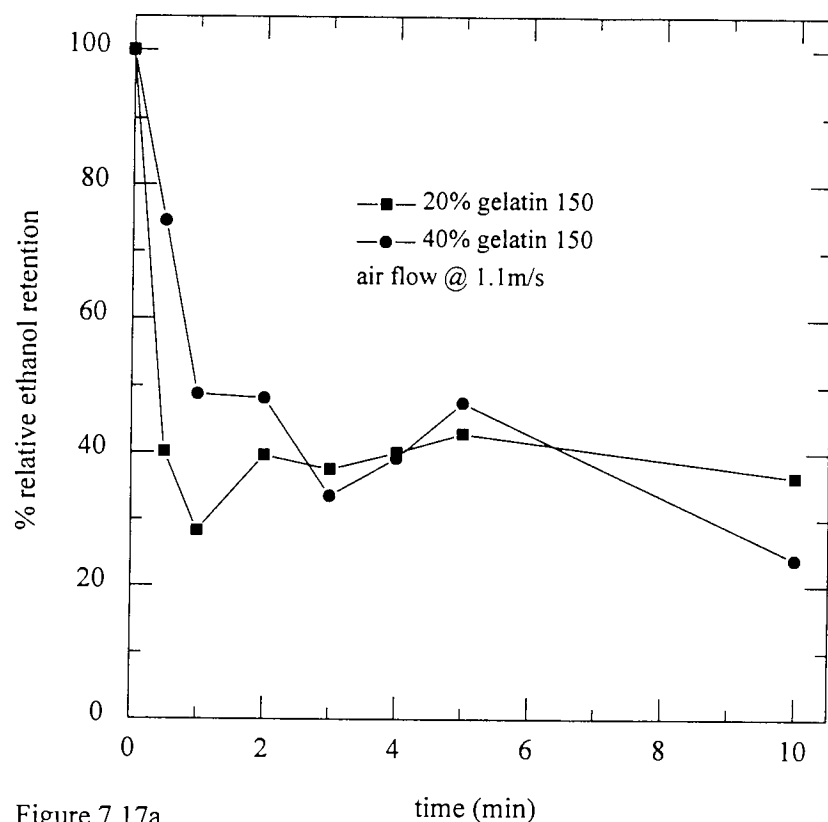


Figure 7.17a

The effect of concentration on the retention of ethanol in gelatin 150 solutions at ambient temperature ($T=25^{\circ}\text{C}$)

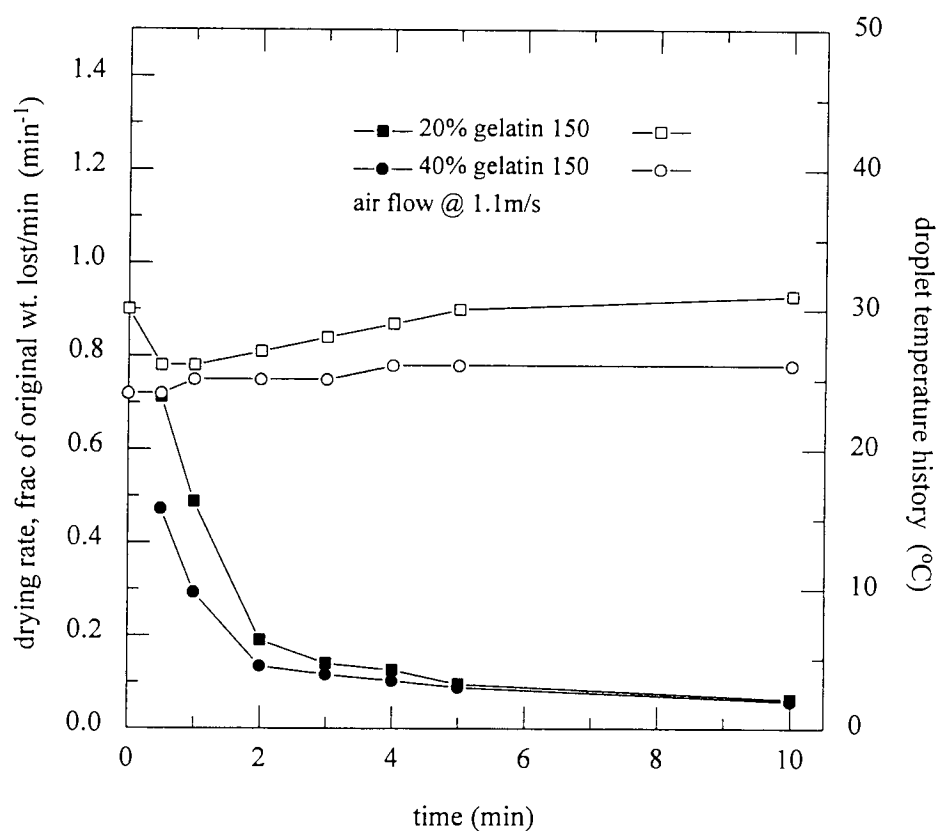


Figure 7.17b

The drying rate [solid symbols] and droplet temperature history [open symbols] for gelatin 150 solutions

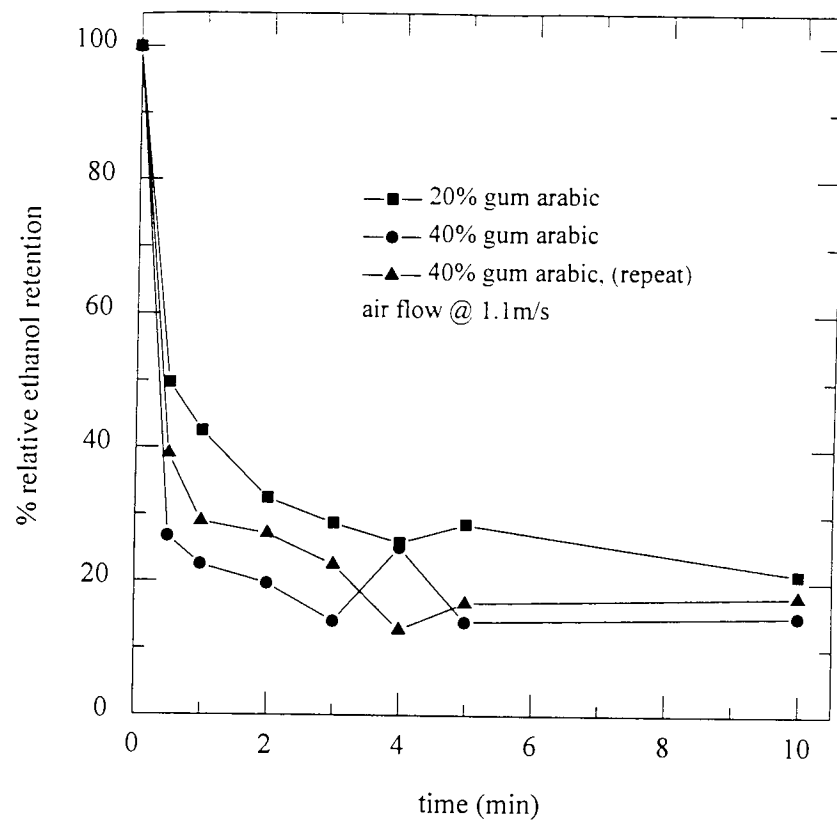


Figure 7.18a

The effect of concentration on the retention of ethanol in gum arabic solution at ambient temperature ($T=25^{\circ}\text{C}$)

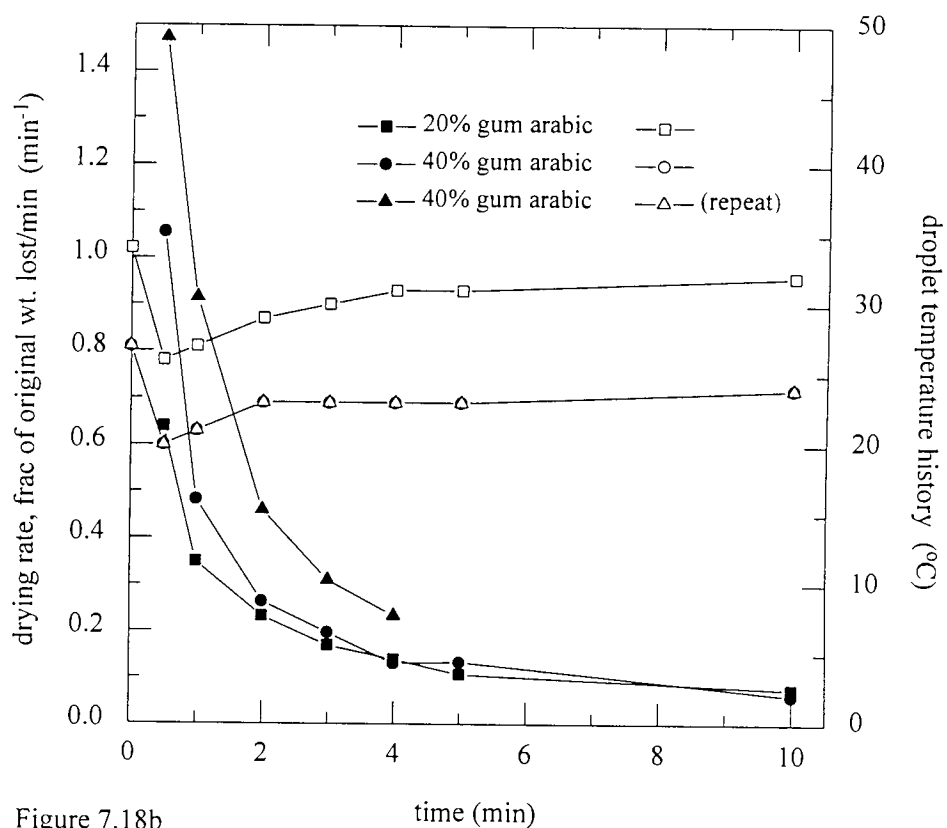


Figure 7.18b

The drying rate [solid symbols] and droplet temperature history [open symbols] for gum arabic solutions

Figure 7.18b shows that there was a fall in droplet temperature to the wet bulb temperature before the gradual increase towards the drying air temperature. This suggests that during the initial stages of drying, evaporation occurs from the wet droplet surface. The subsequent increase in temperature would suggest that there was formation of a skin resistant to mass transfer, resulting in the increased retentions of ethanol. The increase observed with the increase in concentration suggests that the skin may have developed more rapidly at the higher concentration.

7.1.2: The effect of air velocity

The effect of air velocity was determined experimentally for the various encapsulants (at 20% w/w solution), and the results are presented graphically.

7.1.2.1: Rice starch

The results illustrated in Figure 7.19a show that at 25°C there was almost no effect of reducing the air velocity from 1.1 m/s to 0.45 m/s. The $t_{1/2}$ increased from approximately 1 minute to almost 1.5 minutes by increasing the air velocity. The final retention value was the same, i.e. <5%, at both velocities .

Figure 7.19b, of the drying rates and the temperature history data shows only one falling-rate period at both the velocities. Both the droplet temperatures fell to the wet bulb temperature before gradually increasing to the drying air temperature. This suggests that initial drying occurred from a wet surface, but as there was no constant-rate period moisture must have been brought rapidly to the surface from the interior of the droplet.

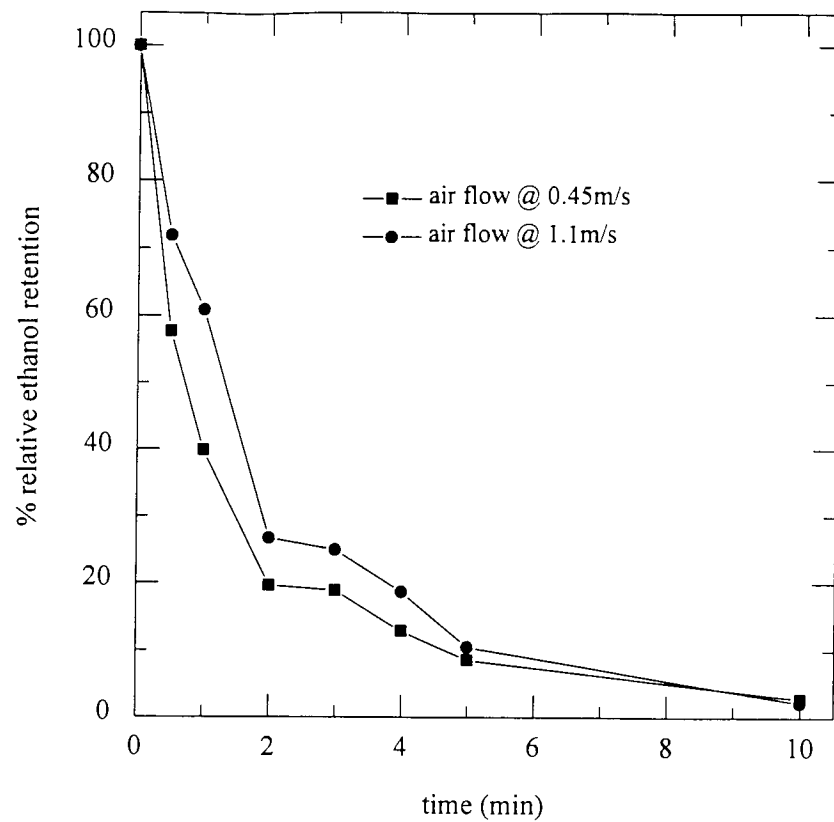


Figure 7.19a

The effect of air flowrate on the retention of ethanol in 20% rice starch solutions at ambient temperature ($T=25^{\circ}\text{C}$)

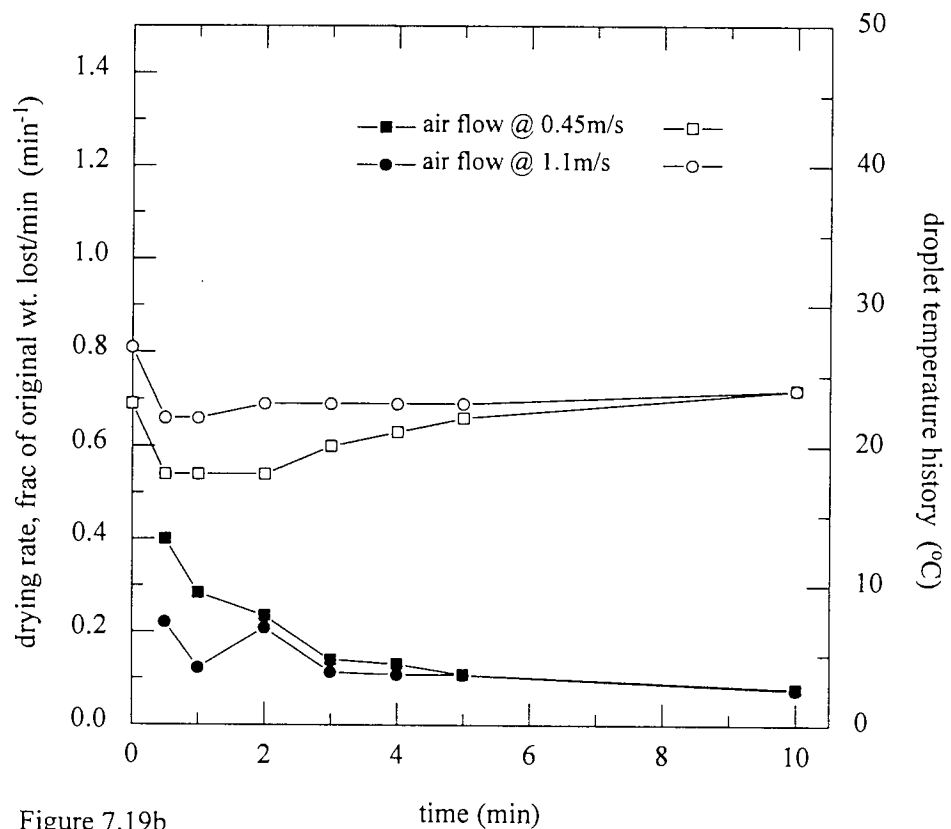


Figure 7.19b

The drying rate [solid symbols] and droplet temperature history [open symbols] for 20% rice starch solutions

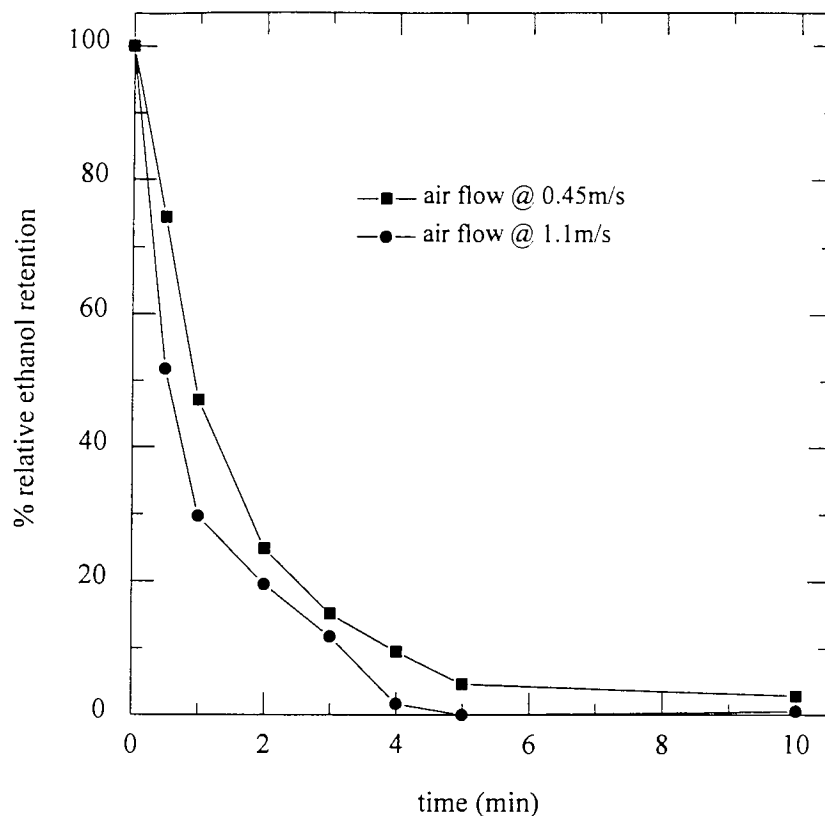


Figure 7.20a

The effect of air flowrate on the retention of ethanol in 20% rice starch solutions at 42°C

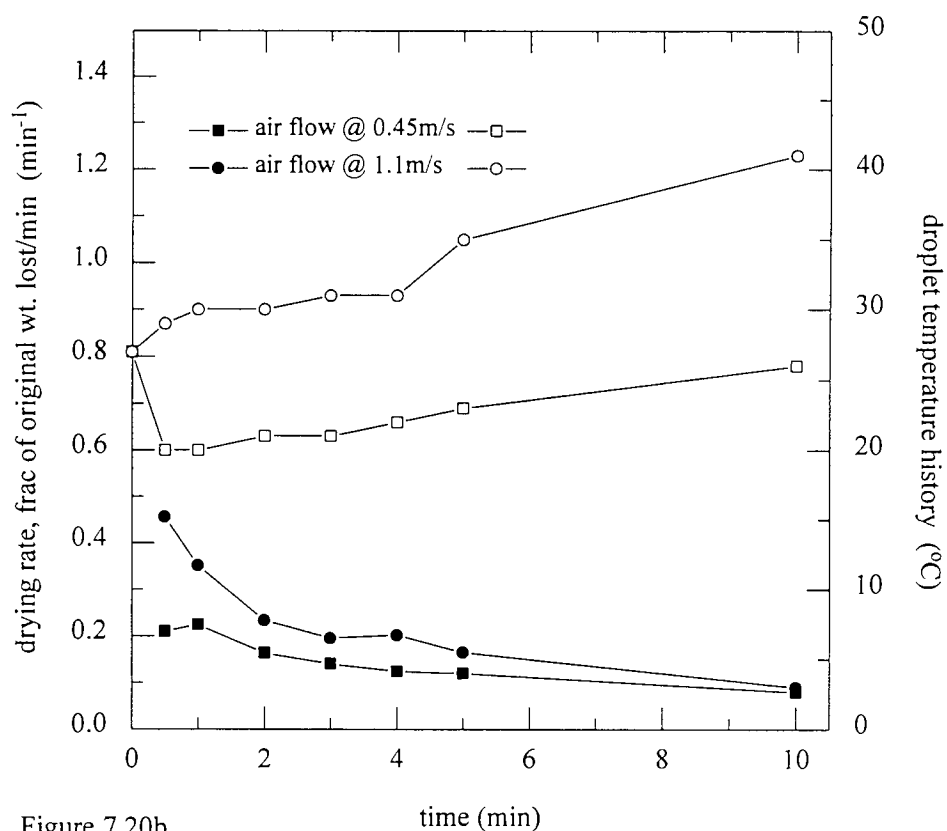


Figure 7.20b

The drying rate [solid symbols] and droplet temperature history [open symbols] for 20% rice starch solutions

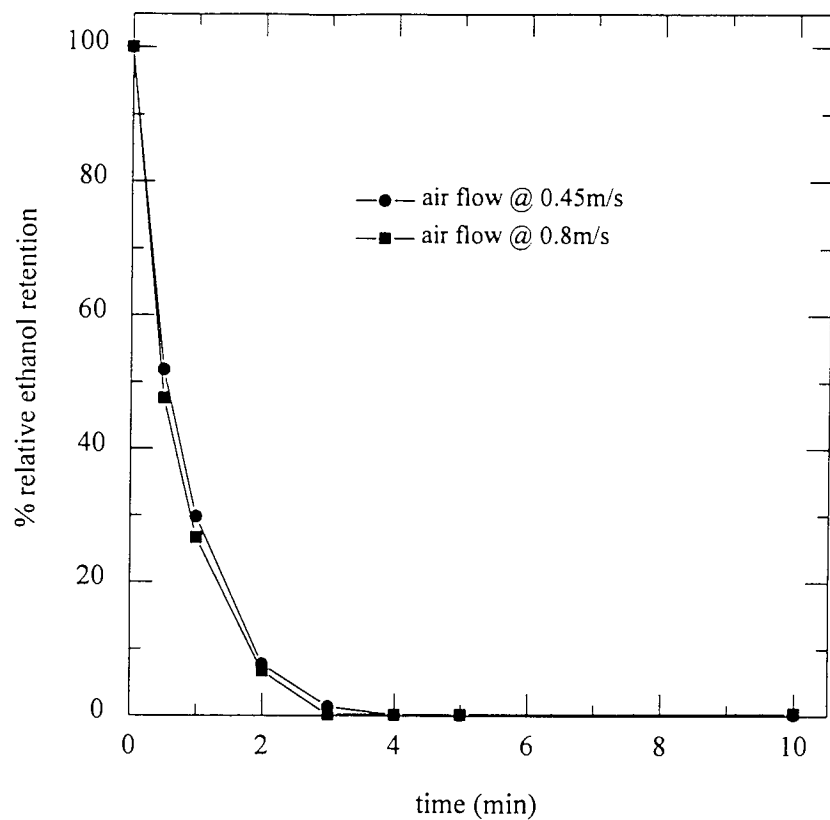


Figure 7.21a

The effect of air flowrate on the retention of ethanol in 20% rice starch solutions at 62°C

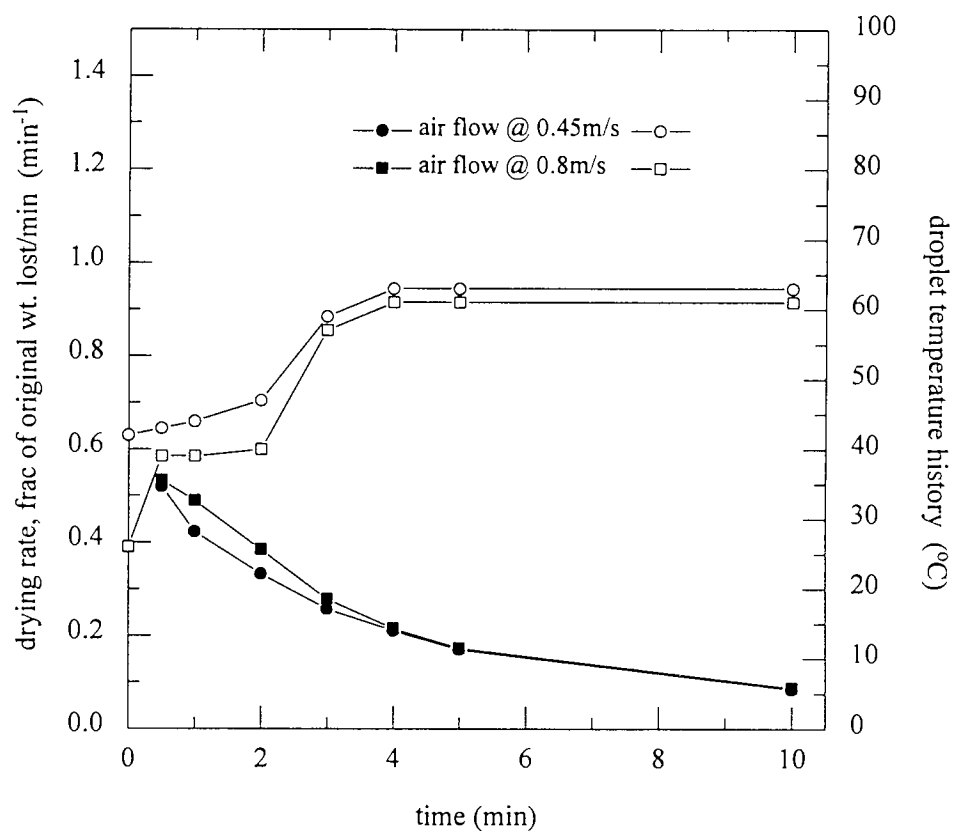


Figure 7.21b

The drying rate [solid symbols] and droplet temperature history [open symbols] for 20% rice starch solutions

An increase in the drying air temperature to 42°C had no effect upon the retention of ethanol at the two air velocities. Both graphs, in Figure 7.20a, show a similar trend, except that the final ethanol content of the droplet reached zero after 5 minutes at 1.1 m/s while at 0.45 m/s the ethanol retention did not reach zero even after 10 minutes.

The drying rate was faster at 1.2 m/s than at 0.45 m/s as shown in Figure 7.20b. The droplet temperature histories show that at 0.45 m/s, the droplet temperature initially fell to the wet bulb temperature before increasing, whereas at the higher velocity, the temperature increased steadily from the onset; i.e. the droplet interior was heated throughout by the drying air.

At 62°C, the ethanol retention trends were similar (Figure 7.21a), with the final value of ethanol retention reaching zero after 4 minutes of exposure to the drying air. This shows that the air velocity, 0.45 m/s and 0.8 m/s, had no effect upon the retention of the ethanol. Figure 7.21b shows that the drying rates at the two velocities were the same. The droplet temperature histories also show a similar trend; there was initially evaporation from a wet surface, shown by the almost constant temperature for the first 2 minutes.

7.1.3.2: Wheat starch

The results shown in Figure 7.22a show that at an air temperature of 25°C, there was no effect of air velocity upon the retention of ethanol, i.e. an increase in the velocity to 1.1 m/s from 0.45 m/s did not result in any enhancement of ethanol retention. The $t_{1/2} = 30$ seconds for both air velocities.

Figure 7.22b demonstrates a fall in droplet temperature to the wet bulb temperature before a gradual increase. The drying rate curves show that drying occurred at a faster initial rate during the first minute at 0.45 m/s than with the

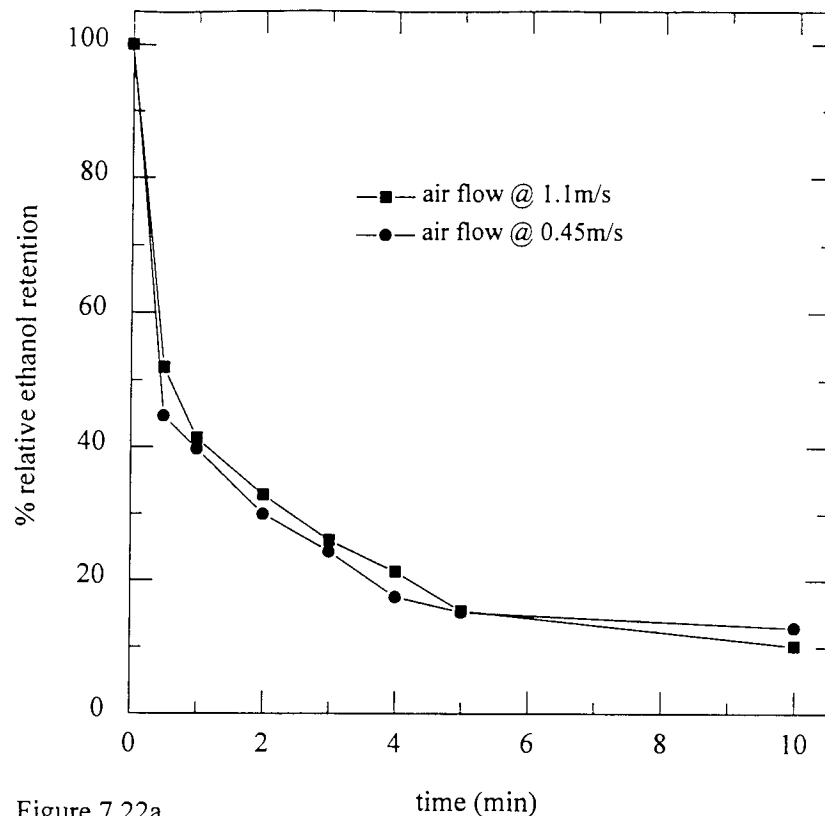


Figure 7.22a

The effect of air flowrate on the retention of ethanol in 20% wheat starch solutions at ambient temperature ($T=25^{\circ}\text{C}$)

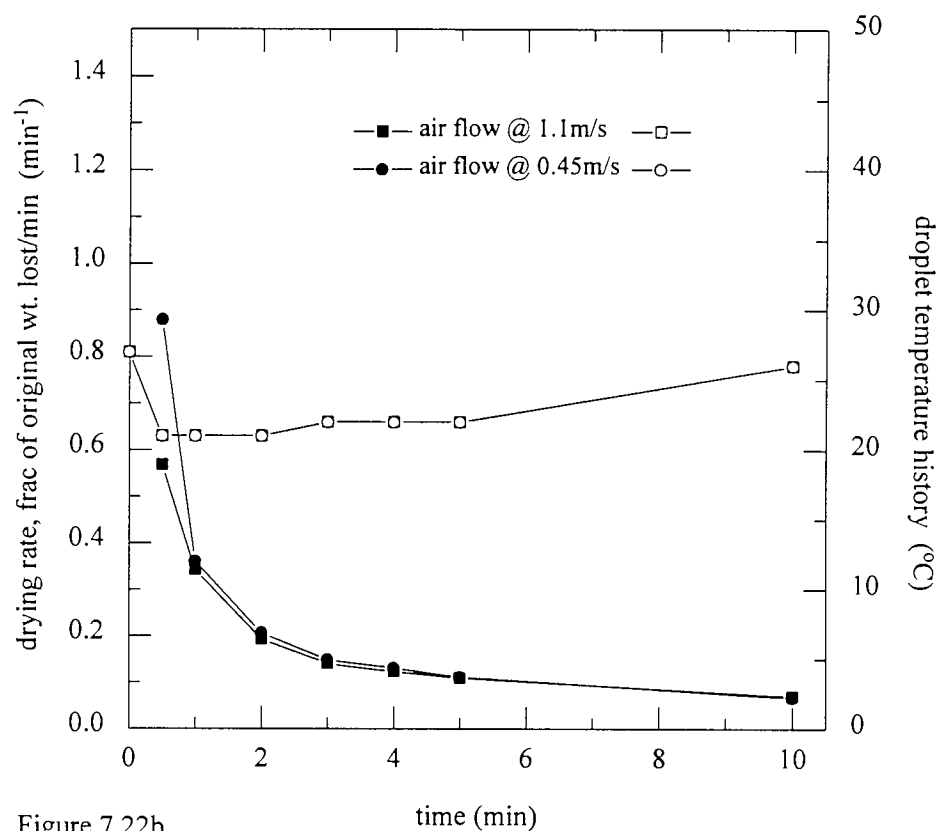


Figure 7.22b

The drying rate [solid symbols] and droplet temperature history [open symbols] for 20% wheat starch solutions

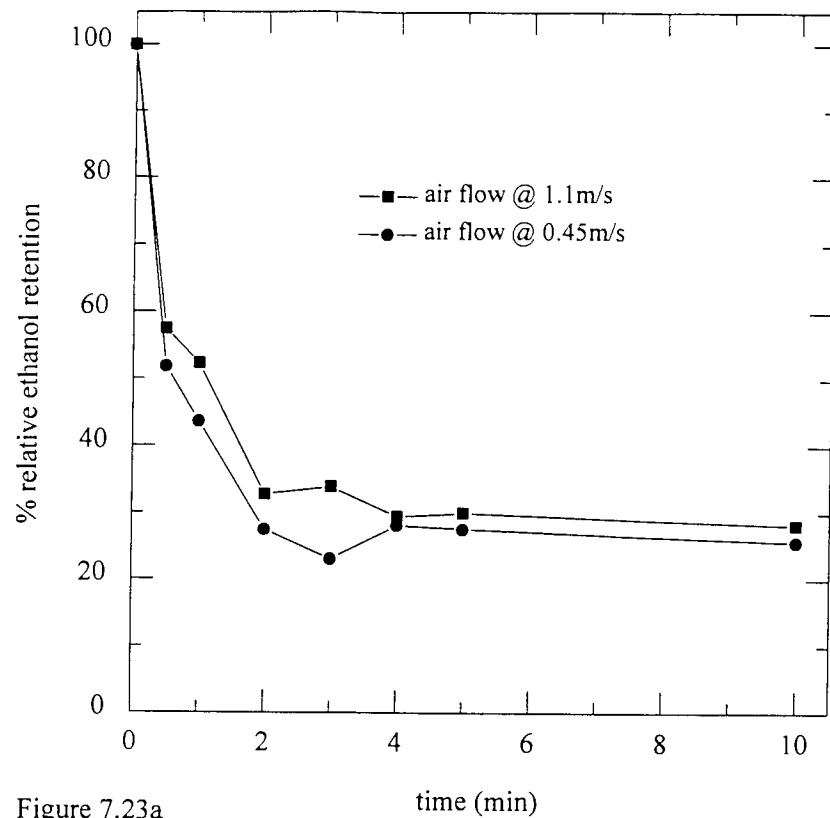


Figure 7.23a

The effect of air flowrate on the retention of ethanol in 20% wheat starch solutions at 42°C

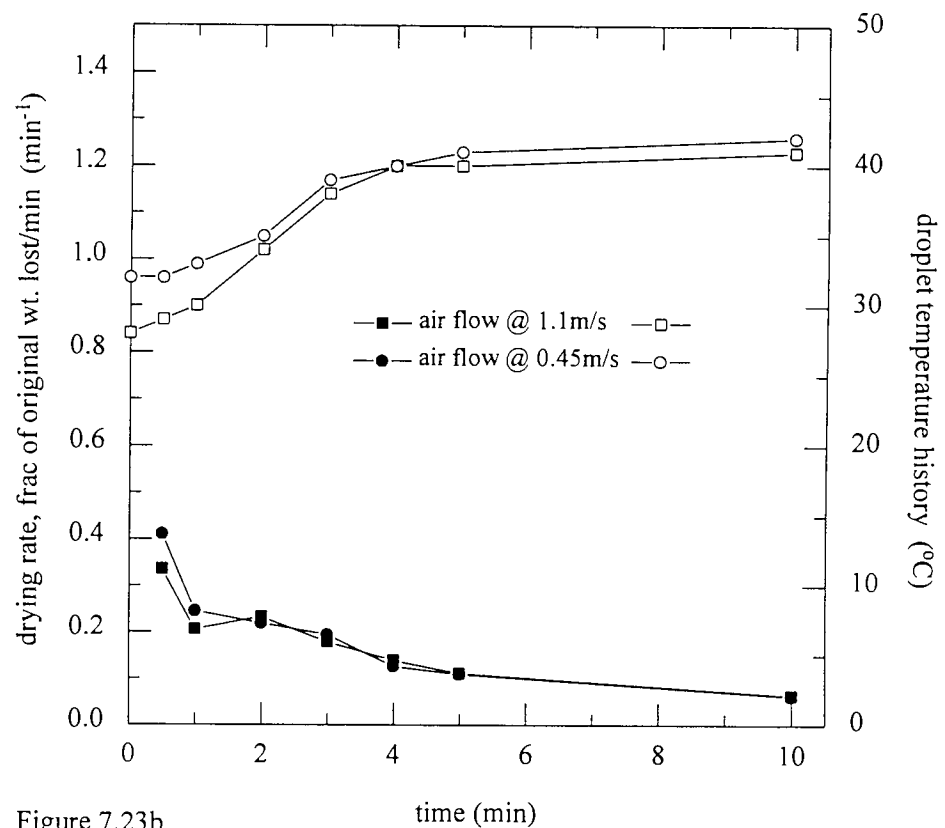


Figure 7.23b

The drying rate [solid symbols] and droplet temperature history [open symbols] for 20% wheat starch solutions

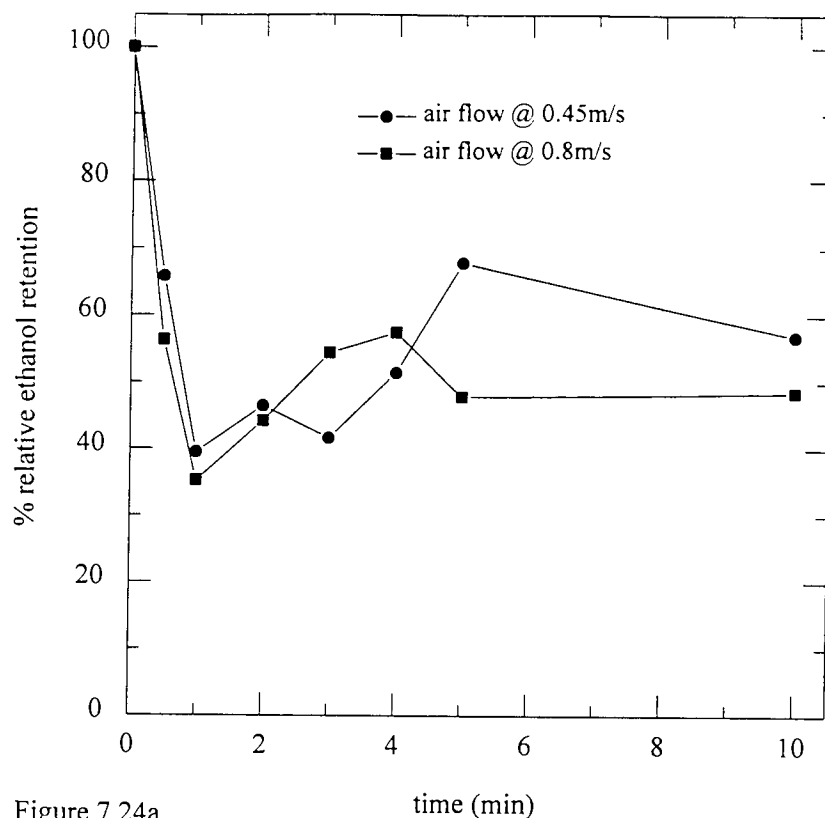


Figure 7.24a

The effect of air flowrate on the retention of ethanol in 20% wheat starch solutions at 62°C

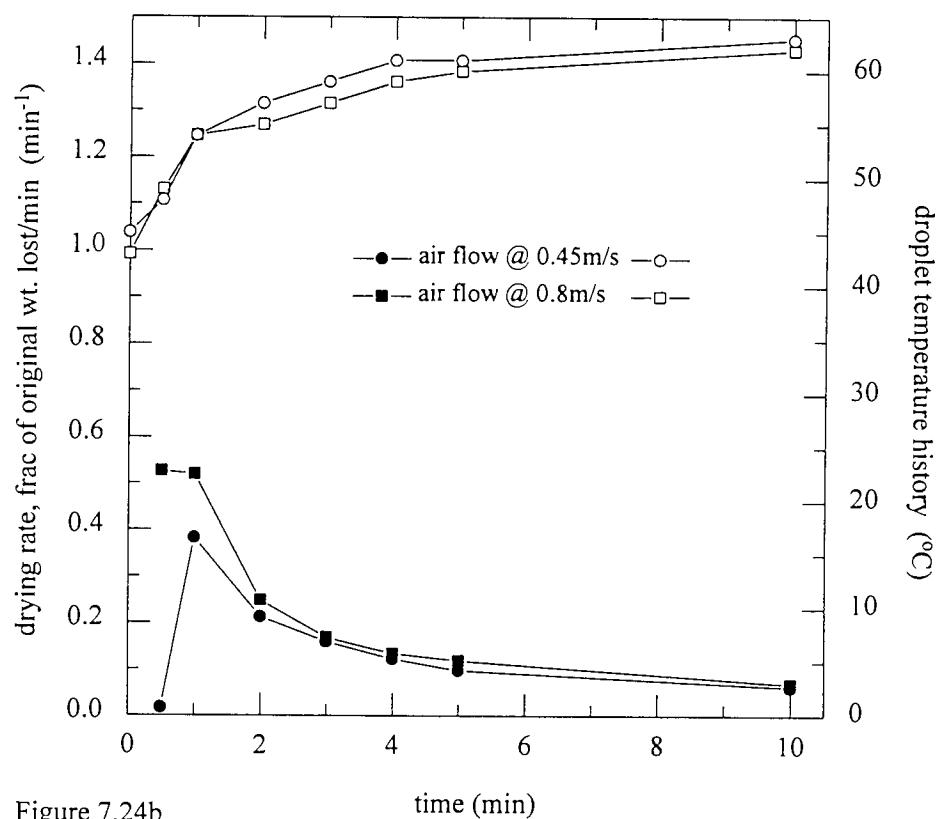


Figure 7.24b

The drying rate [solid symbols] and droplet temperature history [open symbols] for 20% wheat starch solutions

air flow at 1.1 m/s before both rates became almost constant after four minutes.

Figure 7.23a shows that again at 42°C, an increase in air velocity from 0.45 m/s to 1.1 m/s did not enhance the retention of the ethanol. Both the final retention values were almost the same ($25\% < \text{retention} < 30\%$), but the $t_{1/2}$ were different; $t_{1/2} = 30$ seconds for the slower velocity and $t_{1/2} = 1$ minute for the faster velocity.

The drying rates were similar at the two air velocities at 42°C, as were the droplet temperature histories, which climbed gradually to the drying air temperature as shown in Figure 7.23b.

At an increased drying air temperature (62°C), a change in the air velocity again had no significant effect upon the final retention of ethanol (as seen in Figure 7.24a); there was a slight increase in final retention from almost 50% at 0.8 m/s compared to approximately 58% at 0.45 m/s. Both the air velocities resulted in $t_{1/2}$ being 1 minute.

Figure 7.24b shows that the drying rates were similar, as were the droplet temperature histories, for the two air velocities. An almost constant drying rate was attained after approximately five minutes.

7.1.2.3: Dextrin

An increase in air velocity from 0.45 m/s to 1.1 m/s, at an air temperature of 42°C, had no significant effect upon the retention of ethanol. Both the graphs, shown in Figure 7.25a, show a similar trend except that at 0.45 m/s the rate of decrease in retention was slightly greater than at 1.1 m/s. The final retention values were 10% and almost 7% for 1.1 m/s and 0.45 m/s respectively. Figure 7.25b confirms this contention i.e. the drying rates and the droplet temperature histories were similar for the two air velocities.

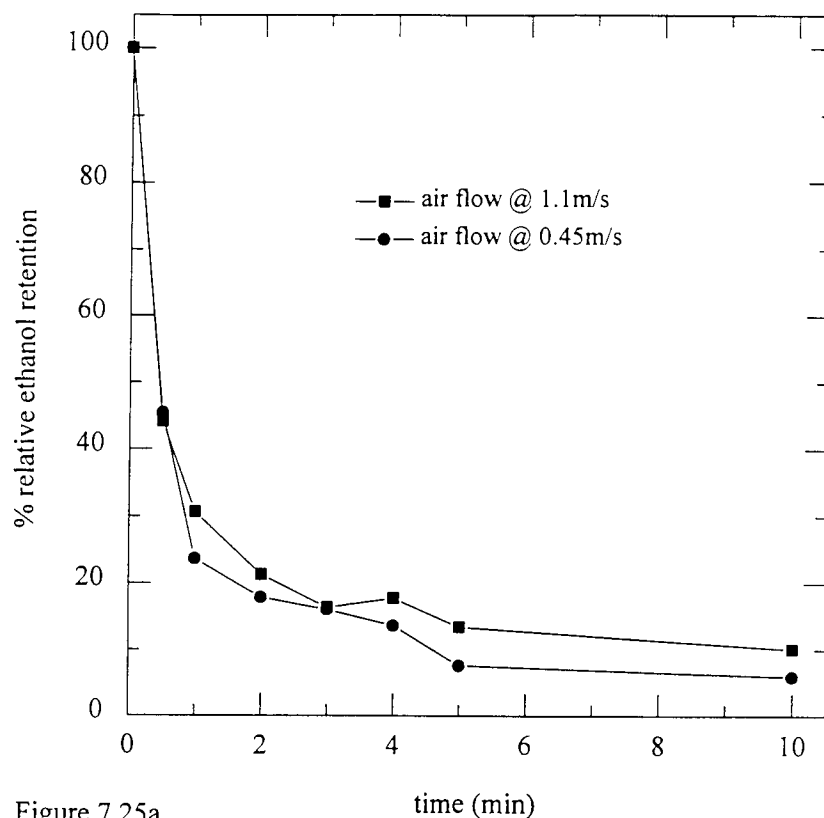


Figure 7.25a

The effect of air flowrate on the retention of ethanol in 20% dextrin solutions

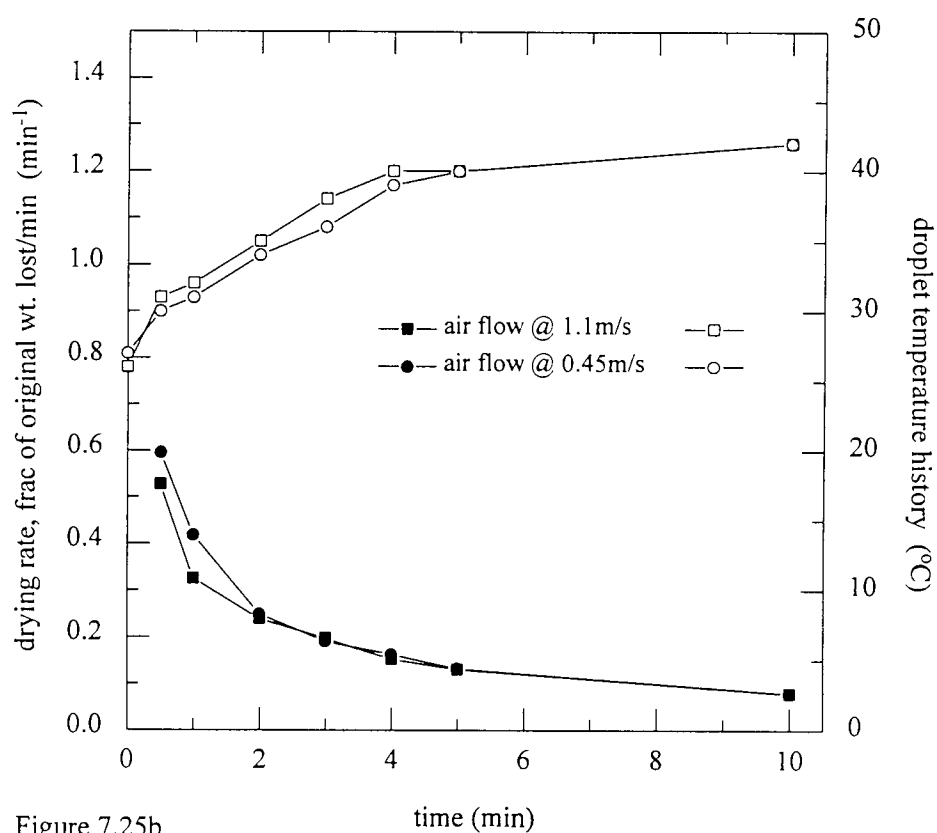


Figure 7.25b

The drying rate [solid symbols] and droplet temperature history [open symbols] for 20% dextrin solutions

7.1.2.4: Fructose

An increase in the air velocity from 0.45 m/s to 1.1 m/s at 25°C had no effect upon the retention of ethanol. The ethanol retention was almost identical at both velocities, (as shown in Figure 7.26a). The $t_{1/2}$ was almost 1 minute for both air velocities. The drying rates shown in Figure 7.26b exhibit one gradual falling-rate period for both velocities, and the droplet temperatures gradually increased to the drying air temperature.

An increase in the velocity at a higher air temperature (62°C), from 0.45 m/s to 0.8 m/s, had no effect upon retention. As illustrated in Figure 7.27a the only difference was the faster loss at the higher temperature, the ethanol content of the droplets had reduced to less than 20% within the first minute of exposure to the drying air at 62°C. The $t_{1/2}$ value here was found to be less than 30 seconds.

The drying rates shown in Figure 7.27b exhibit only one falling-rate period at both velocities, but the gradient of these curves is markedly steeper than at the lower air temperature. There was also a more rapid increase in the droplet temperature upon exposure to the drying air.

7.1.2.5: Sucrose

As shown by Figure 7.28a, the increase in air velocity from 0.45 m/s to 1.1 m/s at 25°C had no significant effect on the ethanol retention. At both velocities, $t_{1/2} = 1$ minute. Figure 7.28b demonstrates only a very gradual falling-rate period associated with a similarly gradual increase in droplet temperature to the drying air temperature for both the air velocities.

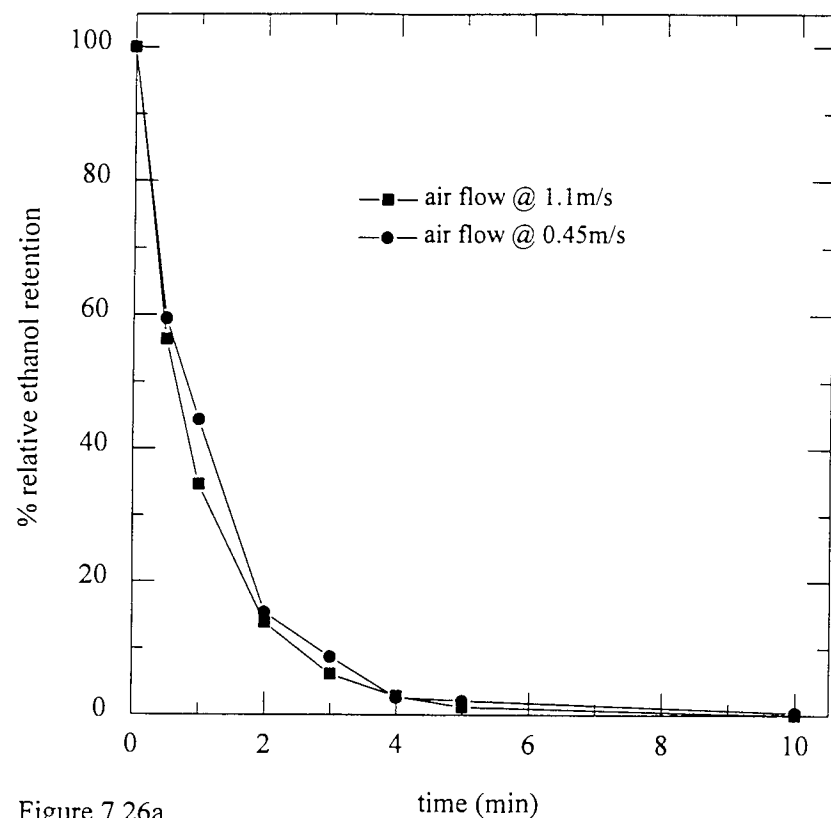


Figure 7.26a

The effect of air flowrate on the retention of ethanol in 20% fructose solutions at ambient temperature ($T=25^{\circ}\text{C}$)

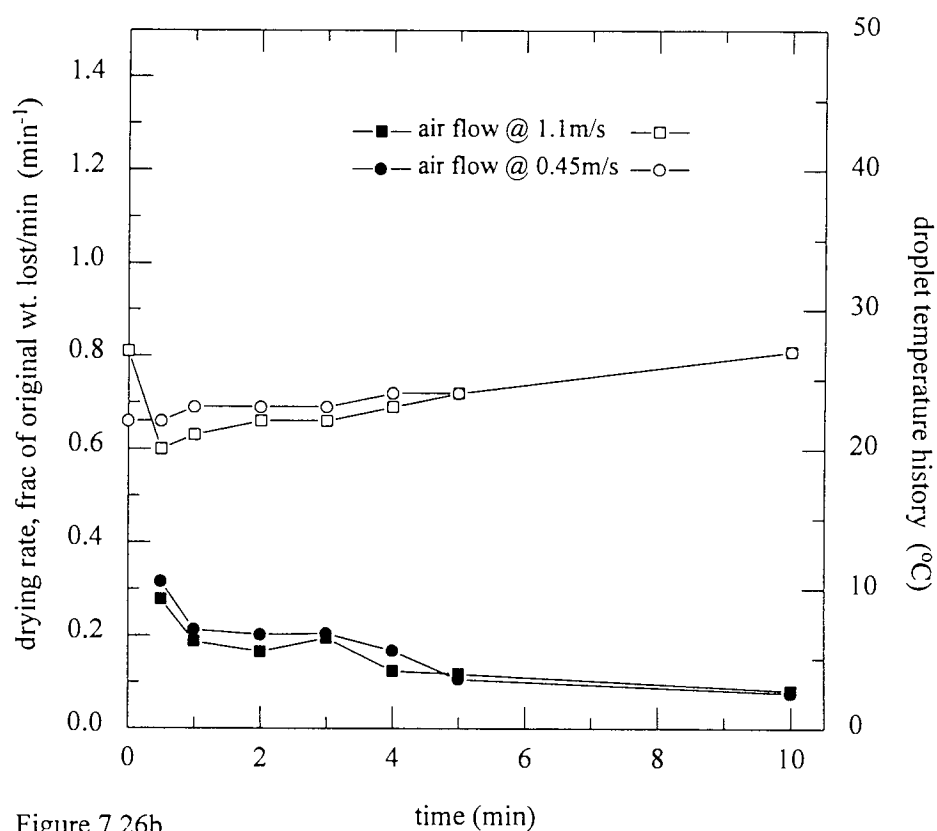


Figure 7.26b

The drying rate [solid symbols] and droplet temperature history [open symbols] for 20% fructose solutions

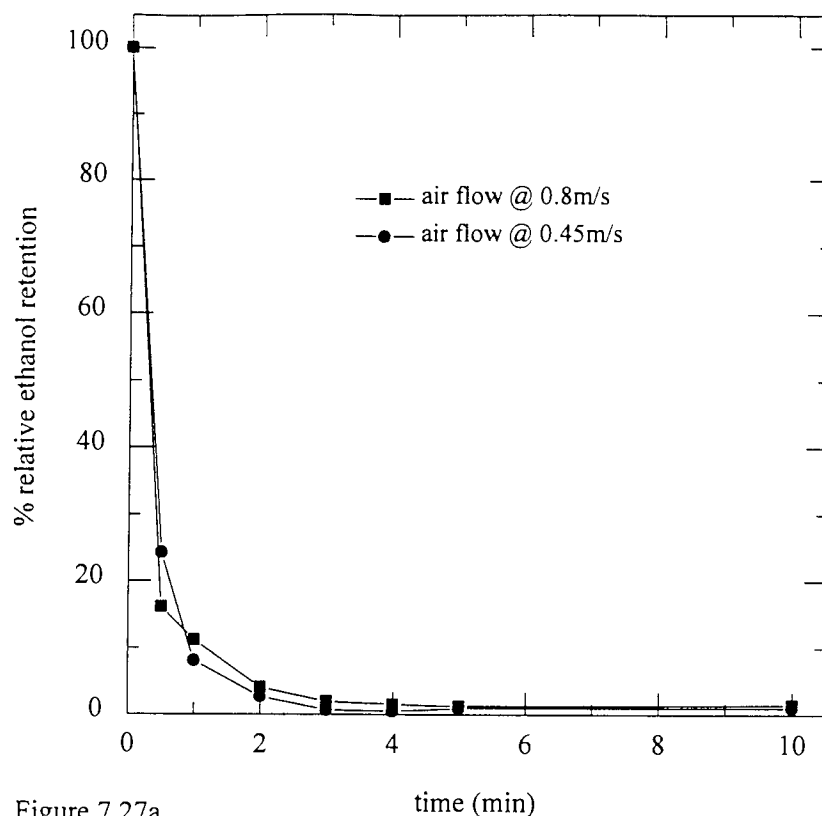


Figure 7.27a

The effect of air flowrate on the retention of ethanol in 20% fructose solutions at 62°C

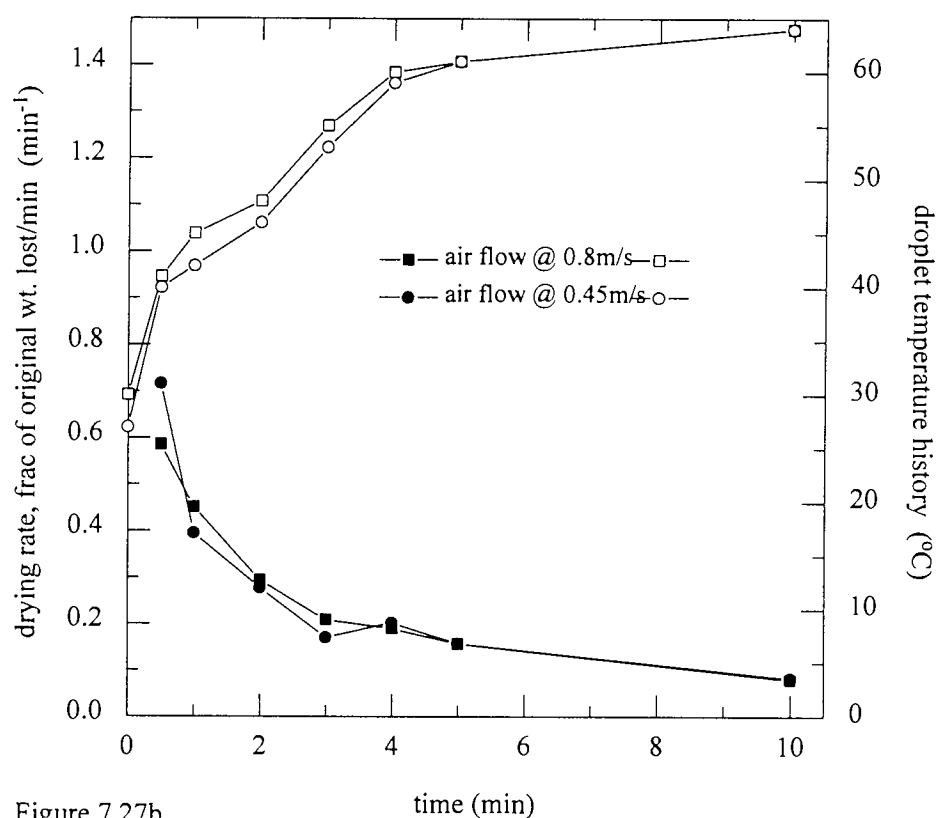


Figure 7.27b

The drying rate [solid symbols] and droplet temperature history [open symbols] for 20% fructose solutions

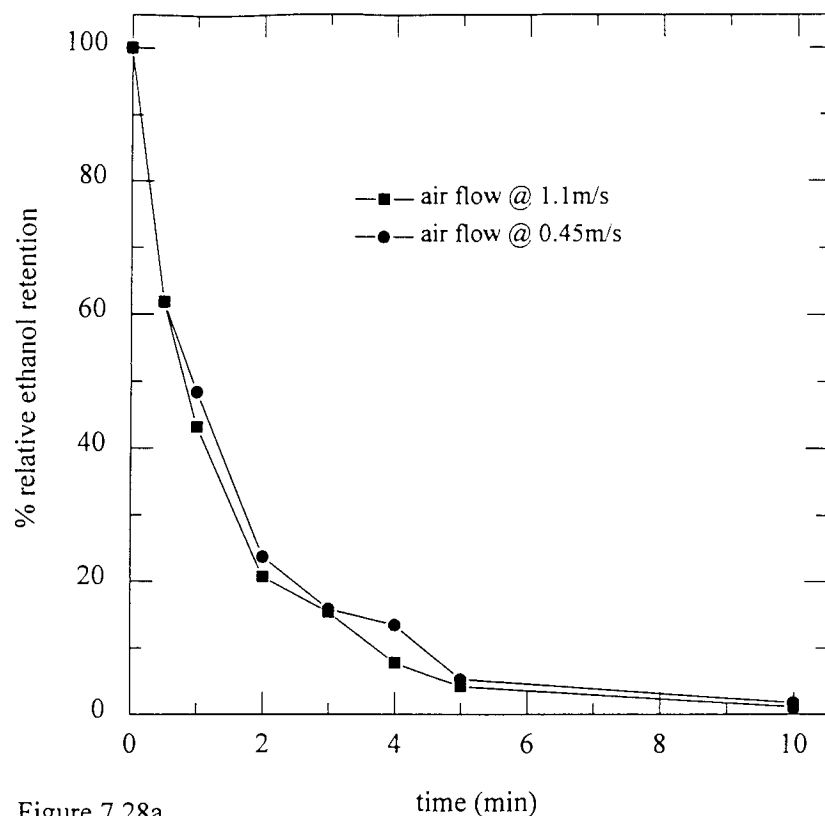


Figure 7.28a

The effect of air flowrate on the retention of ethanol in 20% sucrose solutions at ambient temperature ($T=25^{\circ}\text{C}$)

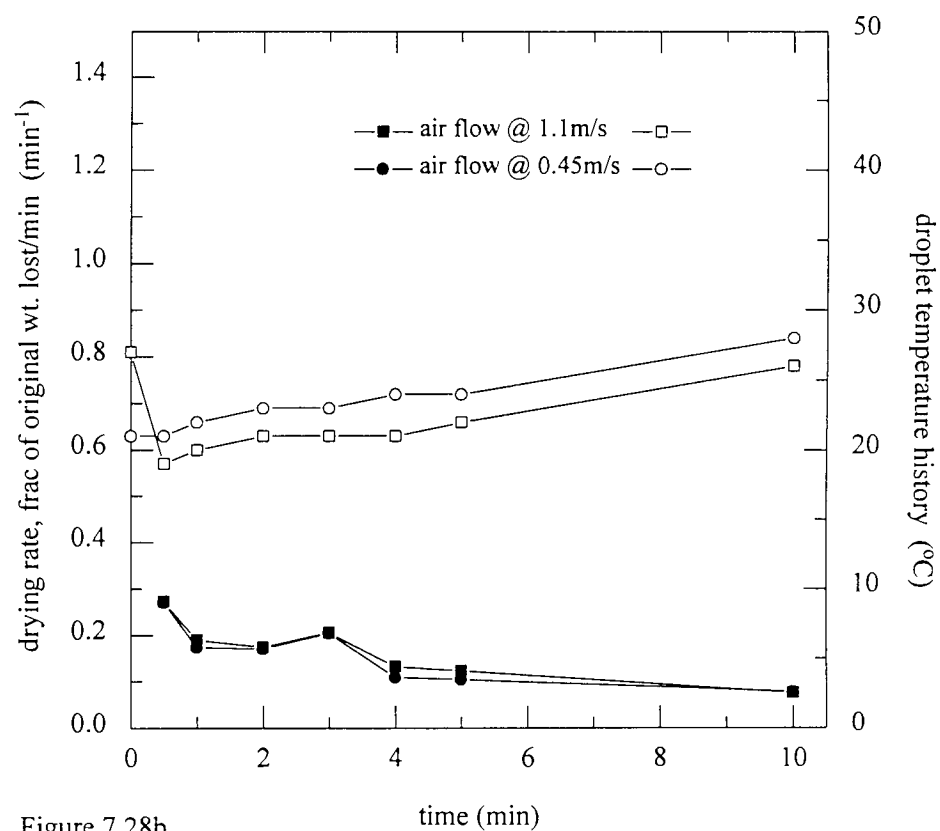


Figure 7.28b

The drying rate [solid symbols] and droplet temperature history [open symbols] for 20% sucrose solutions

7.1.3.6: Skim milk

Figure 7.29a illustrates the effect of air velocity upon the retention of ethanol in a droplet of skim milk at 25°C. Clearly a change in the velocity from 0.45 m/s to 1.1 m/s produced no significant difference in the retention of ethanol, with $t_{1/2} = 1$ minute for both air velocities. The final ethanol content was almost the same for both (<10%). Figure 7.29b shows that the drying rates and the droplet temperature histories were similar at both air velocities. One falling-rate period was observed, and the droplet temperatures increased very gradually to the drying air temperature.

The loss of ethanol was more rapid at the elevated temperature of 62°C, as shown in Figure 7.30a, with $t_{1/2} < 1$ minute for 0.45 m/s and 1 minute for 0.8 m/s. After approximately 1 minute's exposure to the drying air, the ethanol retention curve fell slower at the higher air velocity compared to that at 0.45 m/s, culminating in a slightly increased final retention of 35% at 0.8 m/s and 25% at 0.45 m/s. After 3 minutes of drying the ethanol content levelled off to its final value, i.e. almost all of the loss of ethanol occurred in the first 3 minutes.

The drying rates shown in Figure 7.30b show one similar falling-rate period at both velocities, but with a steeper gradient than at 25°C. The droplet temperature histories are almost identical and the droplet temperature increased rapidly to that of the prevailing drying air. The increase in droplet temperature is indicative of no moisture evaporating from the surface, implying the existence of a moisture impervious skin.

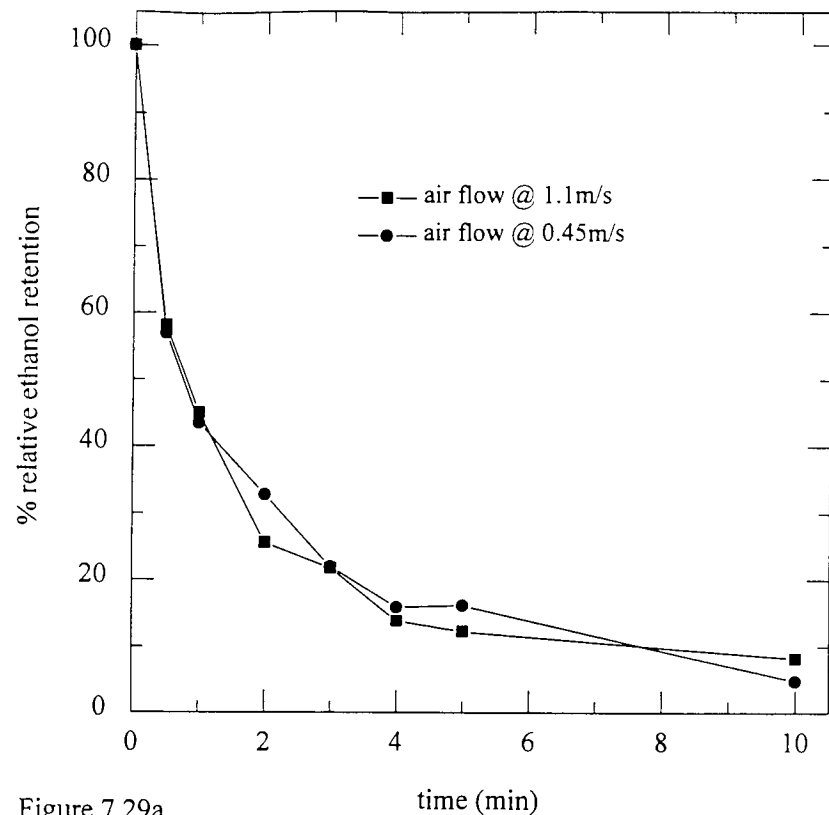


Figure 7.29a

The effect of air flowrate on the retention of ethanol in 20% skim milk solutions at ambient temperature ($T=25^{\circ}\text{C}$)

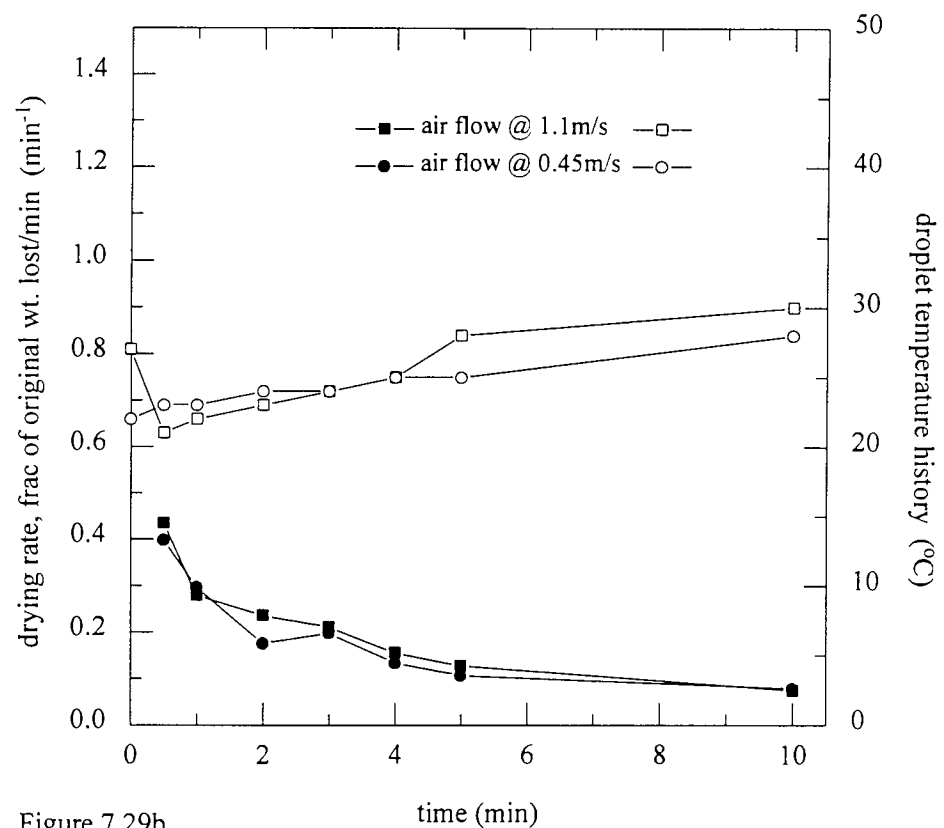


Figure 7.29b

The drying rate [solid symbols] and droplet temperature history [open symbols] for 20% skim milk solutions

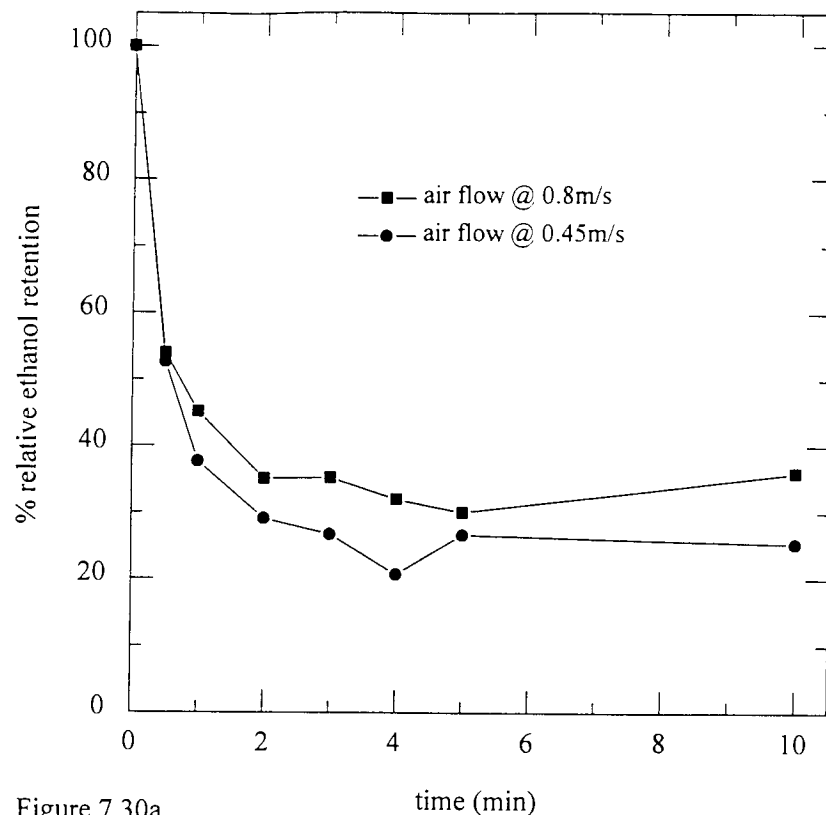


Figure 7.30a

The effect of air flowrate on the retention of ethanol in 20% skim milk solutions at 62°C

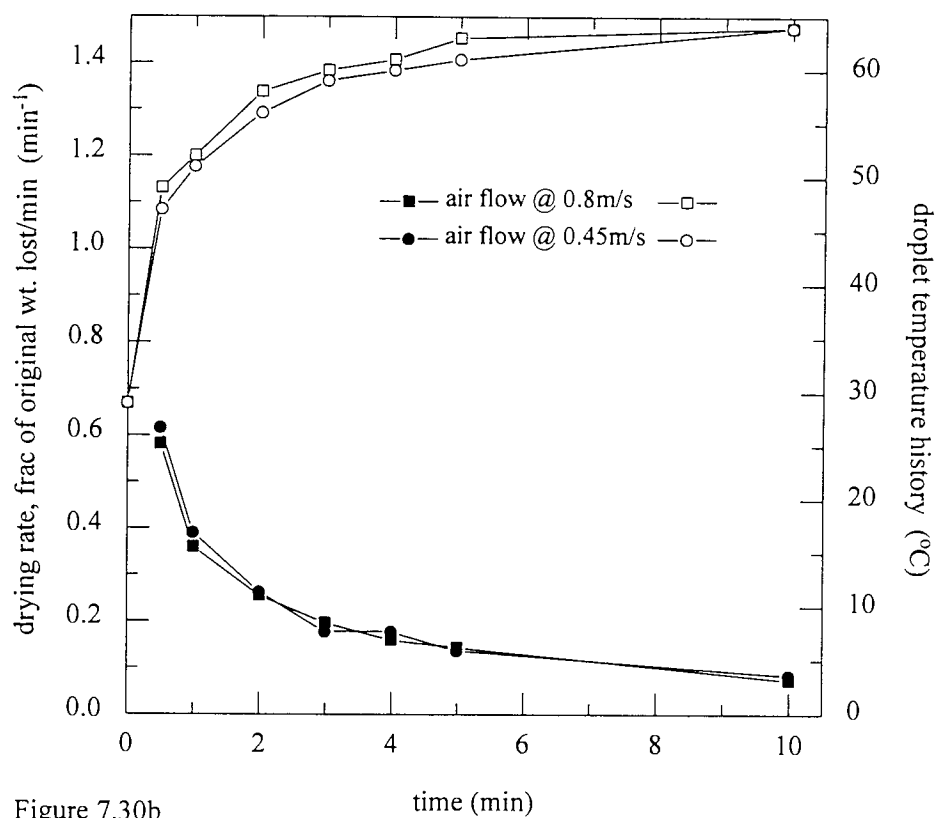


Figure 7.30b

The drying rate [solid symbols] and droplet temperature history [open symbols] for 20% skim milk solutions

7.1.2.7: Coffee

At 25°C it is evident, from Figure 7.31a, that drying at a lower air velocity (0.45 m/s) resulted in a slightly improved final retention of ethanol compared to that at 1.1 m/s. Although the general trend is downwards with the final ethanol retention of approximately 30-34% for both velocities, the gradients of both the graphs show that the rate of loss of ethanol was faster at 1.1 m/s. This is confirmed by the $t_{1/2}$ values of 2 minutes and 5 minutes for 1.1 m/s and 0.45 m/s respectively.

The drying rates (Figure 7.31b) were different at the two air velocities, with that at 1.1 m/s being slightly greater. The droplet temperatures initially fell to the wet bulb temperature at 0.45 m/s followed by a gradual increase. This effect was not present at 1.1 m/s at which from the onset the temperature gradually increased to the drying air temperature.

At an air temperature of 62°C, the effect of increasing the air velocity again became insignificant. Both graphs in Figure 7.32a demonstrate almost the same trend, with $t_{1/2} = 1.5$ minutes for both air velocities. The final retention values for ethanol were also similar at 25%. The drying rates were similar (as shown in Figure 7.32b) and there was a rapid increase in droplet temperature. This suggests early formation of an impervious skin.

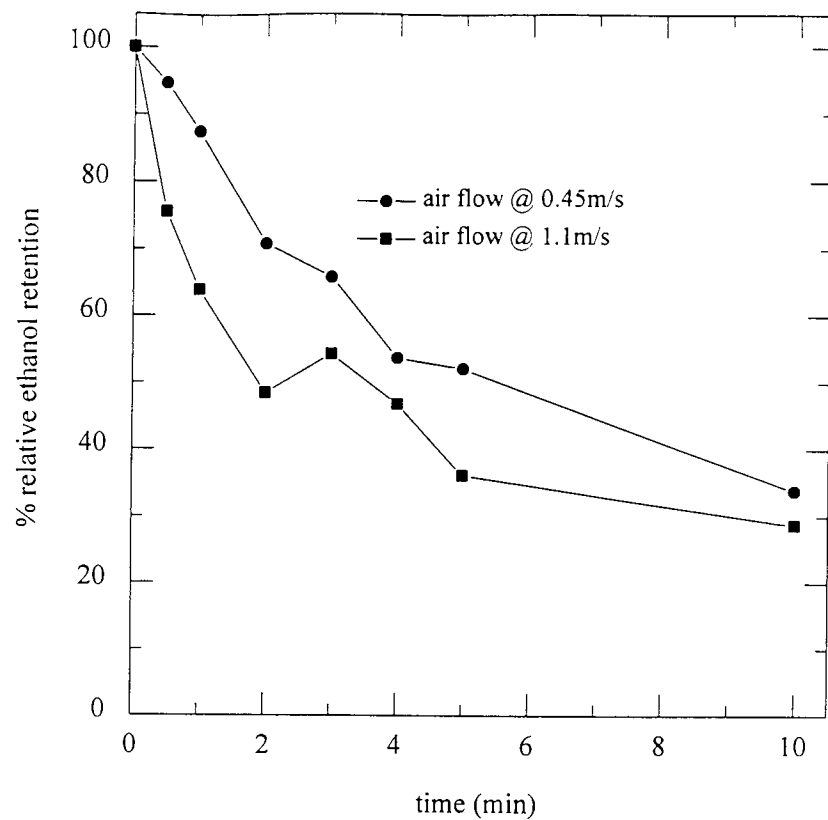


Figure 7.31a

The effect of air flowrate on the retention of ethanol in 20% coffee solutions at ambient temperature ($T=25^{\circ}\text{C}$)

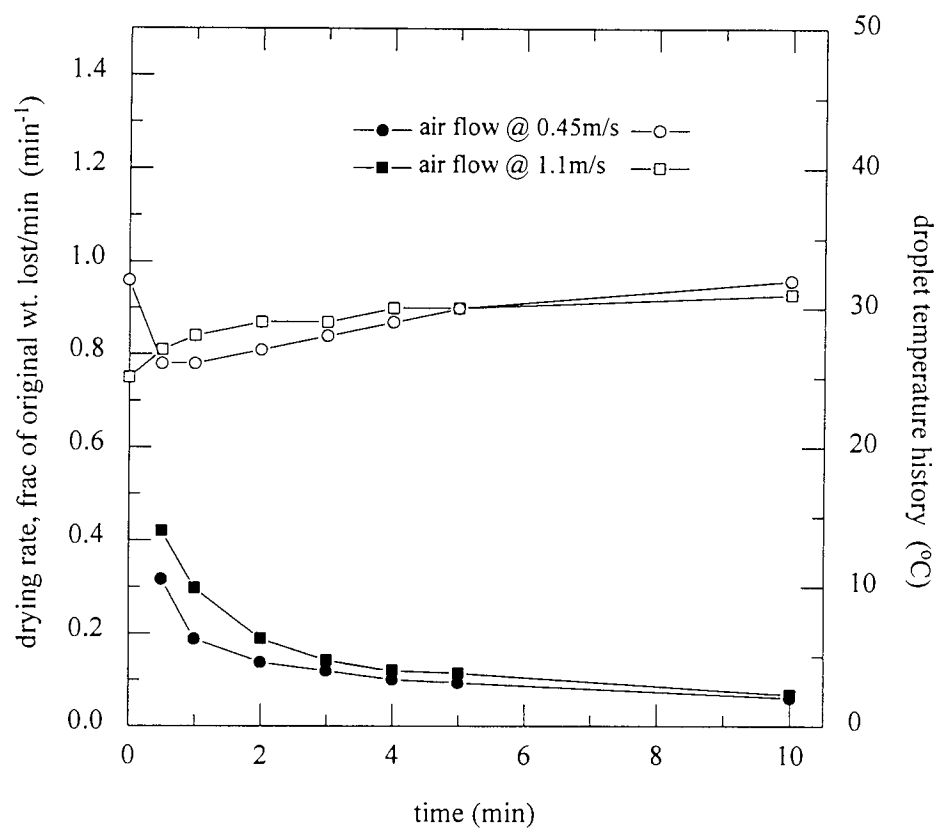


Figure 7.31b

The drying rate [solid symbols] and droplet temperature history [open symbols] for 20% coffee solutions

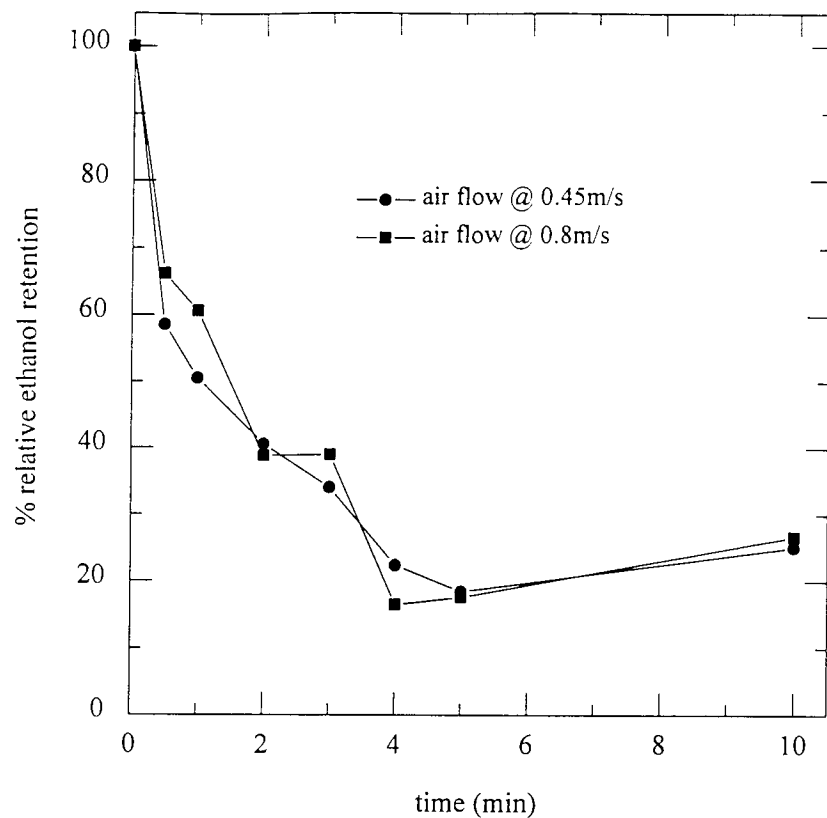


Figure 7.32a

The effect of air flowrate on the retention of ethanol in 20% coffee solutions at 62°C

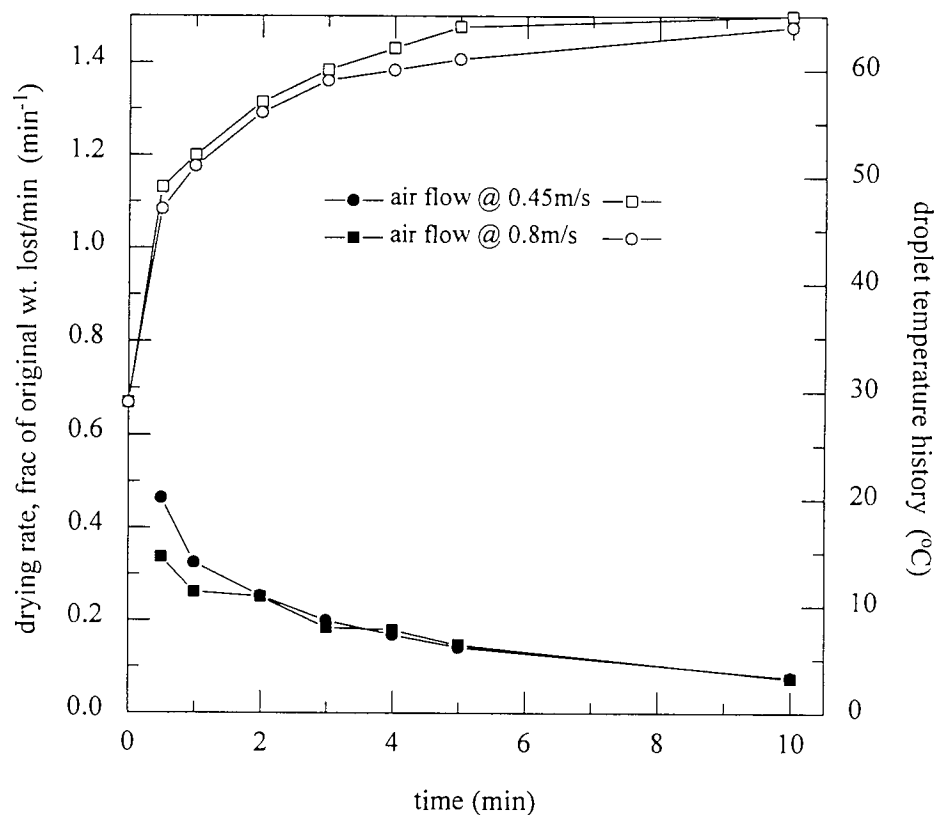


Figure 7.32b

The drying rate [solid symbols] and droplet temperature history [open symbols] for 20% coffee solutions

7.1.2.8: Gelatine 60

Figure 7.33a shows that at 25°C, there was no significant effect of increasing the air velocity from 0.45 m/s to 1.1 m/s, with $t_{1/2} < 1$ minute for both. The final values of retention were different, approximately 10% for 1.1 m/s and almost 18% for 0.45 m/s.

The drying rates (Figure 7.33b) show that there was no difference between the drying rates and temperature histories at the two air velocities. There were two falling-rates, the first almost vertical falling-rate coincided with the initial fall in the ethanol content of the droplets. The second falling-rate was more gradual, and associated with the subsequent gradual fall in the ethanol content of the droplets. The droplet temperature histories show an initial fall to the wet bulb temperature followed by a gradual increase to the prevailing drying air temperature.

7.1.2.9: Gelatine 150

The results illustrated in Figure 7.34a show that both the air velocities provided significantly different values of the final retention although both $t_{1/2} < 30$ seconds. The final retention value was almost 40% for 1.1 m/s and approximately 15% for 0.45 m/s.

Figure 7.34b shows the drying rates and the droplet temperatures for the two air velocities. There were two falling-rate periods, the first associated with the rapid loss of ethanol and the second coinciding with a more gradual loss. The occurrence of the second falling-rate period may coincide with the formation of a skin to hinder mass transfer. There was an initial fall to the wet bulb temperature, suggesting that initially there was evaporation from a saturated surface. The subsequent increase would suggest that this surface evaporation was reduced as a result of the formation of an impervious skin.

7.1.2.10: Gum arabic

With an air temperature of 25°C, the effect of increasing the air velocity from 0.45 m/s to 1.1 m/s had a slight effect upon the retention of ethanol, as shown in Figure 7.35a. The rate of loss of ethanol was marginally faster at the slower air velocity, with $t_{1/2} < 30$ seconds for both. After the initial rapid decrease in ethanol content, the rate of loss became markedly slower after the first 2 minutes of drying, resulting in final values of approximately 20% and 15% for 1.1 m/s and 0.45 m/s respectively.

Two falling-rate periods were exhibited as illustrated by Figure 7.35b. The first falling-rate period was associated with the rapid loss of ethanol from the droplets; the second period involved a more gradual falling-rate which was coincident with reduced ethanol loss. The droplet temperatures are indicative of initial evaporation from a saturated surface as shown by the fall to wet bulb temperature, followed by a gradual increase in temperature. This would suggest that an impervious skin had gradually formed which reduced the internal transfer of moisture for evaporation giving rise to the gradual increase in temperature.

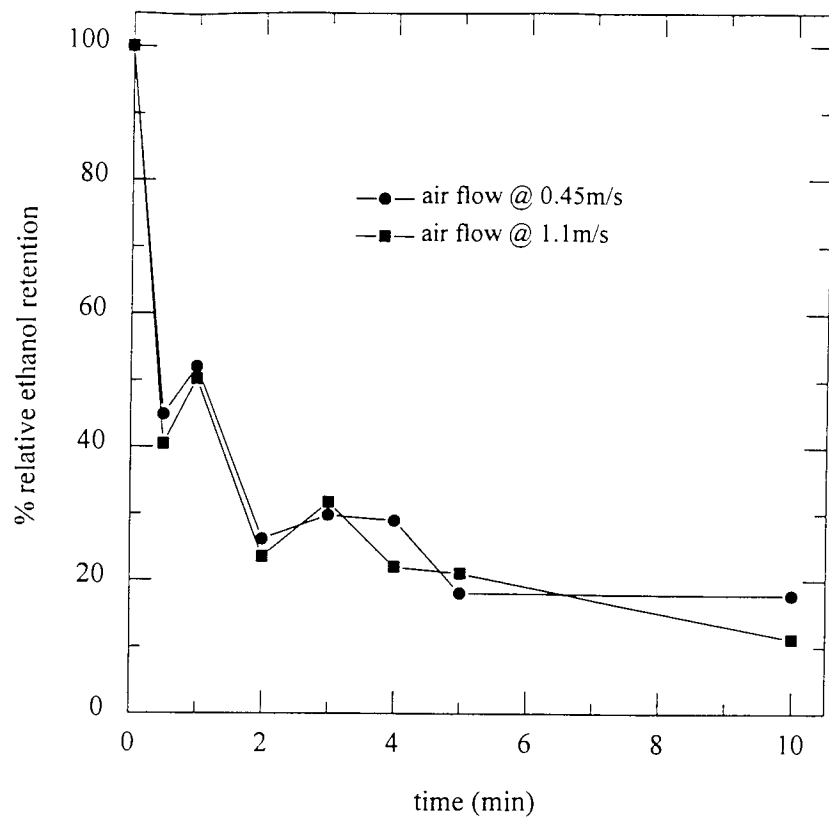


Figure 7.33a

The effect of air flowrate on the retention of ethanol in 20% gelatin 60 solutions at ambient temperature ($T=25^{\circ}\text{C}$)

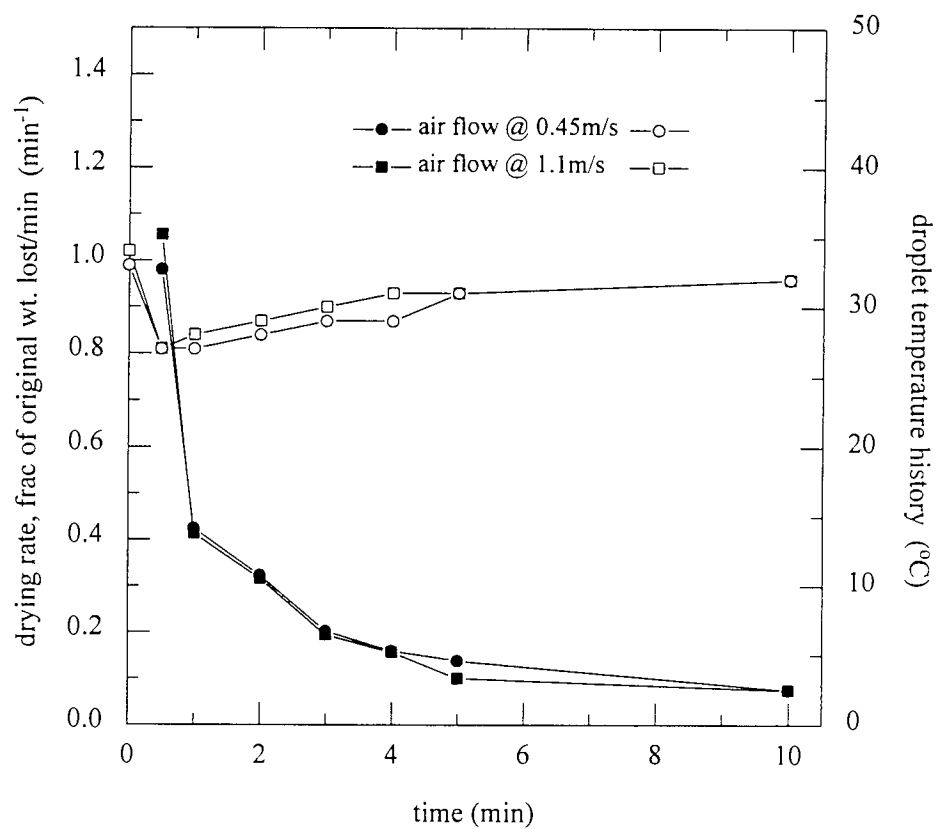


Figure 7.33b

The drying rate [solid symbols] and droplet temperature history [open symbols] for 20% gelatin 60 solutions

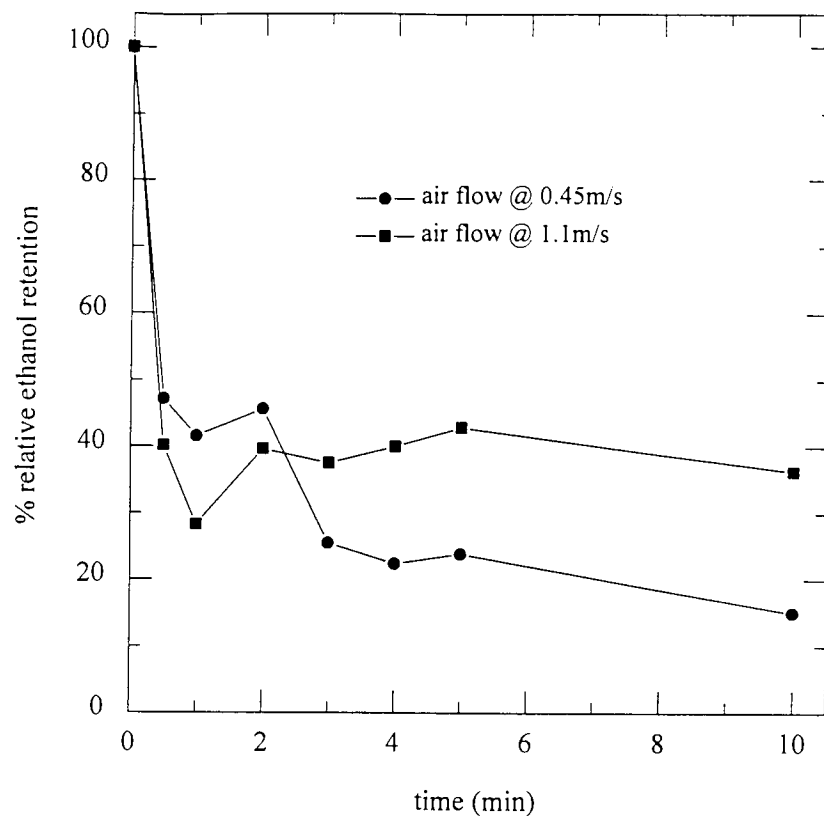


Figure 7.34a

The effect of air flowrate on the retention of ethanol in 20% gelatin 150 solutions at ambient temperature ($T=25^{\circ}\text{C}$)

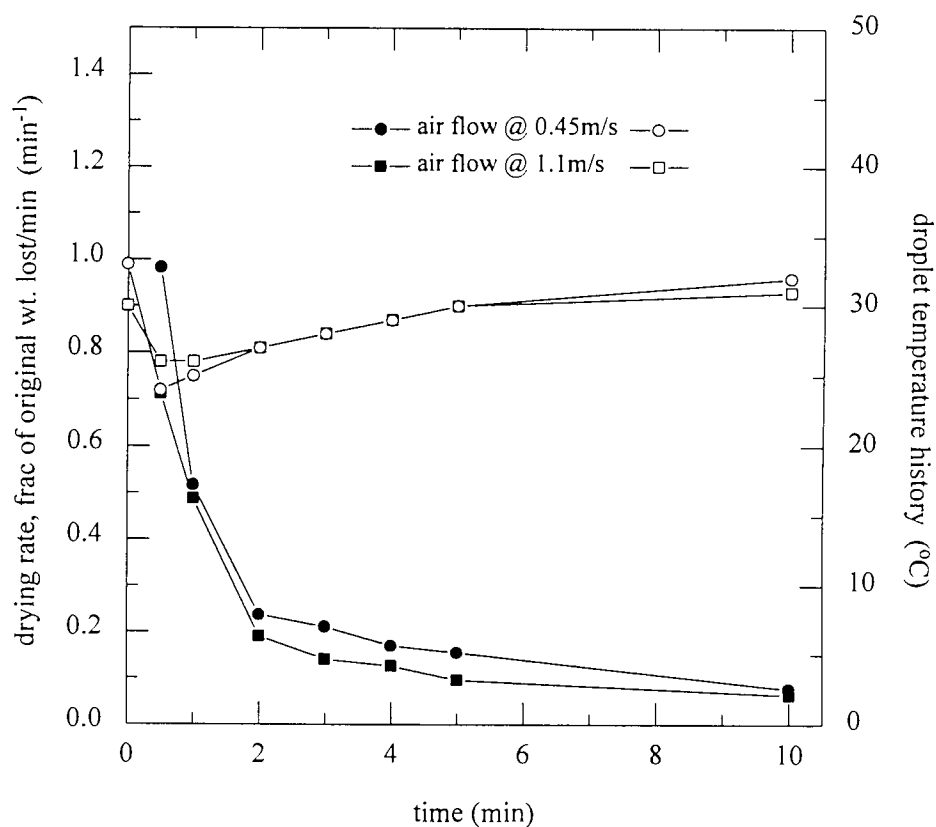


Figure 7.34b

The drying rate [solid symbols] and droplet temperature history [open symbols] for 20% gelatin 150 solutions

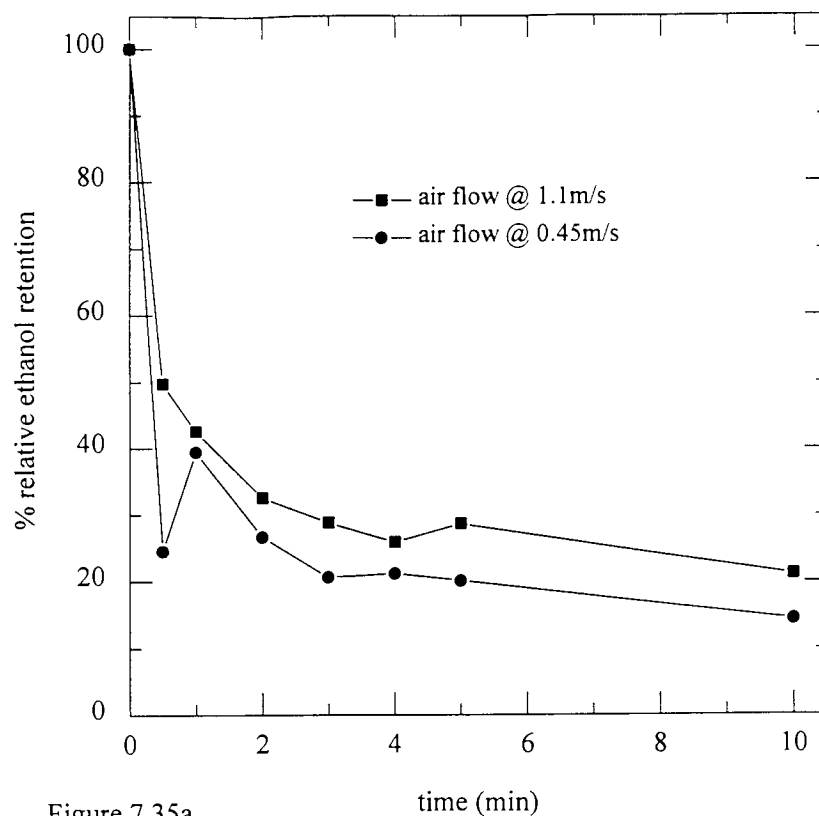


Figure 7.35a

The effect of air flowrate on the retention of ethanol in 20% gum arabic solution at ambient temperature ($T=25^{\circ}\text{C}$)

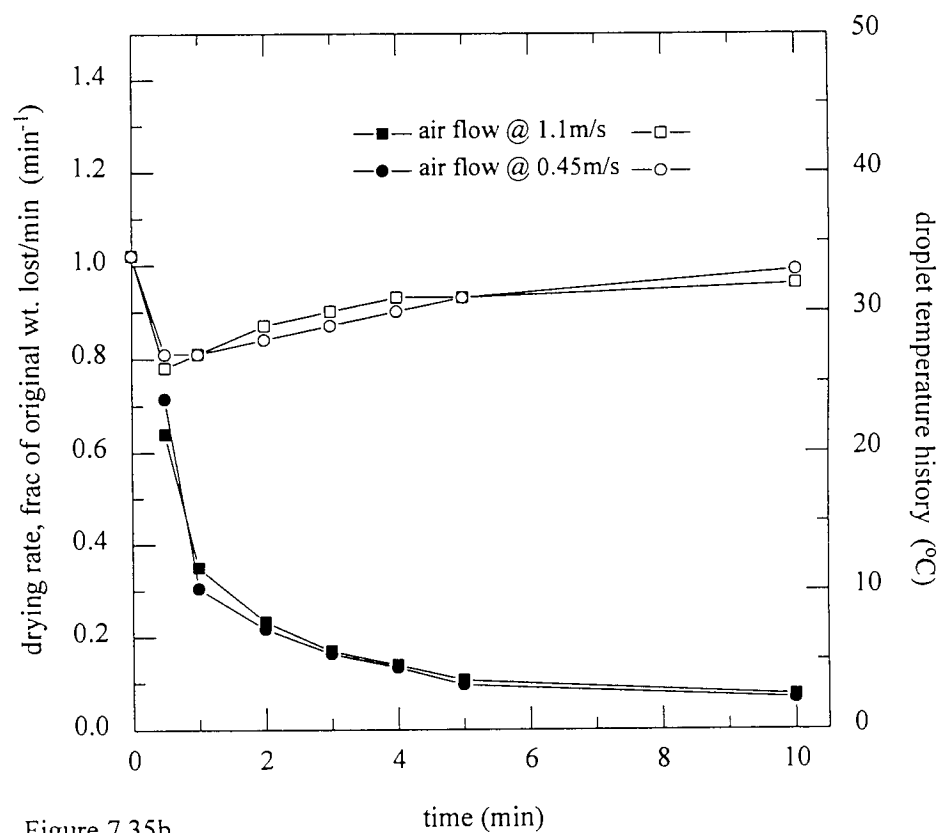


Figure 7.35b

The drying rate [solid symbols] and droplet temperature history [open symbols] for 20% gum arabic solutions

7.1.3: The effect of temperature

The effect of drying air temperature was determined experimentally for a 20% w/w solution of each encapsulant.

7.1.3.1: Rice starch

Figure 7.36a shows that an increase in the air temperature from 25°C to 42°C (at a velocity of 1.1 m/s) resulted in a more rapid loss of ethanol with the retention reducing to 0% after 5 minutes at 42°C. The final retention of ethanol at 25°C was less than 5%; the $t_{1/2}$ was almost 1 minute for both temperatures.

Figure 7.36b shows that at 25°C the droplet temperature initially fell to the wet bulb temperature; subsequently it increased extremely slowly, indicative of evaporation from a saturated surface. When the temperature was increased to 42°C there was, from the onset, a gradual increase in droplet temperature to the air temperature. The drying rates at each temperature showed only one falling-rate period corresponding to evaporation from localised wet spots on the droplet surface. The drying rate at the higher temperature was more rapid.

An increase in the drying air temperature to 62°C and 89°C (with a velocity of 0.8 m/s), resulted in no ethanol retention after 3 minutes and 2 minutes at 65°C and 89°C respectively (as shown in Figure 7.37a). The rate of ethanol loss was more rapid at the higher temperature, indicating that the temperature driving force was probably the major factor affecting the process.

The droplet temperature histories, (Figure 7.37b), show that at 62°C there was initial evaporation from a wet surface, so that the droplet temperature remained constant from $t = 30$ seconds to $t = 2$ minutes, before a rapid increase to the air temperature at $t = 4$ minutes. With a drying air temperature of 89°C the droplet temperature increased rapidly from the onset and attained

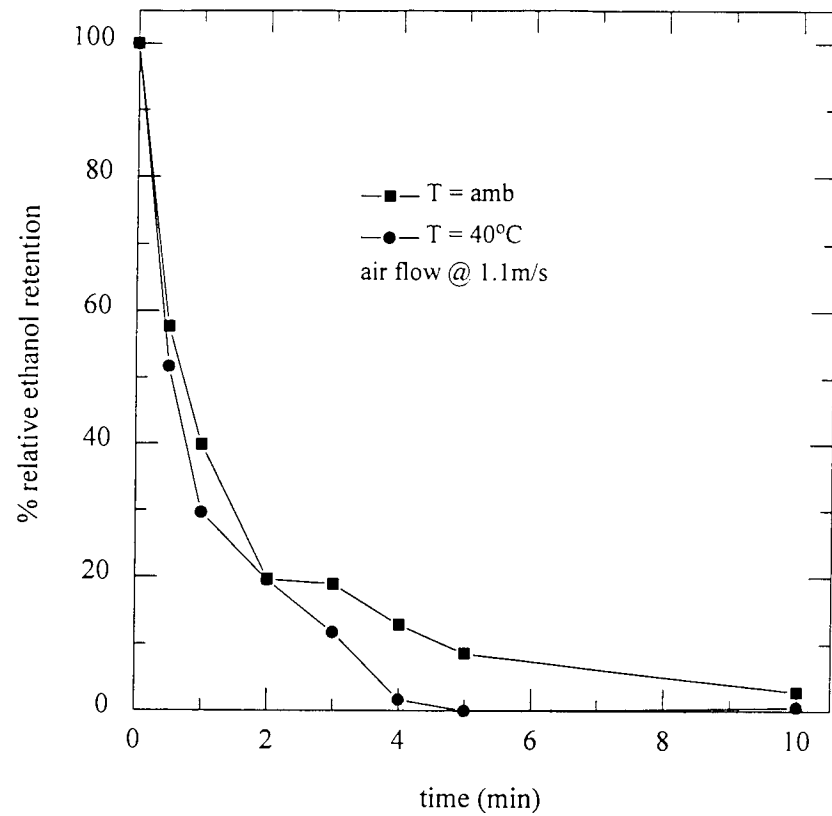


Figure 7.36a

The effect of temperature on the retention of ethanol in 20% rice starch solutions

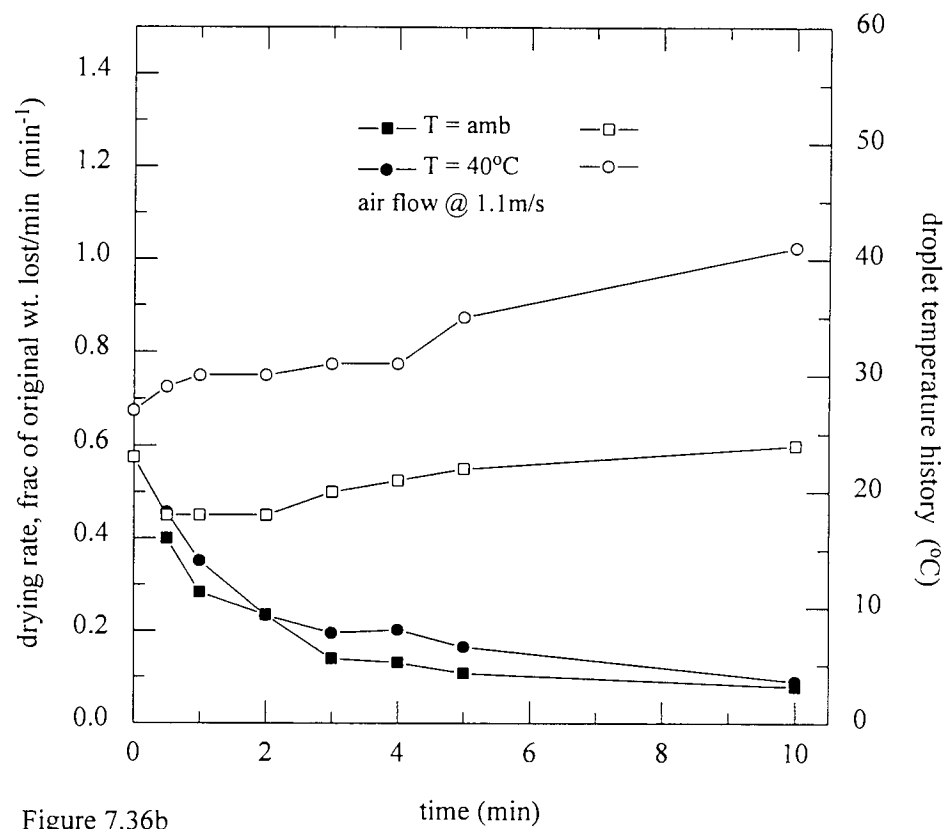


Figure 7.36b

The drying rate [solid symbols] and droplet temperature history [open symbols] for 20% rice starch solutions

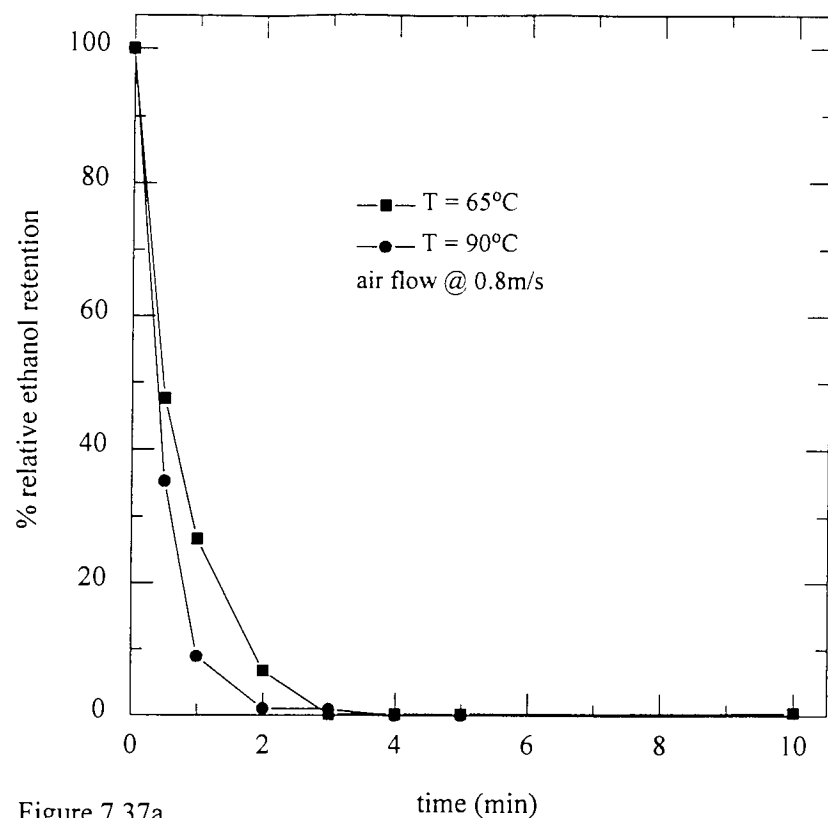


Figure 7.37a

The effect of temperature on the retention of ethanol in 20% rice starch solutions

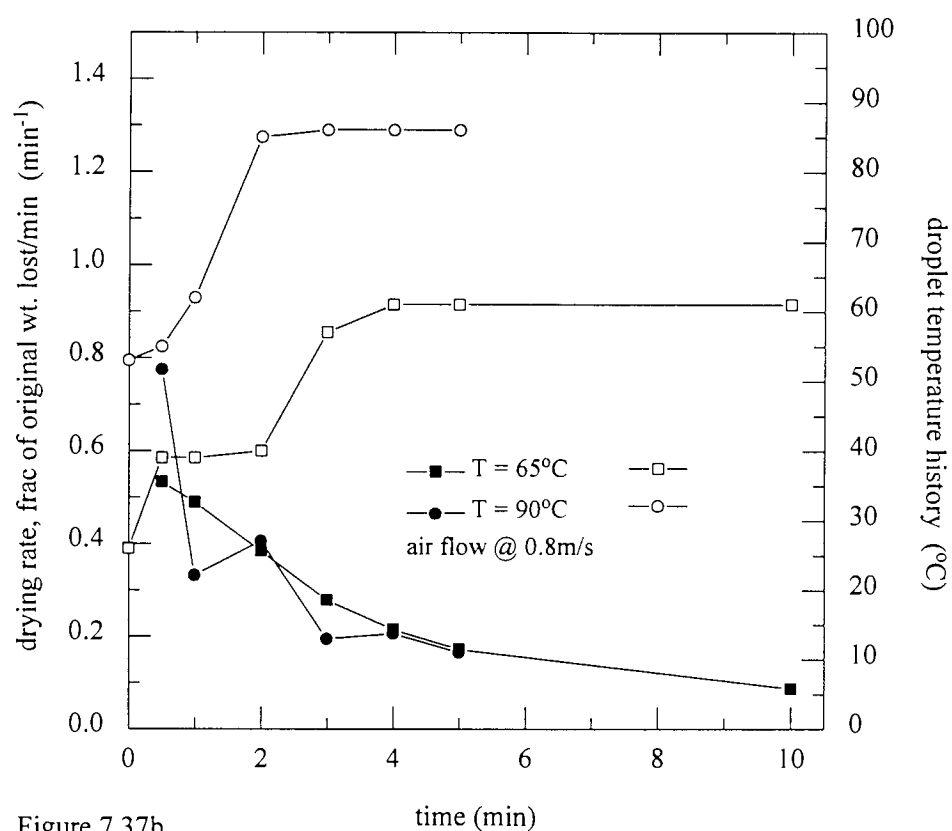


Figure 7.37b

The drying rate [solid symbols] and droplet temperature history [open symbols] for 20% rice starch solutions

the air temperature at $t = 2$ minutes. There was only one falling-rate drying period at each temperature, the rate at the higher temperature being more rapid.

7.1.3.2: Wheat starch

An increase in air temperature from 25°C to 42°C, (with an air velocity of 1.1 m/s), had a significant effect upon retention in the droplets of wheat starch, as illustrated in Figure 7.38a). The final retention of the ethanol was enhanced at the higher temperature, increasing from 10% at 25°C to almost 30% at 42°C. The $t_{1/2}$ were also different with $t_{1/2} \cong 30$ seconds for 25°C and $t_{1/2} \cong 1$ minute for 42°C.

Figure 7.38b shows that at 25°C there was an initial fall in droplet temperature to the wet bulb temperature, followed by an almost constant temperature for 4.5 minutes before a gradual increase in the remaining time of drying. The constant temperature period suggests that evaporation must have occurred from a saturated surface. This implies that the skin formed on the droplet surface was sufficiently porous to allow the passage of moisture from the interior to the surface. The increase in droplet temperature with air temperature at 42°C is indicative of evaporation from an unsaturated surface. This implies that an impervious skin had developed on the surface which prevented the moisture from migrating from the droplet interior. The drying rates show that drying initially occurred at a faster rate at the lower temperature, which also suggests that the skin formed at the higher temperature was more resistant to mass transfer.

Conversely, as shown in Figure 7.39a, an increase in temperature from 62°C to 89°C (air velocity = 0.8 m/s) had the effect of reducing ethanol retention from almost 50% at 62°C to less than 10% at 89°C. The explanation for this reduction in ethanol content is that at the higher temperature there was case hardening of the droplet. The remaining moisture inside the droplet expanding

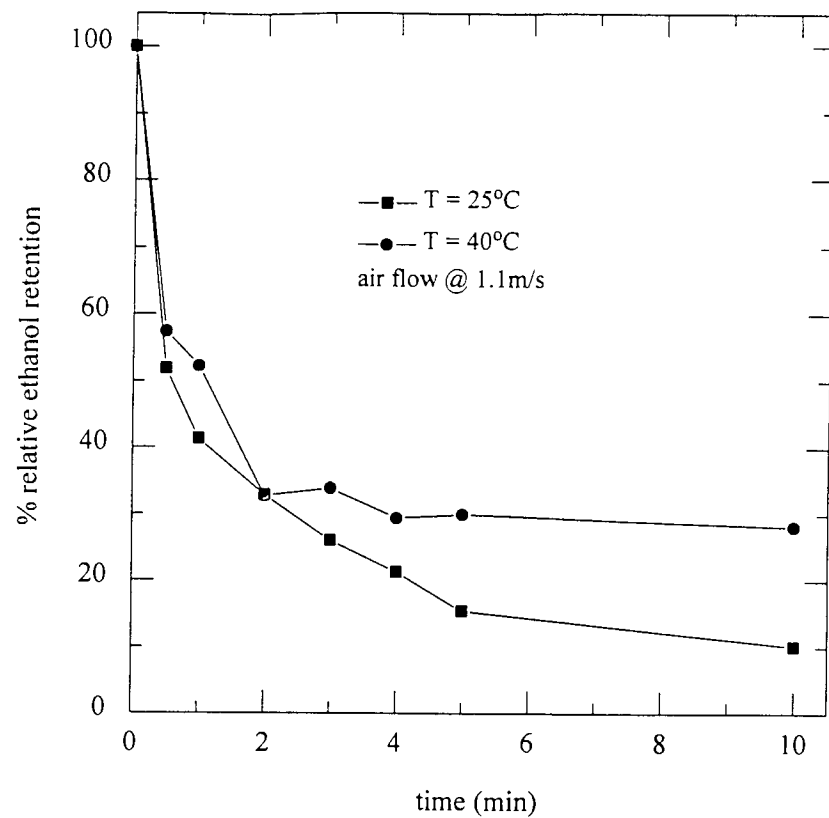


Figure 7.38a

The effect of temperature on the retention of ethanol in 20% wheat starch solutions

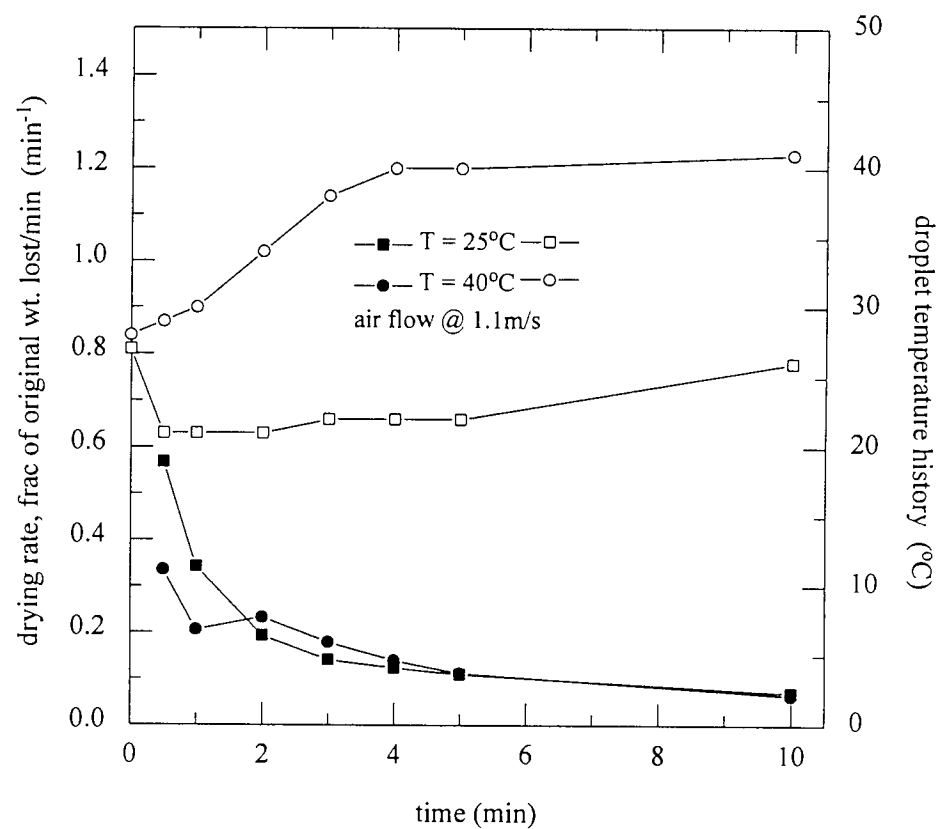


Figure 7.38b

The drying rate [solid symbols] and droplet temperature history [open symbols] for 20% wheat starch solutions

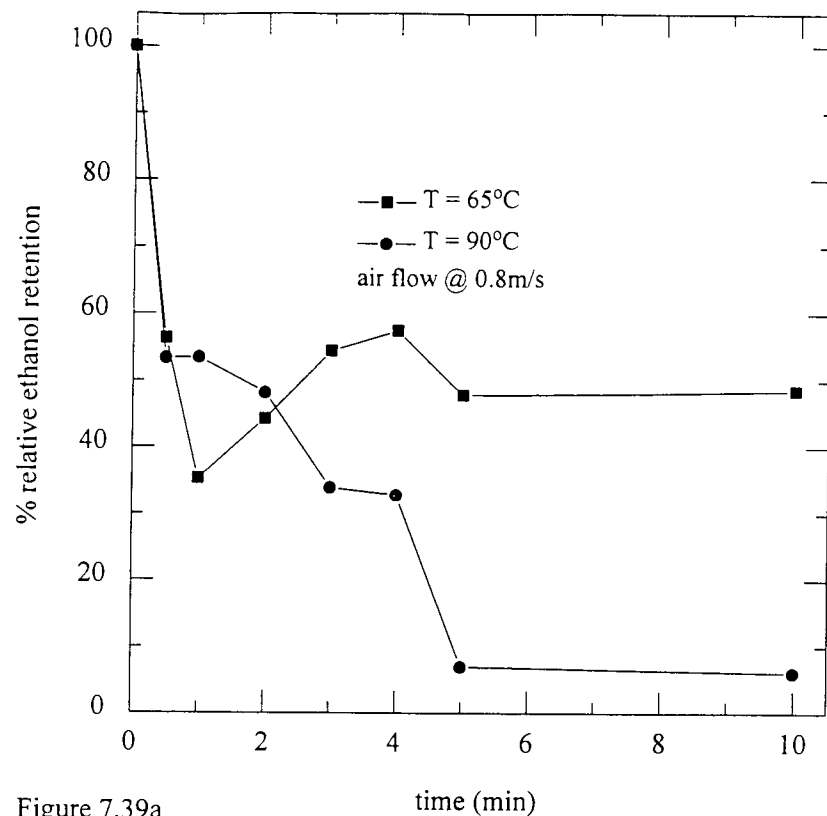


Figure 7.39a

The effect of temperature on the retention of ethanol in 20% wheat starch solutions

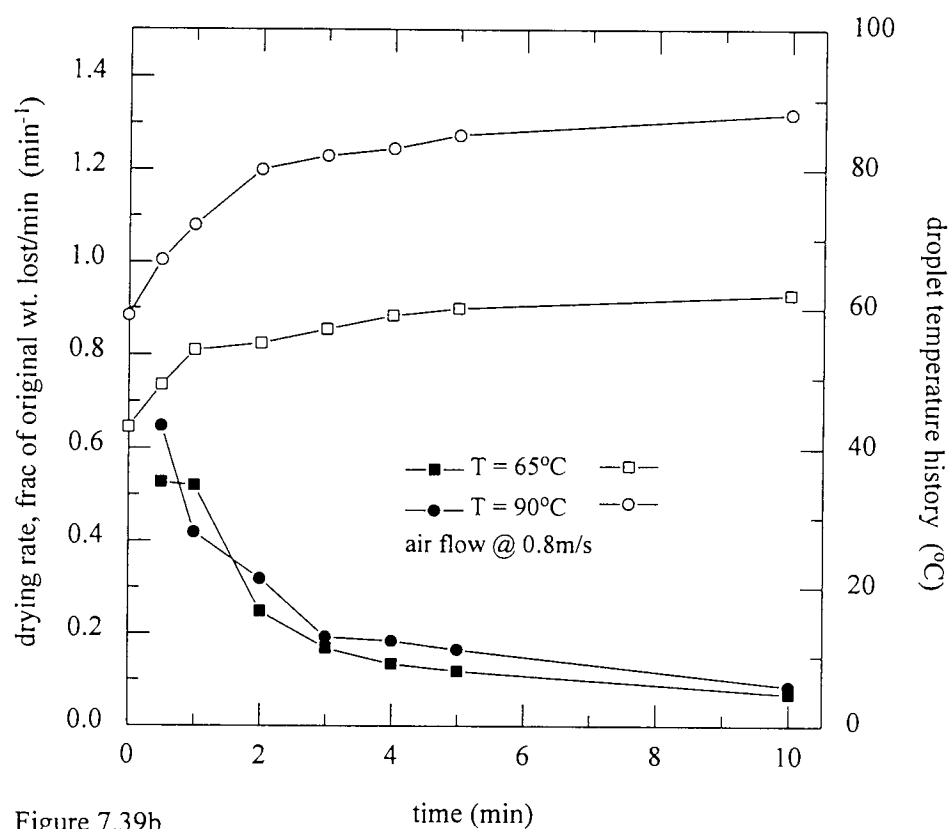


Figure 7.39b

The drying rate [solid symbols] and droplet temperature history [open symbols] for 20% wheat starch solutions

as the droplet was being heated, caused cracking of the impervious skin thus allowing the ethanol to escape resulting in a reduction in ethanol retention (Sayed *et. al.*, 1995 (a)).

Figure 7.39b shows that at both these temperatures, there was a rapid increase in core temperature from the onset of drying. The increase in temperature is indicative of the formation of an impervious skin which hindered mass transfer. The drying rate was highest at 89°C, and there was only one falling-rate period at each temperature.

7.1.3.3: Dextrin

Figure 7.40a shows that an increase in temperature from 25°C to 42°C had no significant difference in the retention of ethanol. The only noticeable difference was the slightly more rapid loss at the higher temperature during the first two minutes of exposure. After 3 minutes, the rate of ethanol loss became almost zero (indicated by the slope of the graph) resulting in a final retention of 10% at both temperatures.

At 25°C the droplet temperature fell to the wet bulb temperature, as shown in Figure 7.40b, and remained there for almost all of the drying period. This suggests evaporation from a saturated surface, i.e. there was no resistance to mass transfer at the surface. However at the higher air temperature the droplet temperature increased suggesting a significant resistance to mass transfer at the surface. The drying rates exhibited only one falling-rate period at each temperature.

An increase in the air temperature to 62°C and 89°C respectively (air velocity = 0.8 m/s), demonstrated no significant difference in retention between them except that the final retention being greater at 62°C (almost 18% compared to approximately 15% at 89°C). As shown in Figure 7.41a, both $t_{1/2}$ values were the same (almost 30 seconds).

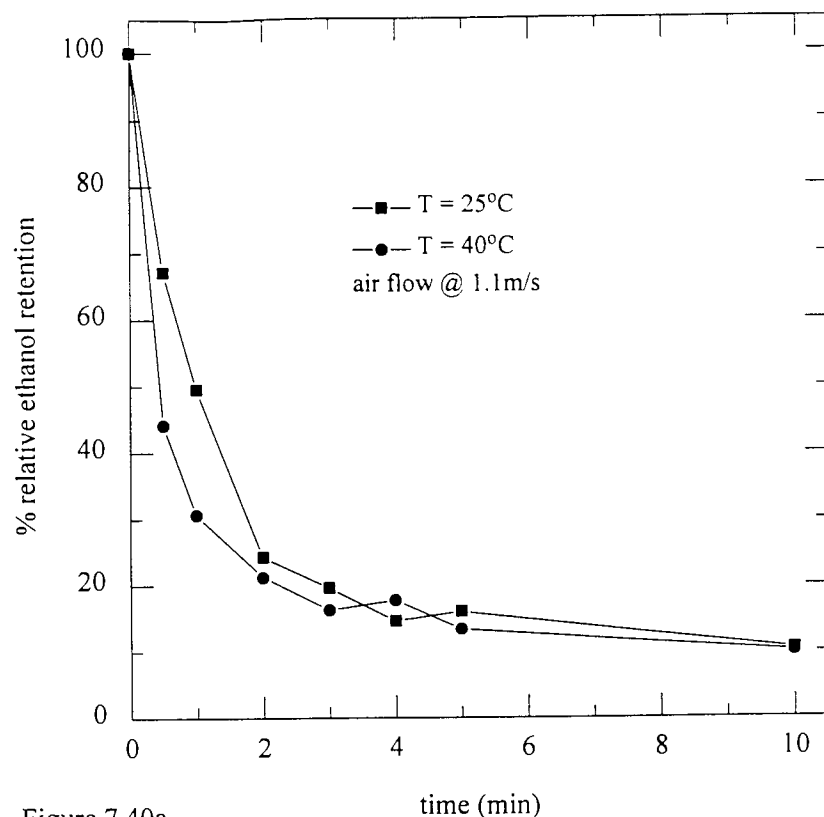


Figure 7.40a

The effect of temperature on the retention of ethanol in 20% dextrin solutions

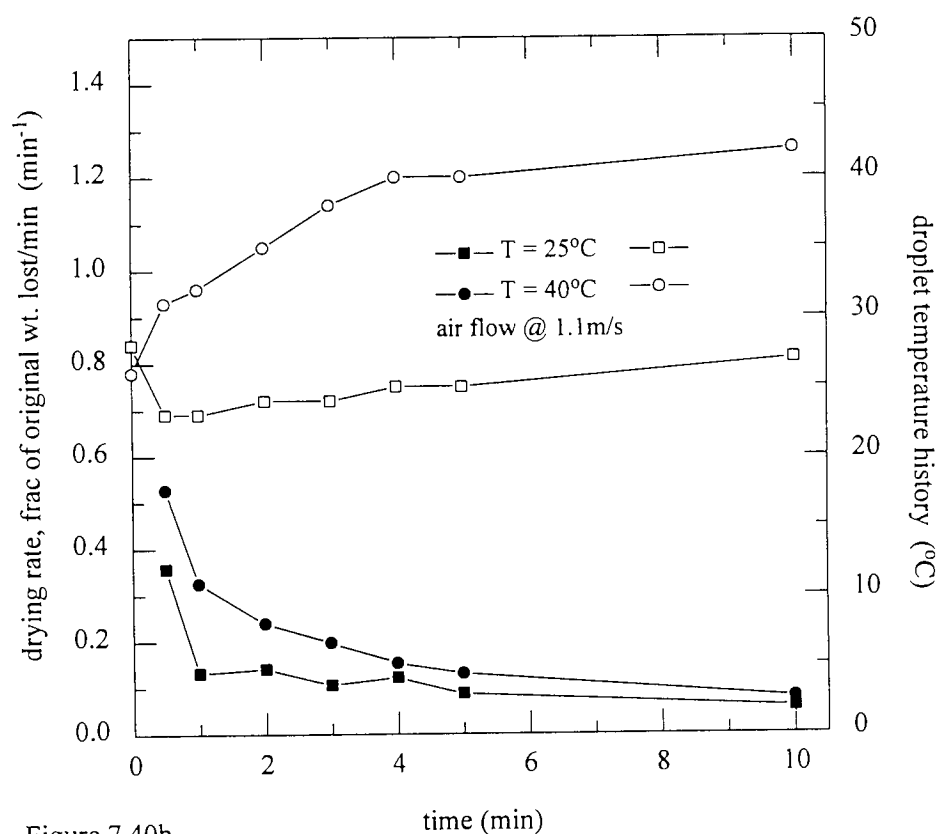


Figure 7.40b

The drying rate [solid symbols] and droplet temperature history [open symbols] for 20% dextrin solutions

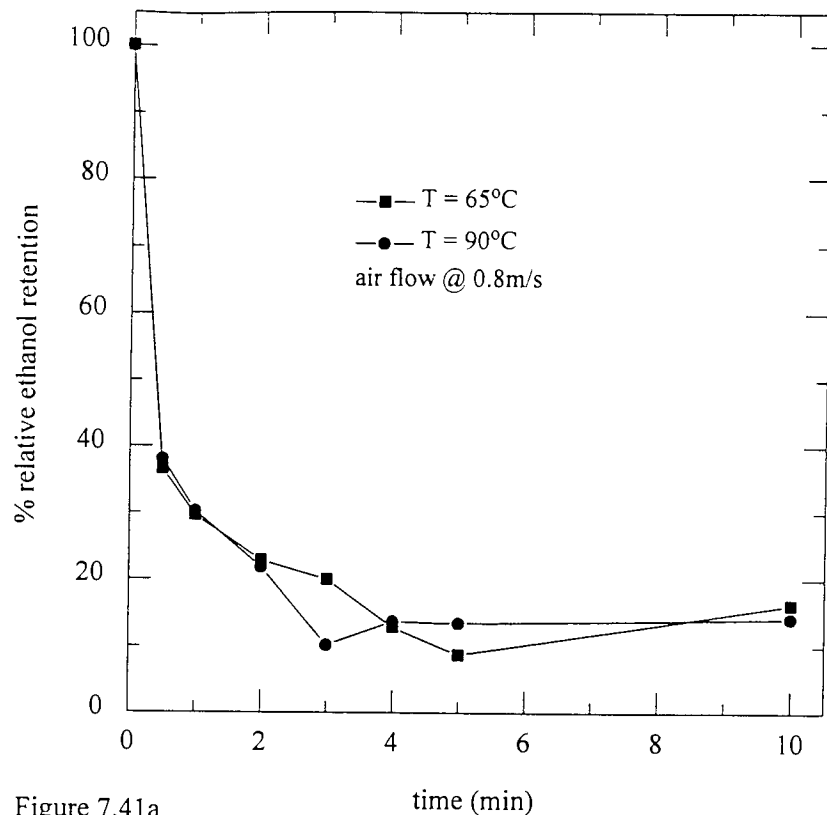


Figure 7.41a

The effect of temperature on the retention of ethanol in 20% dextrin solutions

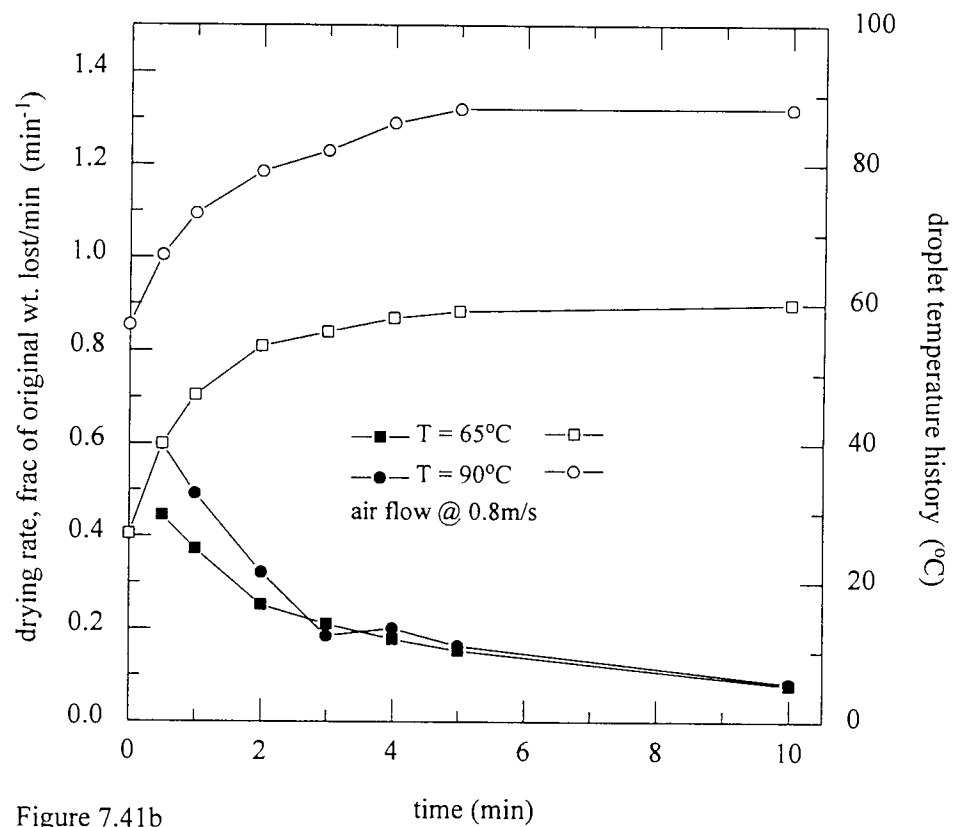


Figure 7.41b

The drying rate [solid symbols] and droplet temperature history [open symbols] for 20% dextrin solutions solutions

The droplet temperatures increased rapidly at both temperatures (Figure 7.41b). This coupled with the one falling-rate period suggests that evaporation occurred from localised wet spots rather than from a completely wet surface.

7.1.3.4: Fructose

No significant difference was found in the retention of ethanol upon increasing the drying air temperature from 25°C to 42°C with the air velocity at 1.1 m/s (as shown in Figure 7.42a). The ethanol content had reduced to its final value (approximately 2%) after three minutes of drying at 42°C, whilst the final value at 25°C was attained after four minutes; the $t_{1/2}$ were 1 minute and 30 seconds at the lower and higher temperature respectively.

Figure 7.42b, illustrates the drying rates and the droplet temperature histories. There was an initial drop to the wet bulb temperature followed by an increase to the drying air temperature. The increase was more rapid at 42°C than at 25°C. The drying rates show one falling-rate period for each temperature

An increase in the air temperature from 62°C to 89°C, with a velocity of 0.8 m/s, had no significant effect upon the retention, as shown in Figure 7.43a; the final retention value was < 5% at each temperature. The only difference was the times at which the final retention value was reached; at 62°C this occurred at $t = 3$ minutes, but at $t = 2$ minutes at 89°C. Within the first minute of drying more than 95% of the initial ethanol content had been lost; $t_{1/2} < 30$ seconds for both temperatures. There was, as shown, no difference in the retention of ethanol with dry air compared with humid ambient air. The dry air was obtained by passing the air through the dessicating section of the apparatus.

Figure 7.43b shows rapid increases which occurred in droplet temperature to the corresponding drying air temperature. The increase from the onset of

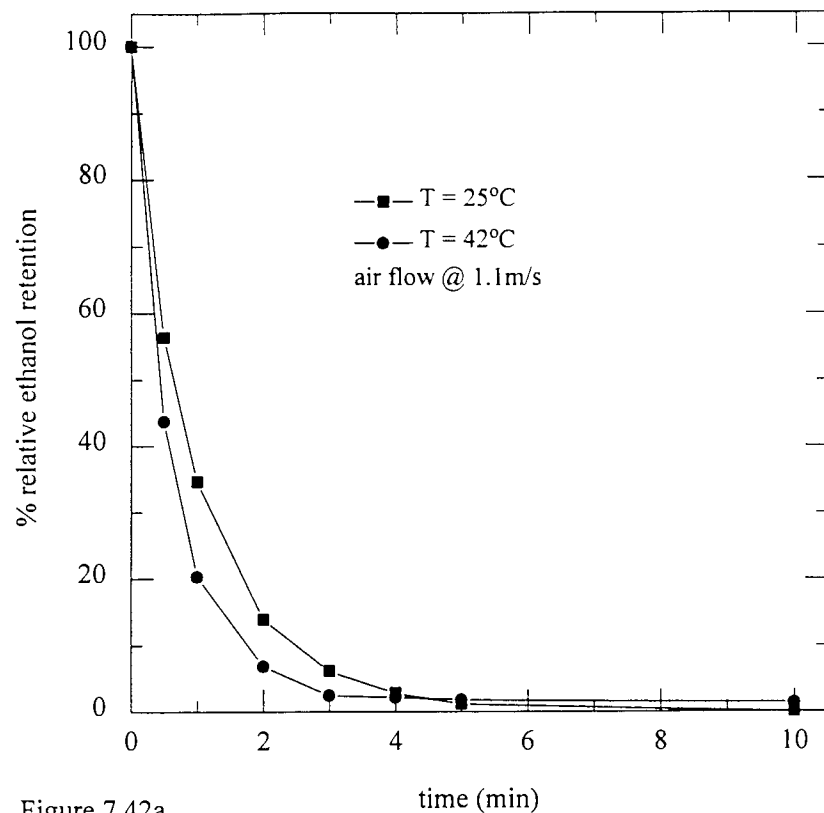


Figure 7.42a

The effect of temperature on the retention of ethanol in 20% fructose solutions

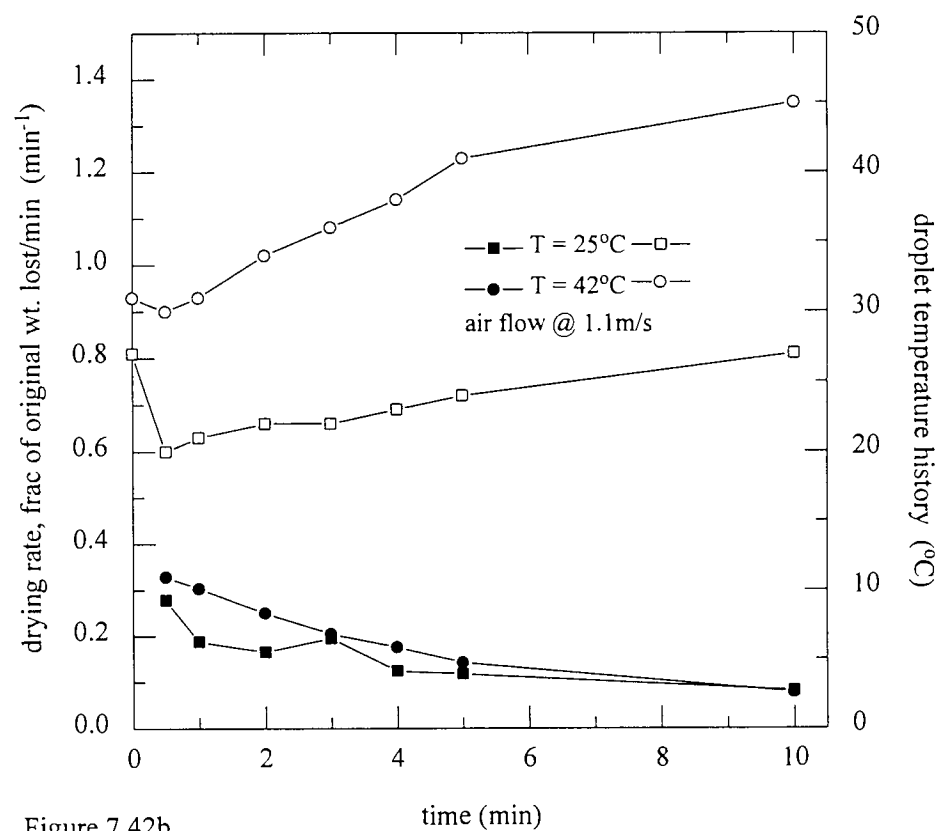


Figure 7.42b

The drying rate [solid symbols] and droplet temperature history [open symbols] for 20% fructose solutions

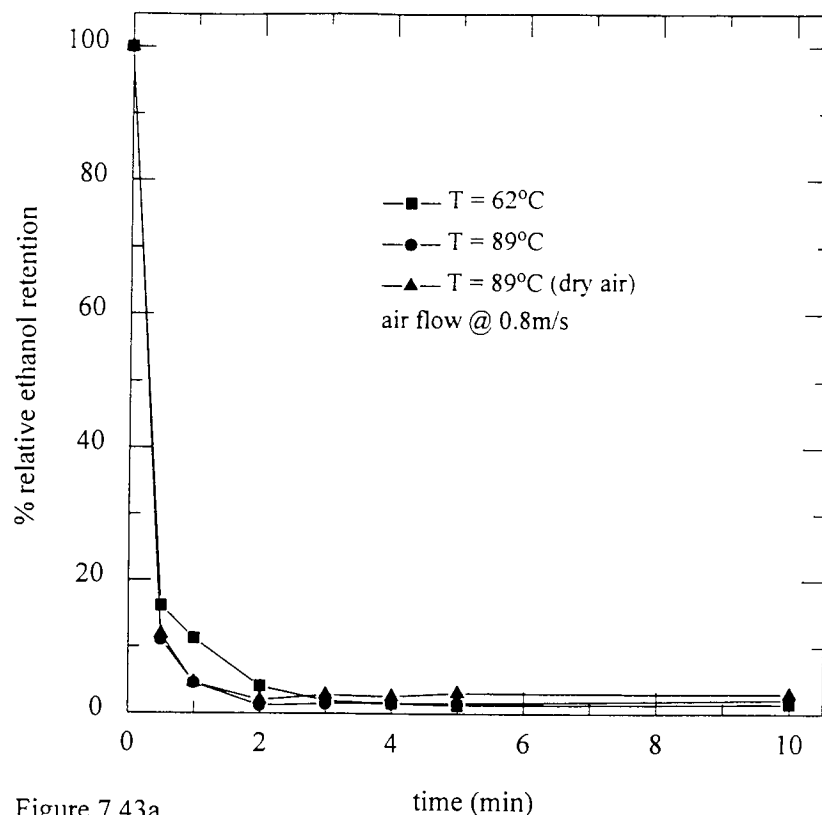


Figure 7.43a

The effect of temperature on the retention of ethanol in 20% fructose solutions

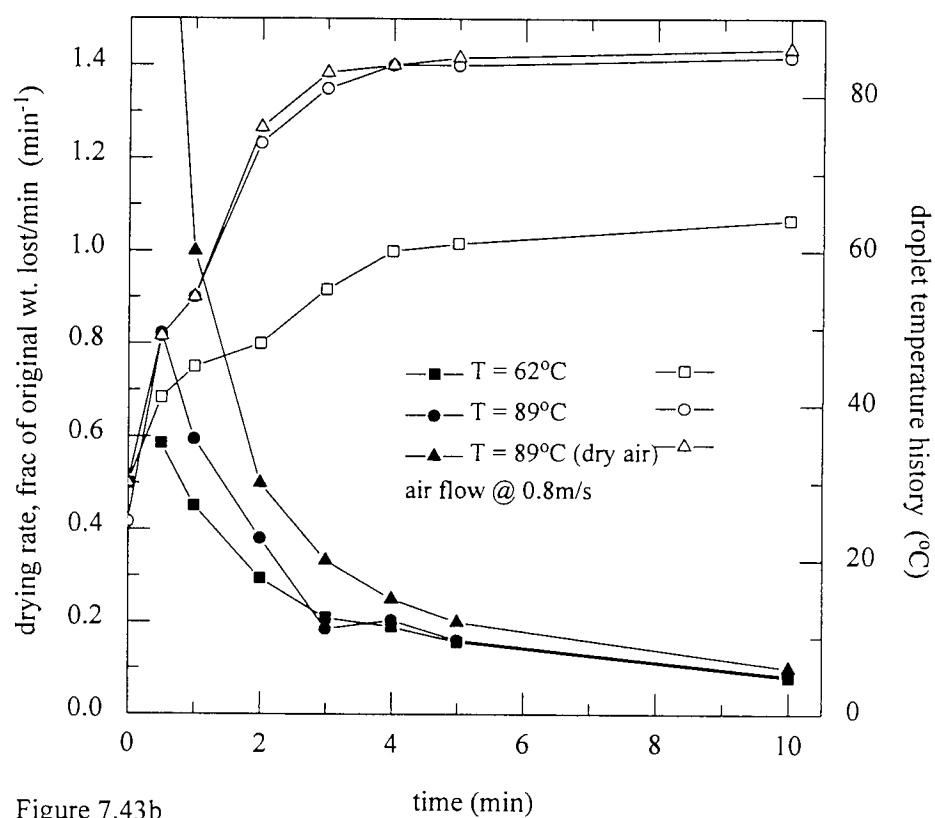


Figure 7.43b

The drying rate [solid symbols] and droplet temperature history [open symbols] for 20% fructose solutions

drying strongly suggests that an impervious skin formed on the droplet. The use of dry air at 89°C produced a similar effect on the droplet temperature to the humid air at the same temperature. Using the dry air resulted in a faster drying rate. Thus the additional driving force to the temperature, viz. the difference in humidity, is an important rate determining factor.

7.1.3.5: Skim milk

An increase in temperature from 25°C to 42°C resulted in an almost quadrupled enhancement in the retention of ethanol from <10% to almost 40%, as shown in Figure 7.44a. The use of dry air at 42°C reduced the final retention value to almost 20%, with $t_{1/2}$ also being similar at one minute.

The temperature histories (Figure 7.44b) show that with the humid air at both temperatures there was an initial fall to the wet bulb temperature before a gradual increase; this initial fall was not observed with dry air. This suggests that initial evaporation was from a wet surface followed by the formation of an impervious skin. The drying rates with humid air were similar at both temperatures with only one falling-rate. However the dry air produced a markedly greater drying rate and two falling-rate periods were present, suggesting the added driving force due to the difference in humidity. The second falling period suggests that there was resistance to the migration of moisture because of the existence of an impervious skin. The drying rates reduced more slowly after $t = 3$ minutes showing the formation of an impervious skin which hinders mass transfer; this is shown by the final value of the ethanol retention reaching its minimum after $t = 3$ minutes (Figure 7.44a).

An increase in air temperature from 62°C to 89°C, (Figure 7.45a), reduced the retention of ethanol from 37% to 10%, with that at 62°C reaching its minimum after one minutes drying and the droplets at 89°C showing a steady downwards trend. This was unexpected because at the higher temperature,

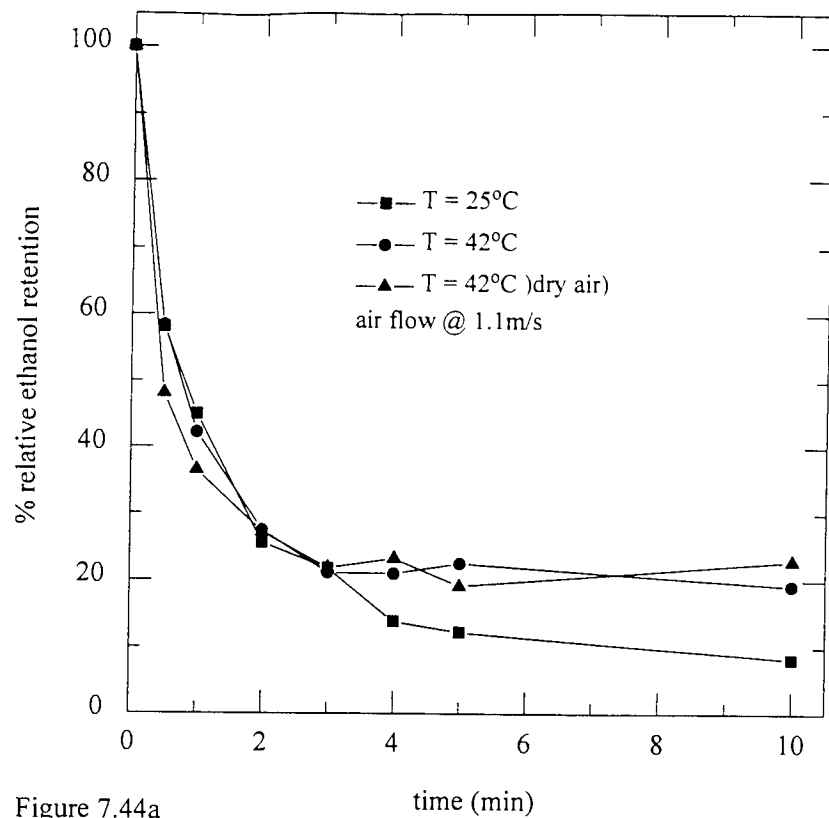


Figure 7.44a

The effect of temperature on the retention of ethanol in 20% skim milk solutions

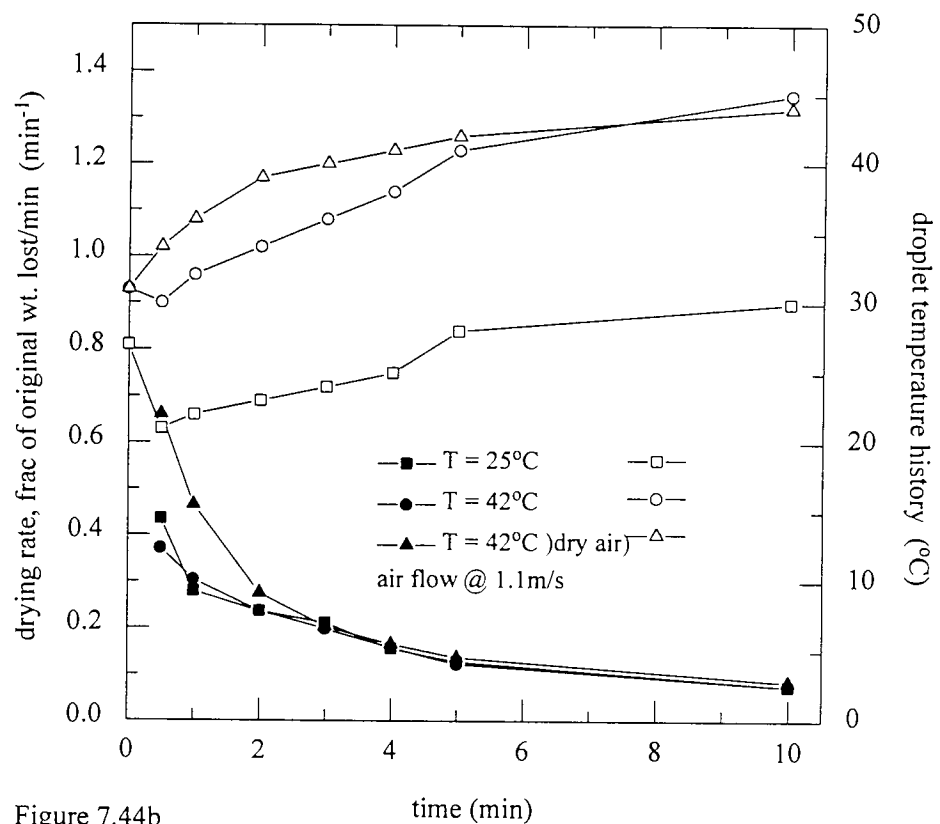


Figure 7.44b

The drying rate [solid symbols] and droplet temperature history [open symbols] for 20% skim milk solutions

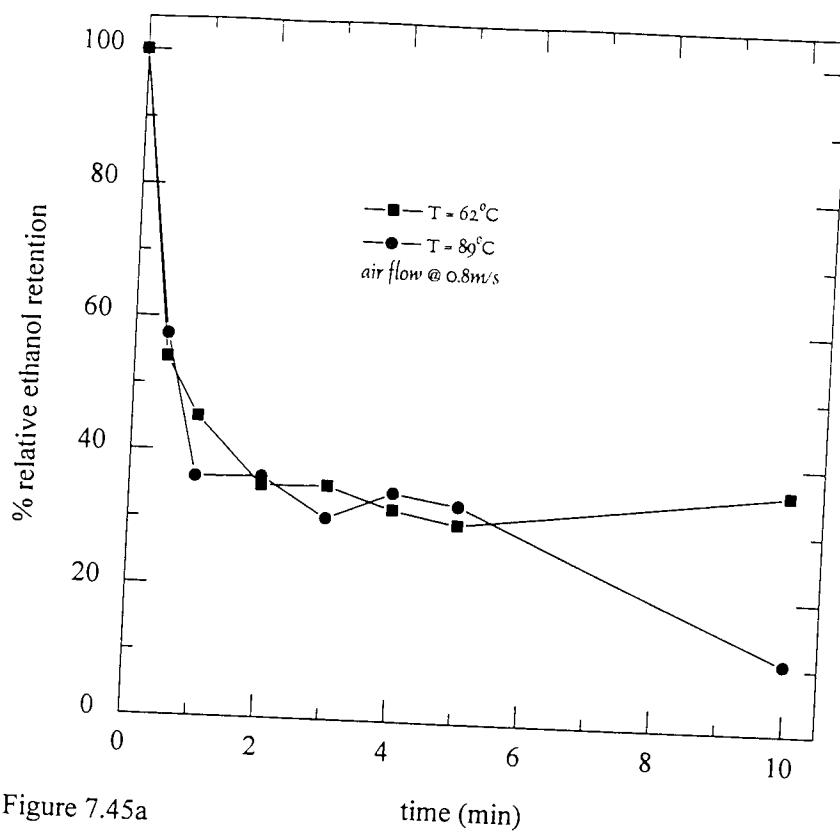


Figure 7.45a
The effect of temperature on the retention of ethanol in 20% skim milk solutions

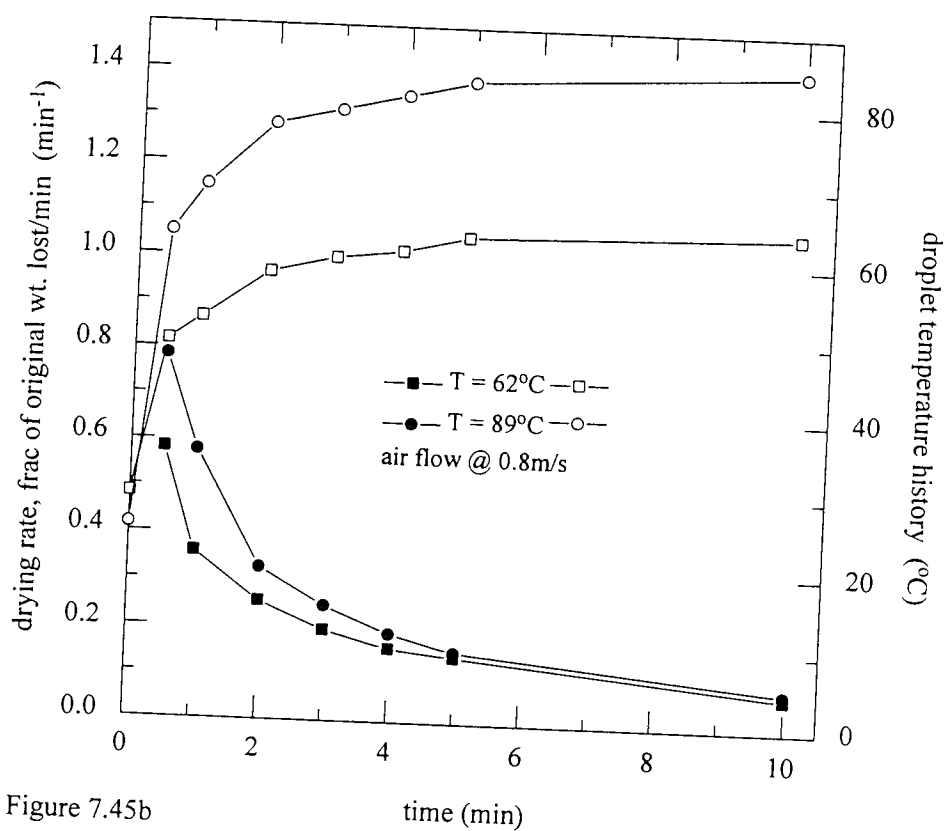


Figure 7.45b
The drying rate [solid symbols] and droplet temperature history [open symbols] for 20% skim milk solutions

there was the formation of a smoother more resistant skin. This reduction in ethanol content can be explained by the appearance of cracks in the smooth surface which would have allowed the ethanol loss to occur (Sayed *et. al.*, 1995 (b)). Both $t_{1/2}$ values are also similar at almost one minute.

Both droplet temperature histories demonstrate a rapid increase to the drying air temperature indicative of the formation of a resistant skin. The drying rates (Figure 7.45b) demonstrate two falling-rate periods, the first period extending upto 2 minutes of drying followed by the second period from $t = 2$ minutes to the end of drying. There was a faster initial drying rate at the higher temperature because of the increased temperature driving force.

7.1.3.6: Coffee

An increase in air temperature from 25°C to 42°C with an air velocity of 1.1 m/s did not significantly effect the retention of ethanol; the only effect was slight reduction in the retention at the higher temperature from almost 30% to 24% as illustrated in Figure 7.46a. The $t_{1/2}$ at both temperatures was almost two minutes.

Figure 7.46b, shows that there was an increase in droplet temperature from the onset of drying. This suggests that surface evaporation was not sufficiently rapid to maintain a constant droplet temperature. The drying rates were identical showing one falling-rate period indicative of some resistance to the migration of moisture to the droplet.

An increase in air temperature from 62°C to 89°C (air velocity 0.8 m/s) reduced the final ethanol content from almost 27% to 10% (Figure 7.47a). The use of dry air at 89°C produced a similar effect to humid air with a final ethanol content of 10%. The $t_{1/2}$ was similar, almost 2 minutes, at both

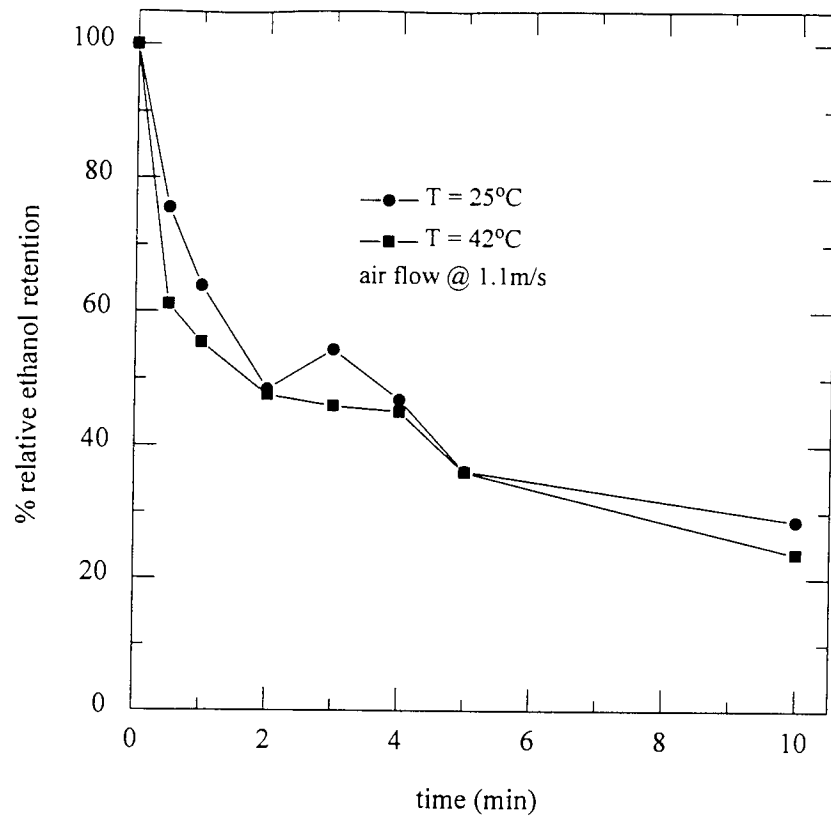


Figure 7.46a

The effect of temperature on the retention of ethanol in 20% coffee solutions

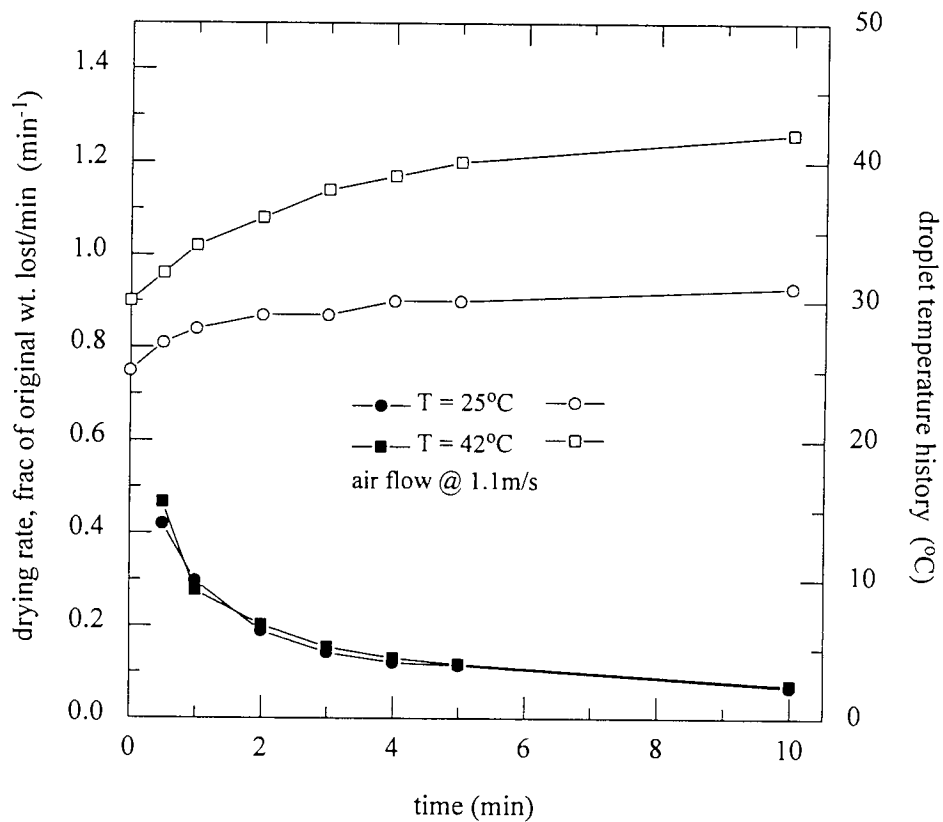


Figure 7.46b

The drying rate [solid symbols] and droplet temperature history [open symbols] for 20% coffee solutions

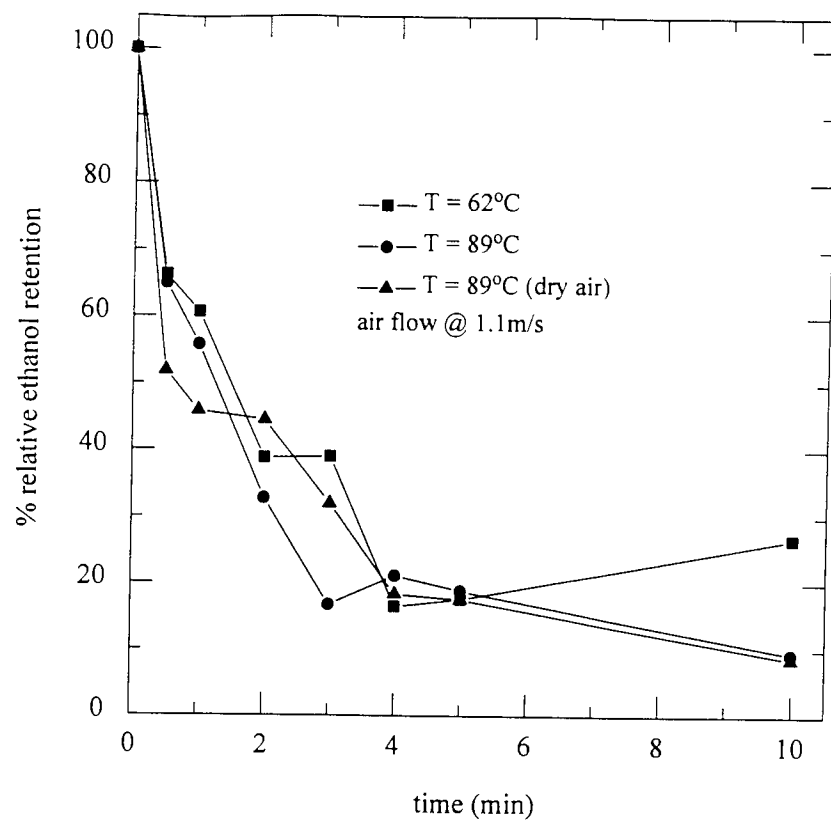


Figure 7.47a

The effect of temperature on the retention of ethanol in 20% coffee solutions

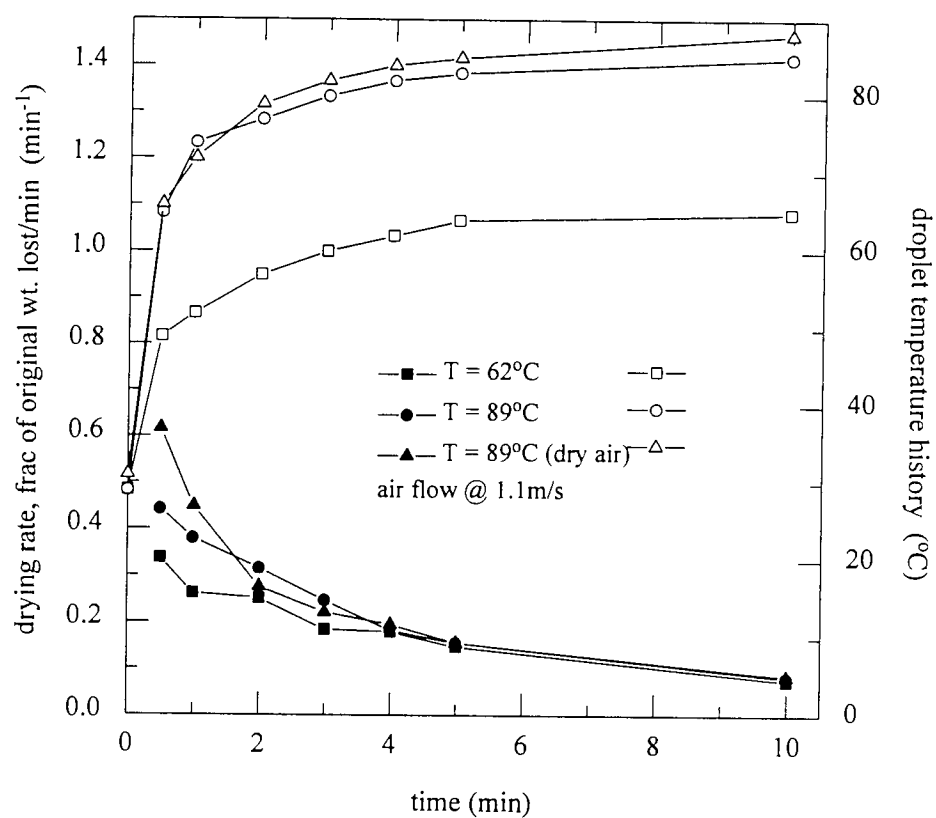


Figure 7.47b

The drying rate [solid symbols] and droplet temperature history [open symbols] for 20% coffee solutions

temperatures with the humid air, but was reduced to < 1 minute with the dry air, reflecting the additional humidity driving force.

Figure 7.47b shows that the droplet temperatures increased rapidly to the drying air temperature, with the humidity having no significant effect upon them. As already discussed the increase in temperature points to the formation of an impervious skin resistant to mass transfer. The drying rate curves show only one falling-rate period for the humid air at each temperature; the dry air provided two falling-rate periods. The drying rates became equal at all three conditions after $t = 4$ minutes of drying; this suggests that after the first four minutes the alteration of drying conditions would have no significant effect upon the drying rate - resistance of an impervious skin is the controlling factor.

7.1.3.7: Gelatine 60

An increase in drying air temperature from 25°C to 42°C at an air velocity of 1.1 m/s made only a slight difference to the final ethanol content of the droplets, i.e. from 10% to almost 18% (as illustrated in Figure 7.48a). The $t_{1/2}$ was < 30 seconds for both temperatures. The droplet temperature histories in Figure 7.48b show that at 25°C there was the initial drop to the wet bulb temperature followed by a gradual increase, i.e there was some evaporation from a saturated surface. This can be explained by the drying rates which show two falling-rate periods. The first indicates evaporation from localised wet spots rather than from a saturated surface; the second is indicative of restricted migration of moisture from within the droplet. At 42°C the droplet temperature increased gradually towards that of the drying air. The drying rates reached steady state at $t = 5$ minutes as indicated by their slopes and by the ethanol content of the droplets having reached the final value by $t = 5$ minutes.

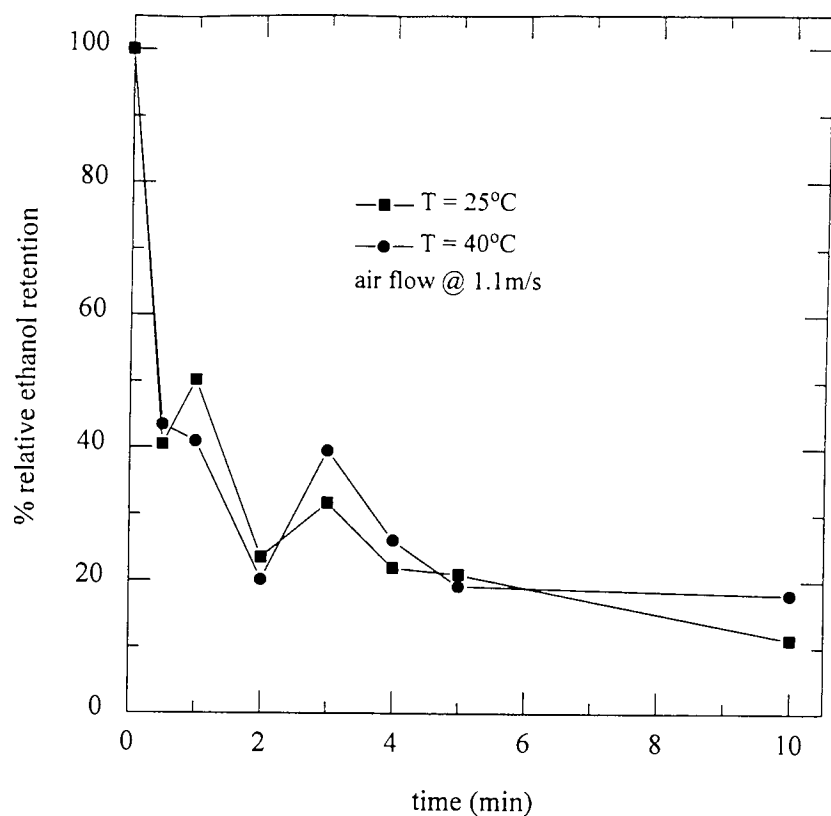


Figure 7.48a

The effect of temperature on the retention of ethanol in 20% gelatin 60 solutions

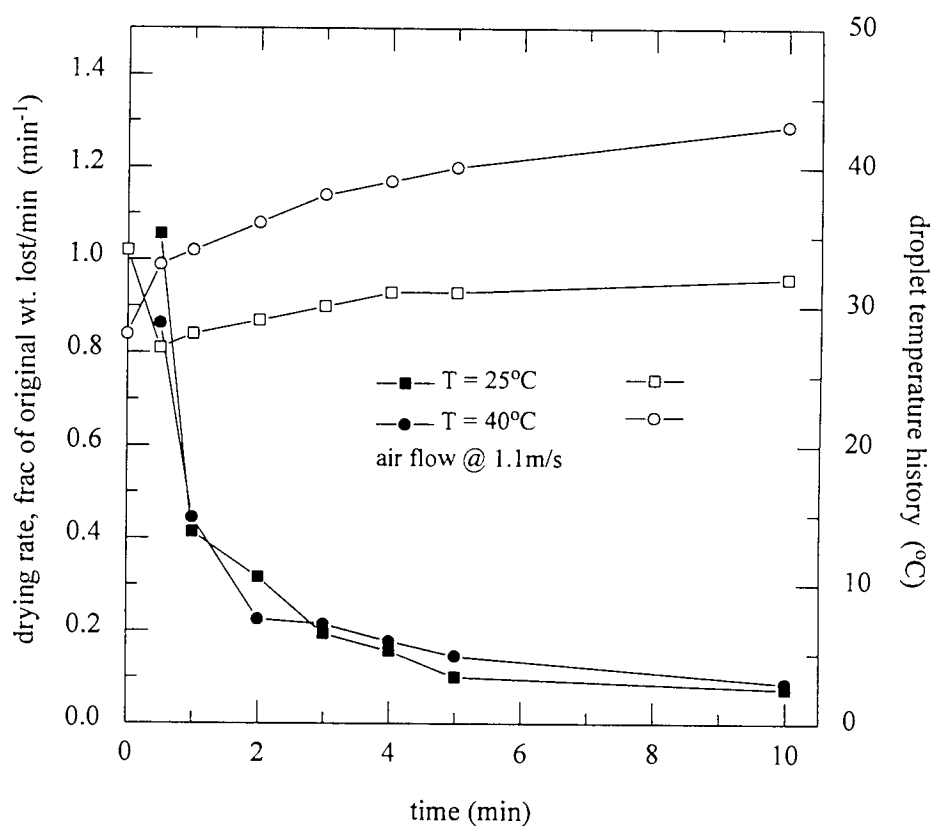


Figure 7.48b

The drying rate [solid symbols] and droplet temperature history [open symbols] for 20% gelatin 60 solutions

An increase in drying temperature from 62°C to 89°C had no significant effect upon the retention of ethanol with the trends being similar until $t = 5$ minutes (Figure 7.49a) after which there was a decrease in retention at the higher temperature from 20% to <5%. This decrease could be explained by droplet expansion at the elevated temperature which would increase mass transfer due to the increase in surface area and reduction in skin thickness. The $t_{1/2}$ was also the same for the two temperatures (< 30 seconds). There was no difference in using dry instead of humid air in the retention of ethanol.

The drying rates shown in Figure 7.49b exhibit two falling-rate periods at each temperature, the first upto $t = 2$ minutes followed by the second period which lasted to the end of drying. The droplet temperature histories show that in all cases there was a rapid increase to the drying air temperature, with the increase at 89°C being more rapid than at 62°C.

7.1.3.8: Gelatine 150

Figure 7.50a shows the effect of drying air temperature upon the retention of ethanol. An increase in temperature from 25°C to 42°C caused a decrease in final retention from 37% to 8%, probably explained by the increased temperature driving force and the formation of a less resistant skin. An increase to 62°C caused an increase in retention to almost 57%, possibly because of the dissolution of the gelatine crystals resulting in a smoother more resistant skin which enhanced ethanol retention. A further increase to 89°C had the opposite effect resulting in a reduction in the retention from 57% to 10%. The use of dry air at 89°C, although for only five minutes drying time, showed that the retention was 30% after five minutes unlike 20% for the humid air. The $t_{1/2}$ values were similar at 25°C and 89°C (< 30 seconds); $t_{1/2} = 1$ and 4 minutes at 42°C and 62°C respectively.

Figure 7.50b illustrates that all the drying rates were similar with two falling-rate periods except for that at 62°C which was virtually constant from the

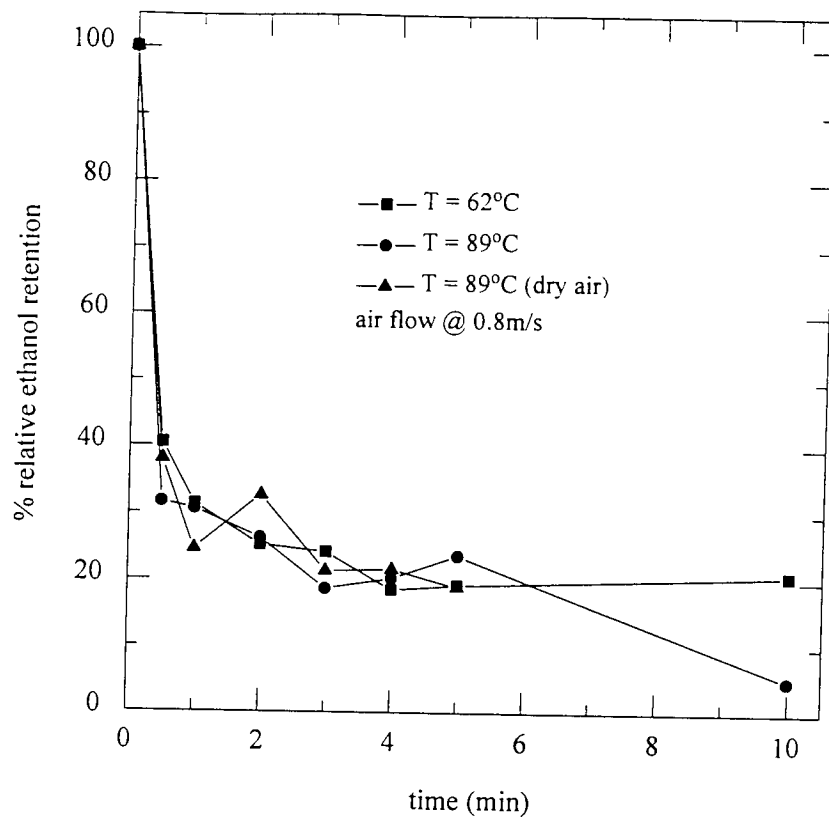


Figure 7.49a

The effect of temperature on the retention of ethanol in 20% gelatin 60 solutions

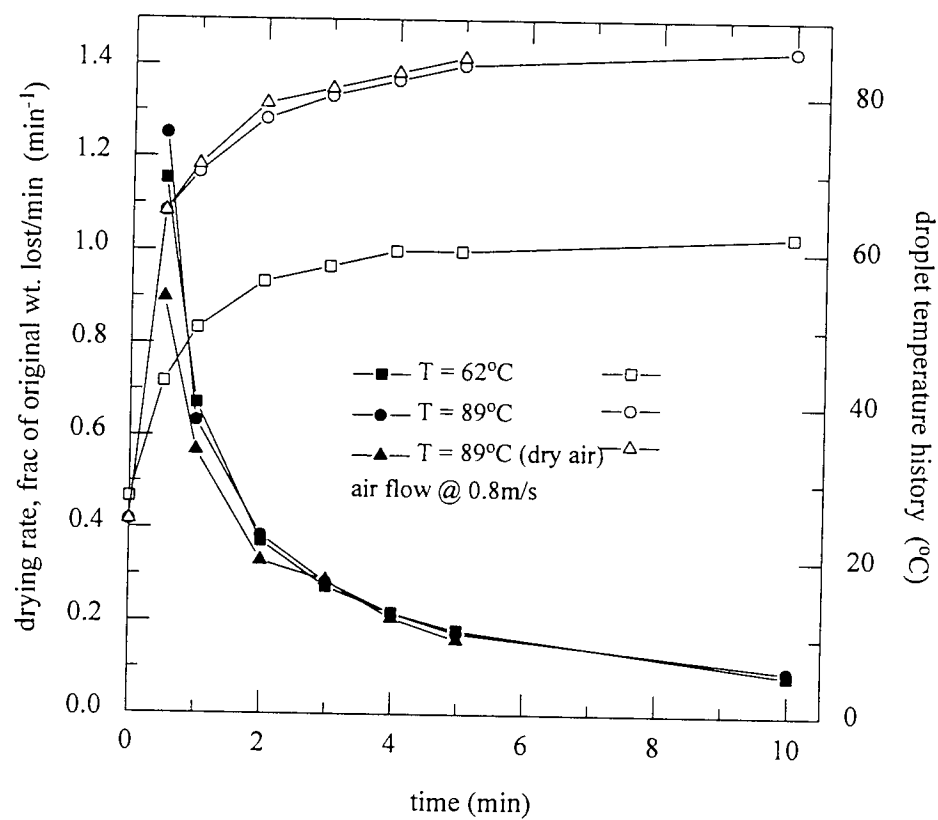


Figure 7.49b

The drying rate [solid symbols] and droplet temperature history [open symbols] for 20% gelatin 60 solutions

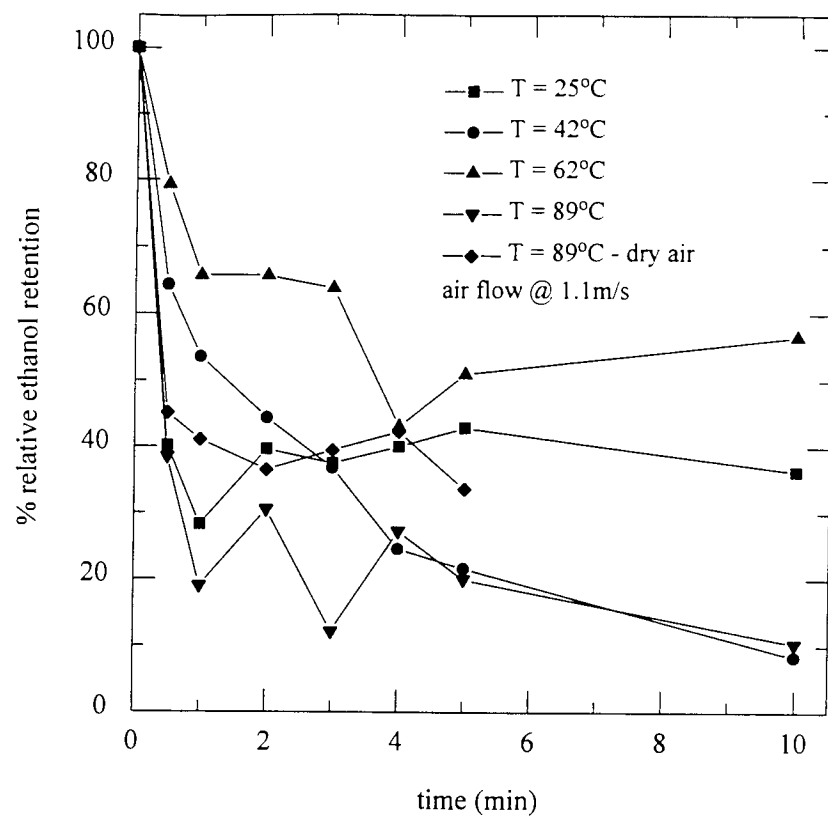


Figure 7.50a

The effect of temperature on the retention of ethanol in 20% gelatin 150 solutions

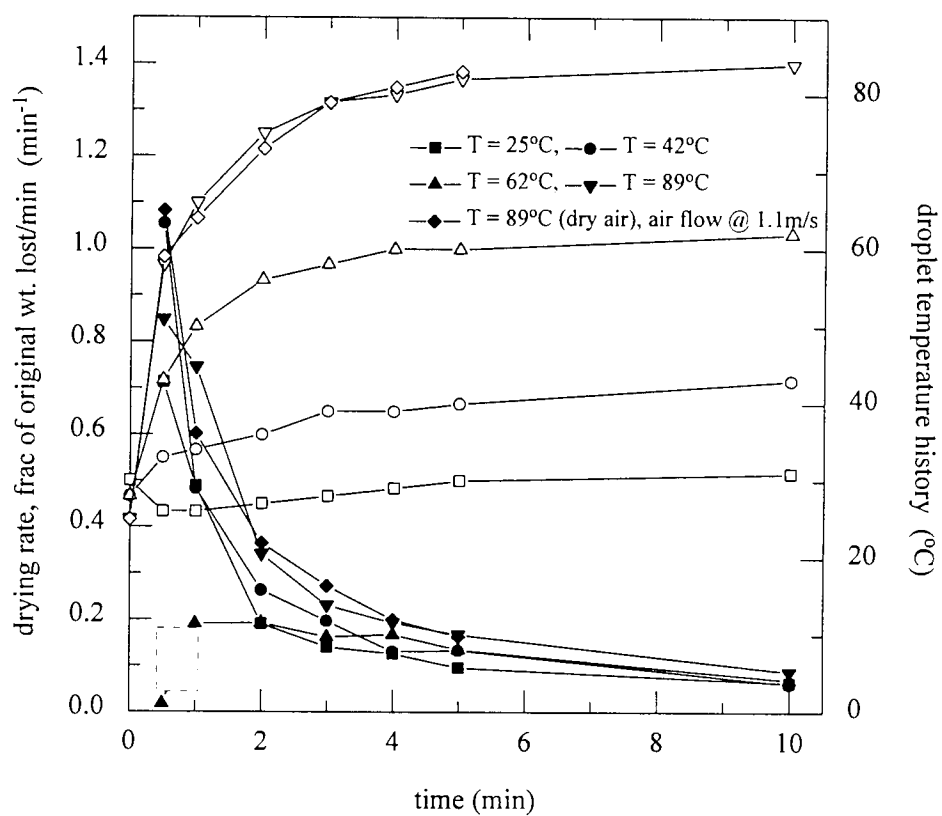


Figure 7.50b

The drying rate [solid symbols] and droplet temperature history [open symbols] for 20% gelatin 150 solutions

onset. This would suggest the rapid formation of a very resistant skin at 62°C. At the higher air temperatures the droplet temperatures increased rapidly. With the air at 25°C drying occurred at the wet bulb temperature. This, coupled with the high retention at this temperature, would suggest that the skin which formed on the droplet was selectively permeable to the water allowing it to escape without the ethanol.

7.1.3.9: Gum arabic

The increase in temperature from 25°C to 42°C had no significant effect upon ethanol retention, as illustrated in Figure 7.51a, with $t_{1/2} = 1$ minute and the final reduction in ethanol concentration to be almost 20%, attained after four minutes drying. Figure 7.51b shows the difference between the drying rates with the rate at 25°C being faster than at 42°C. This would suggest that at 25°C there was an initial rapid loss of moisture before the formation of a skin which then hindered the mass transfer; this skin probably formed after three minutes drying. At 42°C there was a slower drying rate indicative of the formation of a resistant skin almost immediately. The droplet temperature histories show an initial fall to the wet bulb temperature followed by a gradual increase (at 25°C) suggesting initial surface evaporation followed by the formation of a skin. The almost immediate increase in droplet temperature at 42°C suggests the formation of an impervious skin which hindered mass transfer.

A reduction of almost 20% in the ethanol content was associated with an increase in temperature from 62°C to 89°C, i.e. from 30% to 10% after five minutes (as shown in Figure 7.52a) with $t_{1/2} < 30$ seconds. At 62°C there was a rapid drop in ethanol content to 40% suggesting that the skin which formed was not initially a hinderance to mass transfer, but with the progress of drying it became more resistant thus resulting in greater retention. With the temperature at 89°C the ethanol content dropped to almost 10% after two minutes of drying, indicative of a skin of lower resistance. This reduction in

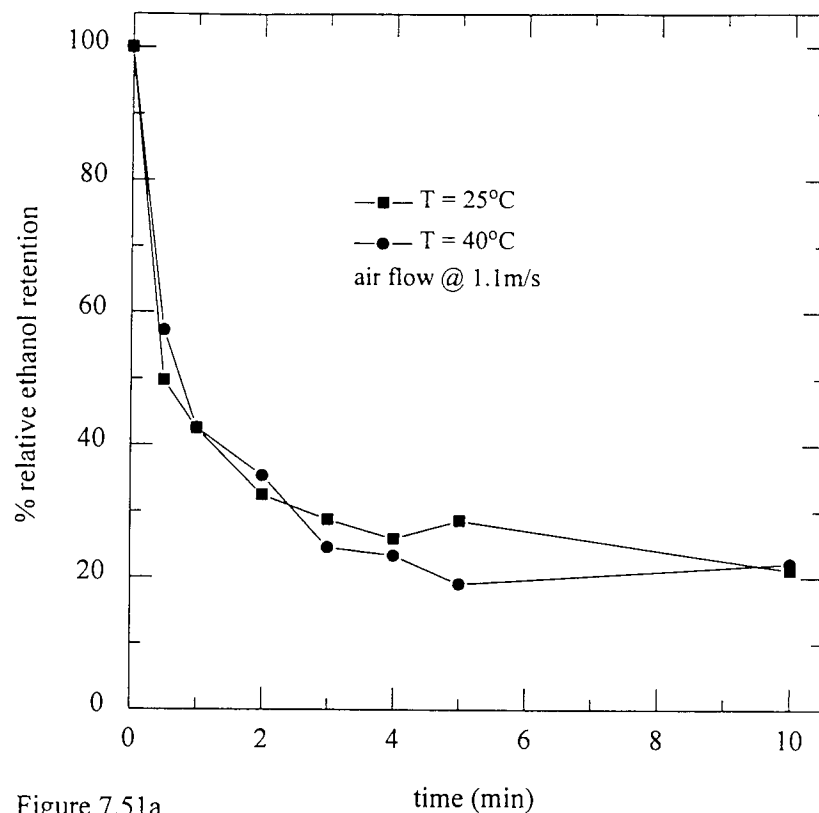


Figure 7.51a

The effect of temperature on the retention of ethanol in 20% gum arabic solution

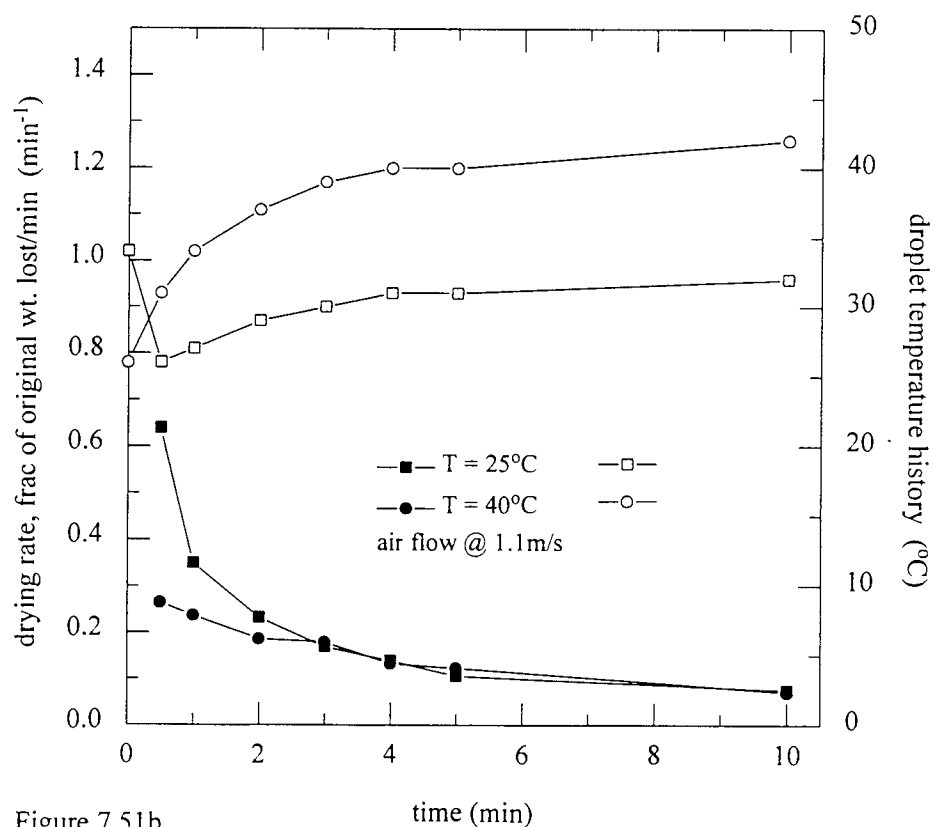


Figure 7.51b

The drying rate [solid symbols] and droplet temperature history [open symbols] for 20% gum arabic solutions

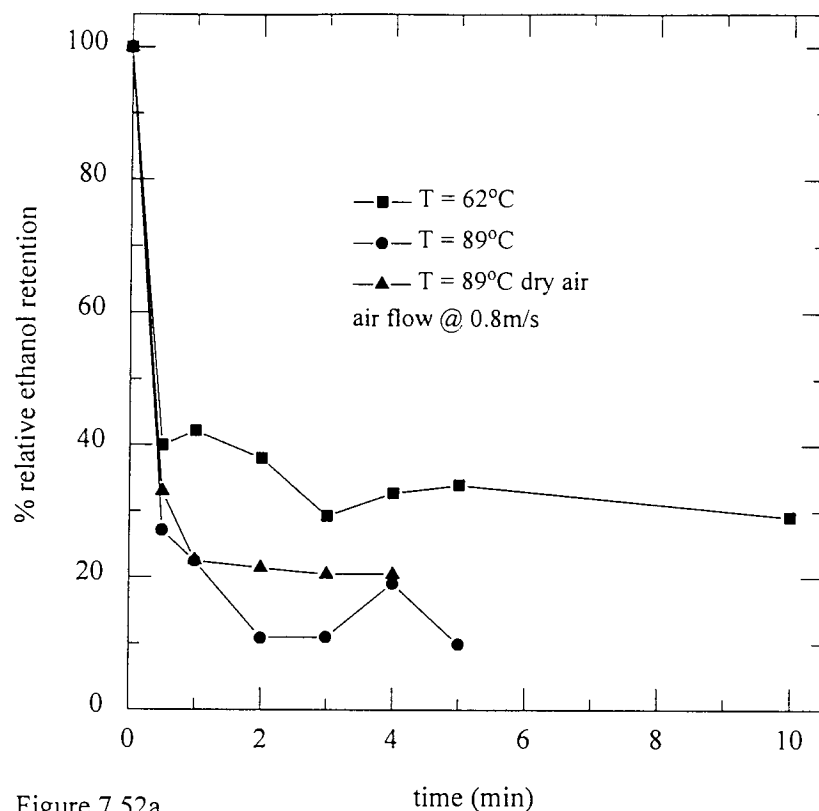


Figure 7.52a

The effect of temperature on the retention of ethanol in 20% gum arabic solution

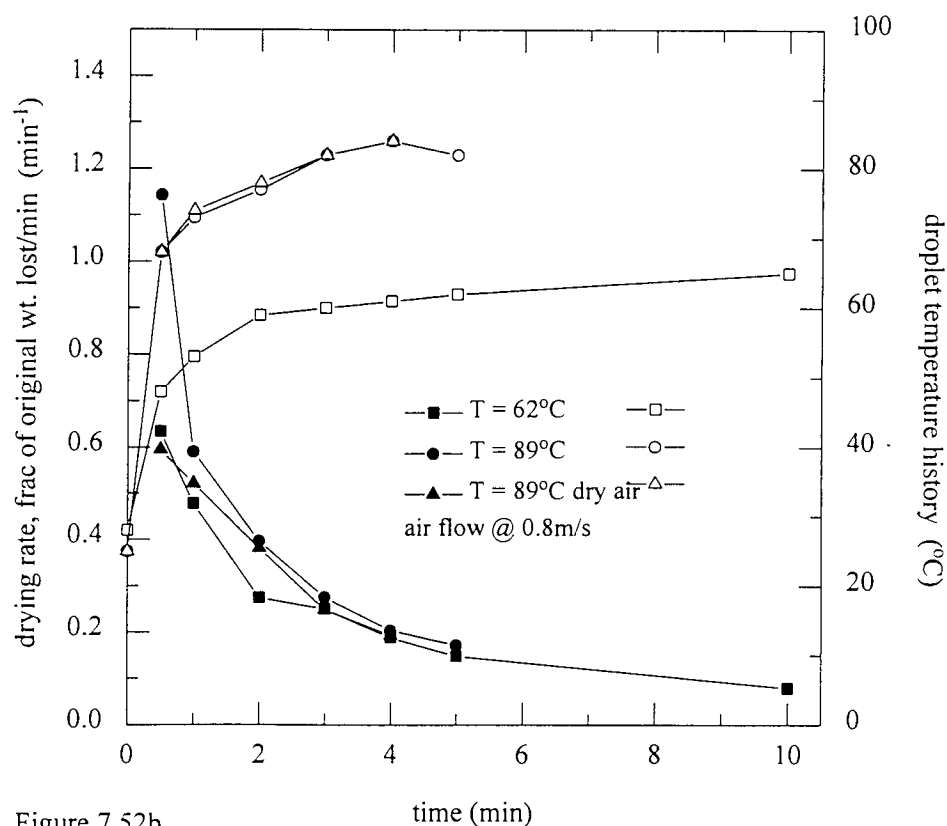


Figure 7.52b

The drying rate [solid symbols] and droplet temperature history [open symbols] for 20% gum arabic solutions

ethanol content is actually due to the skin being resistant to mass transfer causing expansion / contraction of the droplets which would enhance mass transfer (El-Sayed *et. al.*, 1990, and Sayed *et. al.*, 1995). The use of dry air at 89°C enhanced the retention of ethanol, the final value (at $t = 5$ minutes) being 20%, suggesting that with dry air there could have been a reduction in the number of expansion / contraction cycles which would have reduced the loss of ethanol.

The drying rates, at 62°C and 89°C (humid air) were similar; the rate for 89°C (dry air) being markedly different. There was a rapid rise in droplet temperature to reach that of the drying air, as shown by the temperature histories, with no significant difference between results with humid and dry air (Figure 7.52b).

7.2: Antibiotics

The selected antibiotics, described in Chapter 6, were dissolved / suspended in distilled water. Individual droplets were suspended from the end of a rotating thermocouple in a drying air stream; after set time intervals they were removed for analysis of their residual potency, expressed as % relative zone diameter. (The method of analysis is detailed in Chapter 6). The final zone diameter was taken as the diameter of the zone produced by an antibiotic droplet which had been dried for ten minutes. The same notation for solution concentrations are used as in Section 7.1, viz. solutions A, B, and C are the 10%, 20% and 40% w/w solutions respectively.

The plates for the assay must be prepared carefully to avoid complications (such as surface wetness which causes re-growth onto the cleared zones, as shown in Plates 7.53 and 7.54), and hence the need to repeat the assay.

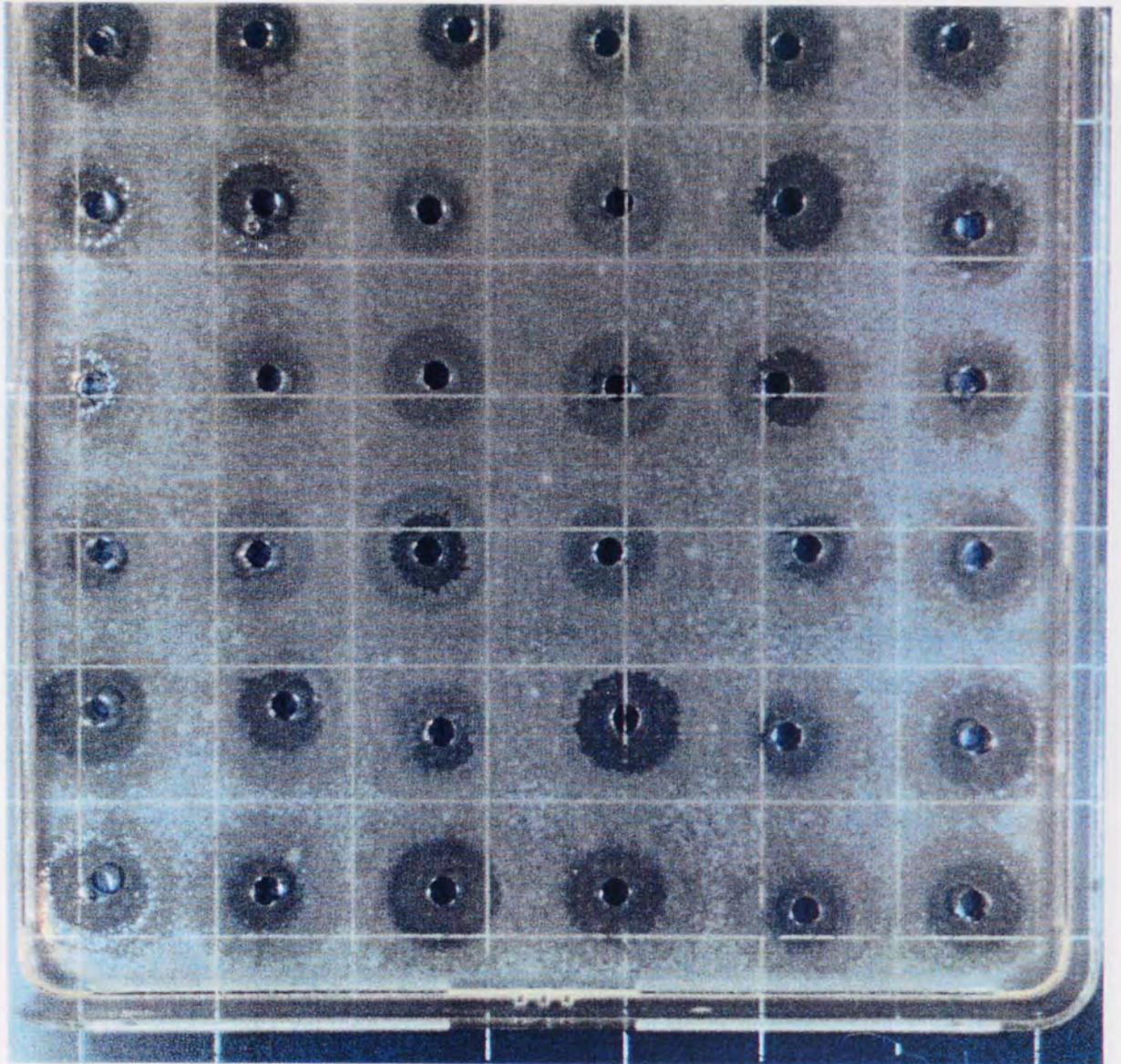


Plate 7.53 Photograph showing re-growth of organisms on previously cleared zones

Figure 7.54: Effect of environmental factors

Figure 7.54 shows the effect of environmental factors on the re-growth of organisms on previously cleared zones. The figure is a photograph of a 6x6 grid of 36 small, square, clear plastic containers. Each container has a small, dark, circular hole in the center. The containers are arranged in a 6x6 grid, with 6 containers in each row and 6 containers in each column. The containers are filled with a dark, granular material, and the holes are filled with a dark, granular material. The containers are arranged in a 6x6 grid, with 6 containers in each row and 6 containers in each column. The containers are filled with a dark, granular material, and the holes are filled with a dark, granular material.

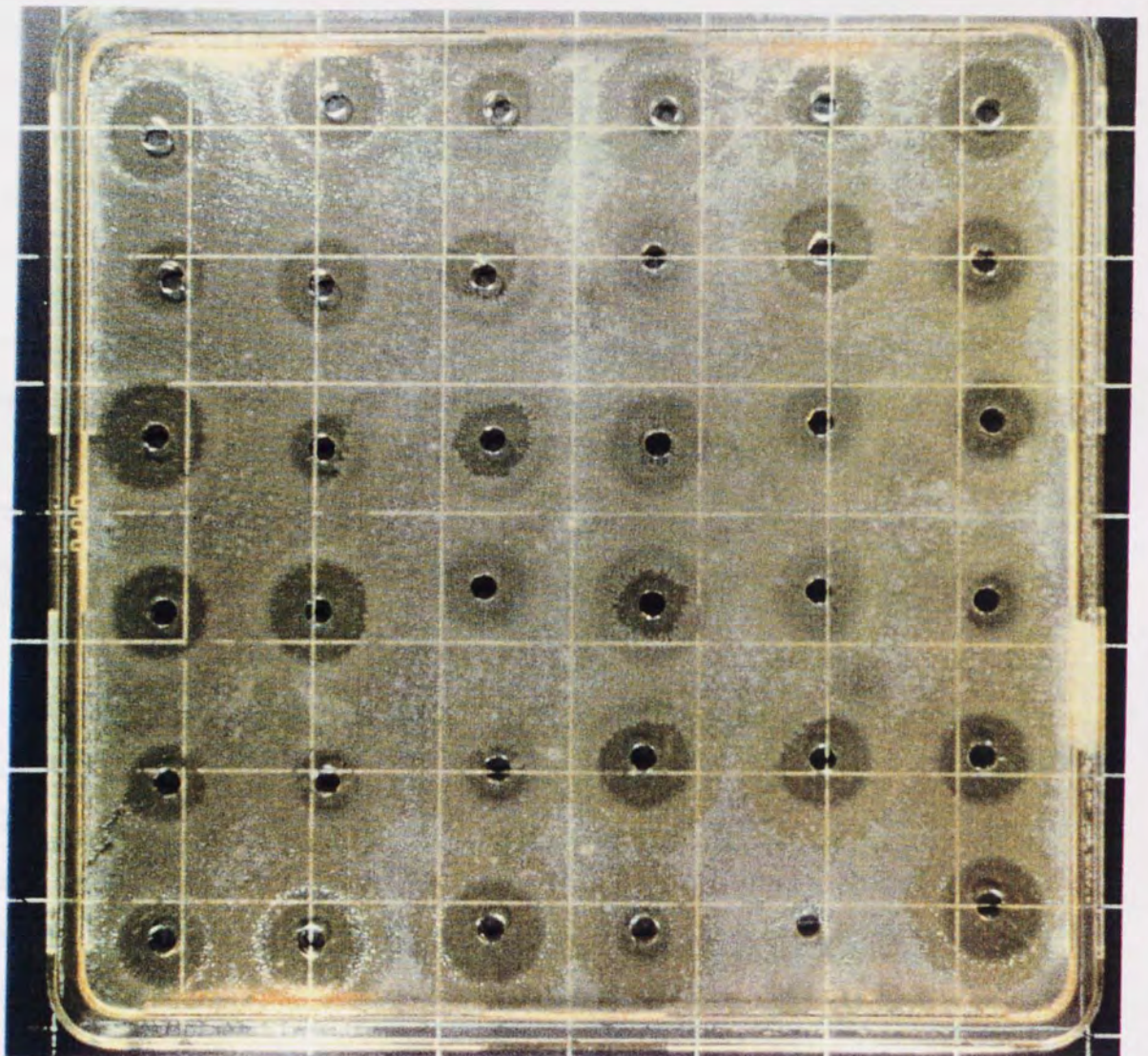


Plate 7.54 Photograph showing re-growth of organisms on previously cleared zones

7.2.1: The effect of initial concentration

The antibiotics were suspended / dissolved in distilled water to give 10%, 20% and 40% w/w solutions, and the effect of initial concentration was determined for each.

7.2.1.1: Ampicillin

Figure 7.55a shows that at 23°C, the zone diameter was independent of initial concentration, with zone diameters (at $t = 10$ minutes) of almost 90% for both solutions B and C and 85% for solution A. The drying rates, shown in Figure 7.55b, were also similar; the temperature histories exhibit an initial fall to wet bulb temperature for the three concentrations.

At 65°C initial concentration had no significant effect upon the zone diameter. Only solution B showed a reduction in zone diameter to 83%, while solutions A and C both remained at 92% (Figure 7.56a). The droplet temperatures increased rapidly to reach the air temperature after two minutes (Figure 7.56b). The drying rates exhibit two falling rate periods, the first lasted upto $t = 2$ minutes.

A further increase in temperature to 90°C, shown in Figure 7.57a, produced a reduction in the zone diameter to 83% for solutions A and B, and to 88% for solution C. There was an initial fall to 87% and 92% within the first minute for solutions A and B respectively followed by a very gradual decrease to the final zone diameter at $t = 10$ minutes. The drying rates exhibit two falling rates, with the first upto $t = 2$ minutes (Figure 7.57b).

The effect of initial concentration was most pronounced at 115°C, as shown in Figure 7.58a; the final zone diameters were 45%, 85%, and 90% for solutions A, B, and C respectively. The loss in potency for solution A occurred between $t = 1$ and 2 minutes during which the zone diameter was reduced from almost

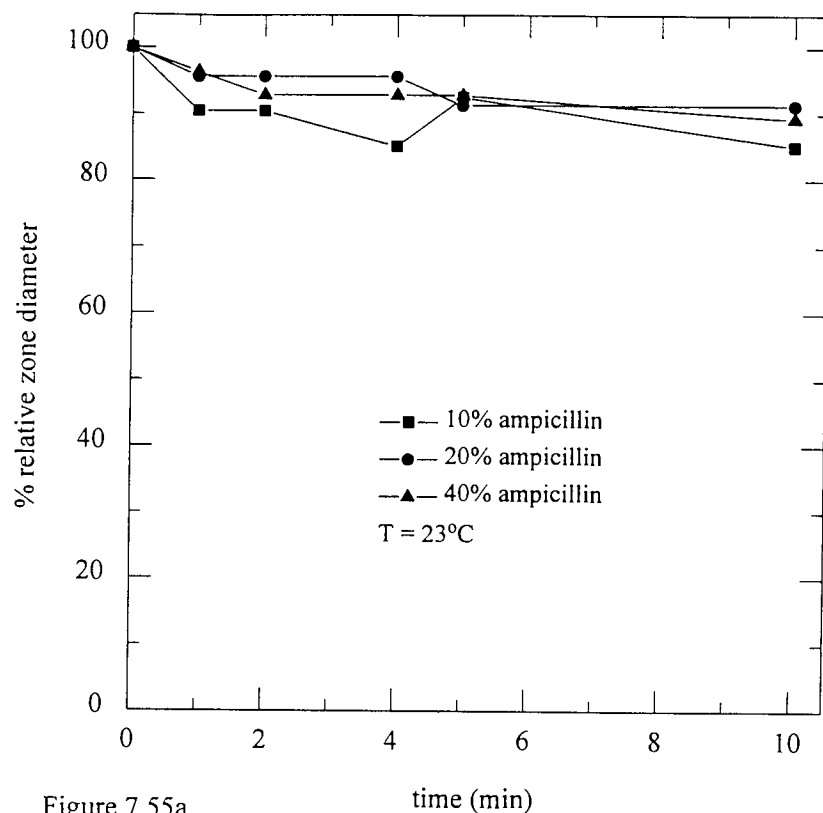


Figure 7.55a

Variation in zone diameter with initial concentration of ampicillin at 23°C air temperature

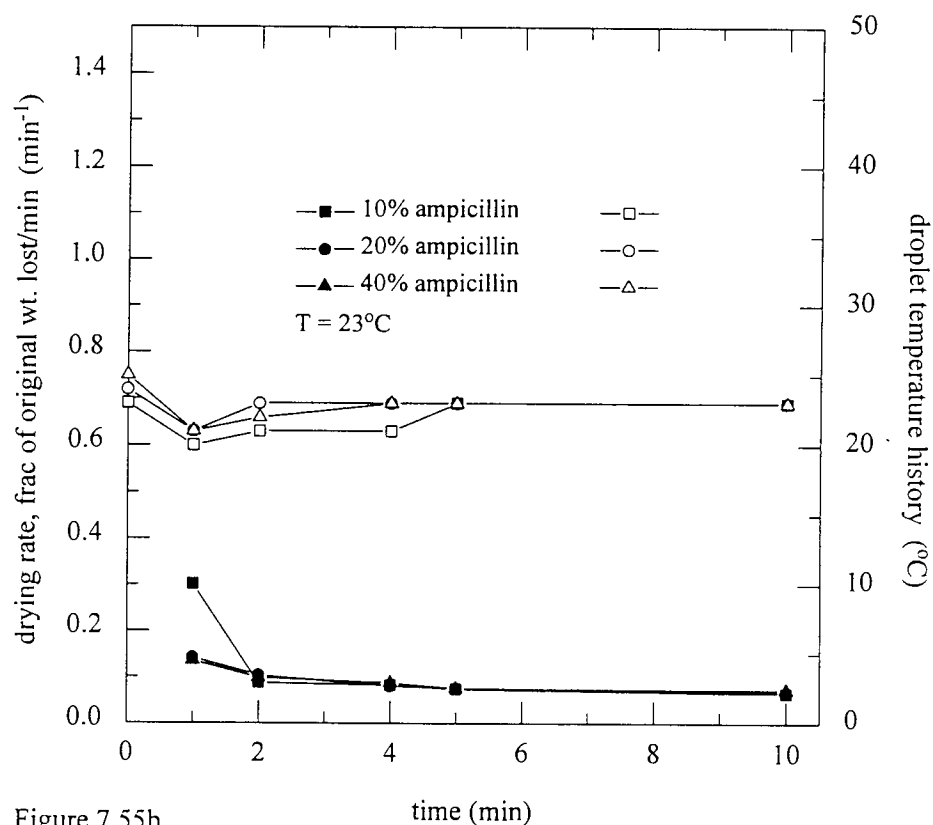


Figure 7.55b

The drying rate [solid symbols] and droplet temperature history [open symbols] for the ampicillin solutions

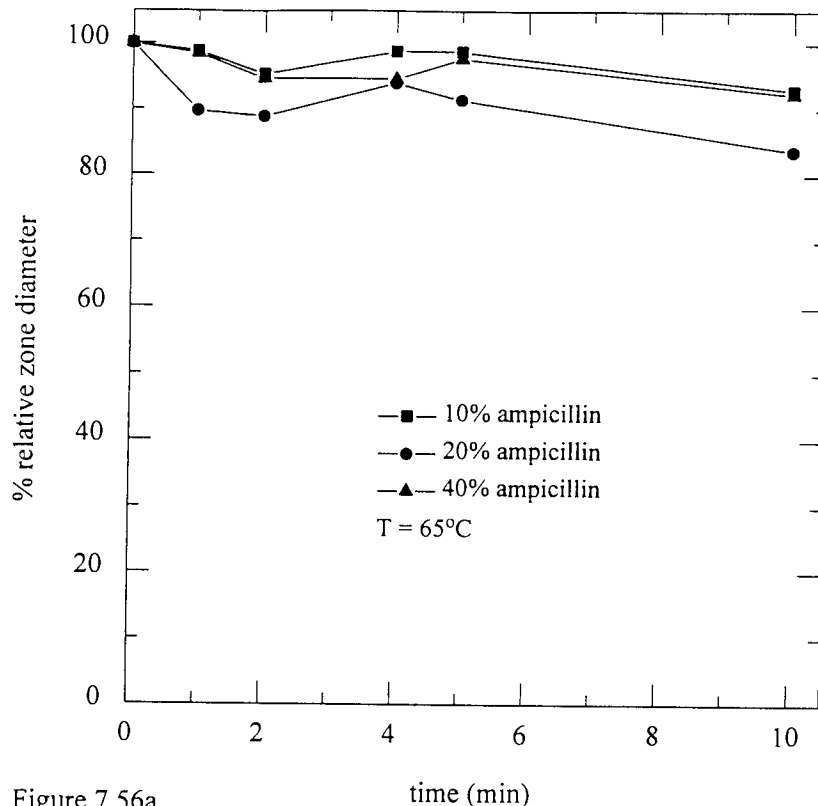


Figure 7.56a

Variation in zone diameter with initial concentration of ampicillin at 65°C air temperature

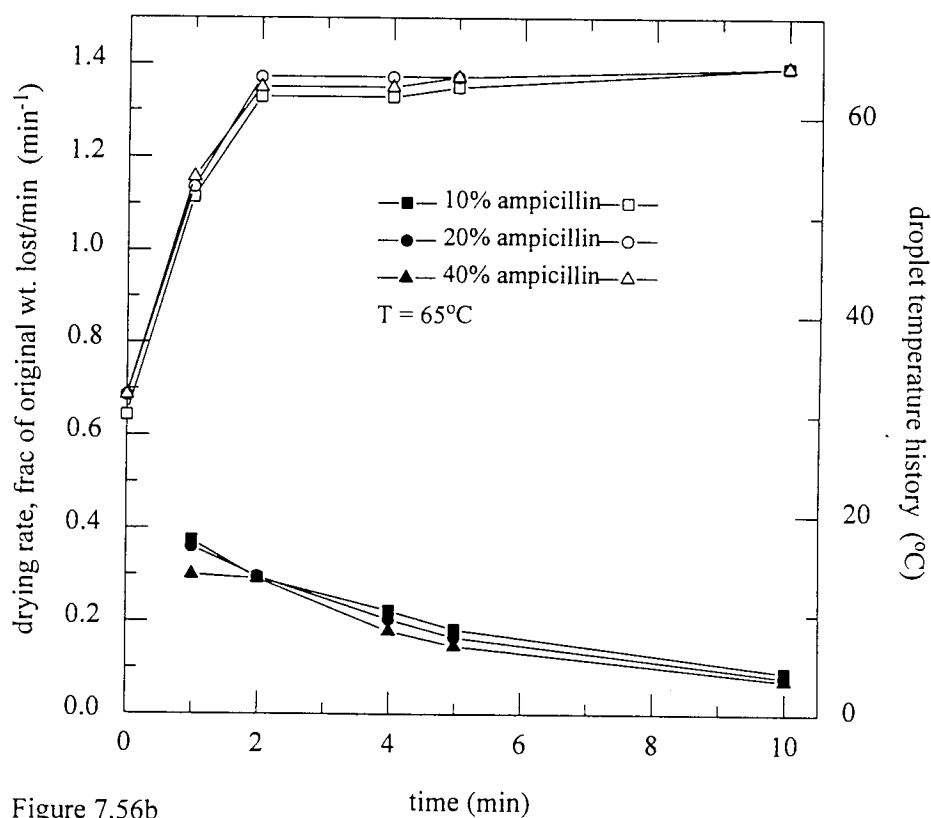


Figure 7.56b

The drying rate [solid symbols] and droplet temperature history [open symbols] for the ampicillin solutions

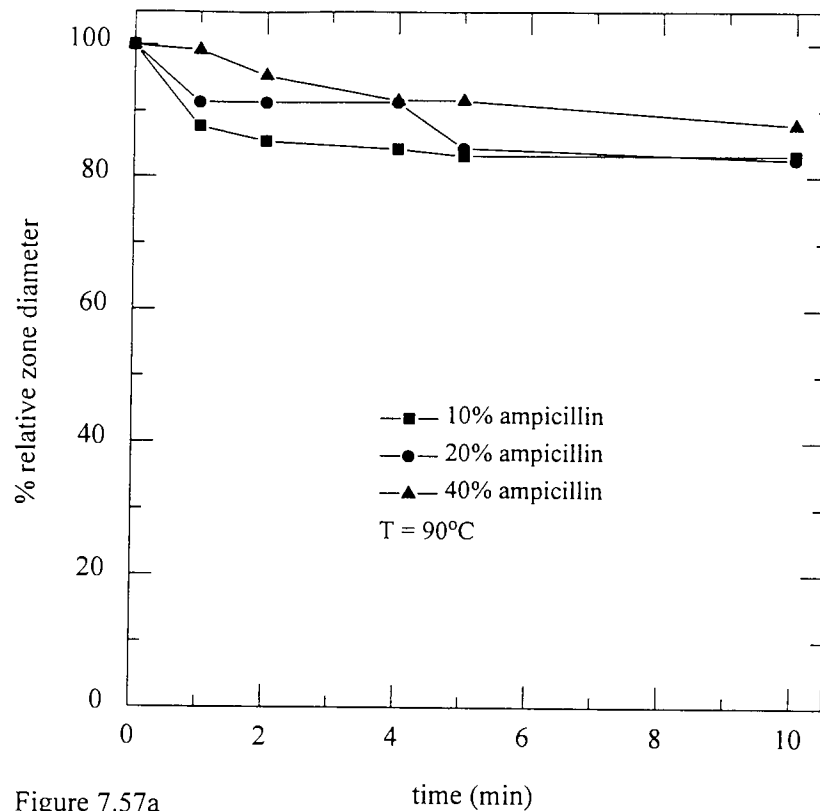


Figure 7.57a

Variation in zone diameter with initial concentration of ampicillin at 90°C air temperature

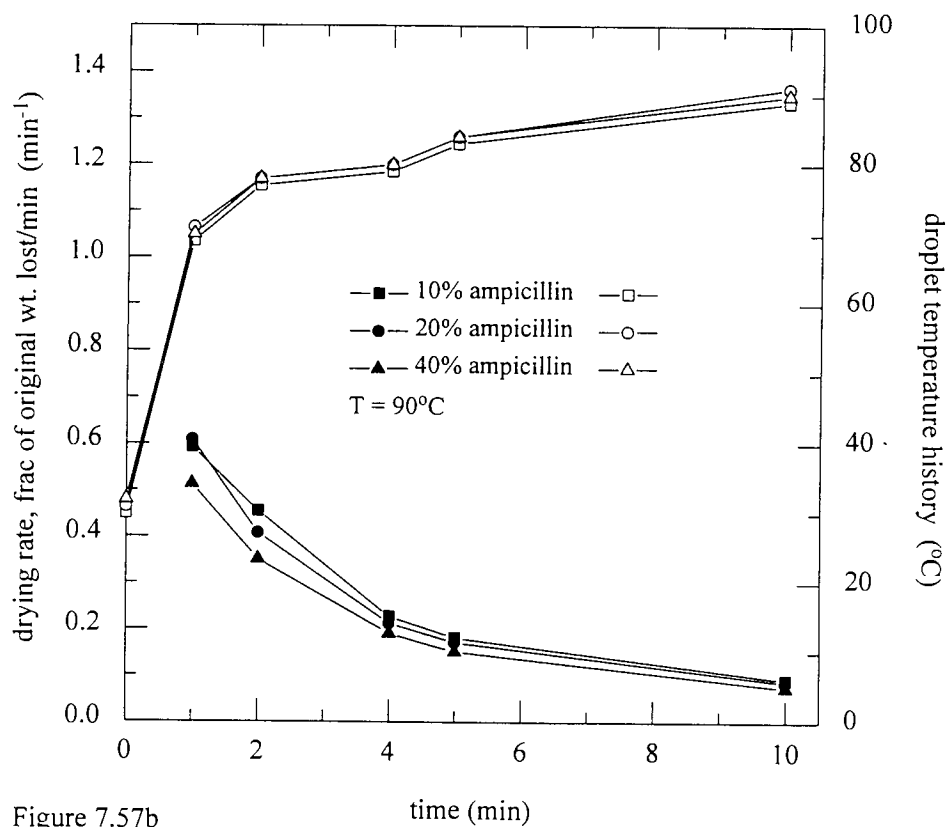


Figure 7.57b

The drying rate [solid symbols] and droplet temperature history [open symbols] for the ampicillin solutions

100% to 65%. Figure 7.58b illustrates the droplet temperature histories; a gradual initial increase was followed by a more rapid increase suggesting that upto $t = 1$ minute there was evaporation from localised wet spots on the droplets; when this ceased coincides with the onset of the rapid increase in droplet temperature. The drying rates exhibit one falling rate period for the three solutions; solution A exhibited a faster initial rate, as would be expected.

7.2.1.2: Chloramphenicol

The effect of initial concentration at 23°C, shown in Figure 7.59a, illustrates a gradual decrease in zone diameter with time, with a fall to almost 80%, 68% and 65% for solutions C, B, and A respectively. The drying rates, shown in Figure 7.59b, exhibit two falling rate periods for all three solutions; again solution A had the faster rate. The droplet temperature histories indicate a fall to wet bulb temperature followed by a gradual increase to the air temperature.

Figure 7.60a shows that an increase in temperature to 65°C caused the zone diameters to fall to 62%, 72%, and 88% for solutions A, B, and C respectively. The droplet temperatures increased rapidly to the air temperature within the first two minutes. This is reflected in the drying rates which show two falling rate periods (Figure 7.60b).

Figure 7.61a shows that initial solids concentration had no significant effect at 90°C, with a fall to only 98% and 95% for solutions B and C. Two falling rates were exhibited by the drying rate curves, Figure 7.61b. The droplet temperatures increase rapidly to reach the air temperature by $t = 4$ minutes.

At 115°C (Figure 7.62a) there was a reduction in zone diameter with a reduction in initial concentration. There was little difference in zone diameter after ten minutes for solution C but a fall to almost 78% with solution B. The drying rates, shown in Figure 7.62b, illustrate two falling rate periods. The droplet temperatures increased rapidly for both solutions.

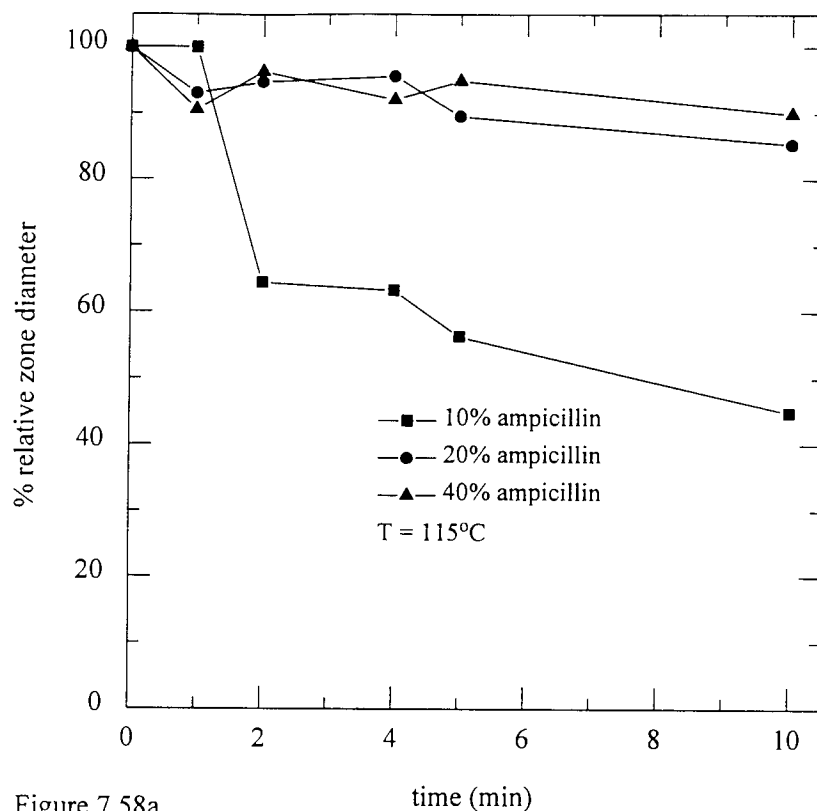


Figure 7.58a

Variation in zone diameter with initial concentration of ampicillin at 115°C air temperature

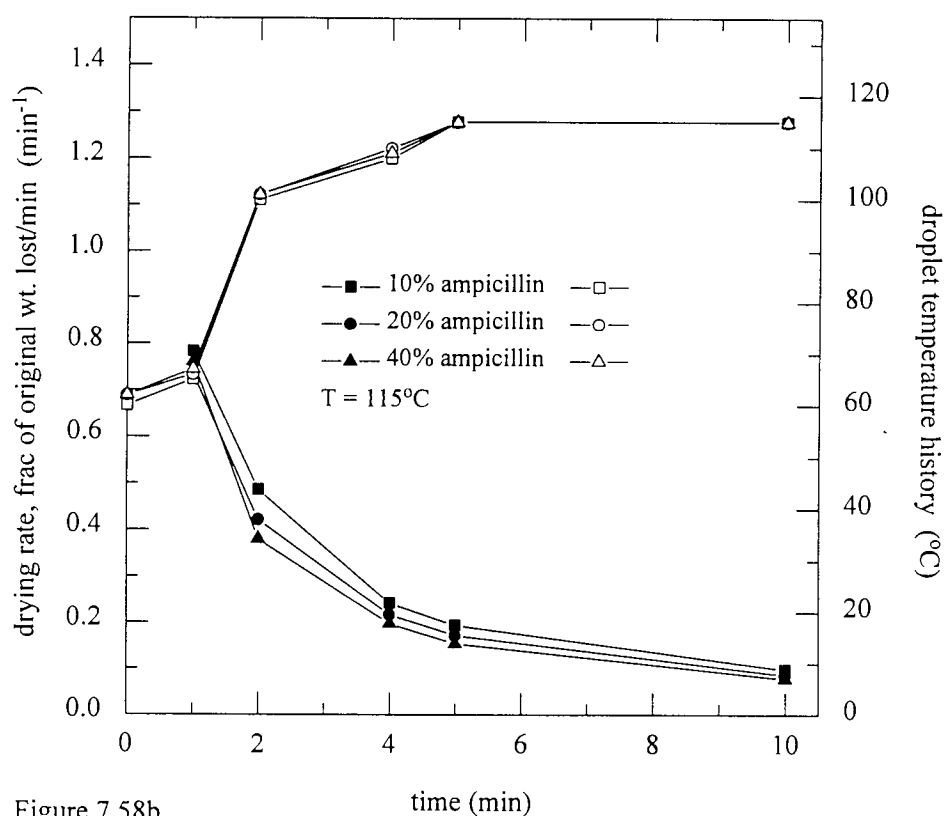


Figure 7.58b

The drying rate [solid symbols] and droplet temperature history [open symbols] for the ampicillin solutions

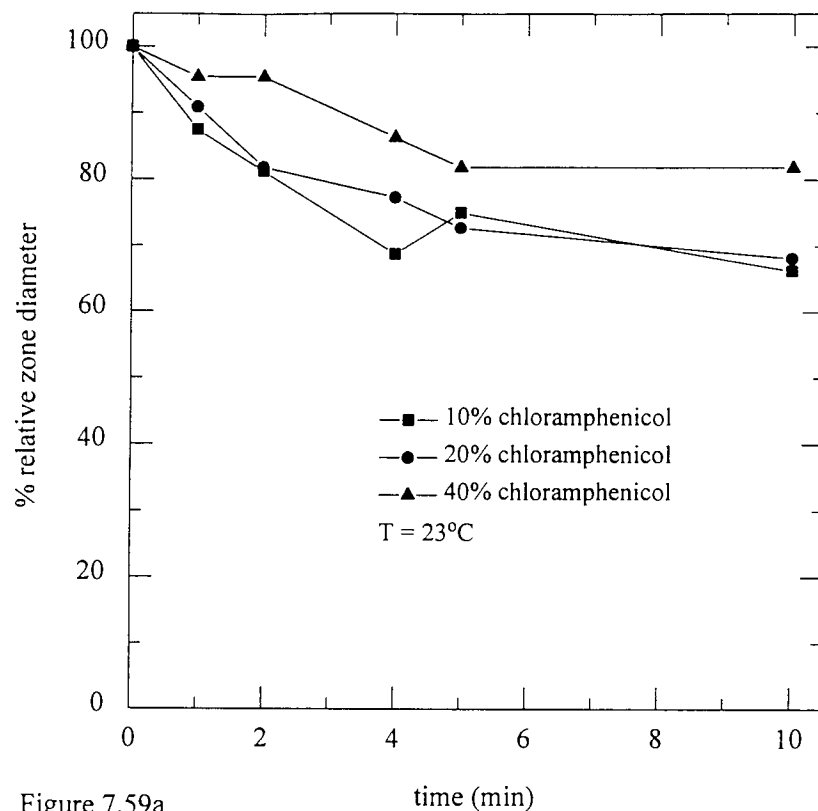


Figure 7.59a

Variation in zone diameter with initial concentration of chloramphenicol at 23°C air temperature

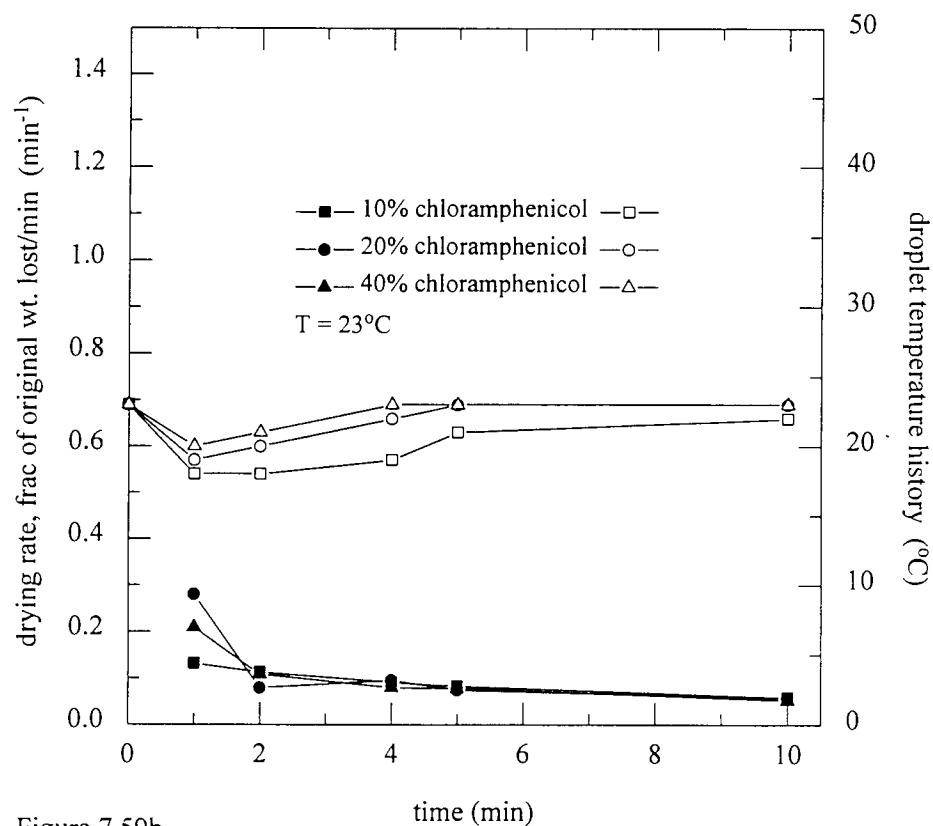


Figure 7.59b

The drying rate [solid symbols] and droplet temperature history [open symbols] for the chloramphenicol solutions

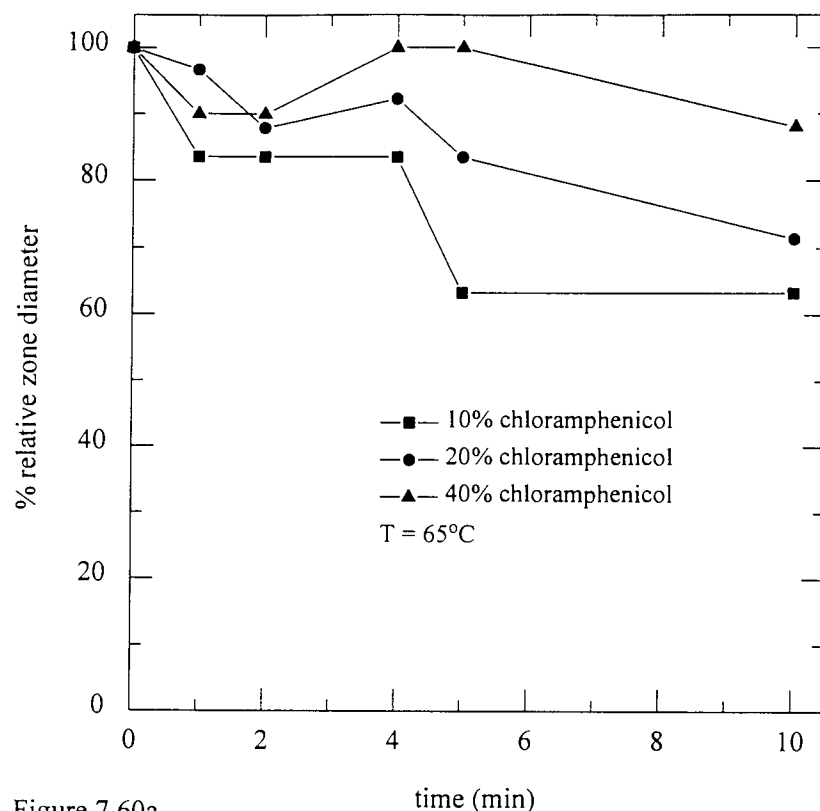


Figure 7.60a

Variation in zone diameter with initial concentration of chloramphenicol at 65°C air temperature

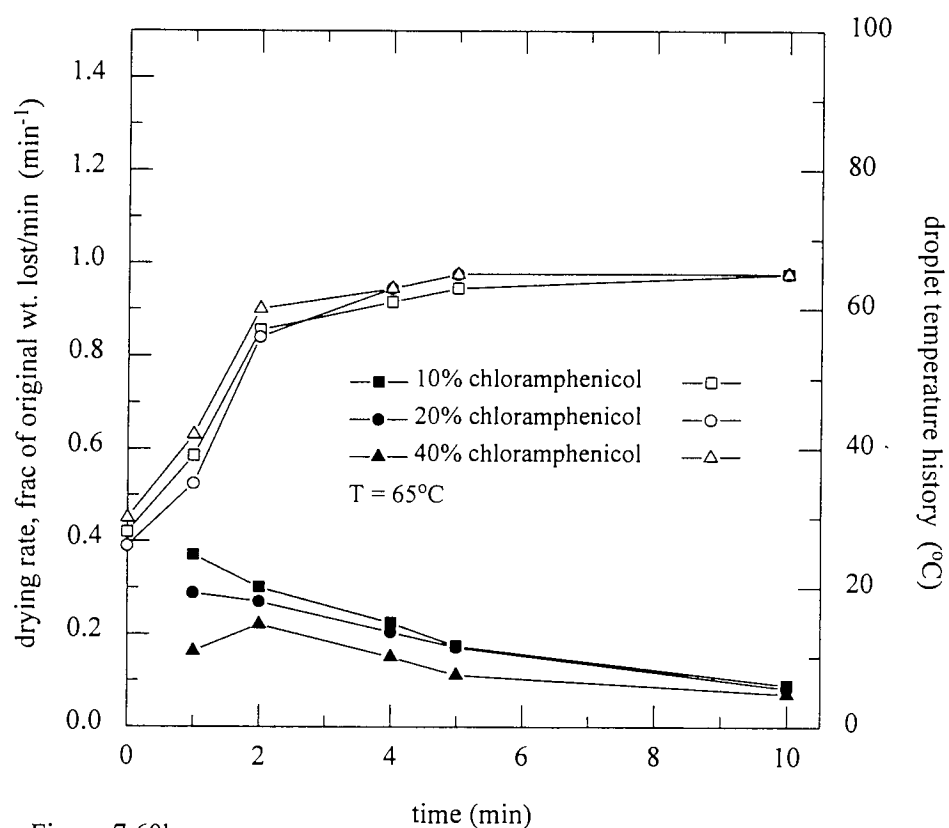


Figure 7.60b

The drying rate [solid symbols] and droplet temperature history [open symbols] for chloramphenicol solutions

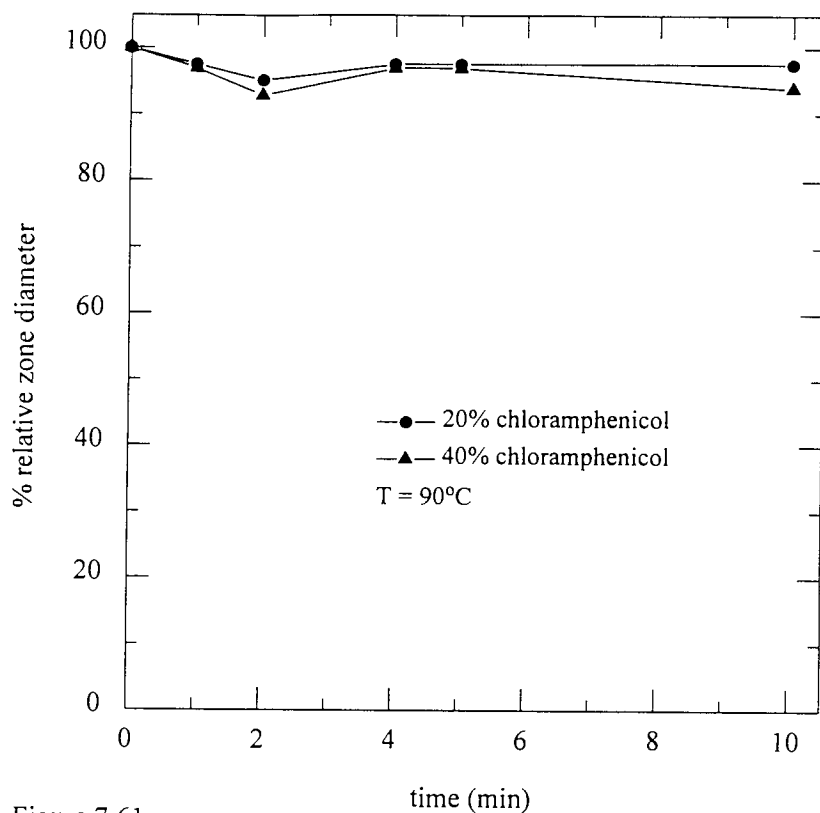


Figure 7.61a

Variation in zone diameter with initial concentration of chloramphenicol at 90°C air temperature

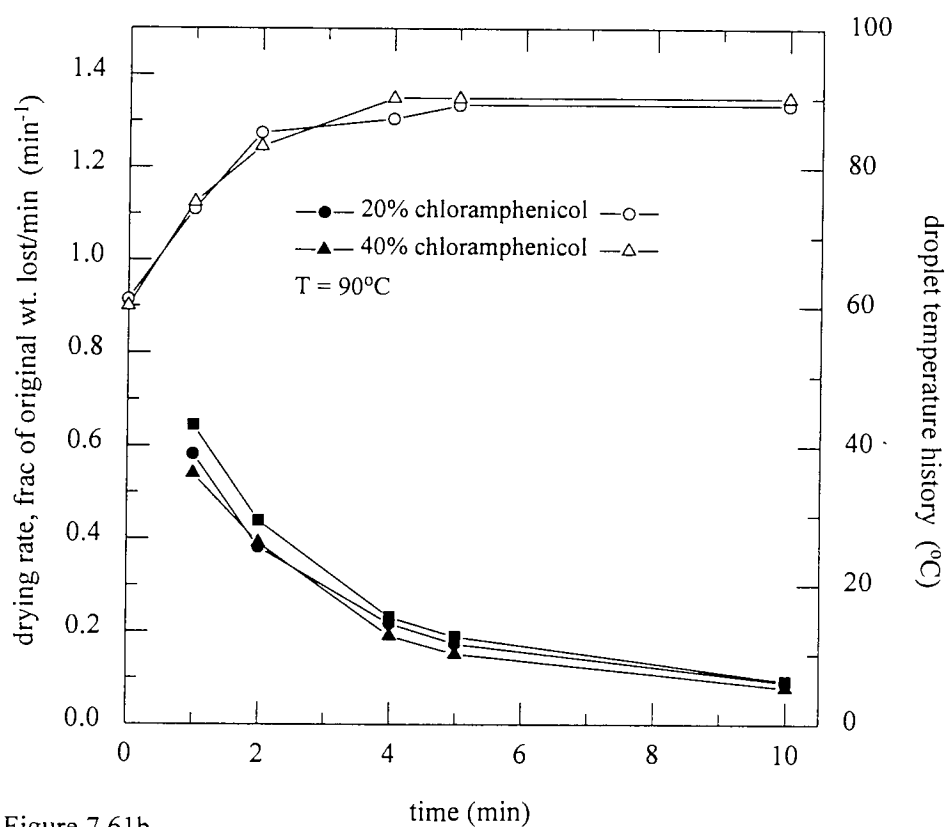


Figure 7.61b

The drying rate [solid symbols] and droplet temperature history [open symbols] for the chloramphenicol solutions

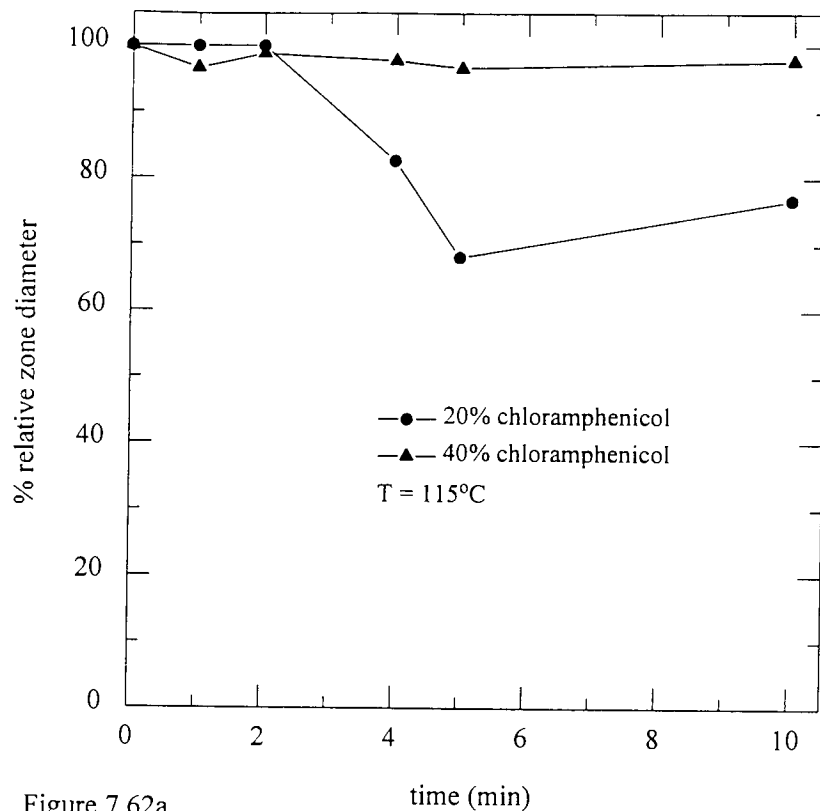


Figure 7.62a

Variation in zone diameter with initial concentration of chloramphenicol at 115°C air temperature

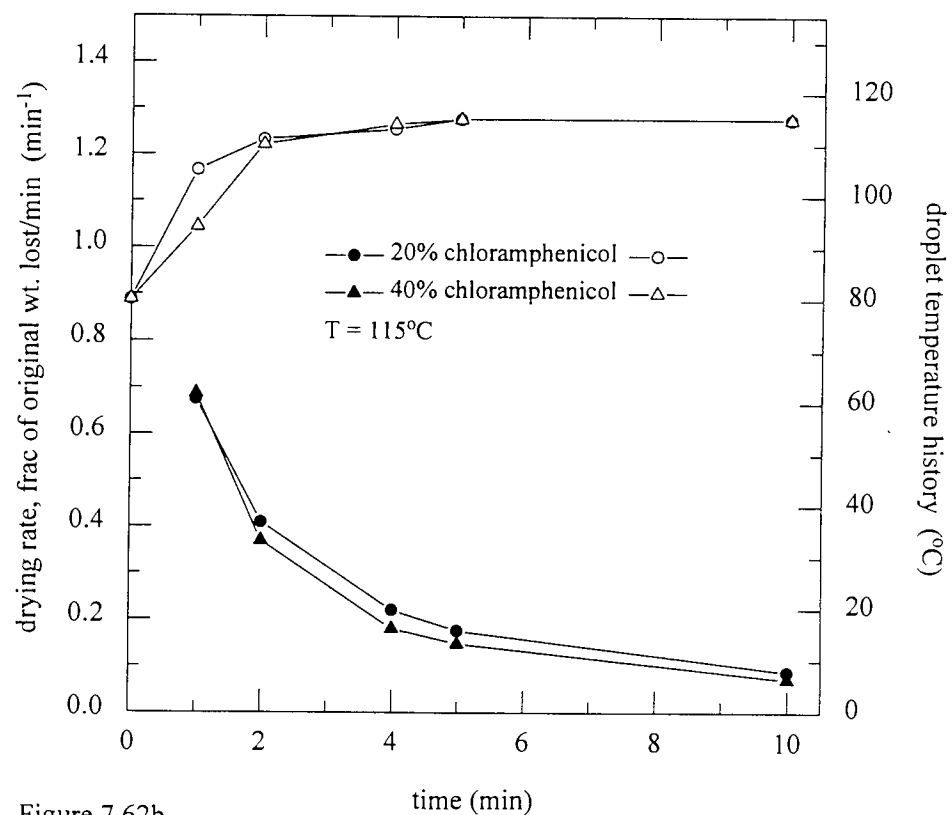


Figure 7.62b

The drying rate [solid symbols] and droplet temperature history [open symbols] for the chloramphenicol solutions

7.2.1.3: Oxytetracycline

Initial concentration was not a significant variable at 23°C as illustrated in Figure 7.63a. Solutions B and C exhibited similar zone diameters of almost 92% and solution A of 84%. There was a fall to the wet bulb temperature, as shown in Figure 7.63b, followed by a gradual increase to the air temperature. Two falling rate periods were exhibited.

At 65°C the zone diameter at the higher concentration was greater than at the lower initial concentration (Figure 7.64a), viz. 76%, 84%, and 88% for solutions A, B, and C respectively. The droplet temperatures exhibited a slow initial rise during the first two minutes followed by a rapid increase to the air temperature. The existence of two falling rate periods (Figure 7.64b) also lends support to the suggestion that initial evaporation was from localised wet spots on the droplet surface.

As the temperature was increased to 90°C the effects of initial solids concentration became more evident. As would be expected, the largest zone diameter corresponded to the highest initial concentration, as shown in Figure 7.65a. With solution C the zone diameter fell to only 96% after ten minutes. The zone diameters for solutions A and B decreased to their final values, 77% and 90% respectively, within the first two minutes of drying. Two falling rates were exhibited by the drying rate curves in Figure 7.65b. The droplet temperatures increased rapidly to the air temperature.

The effects of initial concentration at 115°C are shown in Figure 7.66a. There is an initial rapid decrease in zone diameter during the first two minutes of drying for both solutions B and C, the rate of decrease being faster for the less concentrated solution. A similar zone diameter, 75%, was attained by both the solutions after ten minutes of drying. The initial rapid reductions in zone diameter correlate well with the first falling rate period and the initial increase in droplet temperature (Figure 7.66b).

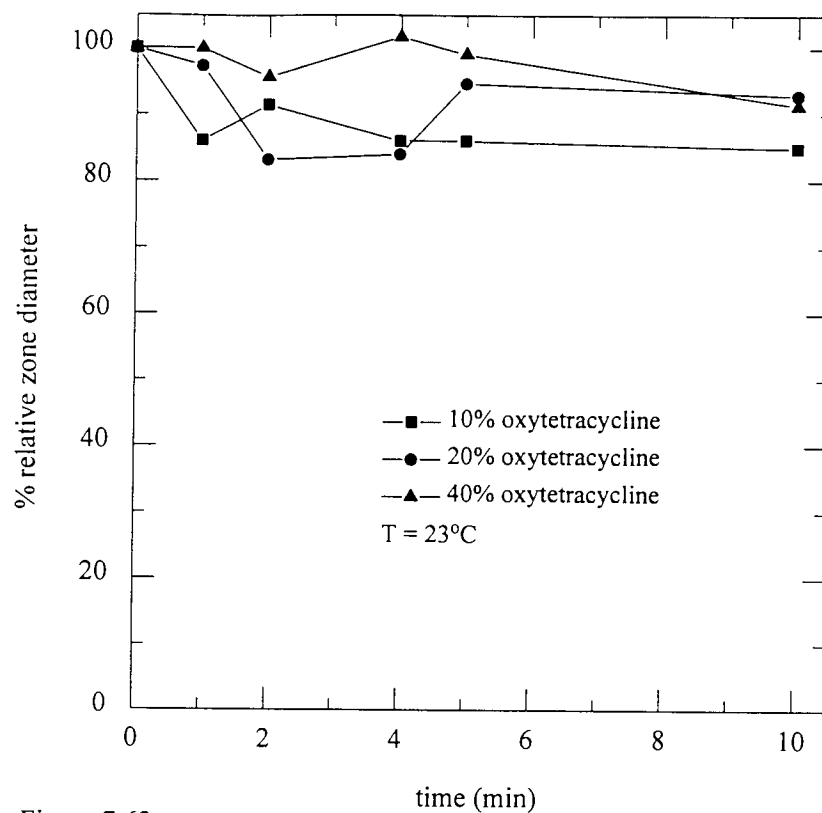


Figure 7.63a

Variation in zone diameter with initial concentration of oxytetracycline at 23°C air temperature

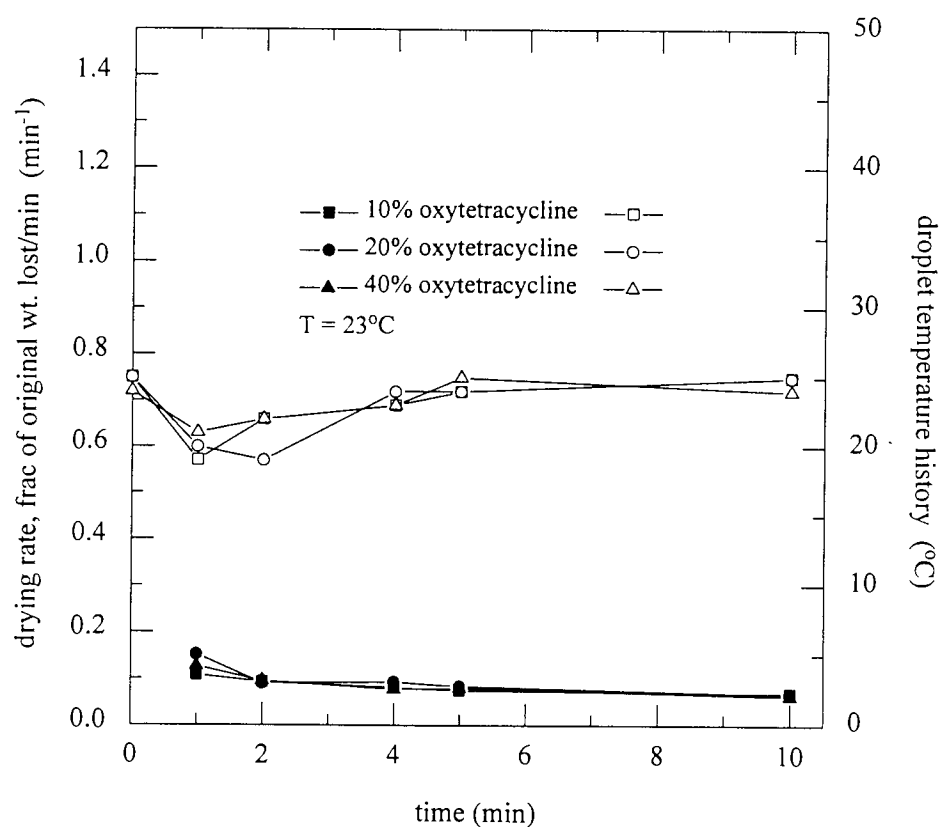


Figure 7.63b

The drying rate [solid symbols] and droplet temperature history [open symbols] for the oxytetracycline solutions

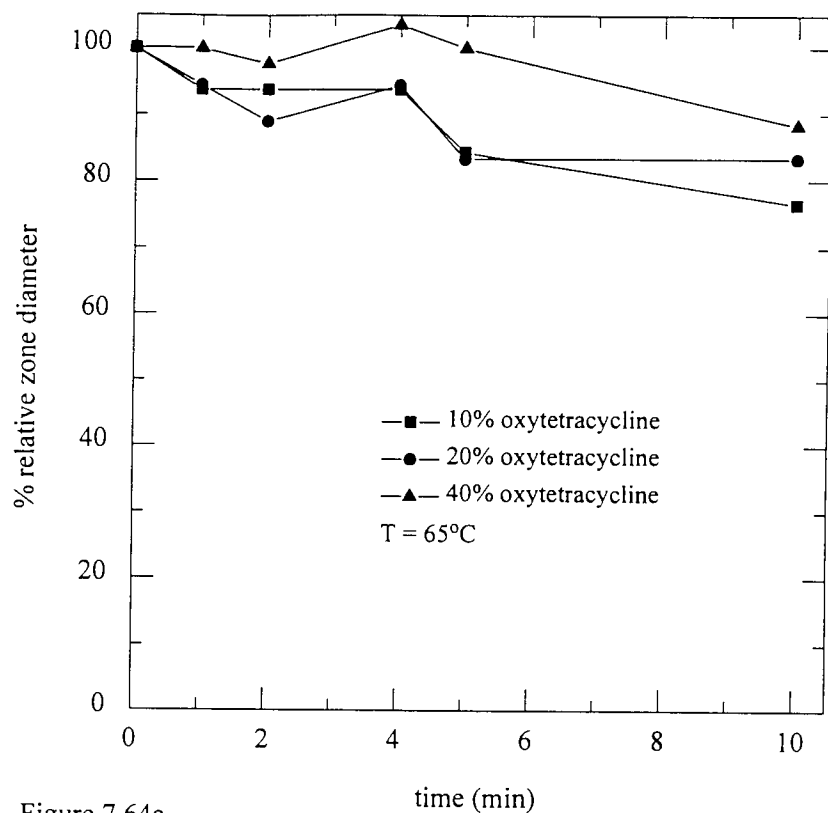


Figure 7.64a

Variation in zone diameter with initial concentration of oxytetracycline at 65°C air temperature

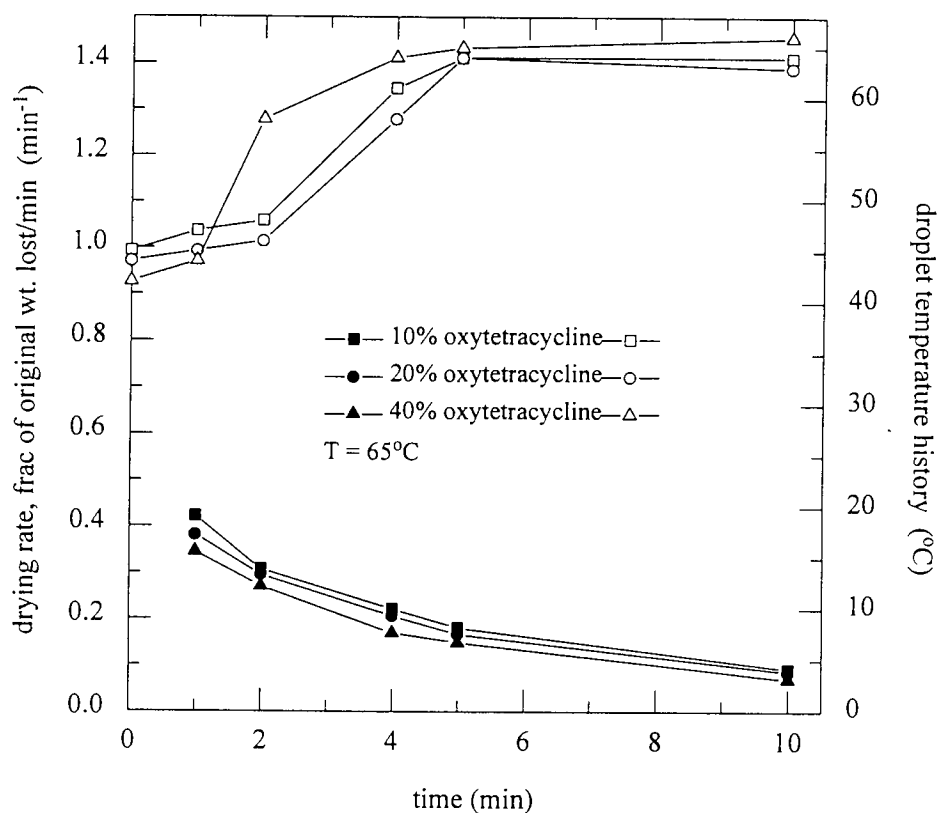


Figure 7.64b

The drying rate [solid symbols] and droplet temperature history [open symbols] for the oxytetracycline solutions

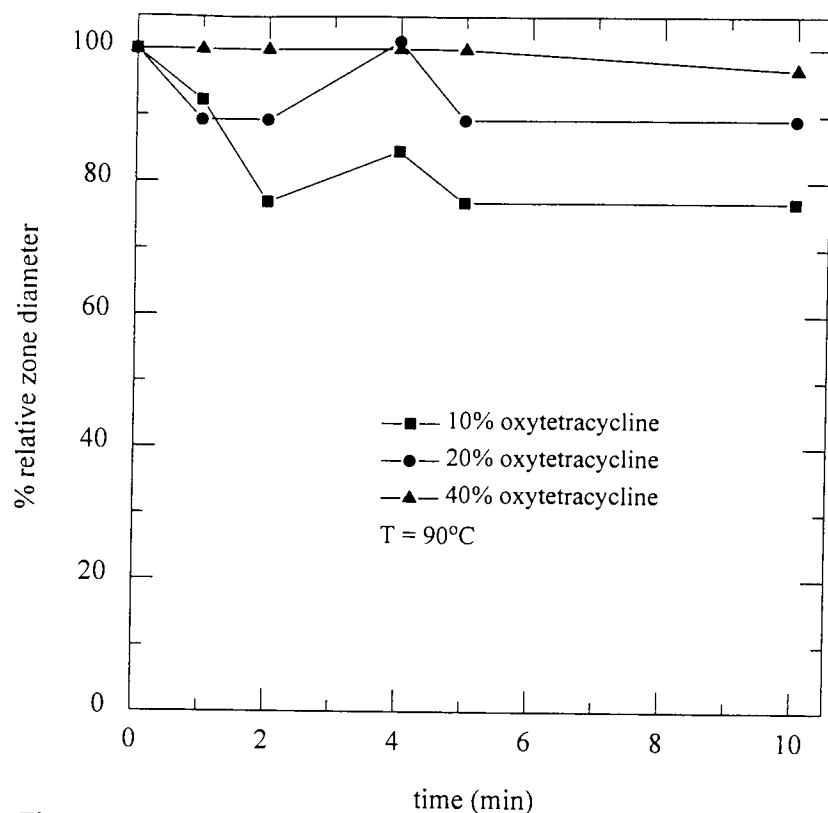


Figure 7.65a

Variation in zone diameter with initial concentration of oxytetracycline at 90°C
ait temperature

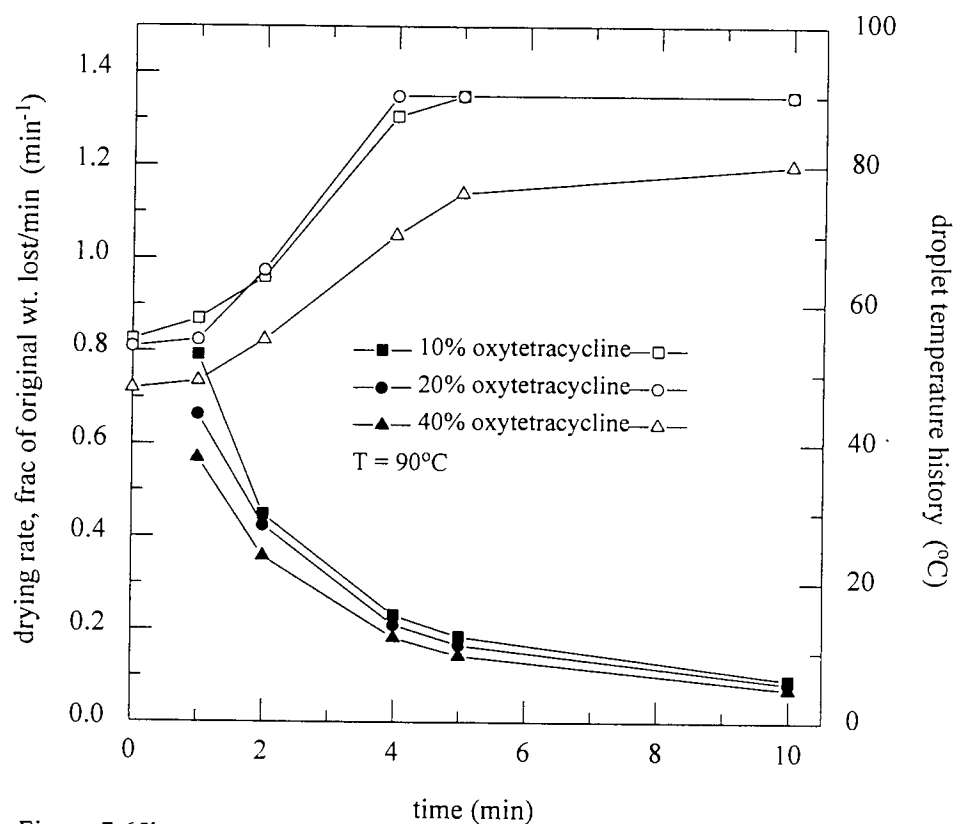


Figure 7.65b

The drying rate [solid symbols] and droplet temperature history [open symbols]
for the oxytetracycline solutions

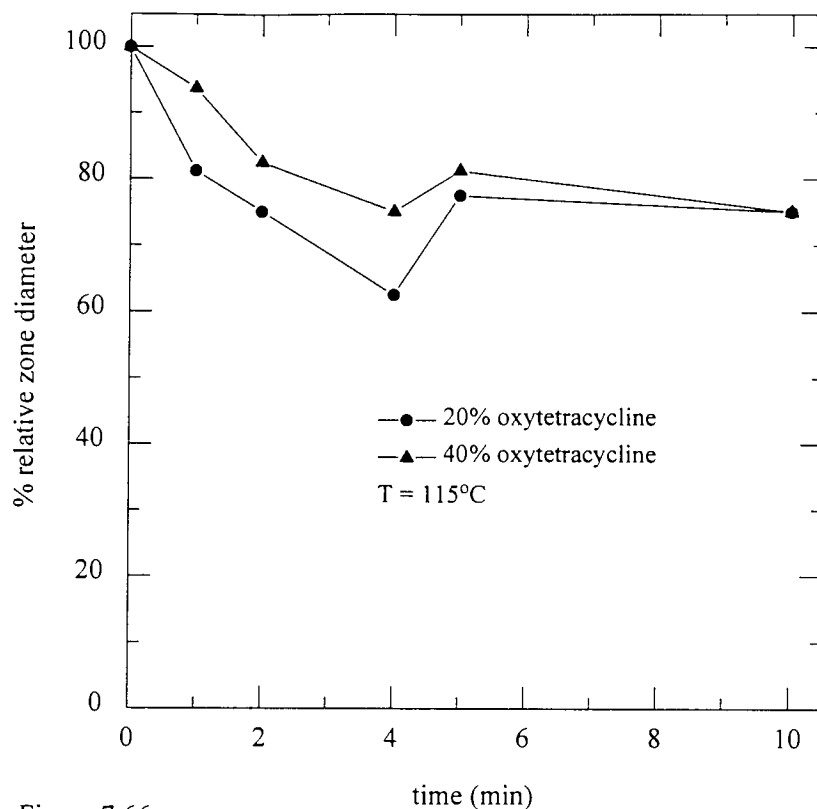


Figure 7.66a

Variation in zone diameter with initial concentration of oxytetracycline at 115°C air temperature

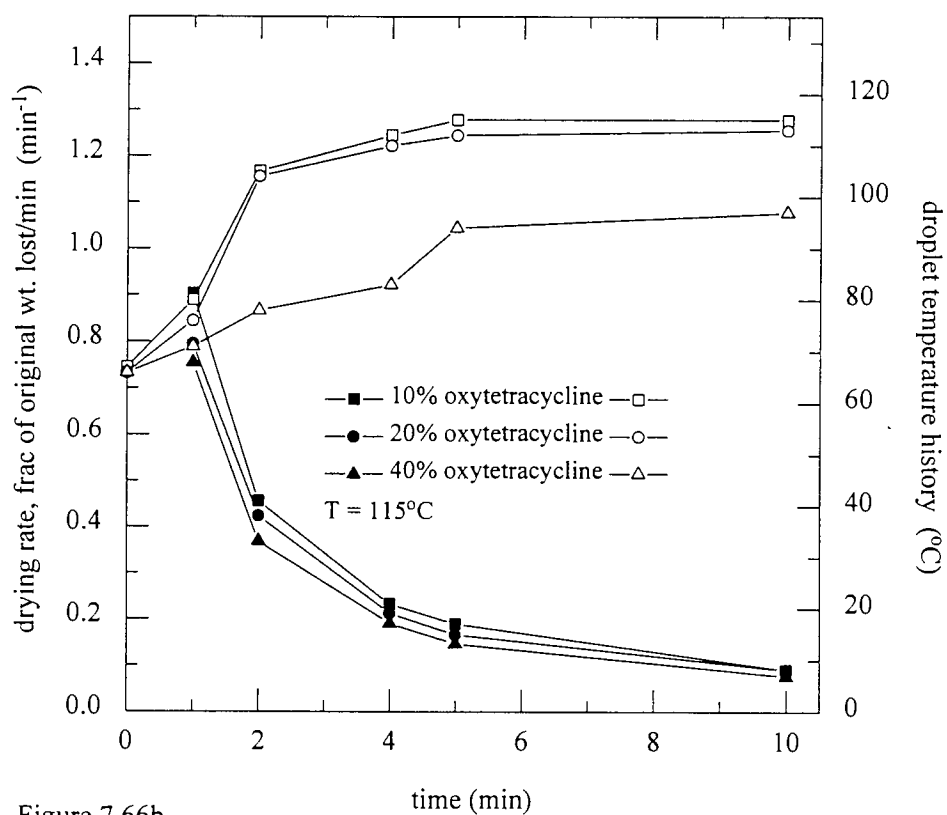


Figure 7.66b

The drying rate [solid symbols] and droplet temperature history [open symbols] for the oxytetracycline solutions

7.2.1.4: Streptomycin

The effect of initial solids concentration at 23°C are shown in Figure 7.67a. There was a greater reduction in zone diameter with decreasing initial concentration, viz. zone diameters of 90%, 87% and 75% for solutions C, B, and A. The lower the initial concentration, the faster the reduction in zone diameter. However, the drying rates were similar, (two falling rate periods were observed with the three solutions). There was a fall to the wet bulb temperature for all three of the solutions before the gradual increase to the air temperature (Figure 7.67b).

Initial solids concentration had no significant effect at 65°C as shown in Figure 7.68a. The zone diameters reduced to almost 93% for both solutions A and B, and only 98% for solution C. The droplet temperatures show a gradual increase to the air temperature. Two falling rate periods are shown by the drying rate curves (Figure 7.68b).

Although there was no significant difference in the zone diameter after ten minutes of drying at 90°C, viz. zone diameters of almost 92% for each of the three solutions, the magnitude of the rate of initial decrease in zone diameter correlated with the initial solids concentration (Figure 7.69a). Similar drying rate curves and droplet temperature histories were obtained for all three of the solutions (Figure 7.69b).

The effect of initial concentration was less pronounced at 115°C as shown in Figure 7.70a. There was a slight reduction in zone diameter for solutions B and C to almost 98%, with a corresponding reduction to 90% for solution A. This reduction for solution A was attained after the first two minutes of drying. The droplet temperatures increased rapidly to the air temperature in each case. The drying rates exhibit two falling rate periods (Figure 7.70b).

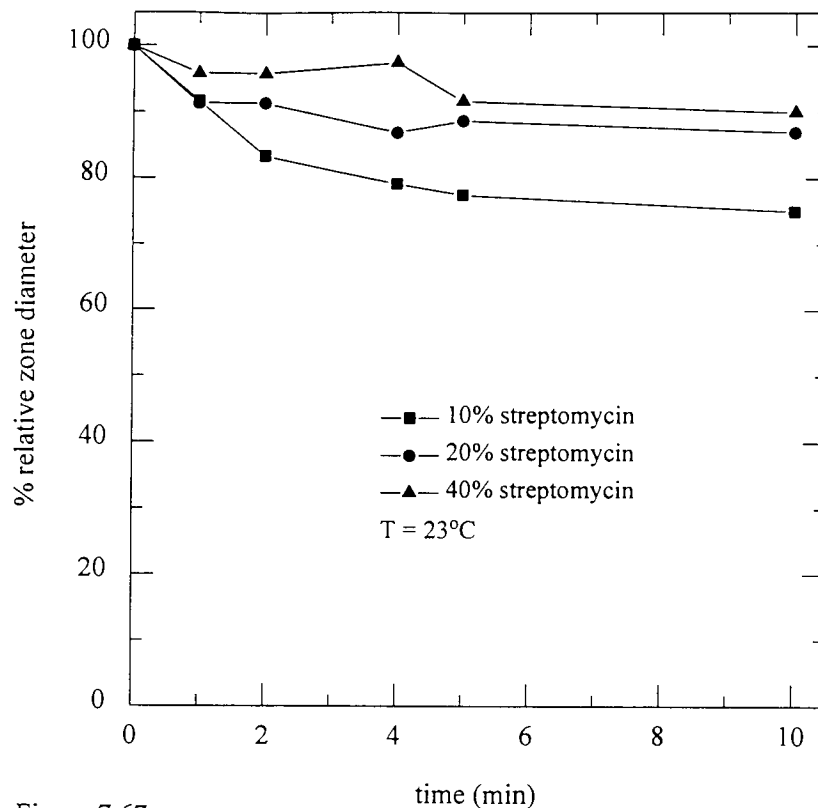


Figure 7.67a

Variation in zone diameter with initial concentration of streptomycin at $T=23^{\circ}\text{C}$ air temperature

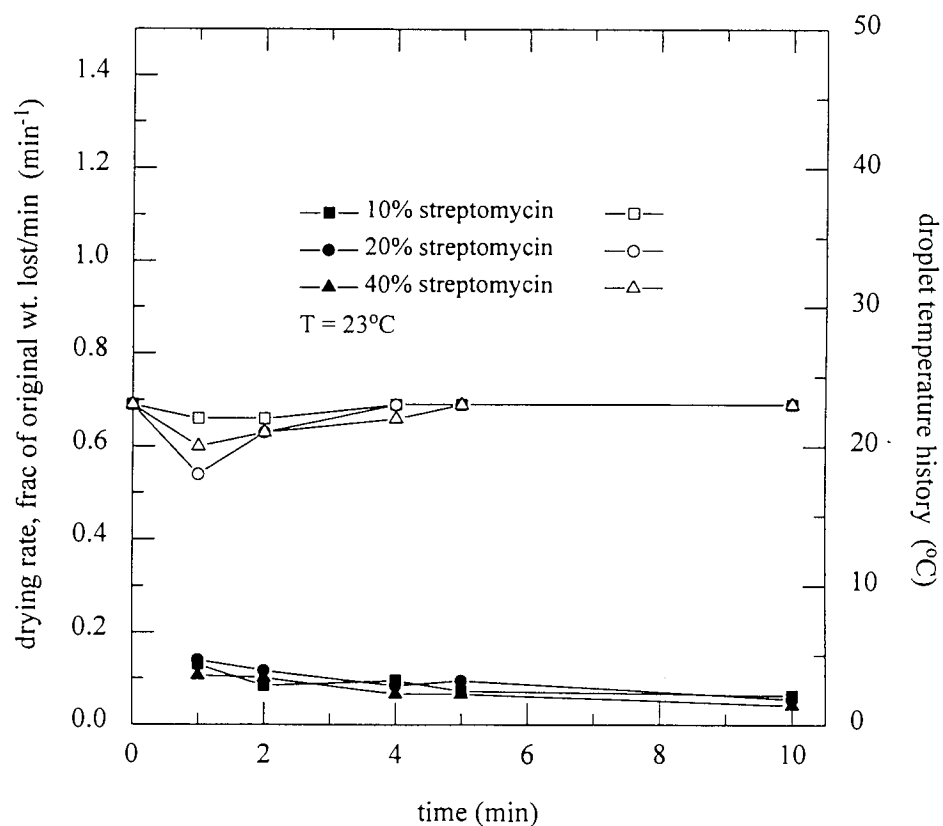


Figure 7.67b

The drying rate [solid symbols] and droplet temperature history [open symbols] for the streptomycin solutions

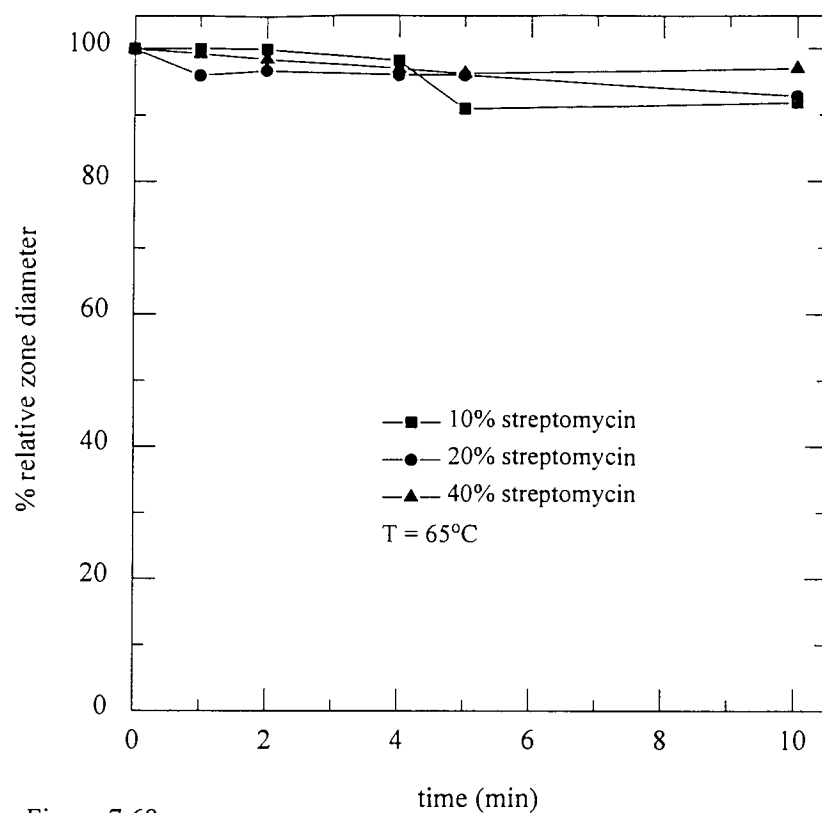


Figure 7.68a

Variation in zone diameter with initial concentration of streptomycin at 65°C air temperature

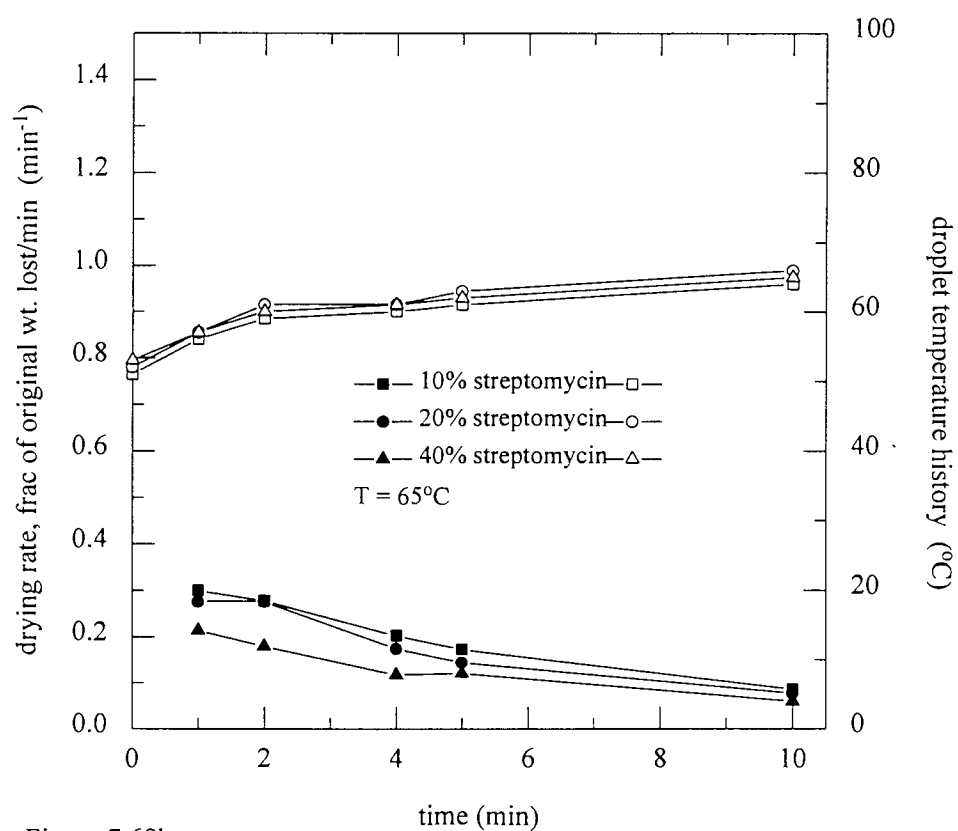


Figure 7.68b

The drying rate [solid symbols] and droplet temperature history [open symbols] for the streptomycin solutions

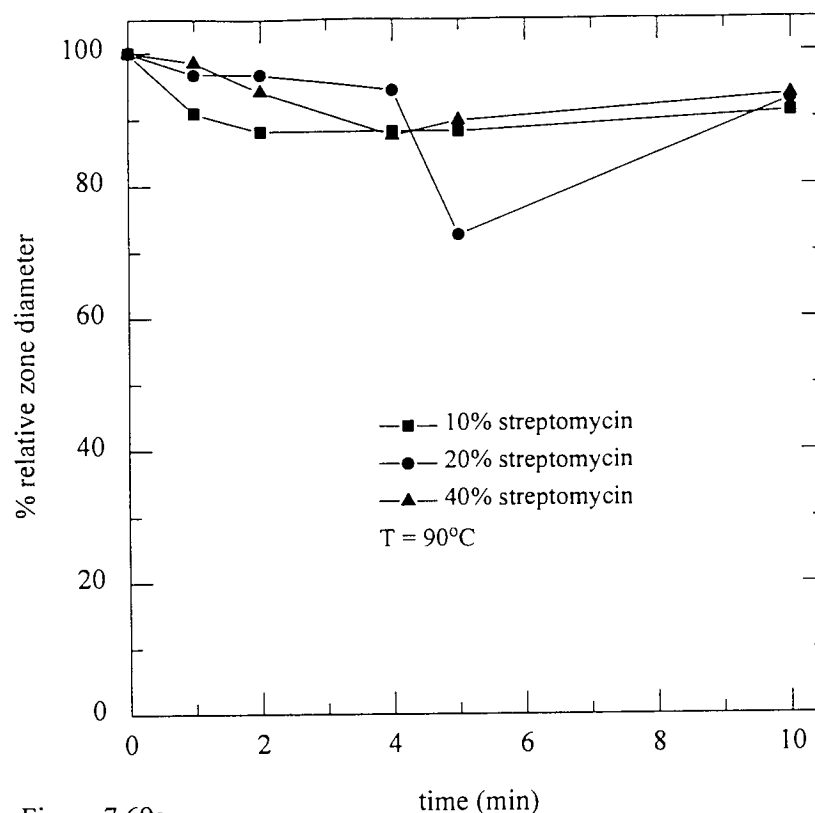


Figure 7.69a

Variation in zone diameter with initial concentration of streptomycin at 90°C air temperature

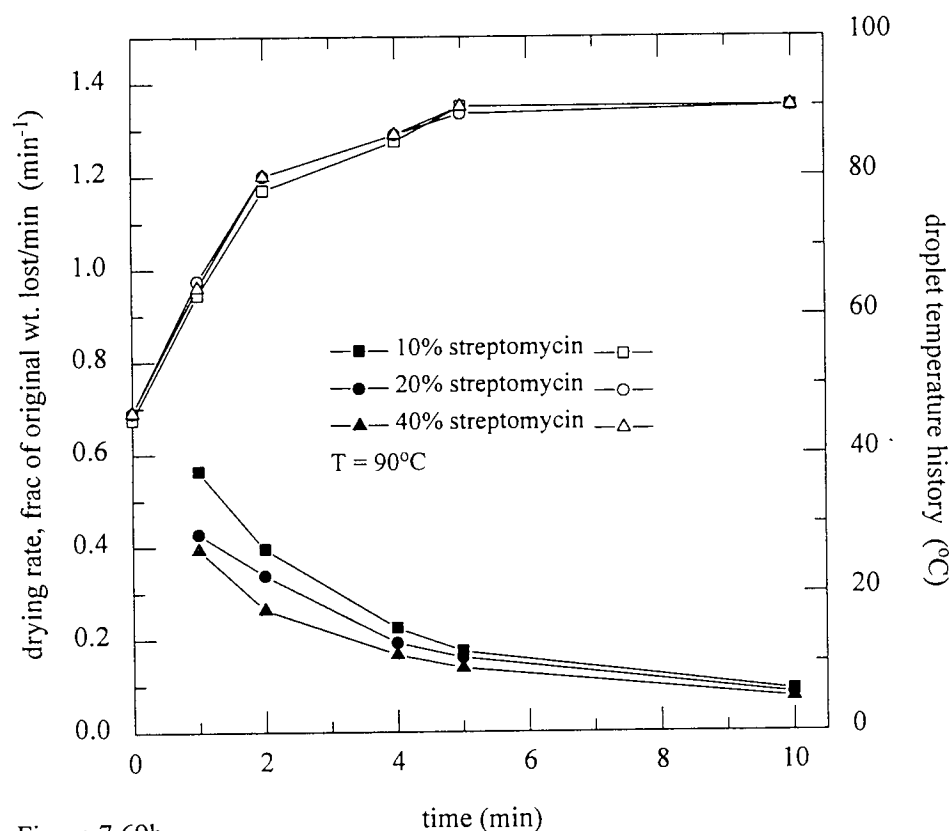


Figure 7.69b

The drying rate [solid symbols] and droplet temperature history [open symbols] for the streptomycin solutions

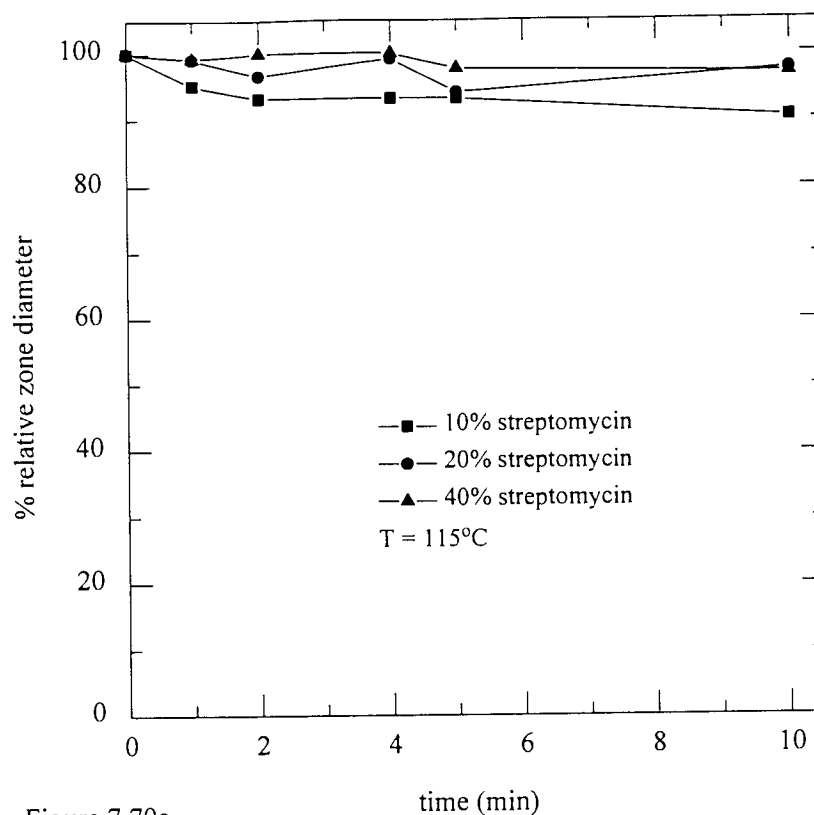


Figure 7.70a

Variation in zone diameter with initial concentration of streptomycin at 115°C air temperature

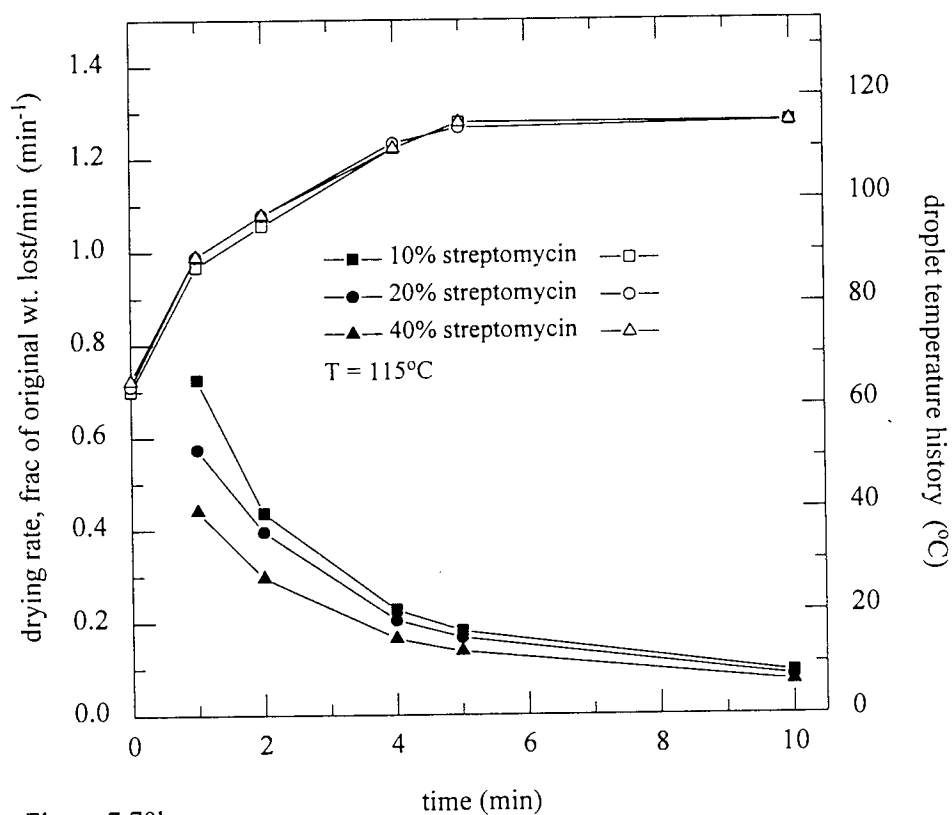


Figure 7.70b

The drying rate [solid symbols] and droplet temperature history [open symbols] for the streptomycin solutions

7.2.1.5: Tetracycline

Variation in initial solids concentration did not effect zone diameter with tetracycline at 23°C (Figure 7.71a), i.e. a similar decrease in zone diameter was apparent for all three solutions, viz. 75%, 78% and 80% for solutions A, B, and C respectively. Similar drying rates, (two falling rate periods), and temperature histories were also exhibited (Figure 7.71b).

No effects due to variation in initial solids concentration were observed with an increase in temperature to 65°C, as shown in Figure 7.72a, i.e. all the zone diameters remaining almost constant throughout. Figure 7.72b shows that there were two falling rate periods, the first indicative of evaporation from localised wet spots on the droplet surface. The droplet temperatures showed a gradual initial increase followed by a rapid increase to the air temperature. The initial gradual increase corresponds to the evaporation from localised wet spots.

Then effects of initial concentration became more evident at 90°C with reductions in zone diameters to 87%, 95%, and 92% for solutions A, B, and C respectively (Figure 7.73a), within the first two minutes of drying. Two falling rates are evident in Figure 7.73b, with the first occurring from the onset upto $t = 2$ minutes followed by the second which proceeded until the completion of drying. The droplet temperature histories show an initial gradual increase followed by a rapid increase to attain the air temperature after almost four minutes of drying.

Figure 7.74a shows that there was a marked effect of initial concentration upon zone diameter at 115°C with the zone for solution A reducing to 72% after two minutes drying. There was almost no effect upon solutions B and C which had the zone diameters reduced to 98% and 95% respectively. The drying rate curves exhibited two falling rate periods for the three solutions. The droplet temperature histories illustrated a rapid increase in droplet temperature to attain air temperature (Figure 7.74b).

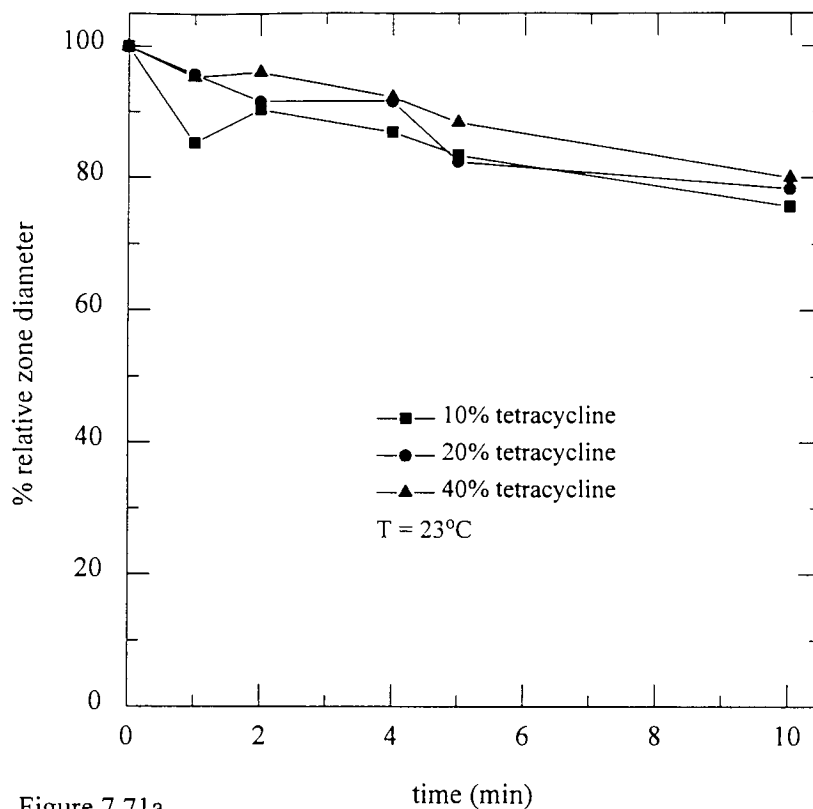


Figure 7.71a

Variation in zone diameter with initial concentration of tetracycline at 23°C air temperature

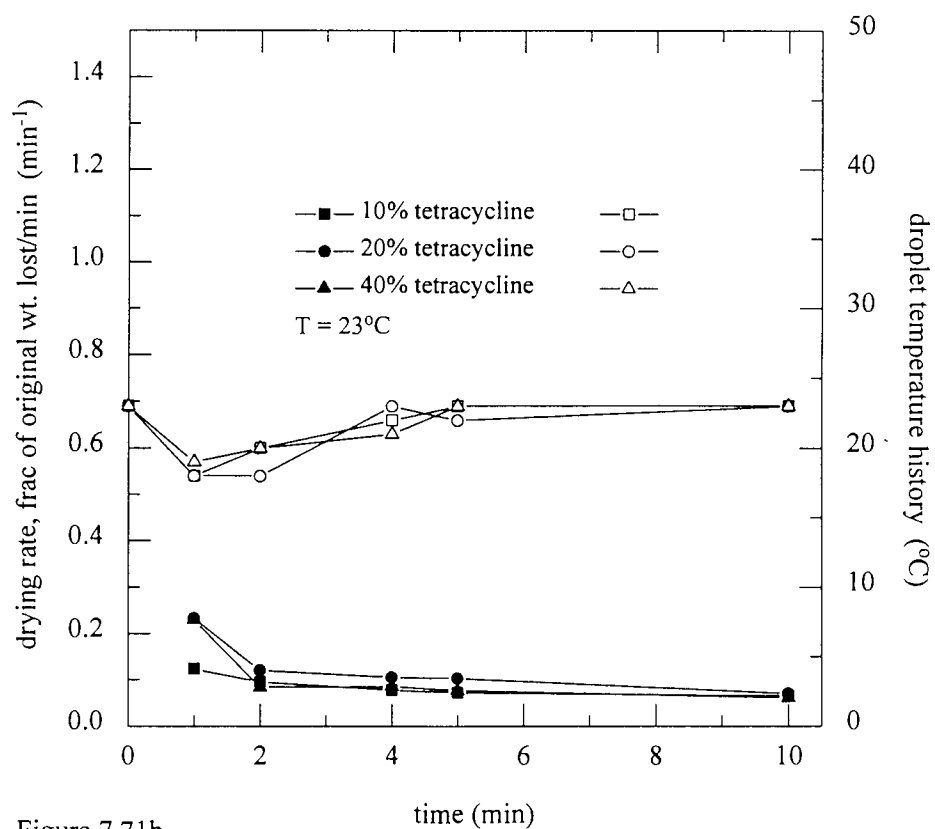


Figure 7.71b

The drying rate [solid symbols] and droplet temperature history [open symbols] for the tetracycline solutions

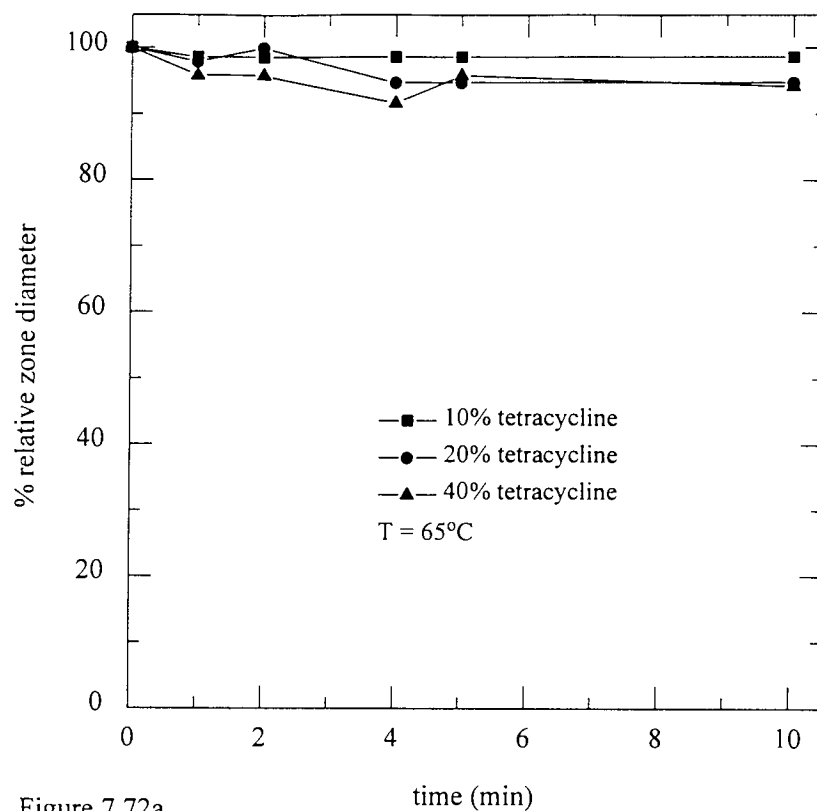


Figure 7.72a

Variation in zone diameter with initial concentration of tetracycline at 65°C air temperature

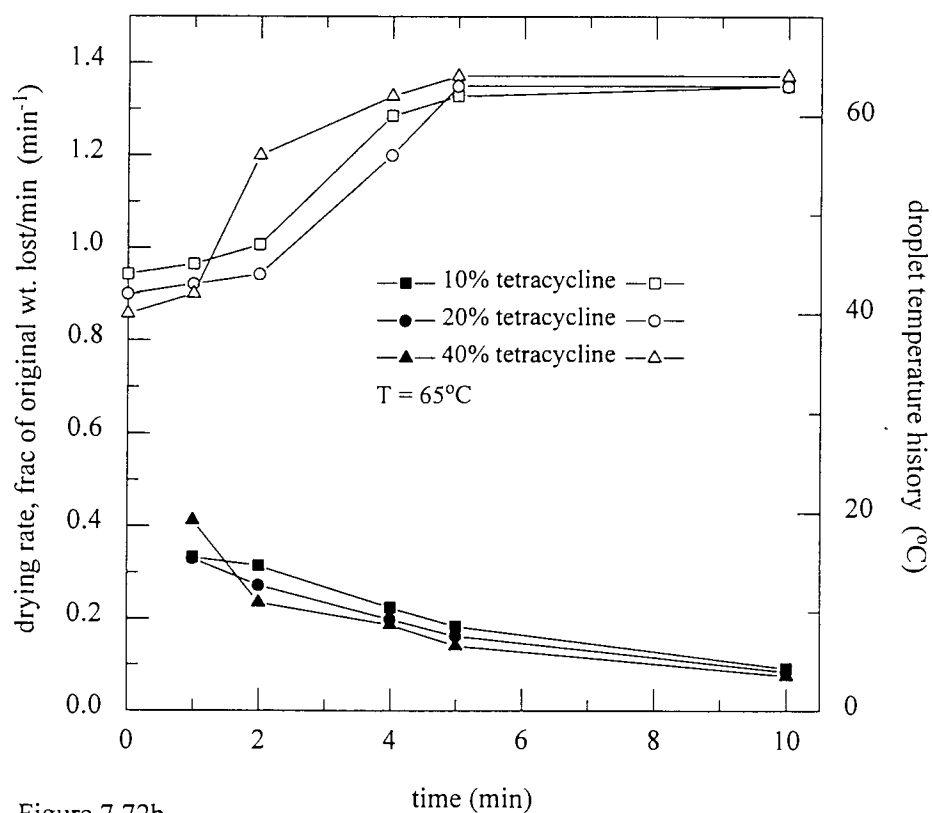


Figure 7.72b

The drying rate [solid symbols] and droplet temperature history [open symbols] for the tetracycline solutions

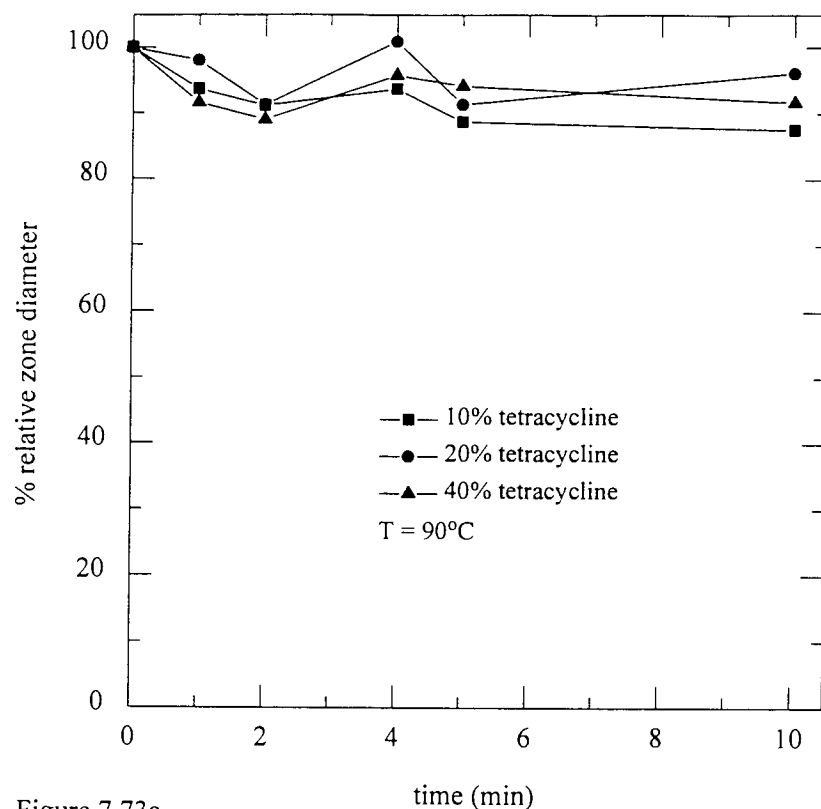


Figure 7.73a

Variation in zone diameter with initial concentration of tetracycline at 90°C air temperature

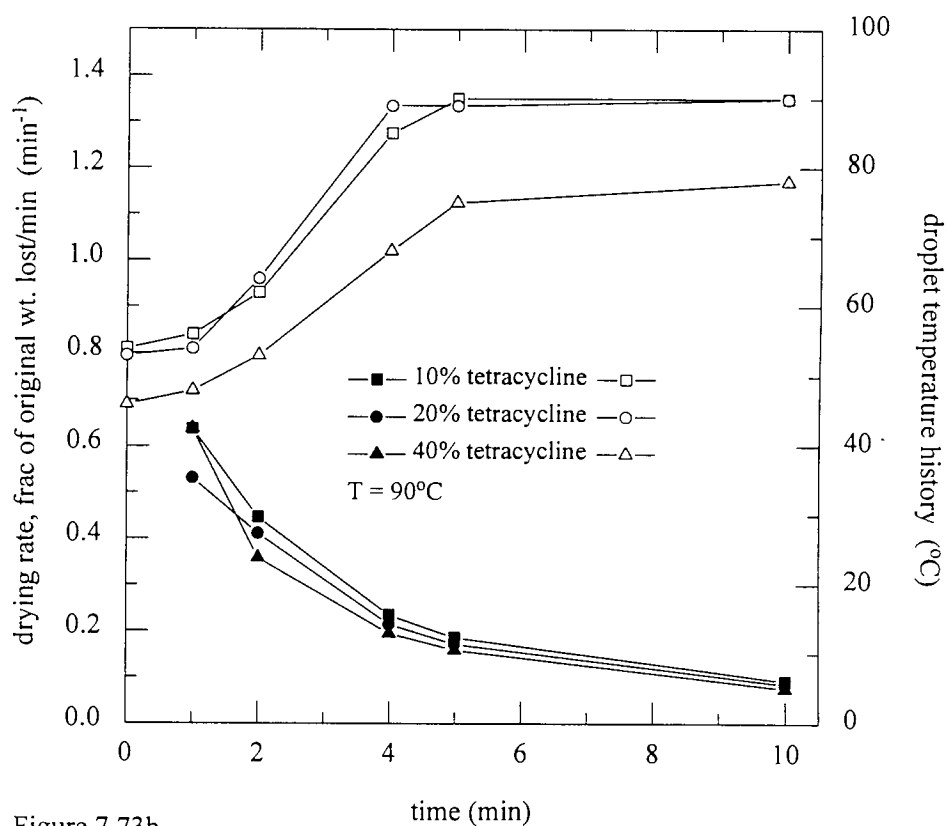


Figure 7.73b

The drying rate [solid symbols] and droplet temperature history [open symbols] for the tetracycline solutions

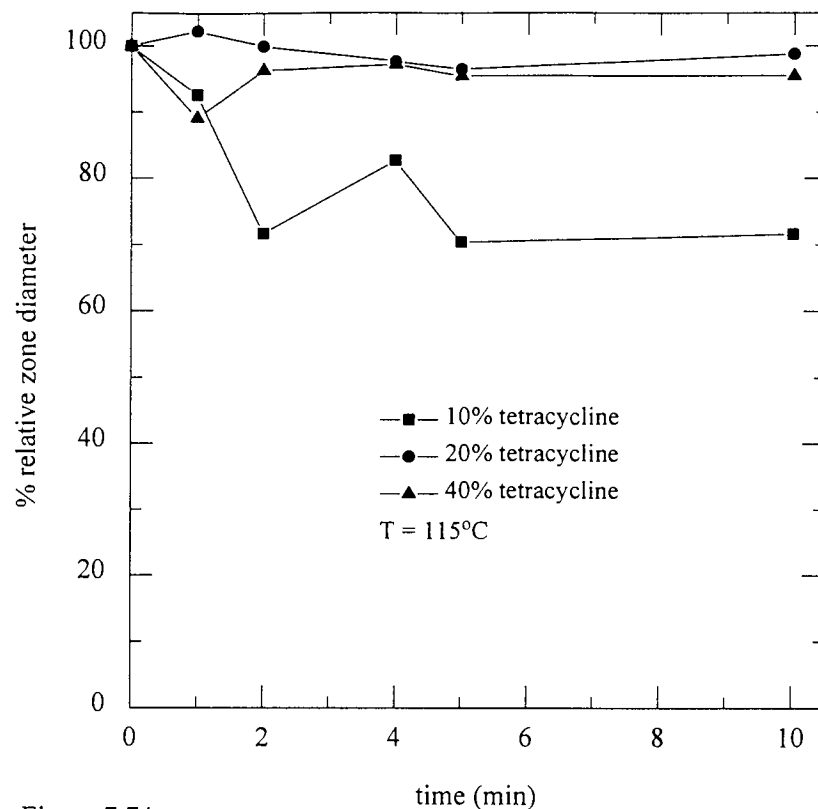


Figure 7.74a

Variation in zone diameter with initial concentration of tetracycline at 115°C air temperature

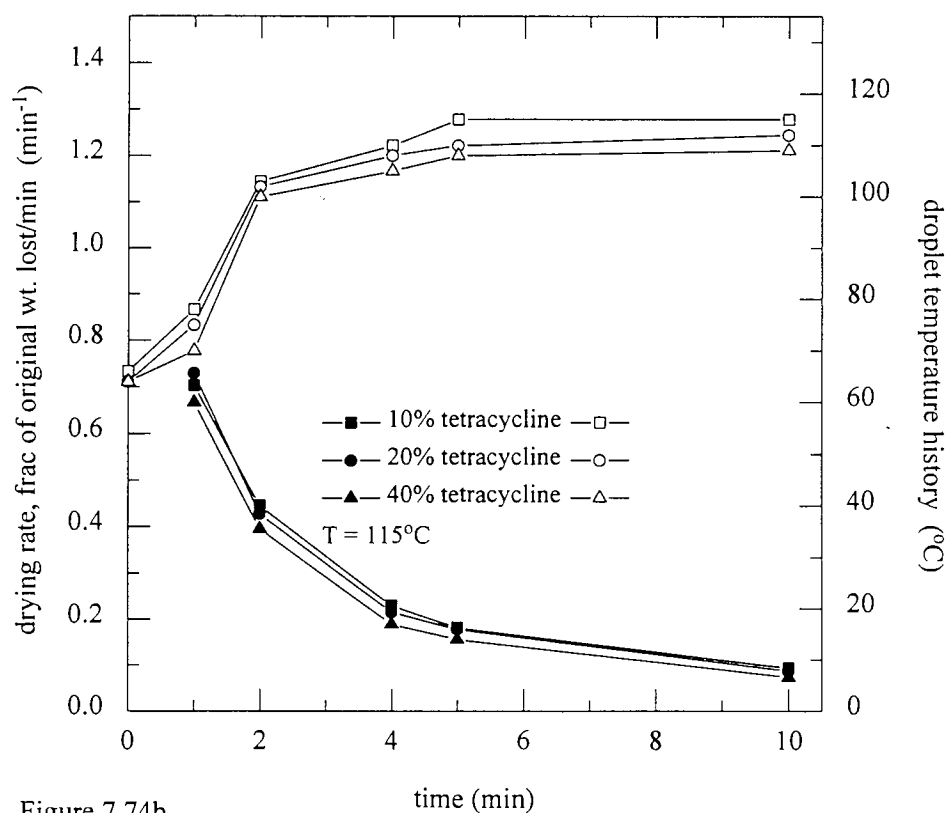


Figure 7.74b

The drying rate [solid symbols] and droplet temperature history [open symbols] for the tetracycline solutions

7.2.2: The effect of temperature

The effect of temperature upon zone diameter was experimentally determined for the various solutions / suspensions of the antibiotics. The drying rate curves showed faster rates with increases in temperature for all the antibiotics, indicating that impervious skin or crust phenomena were absent.

7.2.2.1: Ampicillin

Figure 7.75a illustrates the effect of temperature on the variation of zone diameter for a 10% w/w suspension of ampicillin. As the temperature was increased from ambient through to 90°C, the zone diameter was reduced to only 82% at 90°C. The increase to 115°C produced a marked reduction in zone diameter, with both ambient air and nitrogen as the drying gas, viz. almost 70% for the nitrogen and 45% for the ambient air. The drying rates, shown in Figure 7.75b, exhibit two falling rate periods; the curves for the ambient air and nitrogen were similar at 23°C and 115°C. The droplet temperatures increased rapidly at the higher air temperatures; the droplet temperatures at 23°C increased gradually after first falling to the wet bulb temperature.

With a 20% suspension of ampicillin, an increase in temperature from 23°C to 115°C resulted in a zone diameter reduction from almost 90% to approximately 82% at 115°C (Figure 7.76a). The droplet temperatures increased rapidly to the prevalent air temperature, except for drying at 23°C which increased very gradually after falling to wet bulb to the air temperature. The drying rate curves shown in Figure 7.76b exhibit two falling rate periods.

Variation of temperature with a 40% suspension of ampicillin had no effect as shown by Figure 7.77a, with the zone diameters reducing to 87% at 115°C and 90% at 23°C. All the droplet temperatures, with the exception of that at 23°C,

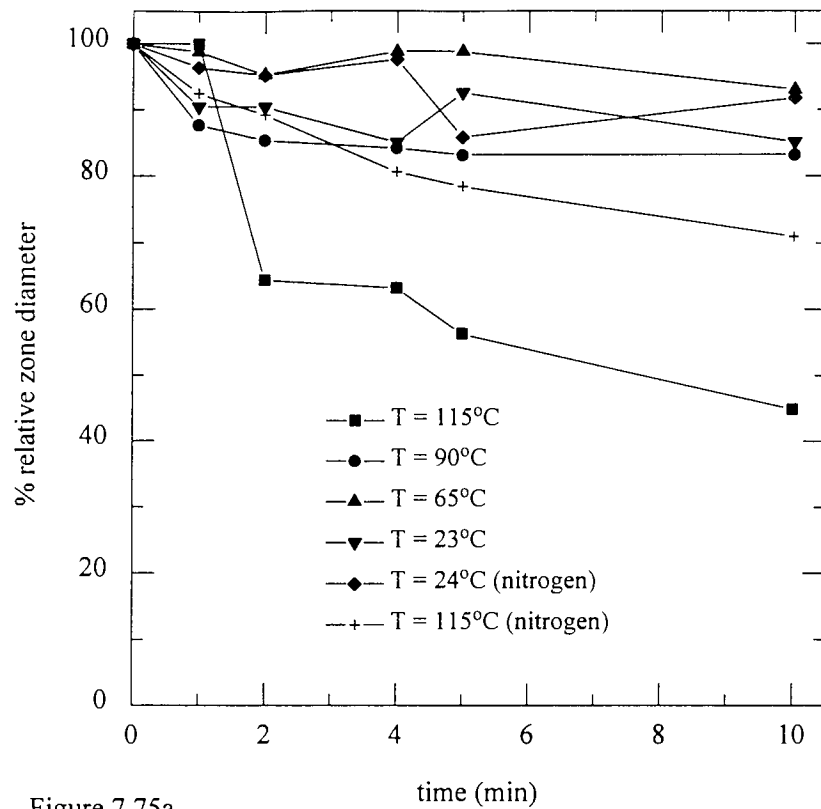


Figure 7.75a

Variation in zone diameter of 10% ampicillin solutions with gas temperature

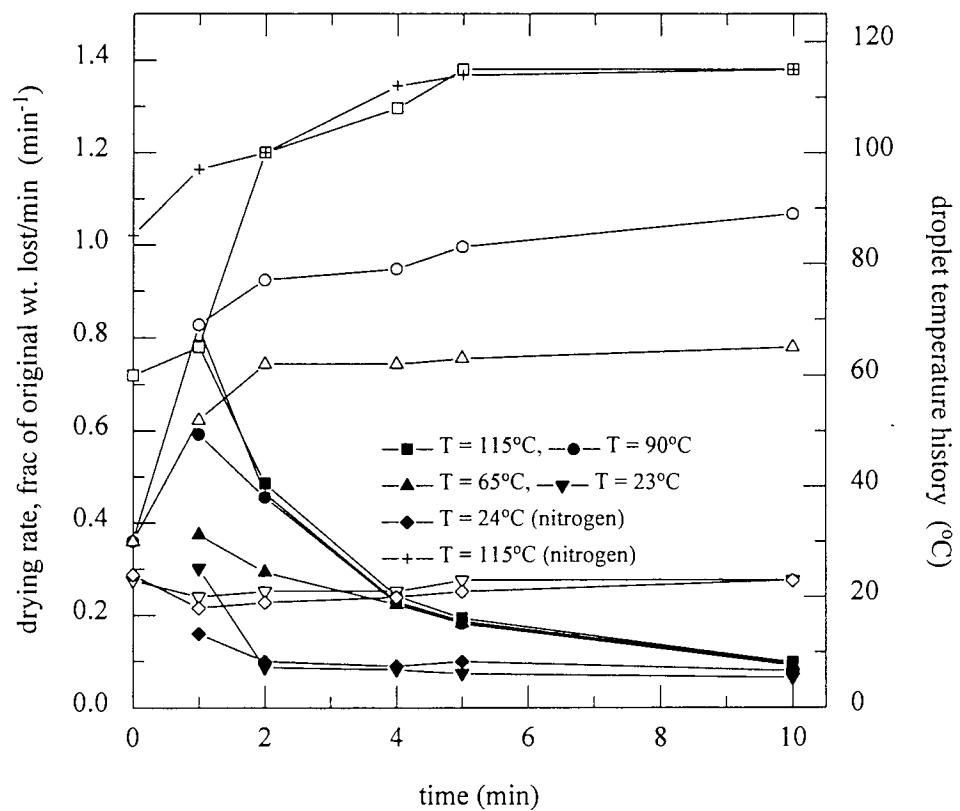


Figure 7.75b

The drying rate [solid symbols] and droplet temperature history [open symbols] for the 10% ampicillin solutions

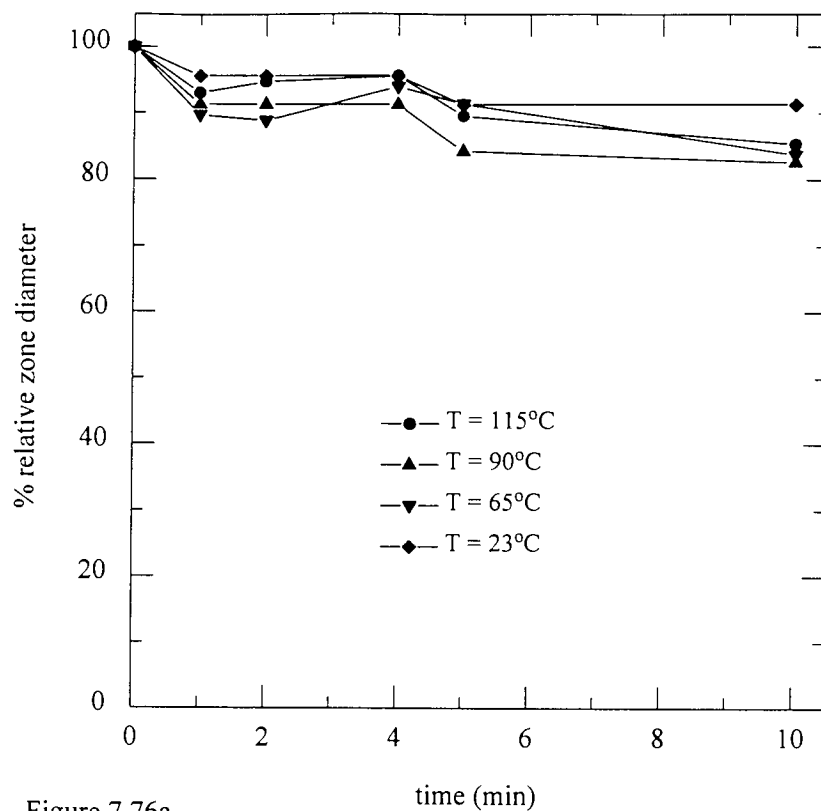


Figure 7.76a

Variation in zone diameter of 20% ampicillin solutions with air temperature

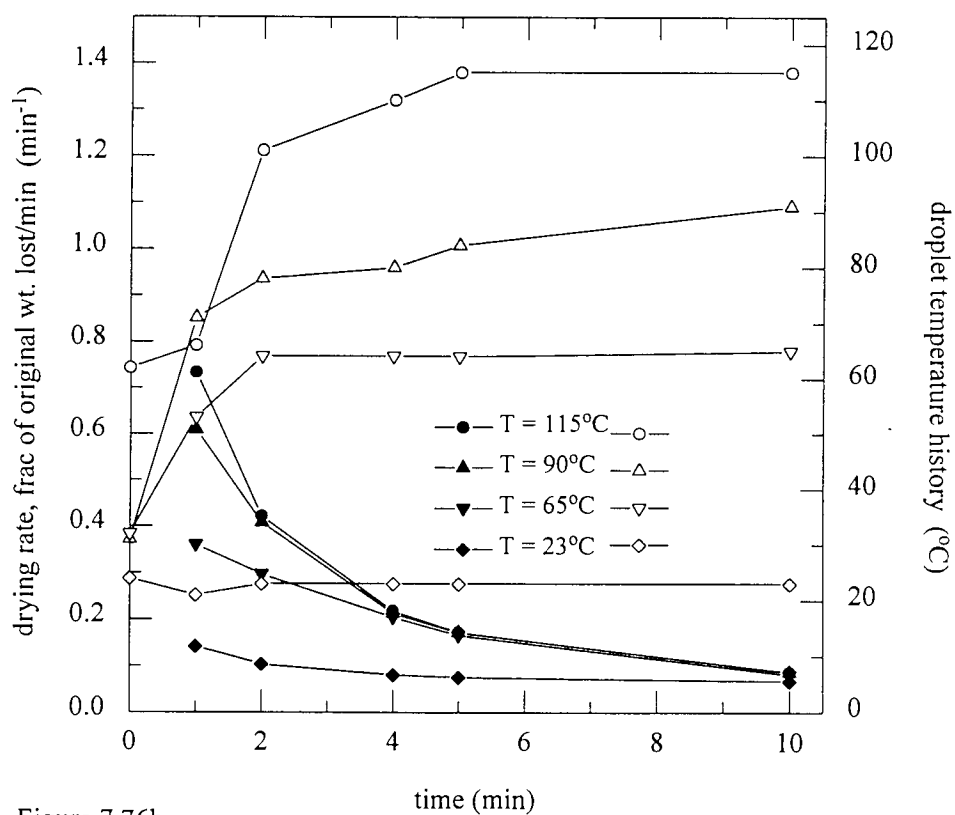


Figure 7.76b

The drying rate [solid symbols] and droplet temperature history [open symbols] for the 20% ampicillin solutions

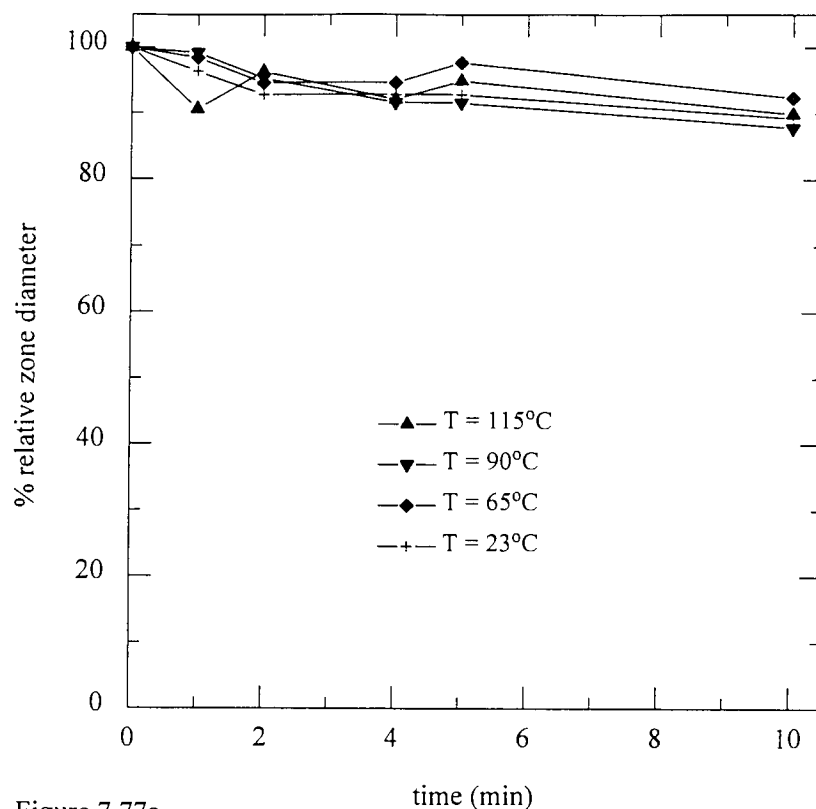


Figure 7.77a

Variation in zone diameter of 40% ampicillin solutions with air temperature

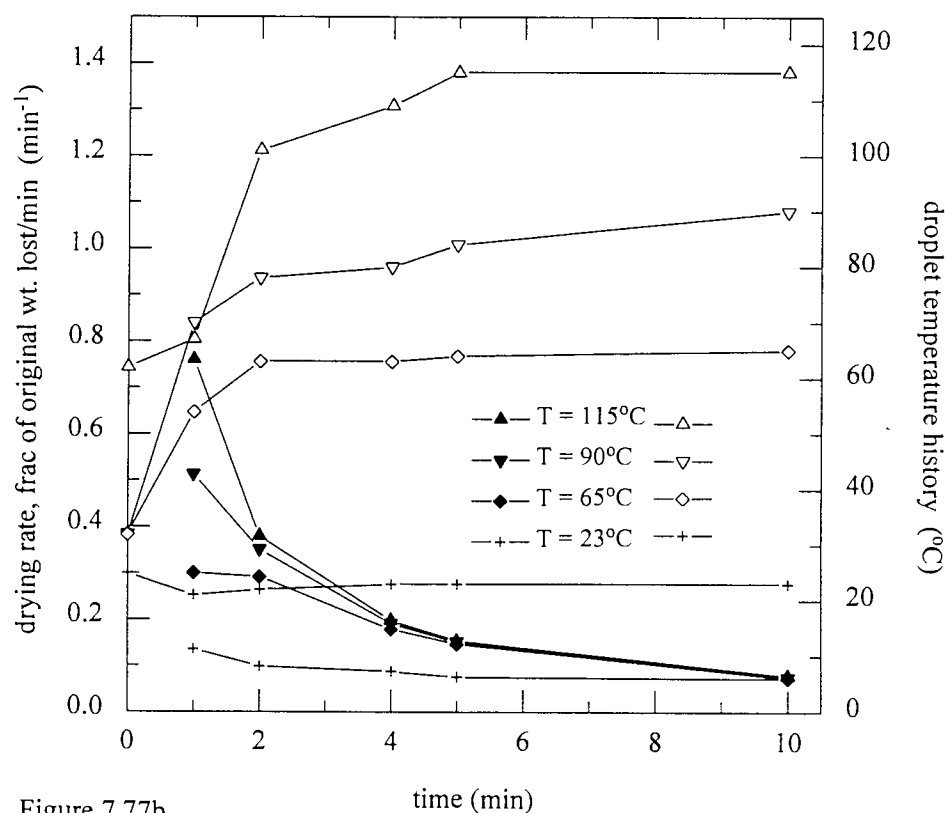


Figure 7.77b

The drying rate [solid symbols] and droplet temperature history [open symbols] for 40% ampicillin solutions

increased rapidly to the prevalent air temperature (Figure 7.77b). Two drying rates were also in evidence.

7.2.2.2: Chloramphenicol

Figure 7.78a illustrates the effect of temperature upon a 10% suspension of chloramphenicol. No zones were evident for the higher temperatures of 90°C and 115°C. Drying the droplet at 24°C in a nitrogen atmosphere resulted in no reduction in the zone diameters, but with air at 23°C there was a marked reduction to almost 64%. An increase in air temperature to 65°C resulted in a similar reduction in the zone diameter. There was a rapid increase in droplet temperature to the prevalent air temperature in all cases except for the gradual increase at 23°C and 24°C with air and nitrogen respectively (Figure 7.78b). Two falling rate periods were in evidence.

The effect of air temperature for a 20% suspension is illustrated in Figure 7.79a which shows that at 90°C there was no effect on the zone diameter. At 23°C the zone diameter had fallen to 68%; an increase to 65°C resulted in a reduction to almost 72%. An increase to 115°C caused a reduction to 77%. Figure 7.79b shows the rapid increase in droplet temperature to attain that of the air by $t = 2$ minutes. The drying rate curves show two falling rates, the first being indicative of evaporation from localised wet spots on the droplet surface, and the second of restrictive migration of internal moisture to the surface.

The effect of temperature, with a 40% suspension of chloramphenicol, on zone diameter is shown in Figure 7.80a. There is little or no effect of increasing the temperature on the zone diameter, with the zones reducing to 98%, 95%, 87%, and 82% for temperatures of 115°C, 90°C, 65°C, and 23°C respectively. The droplet temperatures show a rapid increase to attain the air temperature after two minutes of drying (Figure 7.80b). Two falling rate periods are evident.

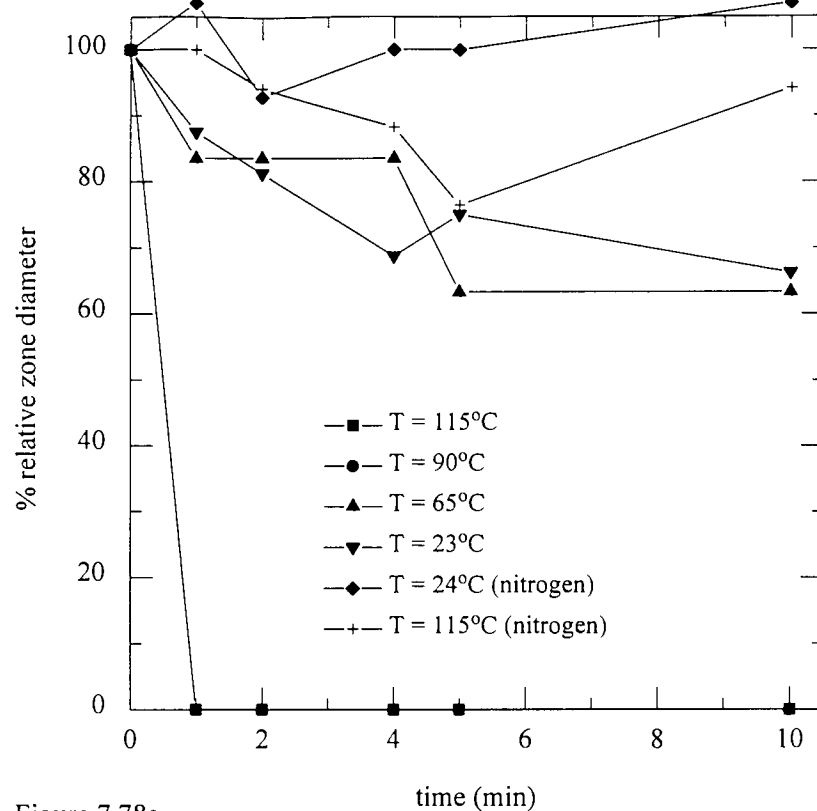


Figure 7.78a

Variation in zone diameter of 10% chloramphenicol solutions with gas temperature

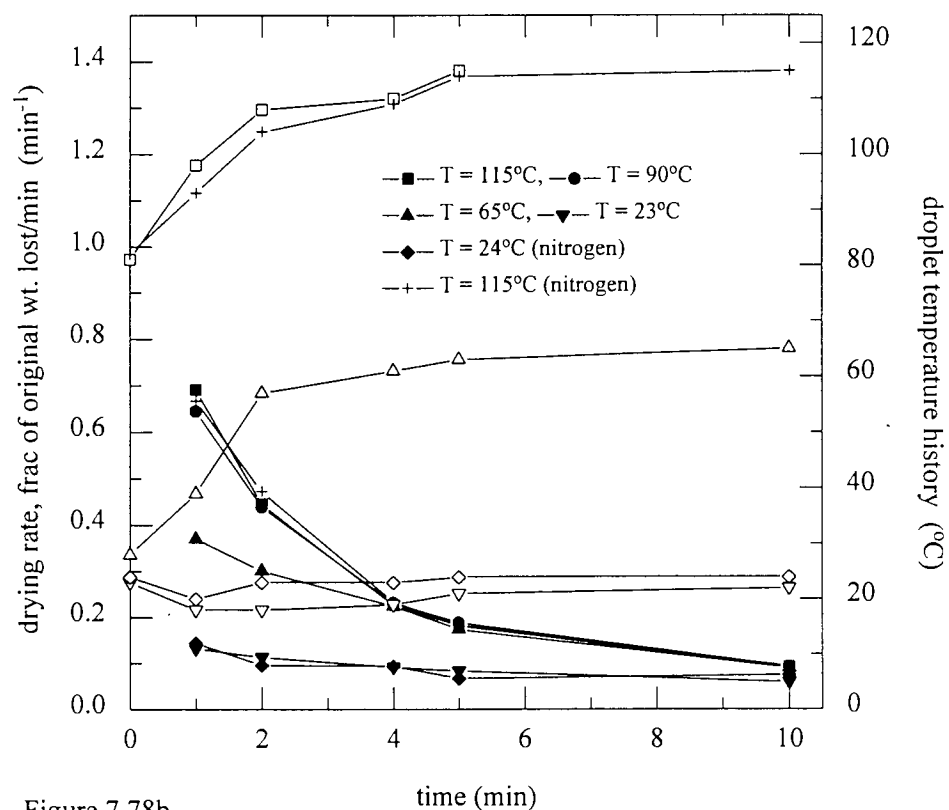


Figure 7.78b

The drying rate [solid symbols] and droplet temperature history [open symbols] for 10% chloramphenicol solutions

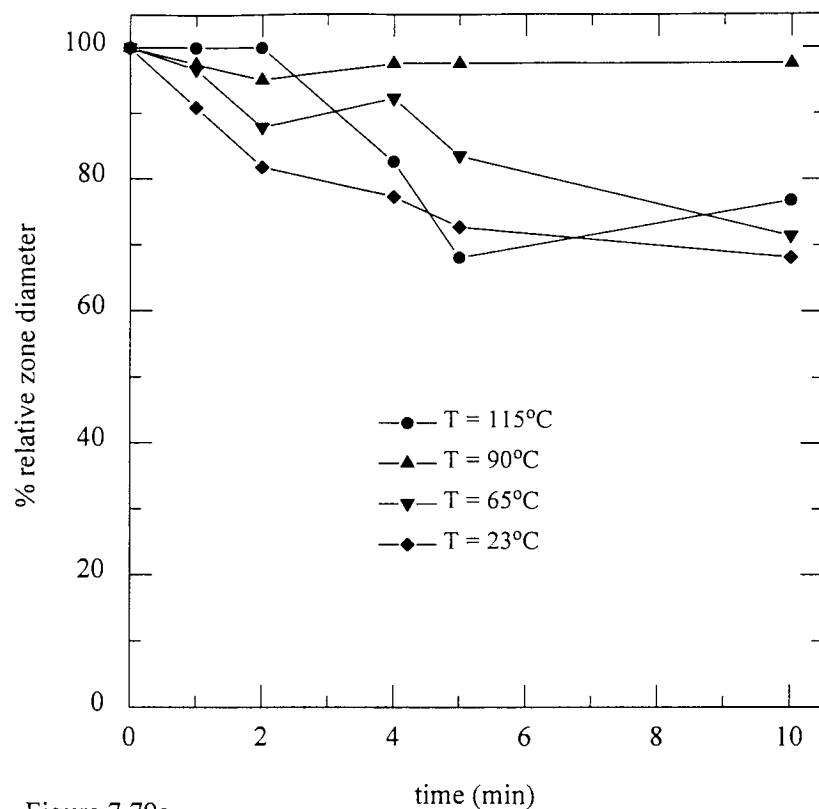


Figure 7.79a

Variation in zone diameter of 20% chloramphenicol solutions with air temperature

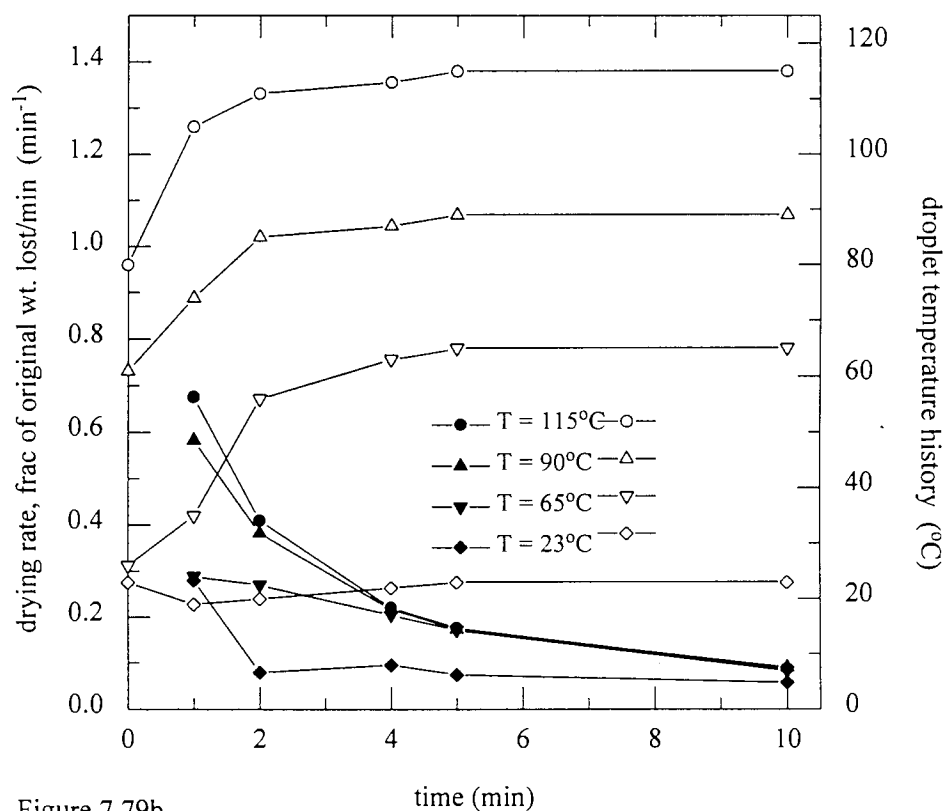


Figure 7.79b

The drying rate [solid symbols] and droplet temperature history [open symbols] for the 20% chloramphenicol solutions

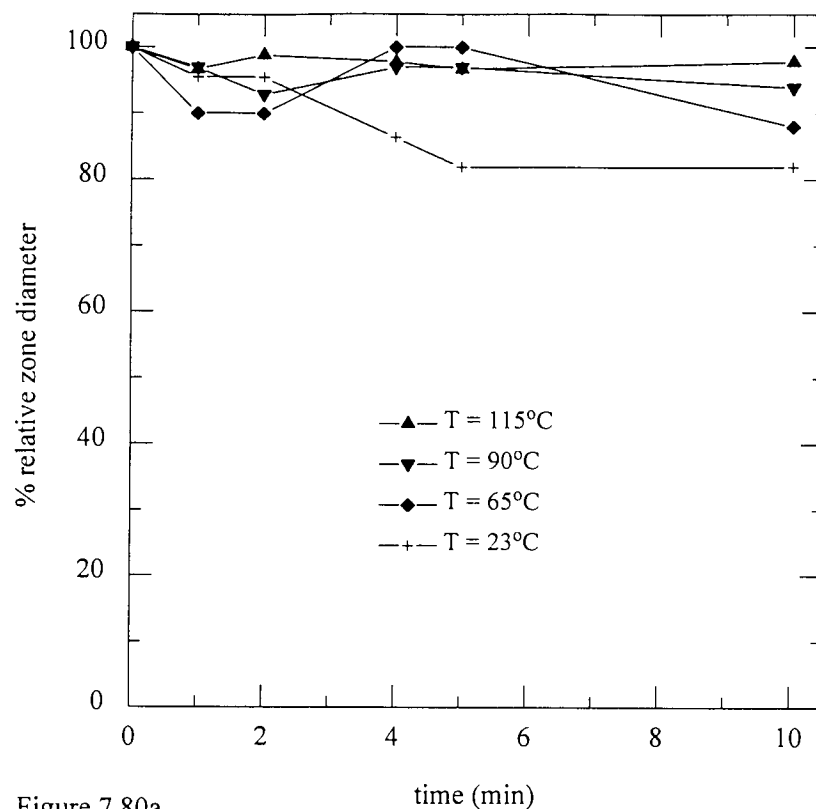


Figure 7.80a

Variation in zone diameter of 40% chloramphenicol solutions with air temperature

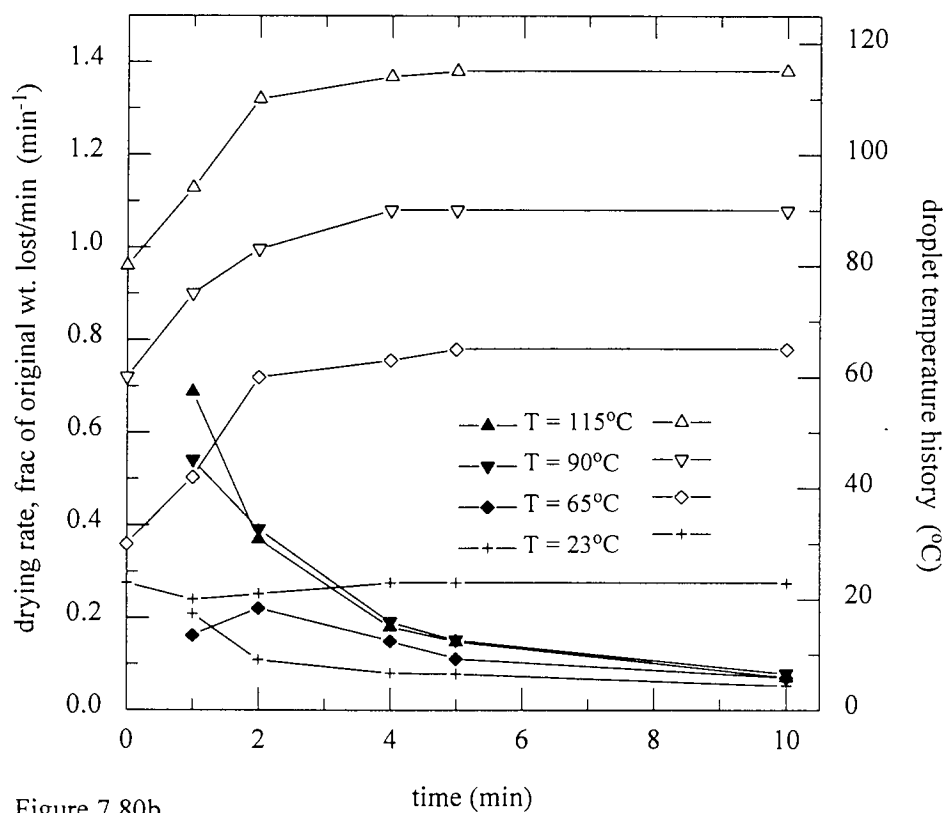


Figure 7.80b

The drying rate [solid symbols] and droplet temperature history [open symbols] for the 40% chloramphenicol solutions

7.2.2.3: Oxytetracycline

A 10% oxytetracycline suspension showed no significant difference in effects of increase in temperature, as shown in Figure 7.81a, which illustrates a decrease in zone diameter from 85% at 23°C to almost 77% at both 65°C and 90°C. The gradual increase in droplet temperature coupled with the drying rates exhibiting two falling rates indicates that the first falling rate corresponded to evaporation from localised wet spots (Figure 7.81b). The second falling rate, accompanied by a rapid increase in droplet temperature, being indicative of restricted migration of internal moisture.

Figure 7.82a shows the effect of increased temperature on zone diameter with a 20% suspension of oxytetracycline. The increase in temperature resulted in a reduction in zone diameter to 93%, 90%, 83% and 75% for 23°C, 65°C, 90°C and 115°C respectively. The zone diameters had decreased to almost their final values at $t = 2$ minutes. This correlates well with droplet temperatures attaining prevalent air temperatures by $t = 2$ minutes and the first falling rate periods which occurred during this time (Figure 7.82b). The initial gradual increase in droplet temperature is indicative of evaporation from local wet spots on the droplet surface which prevented a rapid increase from the onset of drying.

With a 40% suspension of oxytetracycline the zone diameters decreased with increasing air temperature, except at 90°C where there was little effect (Figure 7.83a), with zones reduced to almost 90%, 88% and 75% for 23°C, 65°C and 115°C respectively. With the exception of the trend at 115°C, which showed a decrease from the onset, the decrease occurred after five minutes of drying. This correlated well with the prevalent air temperatures being attained after $t = 5$ minutes. The gradual increase in droplet temperatures, as shown in Figure 7.83b, coupled with the two falling rate periods, indicate that during the first falling rate period there was unsaturated surface evaporation.

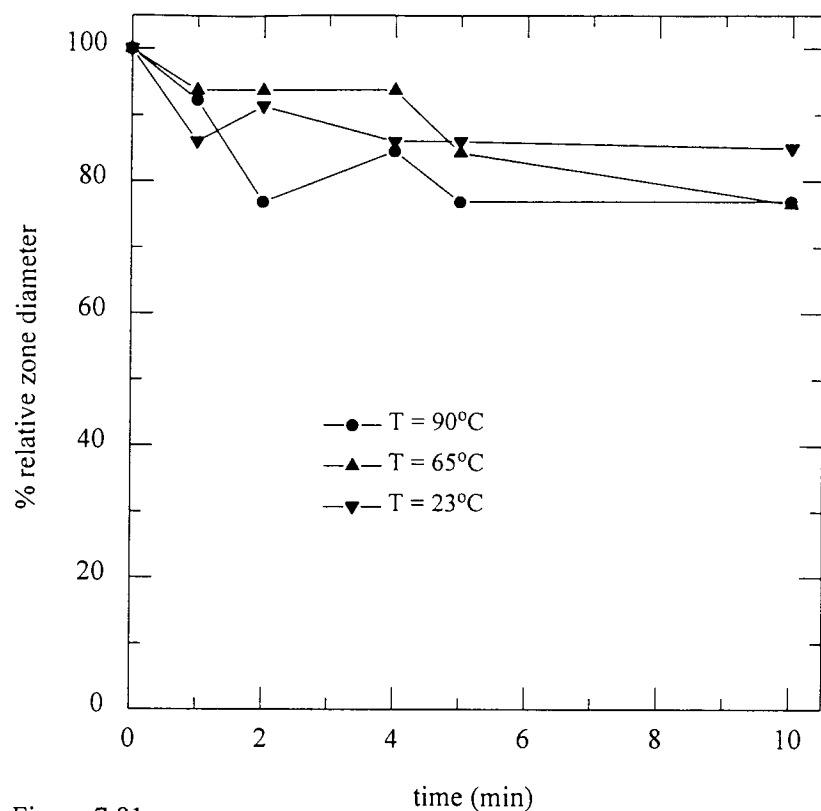


Figure 7.81a

Variation in zone diameter of 10% oxytetracycline solutions with air temperature

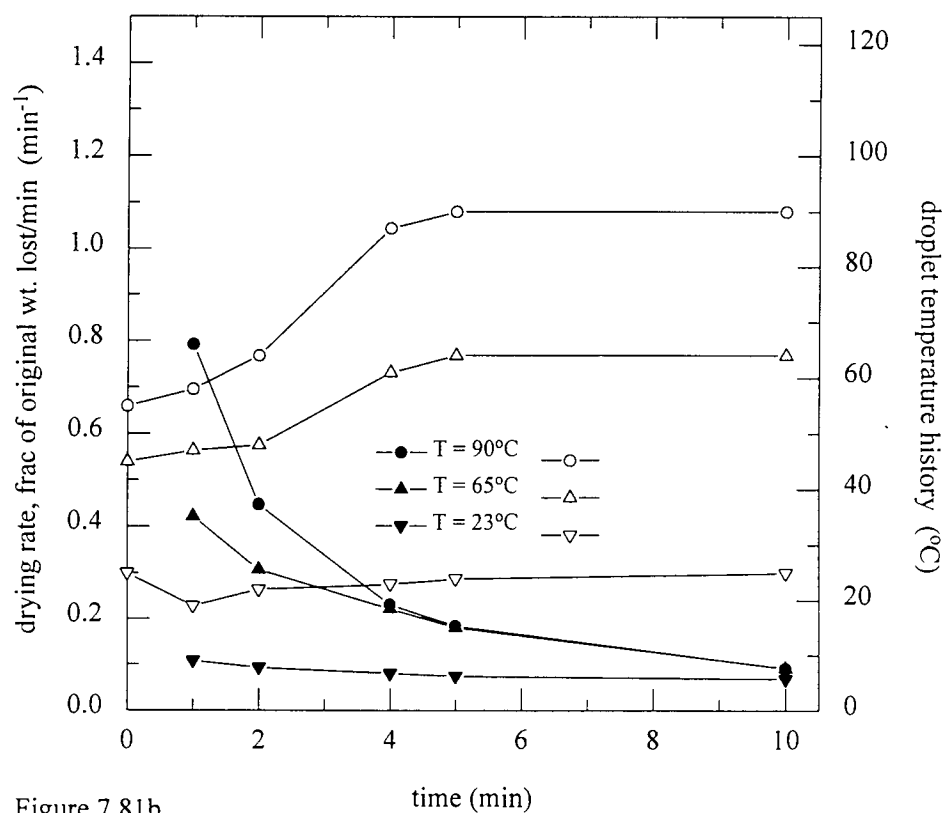


Figure 7.81b

The drying rate [solid symbols] and droplet temperature history [open symbols] for 10% oxytetracycline solutions

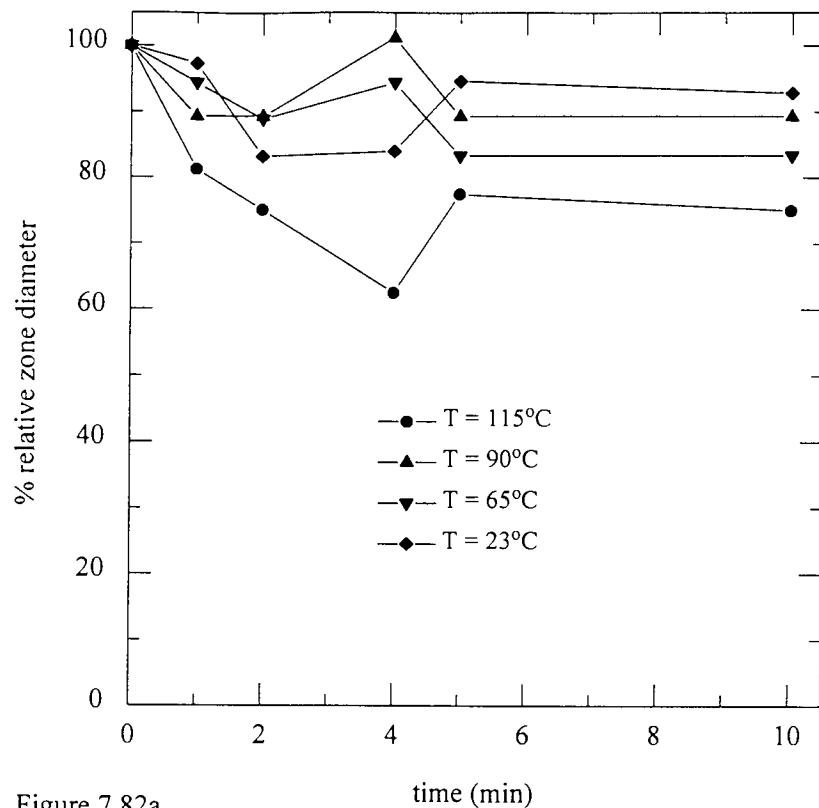


Figure 7.82a

Variation in zone diameter of 20% oxytetracycline solutions with air temperature

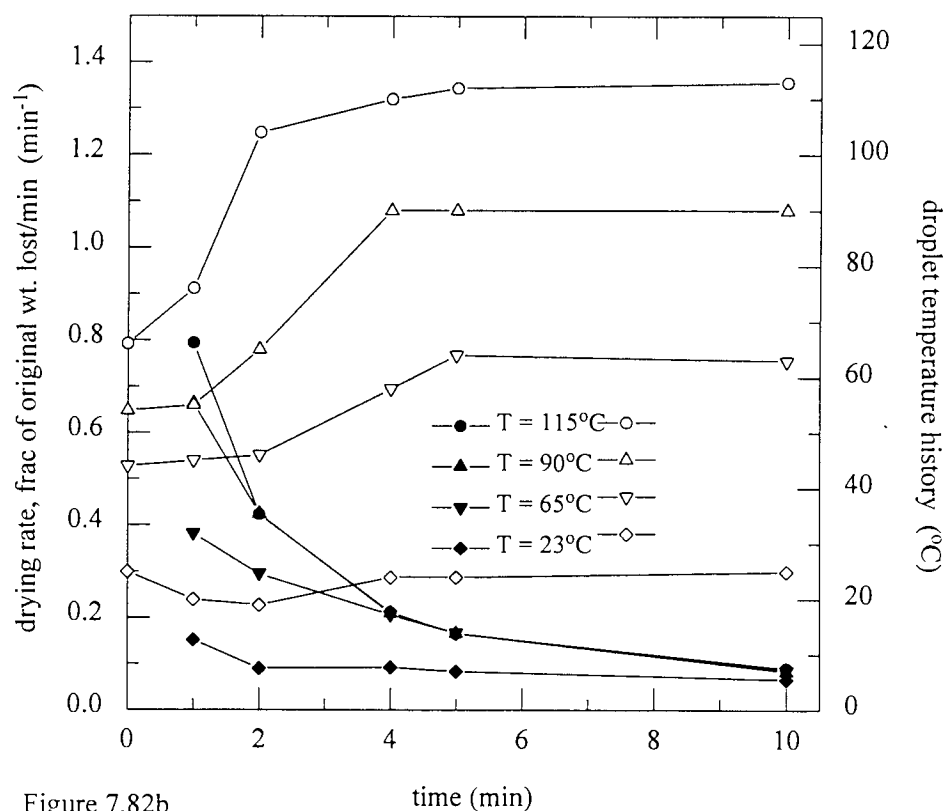


Figure 7.82b

The drying rate [solid symbols] and droplet temperature history [open symbols] for 20% oxytetracycline solutions

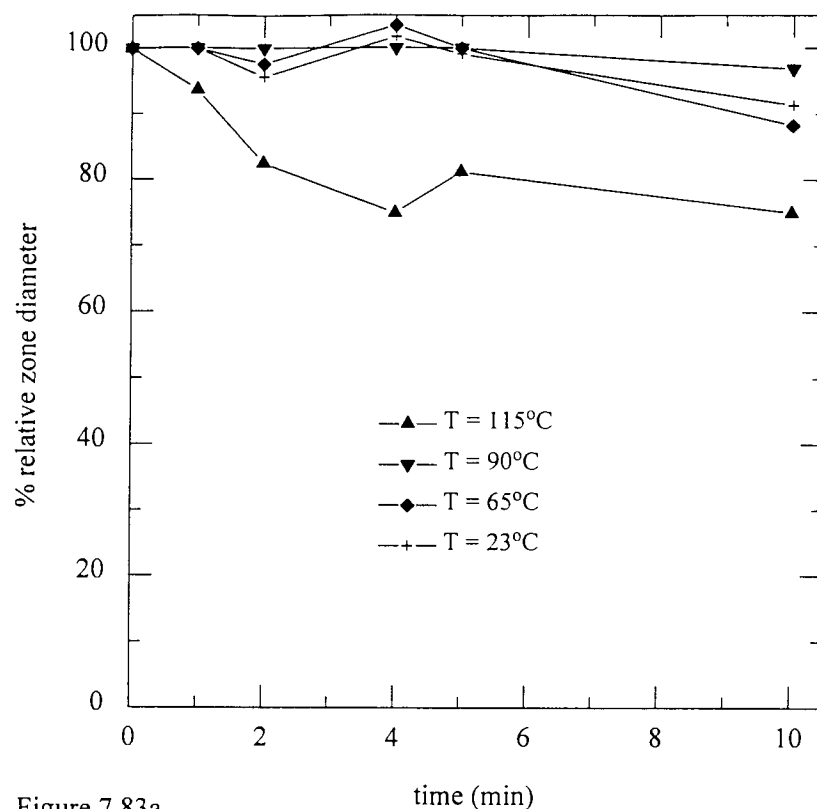


Figure 7.83a

Variation in zone diameter of 40% oxytetracycline solutions with air temperature

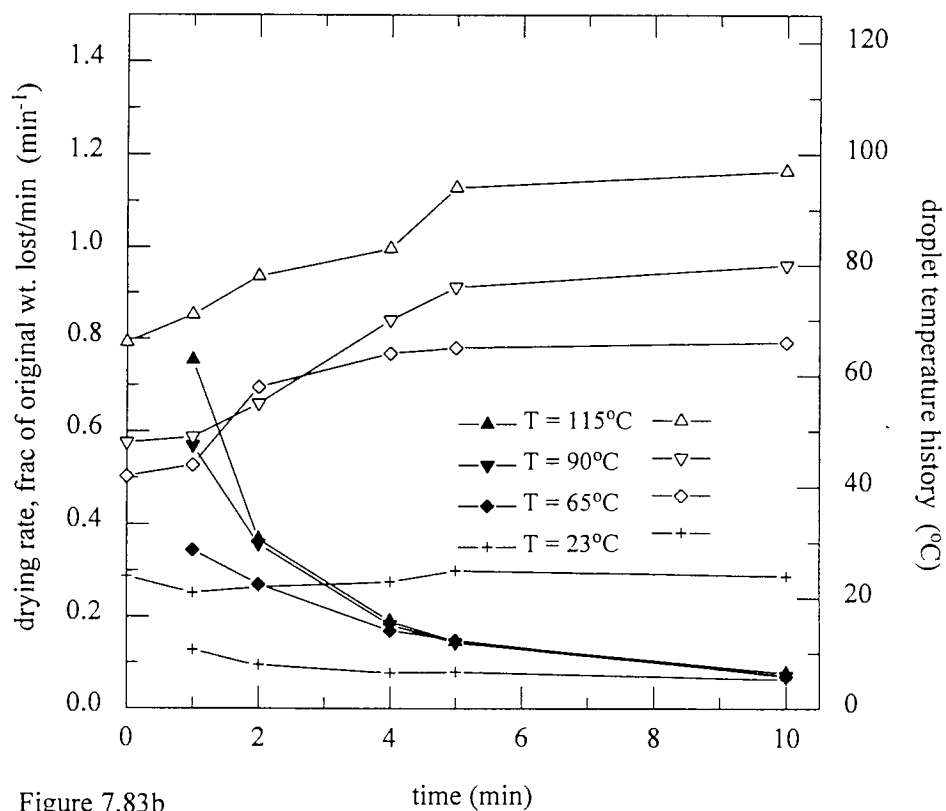


Figure 7.83b

The drying rate [solid symbols] and droplet temperature history [open symbols] for 40% oxytetracycline solutions

7.2.2.4: Streptomycin

Figure 7.84a, shows the effect of temperature on a 10% solution of streptomycin. There was a decrease in zone diameter with an increase in air temperature with the exception of 23°C which showed a greater reduction in zone diameter. The decreases in diameter, achieved within the first two minutes of drying, correlated well with the droplets attaining the prevalent air temperatures within the first two minutes. The first falling rate periods also occurred during this time (Figure 7.84b). The use of an inert drying medium (nitrogen) had no significant effect upon zone diameter.

An increase in temperature with a 20% solution resulted in no significant reduction of the zone diameters, except at 23°C the zones did decrease to 87% (Figure 7.85a). The rapid increase in droplet temperatures and the faster drying rates for the higher temperatures (i.e. 65°C, 90°C and 115°C) are illustrated in Figure 7.85b.

A 40% solution exhibited no significant effects of temperature upon zone diameter as shown in Figure 7.86a, with the zones at 23°C shown to be the most affected (i.e. zone diameters decreased to 90%). The droplet temperatures increased rapidly, corresponding to the first falling rate period (Figure 7.86b).

The apparent decrease in zone diameters at 23°C may be attributable to the difficulty in removing the complete droplet, which remained liquid after ten minutes of drying, from the end of the thermocouple.

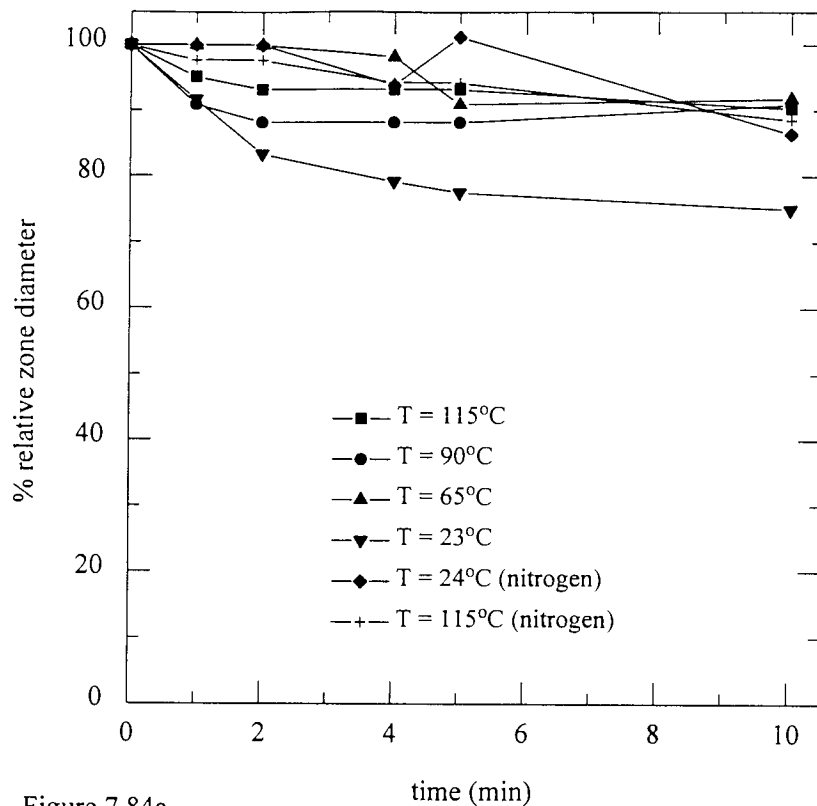


Figure 7.84a

Variation in zone diameter of 10% streptomycin solutions with gas temperature

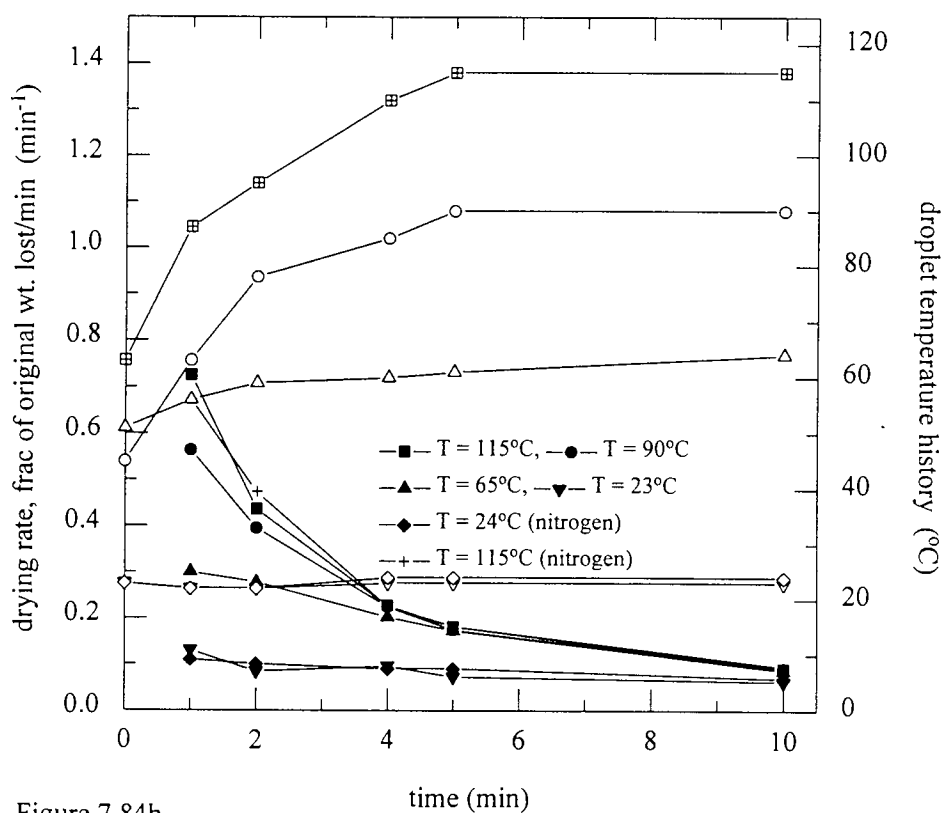


Figure 7.84b

The drying rate [solid symbols] and droplet temperature history [open symbols] for 10% streptomycin solutions

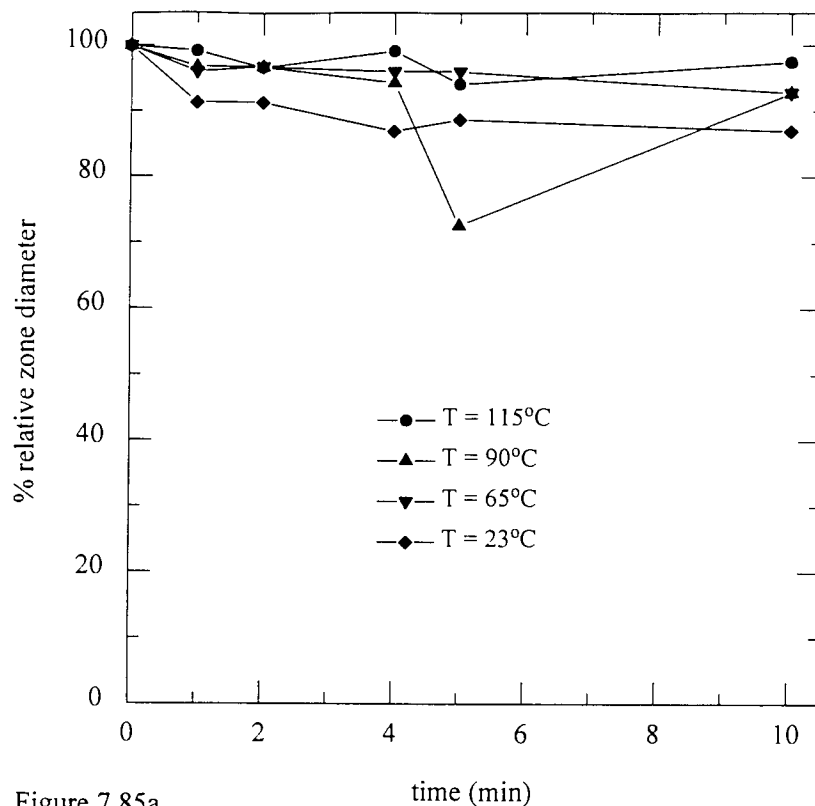


Figure 7.85a

Variation in zone diameter of 20% streptomycin solution with air temperature

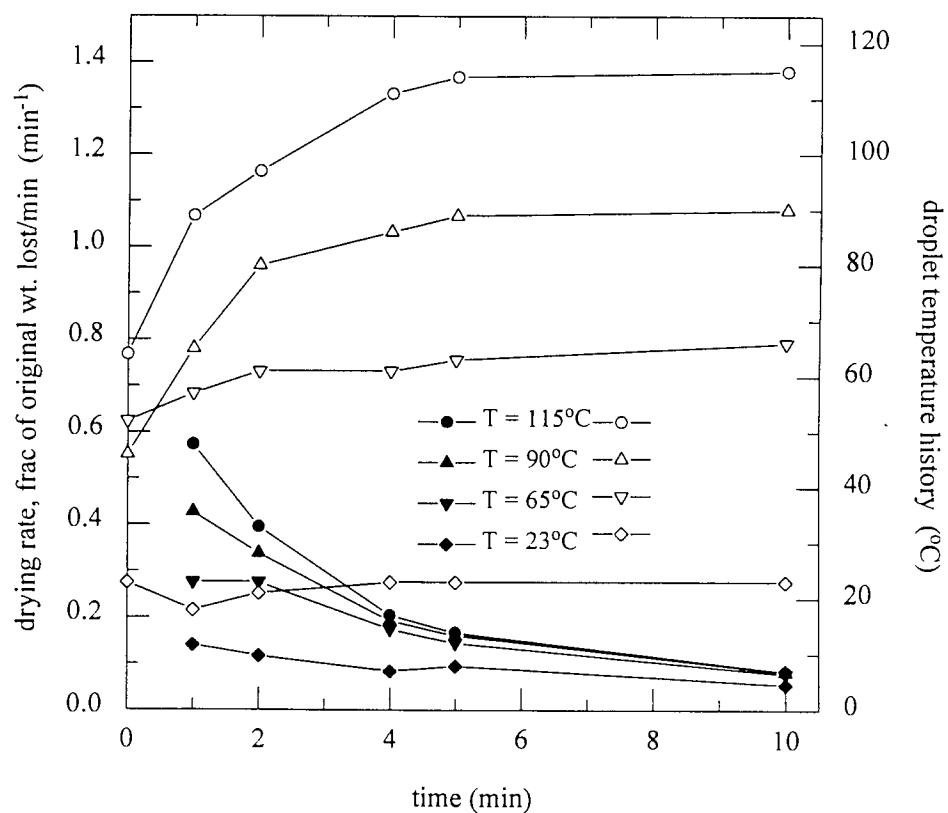


Figure 7.85b

The drying rate [solid symbols] and droplet temperature history [open symbols] for 20% streptomycin solutions

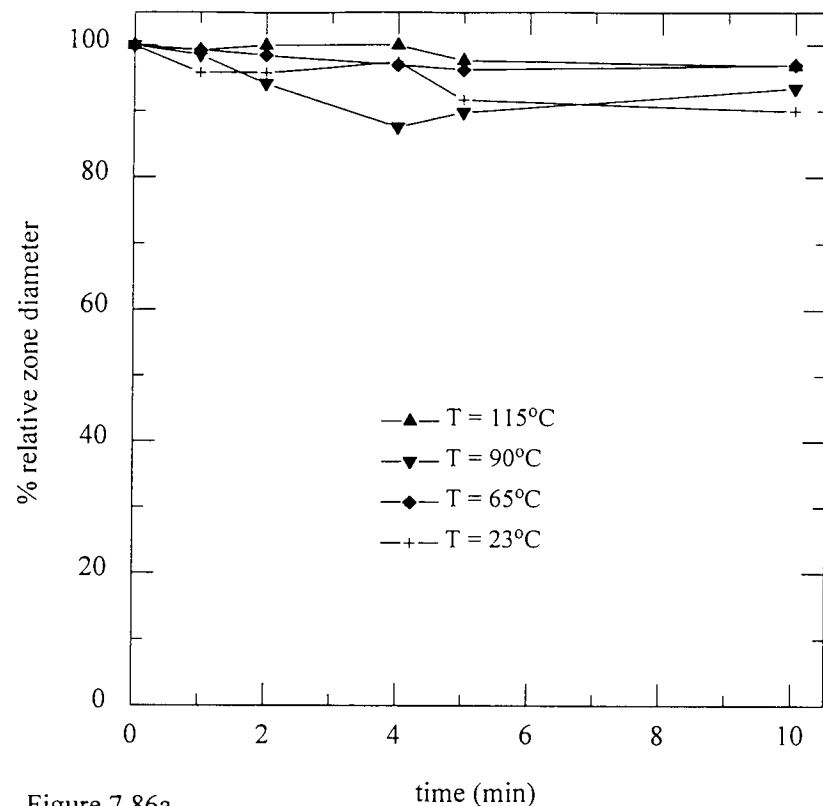


Figure 7.86a

Variation in zone diameter of 40% streptomycin solutions with air temperature

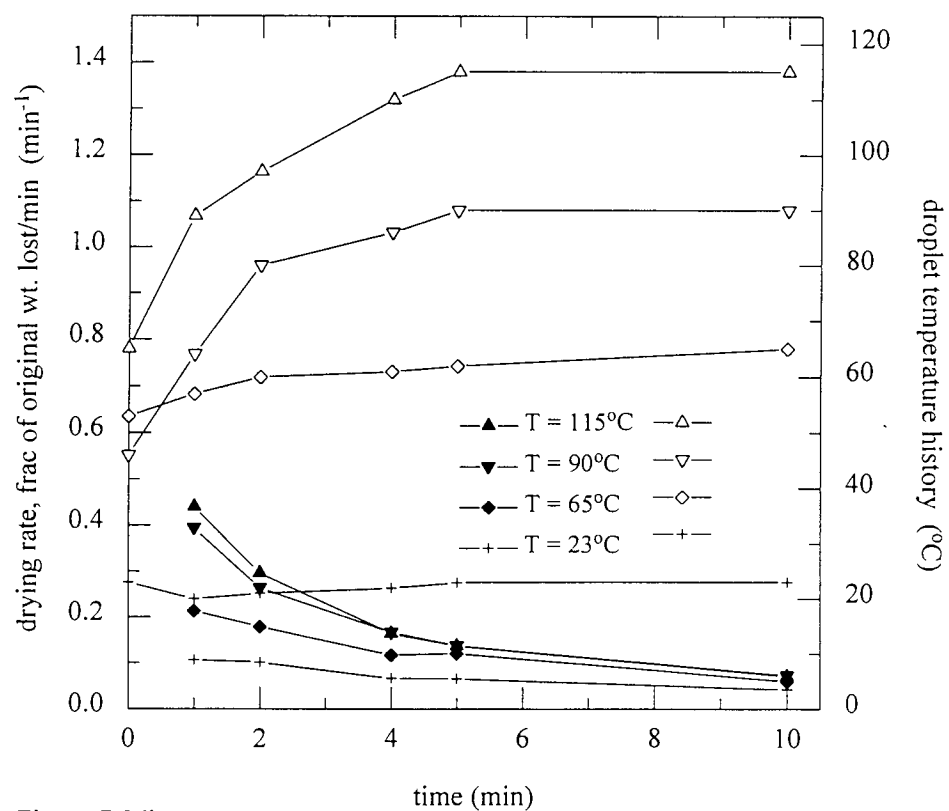


Figure 7.86b

The drying rate [solid symbols] and droplet temperature history [open symbols] for 40% streptomycin solutions

7.2.2.5: Tetracycline

The variation of zone diameter with increasing temperature was most evident with the air temperature at 115°C (Figure 7.87a) with the zone diameter decreased to 72%. The use of an inert drying medium (nitrogen) at both 24°C and 115°C had no effect upon zone diameter. The gradual increase in droplet temperatures to the prevalent air temperature is indicative of unsaturated surface evaporation, which coincides with the first falling rate periods, as shown in Figure 7.87b.

Figure 7.88a shows that temperature had an interesting effect upon zone diameters for a 20% suspension; all final zones were between 95% and 99%, with the exception of that at 23°C which decreased to 78%. The temperature histories, in Figure 7.88b, show a gradual increase in droplet temperature to that of the air. The drying rate curves show two falling rate periods with the first falling rate periods exhibiting a faster rate at elevated temperatures.

A 40% suspension of tetracycline showed no significant effects of increasing the air temperature, as shown in Figure 7.89a, with the exception of the droplets at 23°C where the zones had decreased to 80%. The zones decreased to 95%, 92% and 95% for 65°C, 90°C and 115°C respectively. The droplet temperature histories showed a gradual initial increase to the prevalent air temperatures (Figure 7.89b); these coupled with the first falling rate periods exhibited at all the temperatures suggest that the initial evaporation occurred from localised wet spots on the droplet surface. The subsequent constant droplet temperatures and the second falling rate periods are indicative of restrictions to moisture migration from the droplet interior.

The apparent decrease in zone diameter exhibited at 23°C may again be spurious.

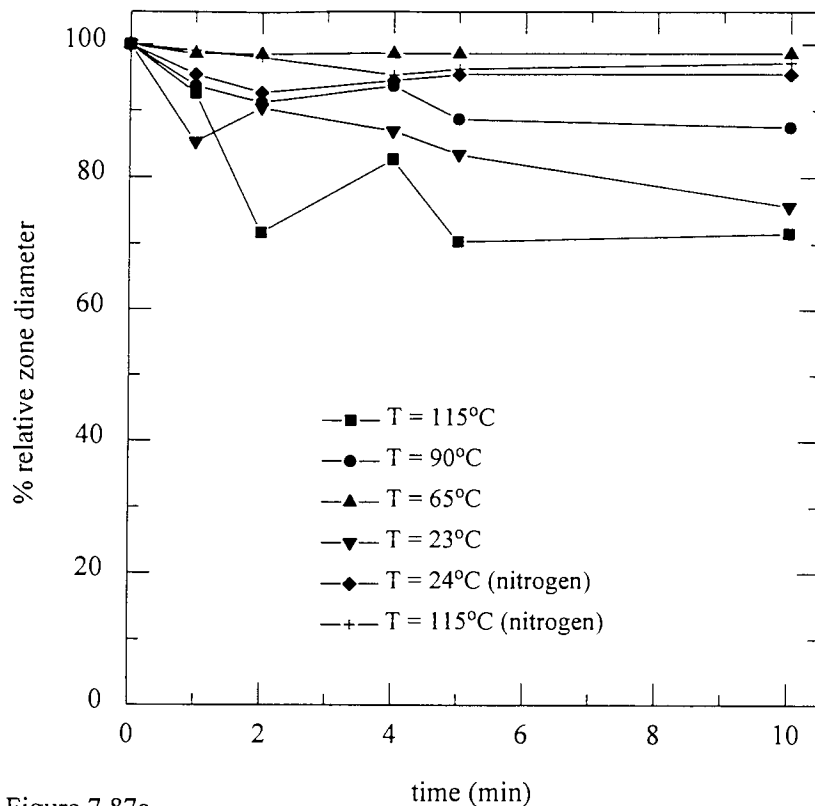


Figure 7.87a

Variation in zone diameter of 10% tetracycline solutions with gas temperature

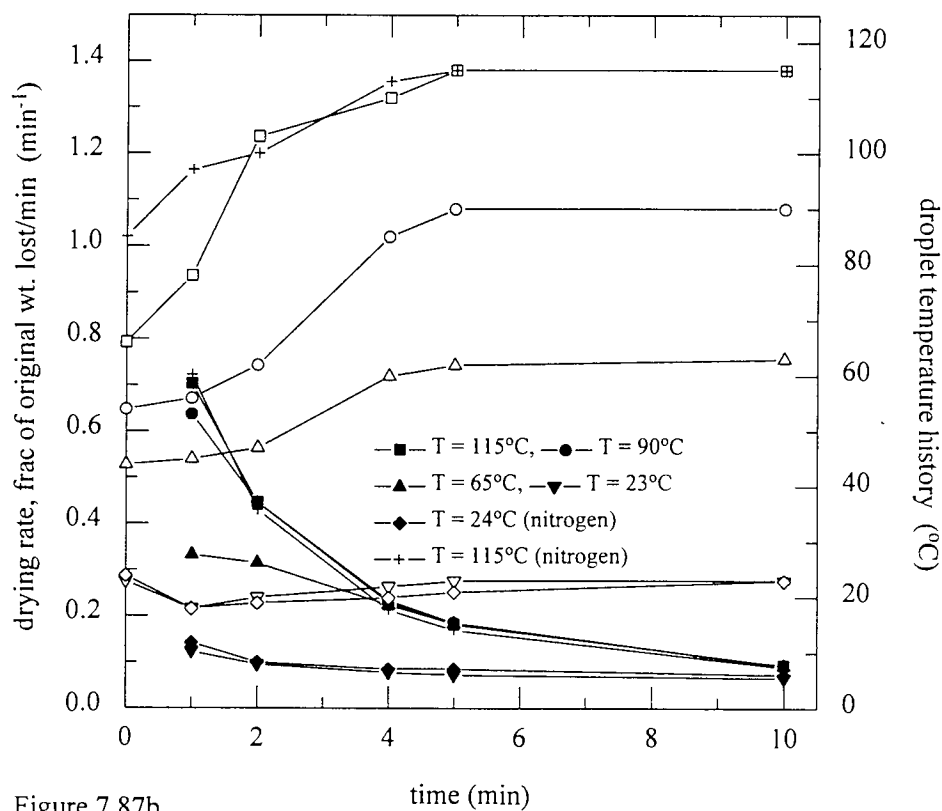


Figure 7.87b

The drying rate [solid symbols] and droplet temperature history [open symbols] for 10% tetracycline solutions

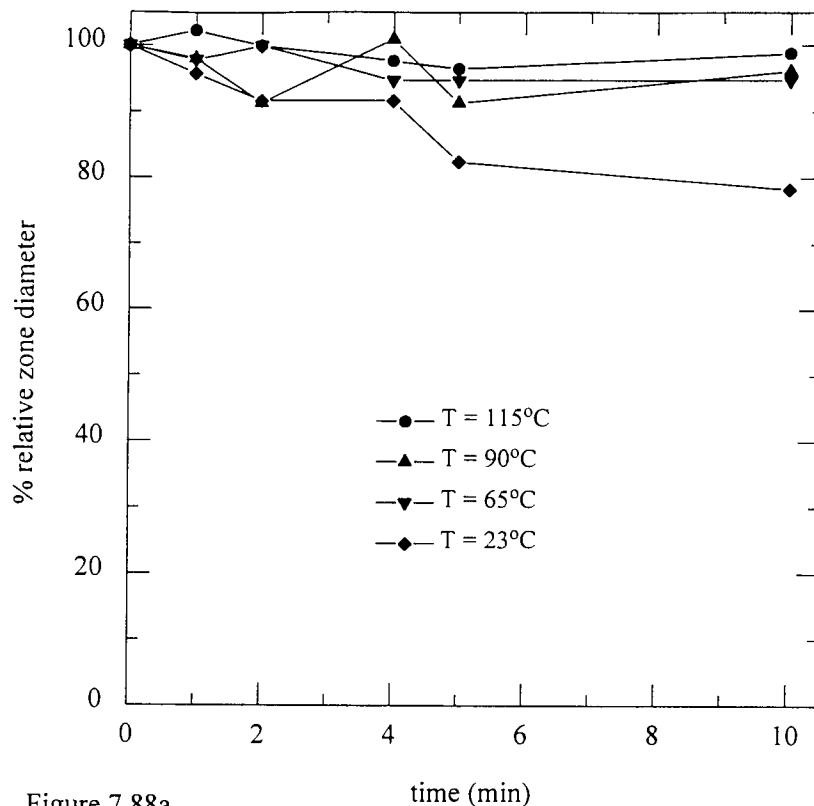


Figure 7.88a

Variation in zone diameter of 20% tetracycline solutions with air temperature

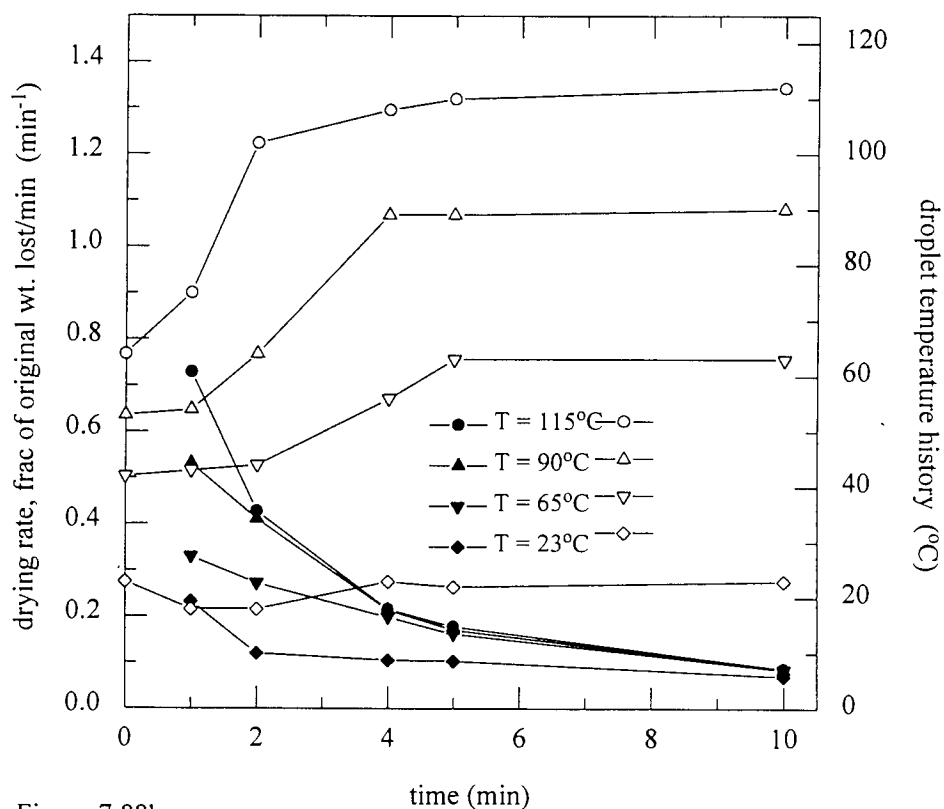


Figure 7.88b

The drying rate [solid symbols] and droplet temperature history [open symbols] for 20% tetracycline solutions

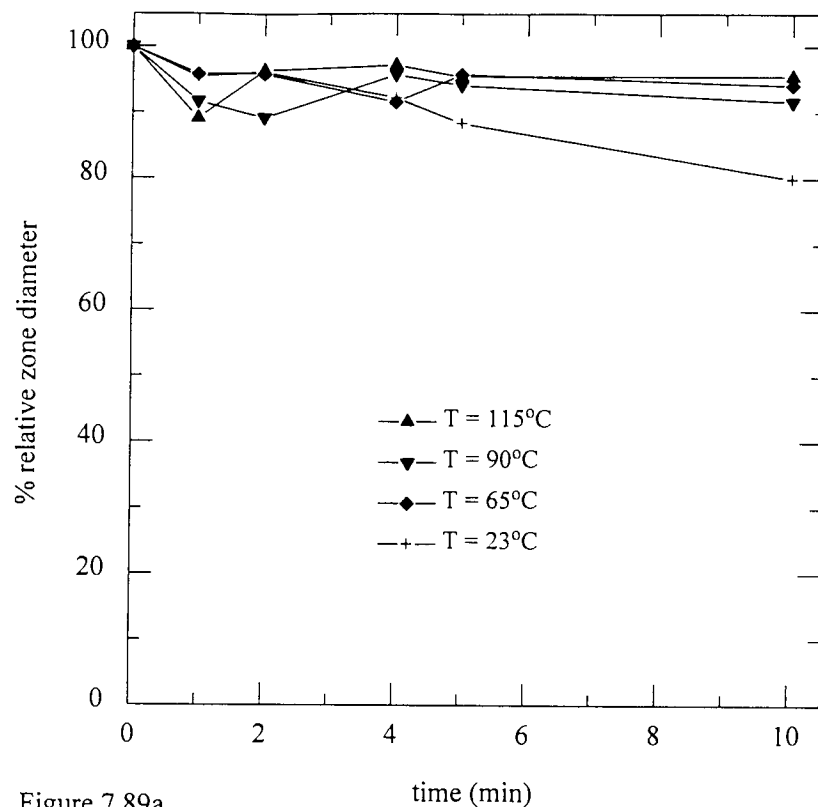


Figure 7.89a

Variation in zone diameter of 40% tetracycline solutions with air temperature

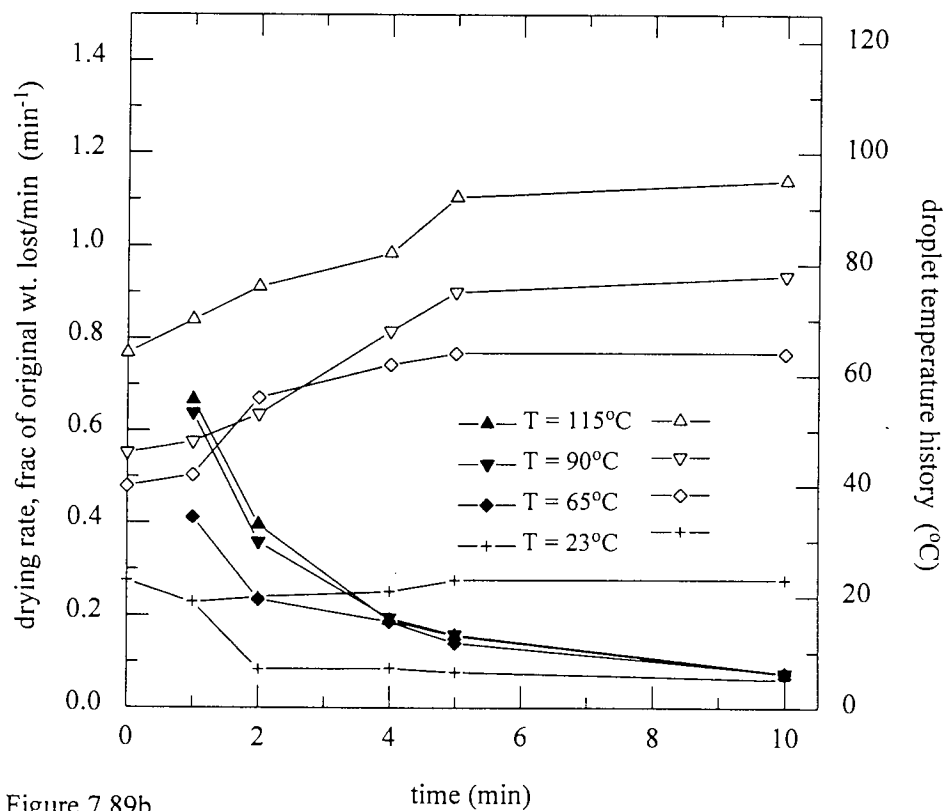


Figure 7.89b

The drying rate [solid symbols] and droplet temperature history [open symbols] for 40% tetracycline solutions

7.2.3: The effect of drying in an inert medium (nitrogen)

To ascertain whether the effects demonstrated by the various antibiotics were caused by the high temperatures or were oxidative effects, the single droplets of the various antibiotics were dried in a nitrogen atmosphere.

7.2.3.1: Ampicillin

There was a slight difference in zone diameter resulting from the use of nitrogen at 24°C compared to air at 23°C, as shown in Figure 7.90a. The final zone diameters were reduced to 85% and 92% for the air and nitrogen atmospheres respectively. The drying rates, shown in Figure 7.90b, were similar with two falling rates. The droplet temperatures initially fell to the wet bulb temperature with both the air and nitrogen before a gradual increase to the air temperature, indicative of unsaturated surface evaporation.

An increase in temperature to 115°C resulted in zone reductions to 70% and 45% for the nitrogen and air respectively, as shown in Figure 7.91a. The decrease with the nitrogen atmosphere was more gradual than with air, where the decrease was from 100% to 65% in the second minute of drying. The drying rates and droplet temperature histories, shown in Figure 7.91b, illustrate a more rapid increase in temperature for the air atmosphere because the initial temperature was low (~60°C) compared to 85°C for the nitrogen. Both drying rates exhibit a similar behaviour.

This difference in zone diameter decrease between the air and nitrogen atmospheres at 115°C suggests that reduced potency was caused by a combination of thermal and oxidative effects.

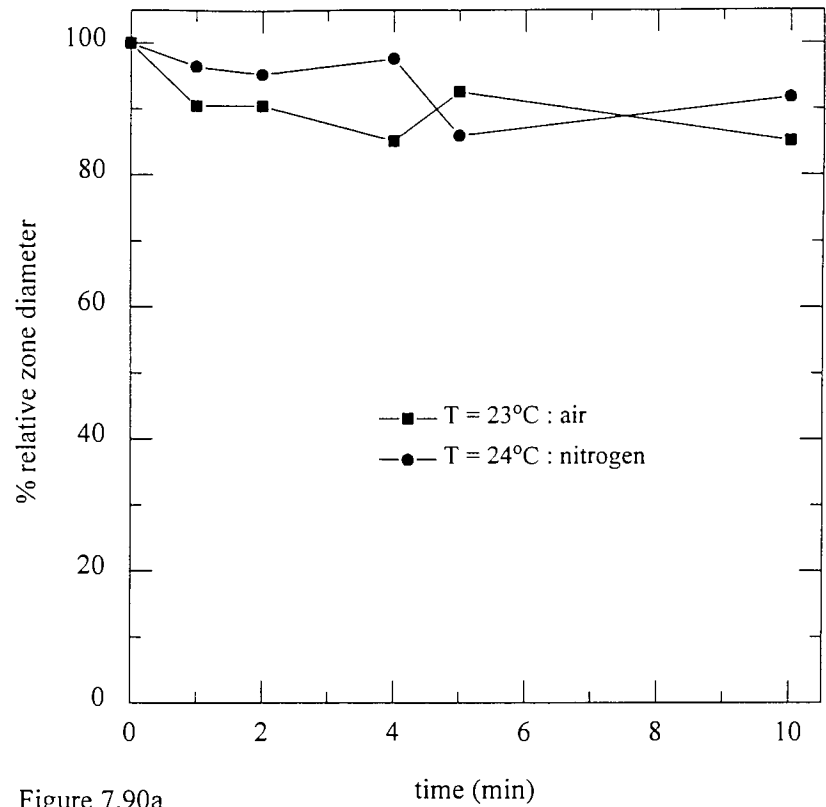


Figure 7.90a
Variation in zone diameter of 10% ampicillin with drying atmosphere at 23°C & 24°C gas temperature

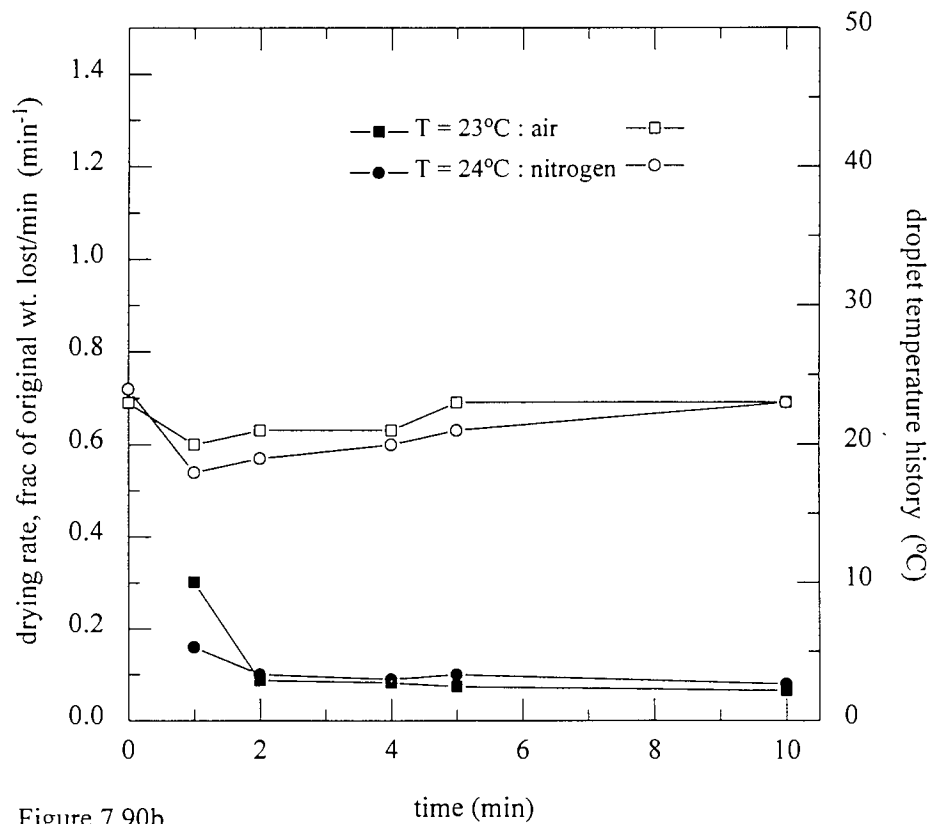


Figure 7.90b
The drying rate [solid symbols] and droplet temperature history [open symbols] for the 10% ampicillin solutions

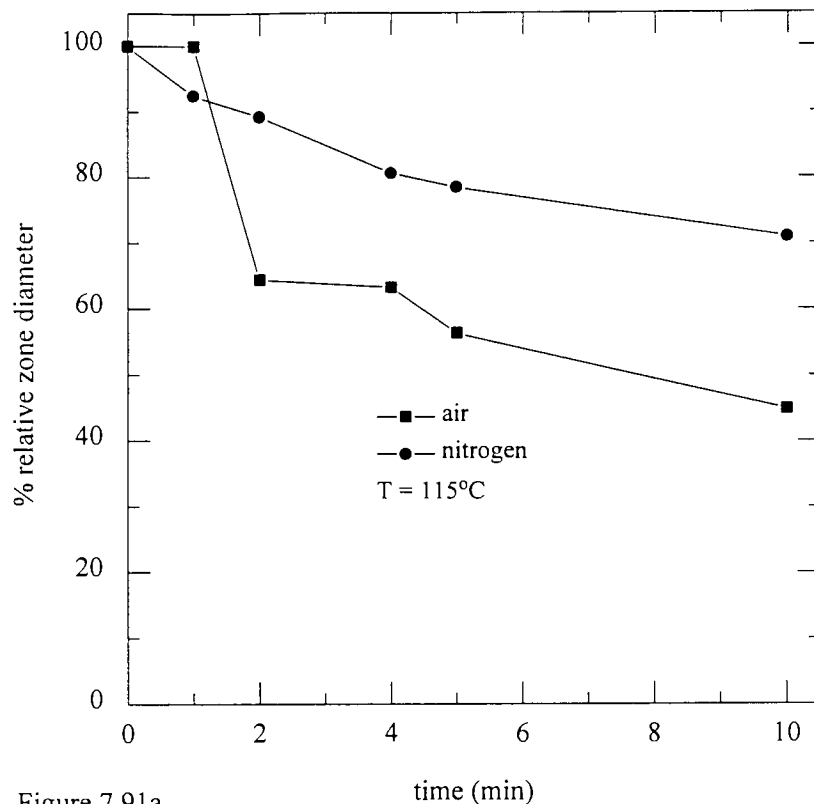


Figure 7.91a

Variation in zone diameter of 10% ampicillin with drying atmosphere at 115°C gas temperature

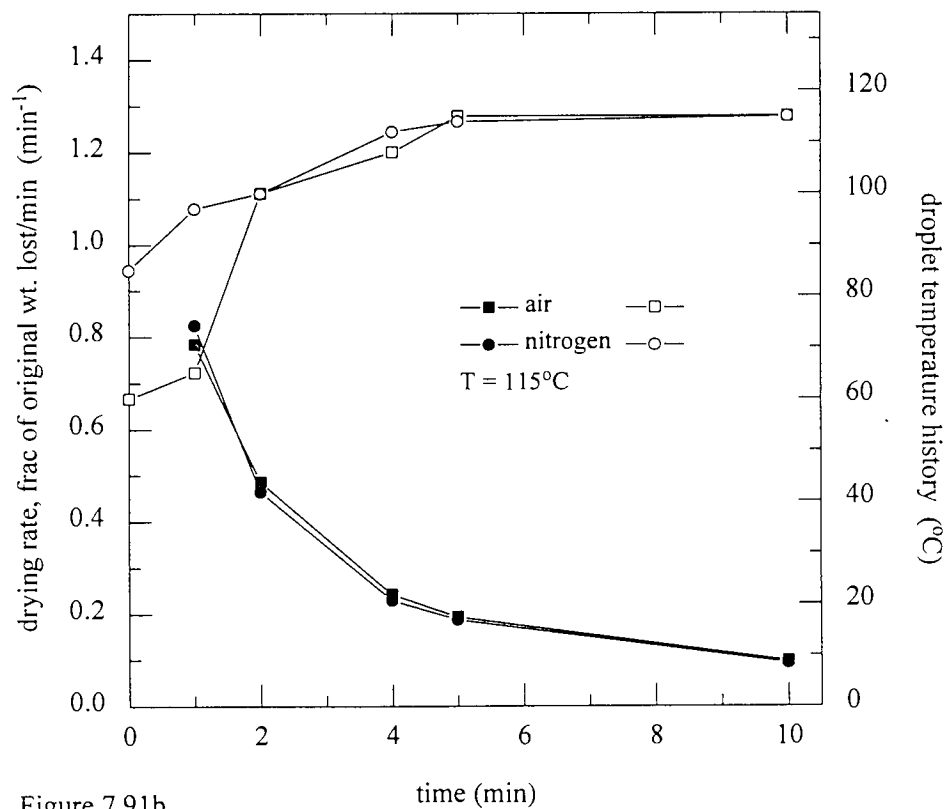


Figure 7.91b

The drying rate [solid symbols] and droplet temperature history [open symbols] for the 10% ampicillin solutions

7.2.3.2: Chloramphenicol

At ambient temperatures, there was a marked decrease in zone diameter for drops dried in air compared to nitrogen, viz. the zones decreased to 67% for the air but were unaffected in nitrogen, as illustrated in Figure 7.92a. Both the drying rates and the temperature histories behaved similarly for both the air and nitrogen (Figure 7.92b).

The decrease in zone diameter to 0% for the air dried droplet compared to only 95% for the nitrogen dried droplets, shown in Figure 7.93a, may have resulted from dilution errors in the DST analysis or the incomplete collection of the dried droplets. Figure 7.93b, showing the drying rates and droplet temperature histories, illustrates the similar behaviour of the drying droplets under both atmospheres.

7.2.3.3: Streptomycin

A decrease in zone diameter was exhibited by the droplets of streptomycin dried in an air atmosphere (75%) compared to 85% with nitrogen (Figure 7.94a). Similar drying rates and droplet temperature histories were obtained in both atmospheres (Figure 7.94b). The greater reduction may have arisen through incomplete removal of the droplet which was still liquid.

This is consistent with the comparable decrease in zone diameters in both the air and nitrogen atmospheres to 90% (Figure 7.95a) at 115°C. Similar temperature histories and drying rates were also obtained (Figure 7.95b).

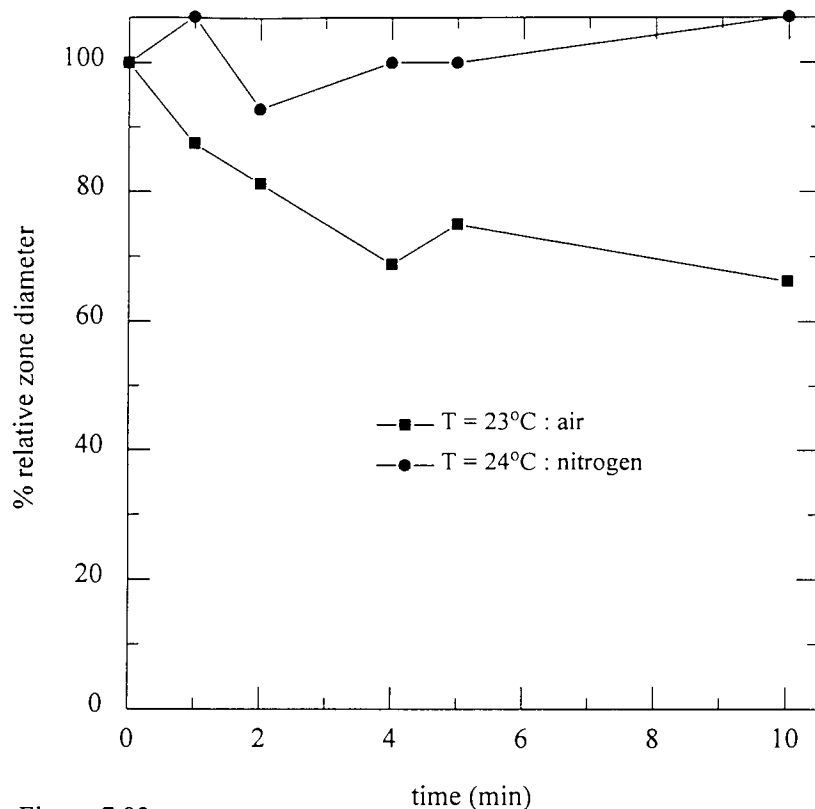


Figure 7.92a

Variation in zone diameter of 10% chloramphenicol with drying atmosphere at 23°C & 24°C gas temperature

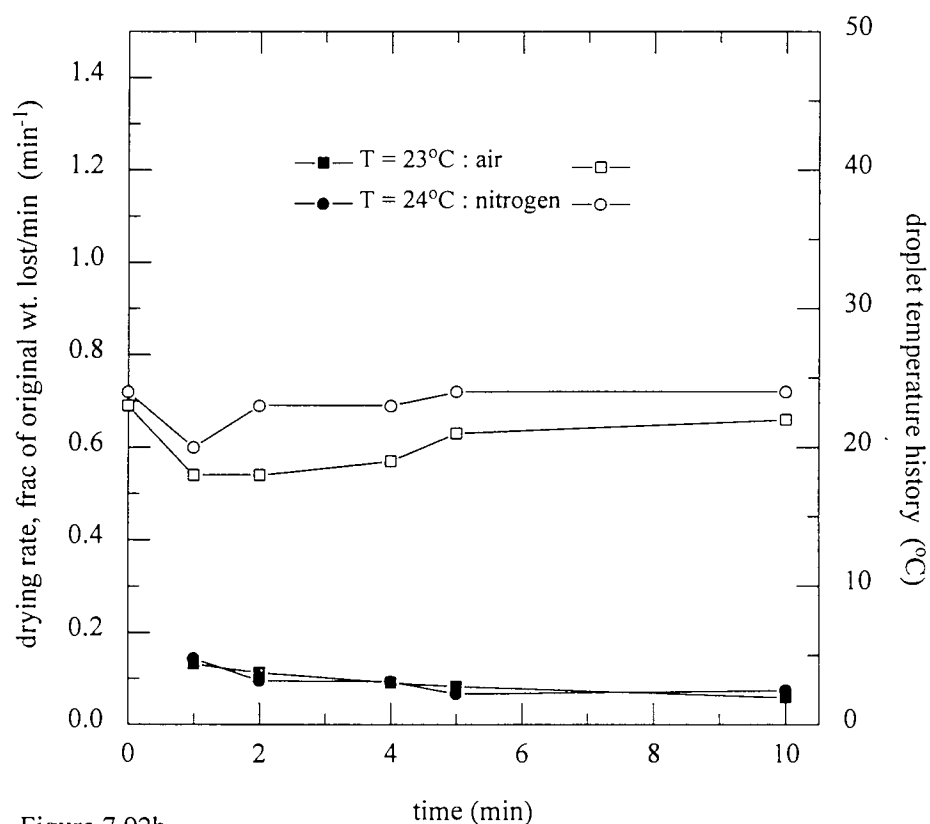


Figure 7.92b

The drying rate [solid symbols] and droplet temperature history [open symbols] for the chloramphenicol solutions

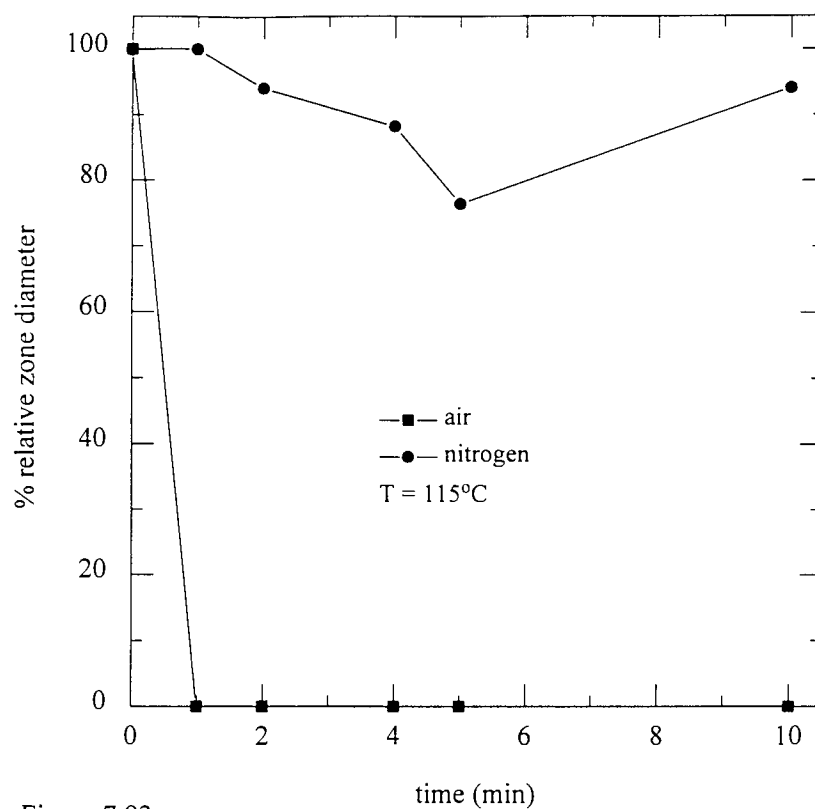


Figure 7.93a

Variation in zone diameter of 10% chloramphenicol with drying atmosphere at 115°C gas temperature

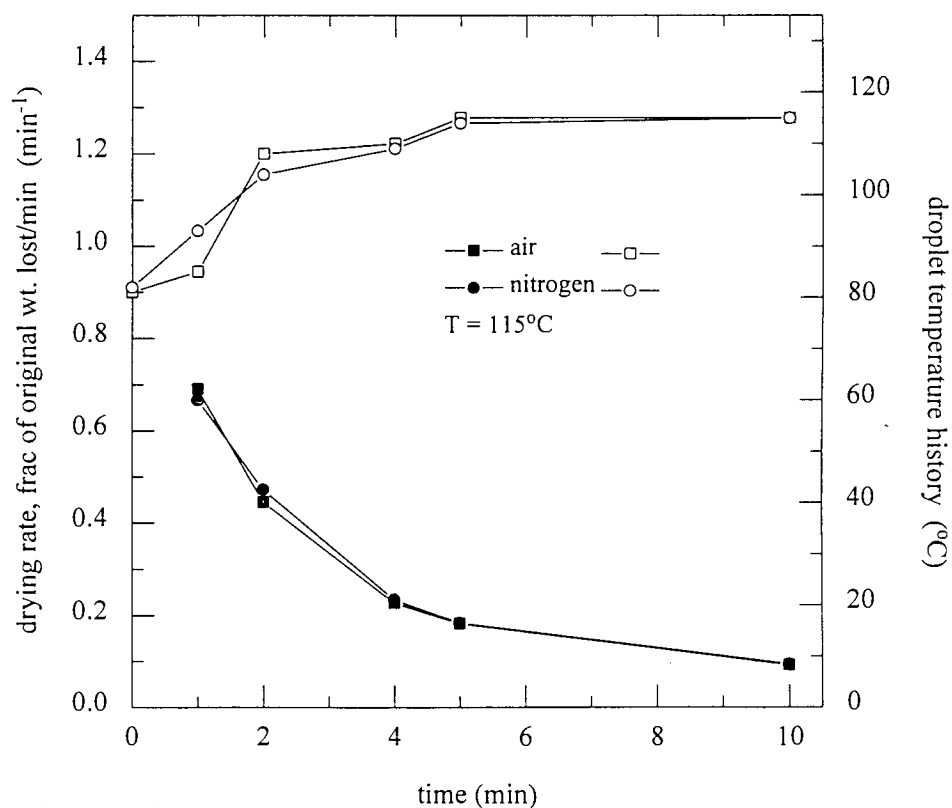


Figure 7.93b

The drying rate [solid symbols] and droplet temperature history [open symbols] for the chloramphenicol solutions

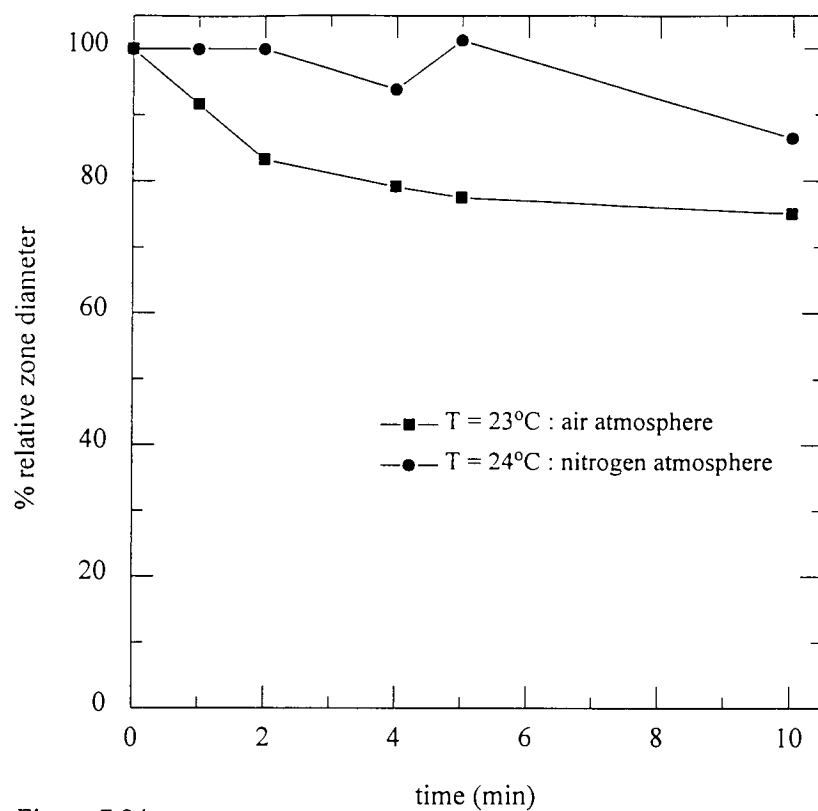


Figure 7.94a

Variation in zone diameter of 10% streptomycin with drying atmosphere at 23°C & 24°C gas temperature

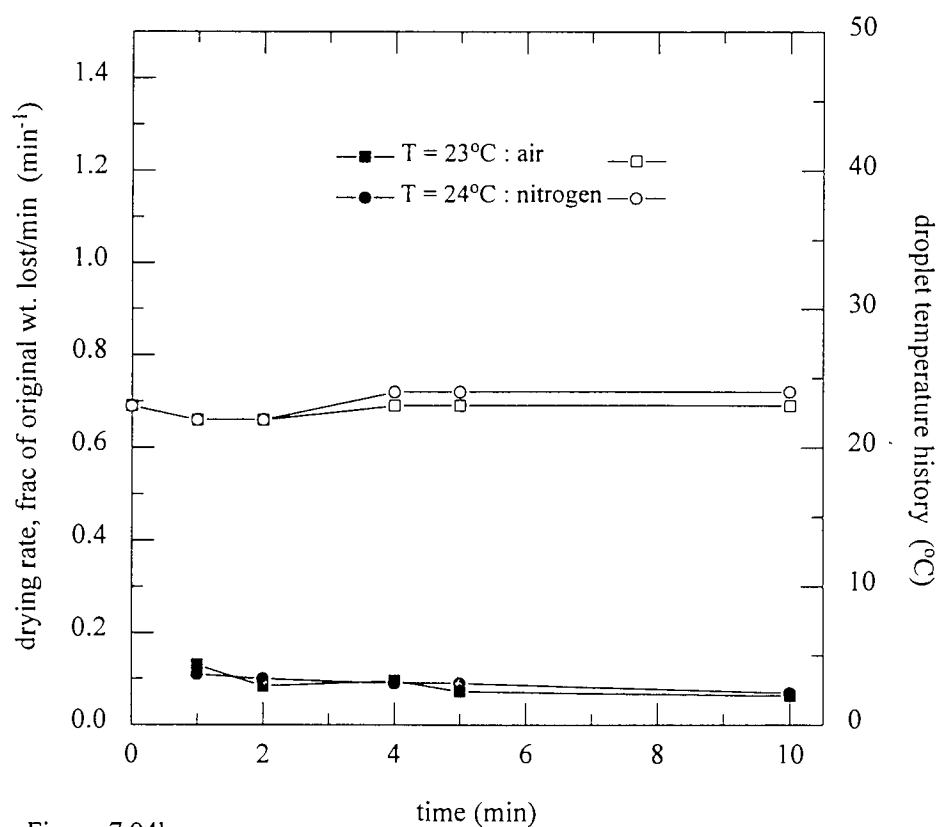


Figure 7.94b

The drying rate [solid symbols] and droplet temperature history [open symbols] for 10% streptomycin solutions

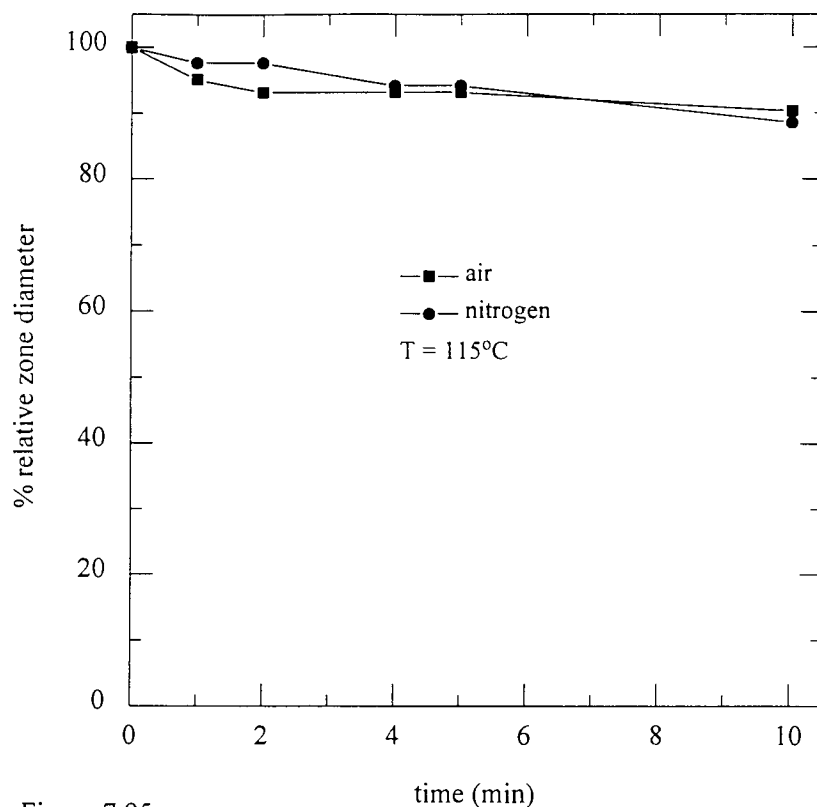


Figure 7.95a

Variation in zone diameter of 10% streptomycin with drying atmosphere at 115°C gas temperature

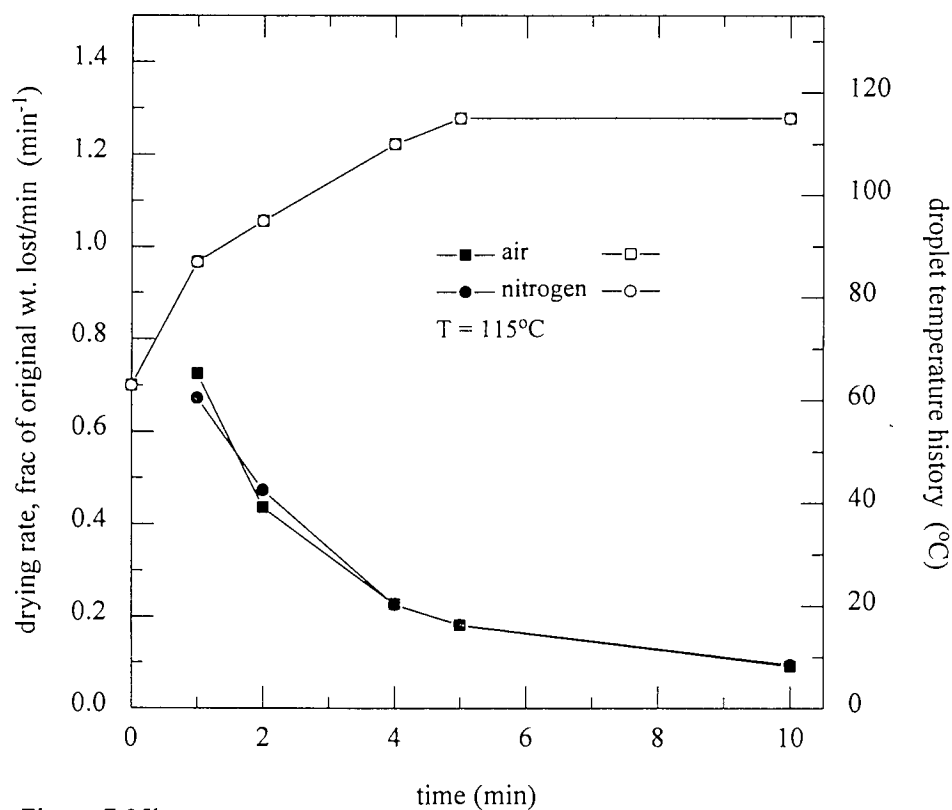


Figure 7.95b

The drying rate [solid symbols] and droplet temperature history [open symbols] for the streptomycin solutions

7.2.3.4: Tetracycline

Figure 7.96a shows the effect of drying in air and nitrogen at ambient temperature; there was a decrease in zone diameter for the air dried droplets to 78% compared to 95% for the nitrogen. The drying rates and droplet temperature histories obtained were similar (Figure 7.96b).

At 115°C there was no difference in zone diameters for either drying atmosphere as shown in Figure 7.97a. The drying rates and droplet temperature histories were similar except for the lower initial temperature for the air dried droplets which showed a rapid increase in droplet temperature (Figure 7.97b).

These results suggest that the apparent decrease in zone diameter at 23°C may have been attributable to difficulty in ensuring complete removal of droplets off the end of the thermocouple.

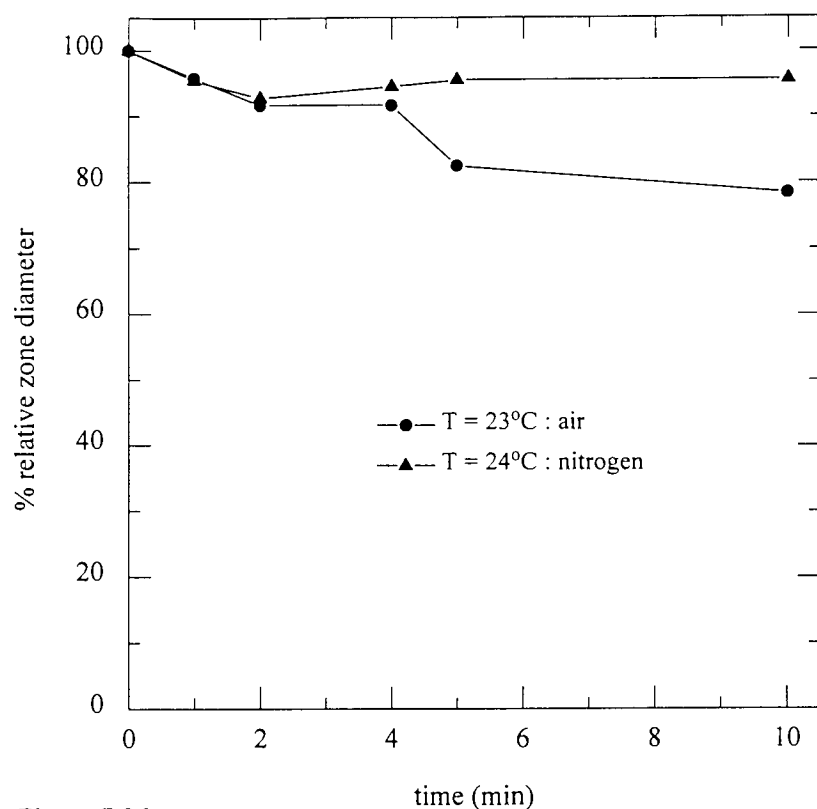


Figure 7.96a

Variation in zone diameter of 20% tetracycline with drying atmosphere at 23°C & 24°C gas temperature

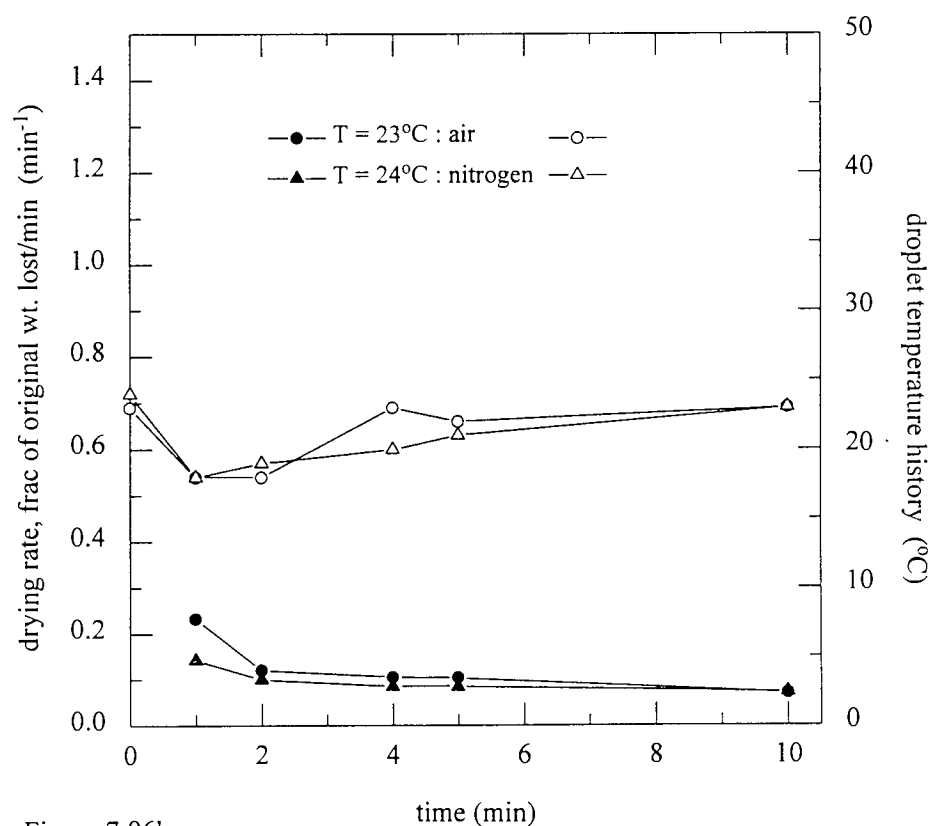


Figure 7.96b

The drying rate [solid symbols] and droplet temperature history [open symbols] for 20% tetracycline solutions

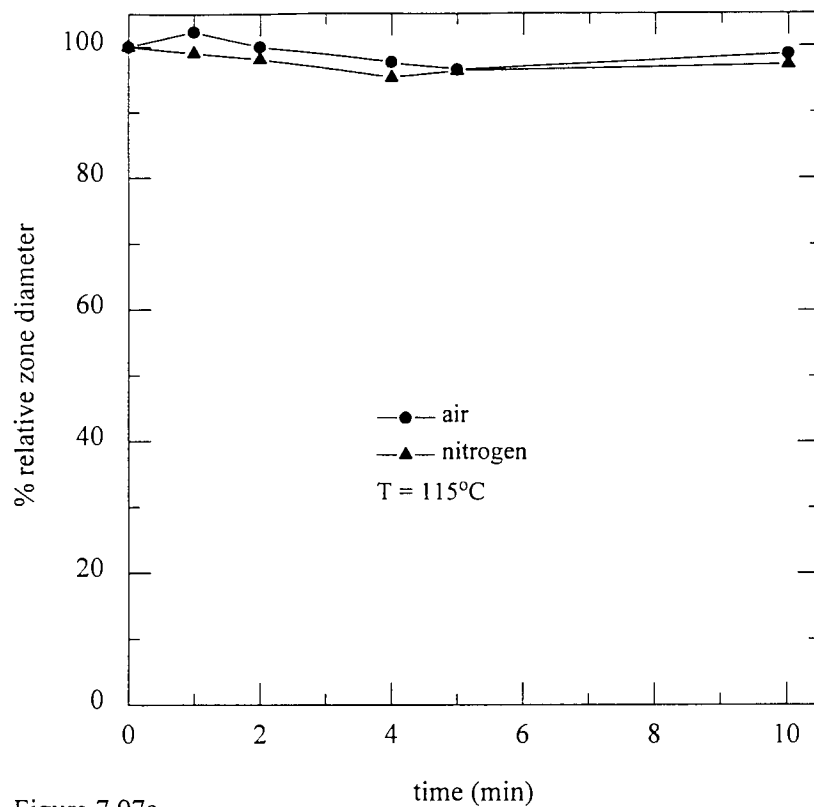


Figure 7.97a

Variation in zone diameter of 20% tetracycline with drying atmosphere at 115°C gas temperature

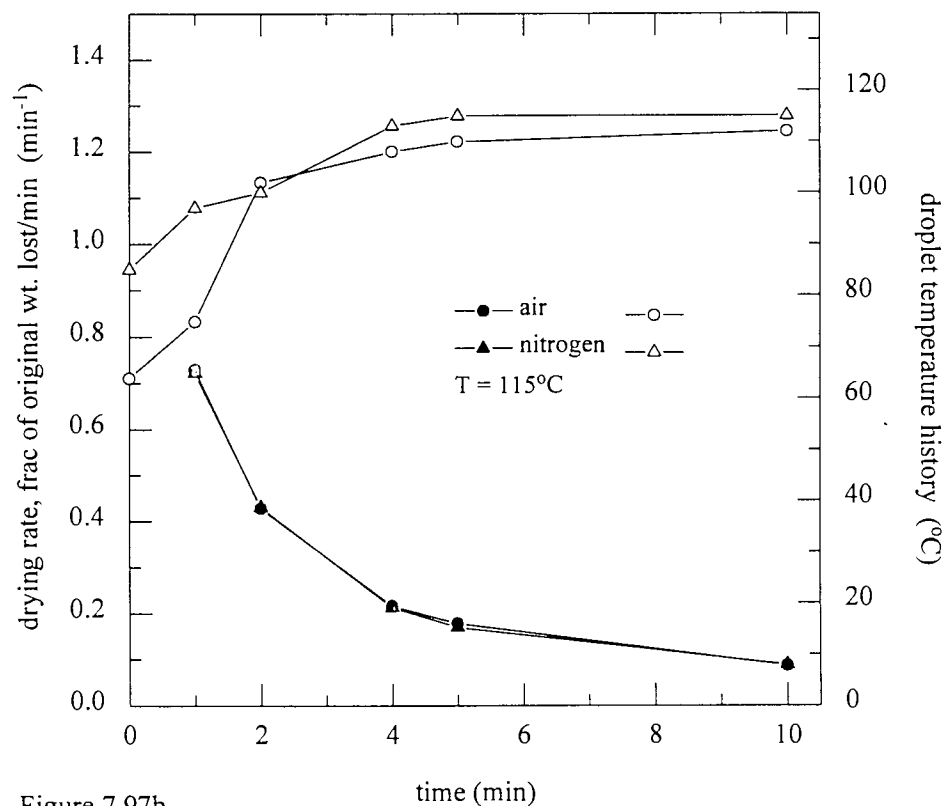


Figure 7.97b

The drying rate [solid symbols] and droplet temperature history [open symbols] for 20% tetracycline solutions

7.3: Enzymes

Because of the constraints of time only two enzymes were chosen in this study, viz. dextran sucrose and invertase, to evaluate the effect of temperature (and drying time) upon enzyme activity. The droplets were pipetted onto the end of the rotating thermocouple, removed after the appropriate drying time and assayed for residual activity (the method of analysis is detailed in Chapter 6).

7.3.1: Dextran sucrose

The enzyme dextran sucrose is very heat-sensitive and has an optimum working temperature of 25°C. The residual enzyme activities are shown in Figure 7.98a and the drying rates and temperature histories in Figure 7.98b.

At an air temperature of 23°C, there was an initial decrease in activity to almost 85% within the first four minutes of drying. In the next minute there was a massive decrease in activity to < 5% at $t = 5$ minutes followed by the activity reaching 0% at $t = 10$ minutes. The droplet temperature at 23°C remained almost constant at the wet bulb temperature from the onset; the drying rate exhibited one falling rate period.

The residual enzyme activity decreased to 15% with air temperature of 65°C before decreasing to 0% by $t = 10$ minutes. This correlated well with the drying rate obtained; the droplet temperature history increased rapidly to the air temperature which resulted in the denaturation of the enzyme.

The enzyme was observed, as expected, to be denatured at the high drying temperatures of 95°C and 115°C. This is evident from the fall in residual activity trends to 0% during the first minute of drying at both temperatures. The drying rates were faster, with that at 115°C being more rapid of the two.

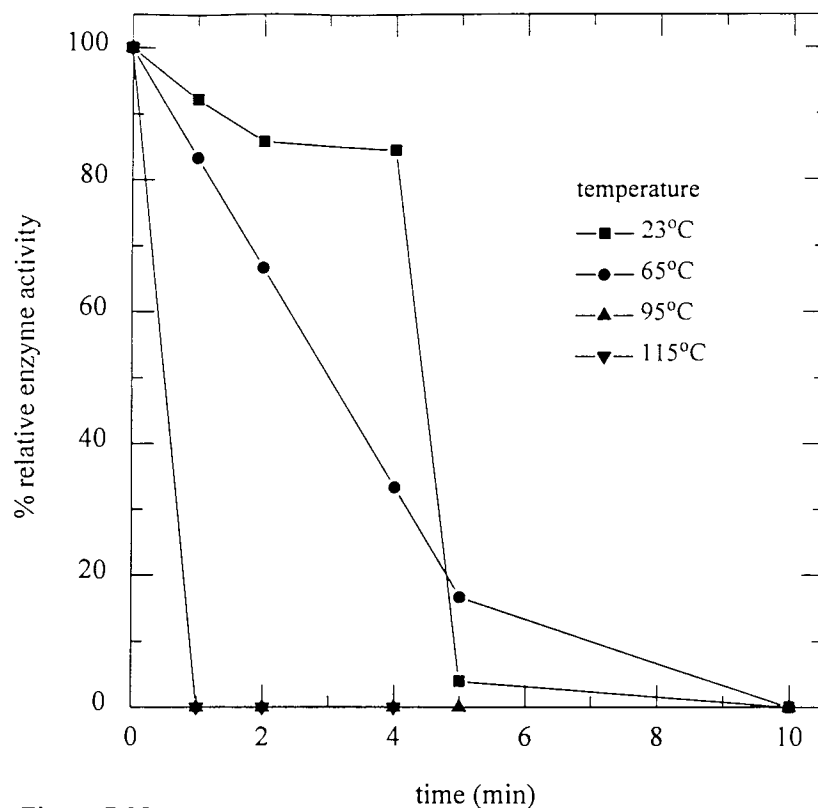


Figure 7.98a

The effect of temperature on the enzyme activity of dextran sucrose solutions

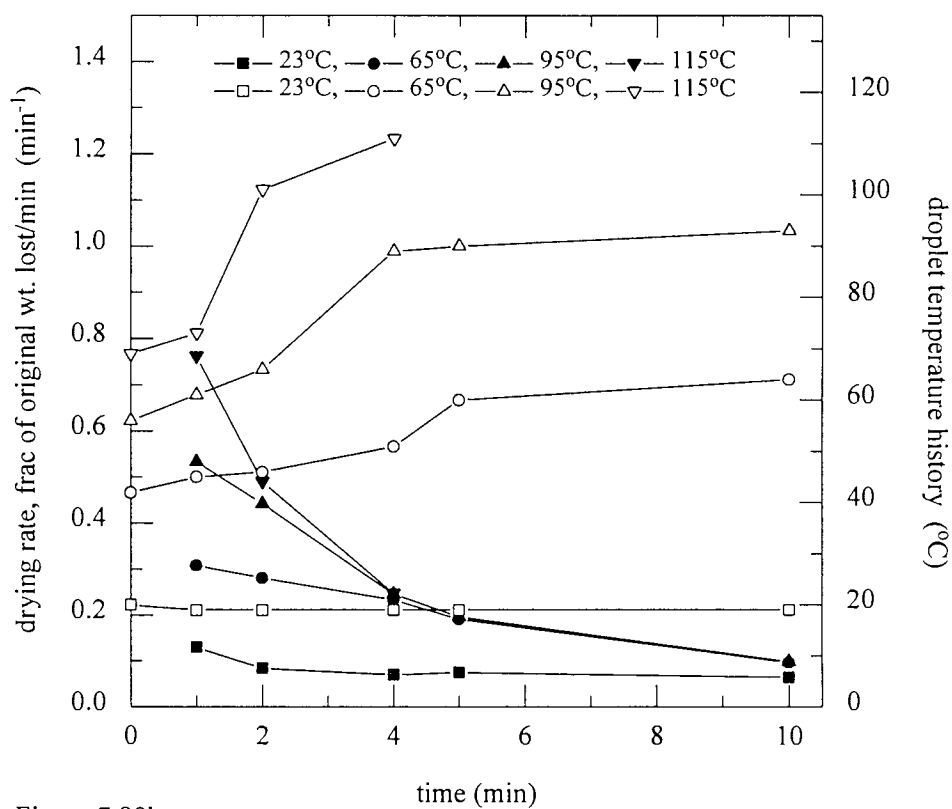


Figure 7.98b

The drying rate [solid symbols] and droplet temperature history [open symbols] for dextran sucrose solutions

Both droplet temperature histories show a rapid increase to the air temperature within the first five minutes, the probable cause of the enzyme denaturation.

7.3.2: Invertase

Invertase is a heat-tolerant enzyme which remains operational at temperatures approaching 60°C. The residual enzyme activities are illustrated in Figure 7.99a and the droplet temperature histories and drying rates are shown in Figure 7.99b.

At 23°C and 65°C the enzyme activity showed little difference, i.e. the residual activity fell to almost 98% and 95% for 23°C and 65°C respectively. At 65°C, the droplet temperature gradually increased to the air temperature whereas it remained at the wet bulb temperature at 23°C. There was a difference in drying rates, with that at 65°C having a more rapid first falling rate period.

The increase in temperature to 95°C and 115°C produced a similar decrease in the residual activity; the decrease at 115°C was always greater than at 95°C, as demonstrated by the activity at $t = 2$ minutes which showed 20% and 10% activity at 95°C and 115°C respectively. The drying rates, showing two falling rates, were similar with, as expected, that at 115°C being more rapid. The increase in droplet temperatures was also more rapid at 115°C, with the air temperatures being attained within the first three minutes.

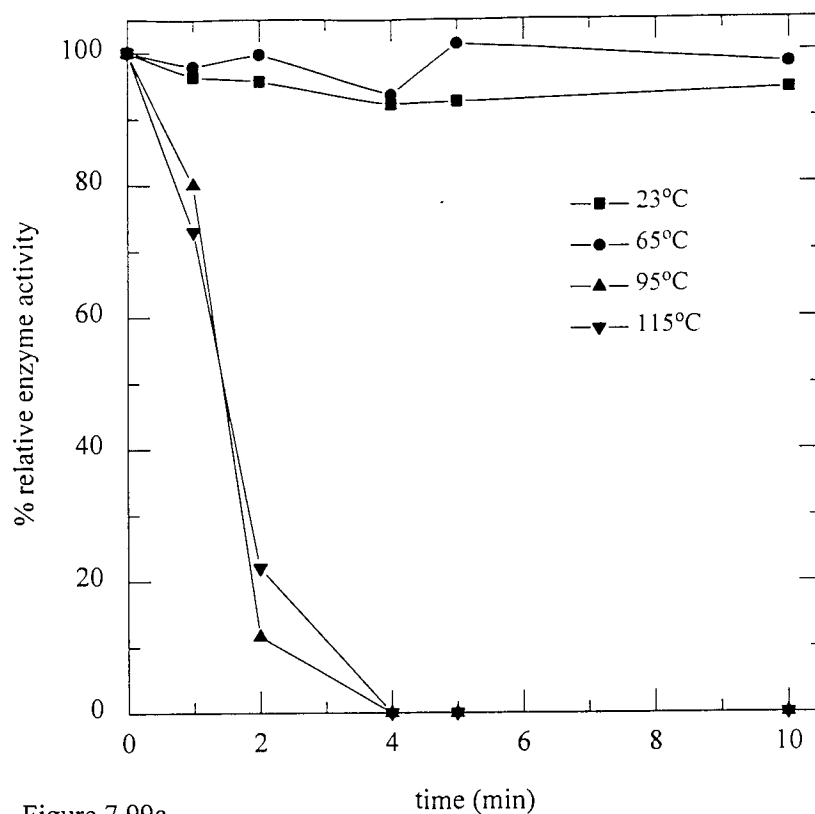


Figure 7.99a

The effect of temperature on the enzyme activity of invertase solutions

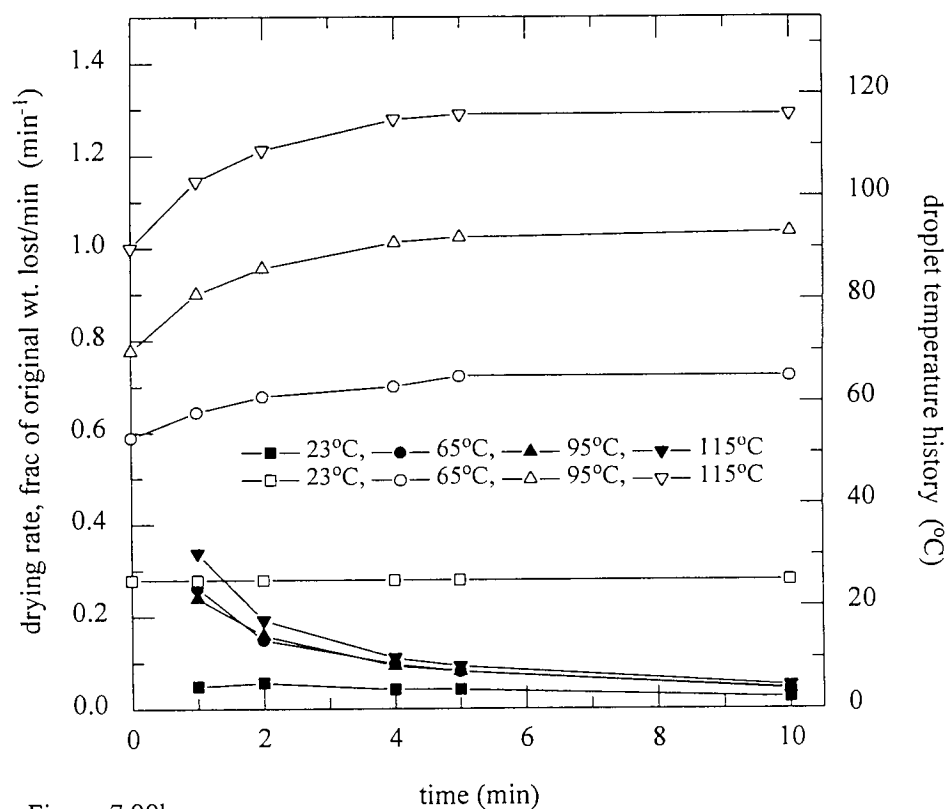


Figure 7.99b

The drying rate [solid symbols] and droplet temperature history [open symbols] for invertase solutions

7.4: Freeze drying

A limited number of experiments were conducted to ascertain the effectiveness of freeze drying for heat-sensitive materials. All the antibiotics were freeze dried and subsequently analysed for their efficacy. Each flavour encapsulant tested for its volatile retention capability during convective drying was also selected to undergo freeze drying to assess the enhancement of volatiles retention possible with freeze drying.

30µl aliquots of each sample tested was dispensed into a 0.5ml micro-centrifuge tube and freeze dried for appropriate periods of time before removal and subsequent analysis. Observation of the contents of the tubes during the freeze drying process showed that with the progression of the drying, the contents of each tube were deposited as a thin film on the walls. This had no apparent effect on the efficacy of the antibiotics, but proved detrimental to the volatiles retention capabilities of the various encapsulants tested as illustrated by the following results.

7.4.1: Antibiotics

Three concentrations of each antibiotic, viz. 10%, 20% and 40% w/w, were freeze dried. The resultant dry powder was reconstituted with distilled water and analysed using the DST methodology used with convective drying. The zone diameters were standardised to be 100% for the untreated samples of each concentration of antibiotic, i.e. an untreated sample always had a zone diameter of 100% regardless of concentration.

7.4.1.1: Ampicillin

Figure 7.100 shows that the zone diameters remained at approximately 100% for all concentrations of ampicillin, although the 10% suspension showed some decrease.

7.4.1.2: Chloramphenicol

The results shown in Figure 7.101 illustrate that the freeze drying resulted in no detrimental effect upon the efficacy of the chloramphenicol suspensions at all three concentrations.

7.4.1.3: Oxytetracycline

Freeze drying of oxytetracycline suspensions resulted in no significant differences between the zone diameters obtained by the DST analysis of the freeze dried drug, as illustrated in Figure 7.102.

7.4.1.4: Streptomycin

The results for streptomycin solution, shown in Figure 7.103, demonstrate a reduction of zone diameter to 90% for a 20% solution. This was not expected, and may have been due to the incomplete reconstitution of the dried drug.

7.4.1.5: Tetracycline

Figure 7.104 demonstrates no detrimental effect of freeze drying on tetracycline suspensions. There was a zone decrease at $t = 4$ minutes but this could be attributable to dilution errors.

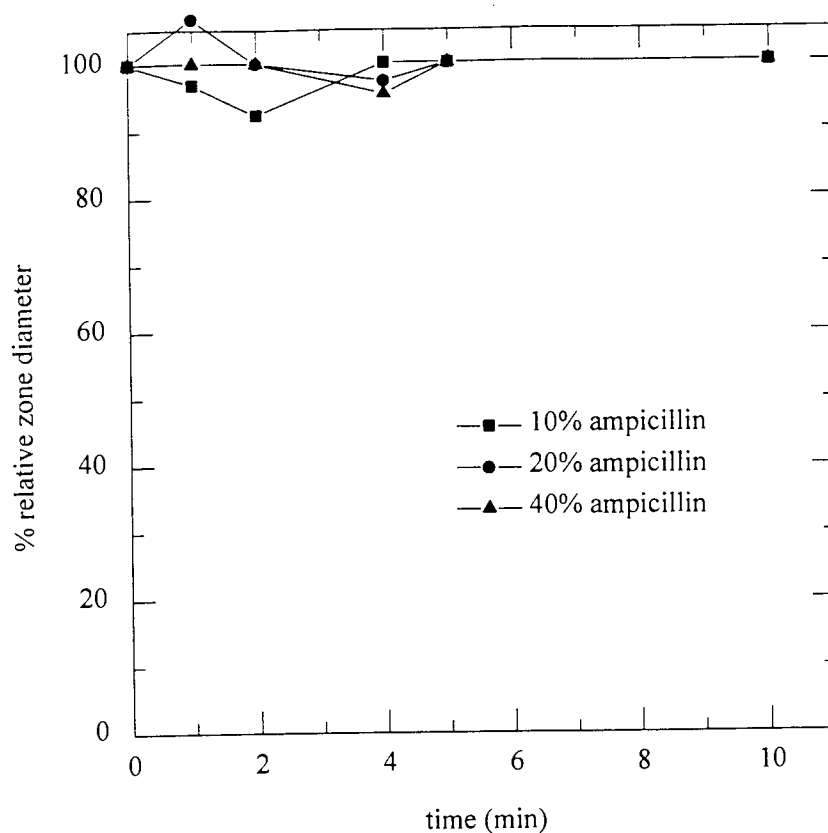


Figure 7.100

Variation in zone diameter with initial concentration of ampicillin

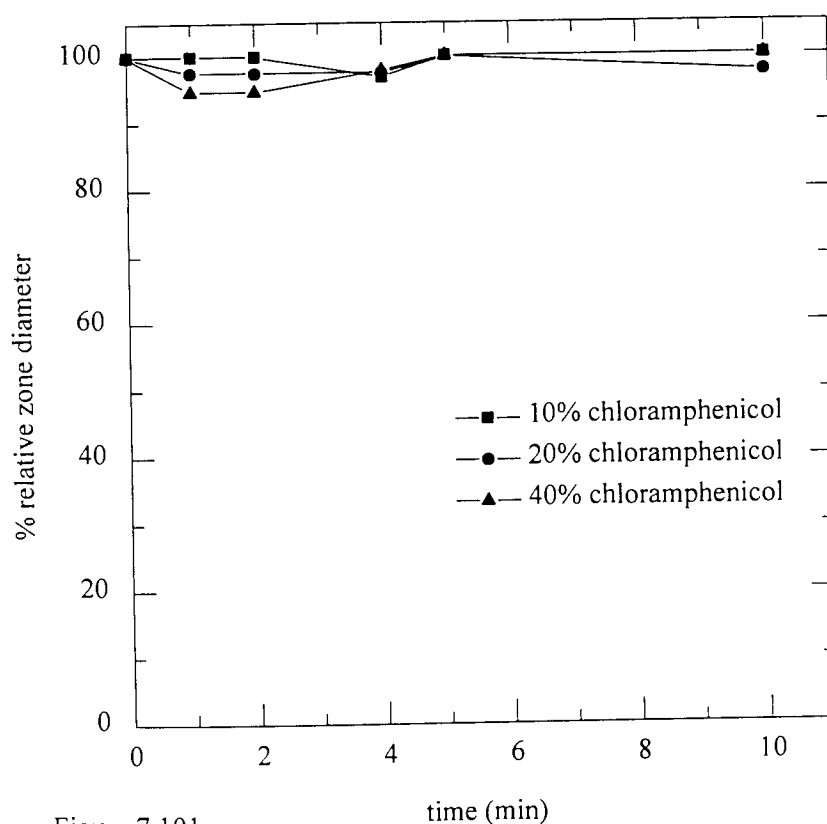


Figure 7.101

Variation in zone diameter with initial concentration of chloramphenicol

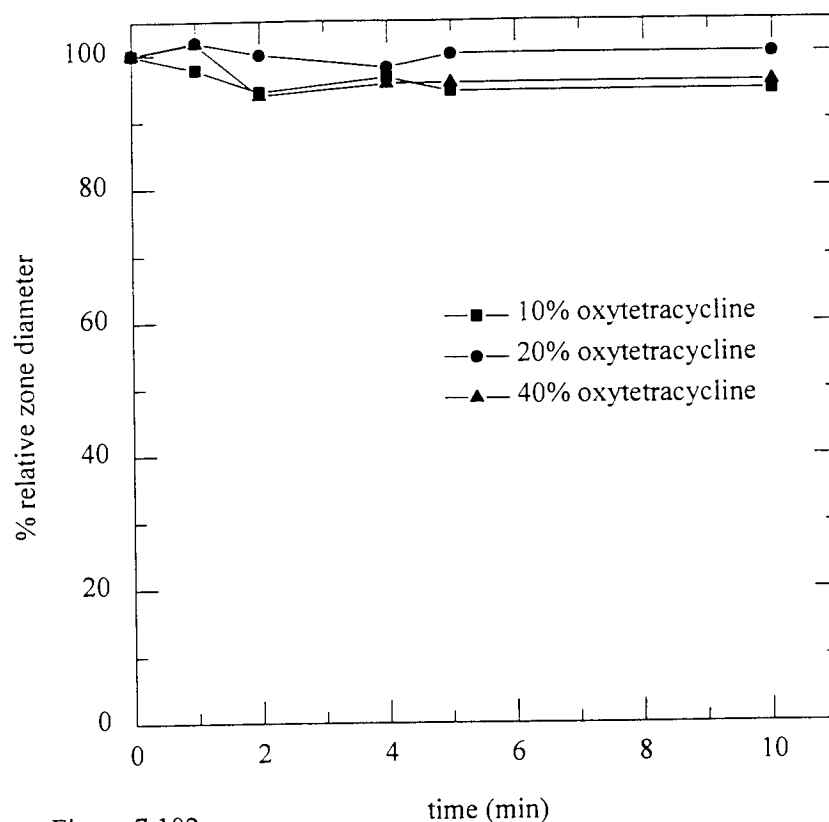


Figure 7.102
Variation in zone diameter with initial concentration of oxytetracycline

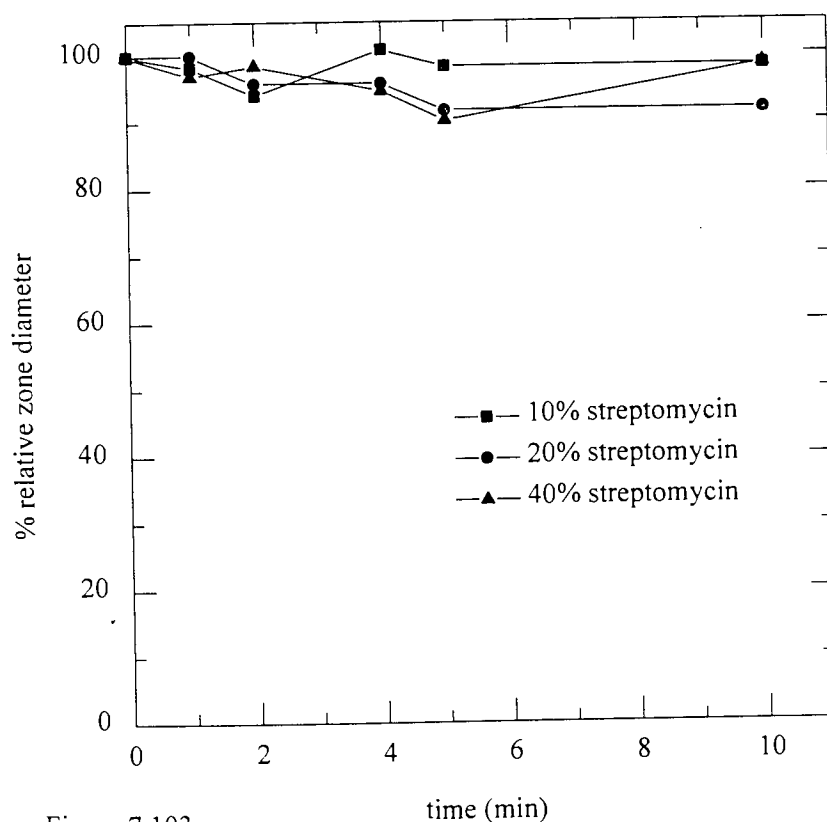


Figure 7.103
Variation in zone diameter with initial concentration of streptomycin

7.4.2: Flavour encapsulants

A 20% concentration suspension / solution was freeze dried as being representative of each encapsulant. As with the convective drying, a $t_{1/2}$ value was allocated to the time at which the retention of ethanol had reduced to 50% of its initial value.

30 μ l aliquots of each encapsulant were dispensed into 0.5ml micro-centrifuge tubes and subjected to freeze drying for appropriate periods of time. After removal from the drying chamber of the freeze dryer, the encapsulants were rehydrated to their original weights with distilled water. The tubes were left to stand overnight in a refrigerator before centrifugation (to separate the supernatant from the particulate material) and subsequent GLC analysis (as detailed in Chapter 6).

Results for ethanol retention, shown in Figures 7.105, 7.106, and 7.107, illustrate that the expected enhancement of ethanol retention with freeze drying did not occur. Figure 7.105 shows that the final retention for both rice and wheat starch decreased to < 5% within the first two minutes and remained at that level for the duration of the drying, with a $t_{1/2} \cong 30$ seconds. The dextrin solution had a longer $t_{1/2}$ ($\cong 1$ minute), and the ethanol content decreased less rapidly after the initial rapid decrease within the first minute; the final ethanol content was 5%.

Figure 7.106, shows the variation of ethanol content with the progression of freeze drying of skim milk and coffee solutions. The skim milk solution had lost almost 95% of its ethanol content within the first minute, with $t_{1/2} \leq 30$ seconds. Conversely, the coffee solution had enhanced ethanol retention; after the initial rapid fall to 62% within the first minute of drying, the ethanol content remained constant for the next three minutes. There was another rapid fall in the fifth minute to 15% followed by another gradual decrease to almost 12% (i.e. in the last five minutes of drying, the ethanol content decreased by

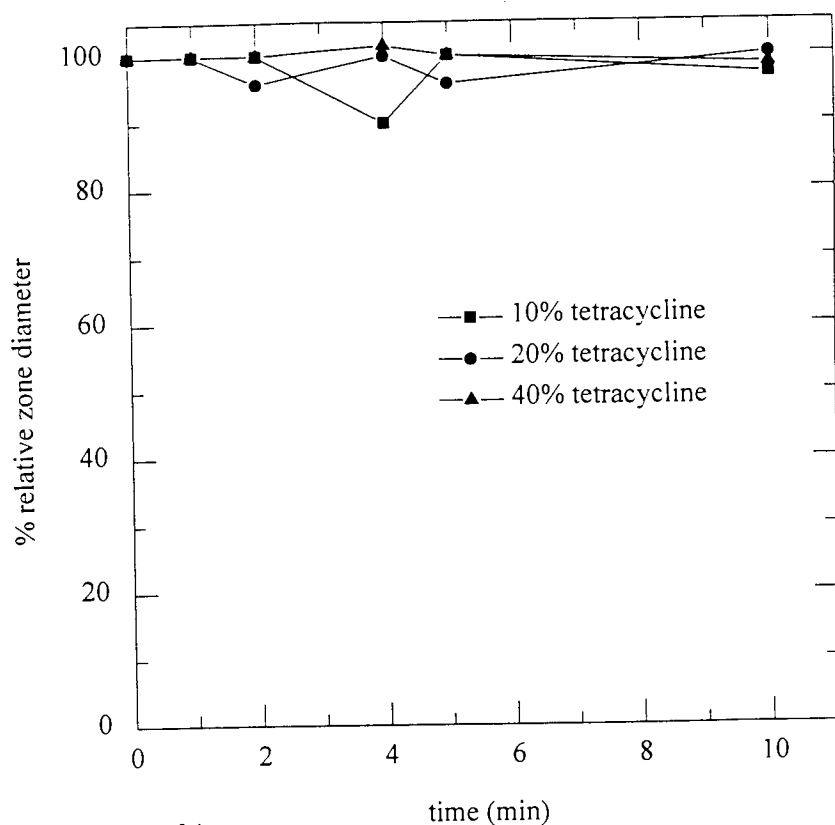


Figure 7.104

Variation in zone diameter with initial concentration of tetracycline

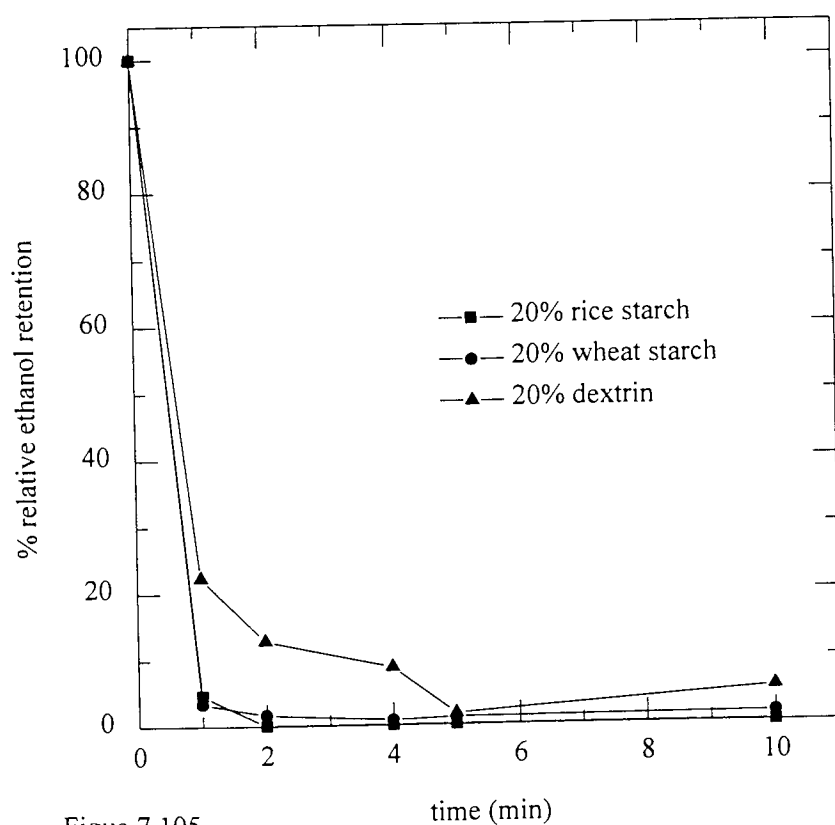


Figure 7.105

The effect of freeze drying on the retention of ethanol in various solutions

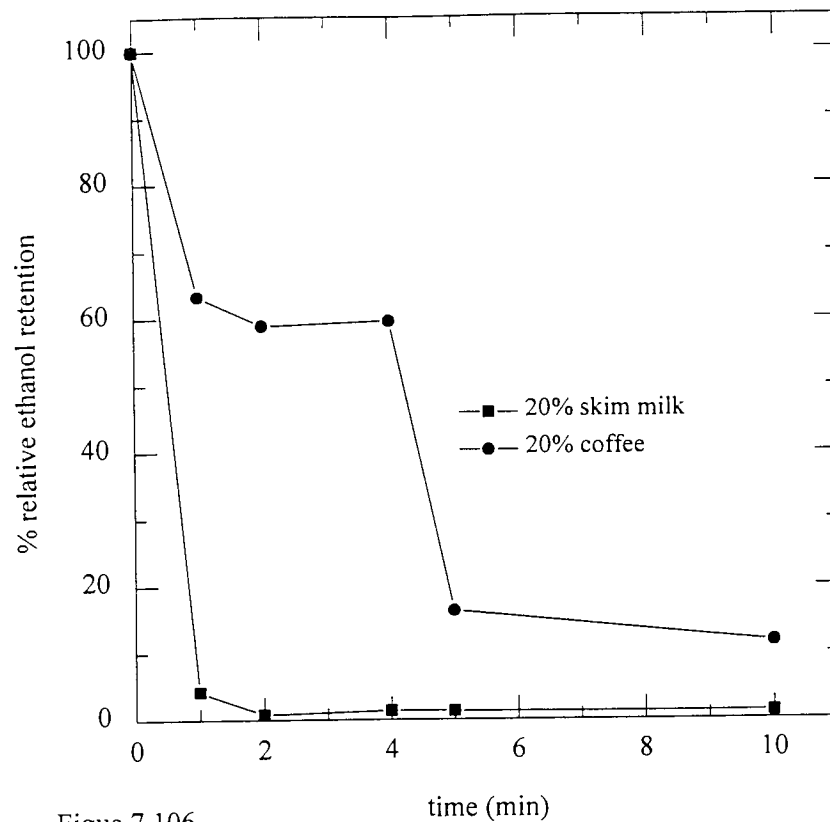


Figure 7.106
The effect of freeze drying on the retention of ethanol in various solutions

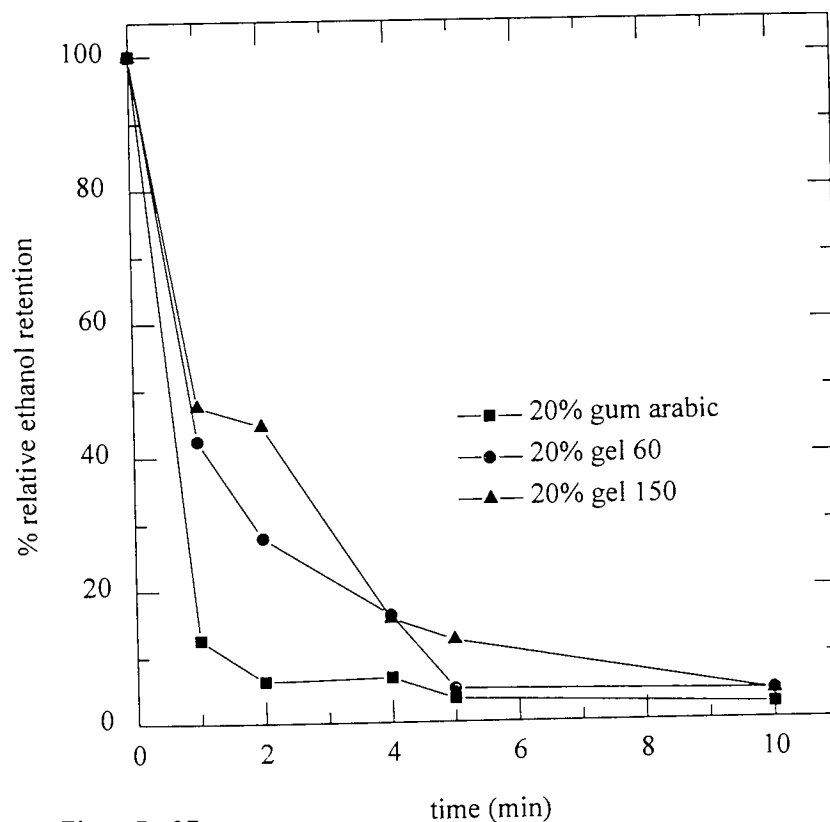


Figure 7.107
The effect of freeze drying on the retention of ethanol in various solutions

only 3%). The $t_{1/2} \cong 4.5$ minutes, and the final ethanol content was 12%. Thus the coffee solution had a more retentive effect than the skim milk.

Figure 7.107, showing the retention of ethanol in gelatine 60 and 150 Bloom and gum arabic gels, demonstrates a reduction in the ethanol retention. The gum arabic appeared to be the poorest encapsulant in this group of materials with almost 87% ethanol loss occurring within the first minute of drying with $t_{1/2} < 1$ minute. The final ethanol content for freeze dried gum arabic was $< 5\%$. There was an initial rapid decrease in ethanol content, to 42% and 48% respectively, with both gelatine 60 Bloom and 150 Bloom in the first minute of drying. In the next minute there was a decrease in ethanol to 38% with gelatine 60 Bloom but with gelatine 150 Bloom it was only to 45% (i.e. a fall of 3%). This could be attributed to the greater gel strength of the gelatine 150 Bloom compared with 60 Bloom. The following three minutes of drying produced a more rapid fall for the 150 Bloom gelatine compared to the 60 Bloom, possibly due to the breakdown of the structure of the gelatine 150 Bloom allowing the ethanol to escape. The ethanol content for both 60 and 150 Bloom gelatine gels was concurrent at 15%, after which each gradually fell to the final value of approximately 5%.

40% solutions of dextrin, rice starch and gum arabic were also freeze dried, and the resultant ethanol retentions are shown in Figure 7.108. All three materials had $t_{1/2} < 1$ minute, and had lost $> 60\%$ of their initial ethanol content within the first minute. The rice starch lost almost 97% of the ethanol during the first two minutes, and retained only 1% of the ethanol at $t = 4$ minutes; this final retention value remained constant for the duration of the drying. The gum arabic solution experienced a rapid initial loss of ethanol of almost 75% during the first minute. There was only a 15% ethanol loss in the remaining time of drying resulting in a final ethanol content of 10%. The ethanol content of the dextrin solution decreased rapidly to almost 30% within the first minute, but then only decreased a further 10% in the next nine minutes of drying. The final retention was almost 20% after 10 minutes.

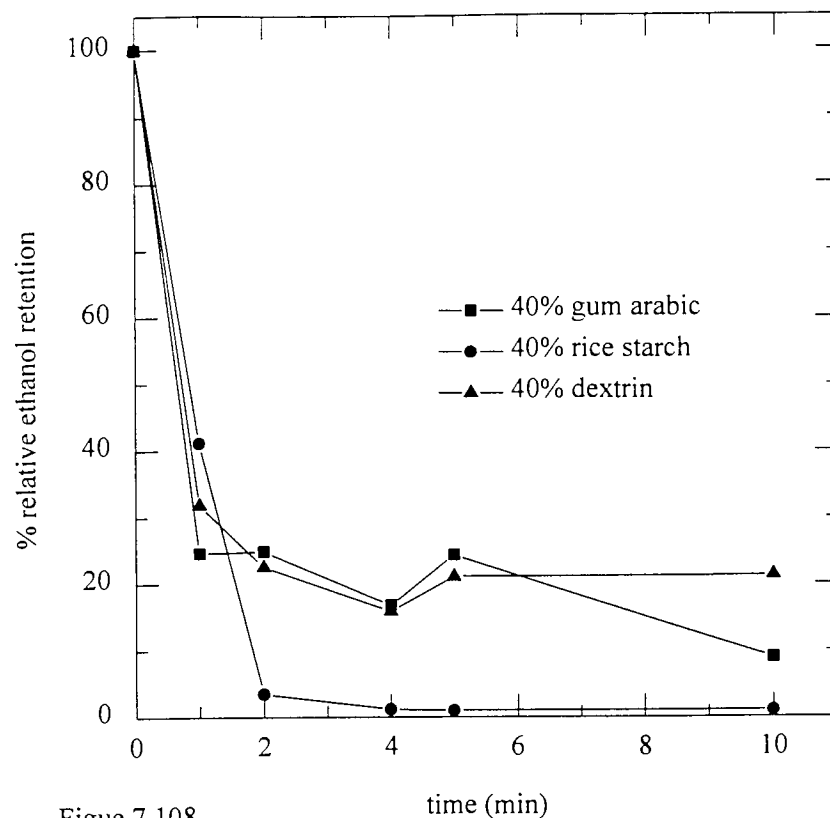


Figure 7.108
The effect of freeze drying on the retention of ethanol in various solutions

7.5: FTIR spectroscopy results

Droplets of the antibiotics were dried at 115°C and stored in a dessicator for several weeks to remove any remaining moisture which would have a peak-masking effect during the analysis, as water absorbs IR radiation. Untreated antibiotic powder was used as the reference for each; 10% and 20% concentrations of each antibiotic were dried for subsequent FTIR analysis. The resultant frequency spectra for the various antibiotic concentrations are shown in Figures 7.109 - 7.113.

Figure 7.109 shows the frequency spectrum for ampicillin. It is evident that some modification occurred to the 10% and 20% suspensions compared to the untreated sample. The peaks between the 3500 cm^{-1} and 3000 cm^{-1} reduced or even disappeared. Similar events occurred between 2500 cm^{-1} and 800 cm^{-1} .

The IR spectra for chloramphenicol, oxytetracycline and tetracycline, shown in Figures 7.110, 7.111, and 7.113 respectively, show that these antibiotics were unaffected by the thermal treatment during the drying process.

Figure 7.112, shows the IR spectrum of streptomycin. There were some changes to the molecule in the 10% solution. as demonstrated by the reduction in the duration of the valleys located at 1700 cm^{-1} and between 1200 cm^{-1} and 1000 cm^{-1} .

These IR spectra confirmed that the antibiotics used were all heat-stable with the exception of ampicillin.

Figure 7.109 FTIR spectra for ampicillin dried at 115°C.

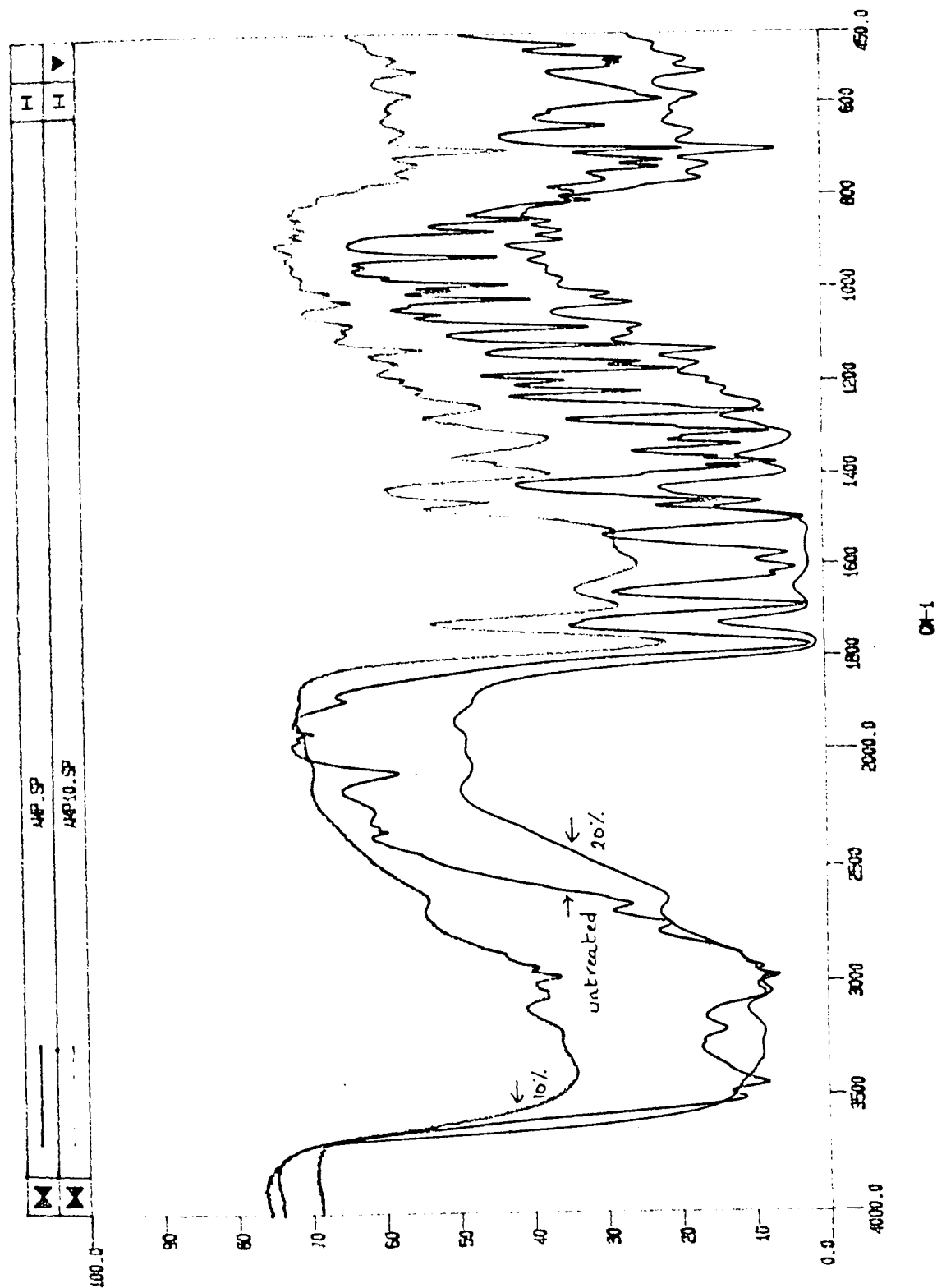


Figure 7.110 FTIR spectra for chloramphenicol dried at 115°C.

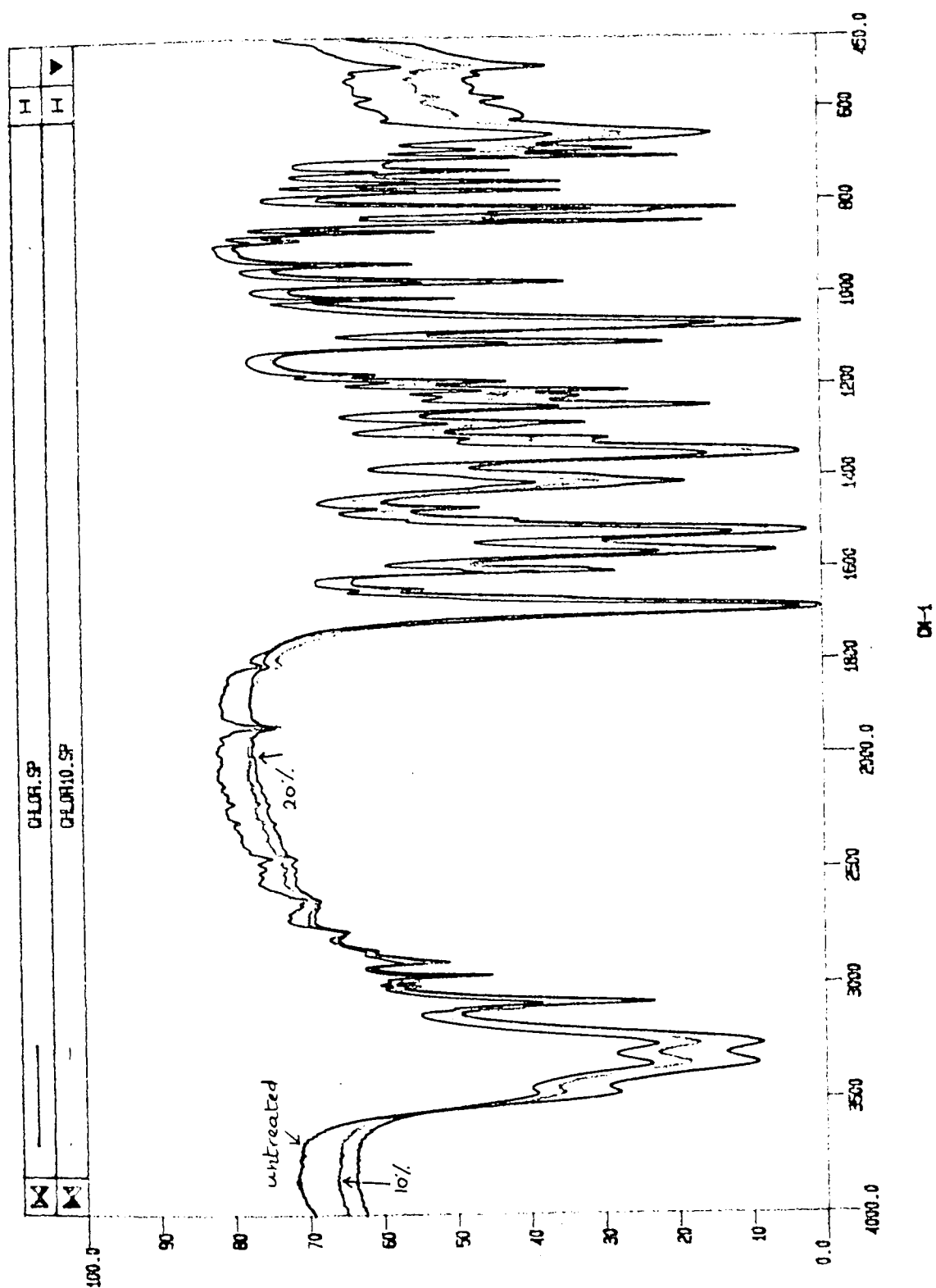


Figure 7.111 FTIR spectra for oxytetracycline dried at 115°C.

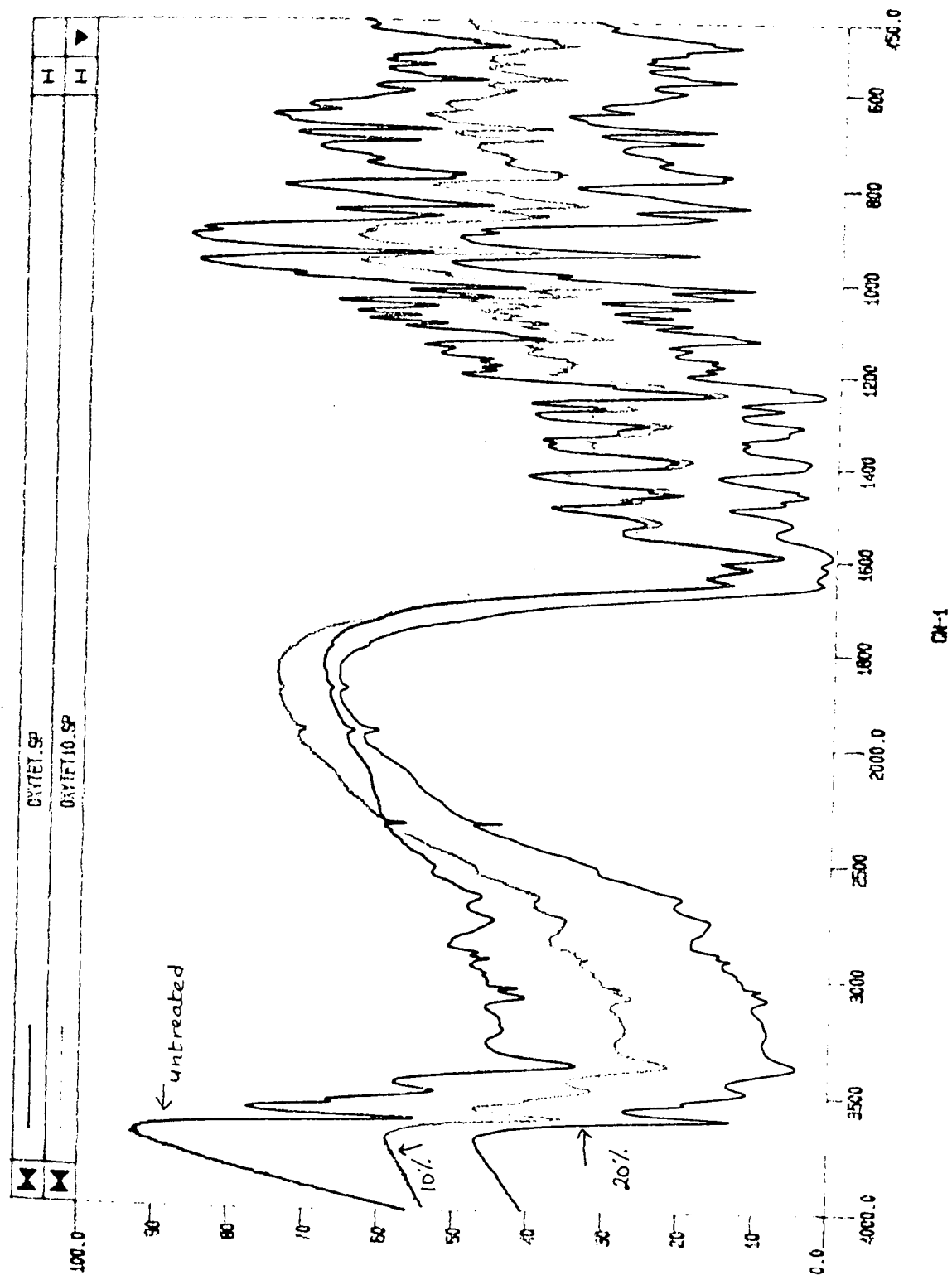


Figure 7.112 FTIR spectra for streptomycin dried at 115°C.

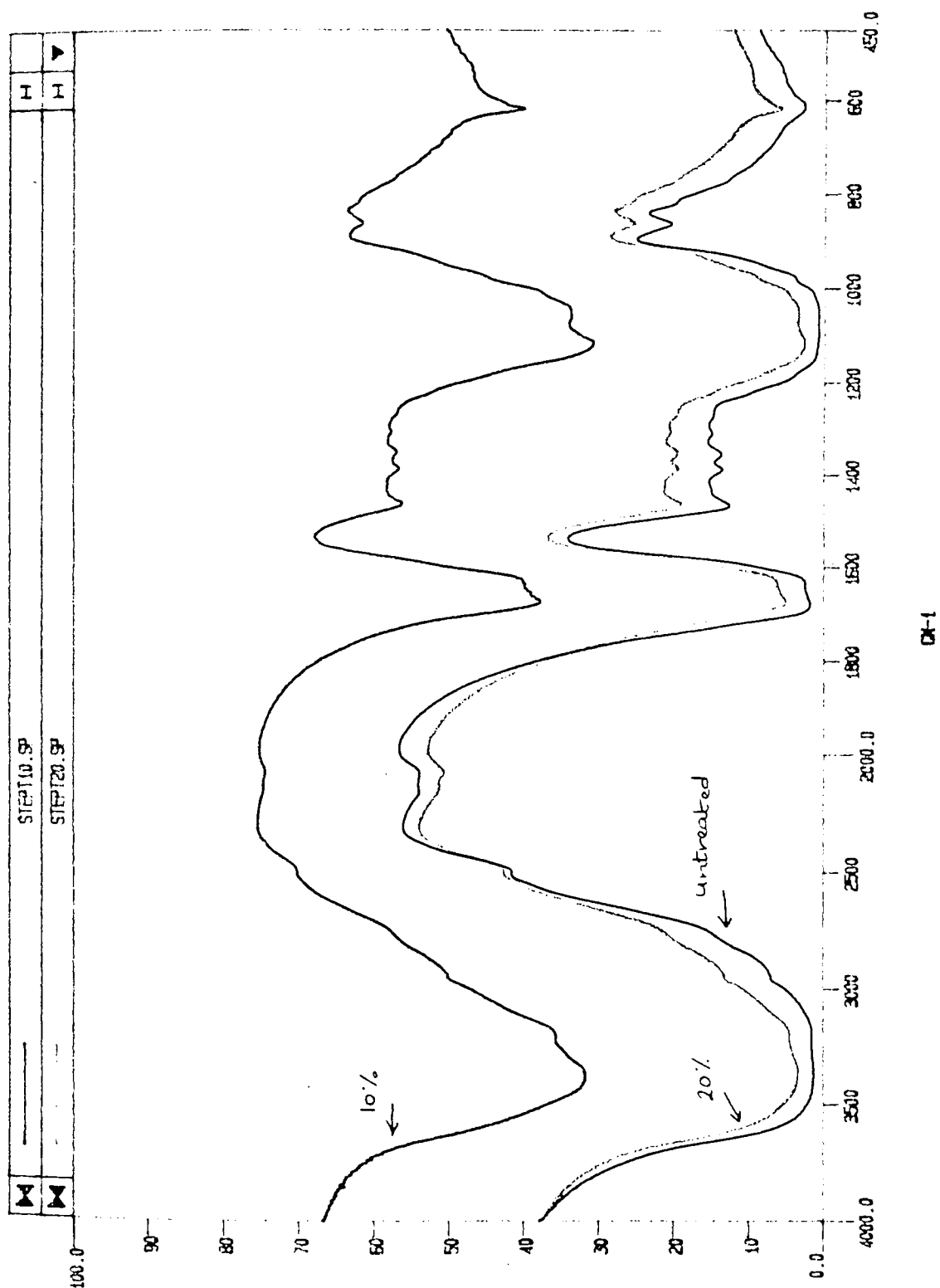
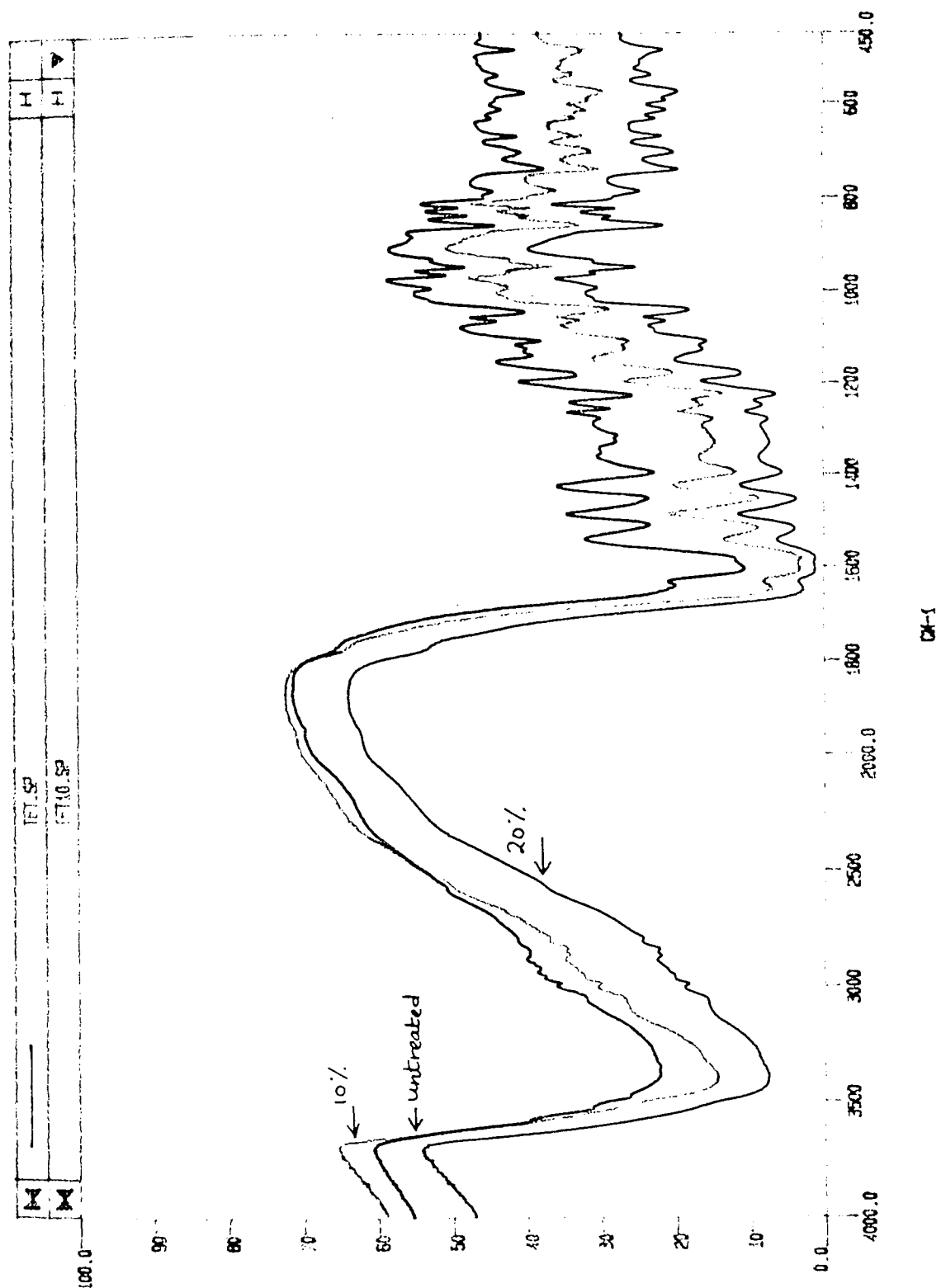


Figure 7.113 FTIR spectra for tetracycline dried at 115°C.



8: Discussion of results

As described earlier, a knowledge of the mechanisms of drying, viz. the heat and mass transfer phenomena, provides some understanding of the drying process in relation to temperature / moisture conditions inside the drying material with respect to the drying gas, as shown in Figure 8.1. The manner of internal moisture transfer and the optimisation of conditions for the desired product properties, e.g. freedom from thermal degradation or loss of required properties such as strength and shape or unsatisfactory morphology, may also be deduced.

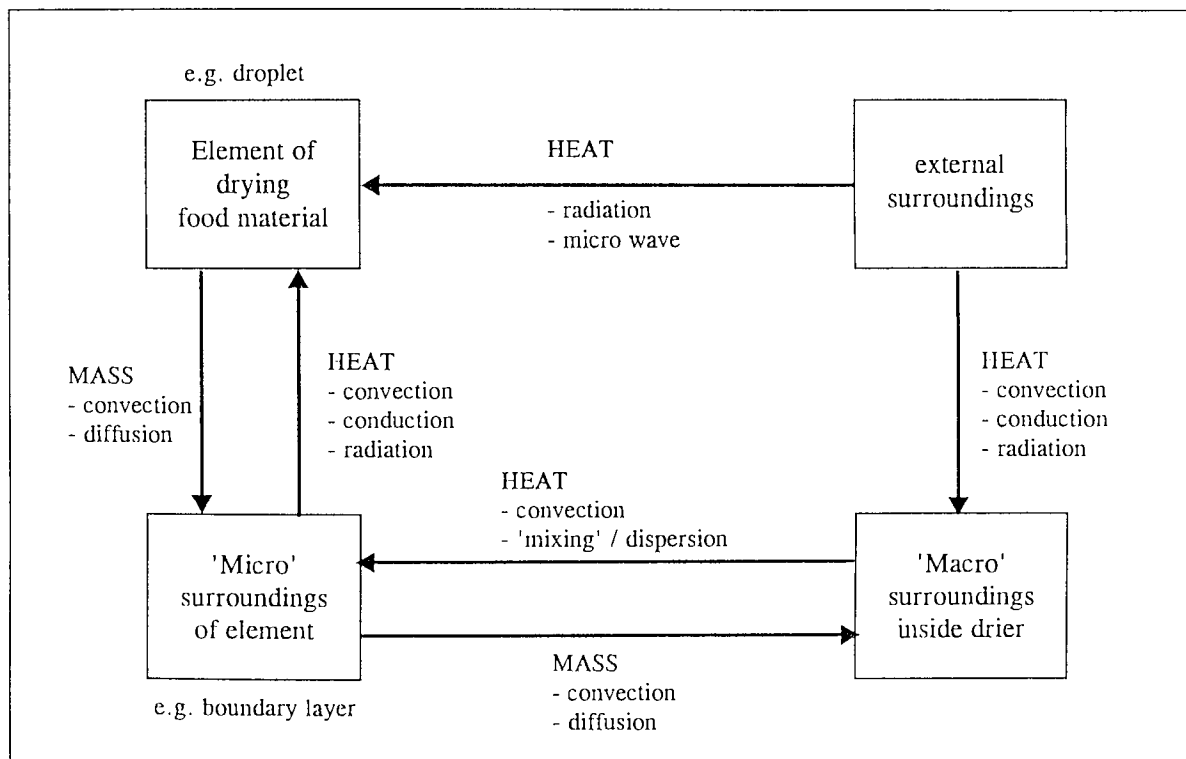


Figure 8.1: The relationship between the drying material and its surroundings (after Bruin & Luyben, 1980)

Heat is transported to the elements of the drying material by radiation, convection, or conduction from the external surroundings. Radiation is transmitted partly from the external surroundings and partly via the 'micro'

and 'macro' surroundings of the drying element, whilst the conductive and convective heat transfer is via the 'micro' and 'macro' surroundings of the drying element alone.

Convection and diffusion, through the micro surroundings of the element and the macro surroundings to the external surroundings, promotes mass transfer from the drying element. Convection and dispersive mixing of the drying medium causes the mass / heat transfer between the micro and macro surroundings. In many practical situations the mass transfer of water from the inside of a drying element, e.g. a droplet or particle, to the surface is the most important transfer because it is rate limiting.

Single droplets suspended in a drying air stream have been extensively studied, e.g. Ranz & Marshall, 1952, El-Sayed *et. al.*, 1987, Verderber & King, 1992, and Walton, 1994, to provide a valuable insight into the fundamentals of drying.

8.1: Experimental technique

This study was an attempt to determine the trends of thermal degradation, in terms of either volatiles-loss or the loss of chemical / biochemical activities, for various heat-sensitive materials when dried as single droplets.

Other workers have reported the use of single droplets to determine volatile component loss e.g. Furuta *et. al.*, 1984, *ibid.*, 1985, etc. but they used different droplets to measure the droplet temperature and volatiles content. Other single droplet work has been done to continuously monitor volatiles loss without the measurement of droplet temperature (Verderber & King, 1992, Sunkel & King, 1993).

In the present study, both the temperature and the volatiles content of the same droplets were measured. Other effects such as residual reactivity were

by the development of a novel rotating thermocouple (see Chapter 6) on which the single droplets were suspended. The apparatus functioned satisfactorily and enabled phenomena to be correlated with temperatures measured simultaneously, rather than in the repeat experiments resorted to in previous investigations. It enabled dried crusts to be collected; not surprisingly if a “liquid” remained, collection became uncertain and a different suspension technique would probably be better, e.g. as demonstrated by Oteng-Attakora (1995).

8.1.1: Loss of volatiles

Volatile flavours (aromas) are lost during the drying of many food products, and this loss of ‘quality’ is crucial both to the customer as well as to the manufacturer. (Losses of volatile constituents when drying non-food products, e.g. detergents, may also result in pollution problems).

In the spray-drying of coffee, there is a loss of more than 90% of its original aroma (Menting & Hoogstag, 1967). To overcome this loss, further process stages, the removal of the flavour components from the feed (usually by steam distillation) and their subsequent re-addition after the spray-drying are added which obviously increase the manufacturing costs. Thus, the need exists to determine techniques which would allow an increased retention of flavours during drying without the costly removal and re-addition stages as presently necessary for coffee.

The effect of particle morphology upon the retention of volatiles has been demonstrated by El Sayed *et. al.*, 1990, Verderber & King, 1992, and Walton 1994. They have shown that the prevention of certain morphological changes, e.g. development of protuberances, droplet ‘ballooning’ effects, etc., could result in the enhancement of flavour retention.

The retention of flavours can be enhanced by other means including the use of less-harsh drying regimes (e.g. freeze-drying and spray-drying) and the use of encapsulants which hold the flavour in an easily soluble shell. An alternative could be very short residence times, e.g. 2s-3s microwave drying.

As previously stated, the encapsulants used during the present study were chosen because of their skin formation characteristics proposed by Hassan (1991). The formation of an outer skin was expected to prevent the loss of the encapsulated flavours.

Figures 8.2 to 8.5 show that the initial losses of ethanol occurred within the first minute of drying regardless of the drying temperature. The initial rate of loss of ethanol was greater with the increased temperature, which would be expected because of the raised vapour pressure. Subsequent ethanol losses were less rapid because of the formation of a skin; the nature of the skin and the drying temperature then affected the final ethanol content.

Rice starch which formed a porous crust lost most of its initial ethanol. Materials which formed a skin resistant to mass transfer, e.g. wheat starch and the gelatines, exhibited cracks on their surface which allowed the loss of ethanol (Sayed, *et. al.*, a,b,c, 1995).

The results confirm that to retain the volatiles it would be desirable to use dryers with very short residence times such as flash dryers, spray dryers, and drum dryers (Table 2.2).

The effect of increasing the initial encapsulant concentration (Figures 8.2 and 8.6) confirm the results observed by others workers such as Furuta *et. al.*, 1984. Increase in initial concentration led to increased ethanol retention. This is the case for materials which form resistant skins. However, increasing the concentration for materials which form porous skins had little if any effect.

Figure 8.2: The retention of ethanol in 20% solutions of the various encapsulants at 25°C

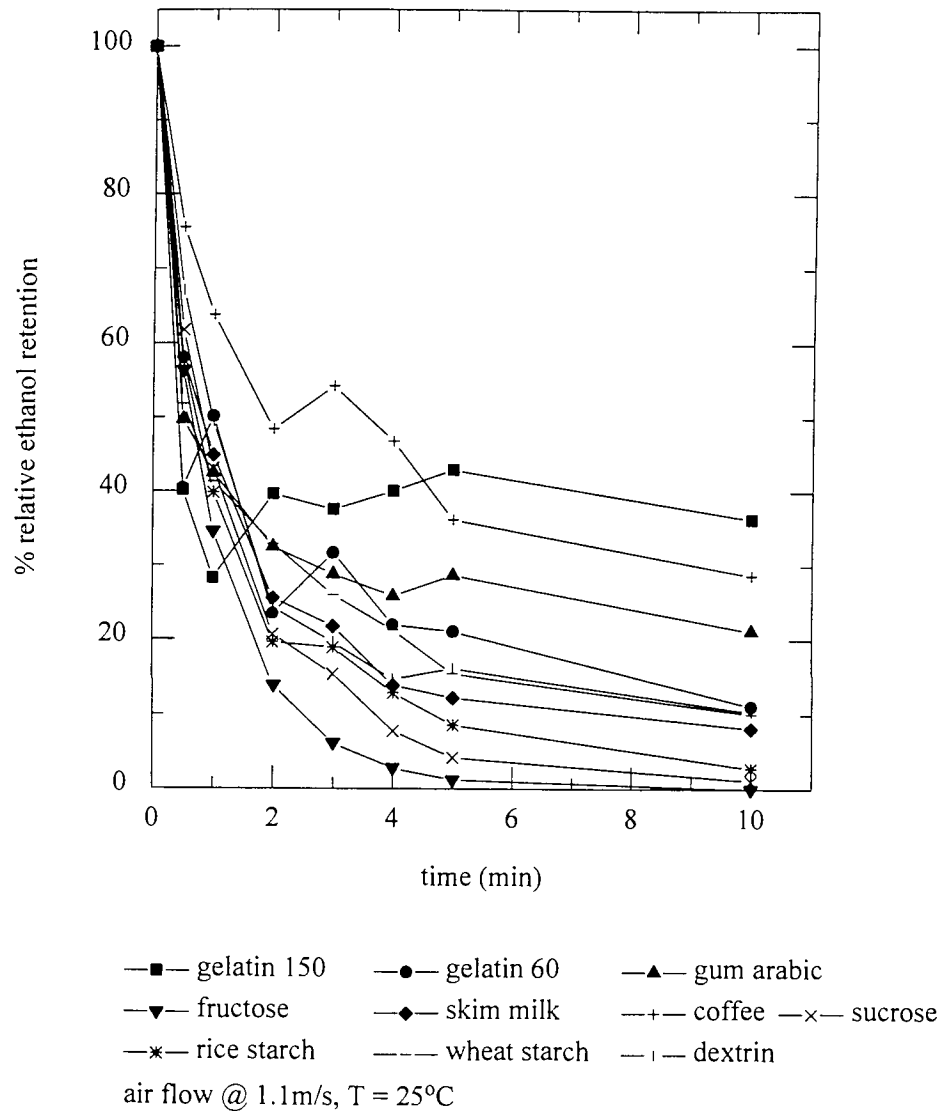


Figure 8.3: The retention of ethanol in 20% solutions of the various encapsulants at 40°C

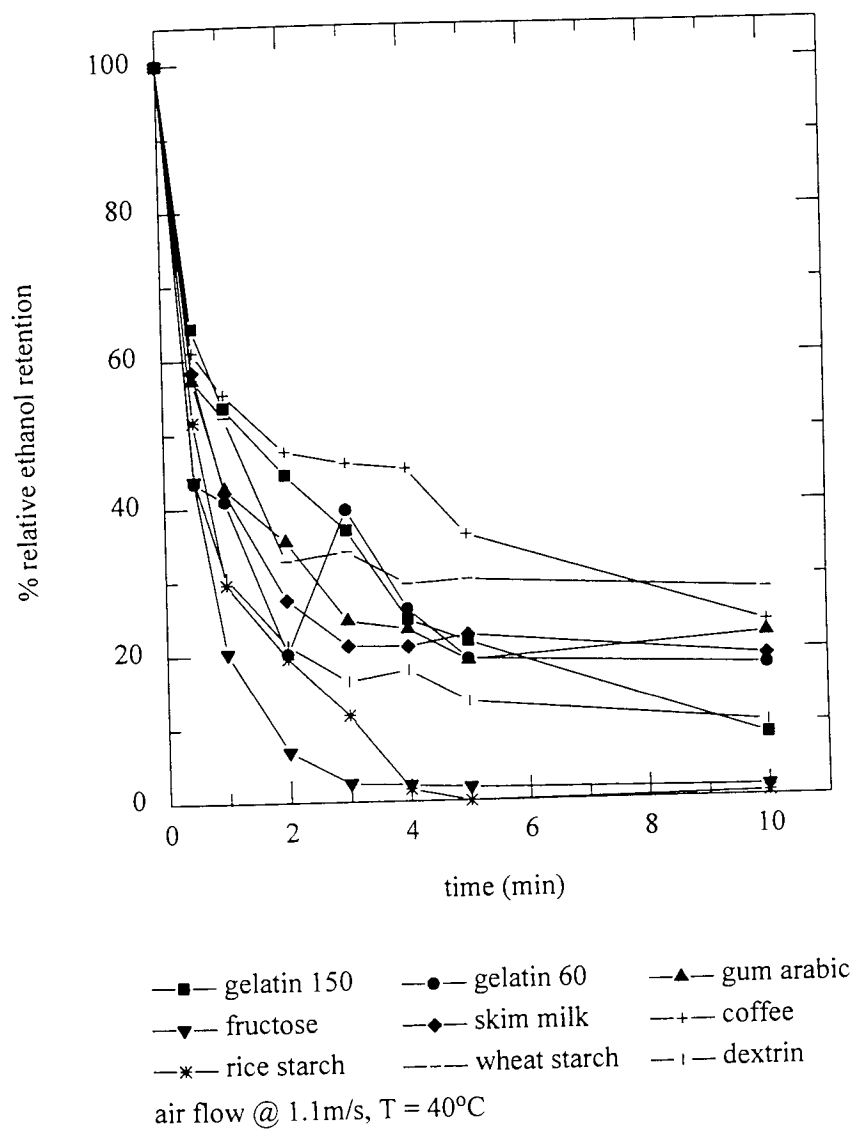


Figure 8.4: The retention of ethanol in 20% solutions of the various encapsulants at 65°C

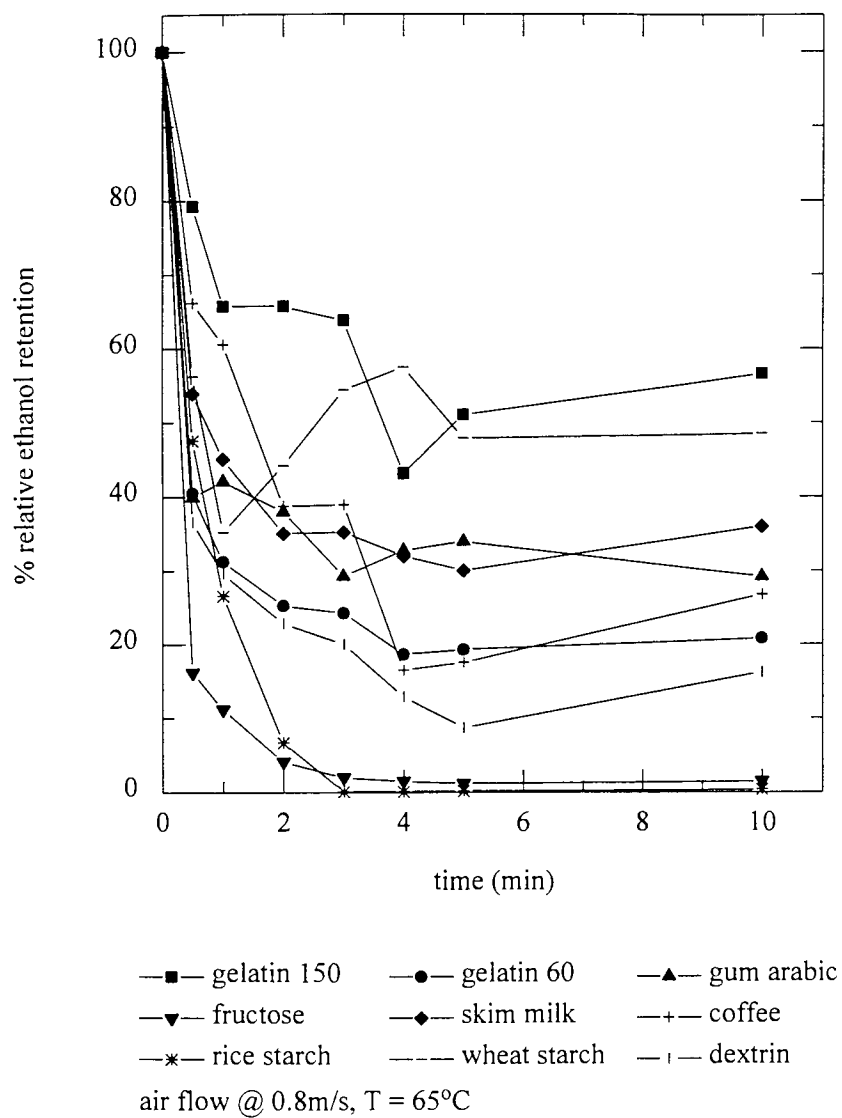


Figure 8.5: The retention of ethanol in 20% solutions of the various encapsulants at 89°C

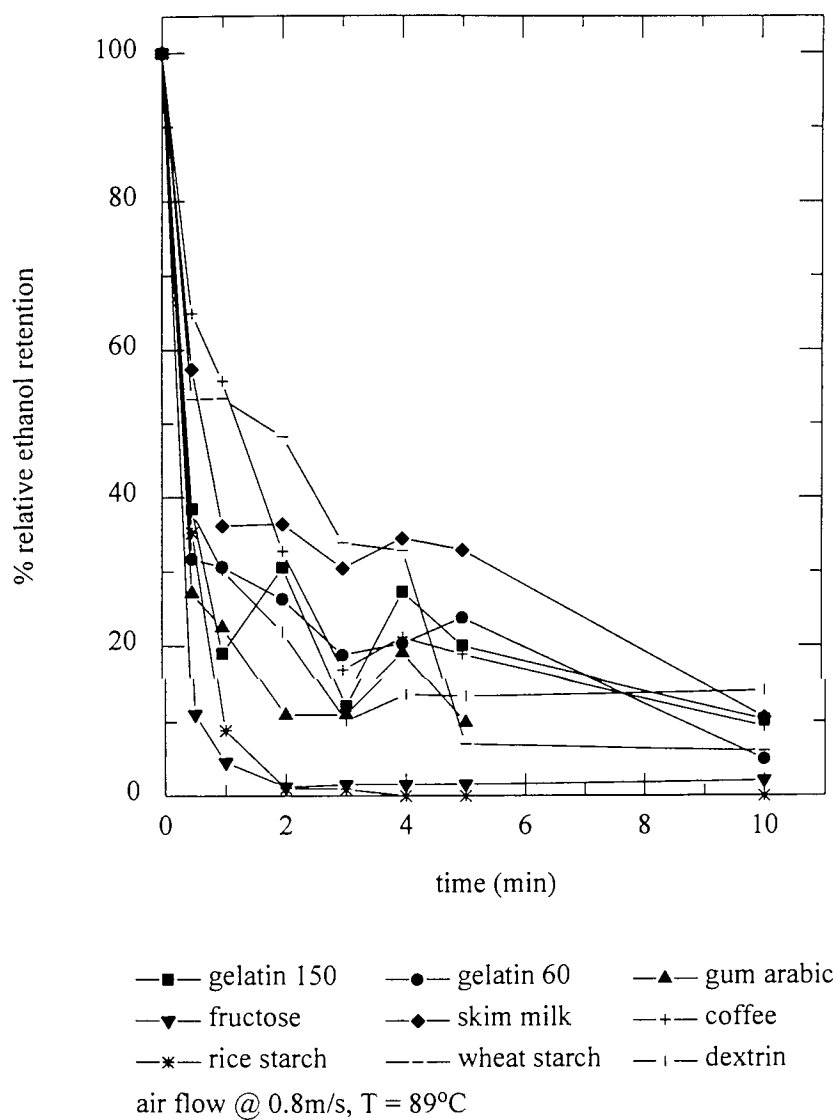


Figure 8.6: The retention of ethanol in 40% solutions of the various encapsulants at 25°C

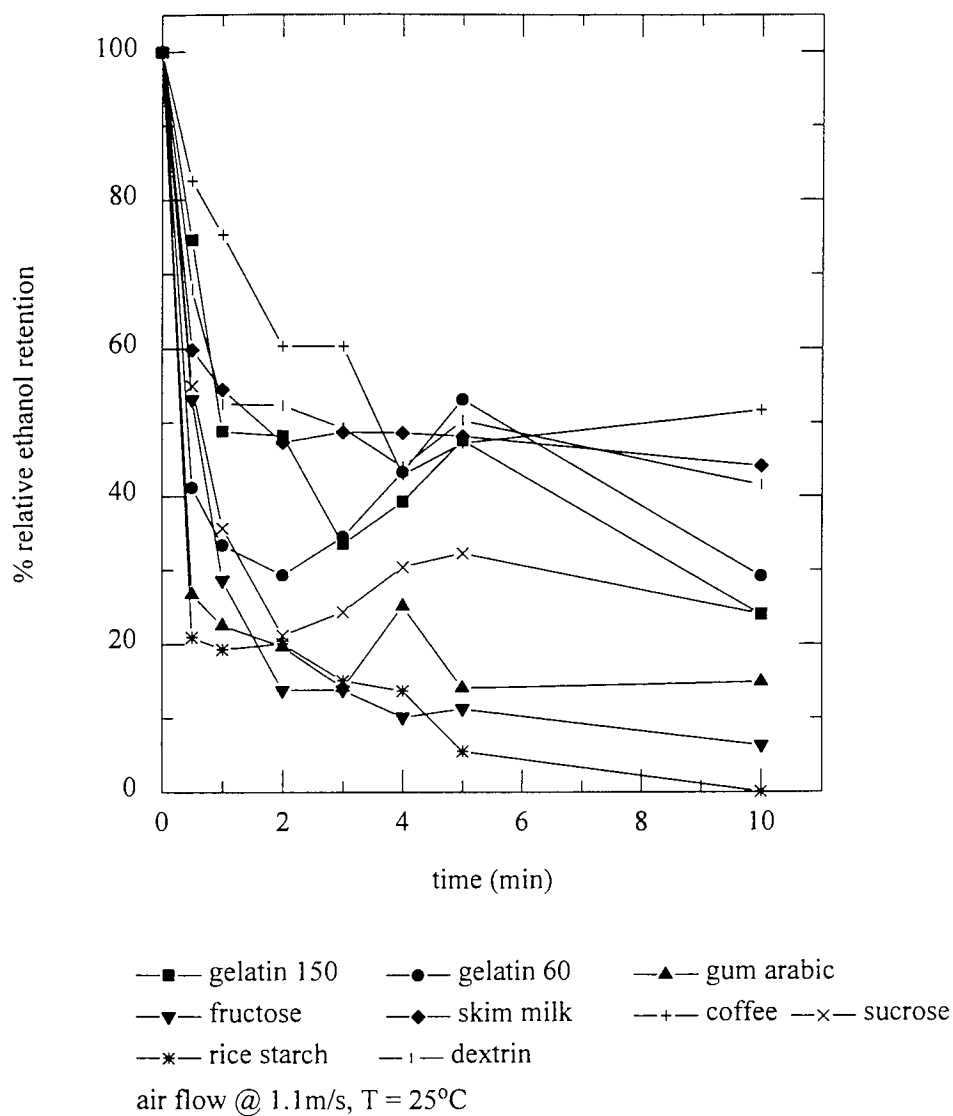
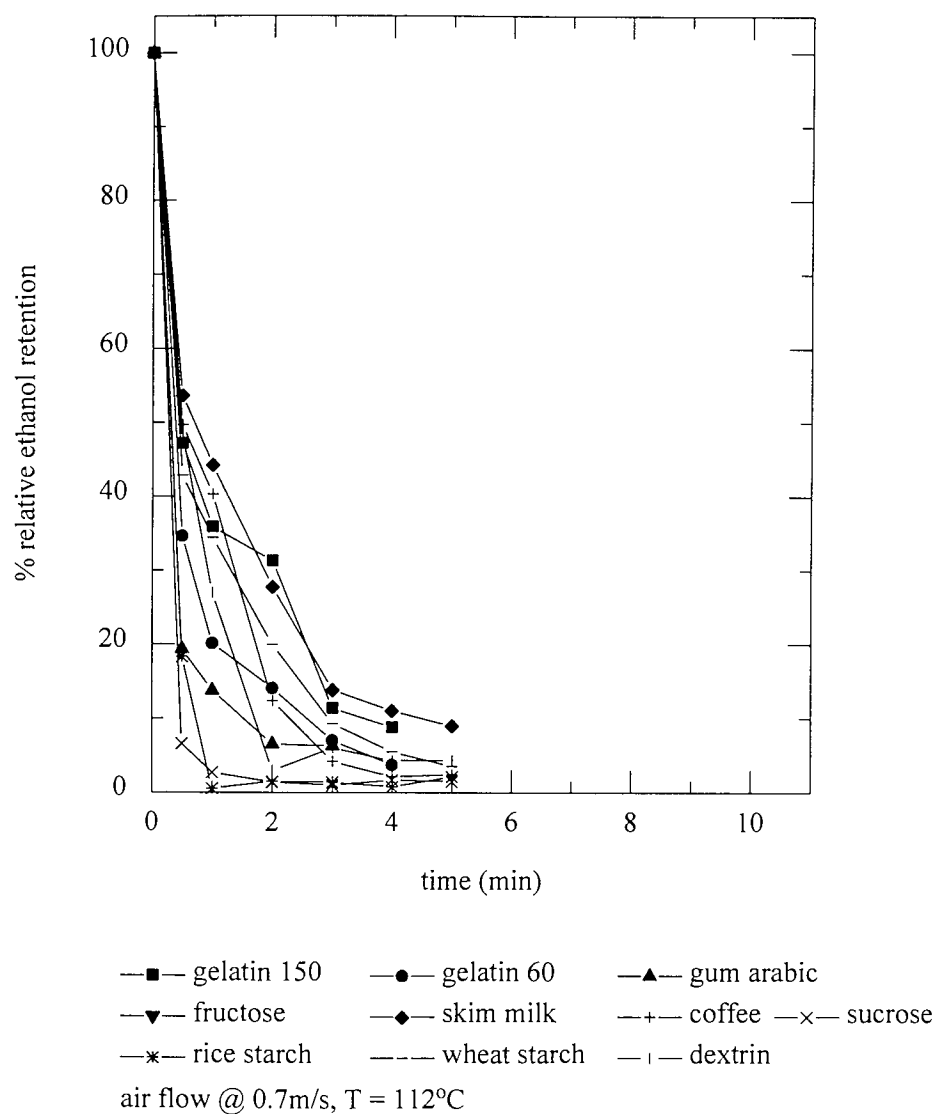


Figure 8.7

The retention of ethanol in 20% solutions of various materials at 112°C



The experiments in which the temperature was varied show that the loss of ethanol occurred within the first minute of drying. Therefore the use of dryers with small residence times is again confirmed to be desirable (Table 2.2).

Figure 8.7, showing the ethanol retention for all the encapsulants at an elevated temperature of 112°C, demonstrates that initial losses in excess of 60% occurred within the first minute of drying. The reduction in final retentions for materials which formed resistant skins compared to that observed at 25°C can be attributed to the appearance of cracks in the droplet surface which allowed the ethanol to evaporate. The elevation of temperature produced no significant differences in the losses observed with rice starch which formed a porous open-structured crust.

Figure 8.6 shows an increase in the retention with the use of coffee and skim milk. This implies that they are more suitable as encapsulants. However, their inherent flavours make them undesirable as they would provide an extraneous flavour. Nevertheless, if the inherent flavours of coffee and/or skim milk could be removed, or even significantly reduced, they might be used as flavour encapsulants.

Gum arabic (which is already a commercially used flavour encapsulant) showed no increase in volatiles retention in this study. An explanation for this would be that the selectively-permeable crust, normally associated with gum arabic, did not form rapidly enough at the given temperatures to retain the ethanol i.e. the formation of the crust has to be rapid to effectively retain the volatiles. Thus there is a possibility that other encapsulants such as carageenan, guar gum, locust bean gum, etc., might prove suitable (BeMiller, 1992).

The results suggest that in order to retain a significant amount of the volatile flavour, the drying needs to occur rapidly i.e. the material needs to experience the relatively high temperatures for very short periods of time; this would allow the use of short residence time dryers which are cheaper than freeze-

drying which is ideal. Clearly in freeze drying, for economic reasons, the initial solids concentration should be the maximum practicable, but pre-drying by a cheaper method would offer no advantage given the volatiles loss is evidently associated with the constant rate periods in this work.

8.1.2: Possible strategies for volatiles retention

As a result of this study and those reported previously, several methods to enhance the retention of volatile flavours can be proposed.

- i) Increasing the initial solids concentration of the feed. This would have two effects: the first would be an increase in viscosity of the feed which would reduce the diffusivity of the volatiles compared to that of the water. Secondly, it would lead to a rapid skin formation and the early onset of selective diffusion.
- ii) The selection of skin forming encapsulants, which would selectively allow the loss of water; here the selection would influence the residence time within a dryer with highly permeable encapsulant having a shorter residence time leading to reduction in physico-chemical degradation.
- iii) The choice of drying parameters which would not allow morphological effects, (such as ballooning, cracking, blow holes, etc.), which enhance volatiles loss to occur. The possible range of morphological changes during spray drying have been summarised by Masters, 1988, and Walton, 1994, as shown in Figure 8.8. However, since in spray drying both the rates of heat and mass transfer to and from individual particles are particle size-dependent, and the particle residence time in the drying zone is similarly size-dependent, such changes are extremely difficult to control given the distribution which is inevitable, commencing from atomisation. Thus, as with moisture content, all that may be achievable is a mean level of volatiles retention for a selected sample of dried materials. An analogy with freeze drying characteristics,

discussed on page 381, does however raise the question as to whether it is feasible to promote a desirable internal particle structure - as distinct from attempting to produce a particular skin or crust structure - by the use of additives. A discontinuous reticulated structure could retain volatiles with the voids. If fluidized bed or pneumatic drying is to be used then the particle pre-forming stage will have a critical effect on the volatiles retention. Partly-formed, cracked or under-sized particles should be avoided.

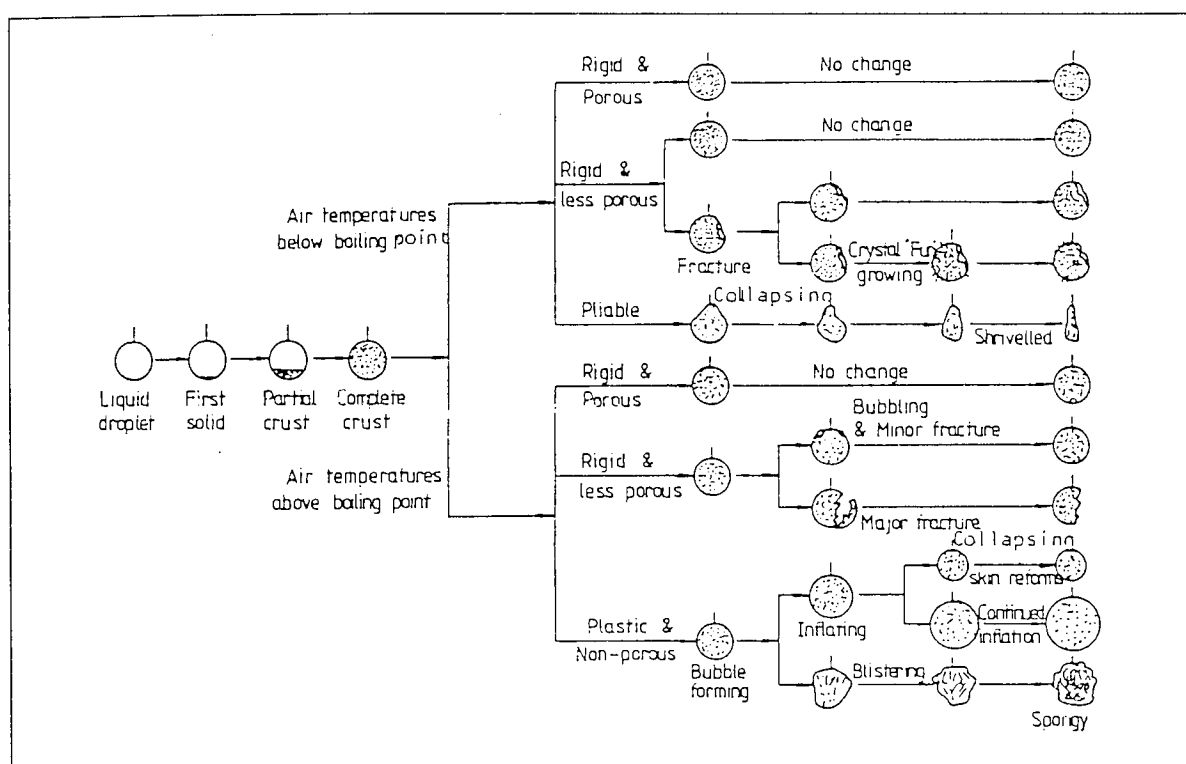


Figure 8.8: Drying characteristics of single droplets

iv) The avoidance of feed aeration (which would allow the formation of bubbles inside the droplets promoting ballooning effects which would lead to increased volatiles loss because of film thinning phenomena) by using commercial anti-foaming agents, e.g. Dow Corning 544 silicone fluid (Walton, 1994), or by slow speed mixing without vortex formation. In some slurry drying processes a de-gassing stage may be introduced prior to drying.

v) The use of solvents in which the volatiles exhibited a reduced vapour pressure (KimHa & Reineccius, 1988).

vi) The use of a second oil phase which would selectively extract the volatile into the oil phase where it would be better retained than in the water (Zakarian & King, 1982).

Additionally, in spray drying, there must be close control of drop size during atomisation to avoid small droplets with high mass / heat transfer coefficients which would rapidly become devoid of volatiles during both the constant-rate (k_g -controlled) and falling-rate (k_c -controlled) periods. As volatiles have been reported to be lost near the atomiser, during the formation and break-up of the liquid sheet, the drops must be formed as quickly as practicable. Recently Otteng-Atakora (1995) has demonstrated conclusively the increase in mass transfer associated with droplets oscillating freely in air; this reinforces the observation regarding volatiles-loss.

The preliminary freeze drying experiments conducted in this study resulted in an unexpectedly high loss of volatiles with all the materials tested. This was attributed to the lack of formation of a structure to entrap the volatiles. (Such a structure also aids in the re-hydration of the material). This suggests that there must be a critical volume / area which must be attained to prevent significant loss of volatiles. Thus the primary advantage of freeze drying is reported to be the formation of such amorphous structures which entrap volatiles in their micro-regions and the subsequent release of the entrapped volatiles when these structures are lost through re-hydration to saturation (Mellor, 1978).

Insofar as particle fragmentation during subsequent handling, e.g. packaging and transport, will expose fresh interior and therefore promote volatiles loss, an improvement could be achievable by increasing inherent particle strength. The manner in which this may be done is by the use of additives, e.g. polymers, has been reviewed by Walton (1994).

8.2: Antibiotics

The drying conditions used in this study had no significant effect upon the efficacy of the various antibiotics (as illustrated in Chapter 7) which were shown to be heat-stable with the exception of ampicillin which was known to be heat-sensitive.

Ampicillin (at 10% w/w concentration) was significantly affected by drying at 115°C (as shown in Figure 7.56a) when the zone diameter decreased rapidly after the first minute.

An inert drying medium, nitrogen, was used to determine the cause of the various effects shown by the dried antibiotics. For ampicillin, the effects were probably due to a combination of thermal and oxidative effects. The other antibiotics were unaffected by the drying conditions under either atmosphere.

The FTIR spectra for the various antibiotics show that there was no significant difference between the untreated and the dried antibiotics (shown by the similar spectra) with the exception of ampicillin which showed major changes in the respective spectra. This suggests the possible loss of functional groups the analysis of which, as a basis for retained efficacy trials, could be the subject of future work.

Freeze drying experiments using the antibiotics demonstrated no difference in the efficacy of the dried antibiotics. This would suggest that the dryer of choice would be a freeze-dryer, but the cost limitations would make this unsuitable except for the expensive materials such as hormones, and vaccines. Thus such heat-stable antibiotics can be dried in vacuum dryers, and short residence time dryers such as spray and drum dryers. Tray or fluidised bed dryers (which have longer residence times (Table 2.2)) cannot therefore be used.

8.3: Enzymes

As expected for the heat-sensitive enzyme, dextran sucrose, the residual activity was greatly affected by temperature, with the activity decreasing to zero very rapidly at temperatures above 65°C. The results for invertase demonstrate its heat-tolerant nature by the enzyme remaining active for longer at temperatures above 65°C.

The limited number of experiments conducted on the temperature effects on enzyme activity show that for heat-sensitive enzymes, such as dextran sucrose, the dryer of choice would be a freeze dryer.

The alternative method of retaining enzyme activity would be through immobilisation of the enzyme prior to drying; this would provide the necessary structural stability to the enzyme which would otherwise become denatured as a consequence of loss of structure (Barzana-Garcia, 1986).

Conversely, for fairly heat-stable enzymes, (such as invertase), which can be dried at 115°C (with only 20% loss of activity in the first minute) other dryers with short residence times can be used e.g. spray dryers, drumdryers, etc.(Table 2.2).

8.4: An explanation for the apparent increase in ethanol retention after 1-2 minutes

Some of the percentage relative ethanol retention data, as plotted, shows an apparent increase in retention after one or two minutes. This is attributable to experimental errors occurring in the removal of more viscous liquid droplets in the period 0.5 to 2 minutes depending upon the feed solution and temperature.

The initial droplets of low viscosity liquids, and the particles, once a crust had formed, were relatively easy to recover. But the viscous droplets tended to be difficult to recover completely. This introduced a weighing and reconstitution error with viscous droplets only.

9: Conclusions and recommendations for further work

9.1: Conclusions

The following conclusions may be drawn:

The apparatus performed satisfactorily in the determination of volatiles loss and thermal degradation with single droplets, proving the technique to be good and reproducible. Therefore, as an improvement on earlier designs, it would be applicable in the type of commercial experimental trials for which they have been used (Walton, 1994) in order to cover a wide range of operating variables prior to the use of expensive pilot plant trials. Such single drop studies are believed to provide a better simulation than slab drying in which “edge effects”, i.e. heat gained via the slab support and shrinkage of the material, can cause discrepancies.

The reproducibility of the technique was shown to be good with a number of repeated experiments exhibiting similar ethanol retentions.

The analytical techniques were also found to be satisfactory:

- a) the modified pharmacological technique (DST) provided results consistent with the FTIR spectra for the antibiotics,
- b) the use of the FTIR was useful to identify possible variations in the spectra which could produce the detrimental effects,
- c) the use of nitrogen as a drying medium proved useful to ascertain which of the effects were due to thermal or oxidative effects, and

d) the use of ethanol as a model volatile, despite its ease of analysis, is now considered to be far from ideal because:

- it is a small molecule in comparison with natural flavours,
- it forms an azeotrope with water at low water concentration, i.e. the azeotrope at 1 bar has the composition 89 mol percent ethanol (Coulson & Richardson, 1977)

The present study has confirmed that the retention of volatiles is a function of selective diffusion and the mechanisms of crust or skin formation on the droplet surface. Whilst the correlation of the effects will always be system-specific the results are novel and have therefore been submitted for publication in the form reproduced as Appendix C (Sayed et. al. 1995 (a, b, c)). From the results of the various experiments, it is evident that the use of rice starch as a commercial encapsulant would be of limited potential because of the open nature of the crusts that were formed upon drying. Wheat starch, despite its increased retention, would be unsuitable as its inherent flavour may render it less preferable. The use of skim milk and coffee, both of which provided enhanced volatiles retention, as commercial encapsulants is of limited potential because their intrinsic flavour and / or colour would be imparted to any product into which they were incorporated. Gum arabic, a known and well used encapsulant, provided no increase in volatiles retention probably because of the moderate temperatures used. There was more volatiles retention with gelatine 150 Bloom than 60 Bloom because of the difference in strengths of the gels produced.

The convective drying of ampicillin above 100°C reduced the efficacy of the antibiotic; conversely, freeze drying had no adverse effect on the antibiotic. The use of an inert drying medium (nitrogen) had less of a detrimental effect than air at the same temperature on the efficacy of ampicillin. The potencies of the other antibiotics, viz. chloramphenicol, oxytetracycline, streptomycin and tetracycline, remained unaffected during both air drying at temperatures

upto 115°C and freeze drying. The results of the drying of enzymes illustrated the heat-sensitive nature of dextran sucrose, which rapidly lost its activity within the first minute at temperatures above 65°C; invertase was shown to be heat-tolerant as it retained its activity for longer at temperatures above 65°C.

9.2: Recommendations for further studies

In order to make better use of the equipment and to gain more insight into the fundamentals of drying, further work is necessary along the avenues proposed below.

Natural volatiles / flavours, such as orange oil, should be used instead of the model volatiles, e.g. ethanol, propanol, etc., normally used. This would probably make the subsequent analysis more difficult as the real flavours are composed of a wide range of components and the determination of loss of a particular component would be difficult.

The air temperatures used in the present study were moderate, with a maximum temperature of 115°C. Subsequent work should be conducted at higher temperatures, e.g. 150°C - 200°C, which would facilitate the rapid formation of the selectively-permeable skin to aid the retention of volatile components, as in the case of gum arabic. At the temperatures used in this study, the encapsulant properties of gum arabic, which are known to be good, proved to be ineffective in the retention of ethanol. There is considerable scope for assessing the effectiveness of the various potential encapsulants using the apparatus and techniques which have been developed. This could start with dextrin, gum arabic and gelatine (Bloom 60 and 150) in the concentration ranges 20% to 50% and at temperatures in the range 150°C to 200°C.

If steam-distillation is a possible mechanism of volatiles loss in any specific case then drying in super-heated steam might offer some advantage. (The

alternative of drying in a recycled air stream pre-saturated with the volatile which it is desired to retain appears less feasible).

The apparatus designed for this study allows the continual monitoring of droplet temperature during drying. There is a need to further modify the apparatus to facilitate the continual downstream monitoring of the drying gas for its volatiles content, such as that used by Sunkel & King, 1992 and Verderber & King, 1993. This would enable a more accurate assessment of the volatiles loss during the progression of drying. The apparatus should be modified to continually monitor the loss of volatiles from a single droplet rather than an assessment of volatiles loss being made from a series of discrete points during drying.

An inert drying atmosphere should be used to determine whether there is any effect of drying atmosphere, coupled with drying temperature, upon the encapsulating properties of the various materials tested. Similarly more of the drying should be conducted with dry gas to monitor the effect of the humidity, and temperature, of the drying gas upon the retentive capabilities of the various encapsulants.

'Neat' enzyme solutions were dried in this study, unlike previous workers who have stabilised the enzymes under test in sugar solutions (Yamamoto & Sano, 1992). Further work, using inert stabilisers, would be useful in order to compare results with other researchers.

To reduce the uncertainty with the removal of the dried droplets from the rotating thermocouple, as shown by the apparent increase in percentage relative ethanol content as the droplets become more viscous (see section 8.4), a 'disposable' or removable thermocouple should be developed which would facilitate droplet collection.

10: Nomenclature

ρ = bulk density of the dry product (kg/m³),

ε = crust porosity

ψ = crust thickness (m)

λ = latent heat of evaporation (J/kg)

ΔH_S = latent heat of sublimation of ice (2840 kJ/kg)

ΔL = thickness of the dry layer (m)

λ = is the latent heat of vaporisation of water (J/kg)

θ = air temperature (°C or K)

ρ_A = density of air at its mean partial pressure (kg/m³)

ΔT is the temperature difference between the air and the surface (°C or K).

θ_w = wet bulb temperature (°C or K)

A = surface area (m²)

C_a = concentration of 'a' (kg/m³)

C_{a_1}, C_{a_2} = molar concentrations of 'a' at y_1 and y_2 (kmol/m³)

C_{pA} = heat capacity of air (J/kg/K)

C_{pF} = heat capacity of the feed (J/kg/K)

C_{pv} = heat capacity of the diffusing vapour (J/kg/K)

D' = average effective diffusivity in the dry layer (m²/s)

D_{ab} = diffusivity of 'a' in 'b' (m²/s)

DN = decomposed compound

D_q = dispersion factor

D_R = the Rosin-Rammler mean diameter (m)

D_v = molecular diffusivity (m^2/s)

dW / dt is the rate of moisture loss (kg/s)

E = activation energy of the reaction (J)

G' = mass flow rate of air (kg/sm^2)

H = humidity of air (kg/kg)

h = external heat transfer coefficient ($\text{W/m}^2\text{K}$)

h = heat transfer coefficient ($\text{W/m}^2\text{K}$)

h_D = mass transfer coefficient ($\text{kgmol/m}^2\text{s}$)

H_w = humidity of saturated air at θ_w (kg/kg)

k = effective thermal conductivity of the dry solid (W/mK)

k = reaction rate constant (dependent upon temperature)

K_G = diffusional transfer coefficient ($\text{kgmol/m}^2\text{s}$)

k_g = external mass transfer coefficient ($\text{kgmol/m}^2\text{s}$)

k_v = thermal conductivity of the film (W/mK)

L_A = air flow rate (m/s)

m = mass flow rate (kg/s)

M_1 = initial moisture content

M_2 = final moisture content in the dry layer

M_{ch} = chamber evaporation capacity ($\text{kgH}_2\text{O/s}$)

M_F = feed flow rate (kg/s)

M_w = molecular mass of water

$\frac{d[N]}{dt}$ = rate of loss of compound N ($\text{kg/m}^3/\text{s}$)

N = original compound

$[N]$ = concentration of compound N (kg/m^3)

$[N]_0$ = the initial concentration of compound N (kg/m^3)

N_a is the molar rate of diffusion per unit area

N_w = water vapour flux ($\text{kgmol/m}^2\text{s}$)

P_{ew} = partial pressure of water vapour in external gas phase (N/m^2)

P_{fw} = partial pressure of water vapour in equilibrium with the sublimation front (N/m^2)

P_s = vapour pressure of water (N/m^2)

P_{sw} = partial pressure of water vapour at surface (N/m^2),

P_w = partial pressure of water vapour in the air stream (N/m^2)

P_{w0} = vapour pressure of water at θ_w (N/m^2)

q = heat flux (W)

R = universal gas constant (J/kmol K)

r_1 = radius of the evaporating droplet (m)

r_2 = outer radius of the gas film (m)

T = average temperature of the dry layer (K)

T_A = air temperature (K)

t_d = drying time (s)

T_e = external temperature of gas (K)

T_F = feed temperature (K)

T_f = temperature of the sublimation layer (K)

T_s = surface temperature of the dry solid (K)

T_{WB} = wet bulb temperature (K)

W = mass evaporation rate (kg/s)

y = distance in the direction of diffusion (m)

11: References

1. Akbar S (1988) PhD Thesis Aston University, Birmingham, England
2. Alexander K & King CJ (1985) *Drying Technology* 3:3;321-348
3. Ali HH (1985) PhD Thesis Aston University Birmingham England
4. Ali HH, Mumford CJ, Jeffreys GV & Bains GS (1988) 6th Int Drying Symp (Drying '88) Versailles France
5. Audu TOK & Jeffreys GV (1975) *Trans Inst Chem Eng* 53;165
6. Audu TOK (1973) PhD Thesis Aston University Birmingham England
7. Bains GS (1990) PhD Thesis Aston University Birmingham England
8. Barker P & Ajongwen N (1991) *Biotech & Bioeng* 37;703-707
9. Barry AL & Fay GD (1973) *Am J Clin Path* 59;196-198
10. Barry AL (1991) in "Antibiotics in Laboratory Medicine" 3rd edition Williams & Wilkins 1-16
11. Barzana-Garcia E, Klibanov AM & Karel M (1986) *Drying* 86 428-432 Hemisphere Publishing
12. BeMiller JN (1992) in "Encyclopedia of Food Sci & Tech" YH Yui (editor) Wiley-Interscience pages 2418 - 2424
13. Bomben JL, Bruin S, Thijssen HAC & Merson RL (1973) *Adv Food Res* 20;2
14. Bootsma HPR, Frijlink HW, Eissens A, Proost JH, van Doorne H & Lerk CF (1989) *Int J Pharm* 51;213-223

References

15. Bowman CW, Ward DM, Johnson AI & Trass O (1961) *Can J Chem Eng* 39;9
16. Bradley EB (1987) in "Instrumental Analysis" 144-160 (see ref 21)
17. Bryan LE & Godfrey AJ (1991) in "Antibiotics in Laboratory Medicine" 3rd edition Williams & Wilkins 599-643
18. Buckingham E (1907) *US Dept Agr Bur Solids Bull*; 38
19. Chandrasekaran SK & King CJ (1972) *AIChEJ* 18:3;513-526
20. Charlesworth DH & Marshall WR Jr (1960) *AIChEJ* 6:1;9-23
21. Christian GD & O'Reilly JE (1987) "Instrumental Analysis" 2nd Edition Allyn & Bacon
22. Coulson JM & Richardson JF (1977, 1978) "Chemical Engineering" Vol 1 (pages 268, 283-294) and 2 (pages 710-762), Pergamon Press
23. Crosby EJ & Stewart WE (1970) *Ind Eng Chem Fund* 9:3;515
24. Daeman ALH & van der Stege HJ (1982) *Neth Milk Dairy J* 36;211-229
25. Daeman ALH, A Kruk & van der Stege HJ (1983) *Neth Milk Dairy J* 37;213-218
26. Davies JE (1991) in "Antibiotics in Laboratory Medicine" 3rd edition Williams & Wilkins 691-713
27. Desrosier NW (1970) in "The Technology of Food Preservation" Avi Publishing Co, Westport, Connecticut
28. Dlouhy J & Gauvin WH (1960) *AIChEJ* 6:1;29-34
29. Eichner K (1975) in "Water Relations of Foods" RB Duckworth (editor) Academic Press 417-434

30. El-Sayed TM, Wallack DA & King CJ (1990) *Ind Eng Chem Res* 29:12;2346-2354
31. Fellows P (1992) in "Encyclopedia of Food Sci & Tech" YH Yui (editor) Wiley-Interscience 2:1234-1241
32. Fortes M & Okos MR (1980) in "Advances in Drying" Vol 1; 119-154
33. Frazier GC Jr & Hellier WW Jr (1969) *Ind Eng Chem Fund* 8;807
34. Frossling N (1938) "On the Evaporation of Falling Drops" English Translation AERE Harwell (1978)
35. Fuchs NA (1959) "Evaporation & Droplet Growth in Gaseous Media" Pergamon Press, London
36. Furuta T, Okazaki M & Toei R (1985) *Drying* 85 338-344 Hemisphere Publishing
37. Furuta T, Okazaki M, Toei R & Crosby EJ (1982) *Drying* 82 157-164 Hemisphere Publishing
38. Furuta T, Tsujimoto S, Okazaki M & Toei R (1984) *Drying Technology* 2:3;311-327
39. Ganetsos G (1990) Undergraduate Lab Handbook Chem Eng Dept Aston University Birmingham England (unpublished)
40. Garner FH & Suckling RD (1958) *AIChEJ* 4:1;114
41. Genskow LR (1988) *Drying* 88 KL63-KL69 6th Int Drying Symp, Versailles, France
42. Githinji PM (1980) *Drying* 80 Vol 2 478-484
43. Goldblith SA, Rey L, & Rothmayr WW (1975) "Freeze Drying & Advanced Food Technology" Academic Press

44. Greenwald CG & King CJ (1982) AIChEJ Symp Series 218:78;101-110
45. Hassan HM & Mumford CJ (1993) Drying Technnology 11:7; 1751-1764
46. Hassan HM & Mumford CJ (1993) Drying Technology 11:7;1165-1782
47. Hassan HM & Mumford CJ (1993) Drying Technology 11:7;1713-1750
48. Hassan HM (1991) PhD Thesis Aston University Birmingham England
49. Heath HB (1985) Food Feb 1985 21-25
50. Heimann W (1980) "Fundamentals of Food Chemistry" Ellis-Horwood Publishers
51. Higbie R (1935) Trans Am Inst Chem Eng 31;365
52. Hoffman TW & Gauvin WH (1960) Can J Chem Eng 129
53. Hsu NT, Sato K & Sage BH (1954) Ind Eng Chem 46;870
54. Inglett GE, Gelbman P & Reineccius GA (1988) ACS Symp Ser 370 29-36
55. James AJ & Martin AJP (1952) Analyst 77; 915
56. Karel M & Flink JM (1983) in "Advances in Drying" AS Mujumdar (editor) Vol 2 103-153
57. Karel M (1988) in " Preconcentration & Drying of Food Materials" S Bruin (editor) Elsevier Publishing
58. Karpov AM & Ulunev AA (1982) Drying of Microbiological Synthesis Products
59. Keey RB (1978) "Introduction to Industrial Drying Operations" Pergamon Press

60. Kerkhof PJAM & Thijssen HAC (1974) *J Food Technol* 4:9;415-423
61. Kieckbusch TG & King CJ (1980) *AIChEJ* 26:5;718-725
62. KimHa J & Reineccius GA (1988) *Perfumer & Flavorist* 13:4;1-4
63. Kinard GE, Manning FS & Manning WP (1963) *Brit Chem Eng* 8;326
64. Kincaid RJ (1987) in "Instrumental Analysis" 212-246 (see ref 21)
65. King CJ (1971) "Freeze Drying of Foods" CRC Press Cleveland Ohio
66. King CJ (1974) in "Advances in Preconc & Dehydration of Foods" A Spicer (editor) *Applied Science* 435-487
67. King CJ (1985) *Drying* 85 59-66 Hemisphere Publishing
68. King CJ (1988) in "Preconcentration & Drying of Food Materials" S Bruin (editor) Elsevier Publishing 147-162
69. King CJ (1990) *Chem Eng Prog* (June) 33-39
70. Kinzer GD & R Gunn (1951) *J Meteor* 81:71
71. Kirby CJ (1990) *Chemistry in Britain* 26:9;847-850
72. Kjaergaard OG (1974) in "Advances in Preconcentration & Dehydration of Foods" A Spicer (editor) *Applied Science* 321-347
73. Lambert P (1992) Personal Communication (Aston University)
74. Langstroth GO, Diehl CH & Winhold EL (1950) *Can J Res* 24A;580
75. Lee CY (1992) in "Encyclopedia of Food Sci & Tech" YH Yui (editor) Wiley-Interscience pages 223-230
76. Lee K & Riley DJ (1968) *J Heat Transfer*;445
77. Lewis WK (1921) *Ind Eng Chem* 13;427

78. Liapis AJ *Drying* 80 Vol 2;224 Hemisphere Publishing
79. Liou JK, Luyben KChAM & Bruin S (1985) *Biotech & Bioeng* 27;109-116
80. Lochmuller CH (1987) in "Instrumental Analysis" 728-764 (see ref 21)
81. Lorian V (1991) "Antibiotics in Laboratory Medicine" 3rd edition Williams & Wilkins Publishers
82. Lyons DW, Hatcher JD, & Sunderland JE (1972) *J Heat Mass Transfer* 15:897-905
83. Mackey BM (1984) *Soc Appl Bacteriology Symp Ser* 12;45-75
84. Majors RE (1987) in "Instrumental Analysis" 658-727 (see ref 21)
85. Marshall WR Jr (1955) *Trans Am Soc Mech Eng* 77;1377
86. Martin AJP & Synge RLM (1941) *Biochem* 35;1358
87. Masters K (1988/1991) "Spray Drying Handbook" 5th edition Longman Scientific
88. Maxwell JC (1890) *Collected Scientific Papers* Cambridge 11;625
89. Mellor JD (1978) "Fundamentals of Freeze Drying" Academic Press
90. Menon AS & Mujumdar AS (1987) in "Handbook of Industrial Drying" 3-46 AS Mujumdar (editor) Marcell-Decker
91. Menting LC, Hoogstag B & Thijssen HAC (1970) *AIChE Symp Ser* 163: 73; 122-24
92. Miura T, S Ohtani & S Maeda (1980) in "Drying 80" Vol 1 Hemisphere Publishing
93. Mujumdar AS (1980) *Drying* 80 Vol 1 Hemisphere Publishing

94. Nesic, S (1988) 6th Int Drying Symp (Drying '88) Versailles France
95. Neu HC (1991) in "Antibiotics in Laboratory Medicine" 3rd edition Williams & Wilkins 714-722
96. Newman AB (1931) Trans Am Inst Chem Eng 27;203
97. Oteng-Attakora (1995) PhD Thesis Aston University Birmingham, England
98. Pace CN (1983) J Am Oil Chem Soc 60;970-975
99. Pei DCT & Gauvin WH (1963) AIChEJ 9:3;375
100. Pei DCT, Narasimhan C & Gauvin WH (1962) Proc Chem Eng 243
101. Perry RH & Chilton CH (1974) Chemical Engineers Handbook 5th edition McGraw Hill
102. Raff AM, Robinson MJ & Svedres EJ (1961) Pharm Sci 50:1;76
103. Randall RC, Phillips GO & Williams PA (1989) in "Food Colloids" Royal Soc Chem pages 386-390
104. Ranz WE & WR Marshall Jr (1952) Chem Eng Prog 48:3;141
105. Ranz WE (1956) Trans Am Soc Mech Eng 78;909
106. Reineccius GA, Anandaram S & Bangs WE (1982) Perfumer & Flavourist Vol 7 Aug/Sept 1982 pages 44-49
107. Rowe TWG & Snowman JW (1978) "Edwards Freeze Drying Handbook" Edwards High Vacuum, Sussex, England
108. Rowe PN, Claxton KT & Lewis JB (1965) Trans Inst Chem Eng 43; T14-T31
109. Rulkens WH & Thijssen HAC (1972) J Food Technol 1:7;95-105

110. Sano Y & Keey RB (1982) Chem Eng Sci 37:6;881-889
111. Schiffman RF (1987) in "Handbook of Industrial Drying" 327-356 AS Mujumdar (editor) Marcell-Decker
112. Schlunder EU (1982) "Handbook of Heat Exchanger Design" Schlunder *et. al.* (editors) Hemisphere Publishing
113. Sherwood TK (1921) Trans Am Inst Chem Eng 13;427
114. Skoog DA & West DM (1986) "Fundamentals of Analytical Chemistry" Saunders Publishing
115. Slichter CS (1897) US Geol Survey 19th Annual Report (1897-98) Part 2, 301
116. Snyder LR & Kirkland JJ (1979) in "Introduction to Modern Chromatography" 2nd edition Wiley-Interscience
117. Steinberger RL & Treybal RE (1960) AIChEJ 6;227
118. Strumillo C & Kudra T (1986) "Drying: Principles, Applications and Design" Gordon & Breach Science Publishers
119. Strumillo C, Grabowski S, Zbicinski I & Bartczak Z (1988) Drying 88 OP515-OP522 6th Int Drying Symp Versailles, France
120. Stuchley AA & Stuchley MA (1983) in "Advances in Drying" volume 2 53-70 Hemisphere Publishing
121. Sud D & Woollatt S (1993) Final Year Project Aston University Birmingham England (unpublished work)
122. Sunkel JM & King CJ (1993) ACS 32:10;2357-2364
123. Takeuchi H, Handa T & Kawashima Y (1989) Drug Dev Ind Pharm 15:12;1999-2016

References

124. Taylor G & Hoare M (1988) Drying 88 OP617-OP623 6th Int Drying Symp, Versailles France
125. Thijssen HAC (1970) 4th Colloq Inst Chim Cafes Verts, 108-117
126. Thijssen HAC (1974) in "Advances in Preconcentration & Dehydration of Foods" A Spicer (editor) Applied Science
127. Toei R & Furuta T (1982) AIChE Symp Ser 78:218;111
128. Toei R, Okazaki M, Kubota K, Ohaski K & Mizata K (1966) Jap Chem Eng 30;43
129. Toor HL & Marchello JM (1958) AIChEJ 4;29
130. Trommelen AM & Crosby EJ (1970) AIChEJ 16:5;857
131. Tsubouchi T & Sato S (1960) Chem Eng Prog Symp Ser 56:269;285
132. Tsujimoto S, Nishikawa M, Furuta T, Okazaki M & Toei R (1985) Drying 85 230-235 Hemisphere Publishing
133. van Brackel J (1980) in "Advances in Drying" Vol.2 AS Mujumdar (editor) 217-268 Hemisphere Publishing
134. van der Bruel AMR, Jenneskens PJ & Mol JJ (1971) Neth Milk Dairy J 25;19-30
135. Verderber PA & King CJ (1992) Drying Technology 11:7;875-891
136. Vidgren P, Vidgren M & Paronen P (1989) Acta Pharm Fenn 98:1;71-78
137. Vidgren M, Vidgren P, Uotila J & Paronen P (1988) Acta Pharm Fenn 97;1870195
138. Walton DE (1994) PhD Thesis Aston University Birmingham England

References

139. Ward DM, Trass O & Johnson AI (1962) *Can J Chem Eng* 40;164
140. Wasserman BP (1984) *Food Tech* 78-89
141. Whitaker JR (1980) in "Enzymes: Interface Between Technology & Economics" JP Dahey & B Wolnak (editors) Marcell-Decker 53-73
142. White J (1973) *Trans Int Microwave Power Inst* 1:40-61
143. Whitfield FB (1992) *Crit Rev Food Sci & Nut* 31:1;1-58
144. Whitman WG (1923) *Chem Eng* 29;147
145. Wiljhuisen AE, Kerkhof PJAM & Bruin S (1979) *Chem Eng Sci* 34;651-660
146. Yada RY, Jackman RL & Smith JL (1992) in "Encyclopedia of Food Sci & Tech" YH Yui (editor) Wiley-Interscience pages 2191-2202
147. Yamamoto S & Sano Y (1992) *Chem Eng Sci* 47:1;177-183
148. Yamamoto S, Okazaki M, Hideo N, & Sano Y (1985) in *Drying* 85 Hemisphere Publishing
149. Yuge T (1960) *Trans Am Soc Mech Eng* 82:series C;214
150. Zakarian JA & King CJ (1982) *Ind Eng Chem Process Dev Des* 21:1;107-113
151. Zaks A & Klibanov AM (1984) *Science* 224:1249-1251

12: Appendices

12.1. Appendix A - Air/water system properties

Some properties of the air - water system, necessary to understand how the drying gases remove the moisture from a drying solid, are listed below:

Humidity, H , is the mass of water carried per unit mass of dry air.

$$H = \frac{\text{kmol of water vapour}}{\text{kmol dry air}} = \frac{P_W}{P - P_W} \cdot \frac{M_W}{M_A}$$

where P_W is the partial pressure of water vapour, P is the total pressure, M_A is the molecular mass of air, and M_W is the molecular mass of water.

The relationship between H and P_W , given by Coulson & Richardson, is:

$$H = \frac{18 P_W}{29 (P - P_W)}$$

Humidity of saturated air, H_o , is the humidity of the air when saturated with water vapour. The air is in equilibrium with water at the given temperature and pressure.

$$\% \text{humidity} = (\text{humidity of air} / \text{humidity of saturated air}) 100\% = (H/H_o) 100\%$$

$$\% \text{ relative humidity} = (\text{partial pressure of water vapour in air} / \text{vapour pressure of water at the same temperature}) 100\%$$

Humid volume, the volume of unit mass of dry air and associated vapour, at atmospheric pressure is

$$(22.4 / 29) (T / 273) + (22.4 / 18) (H) (T / 273) \text{ m}^3/\text{kg}$$

where T is in degrees K.

Saturated volume is the volume of unit mass of dry air together with the water vapour required to saturate it.

Humid heat is the heat required to raise unit mass of dry air and the associated moisture vapour through 1 degree K at constant pressure ($= 1 + 1.88H \text{ kJ} / \text{kg K}$)

Dew point is the temperature at which condensation will first occur when air is cooled.

Wet bulb temperature - If a stream of air flows rapidly over the surface of water, vaporisation occurs (if the water temperature is above the dew point of air). The temperature of water falls and heat flows from the air to the water. If the surface is small enough for the condition of the air to change inappreciably, and if the air velocity is in excess of 5 m/s, the water reaches the wet bulb temperature θ_w at equilibrium.

12.2. Appendix B - Material specification sheets

12/09/94 11:04AM Sigma Chemical Co

PAGE (

ASTON UNIVERSITY
CHEMICAL ENGINEERING
ATTN: A SAYAD



DATE: 12/09/94

SPECIFICATION

PRODUCT NAME: AMPICILLIN TRIHYDRATE

PRODUCT NUMBER: A6140

FORMULA: $C_{16}H_{19}N_3O_4S \cdot 3H_2O$

FORMULA WEIGHT: 403.4

APPEARANCE WHITE TO WHITE WITH A FAINT YELLOW
CAST POWDER

SOLUBILITY CLEAR COLORLESS TO FAINT YELLOW
SOLUTION AT 200 MG PLUS 4 ML OF
1 M HYDROCHLORIC ACID

WATER CONTENT BY NOT MORE THAN 15.0%
KARL FISCHER

ELEMENTAL ANALYSIS 46.7 TO 48.6% CARBON
10.1 TO 10.7% NITROGEN

PURITY BY PERCHLORIC NOT LESS THAN 98%
ACID TITRATION

APPROVED HAM 12/11/92

JEFFREY HOWARD, PH.D.
ANALYTICAL DEPARTMENT
390/941209#1/MXC3

SIGMA WARRANTS THAT THIS PRODUCT WILL CONFORM TO THE ABOVE INFORMATION WHICH IS APPLICABLE AT THIS TIME. WHEN ORDERED, PURCHASER SHOULD ASK FOR SPECIFIC INFORMATION FOR THE LOT NUMBER OF THE PRODUCT ACTUALLY PROVIDED. PURCHASER MUST DETERMINE THE SUITABILITY OF THE PRODUCT FOR ITS PARTICULAR USE. SEE REVERSE SIDE OF INVOICE OR PACKING SLIP FOR ADDITIONAL TERMS AND CONDITIONS OF SALE.

----P.O. BOX 14508, ST. LOUIS, MO 63178 USA PHONE: 1-800-325-5832----

1 OF 1

12/09/94 01:18PM Sigma Chemical Co

PAGE 1

ASTON UNIVERSITY
CHEMICAL ENGINEERING
ATTN: A SAYAD



DATE: 12/09/94

SPECIFICATION

PRODUCT NAME: AMPICILLIN TRIHYDRATE

PRODUCT NUMBER: A6140

FORMULA: $C_{16}H_{19}N_3O_4S \cdot 3H_2O$

FORMULA WEIGHT: 403.4

APPEARANCE	WHITE TO WHITE WITH A FAINT YELLOW CAST POWDER
SOLUBILITY	CLEAR COLORLESS TO FAINT YELLOW SOLUTION AT 200 MG PLUS 4 ML OF 1 M HYDROCHLORIC ACID
WATER CONTENT BY KARL FISCHER	NOT MORE THAN 15.0%
ELEMENTAL ANALYSIS	46.7 TO 48.6% CARBON 10.1 TO 10.7% NITROGEN
PURITY BY PERCHLORIC ACID TITRATION	NOT LESS THAN 98%

APPROVED HAM 12/11/92

Jeffrey Howard

JEFFREY HOWARD, PH.D.
ANALYTICAL DEPARTMENT
390/941209#1/AMK1

SIGMA WARRANTS THAT THIS PRODUCT WILL CONFORM TO THE ABOVE INFORMATION WHICH IS APPLICABLE AT THIS TIME. WHEN ORDERED, PURCHASER SHOULD ASK FOR SPECIFIC INFORMATION FOR THE LOT NUMBER OF THE PRODUCT ACTUALLY PROVIDED. PURCHASER MUST DETERMINE THE SUITABILITY OF THE PRODUCT FOR ITS PARTICULAR USE. SEE REVERSE SIDE OF INVOICE OR PACKING SLIP FOR ADDITIONAL TERMS AND CONDITIONS OF SALE.

-----P.O. BOX 14508, ST. LOUIS, MO 63178 USA PHONE: 1-800-325-5832----

1 OF 8

12/09/94 01:19PM Sigma Chemical Co

PAGE 1

ASTON UNIVERSITY
CHEMICAL ENGINEERING
ATTN: A SAYAD



DATE: 12/09/94

SPECIFICATION

PRODUCT NAME: STREPTOMYCIN SULFATE

PRODUCT NUMBER: S6501

FORMULA: $(C_{21}H_{39}N_7O_{12})_2 \cdot 3H_2SO_4$

FORMULA WEIGHT: 1457.4

APPEARANCE WHITE TO WHITE WITH A LIGHT YELLOW
 CAST POWDER

SOLUBILITY CLEAR COLORLESS TO LIGHT YELLOW
 SOLUTION AT 50 MG/ML IN WATER

MOISTURE CONTENT NOT MORE THAN 8%

ELEMENTAL ANALYSIS 33.6 TO 35.7% CARBON **
 13.1 TO 13.9% NITROGEN **
 ** ANHYDROUS BASIS

PURITY BY THIN LAYER
CHROMATOGRAPHY NOT LESS THAN 98%

POTENCY * NOT LESS THAN 730 UNITS/MG
 * SUPPLIER INFORMATION.

APPROVED DLT 8/18/89

REVISED HAM 4/7/92

Jeffrey Howard

JEFFREY HOWARD, PH.D.
ANALYTICAL DEPARTMENT
390/941209#1/AMK1

CONTINUED ON NEXT PAGE-----

2 OF 8

12/09/94 01:20PM Sigma Chemical Co

PAGE 1

ASTON UNIVERSITY
CHEMICAL ENGINEERING
ATTN: A SAYAD



DATE: 12/09/94

SPECIFICATION

PRODUCT NAME: TETRACYCLINE FREE BASE

PRODUCT NUMBER: T3258

FORMULA: $C_{22}H_{24}N_2O_8$

FORMULA WEIGHT: 444.4

APPEARANCE	YELLOW TO YELLOW WITH A BROWN CAST POWDER
SOLUBILITY	CLEAR TO SLIGHTLY HAZY YELLOW TO ORANGE-BROWN SOLUTION AT 200 MG PLUS 4 ML OF 1 M HYDROCHLORIC ACID
WATER CONTENT BY KARL FISCHER	NOT MORE THAN 13.0% (4 MOLES/MOLE)
PURITY BY THIN LAYER CHROMATOGRAPHY	NOT LESS THAN 98%

APPROVED HAM 5/19/92

REVISED JLH 4/23/93

Jeffrey Howard

JEFFREY HOWARD, PH.D.
ANALYTICAL DEPARTMENT
390/941209#1/AMK1

SIGMA WARRANTS THAT THIS PRODUCT WILL CONFORM TO THE ABOVE INFORMATION WHICH IS APPLICABLE AT THIS TIME. WHEN ORDERED, PURCHASER SHOULD ASK FOR SPECIFIC INFORMATION FOR THE LOT NUMBER OF THE PRODUCT ACTUALLY PROVIDED. PURCHASER MUST DETERMINE THE SUITABILITY OF THE PRODUCT FOR ITS PARTICULAR USE. SEE REVERSE SIDE OF INVOICE OR PACKING SLIP FOR ADDITIONAL TERMS AND CONDITIONS OF SALE.

----P.O. BOX 14508, ST. LOUIS, MO 63178 USA PHONE: 1-800-325-5832----

4 OF 8

12/09/94 01:21PM Sigma Chemical Co

PAGE 1

ASTON UNIVERSITY
CHEMICAL ENGINEERING
ATTN: A SAYAD



DATE: 12/09/94

SPECIFICATION

PRODUCT NAME: OXYTETRACYCLINE DIHYDRATE

PRODUCT NUMBER: 05750

FORMULA: $C_{22}H_{24}N_{2}O_9 \cdot 2H_2O$

FORMULA WEIGHT: 496.5

APPEARANCE	LIGHT YELLOW TO YELLOW-TAN POWDER
SOLUBILITY	CLEAR TO VERY SLIGHTLY HAZY, YELLOW TO YELLOW-ORANGE SOLUTION AT 200 MG PLUS 4.0 ML OF 1 N HYDROCHLORIC ACID
IR SPECTRUM	CONSISTENT WITH STRUCTURE
WATER CONTENT BY KARL FISCHER	6.0 TO 9.0% WATER
ELEMENTAL ANALYSIS	52.2 TO 54.2% CARBON 5.3 TO 5.9% NITROGEN
PURITY BY THIN LAYER CHROMATOGRAPHY	NOT LESS THAN 98%

APPROVED JLH 7/6/94

Jeffrey Howard

JEFFREY HOWARD, PH.D.
ANALYTICAL DEPARTMENT
390/941209#1/AMK1

SIGMA WARRANTS THAT THIS PRODUCT WILL CONFORM TO THE ABOVE INFORMATION WHICH IS APPLICABLE AT THIS TIME. WHEN ORDERED, PURCHASER SHOULD ASK FOR SPECIFIC INFORMATION FOR THE LOT NUMBER OF THE PRODUCT ACTUALLY PROVIDED. PURCHASER MUST DETERMINE THE SUITABILITY OF THE PRODUCT FOR ITS PARTICULAR USE. SEE REVERSE SIDE OF INVOICE OR PACKING SLIP FOR ADDITIONAL TERMS AND CONDITIONS OF SALE.

----P.O. BOX 14508, ST. LOUIS, MO 63178 USA PHONE: 1-800-325-5832---

5 OF 8

12/09/94 01:22PM Sigma Chemical Co

PAGE

ASTON UNIVERSITY
CHEMICAL ENGINEERING
ATTN: A SAYAD



DATE: 12/09/94

SPECIFICATION

PRODUCT NAME: CHLORAMPHENICOL

PRODUCT NUMBER: C0378

FORMULA: $C_{11}H_{12}Cl_2N_2O_5$

FORMULA WEIGHT: 323.1

APPEARANCE WHITE TO WHITE WITH A YELLOW CAST
POWDER

SOLUBILITY CLEAR, COLORLESS TO LIGHT YELLOW
SOLUTION AT 50 MG/ML IN ETHANOL

ELEMENTAL ANALYSIS 40.1% TO 41.7% CARBON
8.5% TO 9.0% NITROGEN

PURITY BY THIN LAYER CHROMATOGRAPHY NOT LESS THAN 98%

APPROVED/DLT/1-13-89

Jeffrey Howard

JEFFREY HOWARD, PH.D.
ANALYTICAL DEPARTMENT
390/941209#1/AMK1

SIGMA WARRANTS THAT THIS PRODUCT WILL CONFORM TO THE ABOVE INFORMATION WHICH IS APPLICABLE AT THIS TIME. WHEN ORDERED, PURCHASER SHOULD ASK FOR SPECIFIC INFORMATION FOR THE LOT NUMBER OF THE PRODUCT ACTUALLY PROVIDED. PURCHASER MUST DETERMINE THE SUITABILITY OF THE PRODUCT FOR ITS PARTICULAR USE. SEE REVERSE SIDE OF INVOICE OR PACKING SLIP FOR ADDITIONAL TERMS AND CONDITIONS OF SALE.

----P.O. BOX 14508, ST. LOUIS, MO 63178 USA PHONE: 1-800-325-5832---

6 OF 8

12/09/94 01:23PM Sigma Chemical Co

PAGE

ASTON UNIVERSITY
CHEMICAL ENGINEERING
ATTN: A SAYAD



DATE: 12/09/94

SPECIFICATION

PRODUCT NAME: GUM ARABIC

PRODUCT NUMBER: G9752

APPEARANCE WHITE WITH A YELLOW CAST POWDER

LOSS ON DRYING NOT MORE THAN 15%

NF TESTS (NF 17):

INSOLUBLE RESIDUE	PASS
STARCH TEST	PASS
TANNIN-BEARING GUMS	PASS

APPROVED HAM 10/22/92

JEFFREY HOWARD, PH.D.
ANALYTICAL DEPARTMENT
390/941209#1/AMK1

SIGMA WARRANTS THAT THIS PRODUCT WILL CONFORM TO THE ABOVE INFORMATION WHICH IS APPLICABLE AT THIS TIME. WHEN ORDERED, PURCHASER SHOULD ASK FOR SPECIFIC INFORMATION FOR THE LOT NUMBER OF THE PRODUCT ACTUALLY PROVIDED. PURCHASER MUST DETERMINE THE SUITABILITY OF THE PRODUCT FOR ITS PARTICULAR USE. SEE REVERSE SIDE OF INVOICE OR PACKING SLIP FOR ADDITIONAL TERMS AND CONDITIONS OF SALE.

-----P.O. BOX 14508, ST. LOUIS, MO 63178 USA PHONE: 1-800-325-5832--

7 OF 8

12/09/94 01:23PM Sigma Chemical Co

PAGE 1

ASTON UNIVERSITY
CHEMICAL ENGINEERING
ATTN: A SAYAD



DATE: 12/09/94

SPECIFICATION

PRODUCT NAME: GELATIN TYPE A FROM PORCINE SKIN
APPROX. 60 BLOOM

PRODUCT NUMBER: G6144

APPEARANCE	YELLOW POWDER
SOLUBILITY	HAZY LIGHT YELLOW AT 50 MG/ML IN WATER
PROTEIN BY BIURET	APPROX. 75%
GEL APPEARANCE OF A 10% AQUEOUS GEL	FIRM HAZY YELLOW GEL

APPROVED FPG 5/25/90

Jeffrey Howard

JEFFREY HOWARD, PH.D.
ANALYTICAL DEPARTMENT
390/941209#1/AMK1

SIGMA WARRANTS THAT THIS PRODUCT WILL CONFORM TO THE ABOVE INFORMATION WHICH IS APPLICABLE AT THIS TIME. WHEN ORDERED, PURCHASER SHOULD ASK FOR SPECIFIC INFORMATION FOR THE LOT NUMBER OF THE PRODUCT ACTUALLY PROVIDED. PURCHASER MUST DETERMINE THE SUITABILITY OF THE PRODUCT FOR ITS PARTICULAR USE. SEE REVERSE SIDE OF INVOICE OR PACKING SLIP FOR ADDITIONAL TERMS AND CONDITIONS OF SALE.
---P.O. BOX 14508, ST. LOUIS, MO 63178 USA PHONE: 1-800-325-5832---

8 OF 8

5-DEC-1994 16:41 FROM MERCK LTD BDH LAB SUPP

TO

0203326284 P.02

RECEIVED 1994 DEC 16 16:41

MERCK

**THIS IS A CONTROLLED DOCUMENT
AND MUST NOT BE COPIED WITHOUT AUTHORISATION**



Aston University

Content has been removed for copyright reasons



BDH Laboratory Supplies
Merck House • Poole • Dorset • DT1 • England
Telephone 01202 610000
Fax 01202 610001
Telex 330800 BDH GB

A Division of Merck Ltd
Registered in England No. 1000000

15-DEC-1994 16:42 FROM: MERCK LTD BLM LAB SUFF

TO

0203326264 P.03

MERCK

**THIS IS A CONTROLLED DOCUMENT
AND MUST NOT BE COPIED WITHOUT AUTHORISATION**

PRODUCT MONOGRAPH

Product No. 44045



Aston University

**Content has been removed for copyright
reasons**

12.3: Appendix C: Papers submitted for publication

The following three papers have been submitted for publication to Drying Technology

Volatiles retention in the drying of skin forming materials.

Part 1: Materials which gelatinise at moderately high temperatures

Abid A Sayed*, Haydar M Hassan, & Clive J Mumford

Chemical Engineering & Applied Chemistry Dept, Aston University, Birmingham B4 7ET, England.



Pgs 413 - 425
Removed.

tion, skin

horizontal
ours under

i simulated
gas liquid
scope. The
flow rates

tent of the
centration,
rative
se in
nsion
also

s and
l the

nount
ie air
ed to

lrying
led to
se the
to the
e, but

on in
adjusted

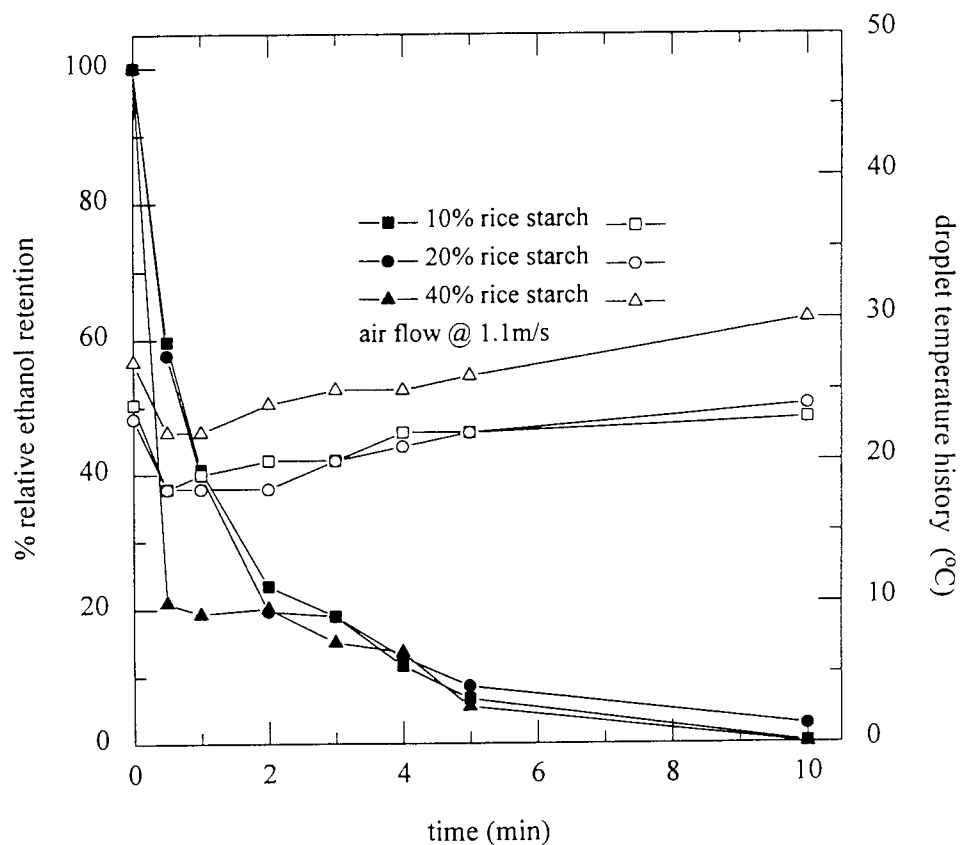


Figure 2

The effect of concentration on the retention of ethanol in rice starch solutions at ambient temperature ($T = 25^{\circ}\text{C}$); droplet temperature history is also shown (open symbols)

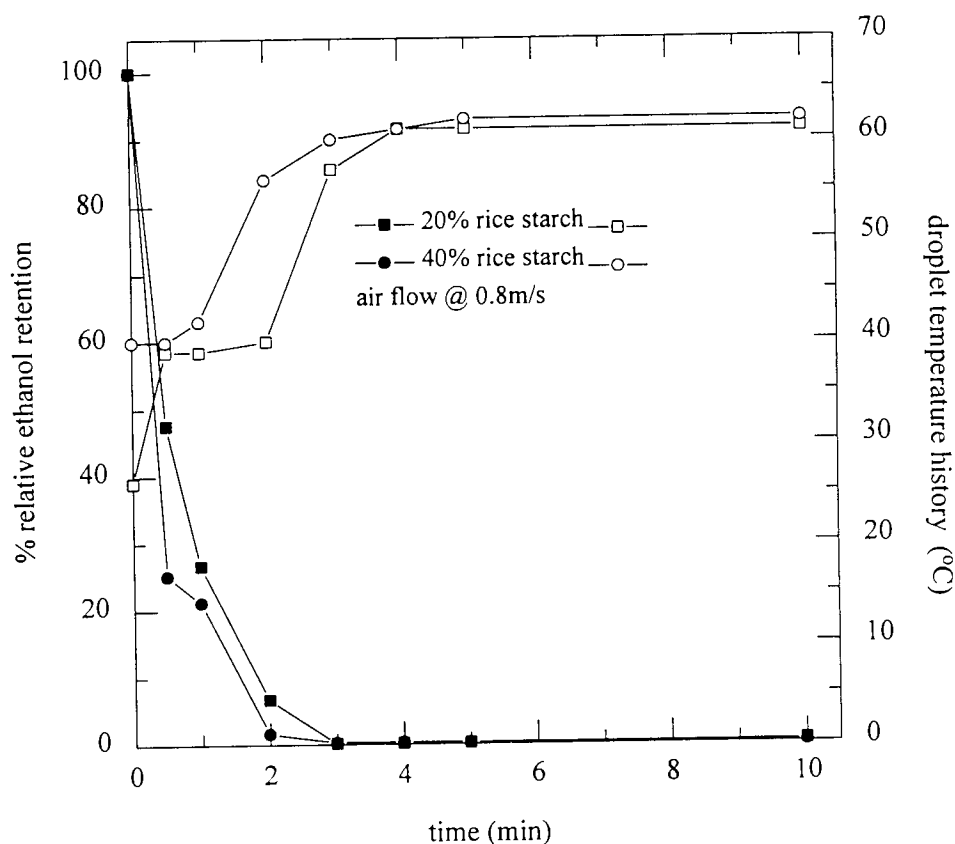


Figure 3

The effect of concentration on the retention of ethanol in rice starch solutions at $T = 62^{\circ}\text{C}$; droplet temperature history is shown (open symbols)

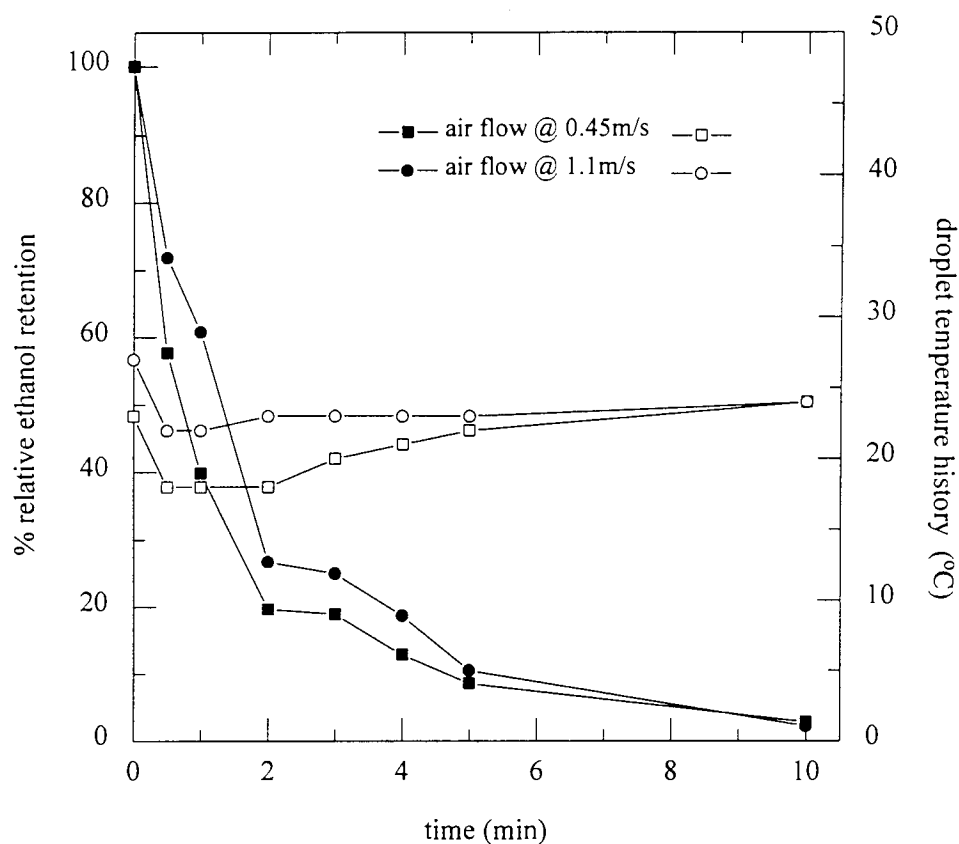


Figure 4

The effect of air flowrate on the retention of ethanol in 20% rice starch solutions at ambient temperature (25°C); droplet temperature history is shown (open symbols)

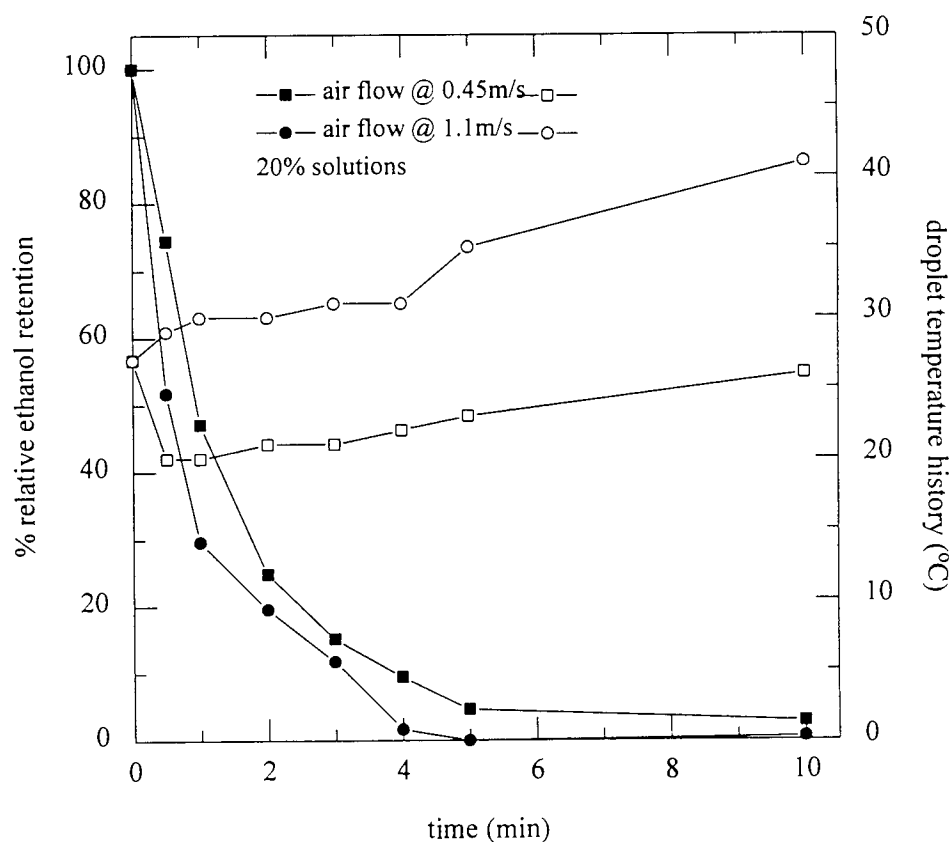


Figure 5

The effect of air flow on the retention of ethanol in rice starch solutions at 42°C; droplet temperature history is shown (open symbols)

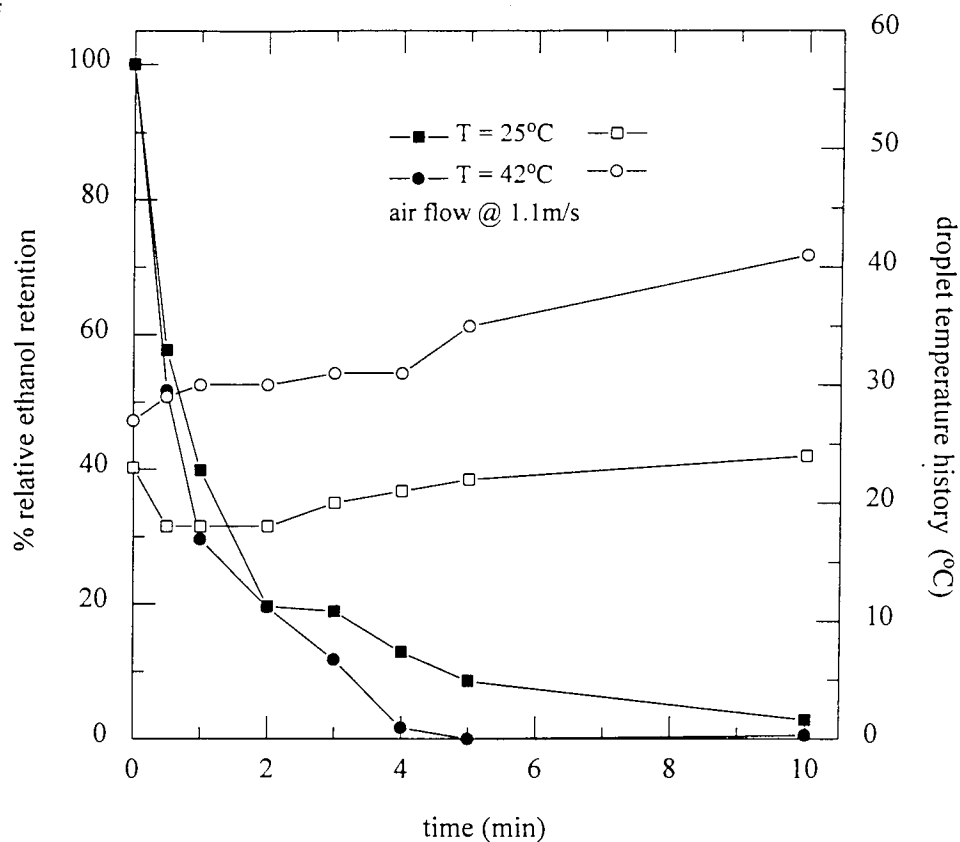


Figure 6

The effect of temperature on the retention of ethanol in 20% rice starch solutions; droplet temperature history is shown (open symbols)

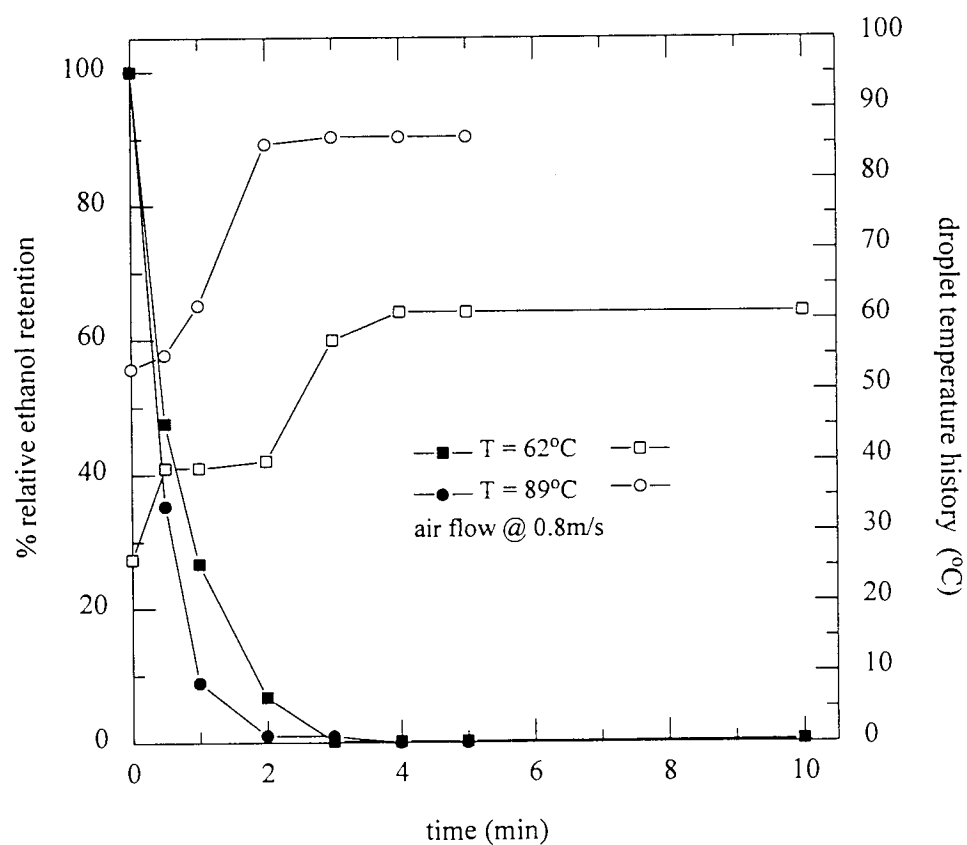


Figure 7

The effect of temperature on the retention of ethanol in 20% rice starch solutions; droplet temperature history is shown (open symbols)

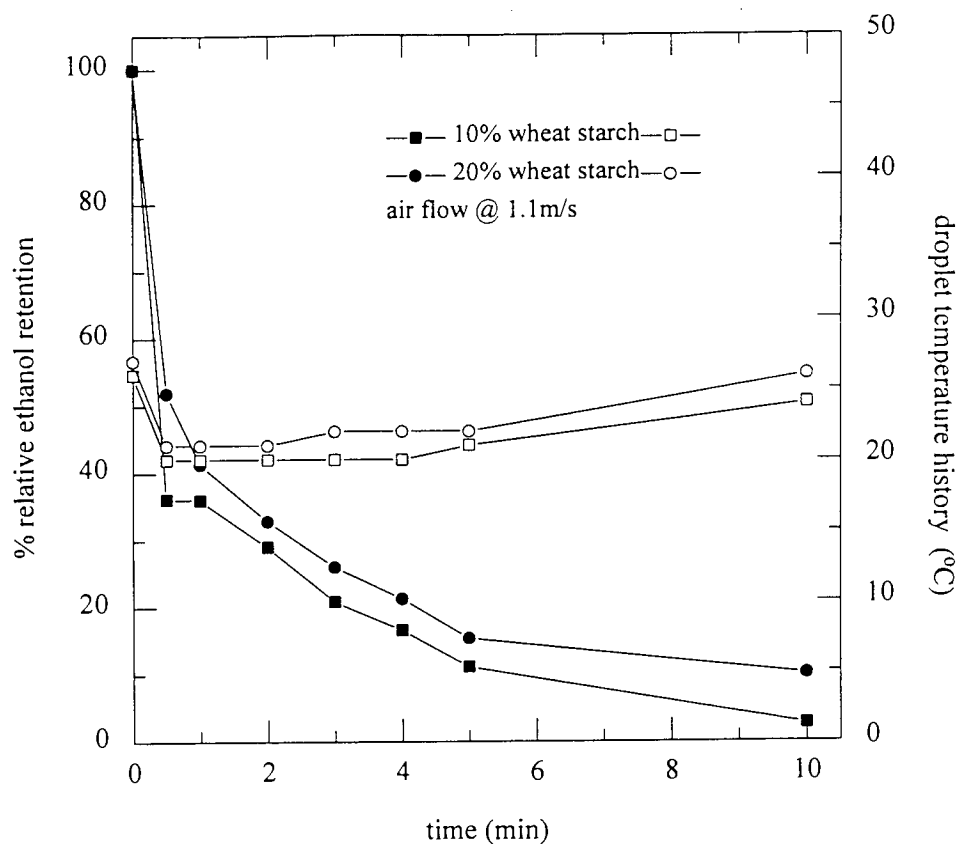


Figure 8

The effect of concentration on the retention of ethanol in wheat starch solutions at $T=25^{\circ}\text{C}$; droplet temperature history also shown (open symbols)

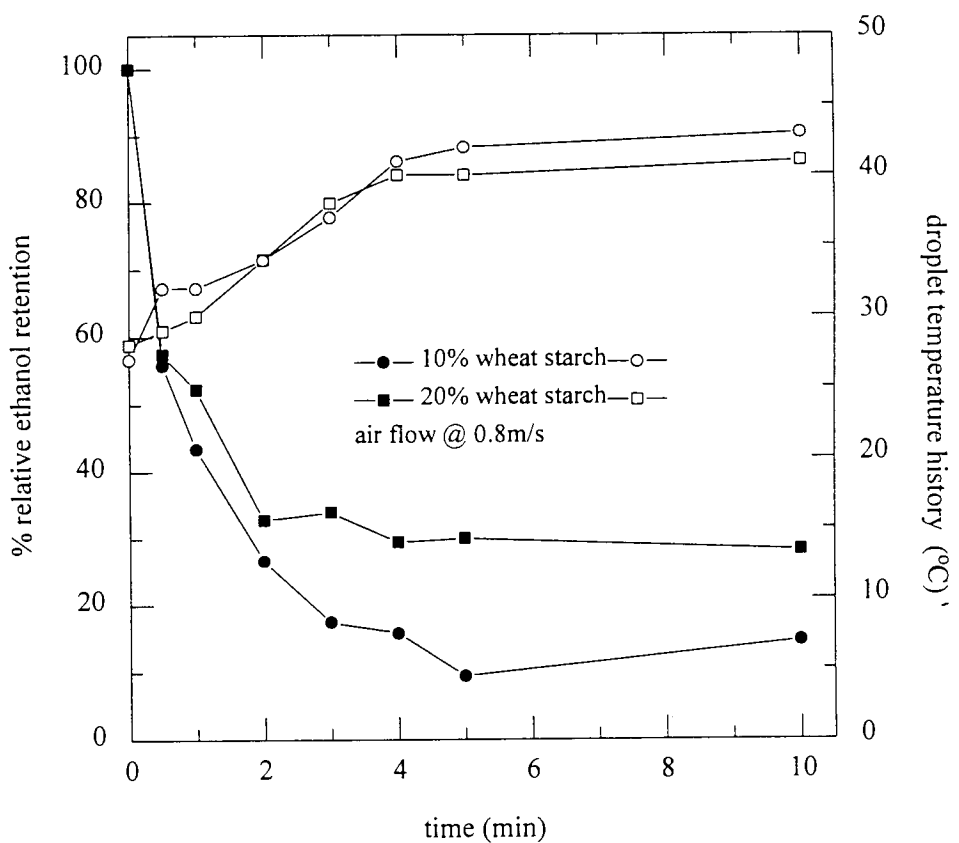


Figure 9

The effect of concentration on the retention of ethanol in wheat starch solutions at 42°C ; droplet temperature history also shown (open symbols)

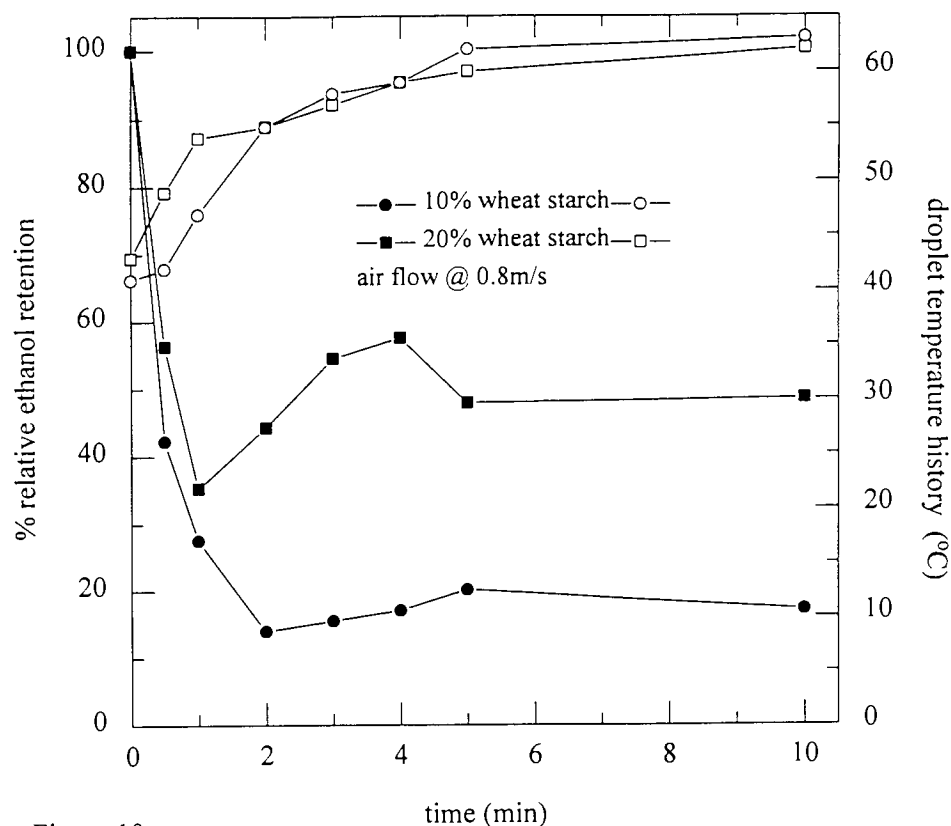


Figure 10

The effect of concentration on the retention of ethanol in wheat starch solutions at 62°C; droplet temperature history also shown (open symbols)

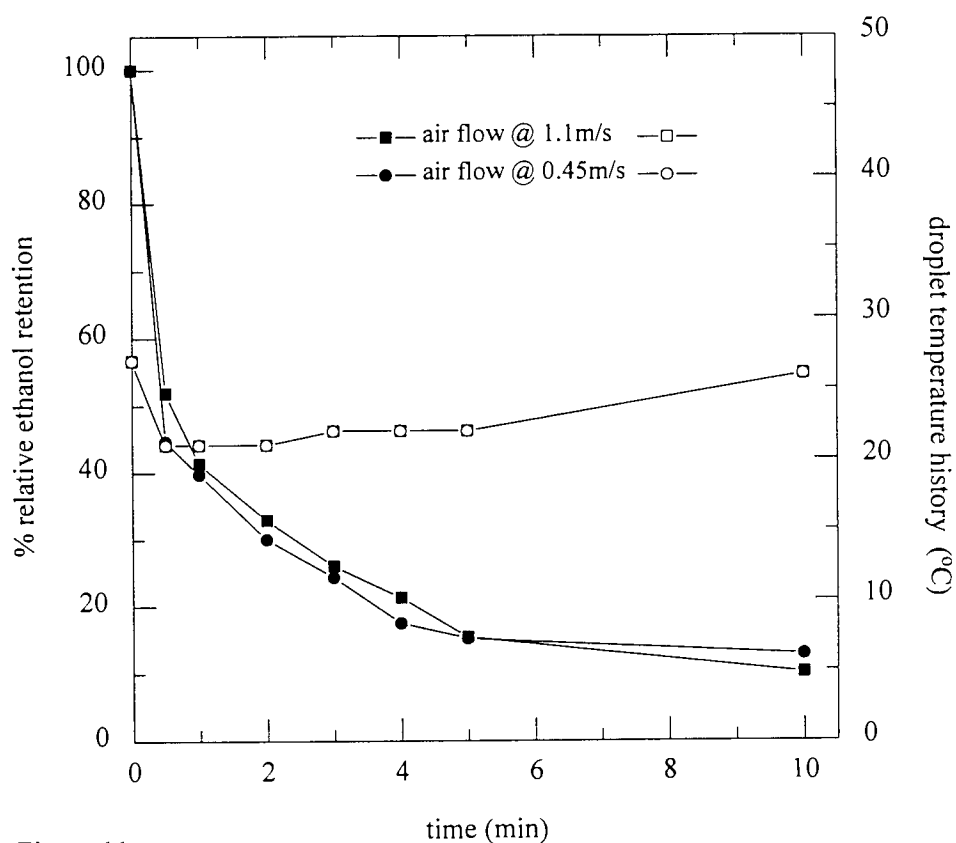


Figure 11

The effect of air flowrate on the retention of ethanol in 20% wheat starch solutions at ambient temperature ($T = 25^{\circ}\text{C}$); droplet temperature history also shown (open symbols)

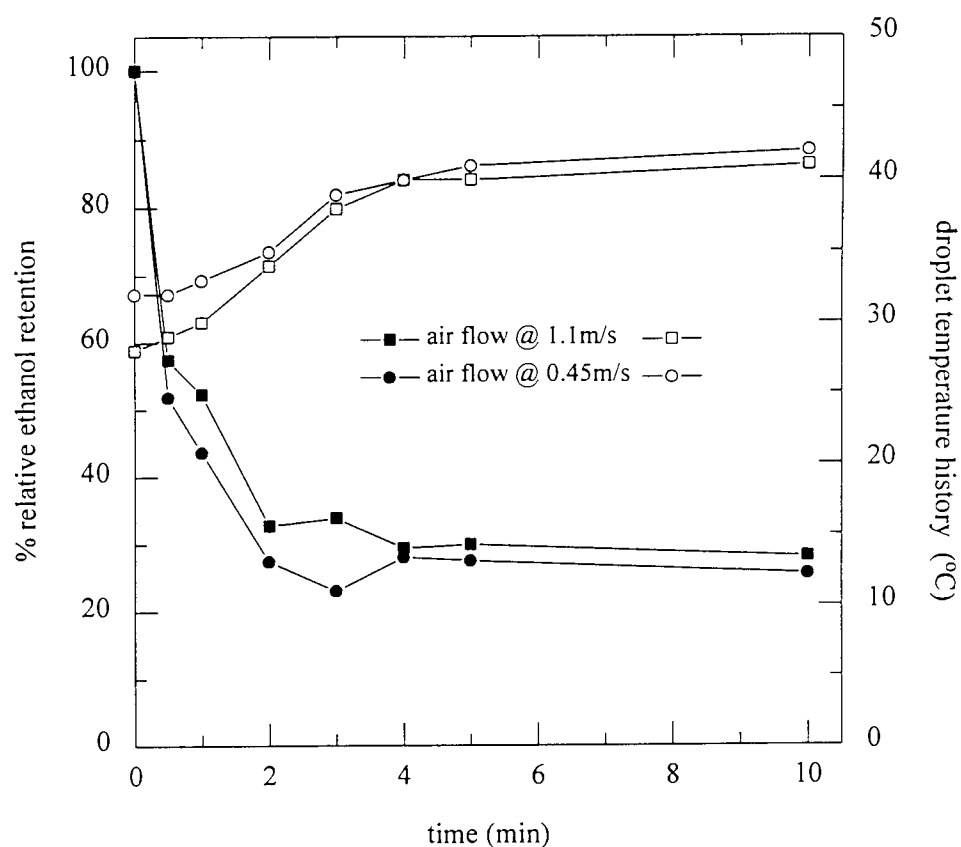


Figure 12

The effect of air flowrate on the retention of ethanol in 20% wheat starch solutions at 42°C; droplet temperature history also shown (open symbols)

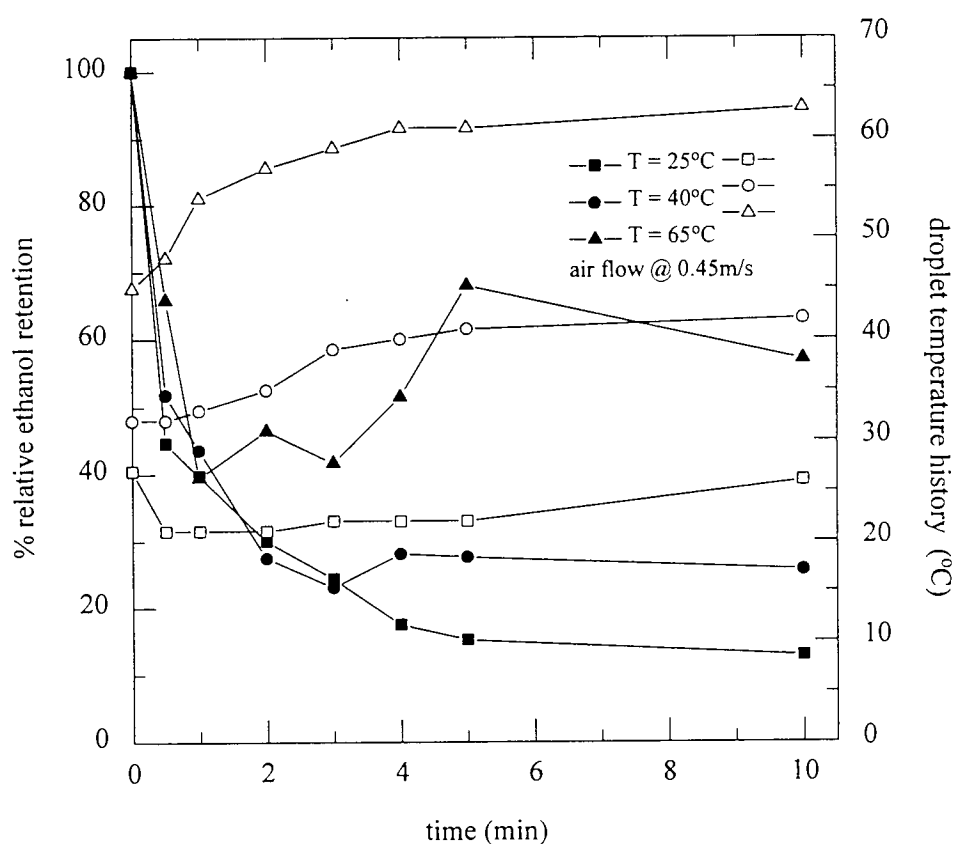


Figure 13

The effect of temperature on the retention of ethanol in 20% wheat starch solutions; droplet temperature history is also shown (open symbols)

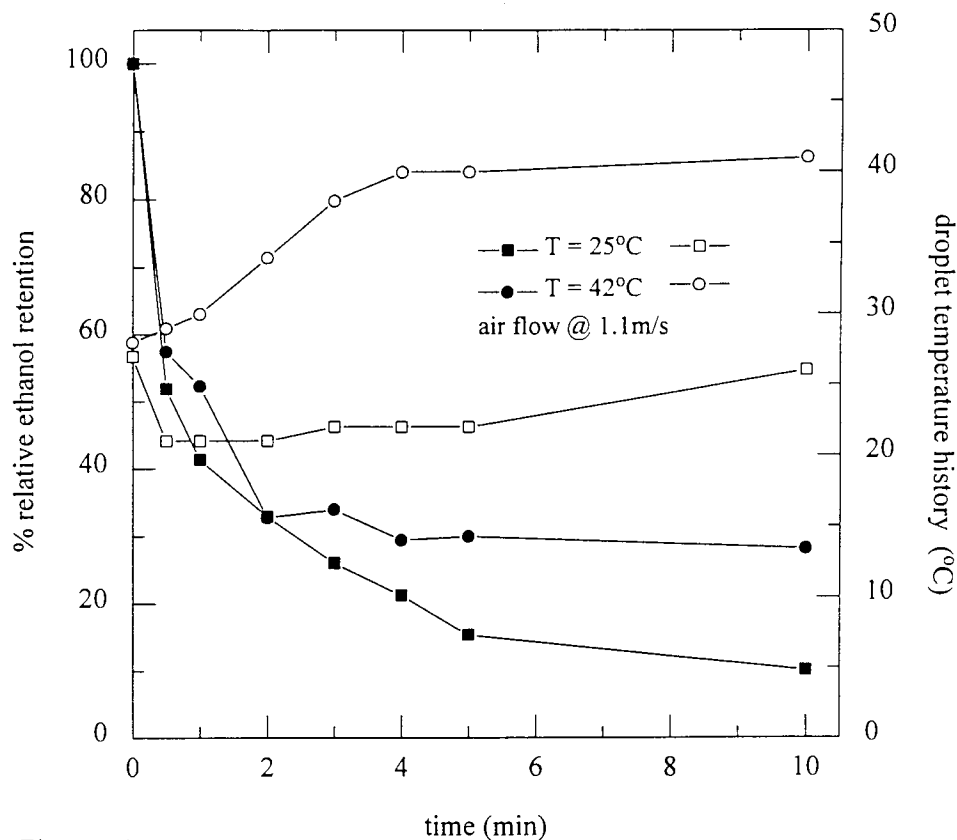


Figure 14

The effect of temperature the retention of ethanol in 20% wheat starch solutions; droplet temperature profile is also shown (open symbols)

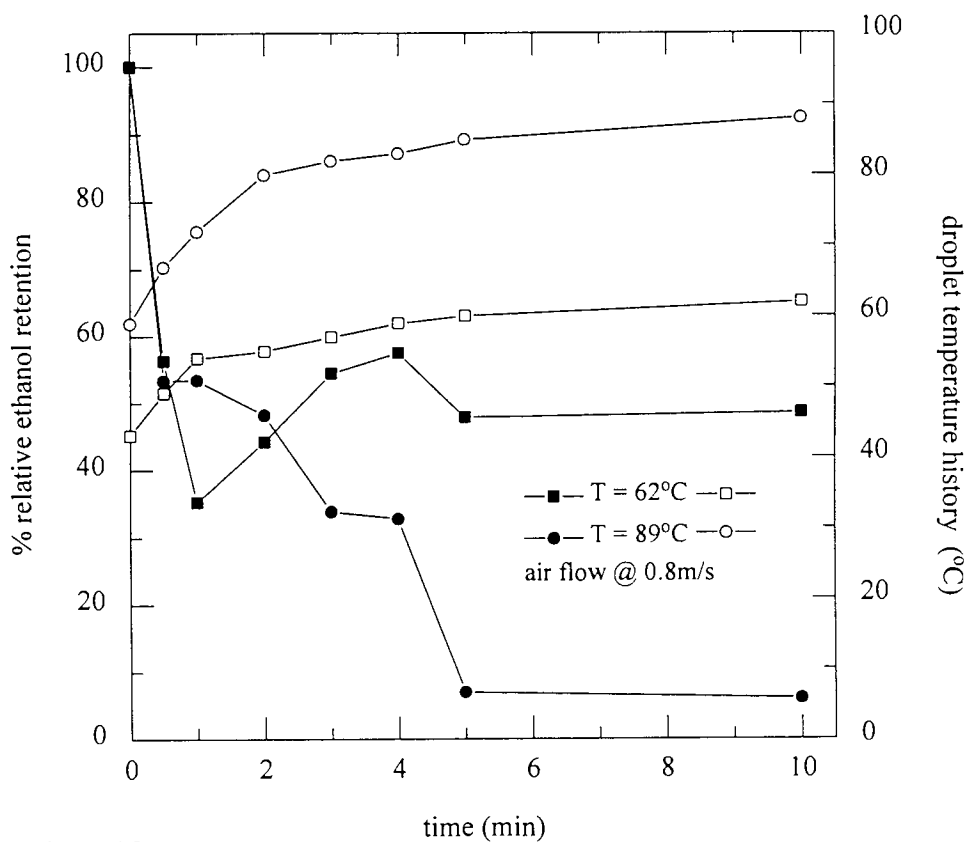


Figure 15

The effect of temperature on the retention of ethanol in 20% wheat starch solutions; droplet temperature history is also shown (open symbols)

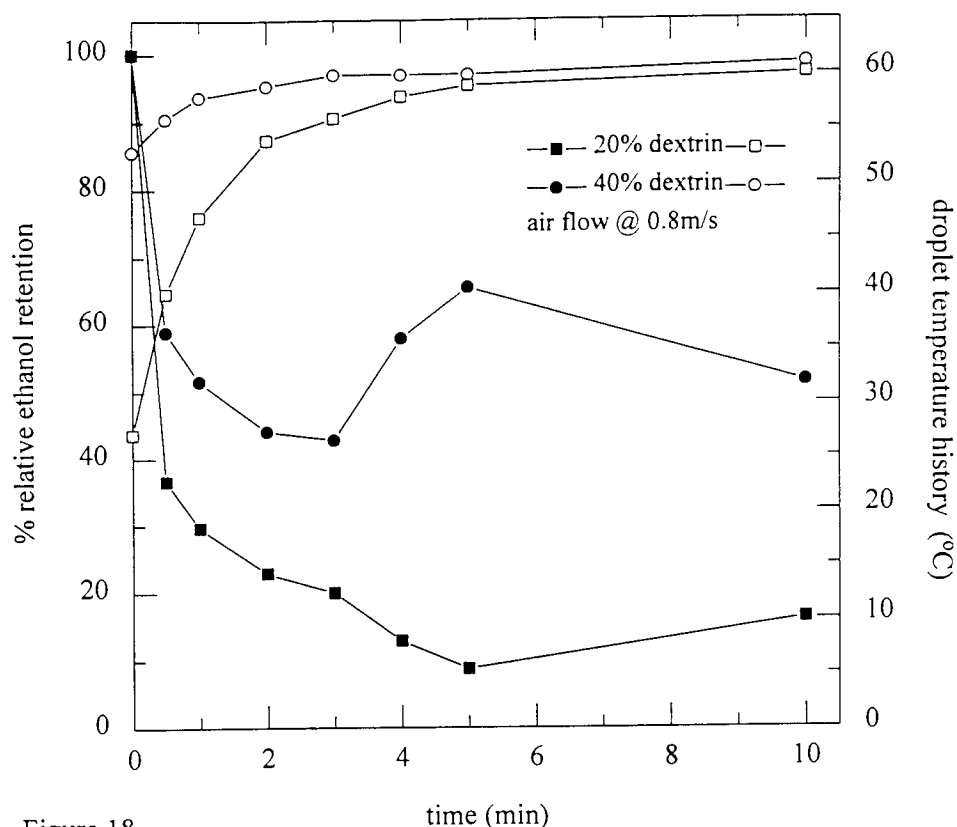


Figure 18
The effect of concentration on the retention of ethanol in dextrin solutions at 62°C; droplet temperature history is also shown (open symbols)

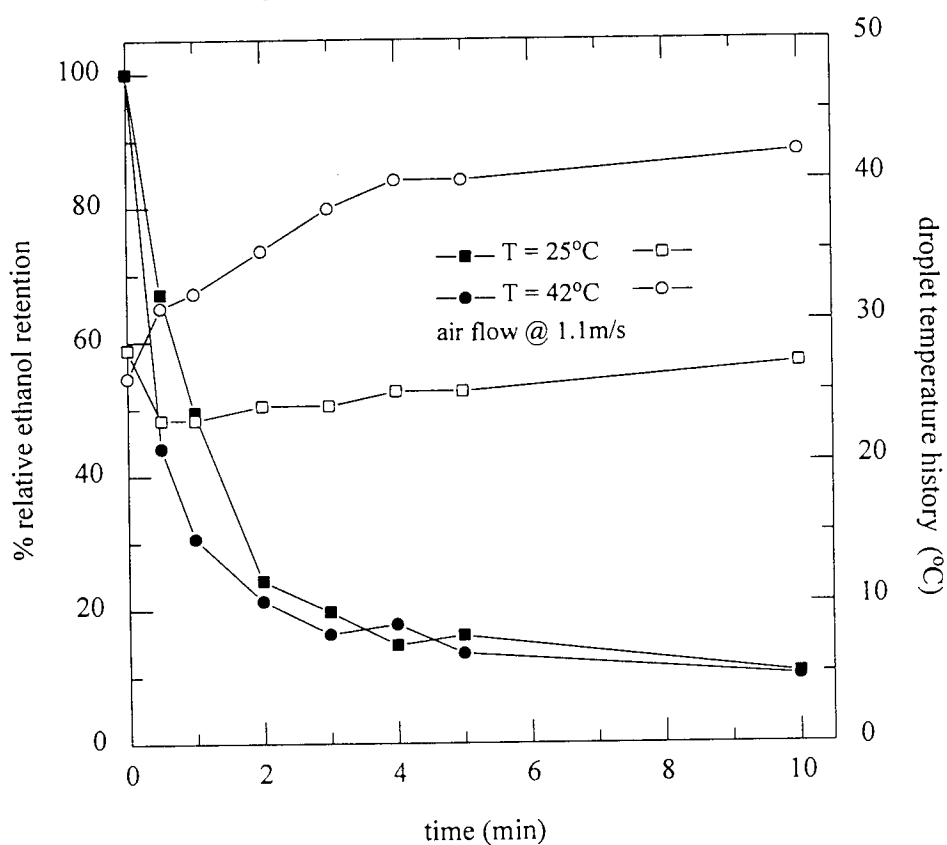


Figure 19
The effect of temperature on the retention of ethanol in 20% dextrin solutions; droplet temperature history is also shown (open symbols)

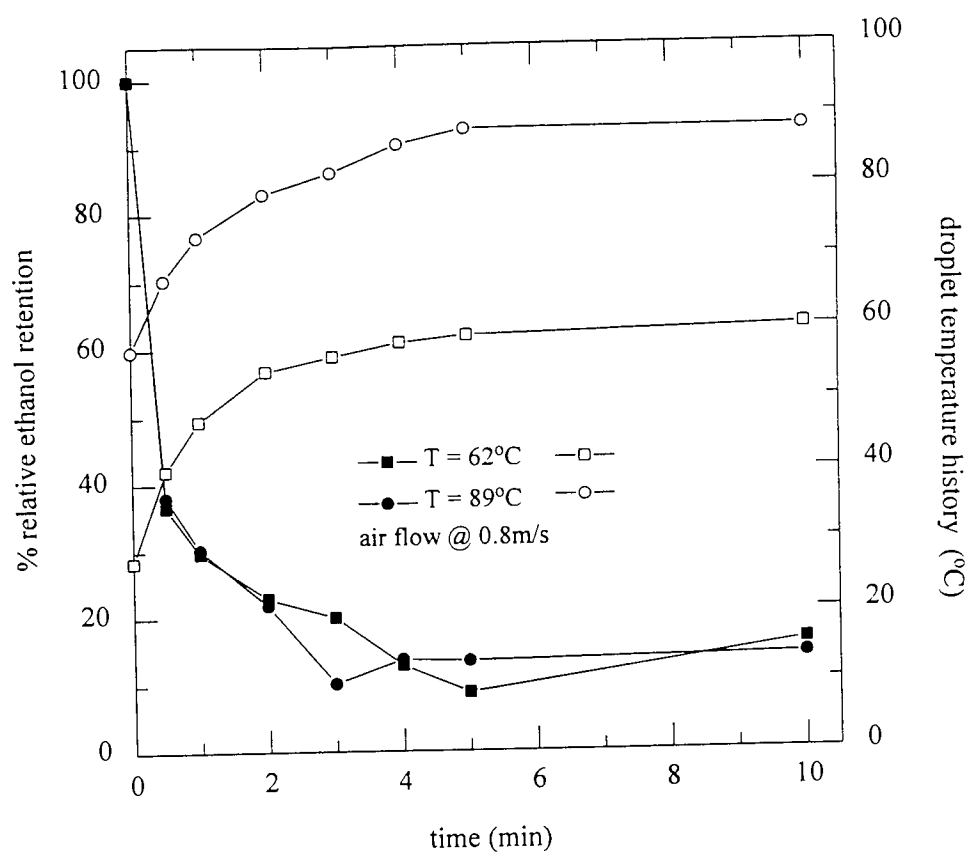


Figure 20
The effect of temperature on the retention of ethanol in 20% dextrin solutions; droplet temperature history is also shown (open symbols)

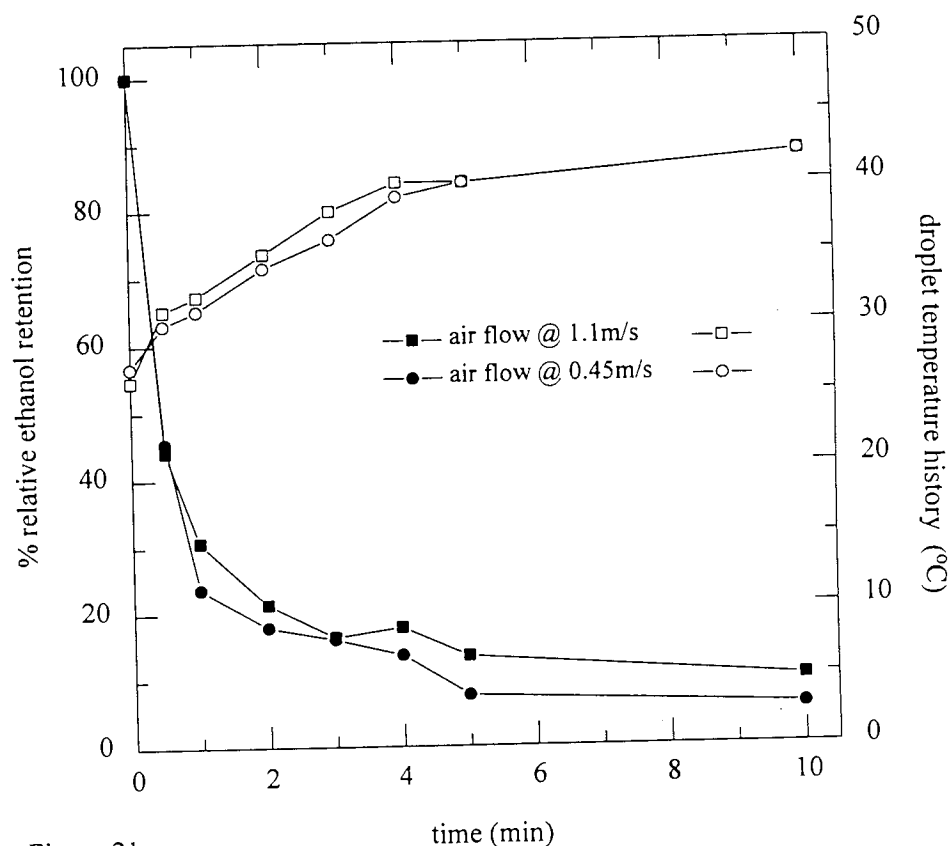


Figure 21
The effect of air flow on the retention of ethanol in 20% dextrin solutions; droplet temperature history is also shown (open symbols)

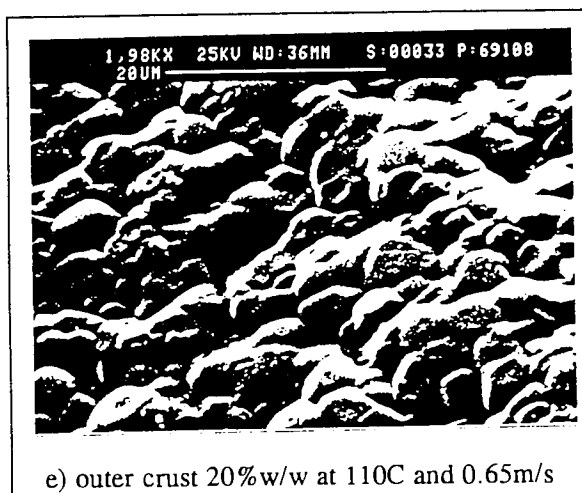
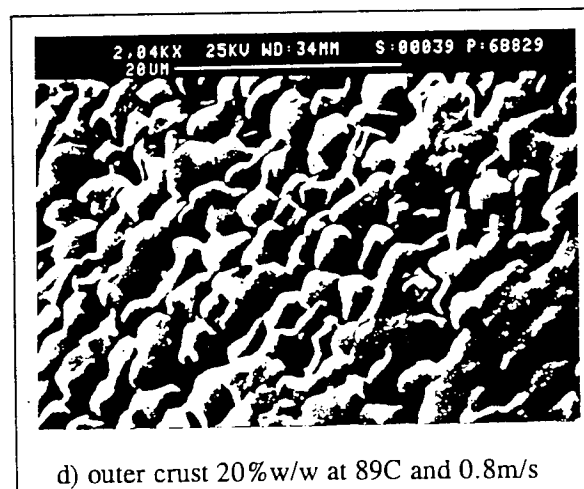
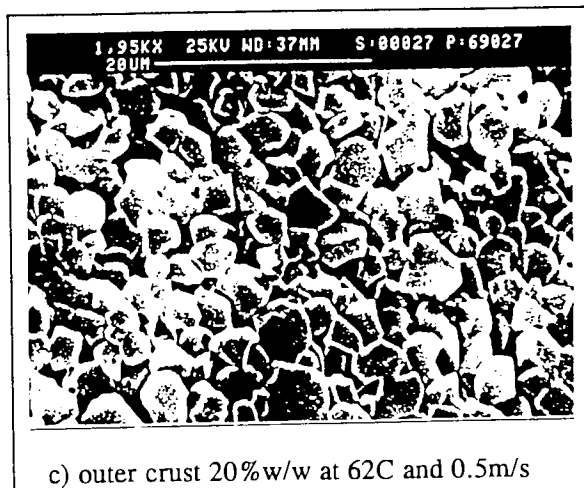
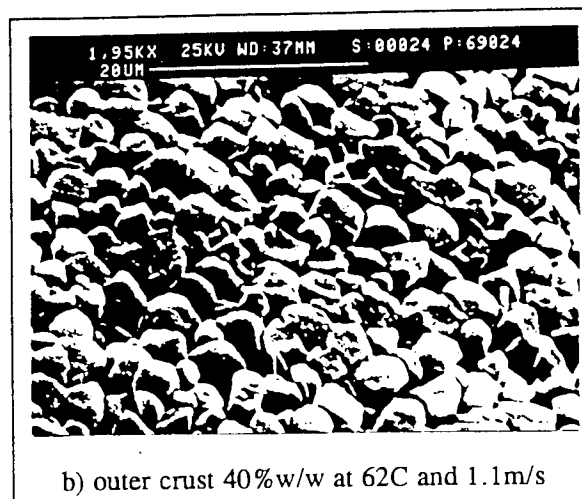
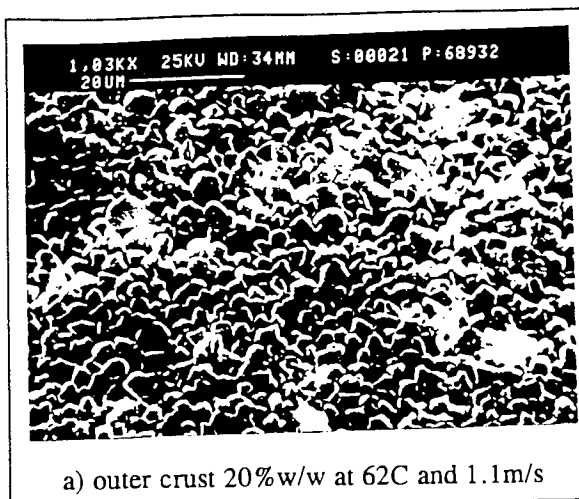


Plate 22

Electron photomicrographs of rice starch showing the effect of initial solids concentration (a,b) and drying temperature upon crust structure (a,c,d & e).

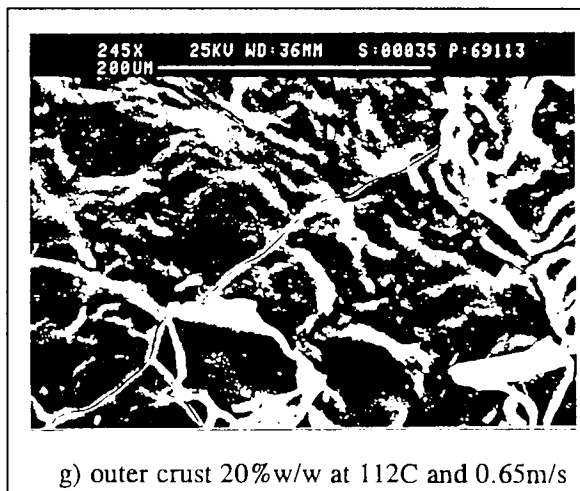
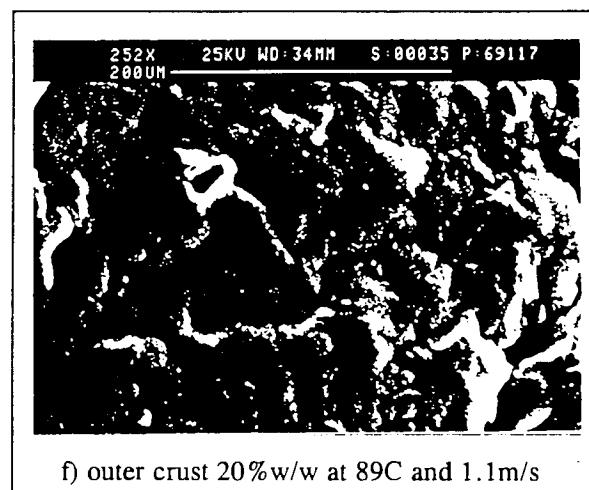
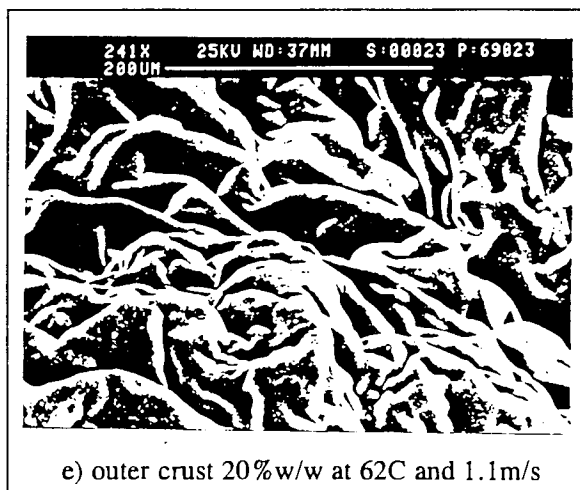
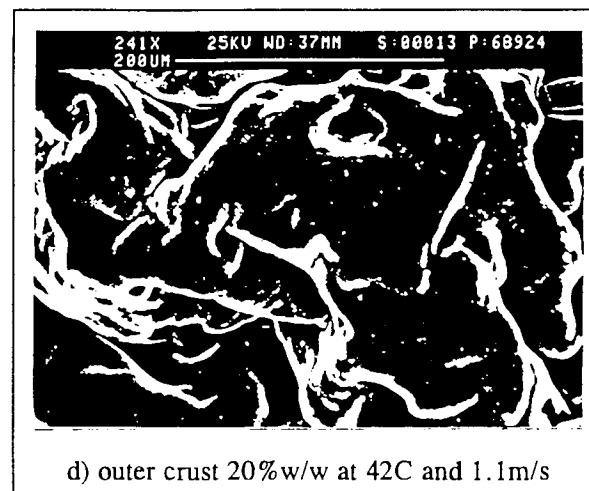
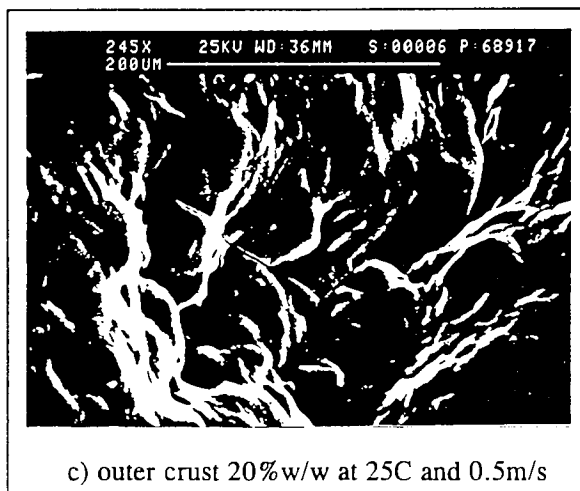
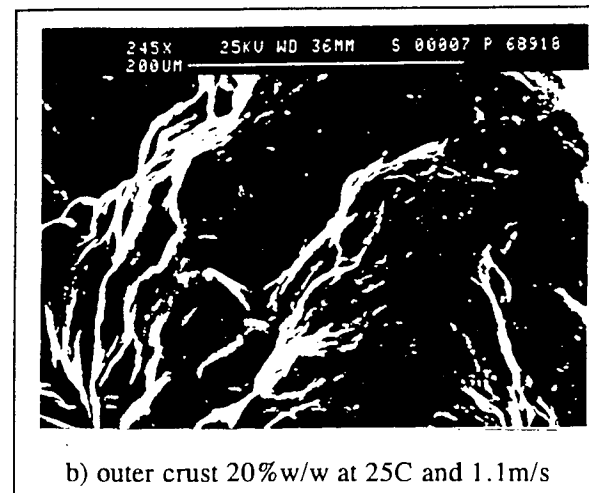
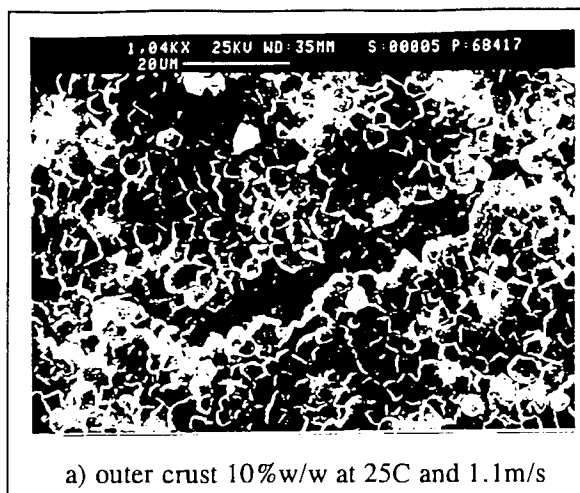


Plate 23

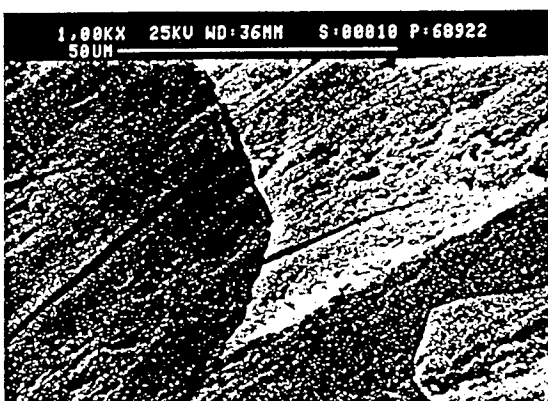
Electron photomicrographs of wheat starch showing the effect of initial solids concentration (a,b), air velocity (b,c) and drying temperature upon crust structure (a,d, e, f & g).



a) outer crust 10%w/w at 25C and 1.1m/s



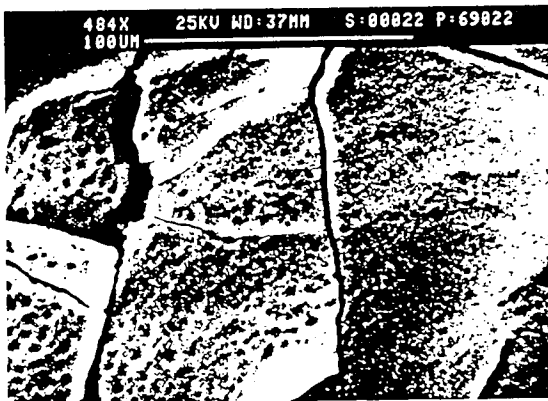
b) outer crust 20%w/w at 25C and 1.1m/s



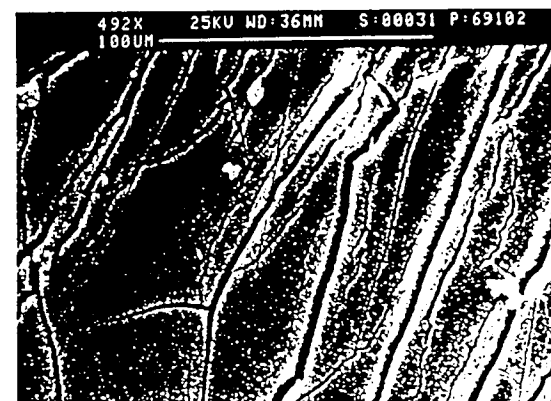
c) outer crust 40%w/w at 25C and 1.1m/s



d) outer crust 20%w/w at 42C and 1.1m/s



e) outer crust 20%w/w at 62C and 1.1m/s



f) outer crust 20%w/w at 89C and 1.1m/s



g) outer crust 20%w/w at 112C and 0.65m/s

Plate 24

Electron photomicrographs of dextrin showing the effect of initial solids concentration (a-c) and drying temperature upon crust structure (b,d, e, f & g).

Volatiles retention in the drying of skin forming materials

Part 2: Natural materials

Abid A Sayed*, Haydar H Hassan & Clive J Mumford

Chemical Engineering & Applied Chemistry Dept., Aston University, Birmingham B4 7ET, England

Keywords: single droplet, volatiles retention, fructose, skim milk, coffee, volatiles retention

Abstract:

The retention of ethanol as a simulated flavour was determined experimentally by drying of coffee and crust


Aston University

Content has been removed for copyright reasons

439 - 453
removed

I
E
F
f
E
A
u
w
di
w
W
ve
30
dr
Tl

demonstrated that
for the increased
viscosity of the 4
water, thus allowi

13

pective

related
omena
effect
would

drying
) The
lowed

) The
cially
e was
tation

opic,

ilarly
10%
The
there

ted a
/2 <
utes
ying.
e 2,
planation
increased
ed to the

Volatiles retention during the drying of skin forming materials

Part 3: Heat-sensitive materials

Abid A Sayed*, Haydar M Hassan and Clive J Mumford

Chemical Engineering & Applied Chemistry Dept, Aston University, Birmingham B4 7ET, England.

Keywords: single droplet, volatiles retention, gum arabic, gelatine, skin formation

Abstract:

Ethanol retention in a single droplet

he
er
st.
de

In

He
dry
con
the
ma
onl
pro

Exp

The
l o
v/w
stat
coll
Blo
fron
gela

The
each

Exp

The
diffe
the g

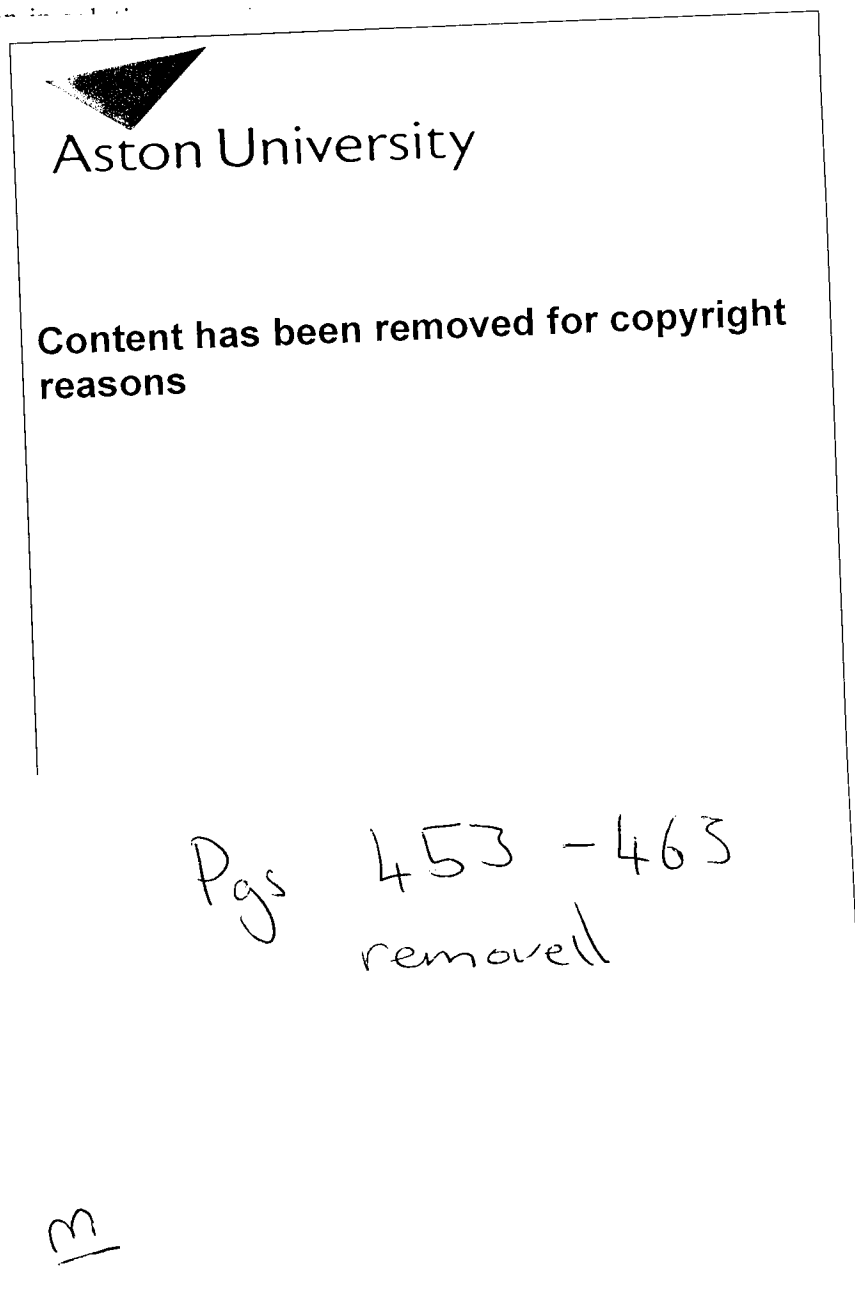
In the
50%

Gelat

Effec

The e
40%,
conce
proba
drople

... a rise to the wet bulb temperature and remained constant for almost 30 seconds, i.e. the initial evaporation was from a saturated surface. This coincided with a rapid loss of ethanol from the droplets during the first minute of drying.



in a
c as
crust
eters

heir
gory
less
the
skin
tive

'art
0%
ise
l a
60
ed
he

of

to
of

to

d
il
s
ne